Urban Adaptation Measures for Climate Change: Study of Urban Wetlands in View of Potential Urban Cooling

by

Abu Taib Mohammed Shahjahan

A thesis submitted
In partial fulfilment of the requirement for the
Degree of DOCTOR OF PHILOSOPHY

Department of Architecture
BANGLADESH UNIVERSITY OF ENGINEERING AND TECHNOLOGY
2018

Department of Architecture
Bangladesh University of Engineering and Technology
Dhaka-1000, Bangladesh.

The thesis titled 'URBAN ADAPTATION MEASURES FOR CLIMATE CHANGE: STUDY OF URBAN WETLANDS IN VIEW OF POTENTIAL URBAN COOLING' Submitted by Abu Taib Mohammed Shahjahan, Roll No. 0410014001 P, Session- April 2010, has been accepted as satisfactory in partial fulfillment of the requirements for the Degree of Doctor of Philosophy on this day February 26, 2018.

BOARD OF EXAMINERS

1. ______________________________ **Chairman**
Dr. Khandaker Shabbir Ahmed
Professor, Department of Architecture, BUET, Dhaka
(Supervisor)

2. ______________________________ **Member (Ex-Officio)**
Dr. Khandaker Shabbir Ahmed
Professor and Head
Department of Architecture, BUET, Dhaka

3. ______________________________ **Member**
Dr. Zebun Nasreen Ahmed
Professor, Department of Architecture, BUET, Dhaka

4. ______________________________ **Member**
Dr. Shayer Ghafur
Professor, Department of Architecture, BUET, Dhaka

5. ______________________________ **Member**
Dr. Muhammad Ashraf Ali
Professor, Department of CE, BUET, Dhaka

6. ______________________________ **Member**
Dr. Ismail Said
Associate Professor, Department of Landscape Architecture
Faculty of Built Environment, Universiti Teknologi,
Malaysia 81310, Sekudai. Johor, Malaysia

7. ______________________________ **Member**
Dr. Ishrat Islam
Professor, Department of URP, BUET, Dhaka

8. ______________________________ **Member (External)**
Dr. Cristian Suau
272 Bath Street, Glasgow, Scotland, G2 4JR, UK
(Ex-Faculty University of Strathclyde)

9. ______________________________ 26.02.2018. **Member (External)**
Prof. Dr. Kazi Md. Fazlul Haq
Department of Geography & Environment
Faculty of Earth and Environmental Sciences
Dhaka University, Dhaka-1000

Signature of the Examining Committee:

1.

____

Chairman

2.

____

Ex-officio

3.

Dr Cristian Suau

____

☐ Internal/ ■ External Member

4.

____

☐ Internal/ ☐ External Member

5.

____

☐ Internal/ ☐ External Member

6.

____

☐ Internal/ ☐ External Member

7.

____

☐ Internal/ ☐ External Member

CANDIDATE'S DECLARATION

It is hereby declared that this thesis has been prepared in partial fulfillment of the requirements for the degree of Doctor of Philosophy in Architecture at Bangladesh University of Engineering and Technology, Dhaka and has not been submitted elsewhere for the award of any degree or diploma.

Abu Taib Mohammed Shahjahan
Student number: 0410014001
Session: April 2010
Department of Architecture
Bangladesh University of Engineering and Technology, Dhaka-1000

Acknowledgements

It is a great pleasure to acknowledge my indebtedness to my supervisor Professor Dr. Khandaker Shabbir Ahmed, Department of Architecture, Bangladesh University of Engineering and Technology (BUET), for his constructive advice, appropriate guidance and support which always helped me in many critical moments in the research. His scientific approach to any problem and quest for exploring new phenomenon of nature always was and will be an inspiration for me. I am grateful to my External Supervisor: Dr. Ismail Said of Associate Professor, Department of Landscape Architecture, Universiti Teknologi Malaysia for his useful and timely comments. His cordiality and enthusiasm was always encouraging in difficult work. I thank the staffs of Department of Architecture, BUET for their sincere support in many official works. Thanks are due to many individuals for their help in my field work.

Finally, I wish to thank my parents for their continuing encouragement and support for my education since childhood. I am greatly indebted to my wife who generously allowed my absence from my duties towards family for an extended period to complete my research work.

ABSTRACT

Urbanization in the developing world took place at an unprecedented rate which outpaced that of the developed world except for few exceptions. Much of the urban areas of the developing world are in the tropical zone, which has gone through an inadvertent environmental modification due to increased built density. This environmental modification due to high built density resulted in an adverse thermal environment in the urban area which is further exacerbated by global warming due to climate change. This adverse thermal environment in the city resulted in a much-reported phenomenon known as Urban Heat Island. An adaptation measure against Urban Heat Island in the tropical cities of the developing world can be use of the natural cycle to cool down the overheated urban fabric.

Dhaka is one of the most densely populated cities in the world, where the juxtaposition of wetlands and built up area coupled together may have an opportunity for creating a viable and distinct character of its own while addressing the challenges of inadvertent environmental modification. Increased built density and reduction of wetlands are making Dhaka’s climate uncomfortable in comparison to its rural surroundings, resulting increasing number of air-conditioned buildings, which in turn elevate urban air temperature and consequent energy demand. Thus, urban land use in Dhaka is directly contributing to Urban Heat Island effect. Coolth produced by urban wetland can be an adaptive measure against urban heat island in Dhaka. This study approaches the problem by identifying wetland as existing and potential cool spot and analyzing their characteristics for cooling efficiency. Remote sensing technique was used to identify the existing and potential cool spot at surface level for analysis. This technique applied to analyze the morphology of the wetland as a producer of coolth with potential to counterbalance for the urban heat. As a part of the study field campaigns were conducted and environmental variables were recorded on the buffer area of selected wetlands indicated in the remote sensing study. Evaluations were undertaken with respect to the design factors such as the orientation of the wetlands, riparian shading characteristics, urban permeability for the cooling effect, as those factors affect the cooling intensity produced by the wetland. Through simulation studies, some aspects are identified which could not be derived from the fieldwork. They are the effect of differential riparian shading on the wetlands, effects of variable temperature and relative humidity on the coolth produced by the wetland. Based on the simulations some urban design recommendations was derived.

The research finding that indicated the relationship between some important factors like the interdependency between fetch and inversion height to control inversion layer over the water surface that regulate the urban cooling effect of the wetland at an urban scale. This relationship informs as to what extent urban wetland design might impact the thermal environment leading to possible urban microclimatic cooling. These findings, in turn, might help in the development of certain policy guidelines for the urban designers and planners to more positively impact the urban thermal environment.

Table of Contents

Data: All the data used in this PhD research is included on the CD attached at the back of the thesis.

Transparent Protractor: A protractor containing the base map of the Dhaka city also attached at the back of the thesis to aid the reading of the Land surface temperature map extracted from the Landsat data.

List of Figures

List of Tables

Chapter 1 : GENERAL BACKGROUND

1.1 Introduction

The world has crossed a historic landmark in 2008, since the construction of earliest urban settlement like Catal Hyuk and Zericho almost 9000 years ago. From 2008 “more than half of the world’s population started living in urban centres than the rural areas and this ratio of urban to rural population continues to grow”. Urbanization in the developing world is dramatic if compared with the standard of today’s urbanized world. Within a short span of time urban population in developing world superseded the developed world. Most of the rural-urban migration in the developing world is for the economic reasons, as city offers better opportunity in terms of livelihood. Many people also migrate to urban areas for the preference of the urban way of life, which is markedly different from the rural. In many parts of the developing world natural disaster like flood, river corrosion, draught often drive away the poorest rural people to the urban area, as they become landless due those natural disaster. Land grab by the social elite or corporations for their economic reasons or exploitation is also contributing to the urban rural migration. Developed world also contributed to the rapid urbanization in the developing world using cheap labours for the mass production of their necessary goods at a lower price. In the recent times, most of rural-urban migrations in the developing world are related to global climate change. All those factors discussed earlier, created the unprecedented urbanization in the developing world, which dwarfed that of the developed world except few exceptions. While Latin America is the world’s most urbanized continent, Asia is distinctive for its rapid transformation into metacities. From a low level of urbanization Africa observed fastest rates of urbanization. Much of the urban areas of the developing world are in the tropical zone, where urbanization is distinctive from climate, demography and cultural point of view. Rapid urbanization in the developing world often went out of control measures putting constraint on necessary infrastructural facilities essential for city life like services, transportation etc. Informal urban areas like slums of developing world are result of the lack of infrastructural facilities and services. “United Nations Population Division” stated that, “the urban population in the global total population has risen dramatically from 13% in 1900 to 46% in 2000” (figure 1.1). UNPD stated that “more than half the world’s population together with its economic activities and built assets are in urban areas” (UNPD, 2014). UN projections also suggest that “Urban centres of Current low- and middle-income nations will contribute to almost all the population increase up of the whole world to 2050” (UNPD, 2014). Global urban population growth is propelled by the growth of all sizes of cities. At 2030 there will be 41 megacities of the population 10 million or more.

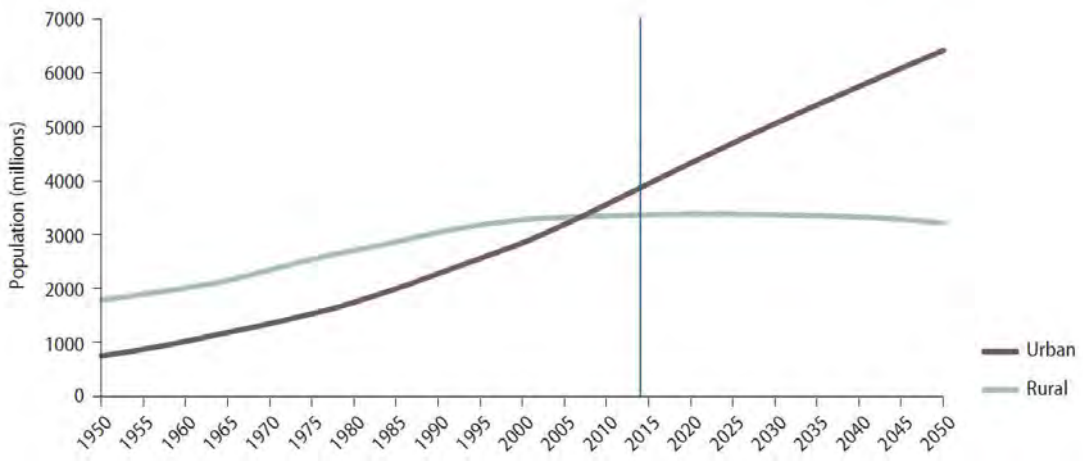

Figure 1.1: Urban and rural population of the world, 1950-2050 (UNPD, 2014)

Nearly half of the urban population will be in the cities in Asia (Figure 1.2).

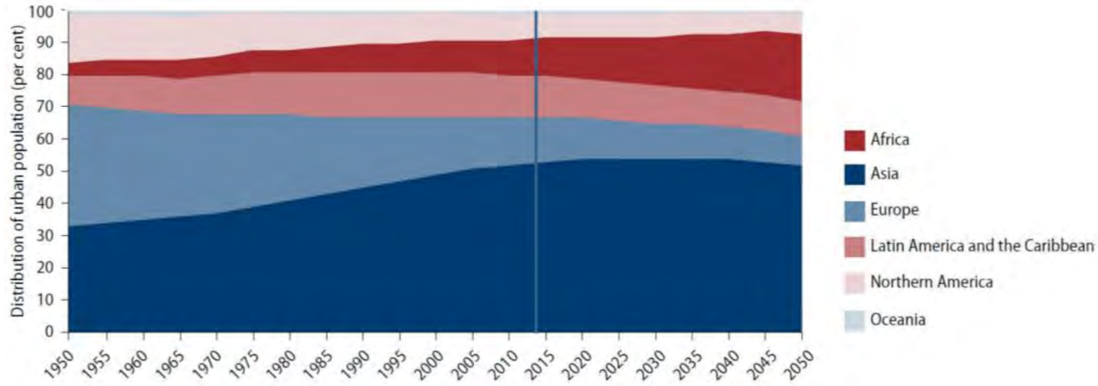

Figure 1.2: Distribution of world's Urban population (UNPD, 2014)

Zhu O. et al., (2012) reported that cities today occupy only 2% of the total land, however, they contribute 70% of the GDP. Carbon emissions from cities and their support systems represent the single largest human contribution to climate change. Over 60% of the Global energy consumption belongs to the urban area. By this energy, consumption cities produce 70% of the greenhouse gas emissions and also the same percentage of global waste. Half of the greenhouse gas emissions are from the mega cities (Zhu O et al., 2012).

1.2 Urbanization and Climate Change

Recent reports of "Intergovernmental Panel on Climate Change (IPCC)" stated with the significant importance that "Climate Change due to anthropogenic activities has caused severe impacts on human and natural systems on all continents, resulting in climate-related extremes" (Revi A. et al, 2014). The examples of such extremes are such as: a. poor air quality, b. extreme heat/cold and human thermal stress, c. hurricanes, typhoons, extreme local winds, d.wild fires, sand and dust storms, e. urban floods, f. sea-level rising level of sea due to global warming, g. energy and water sustainability h. public health problems caused by the extreme hazard events.in a recent study. Missirian A. et al (2017) related increase in temperatures in developing countries to an increase in asylum applications to the EU. They also expect this larger surge in migration continue to increase in future with the warming climate.

According to the IPCC, Bangladesh is the sixth most vulnerable country to the Climate Change (IPCC, 2014). At present the capital of Bangladesh Dhaka is the densest and 'one of the most populated cities in the whole world'. In 1948, Dhaka was a city with an area of approximately 50 sq.km and with a population of 250,000 and in 1993 the population of Dhaka grew to 7.4 million with an area of 300 sq.km and at present, the population is more than 14 million [Ahmed R. 1993; BBS, 2016]. Wetlands and green spaces are diminishing due to unprecedented and often unplanned urbanization, in addition to pressure from the housing sector. Within a span of 20 years (1989-2009), urban wetlands in Dhaka metropolitan area has been reduced from 26.68% of the total area to 9.27% of the total city area, which is approximately a 65% reduction [Ahmed B., et al, 2013]. Increased build density and reduction of public open spaces and wetlands are making Dhaka's climate uncomfortable in comparison to its rural surroundings. Number of air-conditioned buildings increases due to high temperature in urban Dhaka. Air-conditioner used in the buildings extracted heat from interior to exterior urban environment, which in turn elevated urban air temperature and consequent energy demand.

1.3 Statement of The Problem

One of the climate-related extreme that we are facing in Dhaka like other megacities in the world is Urban Heat Island (UHI) which are exacerbated by growing global temperature. From numerous study on UHI mitigation, it can concur that "Urban water bodies can play an effective role in mitigating UHI through microclimatic cooling of the urban area by creating cool spots". As these cool spots can transport coolth inside the urban fabric, they can be termed as Urban Cooling Islands (UCIs). Besides the wetland urban parks can also act as UCIs for the evapotranspiration effect and shading of the trees. As the Heat content capacity of the water is high it could counteract the UCIs effect if kept unshaded. Urban wetland Shaded by Built environment, topography and shade trees can have a proficient effect on microclimatic cooling, whereas riparian shade is having a positive effect on the UCIs as well as on the water quality. The effect of riparian shade on the water body is mostly observed on the linear and narrow streams having urban area barely on either side (Sun R. et al., 2012). There are very few detail studies about the effect of riparian shade on the wider water body. Also, most of the study suggesting a small area and regular (Euclidean shape) shape water body distributed in the regular interval in an urban area for better Urban Cooling Island (UCIs) intensity. Hence the Major research questions are:

- How could the negative impact of the Heat capacity of the reservoirs on UCIs be moderated by the introduction of riparian shade?
- Could the large water body with fractal shape moderate the impact of the heat capacity of the reservoirs on UCIs?
- What is the link between 'UCIs' and the "water quality" of the urban wetland?

Also, it was essential to investigate if it was possible to lower the minimum water temperature of wetland below the temperature of the air immediately above it by providing continuous shading of the water surface, at least during the hot and dry period.

1.4 Methodology

Hence, the specific aims of this PhD research was to develop a sustainable path to transform potential wetlands of Dhaka into "Urban Cooling Islands (UCIs)" to address warming issues of Climate Change which will also promote waterfront ecology with leisure and park amenities as they relate to the urban environment. There is growing energy crisis in the city due to the high cooling energy demand. Therefore, Urban cooling will be an effective way forward as an adaptation measure against climate change. This multidisciplinary research also aims to form an area of co-existence between natural and manmade structures in Dhaka.

1.4.1 Objectives of the research

i. To investigate the factors of Urban Wetland that contribute to Urban Cooling Islands (UCIs) in Dhaka.

ii. To evaluate the impacts of wetland area, shape complexity, location and riparian shading potential on UCIs intensity in Dhaka.

The research can potentially indicate the parametric relationship between the factors that regulate the Urban Cooling Island (UCI) effect of the wetland at an urban scale. This relationship will give insight to what extent urban wetland design might impact the thermal environment leading to possible Urban Microclimatic cooling. These findings, in turn, might help in the development of a tool for the urban designers and planners to more efficiently manage the Urban Thermal Environment. This research will follow the strategy of field study to support simulation and modelling research:

1.4.2 Remote sensing of Urban Cooling Island

Through the study, the existence and intensity of potential Urban Cooling Island (UCI) formed by the wetlands were identified. Spatial information on the land cover and Land Surface Temperature (LST) was extracted using the data obtained from Earth-observing satellites Landsat. Land remote sensing data, obtained by Landsat satellite is the longest continuously acquired moderate-resolution data in terms of time span. Landsat is a joint initiative between the "U.S. Geological Survey (USGS)" and "NASA". The data obtained by Landsat Project is freely available for all types of use, irrespective of governmental, commercial, industrial, civilian, military, and educational purpose worldwide. One of the main rationale to select Landsat data was that it allows to compare and analyze the long-time change in Urban surface temperature due to data availability.

1.4.3 Field measurement of Urban Cooling Island

Based on the previous study conducted by Bangladesh Meteorological Department and Shahjahan et.al (2016), two wetlands of Urban Dhaka were selected for the field study. They were Dhanmondi and Hatirjheel lake. The rationale for selecting wetland sites are given below:

i. These two wetlands are accessible up to their inner periphery without any hindrance.
ii. Both the wetlands have radiating roads leading into the surrounding urban fabric having potentials for studying impact of wetland on surrounding area.
iii. To enable the analysis of the effect of riparian shade, Dhanmondi Lake was selected for its significantly visible riparian shade and Hatirjheel lake was chosen for the absence of visible riparian shade.
iv. The watershed characteristics of both the lakes are comparable in terms of area.
v. Both the lakes are located on the same physiographic condition (Brammer H., 2012). Agro ecological zone for both the lake are also same (FAO/UNDP,1988).
vi. Both the lakes are located on the same overall geothermal gradient zone (Akbar M.A.,2011).

These two existing urban wetlands in Dhaka were studied to discern the relation among the factors such as- UCI intensity and extent; wetland area, shape, location and heat capacity; Riparian buffer width and type for the Riparian shade of the wetland. A buffer zone of 0.5 km from the edge of the wetlands were taken into consideration for the field measurement. Within the buffer zone multiple points starting from the water edge to the deep inside urban fabric were selected for microclimatic measurement in line with other studies performed in this field [Sun R. et al, 2012; Robitu M.et al, 2006; Hwang S.J.et al, 2007].

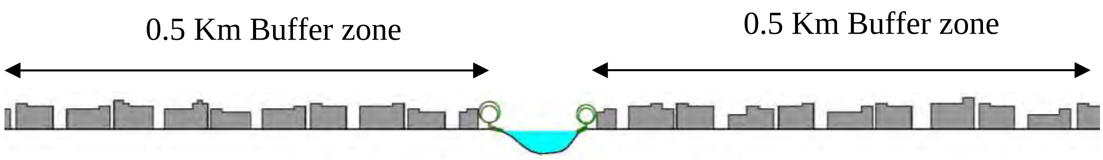

Figure 1.3: Buffer zone for field measurement

Measurement were performed by the following methods:

Choosing the location for an urban station:

The Urban data logging station inside the urban area around these two wetlands were selected with the intent to detect the greatest impact of those wetlands on the microclimate of the encompassing urban fabric. Surrounding area uniform in nature or more representative at least with in a half km buffer zone. The Areas has been selected based on the Urban Climate Zone (UCZ) types given by Oke (2017) expecting the highest probability of finding maximum effects in the Urban Canopy Layer (UCL).

Extensive areas of similar urban development were closely investigated to select a typical urban station. The second step of the search was conducting spatial surveys of air temperature and humidity through traversing the areas of interest surrounding the wetlands carrying the sensor on foot. Cross sections or isoline maps have been drawn after several repetitions of traverse. These cross sections and isoline maps revealed the areas of thermal and moisture anomaly. Those anomalies were the point of significance. Traversing had been done during calm airflow and cloudless skies as recommended by Oke (2006) .Calm airflow and cloudless sky condition increase the potential to differentiate micro- and local climate. The aim was to monitor local effect of urban wetland. For this reason, locations of urban data logging stations were subjected to such local effect. The network of the urban stations designed specifically to sample specific local effects on the urban climate, such as the amelioration of an overly hot urban area by lake breezes.

1. **Air temperature:**

The air temperature around the selected water bodies were measured using air temperature measuring thermometer/data logger.

Response times of thermometers:

Thermometers with a very small lag coefficient or time-constant records temperature readings which fluctuates rapidly within a few seconds up to one or two degrees. A good number of readings should be averaged to get a representative reading from these fluctuating readings. So, for routine measurement there is no benefit of using thermometer of small time constant. A reasonably larger time-constant of thermometer will smooth out these rapid fluctuations. But if the time-constant is too long it may result in errors in case of long-period changes in temperature. It is recommended by Oke (2006) that "the time-constant, defined as the time required by the thermometer to register 63.2 percent of a step change in air temperature, should be 20 s. The time constant depends on the air-flow over the sensor".

Recording the circumstances in which measurements are taken:

Temperature is one of the meteorological quantities whose measurements are particularly sensitive to exposure. WMO stated that "for climate studies temperature measurements are affected by the state of the surroundings such as vegetation, presence of buildings and other objects such as ground cover". The condition of the shield and the modification in the design of the radiation shield or screen, or by some other changes in equipment can also affect temperature measurements. It is important that records should be kept not only of the temperature data but also of the circumstances in which the measurements are taken. Such information is known as metadata (data about data).(Organization & WMO, 2008). The metadata for all the urban stations in both the wetlands were collected.

Radiation shields:

Screens to use as radiation shields for the data logger was made from a Thermally insulating material (e.g. particle board), as the system relies on natural ventilation. The size and construction of the perforated screen constructed, to keep the heat capacity as low as practicable and allows ample space between the instruments and the walls. Direct contact between the sensing elements and the thermometer mounting was avoided. only one door is kept, with the screen being placed so that the sun does not shine on the thermometers when the door is open at the times of observation and the screens are made of plywood.

Observation Period:

To investigate ‘urban microclimate’ dynamics and the “urban heat island”, selected observation days were chosen to typify a range of different weather status, like the three design seasons in Dhaka other than rainy days. It was essential to attain data of high geographical and temporal resolution. But, taking account of our limited budget and manpower, we were only able to collect 12-h samples of data on six occasions, starting from October to February, which were adequate for the research. The variables measured were air temperatures, humidity and wind speed at 1.5–2.0-m height in the middle of Urban Canopy Layer and wetland edge from 07:00 am of one day till 06:00 pm of the same day. Except in one case where the data logger was placed with the Bangladesh Meteorological Department (BMD) instruments for three days for validation purpose. Wind direction and velocity, in our case, were measured just at the edge of the wetland. (Huang, Li, Zhao, & Zhu, 2008)

For air temperature, two types of measurements had been carried out, one is traverse measurement and the other is continuous data logging in the Urban Canopy Layer (UCL) at a selected location based on the Buffer analysis. The position of the data logger in the Urban Canyon and the Wetlands is shown in the figure below:

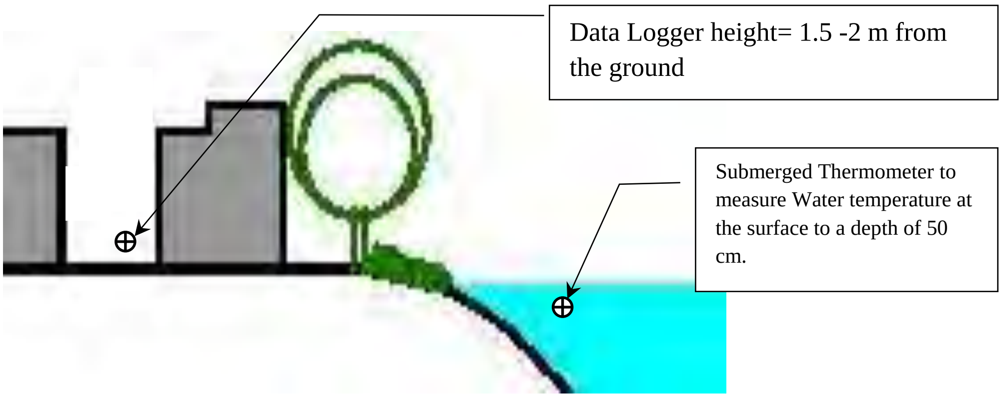

Figure 1.4: Installation of the data loggers on the site.

2. **Water Temperature:** Water temperature of the selected water bodies were measured using thermometer.
3. **Wind speed:** Wind velocity around the wetland within the buffer zone were measured by traverse measurement.

4. **Wetland area, location and Riparian buffer:** Continuous buffers around each wetland was identified with appropriate interval using the spatial analytical module in ArcGIS software. Location and area of the urban wetland were determined from the GIS data of Dhaka. Riparian buffer width and type were determined from GIS data.
5. **Shape complexity of the wetland:** FRAGSTATS, a "spatial pattern analysis program for quantifying landscape structure" were used to determine shape complexity of the selected water bodies of Dhaka. There are several indices to measure the shape complexity, originally developed by Mandelbrot. Perimeter (P) to Area (A) ratio is one of the first measurement of shape complexity of a landscape feature. Several shape complexity indices were integrated in FRAGSTATS software. Among them, "Fractal Dimension Index (FRAC) used to measure the shape complexity of Urban Wetland" [Mandelbrot B. B., 1982. McGarigal K.et al,1995].

1.4.4 Simulation and modelling

Numerical model quantifying shading by riparian vegetation, topography and built-form were built. "Computational Fluid Dynamics (CFD) simulations of the evaporative and radiative cooling effect from water surfaces, buoyancy-driven flow to the wetland and from the wetland in a micro-scale urban environment was evaluated with various configurations" (Robitu M. et al ,2006). The model was used to estimate the influence of wetlands in the micro-climate of surrounding area in real situations.

Problem modelling:

Data obtained from the field study of the two wetlands were entered into the COMSOL–Multiphysics software as a part of problem modelling study. Water and Air temperature, Relative humidity and Wind speed are primary inputs for the simulation besides types of ground cover and the built form. Once the problem modelling is done, the model will be projected to test the specific effect of each contributing factor of Urban Cooling Island (UCI) described above. The principal assumption which had been tested in the simulation model was that the water in the wetland will be cooled down with the help of continuous shading and evaporation to act as UCI, which in turn will cool down the air above it and create high-pressure zone. This cool air will then flow towards the nearest urban centre with low-pressure zone owing to the UHI (Figure 1.5).

The modules of the COMSOL-Multiphysics that are to be combined to model the Urban Cooling Island Effect of the urban wetland is:

i. CFD module: Fluid Flow-Single phase flow
ii. Heat Transfer Module: Heat Transfer in Fluids and Heat Transfer with Surface to Surface Radiation (ht)
iii. Chemical Species Transport: Transport of Diluted species (tds).

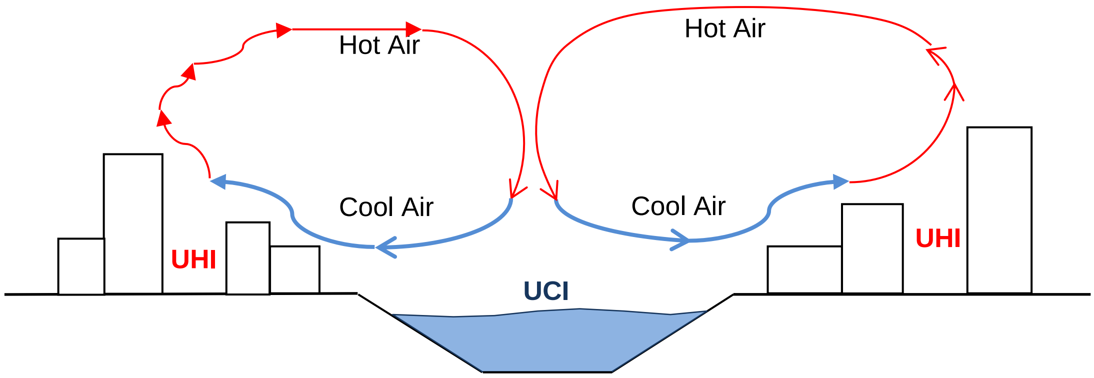

Figure 1.5: Model of Buoyancy Flow

1.4.5 Research framework

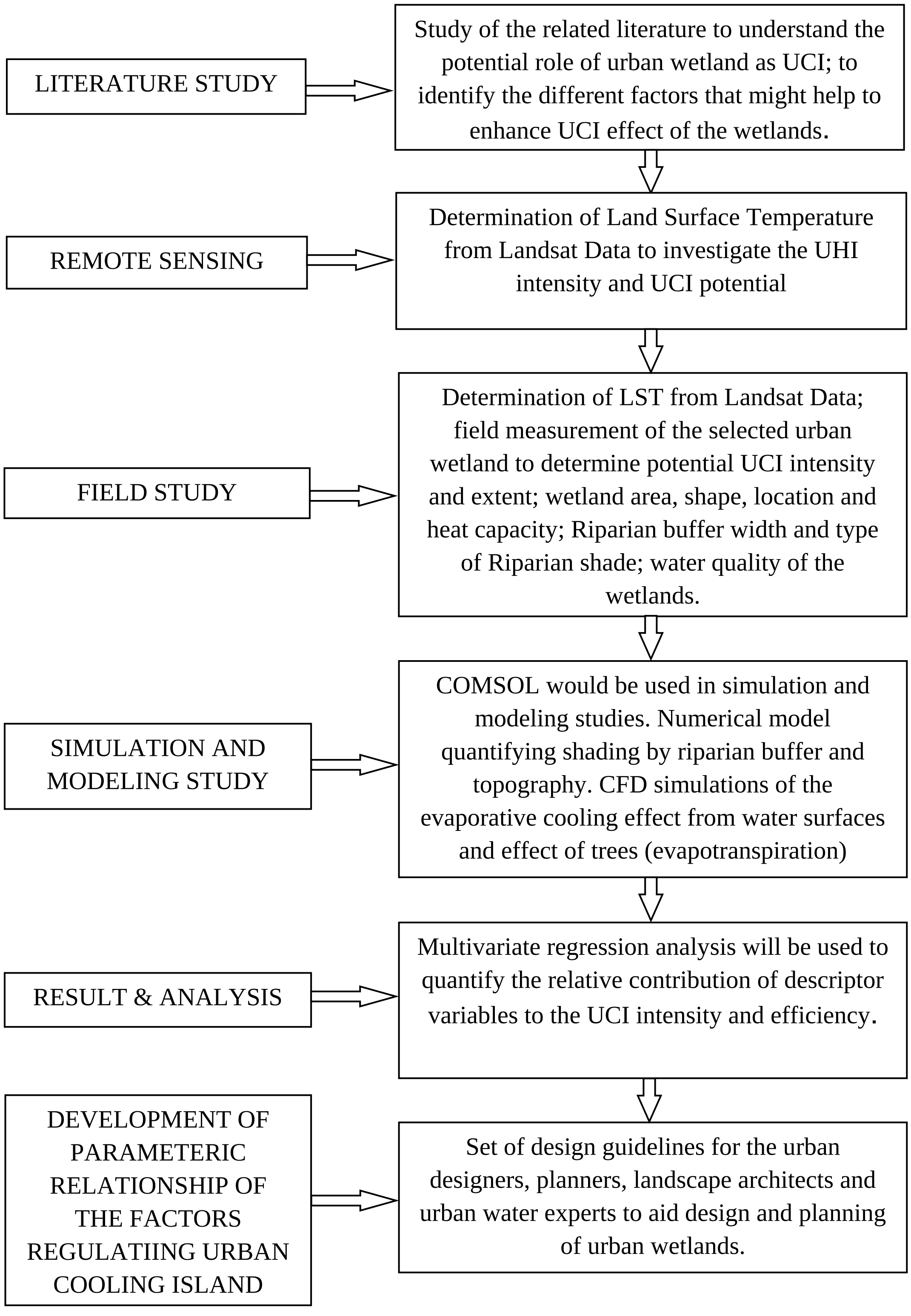

Figure 1.6: Research Framework

1.5 Structure of The Thesis

Chapter one starts with a brief introduction to the urbanization trends of the whole earth and then describes the major impact of the climate due to rapid urbanization. Then the Statement of the problem is given followed by the research objectives. Then a detail description of the methodology to conduct the research are explained. The related references to this chapter are given at the end.

Chapter two begins with the brief description of the Urban Boundary Layer (UBL) followed by brief discussion of the physics behind the Urban Energy Balance. Then the formation of Urban Heat Island (UHI) is explained followed by the category of UHI and its spatial structures and causes of UHI. An Urban Heat Island studies at surface level in Dhaka is presented at this chapter. At the second part of the Chapter there are description of UHI mitigation strategies identifying the role of the Urban wetland as Urban Cooling Islands (UCIs) to mitigate Urban Heat Island effect. This chapter then elaborates the morphology of UCI through identifying its necessary parameters. At the end, the related references are given.

Chapter three elaborate the role of riparian shading in the formation of UCIs. It also indicates the methods of creating riparian shading besides identifying the other ecological services provided by trees including carbon sequestration. Second part of the Chapter explains the mechanism which transports the cooling effect from the source. At the end of the chapter related references to this chapter are given.

Chapter four starts with the objectives of remote sensing technique used for the study. It then explains the methods and the necessary equation for remote sensing. After that, it analyses the UCI with the help of LST and other parameter derived through remote sensing. Related references are given at the end.

Chapter five starts with the objectives of field measurement conducted for the study of UCI. It then explains the field measurement methods, analysis of data obtained from the field and results from field measurement followed by related references.

Chapter six starts with the objective of the simulation study for the research. It then explains the platform chosen for simulation study and simulation model itself. After that result obtained from the simulation are analysed and findings are presented followed by references to related literature

Chapter seven brings together all the findings specially from remote sensing, field measurement and simulation study to explain all the parameters required for the formation of Urban Cooling Islands (UCIs). It then elaborates the techniques obtained from the research to transform Urban wetlands into UCIs as an adaptation strategy against the Urban Heat Island effects.

1.6 References

1. Ahmed R. (1993). "*In search of the impact of urbanization on the thermal environment of the city of Dhaka, Bangladesh, during the pre-monsoon hot season from 1948 through 1987*". Report of the Technical Conference on Tropical Urban Climates Dhaka, Bangladesh, 28 March - 2 April 1993, World Meteorological Organization (WMO).
2. Ahmed B., Kamruzzaman M., Zhu X., Rahman S.M. and Choi K. (2013). *"Simulating Land Cover Changes and Their Impacts on Land Surface Temperature in Dhaka, Bangladesh". Remote Sens.*, 5, 5969-5998; doi:10.3390/rs5115969
3. Akbar, M. A. (2011). "*An assessment of the geothermal potential of Bangladesh*". (pp. 1-33, Rep. No. 5). Reykjavik, Iceland: United Nations University.
4. Brammer H. (2012). "*The physical geography of Bangladesh*". First edition, The University press limited, Dhaka.
5. Bangladesh Bureau of Statistics. (2016) "*Community Report, Dhaka Zila, June 2012"*. Population and Housing Census 2011, Statistics and Informatics Division, Ministry of Planning. *Bbsgovbd*. Retrieved 29 March 2016, from http://www.bbs.gov.bd/PageSearchContent.aspx?key=statistical yearbook.
6. FAO/ UNDP (1988). "*land resources appraisal of Bangladesh for Agricultural Development Report 2: Agro-ecological regions of Bangladesh*". (Rep. No. 2). (1988). FAO.
7. Huang L., Li J., Zhao D., Zhu J (2008). "*A fieldwork study on the diurnal changes of urban microclimate in four types of ground cover and urban heat island of Nanjing, China".* Building and Environment 43, 7–17.
8. Hwang S.J., Lee S.W., Sona J.Y., Park G.A., Kim S.J. (2007). "*Moderating effects of the geometry of reservoirs on the relation between urban land use and water quality*." Landscape and Urban Planning 82, 175–183, Elsevier.
9. Hossain M.E. and Nooruddin M.*"Some aspects of urban climates of Dhaka city".* Report of the Technical Conference on Tropical Urban Climates Dhaka, Bangladesh, 28 March - 2 April 1993, World Meteorological Organization (WMO).
10. IPCC. (2014). Climate Change 2014: Synthesis Report. Contribution of Working Groups I, II and III to the Fifth Assessment Report of the Intergovernmental Panel on Climate Change [Core Writing Team, R. K. Pachauri and L. A. Meyer (eds.)]. IPCC, Geneva, Switzerland, 151 pp.
11. Kadygrov, E.N. 2006. "*Operational Aspects of Different Ground-Based Remote Sensing Observing Techniques for Vertical Profiling of Temperature, Wind, Humidity and Cloud Structure"*. IOM Report No. 89, WMO/TD No. 1309. Available from: http://www.wmo.int/web/www/IMOP/publications-IOM-series.html
12. Missirian A., Schlenker W. (2017). "*Asylum applications respond to temperature fluctuations".* Science 358 (6370), 1610-1614
13. Mandelbrot, B. B. 1982. *"The Fractal Geometry of Nature".* W. H. Freeman and Co., New York.
14. McGarigal, K., Marks, B.J., 1995. *"Fragstats: Spatial Pattern Analysis Program for Quantifying Landscape Structure"*. General Technical Report PNW-GTR- 351, USDA Forest Service, Pacific Northwest Research Station, Portland, OR.
15. Oke, T.R. 2006. "*Initial Guidance to Obtain Representative Meteorological Observations at Urban Sites". World Meteorological Organization, Instruments and Observing Methods*, IOM Report No. 81, WMO/TD-No. 1250 Available from: http://www.wmo.int/web/www/IMOP/publications-IOM-series.html
16. Robitu M., Musy M., Inard C., Groleau D. (2006). *"Modeling the influence of*

vegetation and water pond on urban microclimate". Solar Energy 80, 435–447.

17. Revi A., Satterthwaite D.E., Durand F. A., Morlot J. C., Kiunsi R.B.R., Pelling M., Roberts D.C., and Solecki W., 2014: Urban areas. In: *Climate Change 2014: Impacts, Adaptation, and Vulnerability. Part A: Global and Sectoral Aspects. Contribution of Working Group II to the Fifth Assessment Report of the Intergovernmental Panel on Climate Change*. Cambridge University Press, Cambridge, United Kingdom and New York, NY, USA, pp. 535-612.
18. Sun R., Chen L. (2012). *"How can urban water bodies be designed for climate adaptation?*" Landscape and Urban Planning 105, 27– 33.
19. Sun R., Chen A., Chen L, Lü Y. (2012). *"Cooling effects of wetlands in an urban region: The case of Beijing"*. Ecological Indicators 20, 57–64.
20. Tominaga Y., Sato Y. and Sadohara S. (2015). "*CFD simulations of the effect of evaporative cooling from water bodies in a micro-scale urban environment: Validation and application studies*." Sustainable Cities and Society 19(2015)259–270.
21. United Nations Population Division | Department of Economic and Social Affairs. (n.d.). Retrieved January 30, 2018, from http://www.un.org/en/development/desa/population/index.shtml
22. Zhu O, Melamed M.L., Parrish D., Gauss M., Klenner L.G., Lawrence M., Konare A.and Liousse C. (2012). "*WMO/IGAC Impacts of Megacities on Air Pollution and Climate"* (Rep. No. 205). (n.d.). Retrieved from http://www.wmo.int/pages/prog/arep/gaw/documents/Final_GAW_205.pdf

Chapter 2 : URBAN HEAT ISLAND AND ADAPTATION MEASURES

2.1 Urban Boundary Layer (UBL)

The lowermost part of the atmosphere of the earth which is in direct contact with earth's surface is known as Atmospheric Boundary Layer (ABL). The depth of the ABL is between 100 m to 3000m from mean sea level and controlled by surface roughness, thermal mixing, injection of air pollutants and moisture from the Earth's surface (Oke, 2017). The Atmospheric Boundary Layer can be divided into two layers: Outer and inner region. In the outer region, thermal effects of the Earth's surface dominate. The inner region is roughly lowest 10% of the ABL is more commonly known as the surface layer (SL). Here flow is dominated by friction with earth's surface. During daytime due to the thermal buoyancy driven flow initiated by the hot earth surfaces air is carried upward until they reach the top of the ABL, where further uplifting is barred by a capping inversion. The atmospheric layer above this capping inversion at height Z_i is known as the Free Atmosphere (FA). The layer just below the FA is called Entrainment Zone (EZ) where buoyant thermals air 'bombard' the underside of the inversion and sometimes overshoot into the FA for their inertia. Then they settle back as cleaner, warmer and drier air. This daytime situation in the outer layer is often termed as Mixed Layer (ML) which is refers to the top 90% of the ABL. Due to the Earth's surface, nocturnal cooling at night ABL shrinks nearer to the surface and settle down as a stagnant layer near to the ground at a depth of 200-400m. (Oke, 2017). This layer is known as the nocturnal boundary layer (NBL).

The Surface Layer (SL):

The lowest 10% of the ABL is known as the surface layer (SL) where surface influences such as heating, cooling, and roughness dominate even more, and frictional forces create most mixing.

Inertial sublayer (ISL):

The upper part of the Surface Layer (SL) where the atmosphere responds to the integral effects of Urban Neighborhoods is known as ISL.

Roughness sublayer (RSL):

The lower layer of the Surface Layer (SL), the flow responds to the nature of the individual roughness elements themselves. It is a zone of substantial flow deflection, zones of up- and downflows, overturning, vortices and plumes arising from facets that are warmer/cooler, moister/dryer, cleaner/more polluted than average. The upper boundary of the RSL is termed the blending height Z_r.

The Urban Canopy Layer:

In a city, "the lower part of the RSL, that is the layer below Z_H," i.e. the height of the main urban elements, is termed the urban canopy layer (UCL) (Oke, 1976, 2017). The UCL is the site of intense human activity and exchange and transformation of energy, momentum, and water. The top of the UCL is defined as the height of the urban elements – buildings and/or trees (Figure 2.1). Oke described that Defining the height of the urban elements is not an easy task, as evidence suggests that a few unusually tall elements (isolated high buildings, tall trees) play a particularly significant role in the generation of roughness and turbulence.

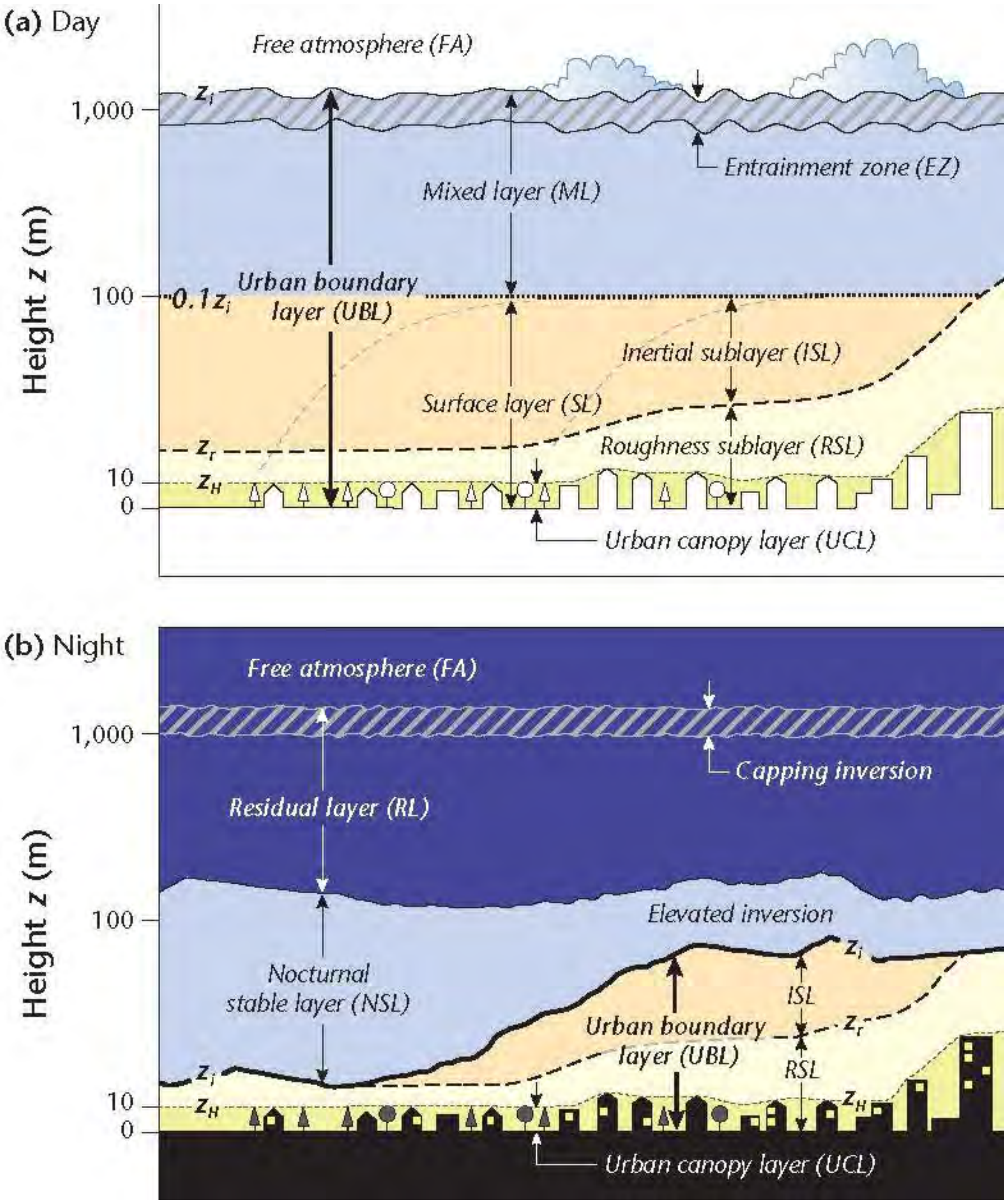

Figure 2.1: Schematic of typical layering of the atmosphere over a city (a) by day, and (b) at night. Note the height scale is logarithmic, except near the surface. (Oke 2017)

2.2 Urban Energy Balance

The relevant flux densities at a non-urban land surface are: the net all-wave radiation $Q*$, the ground heat flux density, that transfers sensible heat by conduction to the substrate (Q_G); the sensible heat flux density Q_H and the latent heat flux density Q_E are the two turbulent heat flux densities that exchange energy between the atmosphere and surface. Energy conservation means those fluxes must balance at a surface (Grimmond and Oke, 1999):

$$Q* = Q_H + Q_E + Q_G \text{ .... } (1)$$

If Anthropogenic heat and energy added or subtracted due to advection are considered, then the equation could be written as (Oke, 1987, 2017):

$$Q* + Q_F = Q_H + Q_E + \Delta Q_S + \Delta Q_A \text{ .... } (2)$$

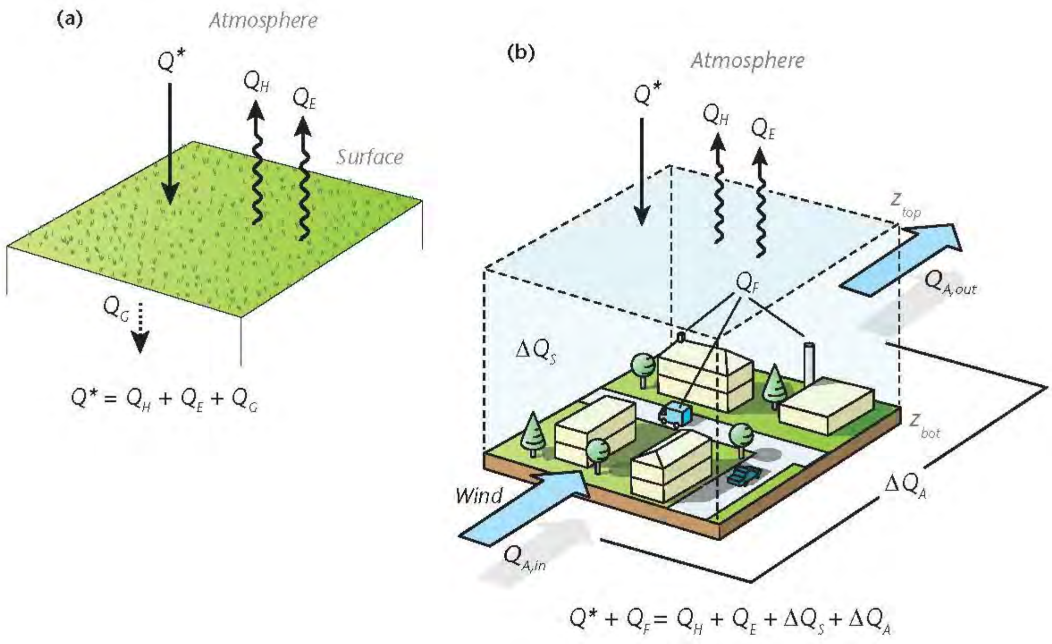

Figure 2.2: Schematic of the fluxes in the SEB of (a) a rural and (b) an urban building-soil-air volume. (Oke, 2017)

A key feature of the Urban Surface Energy Balance is the relation between $Q*$ and ΔQ_S. As the sunrise in the morning, a large fraction of $Q*$ transferred into the heat storage (ΔQ_S). but after the noon more energy is channeled into the two turbulent fluxes Q_H and Q_E, at night the turbulent fluxes subside, the heat that stored in the urban fabric released again and in the dense urban districts fuels continued positive Q_H into the atmosphere during the night.

2.3 Urban Heat Island (UHI)

"The rapid urbanization is accompanied by high levels of concentration of the urban population and built-up areas in many countries" (Oke,2017). One of the environmental manifestations of such an increase in urbanization is the formation of heat islands in urban domain commonly known as Urban Heat Island (UHI). This phenomenon that the Air temperature in a city is often higher than surrounding countryside was first observed by Luke Howard at 1833 (Oke, 1982, 2017). Miao S. et al, 2009 observed for Beijing area the monthly mean UHI intensity for August 2005 is maximum 1.128°C at 1300 UTC. For 14 no-rain days during in August 2005, the nighttime intensity reached the maximum of 1.628°C. Using UrbClim model Lauwaet D. et al, 2015 found the nighttime UHI of Brussels at 0000 LT over all summer periods during 2000-2009 is 3.15°C.

2.3.1 Type of Urban Heat Island

UHI can be distinguished into four types (table 2.1, Oke, 2017):

1. Surface Heat Island (UHI_{Surf})
2. Canopy layer heat island (UHI_{UCL})
3. Boundary layer heat island (UHI_{UBL})
4. Subsurface heat island (UHI_{Sub})

Table 2.1: Summary of UHI types, scales, thermal processes, modeling approach, direct and remote measurement techniques used to observe them (Oke, 2017).

UHI Type	Scale	Processes	Models	Direct Measurement	Remote sensing
Surface heat island (UHI_{Surf})	Micro	Surface EB	Surface EB and equilibrium surface temperature	Temperature sensors attached to the surface	Satellite/ aircraft sensors
Canopy layer heat island (UHI_{UCL})	Local	Surface EB and EB of UCL air volume Canopy and RSL scheme incl.	interactions with subsurface and overlying BL	Temperature sensors at fixed points, arrays and mobile in UCL and rural SL	Mini-sodar(1), mini-lidar
Boundary layer heat island (UHI_{UBL})	Local and meso	EB at top of RSL and BL EB	BL scheme incl. interaction with RSL/surface and free atmosphere	Temperature sensors mounted on aircraft, balloons and tall towers	Sodar, lidar, RASS profiler
Subsurface heat island (UHI_{Sub})	Local	Subsurface Energy Balance (EB)	Heat (water) diffusion in solid	Temperature sensors within the substrate	

Subsurface urban heat island (UHI_{Sub}):

Differences between temperature patterns in the ground under the city, including urban soils and the subterranean built fabric, and those in the surrounding rural ground.

Surface urban heat island (UHI_{Surf}):

Temperature differences at the interface of the outdoor atmosphere with the solid materials of the city and equivalent rural air to the ground interface. Ideally, those interfaces comprise their respective complete surfaces (i.e. λc)

Canopy layer urban heat island (UHI_{UCL}):

Urban canopy layer (UCL) is the layer in between the urban surface and roof level, that is the exterior UCL. "Canopy layer urban heat island is the difference between the temperature of the air contained in the urban canopy layer (UCL), and the corresponding height in the near-surface layer of the countryside. The upper boundary just of the UCL heat island is just the below roof level and it consists of the air between the roughness elements such as buildings and tree canopies".

Boundary layer urban heat island (UHI_{UBL}):

"Boundary layer urban heat island is the difference between the temperature of the air in the layer between the top of the UCL and the top of the urban boundary layer (UBL), and the temperature at similar elevations in the atmospheric boundary layer (ABL) of the surrounding rural area". The UBL Heat Island located above the **UHI_{UCL}**. But the lower boundary of **UHI_{UBL} is** subject to the influence of urban surface.

2.4 Surface Temperature and Surface Energy Balance

Every surface possesses a unique single temperature due to its unique SEB at its interface with the air. the surface temperature T_0 satisfies its combination of radiative, conductive and turbulent fluxes. This temperature is the common boundary in the temperature gradients that generate a sensible heat flux density (Q_H) upwards into the atmosphere and similarly conducts a sensible heat flux downward into the substrate (Q_G). Equation 3 represents the SEB for a surface, as a function of the change of T_0 with time for a layer of thickness z with heat capacity C:

$$C\frac{\partial T_0}{\partial t}z = Q^* - Q_H - Q_E - Q_G \quad (3)$$

Five surface properties exert particularly strong control on Equation 1 and therefore on T_0:

- Geometric,
- Radiative,
- Thermal,
- Moisture and

- Aerodynamic.

Naturally, the surface temperature (T_0) remains critically important to that of the lowest layer of air (Ta), however, while the two are closely linked, the relationship is not linear Geometric properties control T_0 by regulating the available Solar irradiance to the facets. Radiative properties control the ability to reflect shortwave (albedo; α) and longwave radiation and to emit longwave radiation (emissivity; ε). Facets with high albedo reduce shortwave radiation gain and thus lower T_0. Aerodynamic properties such as aerodynamic roughness length z_0 and shelter from wind influence T_0. Highest T_0 occur on facets that are smooth with little turbulence, and facets sheltered from the wind, while lower T_0 are observed over rough facets well coupled with wind. A heat island effect of Putrajaya, Malaysia has identified that shading from built structure could be more effective in reducing urban surface temperature than tree canopies. This reduction in surface temperature by built environment shading has been observed at a magnitude of 3-5°C during the noon (Ahmed A.Q. et al, 2015).

Traditionally Urban Heat Island studies have been conducted for isolated locations with the air temperatures recorded in site. Satellite remote sensing technology has made it possible to study UHI_{Surf} for large areas of cities. Local building geometry and materials influence the “canopy layer urban heat island”. On the other hand, “Heated air from upwind urban areas and the underlying canopy layer in which the canopy urban heat island occurs generates the boundary-layer urban heat island” (Soushi Kato et al., 2007).

2.5 Near Surface Urban Heat Island Under ‘Ideal’ Condition

The temperature cross-section and iso-therm map in figure 2.3 clearly show a number of common features of the heat island morphology as described by Oke (1980, 2017). If the surrounding topography doesn’t have any significant effect the heat island effect sharply protrudes against background rural temperature field. Windward side of the urban/rural boundary area has the “cliff” of the heat island and it follows closely the built-up area for much of the city perimeter. Horizontal Temperature Gradient due to the UHI is slacker for most of the urban area, except we can expect “warm spot” due to anomalously high-density urban area, industrial area, apartment complex, shopping node or the city central area, as these areas are relatively warmer than the other urban areas. Again, we can expect “cool spot” due to the presence of park, wetlands or anomalously low-density urban areas, as these areas are relatively cooler than the other urban areas. These thermal features of the UHI might shift a little bit downwind from their source area due to advection process with wind flow.

Time-dependent aspects of UHI explained by Oke as shown in fig 2.4. Due to the different rates of near-surface warming and cooling, there are different distinctive diurnal air temperature regimes in the Urban and Rural area. At a given time the difference between the Urban and rural temperature defines the UHI intensity. Heat island intensity is maximum around 3-5 hours later after sunset due to diverging rates of cooling of the urban and rural environment. After that slightly greater urban cooling reduces the intensity. At the early daytime due to rural heating UHI intensity almost diminished. At this time some cities even reported observing slightly lower temperature ('cool' islands) in the central area than the surrounding countryside.

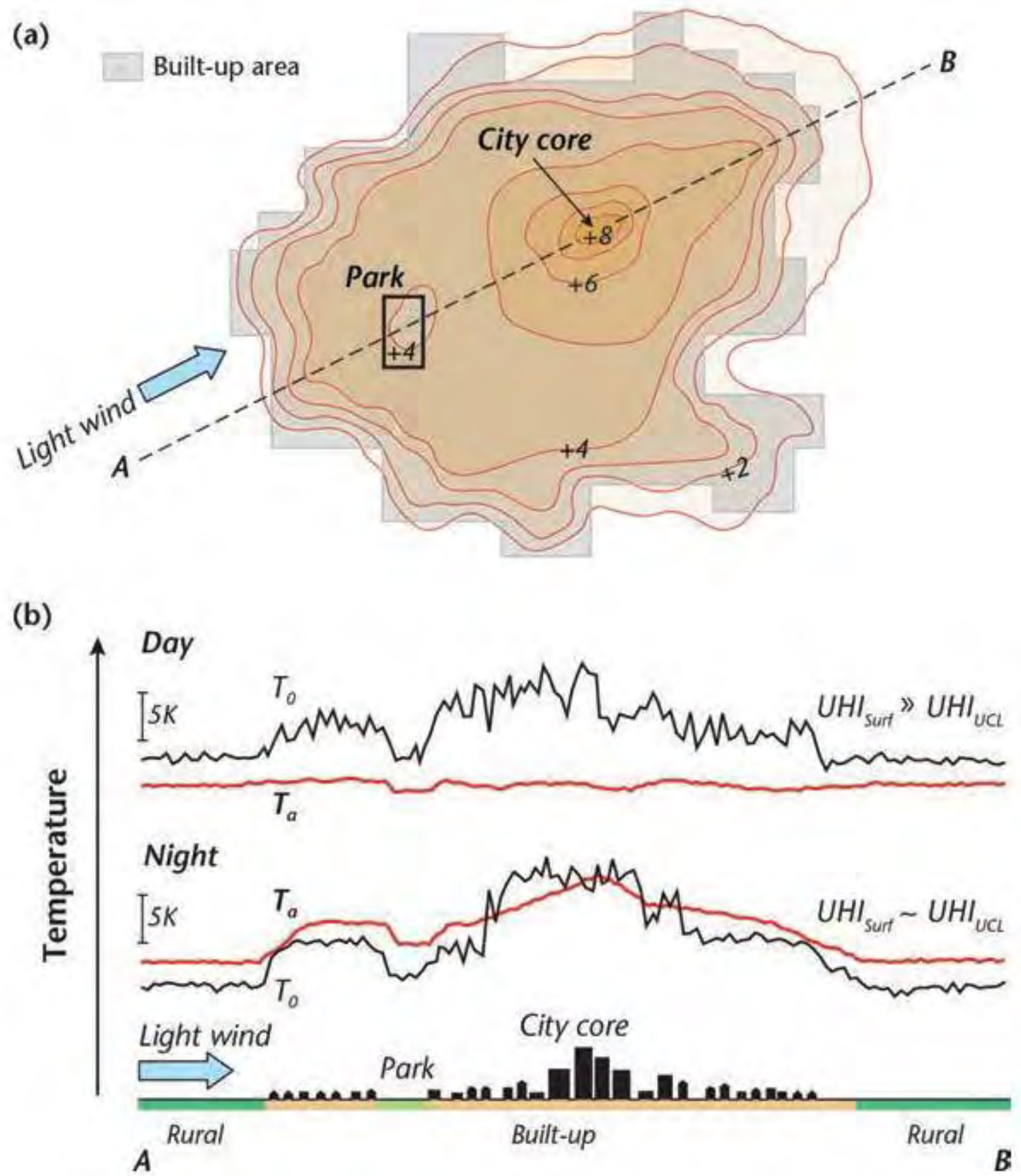

Figure 2.3: Schematic depiction of a typical UHI_{UCL} at night in calm and clear conditions in a city on the relatively level terrain. (a) Isotherm map illustrating typical features of the UHI and their correspondence with the degree of urban development. (b) 2D cross-section of both surface and screen-level air temperature in a traverse along the line A–B shown in (a). (Oke, 2017)

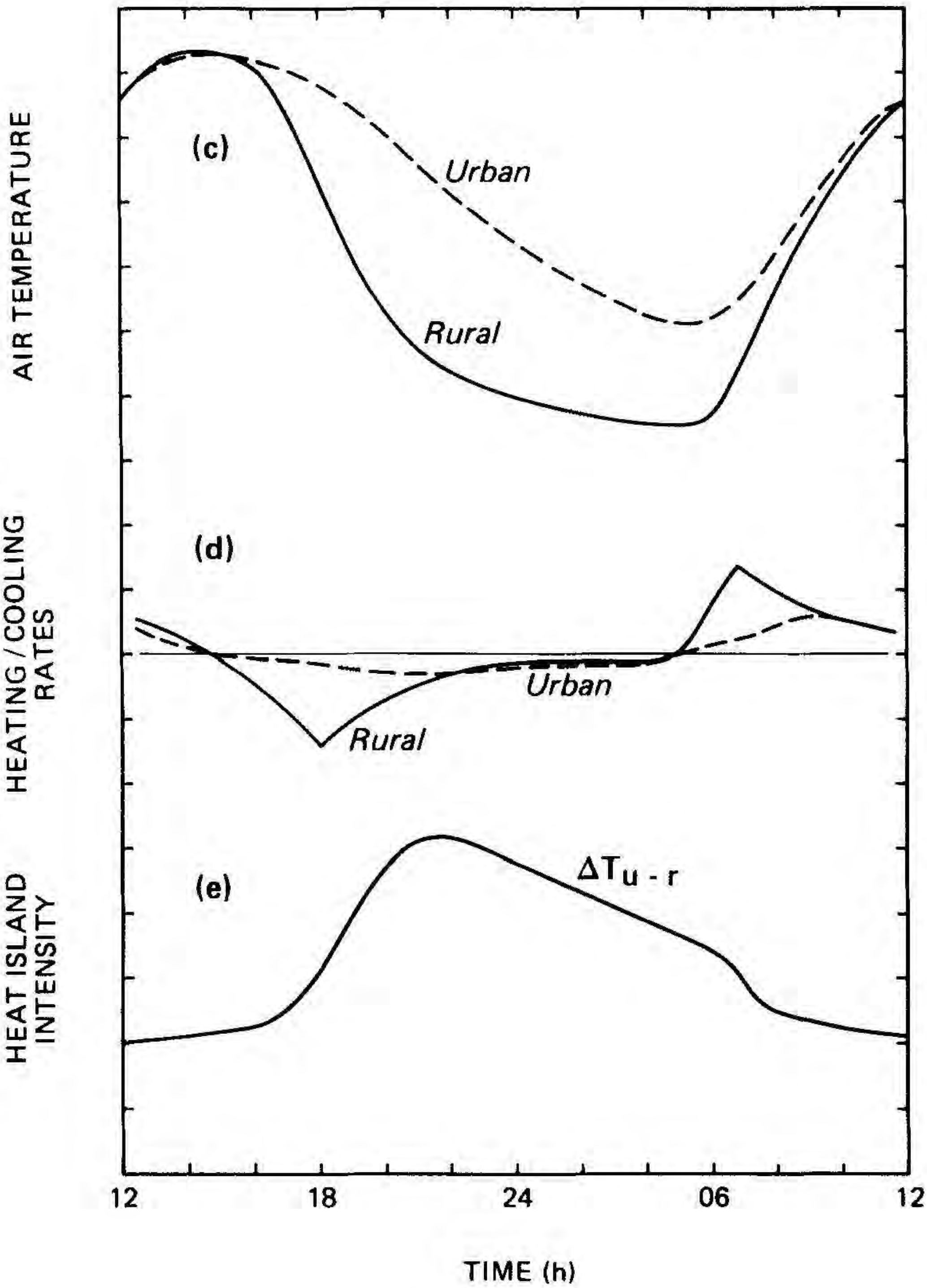

Figure 2.4: Temporal Variation of Urban and Rural (c) air temperature (d) heating/cooling rates and (e) the resulting heat island intensity (Oke, 1980)

Vertical Structure of the UHI:

Under the calm condition, Urban Canopy Layer UHI creates a self-contained urban heat ‘dome’, which due to the wind flow creates an urban boundary layer in the direction of the wind as shown in fig 2-5.

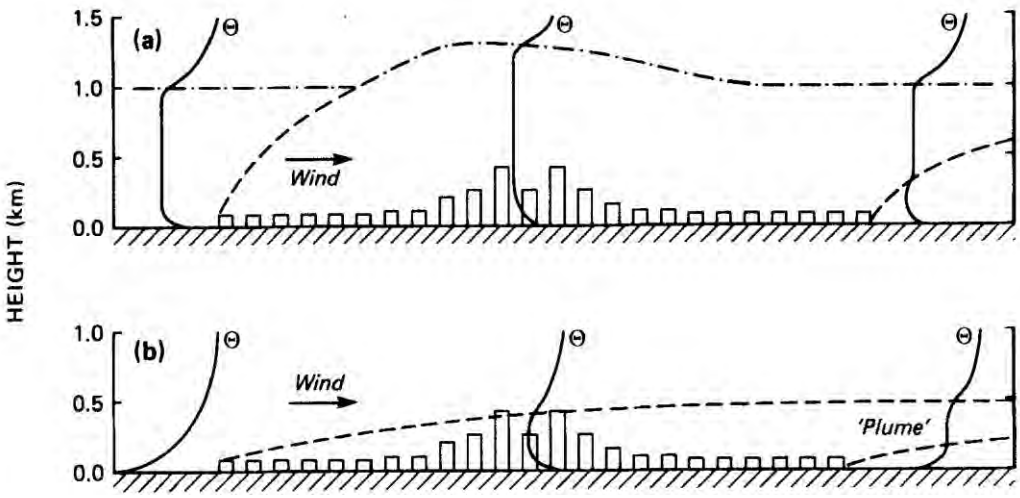

Figure 2.5: Generalized form of UBL thermal structure in a large mid-latitude city during fine summer weather (a) by day, including schematic profiles of potential temperature (θ) and the depths of the urban and rural internal boundary layers (---) and the daytime mixed layer (-·-) and (b) at night. (Oke,1981)

UBL increases as the day progress and by mid-afternoon may reach up to .5-1.5 km in depth depending on surface sensible heat flux and stability of the air mass (Oke, 1980). Downwind of the city a new rural internal boundary layer creates and makes the urban effected air aloft as a heat 'plume', often extending for tens of kilometers (Oke, 1980). The most significant variables that effects UHI intensity is wind speed and cloud cover. Oke (1973) examined the effects of wind speed on UHI intensity which is non-linear and approximately inverse square root of UHI intensity. In case of cloud cover, the cloud type as well as amount also have effects on UHI intensity. It has been observed that low cloud is more effective than an equal amount of high cloud in limiting the UHI intensity.

2.6 Reasons For Urban Heat Island

Transformation of cities natural land with impervious surfaces, buildings, and other infrastructure generates the "urban heat island" (UHI) effect. The UHI is one of the most compelling and crucial concerns of city sustainability. "Although, the urban heat island arises due to many factors, the nature of the surface and its conditions is the strongest among the reason. Lack of evapotranspiration due to the absence of vegetation and water bodies in urban areas and the changes in the thermal properties of surface materials are the main reasons for UHI". "Urban microclimate is closely correlated with the types and patterns of landscape existing in the urban environment" (Sun R. et al,2012 and Steeneveld G.J. et al, 2014). But UHI is not only related to simply an urban-rural comparison of thermal properties, moisture availability and geometric structure also plays part in it.

Oke, (2017) explained four thermal properties that are pertinent to explain UHI.

a. **Heat capacity** (C, in J m^{-3} K^{-1}) expresses a materials ability to store heat and gives the temperature change to expect due to uptake or release of sensible heat. It is the product of density (ρ) and specific heat (c, in J kg^{-1} K^{-1}) of a material (i.e. $C= \rho c$).
b. The ability of a substance to conduct a heat flux density (Wm^{-2}) by passing energy from one molecule to another along a given temperature gradient (Km^{-1}) is known as the **Thermal conductivity** (k, in W m^{-1} K^{-1} Relatively large amounts of heat will be transmitted for a given temperature gradient if the k is high whereas heat transmission will be low for the same temperature gradient if the k is low.
c. The ease with which temperature signals are transmitted through the material is known as **Thermal diffusivity** (κ, in m^2 s^{-1}). κ controls the speed of the movement of temperature wave. With κ the depth of the layer involved in thermal changes could be estimated. The ratio of the Thermal conductivity to the heat capacity is Thermal diffusivity (i.e. $\kappa = k/C$). So, "thermal activity is directly related to the ability of a material to conduct heat, but it has an inverse relationship with the total heat required to cool or warm the substance". Rapid penetration of surface temperature changes in a thick layer of material will require high κ, but if the change is restricted to a shallow layer it means low κ.
d. **Thermal admittance** (μ, in J m^{-2} K^{-1} $s^{-1/2}$; also called 'thermal inertia') is a property of interface of two material surface. Previous three measures are related with volume of the subsurface material itself whereas this property is for the interface of the surfaces. Each of the substance forming the interface has its own μ value. In case of an urban area it is the construction material or ground surface and the surrounding air. Thermal admittance for air (μ_a) depends on the thermal diffusivity of the atmosphere and therefore turbulence. So, μ_a is highly variable. But for soil or construction materials of the built form the value is more stable. Again, in case of wetland the two-material forming the interface is air and water. simply involving the other thermal properties, the expression for thermal admittance is:
$\mu = \sqrt{kC} = C\sqrt{k}$ ………………………………………………………………… (4)

"Various studies put Thermal admittance (μ) is the most important thermal property of the material". Because Large Thermal admittance sequester heat in the material resulting is a relatively small change in the surface temperature throughout the day. Again, a material with low Thermal admittance undergoes large temperature variation throughout the day due to the shedding of a "large amount of heat in the atmosphere". There is a large difference in urban and rural Thermal admittance (oke, 2017). So, it could be concurred that urban area with material with low thermal admittance can end up with significantly higher Urban Surface Heat Island (UHI_{SURF}) In case of Dhaka till now there is no investigation of urban material in terms of Thermal admittance. But the Urban Surface Heat Island (UHI_{SURF}) study presented later in this chapter might be able to explain about the 'thermal admittance' of the urban material of Dhaka. Oke described the following reasons (table 2-2) for Urban Canopy Layer Heat island.

Table 2.2: suggested causes of UHI (Oke, 2017)

Cause	Description of cause
Canopy layer heat island (UHI_{UCL})	
Surface geometry	(a) Increased surface area ($\lambda c > 1$) (b) Closely-spaced buildings – multiple reflections and greater shortwave absorption (lower system albedo); – small sky view factor ($\psi_{sky} < 1$) reduces net longwave loss, especially at night; – wind shelter in UCL reduces heat losses by convection and advection.
Thermal properties	Building materials often have a greater capacity to store and later release sensible heat.
Surface state	(a) Surface moisture-waterproofing by buildings and paving reduces soil moisture and surface wetness. (b) Convection favors sensible (Q_H) over latent heat flux density (Q_E). (c) If snow – lower albedo in the city gives a relative increase of shortwave absorption compared to rural areas.
Anthropogenic heat	Anthropogenic heat release due to fuel combustion and electricity use is much greater in the city.
Urban 'greenhouse effect'	Warmer, polluted and often moister urban atmosphere emits more downward longwave radiation to UCL.

A significantly important observation from the numerous UHI study is the existence of "Cool Island in the middle of the day in the city center" due to the shading of the Urban canyon as shading prevents direct solar radiation gain. "Incoming longwave radiation at the surface of the city is often slightly greater". In general, daily $\Delta L_{\downarrow U\_R}$ in a large city is typically about 20 W m^{-2}, which translates to an increase of 5–10% (Oke et al, 2017). The physical cause of the increase in $L_{\downarrow}$ is attributed to the air pollutants. It was assumed that pollution was chiefly responsible for creating urban warming by absorbing much of the outgoing longwave from the surface and re-emitting a significant fraction back which could be described as an urban 'greenhouse' effect. Although the effect is minor than the UHI, it appears the extra $L_{\downarrow}$ originates from an atmosphere warmed largely by non-radiative processes. (Oke et al,2017). This is a serious concern for the Dhaka as it is one of the most polluted city with the high density of pollutant in the air which could absorb outgoing longwave $L_{\uparrow}$ radiation and re-emit a significant portion back. This might be exacerbating the UHI effect in Dhaka.

Urban green spaces show relatively lower air and surface temperature than their urban surroundings due to the availability of moisture, the sky view factor and the presence of vegetation and/or water. These properties affect both the daytime heating, nocturnal cooling rates and the relative coolness or warmth of the thermal climate relative to that of the surrounding urban area in which it is embedded. The difference sometimes called the **'park cool island' (PCI)** has been studied in the parks of several cities located in different climatic zones. Like the UHI_{UCL}, the PCI is usually largest on nights with 'ideal' weather and its influence declines roughly exponentially with distance from the park edge, this limits its effective impact to a distance of about one park width (diameter) into its surrounds. The largest PCI differences reported are about 5 K (Spronken-Smith and Oke 1998, Upmanis et al., 1998). The results from tropical cities, while fewer in number, suggest similar effects to those of mid-latitude parks.

Following properties modify air temperature in the UCL at the micro- and local scale:

1. Street geometry, because it affects radiation receipt, loss, and air flow.
2. Building fabric, because it affects heat storage, release and waterproofing.
3. Vehicle traffic and space heating/cooling, that release Q_F

The magnitude of the largest observed UHI_{UCL} that is passively-driven (i.e. not due to larger than normal Q_F) is about 12 K (Oke, 2017). If the urban canyon H/W ratio exceeds some threshold, increased shade within the canyon could limit daytime heat storage uptake and this can outweigh the nocturnal thermal benefit due to the reduced longwave radiation loss. Wind speed reduces the magnitude of UHI_{UCL} while wind direction changes the shape of UHI_{UCL} which is strongly affected by city's internal structure. Due to the wind flow, UHI might advect beyond the city boundary like a plume towards the downwind direction of the wind flow.

Cloud cover fraction affects the UHI_{UCL} by reducing solar receipt and trapping longwave radiation. Cloud type such as cirrus (Ci), altocumulus (Ac); cumulus (Cu) and stratus (St) etc. influence the growth of UHI_{UCL}. The combined effect of cloud type and a cover fraction on net longwave radiation cooling at night are given by Bolz relation:

$L^*=L^*_{clear}(1-kn^2)$ (W/m^{-2}) ……………………………………………………… (5)

Where,

L^*_{clear} = net longwave radiation with cloudless skies

k= cloud type factor accounting for the decrease in cloud base temperature with increasing height.

n= cloud amount (in tenths).

Oke (2017) described that in case of complete cloud cover (n=1.0), relatively warm stratus cloud low cloud base reduces the drain of heat by L* by about 90% (average of low clouds – those with bases below approximately 1.5 km). so, the UHI potential is severely curtailed. For middle height altus types cloud the energy sink is cut by about 75% and with high altitude cirrus clouds, consisting of ice crystals, even with overcast L* is only reduced by about 25%. The effect of cloud on UHI potential is a severe concern for Dhaka as six (6) months of the year is Warm and humid characterized by low cloud cover as this restricts the longwave heat loss of the urban fabric through the atmosphere at specifically at night.

2.7 Effects of Urban Heat Island

flooding, landslides, drought, increased aridity, water scarcity, and air pollution has widespread negative impacts on people's health, livelihoods, and assets". It has also been observed by IPCC that "intensity of urbanization is closely associated with long-term trends in surface air temperature in urban centers". It has been stated by IPCC that "climate change can strengthen and/or increase the range of the local urban heat island (UHI), altering small-scale processes, such as a land-sea breeze effect, katabatic winds, etc., and modifying synoptic scale meteorology (e.g. changes in the position of high-pressure systems in relation to UHI events)". From the IPCC reports it is also palpable that "increased frequency of hot days and warm spells are already exacerbating urban heat island (UHI) effects, causing heat-related health problems, increased air pollution, as In the most recent assessment report, IPCC stated that increasing "Urban climate change-related risks, such as heat stress, extreme precipitation, inland and coastal well as an increase in energy demand for warm season cooling of the buildings in a variety of cities in subtropical, semiarid, and temperate sites" (Revi et al, 2014).

In hot regions, the UHI adds to the number of cooling degree-days thereby increasing the cost of air conditioning buildings. UHI adds to the burden of hot weather for inhabitants of cities in the tropics because many cities in this climatic region are from Low and middle income. Most of the people in these cities have no access to air conditioning the UHI is an added threat to their health. Heat stress is the leading cause of mortality from weather-related hazards in various part of the world greater than more violent phenomena like hurricanes (typhoons), tornadoes and floods. Prolonged exposure to excessive heat is particularly dangerous because the human body requires regular periods of sufficient coolness in which to recover. One of the major concern about UHI is that it ramps up during the evening when people sought respite after the day's heat.

The various types of UHI induce other climatic phenomena, such as the extra warmth shifts the thermal structure of the boundary layer towards neutrality and instability, which encourages vertical mixing. This modified temperature structure generates country-breezes. This is an urban heat island circulation (UHIC) that draws air towards the city center at a low level where it converges, rises, flows outwards at a higher level and sinks away from the city over adjacent rural areas.

2.8 Urban Heat Island Observation in Dhaka

"Dhaka is one of the most populated and polluted cities in the world, where the juxtaposition of wetlands and urban context have an opportunity for creating a viable and distinct character of its own. Urban wetland and green space are diminishing due to pressure from the housing sector and unplanned urbanization" (Shahjahan A.T.M. et al, 2016). The first ever city-wide Canopy Layer Urban Heat Island **(UHI_{UCL})** study was done by Bangladesh Meteorological Department (BMD) during the year1992.

Urban air temperature at 0600 hours BST and 1800 hours BST and Humidity at 0600 hours BST of the two dates 03 January 1992 and 08 June 1992 are measured. Thermometers and Assman Psychrometers are used. Air temperature and Humidity observations at fixed hour 0600 BST (morning) and 1800 BST (evening) are considered to find out the thermal and humidity distribution patterns over Dhaka city. The heat island study is based on mobile survey data during the winter months and the month of June and July over Dhaka city which is fast expanding and developing. A network of 10 points is selected for the study which is (1) Agargaon, (2) Tejgaon (3.) Motijheel (4) Dhanmondi (5) Nowabgonj (6) Mirpur (7) Kallayanpur (8) Gulshan (9) Bakshibazar and (10) Airport, these include two meteorological observing station, one at Agargaon and other at Hazrat Shah Jalal International Airport, rest are mobile Survey points. The locations were chosen keeping in view the altitude, exposure, site peculiarities, population density and industrial sites to work out the effects of various "factors on heat island.” Figure 2-6 represents the observed heat island intensity during 1992 at the time of minimum temperature epoch [0600 hours BST] at Dhaka city in January was 3.8°, in April was 2.5° and that of July was 0.6° [Hossain et al,1993, Khaleque et al 1993, Ahmed,1993]. The maximum intensity of heat island or warm pocket is observed to be of the order 3.8°C at Old Dhaka and Motijheel Commercial area.

Figure 2-7 represents the isothermal pattern of 03 January 1992 at 1800 hours BST. The pattern more or less resembles the 0600 hours BST pattern but its heat island intensity decreases from 3.8°C to 2.8°C, during summer months isothermal pattern of 08 June 1992 shows heat island intensity is in order of 0.08°C. [Hossain et al,1993, Khaleque et al 1993, Ahmed,1993]. The Isothermal pattern-shows Warm pockets at Tejgaon Industrial Area, Mirpur and Azimpur because of high-density urban dwellings; among the cool areas that had been observed were Agargaon area, Dhanmondi residential area, Shahjalal International Airport and over outer "boundary of the city”. “Dhanmondi residential area was under the grip of cool pools due to the presence of large water body within the area and more greenery” (Shahjahan A.T.M. et al, 2016).

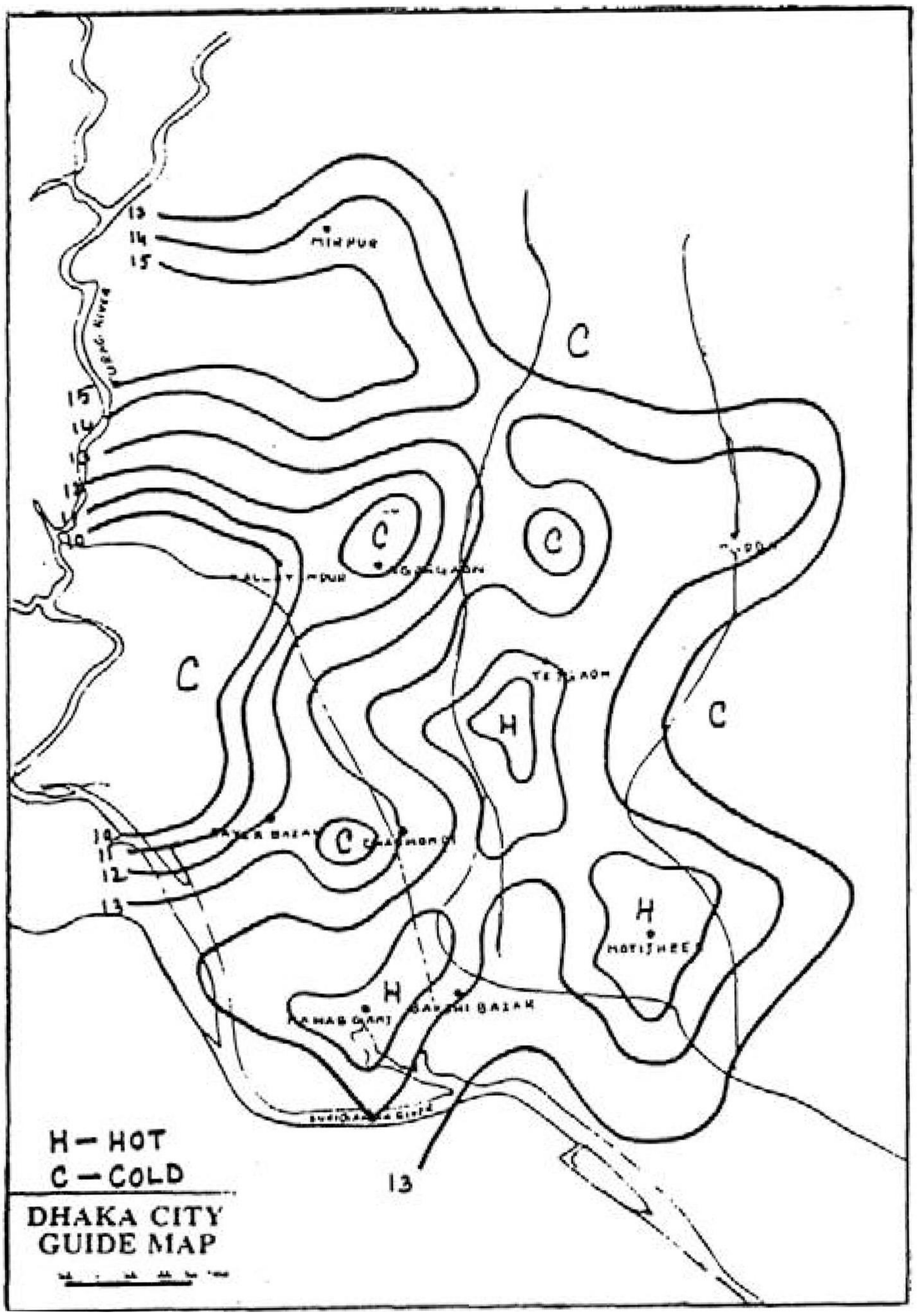

Figure 2.6: Temperature distribution at 0600 BST of 03 January 1992 over Dhaka city (source BMD)

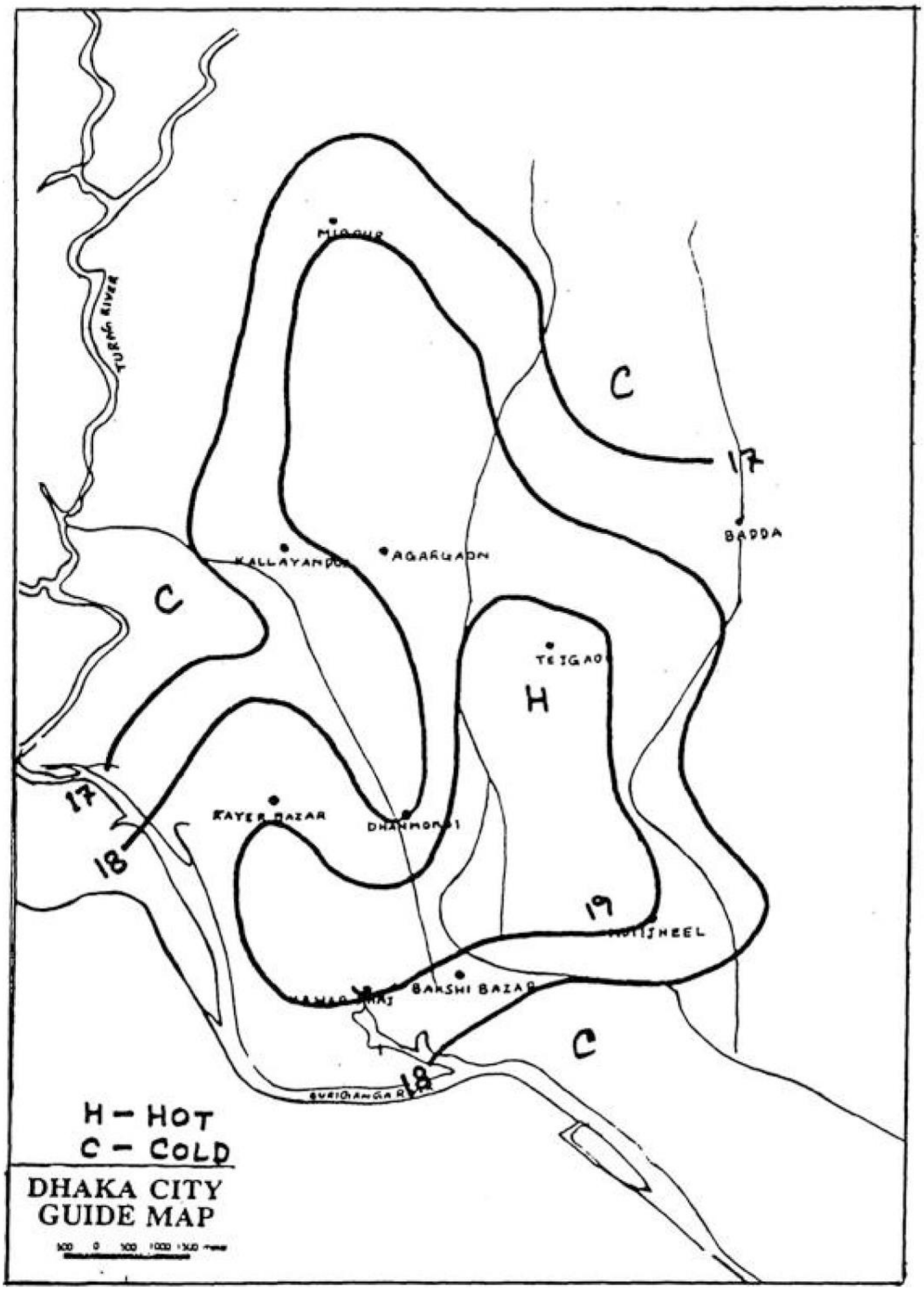

Figure 2.7: Temperature distribution at 1800 BST of 03 January 1992 over Dhaka city (source BMD).

Two peaks of heat island intensity are observed one at early morning and another at early night, but early morning heat island intensity is stronger than early night heat island. During summer months heat island effect is insignificant to consider. Humidity Island (Fig 2-8) has an inverse relation to heat island whenever moisture is less but followed heat island intensity whenever moisture is high.

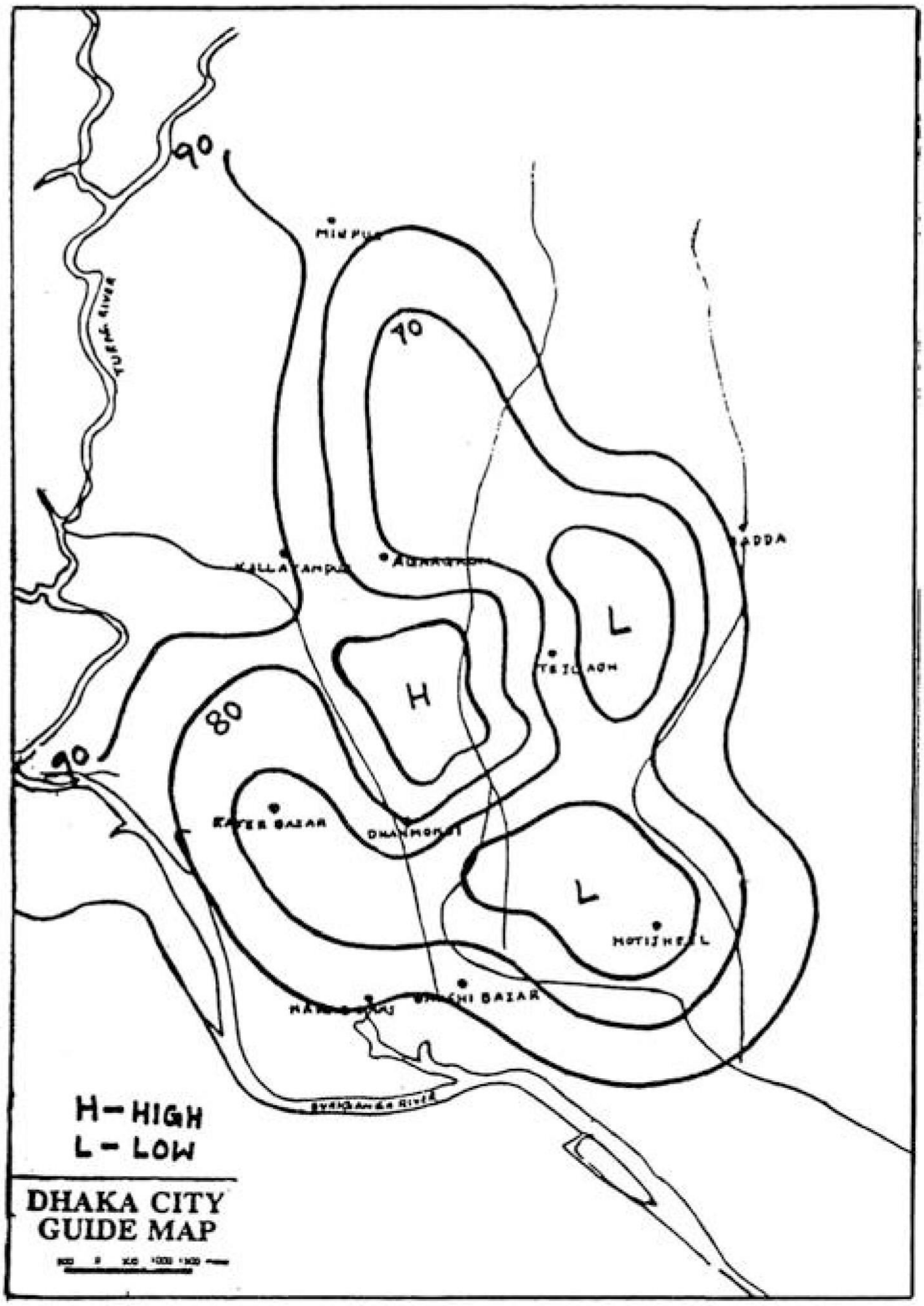

Figure 2.8:Humidity field analysis at 1600 BST of 03 January 1992 over Dhaka city (source BMD).

2.9 Surface Urban Heat Island Study in Dhaka

In regard to Dhaka city, it has been reported that changing of Land Surface Temperature (LST) is found to be directly correlated with Land Cover transition. It had been observed that LST had increased in areas with growing urban development where hard, impermeable pavement and dark surface are replacing natural Land Cover

(LC) like the vegetative land cover and the wetlands (Raja et al, 2013). "Thus, urbanized land use due to rapid urbanization in Dhaka has a direct impact on its urban microclimate which is exacerbating Urban Heat Island Effect" (Shahjahan A.T.M. et al. 2016). Several studies reported that Dhaka city "land surface temperature (LST)" is about 2 - 4°C higher than the LST of its suburbs (Khaleque et al 1993, Raja et al, 2013).

A "Surface Urban Heat Island (UHI_{surf})" study has been done in this research by extracting LST from the data obtained from the Earth-observing Landsat-8 and 5 TM satellite of NASA. The data has been obtained through web-based earth-explorer service of the USGS. Detail method and equation used in this UHI_{surf} analysis has been elaborated in chapter 4. Two dates have been selected to extract LST from the TIR band of Landsat satellite. The first date is 12th December 1991 which is a similar day like the date chosen by Bangladesh Meteorological Department (BMD) for UHI_{UCL} study in Dhaka as stated before and the second date is 16th December 2016. The reason to choose these two dates are to compare the UHI_{surf} as Dhaka has gone under rapid urbanization process after 1990 in this time period of a quarter of a century. So, there will be definitely a relation between the LST change and the urban development process of this quarter century time period which have seen rapid transformation of natural land cover with artificial man-made material.

Base map of the Dhaka city is given in the figure to aid reading the extracted Land Surface Temperature map in figure 2.10, 2.11 and 2.12. From Fig. 2.10 we can see the LST of 12 December 1991, which fairly corresponds with the UHI_{UCL} observed by the BMD. This correspondence with BMD observation is important for the research because subsequent work finding the change in urban surface layer heat island derived based on the value of this date. The highest LST (26.21°C) could be found in Old Dhaka and Tejgaon industrial area and some pockets in Mirpur and Motijheel commercial area. Dhanmondi residential area exhibited lowest LST (21.03°C) which is almost equivalent to the LST of surrounding rural/ peri-urban area. The time of the Landsat pass over Dhaka is around 10:30 am in the morning. So, the Landsat estimated UHI_{surf} for Dhaka on 12 December 1991 is 5.18°C. From Fig. 2.11 we can see the LST of 16 December 2016, which significantly demonstrate the Urban surface change in this 25 years of time. The highest LST (28.20°C) could be found in the new sand filled area for the new residential area in north-east (Bashundhara Residential area) and north-west part of Dhaka, Tongi industrial area. As before motijheel commercial area, Old Dhaka, Mirpur and Tejgaon industrial also exhibited Higher LST around 26.56°C. Like before Dhanmondi residential area exhibited lowest LST (22.4°C). Although LST of Dhanmondi residential area also increased, but it is still nearer to the LST of surrounding rural/ peri-urban area, which is around 21.13°C The time of the Landsat passes over Dhaka are around 10:30 am in the morning. So, the Landsat estimated UHI_{surf} for Dhaka on 16 December 2016 is 7.07°C. From these data, it can be concurred that within the period of 25 years Landsat estimated UHI_{surf} for Dhaka increased around 2°C.

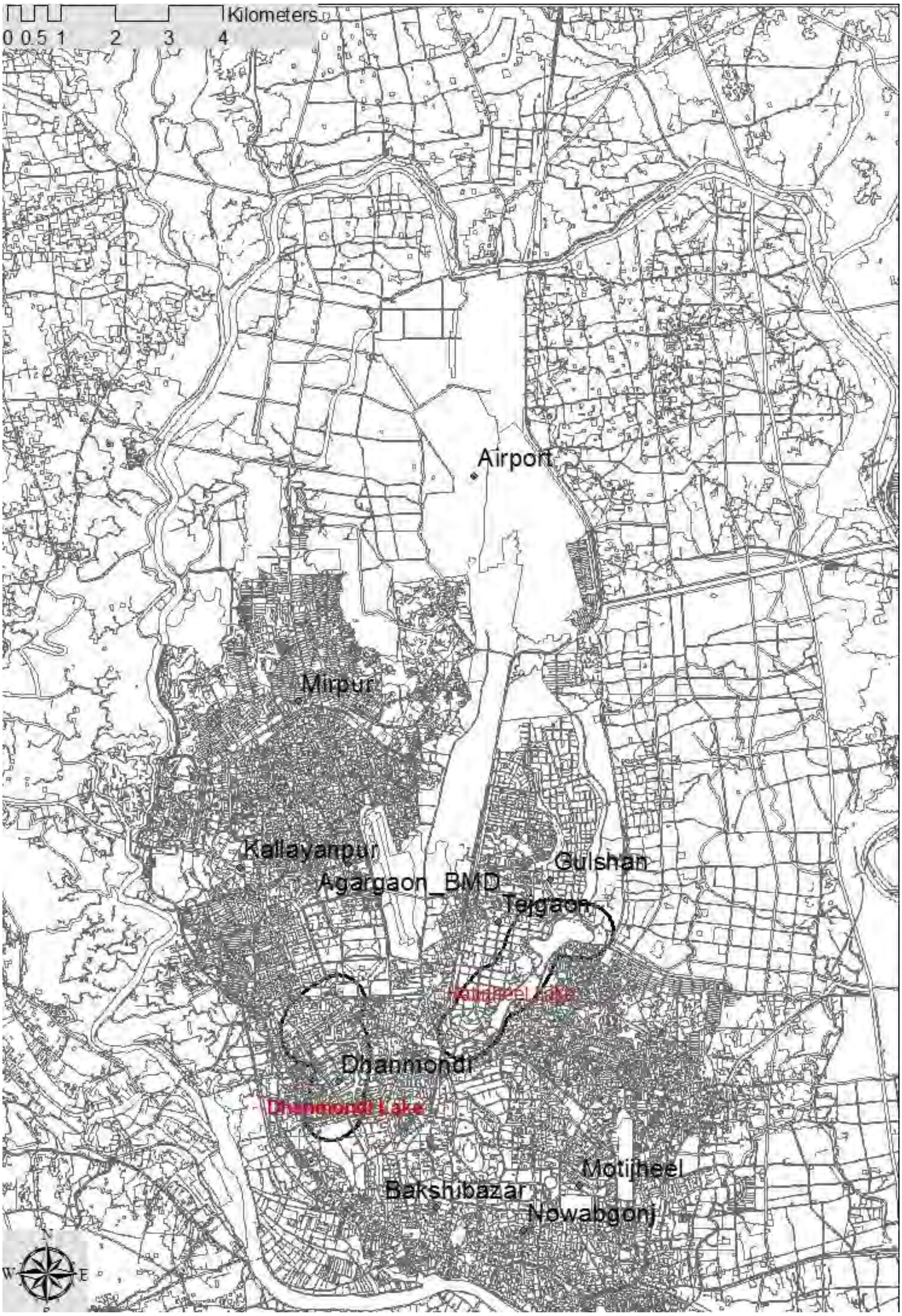

Figure 2.9: Dhaka city Base Map (source RAJUK).

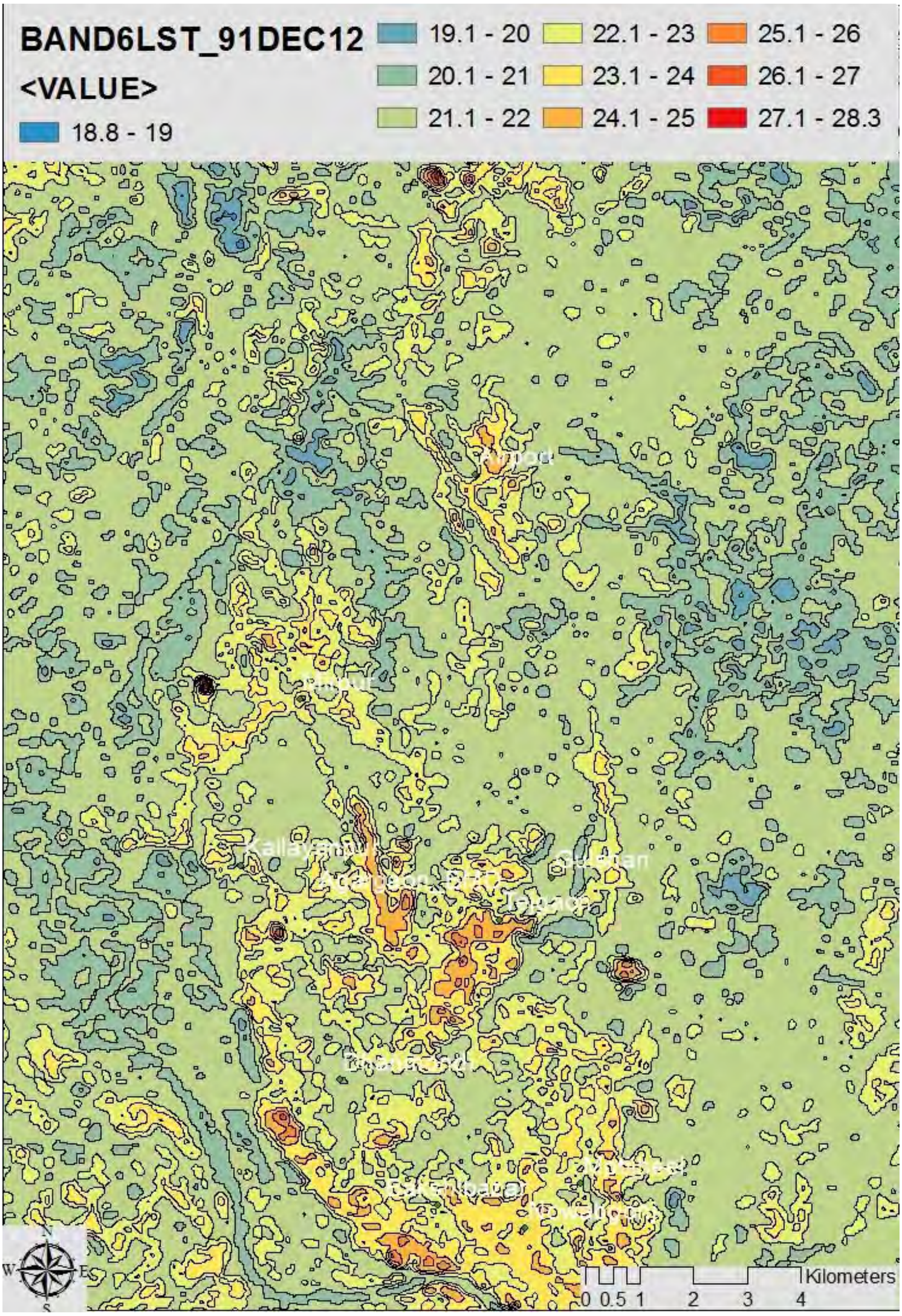

Figure 2.10: Land Surface Temperature_ LST (T_0) of Dhaka at 12 DEC 1991 derived from Landsat 5 TM data (map overlay is provided in the back of this thesis)

From Fig 2.12 the change in LST for the whole urban area of Dhaka in the last 25 years are estimated by deducting the Landsat LST map of 12 December 1991 from the that of 16 December 2016. Some conclusion could be drawn from this analysis of LST change.

a. The newly developed urban area has shown highest increase in LST, hence exhibited the greatest change in $UHI_{surf.}$ The change in LST is in a magnitude of 8.2°C.
b. Industrial area also exhibited LST increase of around at a maximum magnitude of 5.46°C.
c. Commercial area also exhibited LST increase of around at a maximum magnitude of 5°C.
d. Some part of Old city and area under Dhaka south city corporation has seen LST decrease of up to 1°C.

Apart from Urban water surface area, there is area also in the Urban Canyon which has exhibited LST decrease. The cause behind this LST decrease could be increasing shading from tall building.

Although Bangladesh environmental protection law prohibits [Ministry of environment and forest, Bangladesh] modification or filling of any area designated as wetland including rivers, canals, ponds, marshland, flood flow plains and water retention areas, there is no definitive guideline on how these wetlands could be included in the Urban Design process to regulate the thermal environment of Dhaka aside from helping to manage stormwater during the wet season.

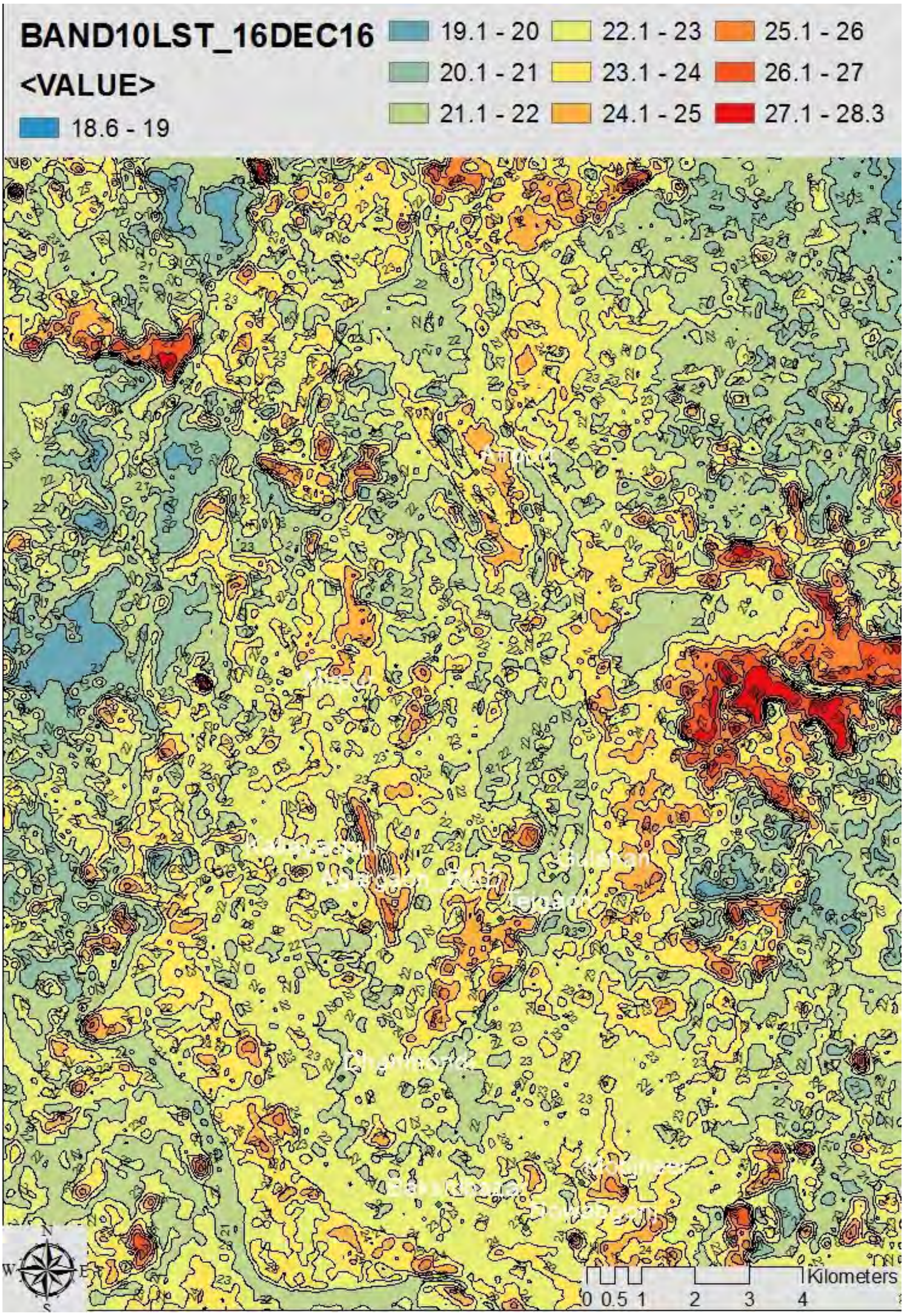

Figure 2.11: Land Surface Temperature_T0 (LST) of Dhaka at 16 DEC 2016 derived from Landsat-8 data(map overlay is provided in the back of this thesis)

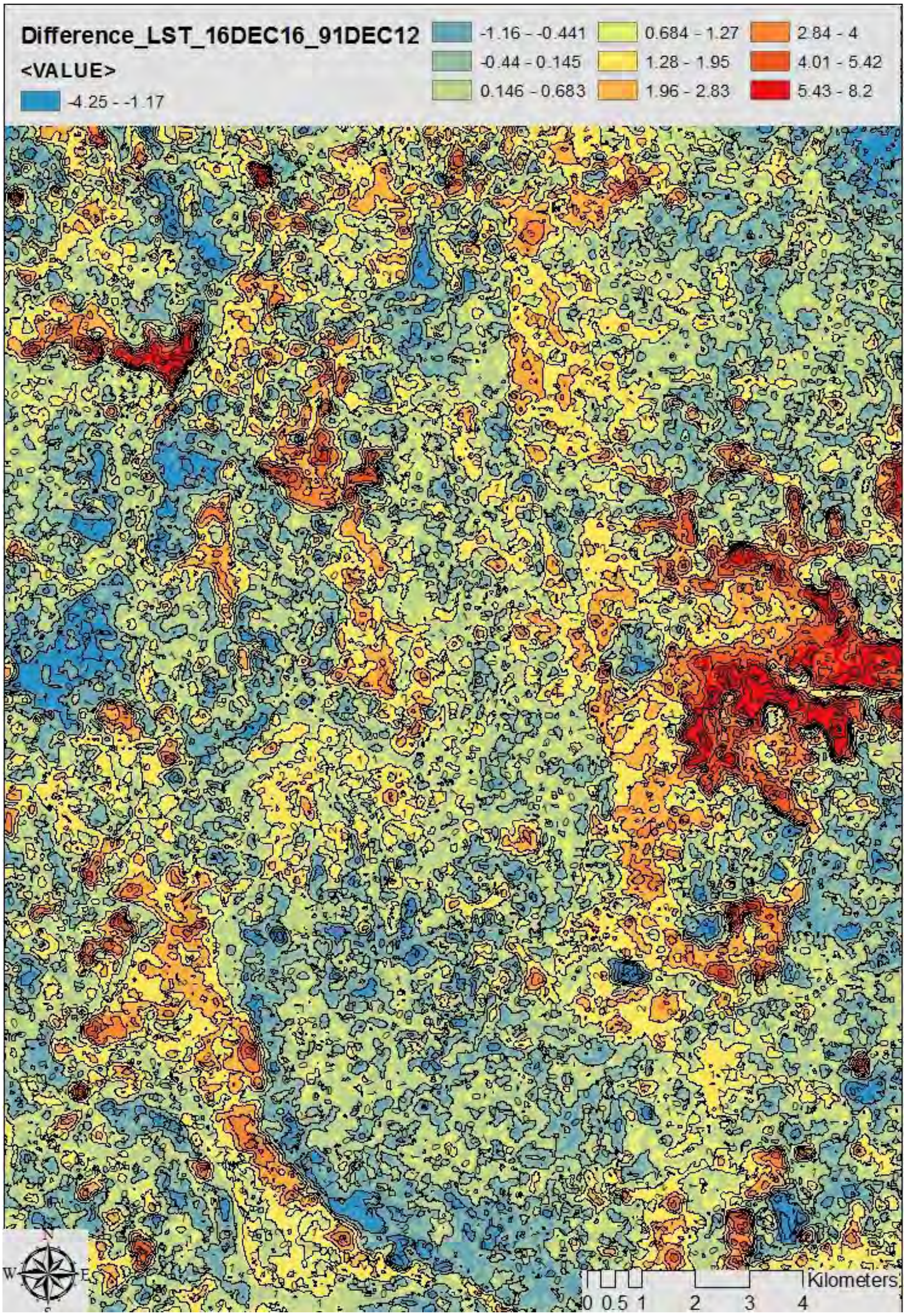

Figure 2.12: Change of Land Surface Temperature T_0 (LST) from 1991 to 2016 (map overlay is provided in the back of this thesis)

2.10 Urban Adaptation Measure for Climate Change: Urban Cooling Islands

Wetlands of Urban areas can have a profound impact on Urban Canopy Layer (UCL) climate levels. Wetlands lower temperature, increases RH and lower Heat Stress Index (HIS) at the downwind side, which is also known as “Lake Effect” (Saaroni H., et al 2003). “Wetlands include reservoirs, lakes, and rivers, and form many Urban Cooling Islands (UCIs)” (Sun R. et al, 2012). This UCI could be an effective adaptation measure against UHI in the urban areas.

Two main processes take place when Hot dry air passes over a wetland. First one is reduction in air temperature due to latent heat absorption of water for evaporation. The second process is sensible heat transfer between the air and underlying water. If the temperature of water is less than that of air, this second process results in temperature drop of air. Also, if the moisture content of the air remains unchanged, there will be an increase in Relative Humidity [RH] with decreasing air temperature (Saaroni H.et al, 2003).

The cooling effect of the urban fabric transported from urban wetlands is widely considered as an important ecosystem regulating service. The environmental benefits of ecosystem regulating services is very valuable in terms of economics. Most of the UHI studies are implemented at the scale of an entire city. For this reason, there are little information available on the effect of individual wetland. Various information on individual wetland such as, the difference of temperature between the wetland and its surrounding landscapes and the transport of cooling effects of wetlands in various spatial scales are not known. The determinants for the existence of UCI such as influence scale of wetlands and the temperature difference are not clearly understood. Also, the factors having impact on the UCI intensity is still not clearly known (Sun R. et al, 2012).

Several strategies have been proposed for the improvement of urban climate like, material with higher albedo, more large trees and vegetative surface or wetlands to promote evaporative cooling. One of the most efficient ways of passive cooling for buildings and urban spaces in hot regions is the Evaporative cooling. “The presence of vegetation and water ponds in cities modify the energy balance, inducing variations in the amount of solar radiation reaching the surface, wind speeds, ambient temperature and air humidity and thus can modify the comfort conditions in urban environment”. [Robitu M. et al, (2006), Taleghani M. et al (2014)].

An investigation by Frey C.M. et al. (2005) from four ASTER satellite scenes with channels from the very near infrared to the thermal infrared showed “a distinct daily cool island for ‘tropical semi desert and desert climate’ city Dubai and daily cooling areas of Abu Dhabi city and its surrounding mangrove areas”. Albedo of a surface controls the net radiation. Although having lower albedo than the surrounding desert, due to the availability water at the parks, golf courses, mangroves these two city exhibits cool island effect (Frey C.M. et al. 2005).

2.11 Inversion Layer Over the Water Bodies

When the air is blowing from the warmer land over the surface of waterbody a shallow stably stratified layer (inversion layer) is produced by a negative (downward) heat flux over the water surface. Moreover, if the advected air is relatively dry, evaporational cooling amplifies the stable layer. Such a shallow inversion layer over the water surface will reduce the evaporation of the reservoir. During spring and summer inversion occurs all times but in winter it occurs only during the day. Inversion can also occur over a well irrigated grass field and can modify the microclimate. Fraedrich K. (1972) developed a simple model of this evaporation process.

Fraedrich indicates many further effects in this inversion effects:

I. Due to the stress between land and lake the air flowing over the water accelerates.
II. Due to the temperature differences between the land and the lake and by **a** pressure increase Because of the cooling inversion layer, secondary flows of thermal origin develop.
III. Increasing moisture in the inversion layer diverge the long wave radiative flux which in turn increase the inversion strength and height.
IV. "Even the air temperature of the environment is equal or less compared with the temperature of the water surface at the shore, inversion can still develop because the water surface temperature decreases due to the interaction between air and water along the air trajectory".

Inversion, increasingly suppresses the evaporation increasing with the travel distance of the air over the reservoir by creating a "vapour blanket".

2.12 Extent of The Cooling Effect of Urban Water Bodies

In the micro-scale environment of the urban heat island, a numerical approach based on computational fluid dynamics (CFD) is now broadly used as an effective analysis tool. 'Computational fluid dynamics (CFD)' simulations can be a powerful analysis tool for determining the potential of the coolth produced from small water surfaces of wetland in micro-scale urban environments and utilizing it in the practical design stage of urban land use. In a study of a residential neighbourhood pond in Japan it has been observed that the "maximum temperature decrease induced by the water surface was approximately 2◦C at the pedestrian level. For a wind velocity of approximately 3m/s at a height of 10m, the effect of the evaporative cooling propagates downwind over an unobstructed distance of 100m." (Tominaga Y. et al, 2015)

A combination of climate and population pressures now threatens the sustainability and security of urban water supplies in many of the cities across the globe. A re-evaluation of alternative approaches to securing a reliable and quality water supply for growing cities is now becoming critical. One of the alternative approaches being explored is 'Water Sensitive Urban Design' (WSUD) or 'Low Impact Design' (LID), the intent of which is to conserve water use by managing design options for reducing and re-using urban waste and storm water.

A study using aquacycle and the single-source urban evapotranspiration interception scheme (SUES) at Canberra, Australia confirms that through passive design strategy to modify urban microclimate like wetland and vegetation maximize evapotranspiration. The subsequent effects on daily maximum air temperatures are estimated using an atmospheric boundary layer budget. Potential energy savings of about 2% in summer cooling are estimated from this analysis (Mitchell V. G.et al, 2008).

Through an optimization study for the thermal comfort of an urban square in France, Robitu et al. (2006) reported that "the presence of water ponds and trees reduced the mean radiant temperature by 35–40℃ at 1.5 m on the top of the ground surface". Using a water pool inside the courtyard or covering the ground of the courtyard with vegetation significantly reduced both the air temperature and mean radiant temperature. Finally, this research suggests using water pool and green areas are the most effective heat mitigation strategies for urban blocks in the Netherlands. (Taleghani M. et al, 2014).

A research work based on weather study by "Dutch hobby meteorologists and a network of stations in Rotterdam (Netherlands, has been observed that water bodies increase rather than decrease the 95 percentile of the daily maximum UHI which is the highest around sunset". This suggest that "water bodies do not a priori act as cooling elements in an urban area, as previously thought", especially during the night and evenings in the late summer, when surface waters are relatively warm. Heat capacity of water bodies are relatively large compared to their milieu which "suppresses the diurnal and annual cycle over water, and water temperatures remain relatively high after evening and season transitions" (Steeneveld G.J. et al,2014).

Theeuwes N. E. et al. (2013) used the "Weather Research and Forecasting (WRF)", a mesoscale meteorological model, "to investigate and quantify the influence of surface water on urban temperature". In this study, how the temperature in the urban area influenced by the spatial distribution of water bodies and water fraction in the city are investigated based on an idealized circular city. The variable of this simulation study was the size and spatial configuration of the surface water cover, and temperature of the water. The result of this simulation study demonstrates "a nonlinear relationship of cooling effect of water bodies with the fractional water cover, size of the water bodies and distribution of water bodies within the city with respect to wind direction". One of the important observation from this simulation study is that although relatively large lakes show more cooling effect close to their edges and in downwind areas, several smaller waterbodies can influence a larger area of the city through their cooling effect if distributed equally within the urban area (Theeuwes et al. 2013). One of the important findings of this simulation study is that, if the water temperature of the wetland stays below the air temperature surrounding it, wetland will always act as a cooling element to the surrounding urban area. In case of the water temperature going above the air temperature, the wetland will act as a warming element for the surrounding urban area. Also, the cooling effect of the wetland varies with the water temperature with the warmer water producing less cooling effect. Another finding is that the lake or wetland has a larger cooling influence on its direct surroundings than on the urban areas further downwind of the wetland (Theeuwes et al. 2013). This study demonstrated obvious relation between the urban temperature and the available wetland surface in an urban area. Also, this study emphasis a further understanding of the role of lakes in the urban climate by investigating different influencing factors including the water body area, shape complexity of the wetland in terms of landscape shape index, distance from the city center as the center of UHI and the properties of the surrounding built-up area.

Wong et al. (2012) conducted a research on the "evaporative cooling performance of water bodies to its surrounding microclimate" at a height of 2m at two locations, Kallang and Sungei Api-api study case area was conducted. Both locations are characterized by "having vast water bodies and encircled by greenery". The cooling effect are likely start at 9am when the solar radiation reaches around 150-200 W/m² in the morning and end at the around 6pm, when the solar radiation was less than 75-100 W/m² in the evening. During daytime, with clear day condition there is a reduction of evaporative cooling impact on the range of 0.1°C - 0.2°C on every span of 35m away from the waterway (Wong et al. 2012).

"Documents of the past manifested that the temperature differences between the city center and its surrounding areas decreased with increasing wind speed and disappeared on clear days" (Rutherford J. C. et al, 2004). Wong N.H. et al, (2011) showed that the effect of wind speed on the temperature difference was small, and did not greatly affect the correlation between urban temperature and land use. Data from field observation at 1.5–2.0-m height which included different weather conditions except rainy days showed the temperatures were also not correlated with the wind speeds, but had a high negative correlation with humidity (Huang et al. 2008).

Kim Y.H. et al. (2008) conducted a study of changes in "local thermal environment by associated with the restoration of an inner-city stream", the Cheonggye stream, in Seoul were investigated in the stream area over several "summertime periods before, during, and after the stream restoration". It has been concurred that the restored stream affects local thermal environment, including temperature mitigation and transformation in sensible heat flux (Kim Y. H. et al. 2008).

A study compared two urban streets found that Urban streets beneficial to the blowing of river wind have better thermal environment than obstructive streets. One street Sanyang Road is spacious and has good natural ventilation while Eryao Street is very narrow and has too many cars to remove heat, resulting in poor natural ventilation. The thermal comfort on Sanyang Road is better than that on Eryao Street. "Through proper adjustment of planning, guiding river wind into urban blocks will play an active role in the improvement of urban thermal environment" (Han G. et al. 2011).

Conventional water facilities, such as canals, fountains and sprays installed in urban areas mainly for landscaping purposes exhibits their cooling effect through evaporative cooling by adjusting relative humidity and air temperature, as well as providing its “landscaping and hydrophilic functions”. so, new water facility for “rather narrow city spaces, such as beside sidewalks and between buildings could be designed that can be adjusted according to the micro-meteorological environment in the living space”. This phenomenon has been investigated by Nomura *et al.*, 1993 in “a field study on the degree of cooling effect that artificial water facilities can produce in relatively-narrow urban areas. In their experiments, a model fountain, which serves as a basic water facility, was established in a wind tunnel to measure the range of cooling effect. Based on the results, they placed new, novel water facilities in the field environment”. “The time of the field measurements were on July 30 and 31st, 1992, when summer conditions were at an average level with clear days with a 2.5 m/ s west-northwesterly sea breeze. The temperature fall area induced by evaporation of water from the spray and water fall operation at the Stage Stone Pillar Pond spreads out to nearly 35m toward leeward from the Stage Stone Pillar Pond. Also, even when the spray is not operated, air temperature is 1 to 2 K lower than the average air temperature in this park, that is, 35.8° C”. “Thus, it was confirmed that spray or water fall operations create an air temperature decline area on the leeward side, and that the degree of temperature decline depends on types of water facilities, but especially water spray facilities are effective for cooling. The result was reproduced in a suction type wind tunnel, 6.4 m long, 0.4 m wide and 0.4 m high for the measuring part with the same atmospheric properties in a wind tunnel as the actual ones in an urban area in order to experimentally study the effect of air temperature decline by urban water facilities” (Nishimura et al. 1998).

Manteghi et al , 2015 observed that the temperature inside some of the street canyons was actually lower in many cases than in the open area (bay point) after the morning hours due to the large heat capacity of the water body compared to its surroundings. This suggests that in high ambient temperatures, these waters also reach a relatively high temperature compared to their surroundings. Due to the distance from the river the four N-S oriented streets showed significantly higher temperatures, even although they enjoy a longer time out of direct sunlight, i.e. solar radiation which suggests that their distance from the river is an important factor in producing lower temperatures. They also observed that the cooling effects of the Malacca River are greater than those of the Malacca Sea which indicates that distance to the sea does not make a significant difference. This study indicates that the relative temperature of the respective body of water is mainly prescribes the temperature change, overriding the effects of cooling owing to evaporation. Thus, lower temperature of the water compare than its surroundings always works as a cooling element; but the converse is also true (e.g. at night). In short, water bodies work as buffers of the diurnal temperature cycle: cooling the environment throughout the day time and warming it at night time. Also, the study showed that the relative humidity of the measured points was lower at the time of high temperature (Figure 3.1) which points to an inverse relationship between air temperature and relative humidity. Overall urban streets open to winds from the river have a better microclimate than streets which block this to a greater extent. The maximum nearest water body point temperature has a delay of few hours was compared to the maximum air temperature of the streets with the higher temperature of the near water body which occurs in the evening (Manteghi et al, 2015).

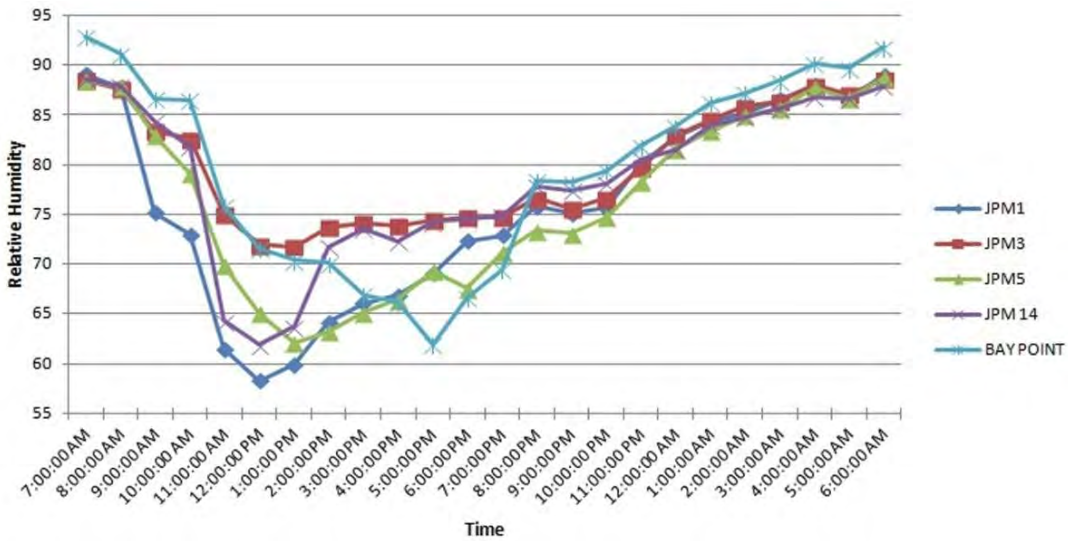

Figure 2.13: Change of Relative Humidity with time (Manteghi et al, 2015)

2.13 Relationship Between Microclimatic Cooling and Shape Complexity of The Urban Water Bodies

On average Urban wetlands are cooler than their surrounding landscapes. This implies that cooling effects of wetlands are significant to cool down hot urban environments. The cooling effect of the wetland should therefore be included in the assessment of wetland ecosystem services. Next observation made by Sun R. et al (2012) is that the UCI intensity does not linearly correlate with wetland area, whereas it is highly correlated with wetland shape. There observation indicates that the cooling effect has a threshold as the wetland area increases. Thus, it is reasonable, to benefit more stakeholders a large water body could be substituted with several small water bodies of the same total area. Their recommendation was "the cooling effect of wetlands may be intensified by constructing them in a small size with relatively regular shape because we do not have enough urban land to create large wetlands with natural complex shape" (Sun R. et al, 2012).

2.14 Relationship Between Water Quality and Shape of The Urban Water Bodies

Hwang S.J. et al observed that "edges of wetland mediate the material flux between adjacent systems. This mediating effect of edges is strongly tied to the complexity of the adjacent shapes of the wetland. Land use within a watershed has a direct impact on the water quality of adjacent aquatic systems. Hydrological processes carry material produced by land-use activities into aquatic ecosystems through the edges of the ecosystem. Therefore, the geometry of aquatic ecosystems theoretically affects the relationship between land use and water quality". With the increment of "shape complexity of wetlands, the concentration of BOD, COD, and TP within reservoir water significantly reduces". They build a "moderation model for BOD, COD, TN, and TP, which suggest that shape complexity can considerably relieve the negative impacts on water quality of urban land use in areas adjacent to reservoirs". (Hwang S.J., et al, 2007).

Research by various author on urban wetlands has addressed matters like "water pollution, eutrophication, sedimentation, and shifts in biotic communities (Birch and McCaskie 1999, Lindstrom 2001, Leavitt et al. 2006, Novotny et al. 2008, Effler et al. 2010, Meter et al. 2011, Van Metre 2012)". "Changes may be mediated by morphological characteristics of water bodies (e.g., size, shape, and type), as well as broader, landscape-scale characteristics of lake districts and flow networks, like water body density and connectivity" (Oertli et al. 2002, Williams 2004, Downing 2010).

The water quality of adjacent urban wetland is profoundly affected by the types of urban area. Downing (2010) defined, "Developed urban open area land cover includes parks, golf courses, and other spaces where the natural vegetation removed or altered, but not necessarily built up. On the other hand, undeveloped category, depending on the region and climate includes areas designated as forest, scrub, or desert". "The size and shape of water bodies has a broad range of effects on their hydrologic and geochemical conditions and their ecological and biogeochemical functions. Small water bodies also differ from larger (and more intensively studied) lakes in terms of physical and biogeochemical conditions and processes" (Downing 2010). For example, "smaller lakes tend to be high in dissolved organic matter and dissolved CO_2 but low in dissolved inorganic carbon and oxygen" (Kelly et al.,2001; Crisman et al.,1998; Hanson et al.,2007). "Lake size has been observed to impact methane production" (Michmerhuizen et al.,1996; Bastviken et al.,2004) and "CO2 efflux" (Cole et al.,2007; Hanson et al.,2007). "Areal rates of organic carbon sequestration are potentially an order of magnitude higher in small lakes" (Downing et al.,2008; Dean et al.,1998; Downing J.A.,2010). In akin to, "lake size also influences regional and global Nitrogen budgets, as small lakes retain double the amount of nitrogen globally than large lakes and are sinks for N via denitrification" (Harrison et al. 2008).

Shoreline development factor (SDF) used to measure the shape of landscape feature. Water body shape measured by the shoreline development factor (SDF) showed it is marginally influenced by land cover. "The median SDF indicated a significant increase in the shoreline-to-area ratio in the urban low-, medium-, and high-intensity land cover classes, meaning that urban water bodies are likely to be longer and tortuous compared to the undeveloped land. The variation in median SDF across cities increased at medium- and high intensity urban land covers. In contrast, the slope of the SDF frequency distribution was significantly lower in high-intensity urban land cover than undeveloped land, indicating that the distribution was shifting to ''rounder'' water bodies in these land covers" (Steele M. K. et al 2014). urban land covers exhibit moderate sized water bodies less connected in comparison of the waterbodies in undeveloped land. Steele suggested that “the differences in the size distributions suggest that the smallest water bodies nearer to an area of 0.5 ha are the most affected by urbanization. Visual observations indicate most of water bodies in all land cover classes were irregular spheroids, but certain shapes were associated with human alteration. Although the impounded dendritic shape was also observed in all land covers urban land cover are associated with simplified shapes. Due to anthropogenic activities, urban wetland is characterized by a reduction of irregularity of the basic shape and a reduction in tortuosity and irregularity of the shoreline. water bodies in the urban land covers are less connected to surface flow lines like streams and rivers compared to water bodies in undeveloped land”. Steele further stated that “although the percentage of water bodies connected to surface flow lines increased as the size of water bodies increased, small water bodies with an area around 0.01 km2 in urban land covers were more likely to be disconnected from flow lines than similar-sized water bodies in the undeveloped land covers”. He suggested “to mitigate the urban heat island and simultaneously influence biogeochemical cycling on a regional level, reincorporation of small water bodies with the water network is necessary”. He also described that “the decrease in connectivity to the greater watershed and the loss of the smallest water bodies together may have substantial implications for both the terrestrial environment and regional and global nutrient and carbon cycling. Small water bodies in urban landscapes are less likely to be connected to streams than in minimally developed landscapes, and patterns of connectivity between lakes and streams reflected an interaction between land use intensity and climate” (Steele M. K. et al ,2014).

2.15 Effects of Water Temperature on Water Quality

A research in Sierra Nevada, California by Ficklin et al (2013) showed, “Warmer temperatures are expected to raise mountain stream temperatures, affecting water quality and ecosystem health”. They “demonstrate the importance of climate-driven changes in hydrology as fundamental to understanding changes in the local water quality”. In their Sierra Nevada case study, they “focused on changes in stream temperature, dissolved oxygen (DO) concentrations, and sediment transport in mountainous, snowmelt-dominated, and water limited systems”. They observed that “stream temperatures are primarily influenced by the amount of heat exchange at the air/water interface and secondarily by the temperature of the contributing hydrologic components to the stream reach such as groundwater, surface runoff, and snowmelt inputs. Stream temperatures in general have shown a strong positive correlation with air temperature” (Ficklin D.L. et al ,2013).

“Increased stream temperatures can cause dissolved O_2 (DO) limitation via increased microbial activity and O_2 demand and reduced O_2 diffusion and solubility” (Somers et al. 2013). “Stream temperature influences growth, metabolism, and reproduction of aquatic biota, and can be lethal if it exceeds thermal limits of aquatic fauna" (Vannote et al. 1980, Hester et al. 2011). "Urbanization elevates water temperature at baseflow and can cause temperature surges during storms. Impervious surface in highly developed watersheds leads to high levels of runoff during storms" (Dunne et al. 1978, Arnold et al. 1996). "The initial runoff from paved surfaces can reach extremely high temperatures because impervious surfaces can be as much as 50°C hotter than the air" (Berdahl et al. 1997).

Somers measured "canopy closure from the ground at the thalweg (a line following the lowest part of a valley whether under water or not) of the stream with concave forest densiometers (Forest Densiometers, Bartlesville, Oklahoma) (Lemmon 1957) at each cross-section to provide an estimate of canopy closure 100 m upstream of the temperature logger". "Densiometer readings are subjective, so field canopy-closure measurements were made by 2 technicians who underwent extensive calibration to ensure their interpretations were consistent". They "also calculated canopy closure from aerial photographs taken in 2008 (NAIP 2008)" and "created a 10 3 10-m grid in ArcGIS that covered the entire study area, overlaid satellite images of each stream reach with the grid, and visually analyzed cover 100 m upstream of the temperature loggers". Than they "counted the grid cells in which the stream was not visible and divided this number by 10. For example, if the stream was clearly visible in 2 of the grid cells, estimated canopy closure is 80%. These estimates were only slightly correlated with densitometer readings (adjusted $R^2 = 0.25$, $p <0.05$), probably because of differences in sampling and photography dates and in resolution between densiometer readings and 30-m grids" (Somers et al. 2013)

2.16 References

1. Ahmed R. "*In search of the impact of urbanization on the thermal environment of the city of Dhaka, Bangladesh, during the pre-monsoon hot season from 1948 through 1987*". Report of the Technical Conference on Tropical Urban Climates Dhaka, Bangladesh, 28 March - 2 April 1993, World Meteorological Organization (WMO).
2. Ahmed A.Q., Ossen D.R., Jamei E., Manaf N.A., Said I., Ahmad M.H. (2015). "*Urban surface temperature behaviour and heat island effect in a tropical planned city"*. Theoretical Applied Climatology 119:493–514.
3. Ahmed K S. 1995. "*Approaches to Bioclimatic Urban Design for the tropics with special reference to Dhaka, Bangladesh*". Ph.D. thesis, Environment and Energy studies Programme, Architectural Association School of Architecture, London.
4. Arnold, C. L., and C. J. Gibbons. (1996). "*Impervious surface coverage: the emergence of a key environmental indicator"*. Journal of the American Planning Association 62:243–258.
5. Berdahl, P., and S. Bretz. (1997). "*Preliminary survey of the solar reflectance of cool roofing materials"*. Energy and Buildings 25:149–158.
6. Bastviken, D., J. J. Cole, M. L. Pace, and L. J. Tranvik. 2004. "*Methane emissions from lakes: dependence of lake characteristics, two regional assessments, and a global estimate"*. Global Biogeochemical Cycles 18:1–12.
7. Birch, S. & McCaskie, J. (1999) "*Shallow urban lakes: a challenge for lake management*". Hydrobiologia 395: 365
8. Crisman, T. L., L. J. Chapman, and C. A. Chapman. 1998. "*Predictors of seasonal oxygen levels in small Florida lakes: the importance of color"*. Hydrobiologia 368:149–155.
9. Cole, J. J., Y. T. Prairie, N. F. Caraco, W. H. McDowell, L. J. Tranvik, R. G. Striegl, C. M. Duarte, P. Kortelainen, J. A. Downing, J. J. Middelburg, and J. Melack. 2007. "*Plumbing the global carbon cycle: integrating inland waters into the terrestrial carbon budget"*. Ecosystems 10:172–185.
10. Coutts, A. M., Tapper, N. J., Beringer, J., Loughnan, M., & Demuzere, M. (2013). *"Watering our cities the capacity for Water Sensitive Urban Design to support urban cooling and improve human thermal comfort in the Australian context". Progress in Physical Geography, 37*(1), 2-28.
11. Dunne, T., and L. Leopold. (1978). "*Water in environmental planning"*. 16th edition. W. H. Freeman and Company, San Francisco, California.
12. Downing, J. A. 2010. "*Emerging global role of small lakes and ponds: little things mean a lot"*. Limnetica 29:9–24.
13. Dean, W. E., and E. Gorham. 1998. "*Magnitude and significance of carbon burial in lakes, reservoirs, and peatlands"*. Geology 26:535.
14. Effler, S. W., S. M. O'Donnell, A. R. Prestigiacomo, D. M. O'Donnell, R. K. Gelda, and D. A. Matthews. 2010. "*The effect of municipal wastewater effluent on nitrogen levels in Onondaga Lake, a 36-year record"*. Water Environment Research 82:3–19.
15. Fraedrich K. (1972). "On the evaporation of a lake in warm and dry environment". Tellus, 24: 116–121. doi:10.1111/j.2153-3490.tb01538.x
16. Ficklin D.L., Stewart I.T., and Maurer E.P. (2013). "*Effects of climate change on stream temperature, dissolved oxygen, and sediment concentration in the Sierra Nevada in California*." Water Resources Research, Vol. 49, 2765–2782, doi:10.1002/wrcr.20248.
17. Frey C.M., Rigo G., Parlow E. "*Investigation of the daily Urban Cooling Island (UCI) in two coastal cities in an arid environment: Dubai and Abu Dhabi (U.A.E)"*. Institute of Meteorology, Climatology and Remote Sensing, Department of Geosciences, University of Basel.
18. Golnoosh Manteghi, Hasanuddin bin limit & Dilshan Remaz. (2015). "*Water Bodies an Urban Microclimate: A Review"*. Modern Applied Science; Vol. 9, No. 6;

19. Grimmond C.S.B, Oke T.R. (1999). "*Heat storage in urban areas: observations and evaluation of a simple model*". Journal of Applied Meteorology 38: 922–940.
20. Hwang S.J., Lee S.W., Sona J.Y., Park G.A., Kim S.J. (2007). "*Moderating effects of the geometry of reservoirs on the relation between urban land use and water quality*." Landscape and Urban Planning 82, 175–183, Elsevier.
21. Hester, E. T., And M. W. Doyle. (2011). "*Human impacts to river temperature and their effects on biological processes: a quantitative synthesis"*. Journal of the American Water Resources Association 46:1–17.
22. Huang L., Li J., Zhao D., Zhu J (2008). "*A fieldwork study on the diurnal changes of urban microclimate in four types of ground cover and urban heat island of Nanjing, China".* Building and Environment 43, 7–17.
23. Han G., Chen H., Yuan L., Cai Y., Han M. (2011). *"Field measurements on micro-climate and cooling effect of river wind on urban blocks in Wuhan city".* Multimedia Technology (ICMT), 2011 International Conference on .10.1109/ICMT.2011.6003331
24. Hanson, P. C., S. R. Carpenter, J. A. Cardille, M. T. Coe, and L. A. Winslow. 2007. "*Small lakes dominate a random sample of regional lake characteristics"*. Freshwater Biology 52:814–822.
25. Hanson, P. C., S. R. Carpenter, J. A. Cardille, M. T. Coe, and L. A. Winslow. 2007. "*Small lakes dominate a random sample of regional lake characteristics"*. Freshwater Biology 52:814– 822.
26. Harrison, J. A., R. J. Maranger, R. B. Alexander, A. E. Giblin, P.A. Jacinthe, E. Mayorga, S. P. Seitzinger, D. J. Sobota, and W. M. Wollheim. 2008. "*The regional and global significance of nitrogen removal in lakes and reservoirs"*. Biogeochemistry 93:143–157.
27. Hossain M.E. and Nooruddin M. *"Some aspects of urban climates of Dhaka city".* Report of the Technical Conference on Tropical Urban Climates Dhaka, Bangladesh, 28 March - 2 April 1993, World Meteorological Organization (WMO).
28. Jáuregui, E. (1991). "*Effects of revegetation and new artificial water bodies on the climate of northeast Mexico City"*. Energy and buildings, 15(3), 447-455.
29. Kim Y. H., Ryoo, S. B., Baik, J. J., Park, I. S., Koo, H. J., & Nam, J. C. (2008). "*Does the restoration of an inner-city stream in Seoul affect local thermal environment"?* Theoretical and applied climatology, 92(3-4), 239-248.
30. Khaleque M.A., Habib A. and Ahmed S. *"Eco-climatic features of Dhaka city due to urbanization".* Report of the Technical Conference on Tropical Urban Climates Dhaka, Bangladesh, 28 March - 2 April 1993, World Meteorological Organization (WMO).
31. Kotthaus S., Grimmond C.S.B. (2014). "*Energy exchange in a dense urban environment – Part I: Temporal variability of long-term observations in central London"*. Urban Climate 10, 261–280, Elsevier B.V.
32. Kelly, C. A., E. Fee, P. S. Ramlal, J. W. M. Rudd, R. H. Hesslein, C. Amena, and E. U. Schindler. 2001. "*Natural variability of carbon dioxide and net epilimnetic production in the surface waters of boreal lakes of different sizes"*. Limnology and Oceanography 46:1054–1064.
33. Lauwaet D., Ridder K.D., Saeed S., Brisson E., Chatterjee F., Lipzig N.P.M. V., Maiheu B., Hooyberghs. H. (2016). *"Assessing the current and future urban heat island of Brussels".* Urban Climate 15, 1–15.
34. Lemmon, P. E. (1957). "*A new instrument for measuring forest overstory density*". Journal of Forestry 55:667–669.
35. Lindstrom, M. 2001. "*Urban land use influences on heavy metal fluxes and surface sediment concentration of small lakes*". Water, Air, and Soil Pollution 126:363–383.

36. Leavitt, P. R., C. S. Brock, C. Ebel, and A. Patoine. 2006. "*Landscape-scale effects of urban nitrogen on a chain of freshwater lakes in central North America"*. Limnology and Oceanography 51:2262–2277.
37. Michmerhuizen, C. M., R. G. Striegl, and M. E. McDonald. 1996. "*Potential methane emission from north-temperate lakes following ice melt"*. Limnology and Oceanography 41:985– 991.
38. Manteghi G., Lamit H.B. and Ossen D.R. (2015)**. "***Influence of Street Orientation and Distance to Water Body on Microclimate Temperature Distribution in Tropical Coastal City of Malacca".* International Journal of Applied Environmental Sciences, Volume 10, Number 2, pp. 749-766
39. Ministry of Environment & Forests (n.d.). Retrieved February 02, 2018, from http://moef.portal.gov.bd/
40. Miao S., Chen F., LeMone M.A., Tewari M., Li Q., and Wang Y. (2009). "*An Observational and Modeling Study of Characteristics of Urban Heat Island and Boundary Layer Structures in Beijing*". Journal of Applied Meteorology and Climatology. Volume 48 No. 3.
41. Mitchell V. G., Cleugh H. A., Grimmond C. S. B. and Xu J. (2008) "*Linking urban water balance and energy balance models to analyse urban design options"*. Hydrological Processes Hydrol. Process. 22, 2891–2900. Published online in Wiley InterScience.
42. Mills, G. 2004. "*The Urban Canopy Layer Heat Island".* Available from: http://www.urban-climate.org/
43. Murakawa, S., Sekine, T., Narita, K. I., & Nishina, D. (1991). "*Study of the effects of a river on the thermal environment in an urban area"*. Energy and buildings, 16(3), 993-1001.
44. Nishimura N., Nomura T., Iyota H. and Kimoto S (1998). "*Novel water facilities for creation of comfortable urban micrometeorology*". Solar Energy Vol. 64, Nos 4–6, pp. 197–207.
45. Novotny, E. V., D. Murphy, and H. G. Stefan. 2008. "*Increase of urban lake salinity by road deicing salt"*. Science of the Total Environment 406:131–144.
46. Oke, T.R. 1982. "The energetic basis of the urban heat island". Quarterly Journal of the Royal Meteorological Society (1982), 108, pp. 1-24
47. Oke T. R., Mills G., Christen A., and Voogt J. A. (2017). "Urban Climates". Cambridge University Press.
48. Offerle B., Grimmond C. S. B. and Fortuniak K. (2005). "*Heat storage and anthropogenic heat flux in relation to the energy balance of a central European city centre"*. International Journal of Climatology. 25: 1405–1419 (2005)
49. Oertli, B., D. A. Joye, E. Castella, R. Juge, D. Cambin, and J. Lachavanne. 2002. "*Does size matter? The relationship between pond area and biodiversity"*. Biological Conservation 104:59–70.
50. Robitu M., Musy M., Inard C., Groleau D. (2006) *"Modeling the influence of vegetation and water pond on urban microclimate"*. Solar Energy 80, 435–447.
51. Revi A., Satterthwaite D.E., Durand F. A., Morlot J. C., Kiunsi R.B.R., Pelling M., Roberts D.C., and Solecki W., (2014): Urban areas. In: *Climate Change 2014: Impacts, Adaptation, and Vulnerability. Part A: Global and Sectoral Aspects. Contribution of Working Group II to the Fifth Assessment Report of the Intergovernmental Panel on Climate Change*. Cambridge University Press, Cambridge, United Kingdom and New York, NY, USA, pp. 535-612.
52. Raja D.R., Neema M.N. "*Impact of Urban Development and Vegetation on Land Surface Temperature*". Computational Science and Its Applications – ICCSA

2013,13th International Conference, Ho Chi Minh City, Vietnam, June 24-27, 2013, Proceedings, Part III. Pages 351-367.Springer

53. Sun R., Chen L. (2012). "*How can urban water bodies be designed for climate adaptation?*" Landscape and Urban Planning 105, 27– 33.
54. Steeneveld G.J., Koopmans S., Heusinkveld B.G., Theeuwes N.E. (2014). "*Refreshing the role of open water surfaces on mitigating the maximum urban heat island effect.*" Landscape and Urban Planning 121,92–96.
55. Saaroni H., Ziv B. (2003). "*The impact of a small lake on heat stress in a Mediterranean urban park: the case of Tel Aviv, Israel*". Int J Biometeorol 47:156–165 DOI 10.1007/s00484-003-01617
56. Spronken-Smith R. A. & Oke T. R. (1998). "*The thermal regime of urban parks in two cities with different summer climates"*. International Journal of Remote Sensing, 19:11, 2085-2104, DOI:10.1080/014311698214884
57. Spronken-Smith R. A. & Oke T. R. (1998). "*The thermal regime of urban parks in two cities with different summer climates"*. International Journal of Remote Sensing, 19:11, 2085-2104, DOI:10.1080/014311698214884
58. Sun R., Chen A., Chen L, Lü Y. (2012). *"Cooling effects of wetlands in an urban region: The case of Beijing"*. Ecological Indicators 20 (2012) 57–64.
59. Steeneveld G.J., Koopmans S., Heusinkveld B.G., Theeuwes N.E. (2014) "*Refreshing the role of open water surfaces on mitigating the maximum urban heat island effect*." Landscape and Urban Planning 121, 92–96.
60. Somers K. A., Bernhardt E.S., Grace J.B., Hassett B. A., Sudduth E.B., Wang S. and Urban D.L. (2013). *"Streams in the urban heat island: spatial and temporal variability in temperature".* Freshwater Science, 32(1):309–326
61. Steele M. K., Heffernan J. B. (2014). "*Morphological characteristics of urban water bodies: mechanisms of change and implications for ecosystem function"*. Ecological Applications, 24(5), pp. 1070–1084.
62. Tominaga Y., Sato Y. and Sadohara S. (2015) "*CFD simulations of the effect of evaporative cooling from water bodies in a micro-scale urban environment: Validation and application studies*." Sustainable Cities and Society 19(2015)259–270.
63. Taleghani M., Tenpierik M., Dobbelsteen A.V.D., and Sailor D.J. (2014) "*Heat in courtyards: A validated and calibrated parametric study of heat mitigation strategies for urban courtyards in the Netherlands*." Solar Energy 103, 108–124. 2014.
64. Theeuwes N.E., Solcerová A. and Steeneveld G.J. (2013). *"Modeling the influence of open water surfaces on the summertime temperature and thermal comfort in the city".* Journal of Geophysical Research: Atmospheres, 118(16), 8881-8896. doi:10.1002/jgrd.50704.
65. United Nations Population Division | Department of Economic and Social Affairs. (n.d.). Retrieved February 03, 2018, from http://www.un.org/en/development/desa/population/
66. Vannote, R. L., And B. W. Sweeney. (1980). "*Geographic analysis of thermal equilibria: a conceptual-model for evaluating the effect of natural and modified thermal regimes on aquatic insect communities"*. American Naturalist 115:667–695.
67. Van Metre, P. C. 2012. "*Increased atmospheric deposition of mercury in reference lakes near major urban areas"*. Environmental Pollution 162:209–215.
68. Williams, P. 2004. "*Comparative biodiversity of rivers, streams, ditches and ponds in an agricultural landscape in Southern England"*. Biological Conservation 115:329–341.
69. Wong N.H., Tan C.L., Nindyani A.D.S., Jusuf S.K. and Tan E. (2011). *"Influence of Water bodies on Outdoor Air Temperature in Hot and Humid Climate".* ICSDC 2011: pp. 81-89. doi:10.1061/41204(426)11

Chapter 3 : PRODUCTION AND TRANSPORT OF COOLING EFFECT

3.1 Characteristics of Water, Water Heating and Cooling

The first and second law of thermodynamics describe "Energy exchange" (Halliday et al. 1988), "which tells us we can transform energy but can't create or destroy. The direction of energy exchange will occur from areas of high concentration towards area of lower concentration". A natural body of water such as lake, river etc. can be heated by two primary sources: "the sun and the ambient radiation emitted by the atmosphere and earth. In a temperate zone on a clear summer day the daily incoming solar radiation would be 332 Wm^{-2} and ambient radiation 330 Wm^{-2}" (Satterlund et al., 1992). "Shade is created by intercepting direct solar radiation and preventing it from reaching the surface of the earth. Approximately 95% of visible radiation will penetrate a column of clear water to a depth of 3 feet and over 75% will penetrate to a depth of 30 feet" (Hollaender 1956, Sellers W.D. 1974). "The interaction of water with visible, near-infrared and ambient radiation vary with the season of the year, time of day, water turbidity and surface turbulence. Energy exchange between water and incoming radiation can be estimated mathematically by the following equation" (Halliday et al., 1988).

$$\tau = \frac{Q}{P} = \frac{Q}{SA}$$

Where,

$$Q = mc(T_f - T_i)$$

"Here τ is time(s); P is the total energy delivered to the water per second (W), Q is the amount of heat deposited in the body of water(J); A is the surface area of the body of water exposed to the radiation (m^2); m is the mass of the body of water (kg); c is the specific heat capacity of water (4,190 Jkg^{-1}@ 288°K); T_f is the final temperature of the body of water(K); T_i is the initial temperature of the body of water; and S is the radiation at the surface of the water (Wm^{-2})" (Halliday et al., 1988).

To accurately estimate the increase of temperature of water body "water surface reflectance, the transparency of the water to visible radiation, heat exchange with other thermal bodies (i.e. soil) and the mixing associated with stream environment need to be considered. Introduction of shade in the urban wetland would end up intercepting direct solar radiation. But the shading will have little effect on diffuse, scattered or ambient radiation sources. To cool down water must convert and radiate its internal energy (in the form of heat) out into the thermal reservoir of the atmosphere. This process is governed by a partial differential equation known as the 'one dimensional heat equation' or the 'diffusion equation' are provided as follows" (Matthews J. et al 1970):

$$\frac{\partial^2 T}{\partial x^2} - \frac{1}{\kappa}\frac{\partial T}{\partial t} = 0$$

Where,

$$\kappa = \frac{k}{\rho c}$$

“Here x is the position in the water column (m), ϰ is a constant depending on the thermal conductivity k, the heat capacity is c and the mass density is ρ”.

From this equation, it can be see that “cooling of water by diffusion is a slow process. It has to remembered that shading doesn’t produce cooling, but rather prevents heating by direct solar radiation” (Larson et al, 1996).

3.2 Effects of Riparian Shade on Water Temperature

“Riparian vegetation may affect the stream micro-climate (e.g., air temperature, humidity, and wind speed), which in turn affect evaporation, conduction, ground temperature, and water temperature” (Rutherford J. C. et al, 1997). Rising water temperature (Tw) due to anthropogenic climate change may have serious consequences for river ecosystems. Conservation and/or expansion of riparian shade could counter the negative effect warming and buy time for ecosystems to adapt. In a field study in UK rivers it has been identified that approximately 0.5 km of complete shade is necessary to off-set T_w (water temperature) by 1°C during July (the month with peak T_w) at a headwater site; whereas 1.1 km of shade is required 25 km downstream (Johnson M. F. et al, 2015).

Riparian vegetation strongly affects stream temperature in small streams. Quinn et al. (1997) found that pasture streams had daily max. temperature 6-7 °C higher than adjacent forest stream. Riparian vegetation absorbs incoming shortwave radiation. On a given day daily minimum temperature occurred almost simultaneously and was similar in magnitude regardless of riparian shading but there were significant differences in daily maximum water temperature between sites depending on the amount of shade. Daily minimum water temperature is largely determined by air temperature, the exchange of long-wave radiation between the atmosphere and the stream at night and heat conduction from the steam bed (Rutherford J. C. et al, 2004).

Bowler explained that “Predicted increases in stream temperature due to climate change will have many direct and indirect impacts on stream biota. A potential intervention for mitigating stream temperature rise is the use of wooded riparian zones to increase shade and reduce direct warming through solar radiation. Bowler conducted a systematic review of the available evidence for the effects of wooded riparian zones on stream temperature to assess the effectiveness of this intervention. This systematic review provides evidence that wooded riparian zones can reduce stream temperatures, particularly in terms of maximum temperatures up to 4.94°C” (Bowler D.E, et al, 2012).

Somers et al. (2013) showed that at “the reach scale, warmer baseflow temperatures were associated with wider streams, whereas cooler baseflow temperatures were associated with greater riparian canopy cover and more habitat transitions. At the watershed scale, warmer temperatures occurred in watersheds with higher road densities, and cooler temperatures occurred in watersheds with higher %forest. Maximum temperature appeared to be most strongly influenced by canopy closure via a direct negative path and by mean width of the channel by a direct positive path. Percent developed land cover and road density significantly influenced maximum temperature via a direct path. A significant indirect path indicated that shading effects of % canopy cover dampened the positive relationship between % developed land and stream baseflow temperatures” (Somers et al. 2013).

3.2.1 Methods of producing riparian shade

Rutherford J. C. et al, (1997) constructed “a computer model for stream water temperature was developed, and tested in a small pasture stream near Hamilton, New Zealand. The model quantifies shading by riparian vegetation, hillsides, and stream banks using three coefficients: canopy angle, topography angle, and canopy shade factor (figure 3.1). Shade was measured directly and found to vary significantly along the channel”.

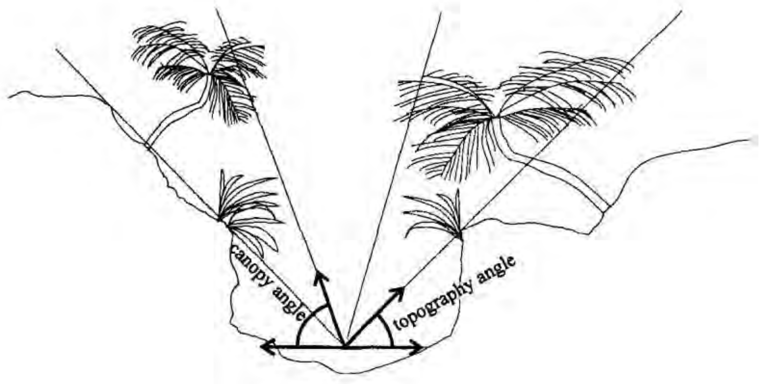

Figure 3.1:Sketch of a typical stream channel cross-section showing topography and canopy angles perpendicular to stream. (Rutherford et al., 1997)

Floating plants/watercress did not prevent solar radiation from reaching the stream, presumably because there is enough water movement through the weed beds. In small streams additional shading may be provided by the banks and groundcover which grows along the edge of the stream, so trees may be planted 10 m apart or more. It is desirable that trees be separated so that enough light reaches the banks to maintain groundcover (e.g., ferns, grasses etc.) along stream banks which help stabilize the channel against erosion. (Rutherford J. C. et al, 1997).

Larson L. L. et al. (1996) reported that “direct sunlight only accounts for approximately 20% of the total, and as a result, shaded areas can receive up to 80% of the total radiative energy available at the surface. Furthermore, the ability of woody vegetation (the physical limitation of height growth) to shade a stream decreases with increasing stream width. A stream running east or west will have an entirely different shading pattern than one running north or south. Shade generated by the topography and/or stream channel will also contribute different levels of shading and exposure for water" (Larson L. L. et al, 1996).

Bowler D.E. et al (2012) suggested that "analysis of riparian shade need to inform on how trees should be planted, in terms of buffer width, length of reach requiring a buffer and the types of trees that should be planted, nor on the roles of stand density/age and nature of understory vegetation. Variables such as stream width and river discharge (thermal capacity), river basin location (headwater or lowlands) and the degree to which the wider catchment is forested are likely to be critical controls on the efficacy of riparian trees as a temperature moderator" (Bowler D.E. et al, 2012).

3.2.2 Width of the riparian buffer to control water temperature

The width of the riparian shading buffer closely effects the temperature of the wetland. Sweeney B. W. et al. (2014) reports that "buffer widths of ≥20 m will keep stream temperatures within 2°C of those that would occur in a fully forested watershed but that full protection from measurable temperature increases is assured only by a buffer width of ≥30 m." (Sweeney B. W. et al, 2014). Figure 3.2 showing a schematic representation of generic riparian buffer area. This buffer is showing "a zone of influence relative to aquatic and upland areas. The intensity of riparian influence is depicted with shading. Material flows refers to energy, organic matter, water, sediment, and nutrient flow". (Riparian areas: functions and strategies for management, 2002).

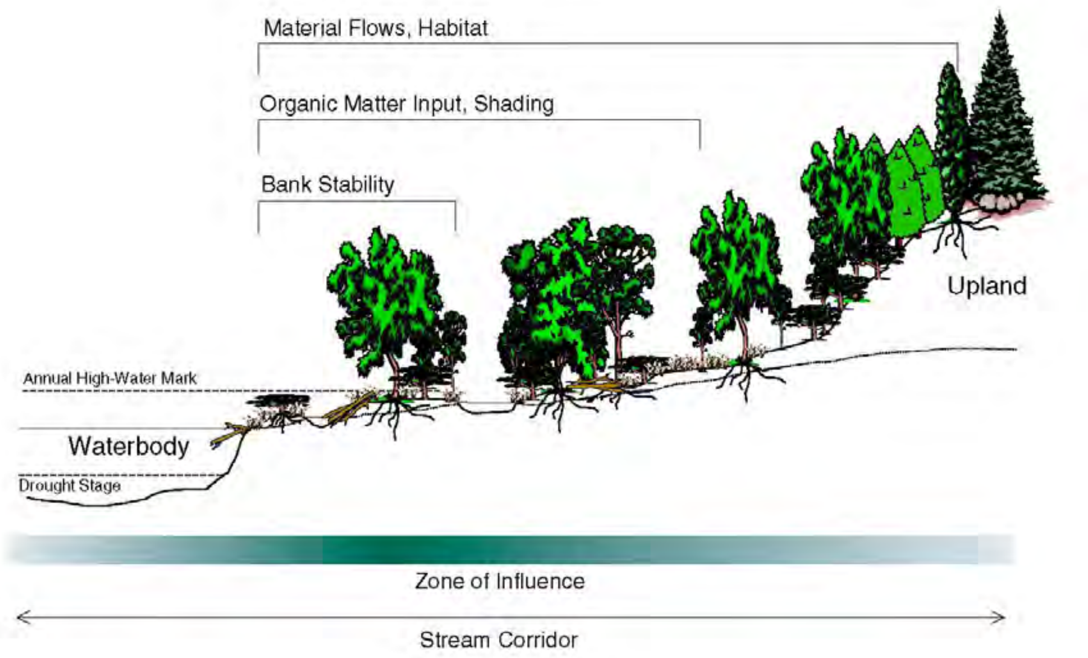

Figure 3.2: Schematic of a generic riparian buffer area (Riparian areas: functions and strategies for management, 2002).

3.2.3 Influence of riparian buffer on removal of nitrogen

Sweeney B. W. et al. (2014) also reports that riparian shading buffers of "at least 30 m wide are needed to protect the physical, chemical, and biological integrity of small streams. A width of 20-30 m should be reasonably effective for removal of nitrogen from surface runoff. effective nitrogen removal at the watershed scale probably requires buffers that are at least 30 m wide and that the likelihood of high removal efficiencies continues to increase in buffers wider than 30 m" (Sweeney B. W. et al, 2014).

3.2.4 Effects of riparian buffer on overland sediment movement

Sweeney B. W. et al. (2014) also reports about several factors influencing the riparian shading buffer effectiveness. Those factors are "soil type, vegetation, slope, sediment load, rainfall intensity, and microtopography influence. Streamside buffers 10 m wide can be expected to trap about 65% of sediments delivered by overland flow, while 30-m buffers can be expected to trap about 85% of sediments. Removal efficiency was maximized at a slope of 9%. A streamside forest of 25 m can maximize the width of small streams but it appears that little or no additional widening occurs in response to forest buffers ≥25 m. An interlocking network of tree roots can increase bank strength and, therefore, resist erosion, streamside forest widths of around 10 m provide some protection, could reduce streambank soil loss and sediment release by 77-97%. Forests on the side of the canal or lake help to reduce bank erosion and channel meandering" (Sweeney B. W. et al, 2014).

3.2.5 Width of riparian buffer to maintain large woody debris and macroinvertebrates

Large woody debris(LWD) in the wetland that naturally accumulated from the forest or large trees by the side of wetland perform some important role on the ecology of the wetland. Sweeney B. W. et al. (2014) in his review of wetland side riparian buffer summed up that "a streamside forest can best provide a natural level of Large Woody Debris to streams if its width is generally ~30 m or equal to the height at maturity of the dominant streamside trees". "LWD provides nutrients and food for aquatic organisms, increases the diversity of instream habitats by forming dams and attendant pools, and helps dissipate the energy of water and keep its sediments from moving downstream". "Role of LWD in channel development, oxygenation, and turbulent mixing of water, organic carbon and nutrient cycling, species habitat". "A streamside forest can best provide a natural level of LWD to streams if its width is generally ~30 m or equal to the height at maturity of the dominant streamside trees". "At least 30m wide buffer of dense streamside forest is needed to protect and support natural levels of macroinvertebrates as well as macroinvertebrate activity in small streams". "A streamside forest of ≥30 m is also needed to protect and maintain fish communities in a natural or near-natural state. Streamside forest buffers ≥30 m wide are also essential to protect water quality, habitat, and biotic features of streams associated with watersheds ≤100 km2, or about fifth order or smaller in size" (Sweeney B. W. et al, 2014).

3.2.6 Carbon sequestration by persistent reedbeds

One study suggests that the maintenance of persistent reedbeds by regular inundation is a means of promoting carbon sequestration. Equally, alterations to flooding regime that lead to the dieback of reedbeds and the drying of soils have the potential to cause considerable losses of carbon to the atmosphere. The management of river hydrology, being an activity of government, is a means by which these carbon fluxes to the atmosphere can be manipulated. Further quantification of gas flux and transfers between soil and water is required to fully articulate a carbon budget relating to phases of wet and dry conditions within the reedbeds of the Macquarie Marshes. The technique developed in this paper of combining the biomass assessment methods of Thursby et al. (2002) with NDVI modeling provides an effective means of assessing changes in aboveground carbon storage associated with flows that could have broader application in environmental water monitoring and evaluation. (Whitaker K. et al, 2015).

So, it is evident that cooling down the water of the wetland with the help of riparian shading is essential to create UCI. The ancient way of ice making in the desert by the Persian (modern Iran) people with help of continuous shading the water is an appropriate example of cooling the water to even below the air temperature with the help of shading only (Asadi F. et al, 2012). So, to keep the water of the wetland in urban area under continuous shading, we need to develop appropriate Urban Solar Envelope (Knowles R. L. et al, 1980**)**.

3.3 Simulating Effect of Water Temperature on Shading

A simulation study had been conducted at a section of Dhanmondi Lake area (approx. 468mX280m) adjacent to the Satmasjid road on South-west and road 6A on the south-east has been selected. One of the day of field measurement in this area, 24 Feb 2017 was used for the sun position in the simulation model. The simulation time was fixed from 9 AM to 16:00 PM of that day. The whole simulation study conducted for three cases depicting three types of ambient condition:

a. Case 1: First simulation study conducted with the water of the lake completely under solar radiation.
b. Case 2: Second simulation study conducted with the fifty percent (50%) water of the lake under solar radiation.
c. Case 3: Third simulation study conducted with the water body completely shaded from solar radiation.

The simulation was conducted using COMSOL-Multiphysics software 5.0. Heat Transfer Module_Heat Transfer with Surface to Surface Radiation (ht) of COMSOL -Multiphysics was used in the simulation. The initial temperature of the water fixed equal the minimum temperature of the day obtained from the field measurement. Detail description about the model are in chapter six. The following figure 3.3 depicts the effect of shading on water surface temperature of the lake.

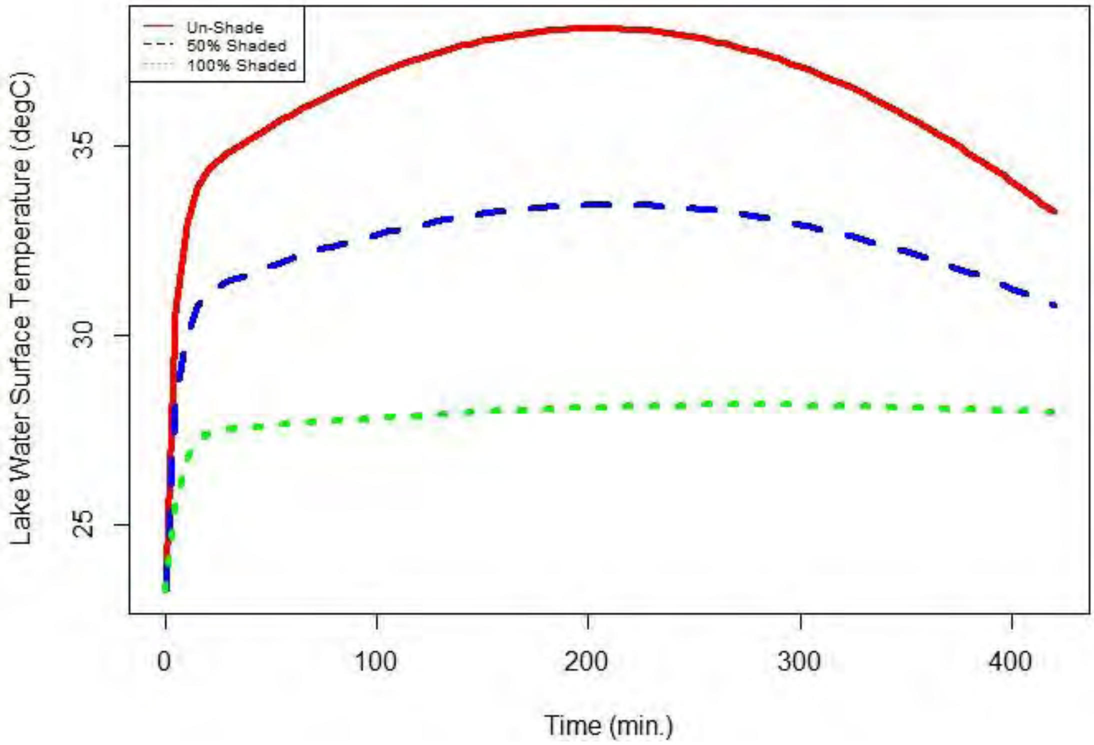

Figure 3.3: Effect of shading on simulated water surface temperature of the lake

From the simulation study it could be concurred that the fully shaded water surface response little with the progressing day temperature as in this case water body can only gain heat from the ambient temperature of the atmosphere**.**

3.4 Relationship of The Different Parameters to Create Urban Cooling Islands

From the study of related literature, it can be concurred that Urban water bodies can play an effective role in microclimatic cooling of the urban area by creating "urban cooling islands" (UCIs). We also can identify several factors that have profound effect on UCIs. They are as follows:

1. Area of the water body
2. Distance of the water body
3. Shape complexity of water body
4. Percentage of Built up area around the water body
5. Heat capacity of Water body
6. Riparian Shade
7. Width of Riparian Buffer
8. Type of Riparian Shade
    1. Riparian vegetation (Canopy angle, Canopy shade factor)
        a. Macrophytes
            i. Floating plants

ii. Emergent

b. Shade trees

c. Ground covers

i. Ferns

ii. Grasses

2. Topography (Topography angle)

a. Hillsides

b. Stream banks

9. Water Quality

1. Removal of nitrogen
2. Overland sediment movement
3. Dissolved oxygen (DO) concentrations

The relationship among the different factors discussed above is shown in the diagram next page. Form the above discussion it is evident that Heat capacity of the water body is counteracting the UCIs effect. Whereas riparian shade is having positive influence on the UCIs and likewise on the water quality. The effect of riparian shade on the water body is mostly done on the linear and narrow streams. There is very few detail studies about the effect of riparian shade on the wider water body. Also, most of the study suggesting small area and regular (Euclidean shape) shape water body distributed in regular interval in urban area for better Urban Cooling Island (UCIs) intensity. So, from the above literature study some Major research questions arises are:

1. How the negative impact of Heat capacity of the reservoirs on UCIs could be moderated by the introduction of riparian shade?
2. Could the large water body with fractal shape moderate the impact of heat capacity of the reservoirs on UCIs?
3. What is the link between “UCIs” and the “water quality of the urban wetland”?

Also, it will be necessary to investigate whether it is possible to lower the minimum water temperature of wetland below that of the air temperature by continuous shading of the water, at least during the hot and dry period. In the figure 3.3 below all the parameters related to the creation of Urban Cooling Island (UCI) are indicated with possible relationship.

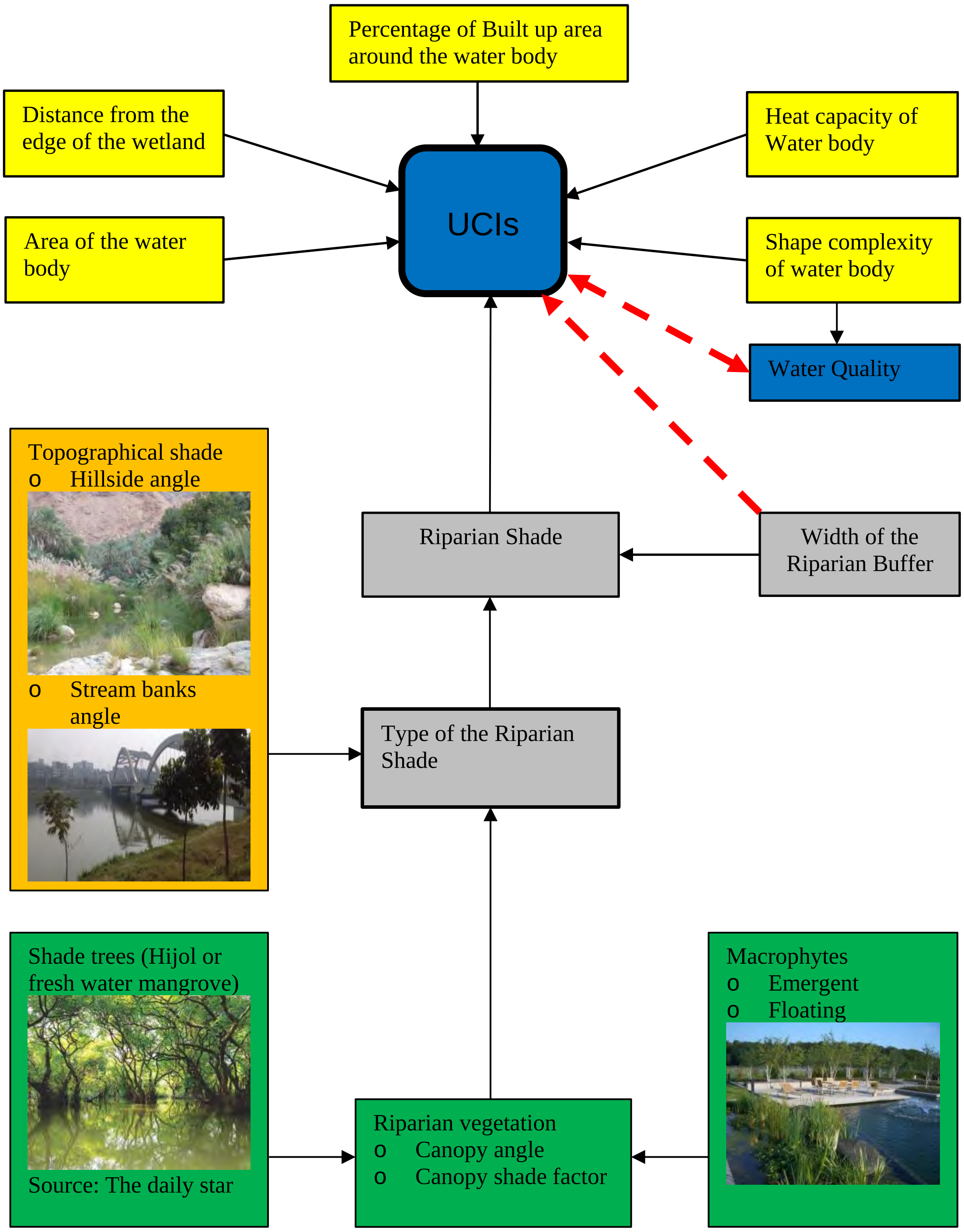

Figure 3.4: Relation of the different parameters related to the creation of UCI

3.5 Transporting Cooling Effect Through Advection

Meteorological office, 1957 in the meteorological glossary stated advection as "the process of transfer by horizontal motion" (Rider N.E. et al, 1963). The term advection could be defined as "the transport of a substance by bulk motion from one region to another in the field of physics, engineering, and earth sciences". In general, most of the advected substance are fluid and the properties of the substance are carried with it. The advected substance carries its conserved properties such as energy through the process. "The advection of variables like temperature, moisture and vorticity are mostly discussed in the meteorology". Warm advection is the process in which the wind blows from a region of warm air to a region of cooler air. Moisture advection which regions are often co-located with regions of warm advection, is horizontal transport of moisture. "Moisture advection plays a very important role in the development of precipitation, because precipitation will not form if there is little moisture availability".

The quantity of a "substance passing through a section perpendicular to a particular direction per unit area and per unit time is called the flux of a substance. The nature of the transporting process determines the amount of substance traversing the cross-section over which the count is performed depends on. In case of the passive entrainment of the substance by the carrying fluid, then the flux can be easily related to the substance concentration and the fluid velocity, as follows:

$$q = \frac{amount}{volume\ of\ fluid} \times \frac{volume\ of\ fluid}{area \times time} = c \times u$$

Where, where u is the entraining fluid velocity, q is flux, c is concentration of the substance. This process is called Advection, a term that simply means passive transport by the moving fluid that contains the substance" (Thayer School of Engineering at Dartmouth).

3.6 Advection in The Earth Science

There are three different advective effects are generally recognized: they are *'clothesline effect',* the *'leading-edge or fetch effect',* and the *'oasis effect'.*

3.6.1 Clothesline effect

When the air flows through a vegetative canopy we can observe this effect. For the ideal conditions of this effect we can consider two vegetative stand borders, one at the edge of a crop field surrounded by warmer and drier ground and the other the edge of a forest bordered by fields. Oke illustrated this effect by the following figure 3.5 of horizontal flow. The air entering crop from the right is warm and dry will increase both the heat supply and the "vapour pressure gradient" between the transpiring leaves and the crop air. As an outcome of this the soil moisture adjacent to the stand border will rapidly deplete due to enhance evaporation rate. As the air enters further into the crop it adjusts to the more typical condition due to moisture acquiring.

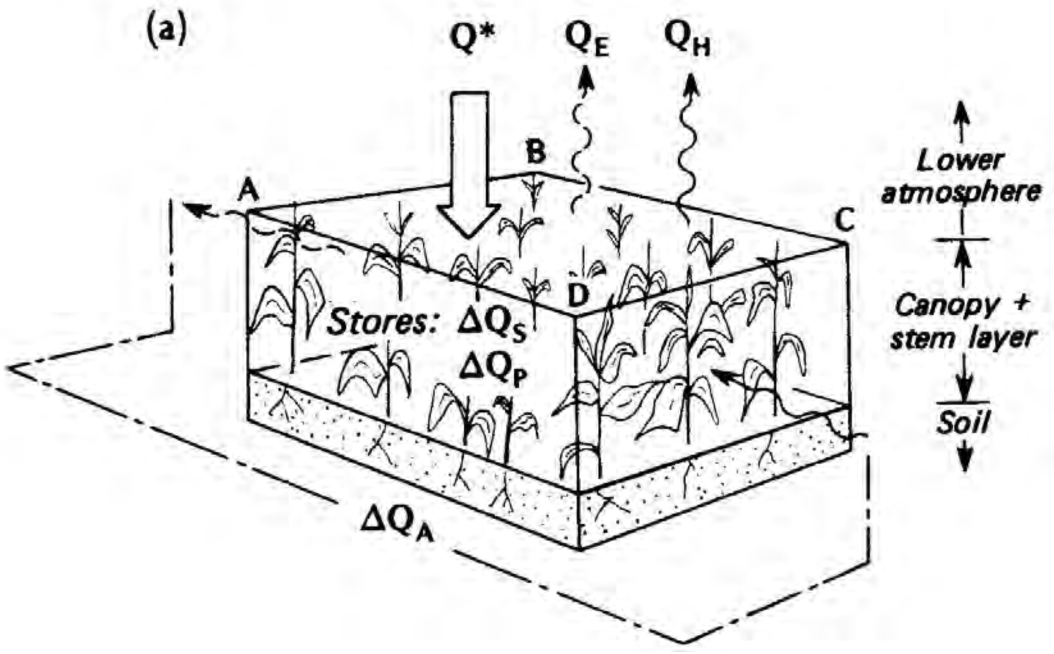

Figure 3.5: Schematic depiction of fluxes involved in the energy balances of a soil-plant-air volume (Oke, 2002)

3.6.2 Leading-edge or Fetch effect

When the air passes from one surface-type to another new and climatically different surface it must adjust to new set of boundary condition. Due to this adjustment a line of discontinuity is created as illustrated in the fig 3.6, which is called the leading-edge. Oke (2002) described that "the adjustment is not immediate throughout the depth of the whole layer, which is generated at the surface and diffuse upward. The layer of the surface whose properties have been affected by the new surface is called as an Internal boundary layer (IBL)". The depth of the internal boundary layer grows with the increasing distance from the starting point of this layer towards the wind direction. As illustrated in figure 3.6 the starting point of the IBL is known as "Leading edge" and the "distance from the leading edge to the downwind direction" known as the "Fetch" (Oke,2002).

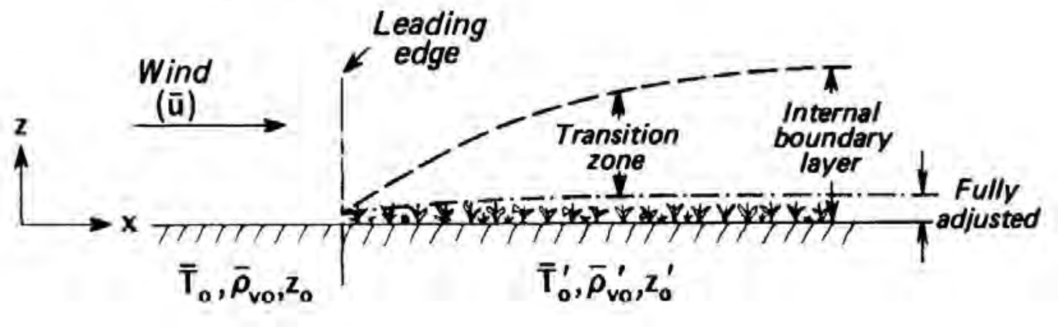

Figure 3.6: The development of an internal boundary layer as air flows from a smooth, hot, dry, bare soil surface to a rougher cooler and more moist vegetation surface (Oke,2002).

Only lower 10% of the new IBL are fully adjusted to the properties of the new surface. The rest of the layer is modified by the new surface but not adjusted to it and is in a transition zone. The properties of the air above the IBL are not determined by the surface immediately below it but with the upwind influences. To illustrate the advection, we may consider air flowing from a dry bare soil surface to a fully moist low vegetation cover. If no major across flow is assumed vertical and along wind (z and x direction) could be analyzed conveniently (figure 3.6). The rate of horizontal moisture transport, A ($kgm^{-2}s^{-1}$) is:

$$A = up_v$$

Where $p_v = vapour\ cotent\ (kgm^{-3}), u = air\ speed\ (m^{-1})$

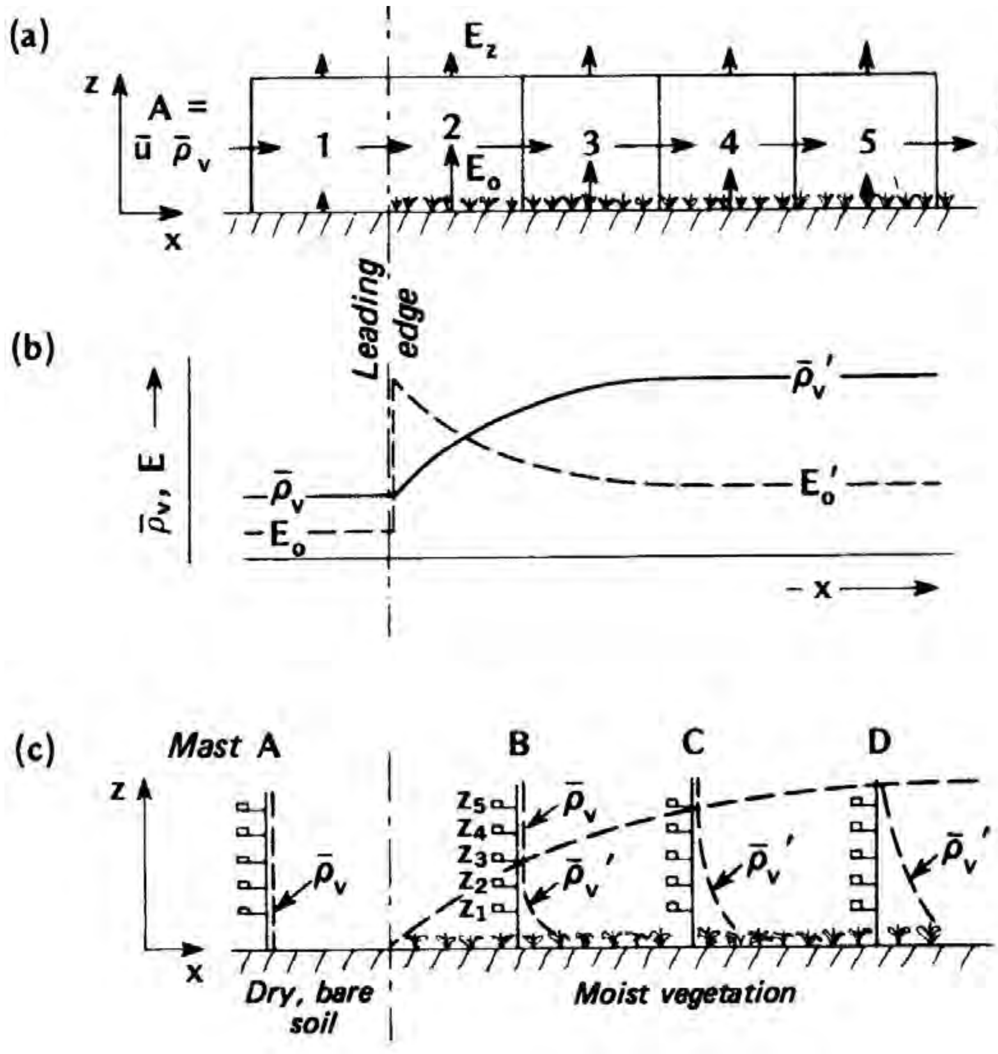

Figure 3.7: Moisture advection from a dry to a wet surface, (a) Evaporation rates and the vapour balance of a surface air layer (fluxes of vapour are proportional to the length of the arrows), (b) Surface evaporation rate (E_0), and mean water vapour concentration of the air layer, (c) Vertical profile of water vapour in relation to the developing boundary layer (Oke, 2002).

The vertical arrows represent the evaporation fluxes, and the horizontal arrows the advective fluxes. Leading-edge effects occur wherever there is a marked discontinuity in surface properties.

3.6.3 Oasis effect

In an arid region, an isolated moisture source always finds itself cooler than its surroundings due to evaporative cooling. The oasis in the desert is an obvious example of this effect known as "Oasis effect".

Due to its limited precipitation semi desert area can consume only small amount of radiant energy through evaporation from the precipitation, leaving a big portion of the radiant energy dissipated as sensible heat to warm the air, and thus exhibiting large Bowen ratio (β). On the other hand, free availability of water in the Oasis permits evaporations to exceed beyond precipitation by one order. To do this the energy needed for the evaporation is much more than the supplied radiant energy (here, Q_E is greater than Q^*). For this reason, in the Oasis sensible heat from the atmosphere contributed to the surface to accomplish exceeding evaporation. Thus, the Oasis is cooler than its surroundings, where it is embedded. In an example of an extreme case of "Oasis effect", the observed ratio $\frac{Q_E}{Q^*} = 2.5$ for shorter period over an irrigated cotton field. In the Oasis the reversal of Q_H due to continual air-to-oasis inversion temperature gradient exhibits negative Bowen ratio (β). The irrigated field of alfalfa near Phoenix, Arizona exhibits the 'oasis-effect' (Figure 3.7). it shows the average daily energy balance components in June following the irrigation in late May. For the first half of June an 'oasis effect' is clear; evapotranspiration exceeds the net radiation, and Q_H is directed towards the crop.

Many types of 'oasis-effect' advective situations can be found. Such as:

i. A cool, moist surface dominated by large-scale warmer, drier surroundings.
ii. A lake in an area with a dry summer climate;
iii. A glacier in a mountain valley;
iv. An isolated snow patch;
v. An urban park;
vi. An isolated tree in a street or on open, bare ground.

3.7 Advective Effects of Urban Wetland and Urban Green

"Several field studies of evaporation from irrigated fields surrounded by semi-arid areas report leading edge effects" (Rosenberg *et al*., 1983). For example, "several observational studies at Davis, CA (near the Sacramento site used here) focus on the case of a step change in moisture availability due to irrigation of grass set in the midst of drier fields" (e.g. Dyer and Crawford, 1965; Goltz and Pruitt,1970). In those studies, "the latent heat flux was estimated from both closure of the energy balance (Q^* and

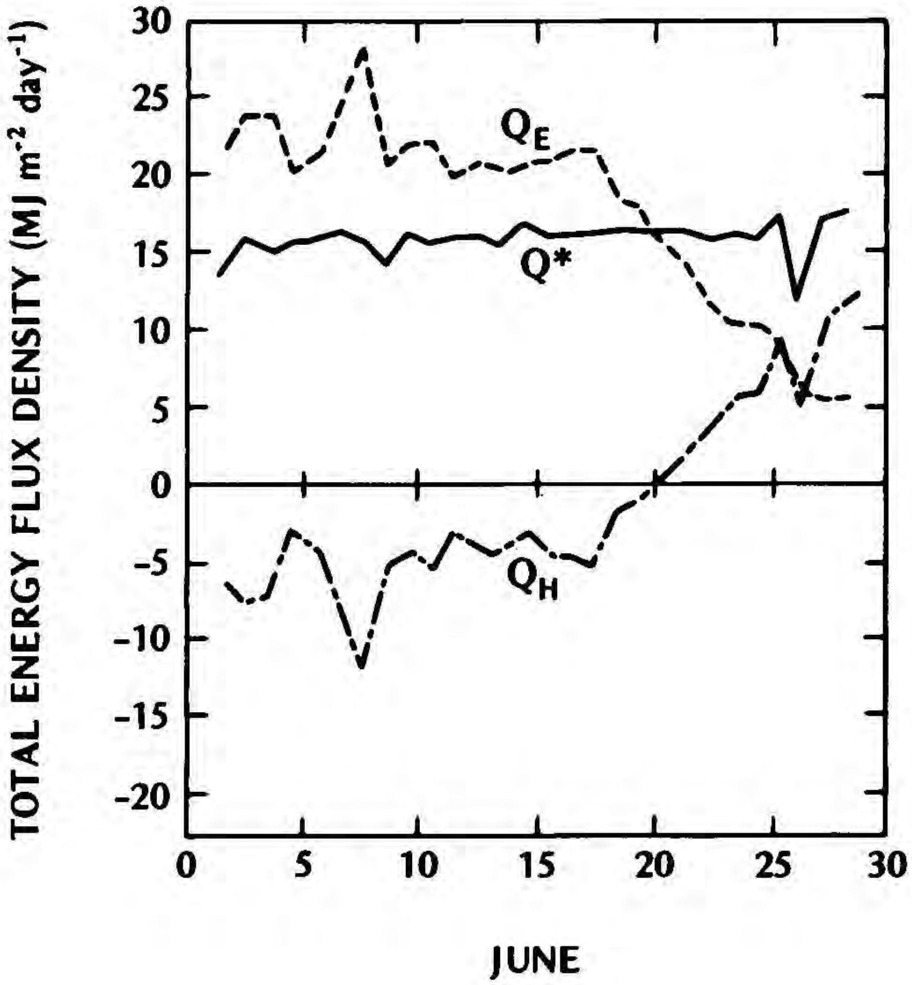

Figure 3.8: Average daily energy balance of an alfalfa crop in June 1964 near Phoenix, Arizona (33°N). The crop was irrigated by flooding in late May and this was followed by drought throughout June (van Bavel, 1967, Oke 2002).

Q_G were measured and Q_H was inferred from changes in a series of air temperature profiles downstream from the leading-edge) and lysimetry". Lang *et al.* (1974) "used lysimetry to study the influence of microscale advection on evaporation from an irrigated field of rice". Rider *et al.* (1963) "measured evaporation from irrigated grass downwind from a paved airport runway at Canberra airport in between 5cm to 150 cm height from the ground. All these studies show sharp increases in evaporation near the step change, followed by exponential decay with increasing fetch, until the surface layer fully adjusts to the new surface moisture, i.e. Q_E becomes approximately constant with distance. Estimates of the horizontal extent of leading edge effects vary widely; from less than 20 m" (Rider *et al.*, 1963) "to as great as 200 m" (Rijks, 1971). Increased evaporation can also occur due to Microscale advection in urban areas. Oke (1979) found "advectively-assisted evaporation over an irrigated suburban lawn in Vancouver, BC".

3.8 Advection of Urban Heat Island

Through Urban Heat Island Circulation (UHIC) rural cool air advected to the urban area during late evening and hence increase cooling rate. Eugensson et al. (1998) described three phases of urban heat island development due to this advection of rural cool air: phase one, differential cooling: differential cooling rate after the sunset in urban and rural area increase the UHI rapidly before the UHIC starts. Phase two, transition: "at the beginning of the second phase, the wind speed slowly increases because of the UHIC and entrainment of the rural cooler air increases the urban cooling rate". After 2-3 hour into the sunset the UHIC is fully developed and the level of advected energy Q_A becomes more stable. Phase three, stabilization: in this final phase, the two cooling rates together with UHI, wind speed and wind direction become stable which last till morning. The UHI and UHIC are dynamic systems pulsating horizontally throughout the night. This is a self-regulating system that requires a $\Delta T_{u-r} \approx 2°C$ to maintain the UHIC (calculated for the whole city).

3.9 Thermal Comfort Zone in The Dhaka City

One of the major objectives of the creation of "Urban Cooling Island" is to create coolth and transport it inside the urban fabric to achieve thermally desirable environment in the urban spaces. Thermal comfort in urban spaces is essential for the liveability of the urban spaces in a city, which depends on the number of environmental variables such as air temperature, radiant temperature, relative humidity and airflow. Through field investigation Ahmed (1995) established the comfort criteria for the outdoor urban spaces of the warm-humid city like Dhaka. The following criteria for outdoor comfort in the urban spaces of Dhaka were summarized from his work:

a. "Under still air conditions, at an average relative humidity of 70% the range of comfort air temperature for people with commonly worn summer clothing and engaged in sedentary activities or stationary in between 28.5°C to 32°C".
b. "Air flow in urban spaces could push the maximum limit of comfort temperature up to 34°C. Airflow also pushes up the upper boundary of acceptable relative humidity. For example, with air flow above 2m/sec the level of humidity for comfort was found to be extended up to 95%".
c. "Shading in urban spaces by any means is most essential for thermal comfort particularly in between 10:30 to 15:30 hours".
d. "To design outdoor spaces for long stay comfort temperature range can swing of ±3°K around the mean, but for the short stay or transient spaces it should be of ±1°K".

   One of the most important implication of the above comfort criterion with respect Dhaka city is that for an ideal configuration of urban outdoor spaces should be aligned with a wind corridor, ensured through judicious urban design, while optimally shaded by built-form or trees. Trees could provide double benefit by evapotranspiration besides direct solar shielding. The thermal effect of such urban spaces could be further enhanced if the air coming through wind corridor is from a shaded wetland, which pre-cool the air by exchanging latent heat of evaporation.

3.10 REFERENCES

1. Asadi F. and Kazemzadeh M. (2012). *"Ancient Refrigerator (Earth Architecture): A Sustainable Solution to Desert Architecture in Iran—Case Study in Kerman"*. ICSDEC 2012: pp. 260-267. doi: 10.1061/9780784412688.031.
2. Ahmed K S. 1995. "*Approaches to Bioclimatic Urban Design for the tropics with special reference to Dhaka, Bangladesh*". Ph.D. thesis, Environment and Energy studies Programme, Architectural Association School of Architecture, London.
3. Bowler D.E., Mant R., Orr H., Hannah D. M. and Pullin A.S. (2012). "*What are the effects of wooded riparian zones on stream temperature*?" Environmental Evidence, 1:3.
4. Dyer A.J., Crawford T.V. 1965. "*Observations of the microclimate at a leading edge"*. Quarterly Journal of the Royal Meteorological Society **91**: 345–348.
5. Ficklin D.L., Stewart I.T., and Maurer E.P. (2013). "*Effects of climate change on stream temperature, dissolved oxygen, and sediment concentration in the Sierra Nevada in California*." Water Resources Research, Vol. 49, 2765–2782, doi:10.1002/wrcr.20248.
6. Goltz S.M., Pruitt W.O. 1970. "*Spatial and Temporal Variations of Evapotranspiration Downwind from the Leading Edge of a Dry Fallow Field"*. Div. Technical Report ECOM68-G10-1, Department of Water Science and Engineering, University of California at Davis.
7. Haeger-Eugensson M. and Holmer B. (1999). "*Advection caused by the urban heat island circulation as a regulating factor on the nocturnal urban heat island*". Int. J. Climatology. **19**: 975–988.
8. Hollaender A. (1956). "*Radiation Biology*". Vol 1-3. McGraw-Hill, New York. Matthews, J. and Walker, R. L. 1970. Mathematical methods of physics. Addison-Wesley Publishing Company, Inc. New York
9. Halliday, D. and R. Resnick. 1988. "*Fundamentals of physics*". 3rd ed. John Wiley & Sons Inc., New York.
10. Johnson M. F., and Wilby R. L. (2015). "*Seeing the landscape for the trees: Metrics to guide riparian shade management in river catchments*." Water Resources Research, 51, 3754–3769, doi:10.1002/2014WR016802.
11. Knowles R. L. and Berry R. D (1980). "*Solar Envelope Concepts: Moderate Density Building Applications: Final Report*". Solar Energy Information Data Bank (U.S.), Solar Energy Research Institute.
12. Lang ARG, Evans GN, Ho PY. 1974. "*The influence of local advection on evapotranspiration from irrigated rice in a semi-arid region"*. Agricultural Meteorology **13**: 5–13.
13. Larson L. L. and Larson S. L. (1996). "*Riparian Shade and Stream Temperature: A Perspective*." Rangelands, Vol. 18, No. 4, pp. 149-152.
14. Matthews J. and Walker R.L. 1970. "*Mathematical methods of physics"*. Addison-Wesley Publishing Company, Inc. New York.
15. Oke, T.R. (2002). "*Boundary layer climates"*. 2nd edition. Routledge, Taylor and Francis Group.
16. Oke TR. 1979. "*Advectively-assisted evapotranspiration from irrigated urban vegetation"*. Boundary-Layer Meteorology **17**: 167–173.
17. Rutherford J. C., Blackett S., Blackett C., Saito L., Colley R.J.D (1997). "*Predicting the effects of shade on water temperature in small streams*." New Zealand Journal of Marine and Freshwater Research, 1997, Vol. 31: 707-721.
18. Rutherford J. C., Marsh N.A., Davies P.M. and Bunn S.E. (2004). "*Effect of patchy shade on stream water temperature: how quickly do small streams heat and cool*." Marine and fresh water research, 55, 737-748.

19. Rider N.E, Philip J.R., Bradley E.F. (1963). "*The horizontal transport of heat and moisture-a micrometeorological study"*. Quarterly Journal of the Royal Meteorological Society **89**: 507–531.
20. Rijks DA. 1971. "*Water use by irrigated cotton in Sudan: III. Bowen ratios and advective energy"*. Journal of Applied Ecology **8**: 643–663.
21. *"Riparian areas: functions and strategies for management"*. (2002). Washington, D.C.: National Academy Press.
22. Rosenberg NJ, Blad BL, Verma SB. 1983. "*Microclimate—the Biological Environment"*. John Wiley and Sons: New York.
23. Satterlund, D. R. and P. W. Adams. 1992. "*Wildland watershed management"*. 2nd ed. John Wiley & Sons inc. New York.
24. Sellers, W. D. 1974. "*Physical Climatology"*. University of Chicago Press. Chicago, Ill.
25. Sweeney B. W. and Newbold J. D. (2014). "*Streamside forest buffer width needed to protect stream water quality, habitat, and organisms: A literature review*." Journal of The American Water Resources Association, Vol. 50, No. 3.
26. Shahjahan A.T.M. and Ahmed K. S. "*Study of urban water bodies in view of potential for micro-climatic cooling and natural purification of waste water*" in the book " Balanced Urban Development: Options and Strategies for Liveable Cities". Edited by: Basant Maheshwari, Vijay P. Singh and Bhadranie Thoradeniya. Springer International Publishing. The Netherlands. 2016
27. Spronken-smith R.A., Oke T.R. and Lowry W.P(2000). "*Advection and the surface energy balance across an irrigated urban park".* International Journal of Climatology. **20**: 1033–1047
28. Spronken-Smith R. A. & Oke T. R. (1998). "*The thermal regime of urban parks in two cities with different summer climates"*. International Journal of Remote Sensing, 19:11, 2085-2104, DOI:10.1080/014311698214884
29. Taleghani M., Tenpierik M., Dobbelsteen A.V.D., and Sailor D.J. (2014) "*Heat in courtyards: A validated and calibrated parametric study of heat mitigation strategies for urban courtyards in the Netherlands*." Solar Energy 103, 108–124. 2014.
30. Thayer School of Engineering at Dartmouth. (n.d.). Retrieved February 02, 2018, from https://thayer.dartmouth.edu/
31. Whitaker K., Rogers K., Saintilan N., Mazumder D., Wen L., and Morrison R. J. (2015). "*Vegetation persistence and carbon storage: Implications for environmental water management for Phragmites australis*." Water Resour. Res., 51, 5284–5300, doi:10.1002/2014WR016253.

Chapter 4 : REMOTE SENSING OF URBAN COOLING ISLAND

4.1 Introduction

Remote sensing technique can capture the data of large area with high spatial resolution at a time, which is very useful for urban meteorological and land cover analysis. Through the remote sensing methodology, the existence and intensity of potential Urban Cooling Island (UCI) formed by the wetland had been identified. Spatial information on the land cover and Land Surface Temperature (LST) were extracted using Landsat - a collection of space-based moderate-resolution land remote sensing data, which is a joint initiative between the U.S. Geological Survey (USGS) and NASA. One of the reasons to choose Landsat satellite data is because this program is the longest-serving earth observing satellites. That’s the reason Landsat data is extremely valuable to grasp the long-time urban thermal environmental change besides observing urban land cover change. Data from the Landsat-5 and Landsat-8 of selected dates were downloaded and processed to find the Normalized Difference Vegetation Index (NDVI), Normalized Difference Built-up Index (NDBI), Normalized Difference Water Index (NDWI), Modified NDWI (MNDWI), Soil Adjusted Vegetation Index (SAVI) and Index-based Built-up Index (IBI) and finally Land Surface Temperature (LST). Using ArcGIS 10.2.1 software, at first, the Landsat images were atmospherically corrected and the NDVI was calculated. Land Surface Temperature was then extracted using several equations in a couple of steps explained in various remote sensing literature. The first date was 12 December 1991, that was chosen for remote sensing to correspond with the first urban heat island study in Dhaka conducted by Bangladesh meteorological department at winter and summer season of 1992.

Albedo for two dates in a span of 25 years were also calculated for the Dhaka city. Albedo is an important property of the Earth surface heat budget which is the average reflectance of the sun’s spectrum. This unitless quantity has values ranging from 0 to 1.0 and will vary based on the land cover. For example, snow would have a high value and coniferous forests a low value. Water also have very low albedo and absorbs lots of heat. Weng (2003) observed the relation between UHI_{surf} and the Fractal dimensions by deriving transect of the urban area form the LST of Summer and springtime. In the calculated Normalized difference vegetation index (NDVI) from Landsat data, a threshold NDVI of 0.35 was applied to all NDVI images to distinguish large canopy trees from non-vegetated surfaces. Because many studies revealed that above 0.35, NDVI is agreed to have a strong correlation to photosynthetic activity and plant evapotranspiration (Mackey C. et al, 2012 and Hung T. et al, 2006).

4.2 Landsat Data

The band from Landsat-8 data that had been used in this study were Band 2 (Blue), Band3 (Green), Band4 (Red), Band5 (NIR), Band 6 (SWIR-1), Band 7 (SWIR-2) and Band 10 (TIR-1). From Landsat-5, the band used were Band 1 (Blue), Band 2 (Green), Band 3 (Red), Band 4 (NIR), Band 6 (TIR)

Table 4.1: List of Bands available in Landsat-7 ETM+ and Landsat-8 OLI and TIRS (source: Landsat Science Data Users Handbook)

Landsat-7 ETM+ Bands (µm)			Landsat-8 OLI and *TIRS* Bands (µm)		
			30 m Coastal/Aerosol	0.435 - 0.451	Band 1
Band 1	30 m Blue	0.441 - 0.514	30 m Blue	0.452 - 0.512	Band 2
Band 2	30 m Green	0.519 - 0.601	30 m Green	0.533 - 0.590	Band 3
Band 3	30 m Red	0.631 - 0.692	30 m Red	0.636 - 0.673	Band 4
Band 4	30 m NIR	0.772 - 0.898	30 m NIR	0.851 - 0.879	Band 5
Band 5	30 m SWIR-1	1.547 - 1.749	30 m SWIR-1	1.566 - 1.651	Band 6
Band 6	60 m TIR	10.31 - 12.36	*100 m TIR-1*	*10.60 – 11.19*	Band 10
			100 m TIR-2	*11.50 – 12.51*	Band 11
Band 7	30 m SWIR-2	2.064 - 2.345	30 m SWIR-2	2.107 - 2.294	Band 7
Band 8	15 m Pan	0.515 - 0.896	15 m Pan	0.503 - 0.676	Band 8
			30 m Cirrus	1.363 - 1.384	Band 9

4.3 Extracting Albedo from Landsat Data

The Landsat Thematic Mapper (TM) and Enhanced Thematic Mapper Plus (ETM+) sensors capture reflected solar energy, convert these data to radiance, then rescale this data into an 8-bit digital number (DN) with a range between 0 and 255. It is possible to manually convert these DNs to ToA Reflectance using a two-step process. The first step is to convert the DNs to radiance values using the bias and gain values specific to the individual scene you. The second step converts the radiance data to ToA reflectance. The Landsat 8 OLI sensor is more sensitive, so these data are rescaled into 16-bit DNs with a range from 0 and 65536. Also, these data had been converted to reflectance, rather than radiance, so DNs can be manually converted to Reflectance in a single step. The input to the albedo calculation was a Landsat image that had been converted from digital numbers to Top of Atmosphere (TOA) reflectance.

OLI Top of Atmosphere Reflectance:

Like the conversion to radiance, the 16-bit integer values in the level 1 product can also be converted to Top of Atmosphere (TOA) reflectance. The following equation was used to convert level 1 DN values to TOA reflectance:

$$\rho\lambda' = M_{\rho} * \mathrm{Q_{cal}} + A_{\rho}$$

where:
ρλ' = Top-of-Atmosphere Planetary Spectral Reflectance, without correction for the solar angle. (Unitless)
M_{ρ} = Reflectance multiplicative scaling factor for the band (REFLECTANCE_MULT_BAND_n from the metadata).
A_{ρ}= Reflectance additive scaling factor for the band (REFLECTANCE_ADD_BAND_N from the metadata).
Qcal = Level 1-pixel value in DN

Correction for the solar elevation angle:

Equation for corrected TOA Reflectance was:

$$\rho_{\lambda} = \frac{\rho'_{\lambda}}{sin\theta}$$

Liang (2000) developed a series of algorithms for calculating albedo from various satellite sensors. His Landsat formula to calculate Landsat shortwave albedo was normalized by Smith (2010) and is presented below.

$$\alpha_{short} = \frac{0.356\rho_1 + 0.130\rho_3 + 0.373\rho_4 + 0.085\rho_5 + 0.072\rho_7 - 0.0018}{0.356 + 0.130 + 0.373 + 0.085 + 0.072}$$

This formula had been implemented in ArcMap using Band Math as:

((0.356*B1) + (0.130*B2) + (0.373*B3) + (0.085*B4) + (0.072*B5) -0.018) / 1.016

Determining NDVI, NDBI, NDWI, MNDWI, SAVI and IBI:

Normalized Difference Vegetation Index (NDVI) is expressed as follows (Purevdorj et al., 1998)

$$NDVI = \frac{NIR - RED}{NIR + RED}$$

Normalized Difference Built-up Index (NDBI) is expressed as follows (Zha et al., 2003)

$$NDBI = \frac{SWIR - NIR}{SWIR + NIR}$$

Normalized Difference Water Index (NDWI) is expressed as follows (McFeeters 1996):

$$NDWI = \frac{GREEN - NIR}{GREEN + NIR}$$

Modified NDWI (MNDWI) can be expressed as follows (Hanqiu Xu 2006):

$$MNDWI = \frac{GREEN - SWIR1}{GREEN + SWIR1}$$

Soil Adjusted Vegetation Index (SAVI) can be expressed as follows (H. XU,2008)

$$SAVI = \frac{(NIR - RED)(1 + l)}{(NIR + RED + l)}$$

Index-based Built-up Index (IBI) can be expressed as follows (H. XU,2008)

$$IBI = \frac{[NDBI - \frac{(SAVI + MNDWI)}{2}]}{[NDBI + \frac{(SAVI + MNDWI)}{2}]}$$

When the NDVI is used instead of the SAVI, the IBI can be rewritten:

$$IBI = \frac{\frac{2MIR}{MIR + NIR} - [\frac{NIR}{NIR + RED} + \frac{GREEN}{GREEN + MIR}]}{\frac{2MIR}{MIR + NIR} + [\frac{NIR}{NIR + RED} + \frac{GREEN}{GREEN + MIR}]}$$

4.4 Determining Land Surface Temperature from Landsat 8

Step 1: Conversion to spectral radiance

$$L_\lambda = M_L Q_{cal} + A_L$$

Where:
L_λ = Spectral radiance (W/ (m2 * sr * µm))
M_L = Radiance multiplicative scaling factor for the band (RADIANCE_MULT_BAND_n from the metadata).
A_L = Radiance additive scaling factor for the band (RADIANCE_ADD_BAND_n from the metadata).
Qcal = Level 1-pixel value in DN

Step 2: TIRS Top of Atmosphere Brightness Temperature

Temperature at satellite

$$T = \frac{K_2}{\ln\left(\frac{K_1}{L_\lambda} + 1\right)}$$

where:

T = Top of Atmosphere Brightness Temperature, in Kelvin.
L_λ = Spectral radiance (Watts/(m2 * sr * µm))
K1 = Thermal conversion constant for the band (K1_CONSTANT_BAND_n from the metadata)
K2 = Thermal conversion constant for the band (K2_CONSTANT_BAND_n from the metadata)

Step 3: Deriving Land Surface Emissivity

(Jose´ A. Sobrino, Juan C. Jimenez-Munoz, 2004)

$$\varepsilon = 0.004P_v + 00.986$$

(Carlson & Ripley, 1997)

$$P_v = \left(\frac{NDVI - NDVI_{min}}{NDVI_{max} - NDVI_{min}}\right)^2$$

where,
P_v = Proportion of Vegetation
ε = Land Surface Emissivity (LSE)

Step 4: Deriving Land Surface Temperature

Land Surface Temperature (LST) (Weng, Lu, & Schubring, 2004)

$$LST = \frac{T}{1 + \left(\lambda \times \frac{T}{\rho}\right) \times \ln(\varepsilon)}$$

Where:

λ = wavelength of emitted radiance (for which the peak response and the average of the limiting wavelengths (λ= 11.5 µm) (Markham & Barker, 1985) will be used),

$\rho = h \times \frac{c}{\sigma}$ (1.438×10^{-2} m K)
σ = Boltzmann constant (1.38 × 10^{-23} J/K),
h = Planck's constant (6.626×10^{-34} J s),
and
c = velocity of light (2.998×10^{8} m/s).

Table 4.2: Landsat 4-5 Thematic Mapper (TM) and Landsat 7 Enhanced Thematic Mapper Plus (ETM+) (source: Landsat Science Data Users Handbook)

Band	Wavelength	Useful for mapping
Band 1 - blue	0.45 - 0.52	Bathymetric mapping, distinguishing soil from vegetation and deciduous from coniferous vegetation
Band 2 - green	0.52 - 0.60	Emphasizes peak vegetation, which is useful for assessing plant vigor
Band 3 - red	0.63 - 0.69	Discriminates vegetation slopes
Band 4 - Near Infrared	0.77 - 0.90	Emphasizes biomass content and shorelines
Band 5 - Short-wave Infrared	1.55 - 1.75	Discriminates moisture content of soil and vegetation; penetrates thin clouds
Band 6 - Thermal Infrared	10.40 - 12.50	Thermal mapping and estimated soil moisture
Band 7 - Short-wave Infrared	2.09 - 2.35	Hydrothermally altered rocks associated with mineral deposits
Band 8 - Panchromatic (Landsat 7 only)	0.52 - 0.90	15-meter resolution, sharper image definition

4.5 Land Surface Temperature Retrieval from Landsat Tm 5

The following equation was used to convert DN's in a 1G product back to radiance units:

$$L_\lambda = \left(\frac{(LMAX_\lambda - LMIN_\lambda)}{(QCALMAX - QCALMIN)}\right) \times (QCAL - QCALMIN) + LMIN_\lambda$$

QCAL = the quantized calibrated pixel value in DN
$LMIN_\lambda$ = the spectral radiance that is scaled to QCALMIN in watts/(meter squared * ster * µm)
$LMAX_\lambda$ = the spectral radiance that is scaled to QCALMAX in watts/(meter squared * ster * µm)
QCALMIN = the minimum quantized calibrated pixel value (corresponding to $LMIN\lambda$) in DN
= 1 for LPGS products
= 1 for NLAPS products processed after 4/4/2004
= 0 for NLAPS products processed before 4/5/2004
QCALMAX = the maximum quantized calibrated pixel value (corresponding to $LMAX\lambda$) in DN = 255

<u>Radiance to Reflectance:</u>

For relatively clear Landsat scenes, a reduction in between-scene variability could be achieved through a normalization for solar irradiance by converting spectral radiance, as calculated above, to planetary reflectance or albedo. This combined surface and atmospheric reflectance of the Earth is computed with the following formula:

$$\rho_P = \frac{\pi \times L_\lambda \times d^2}{ESUN_\lambda \times \cos\theta_s}$$

Where:
ρ_P = Unitless planetary reflectance
L_λ = Spectral radiance at the sensor's aperture
d = Earth-Sun distance in astronomical units from an Excel file or interpolated from values listed in Table 4.4
$ESUN_\lambda$ = Mean solar exoatmospheric irradiances from Table 4.3
θ_s = Solar zenith angle in degrees [cos (Solar zenith angle) = sin (Sun_Elevation)]

Table 4.3: ETM+ Solar Spectral Irradiances

ETM+ Solar Spectral Irradiances (generated using the ChKur* solar spectrum)	
Band	watts/(meter squared * µm)
1	1970
2	1842
3	1547
4	1044
5	225.7
7	82.06
8	1369

*ChKur is the combined Chance-Kurucz Solar Spectrum within MODTRAN 5 (2011, Berk, A., Anderson, G.P., Acharya, P.K., Shettler, E.P., MODTRAN 5.2.0.0 User's Manual, available http://modtran5.com)

Table 4.4: Earth-Sun Distance in Astronomical Units

Earth-Sun Distance in Astronomical Units									
Day of Year	Distance	Day of Year	Distance	Day of Year	Distance	Day of Year	Distance	Day of Year	Distance
1	.98331	74	.99446	152	1.01403	227	1.01281	305	.99253
15	.98365	91	.99926	166	1.01577	242	1.00969	319	.98916
32	.98536	106	1.00353	182	1.01667	258	1.00566	335	.98608
46	.98774	121	1.00756	196	1.01646	274	1.00119	349	.98426
60	.99084	135	1.01087	213	1.01497	288	.99718	365	.98333

Band 6 Conversion to Temperature:

$$T = \frac{K_2}{\ln\left(\frac{K_1}{L_\lambda} + 1\right)}$$

Where:
T = Effective at-satellite temperature in Kelvin

K2 = Calibration constant 2 from Table 11.5
K1 = Calibration constant 1 from Table 11.5
L = Spectral radiance in watts/ (meter squared * ster * µm)

Table 4.5: ETM+ and TM Thermal Band Calibration Constants

ETM+ and TM Thermal Band Calibration Constants		
	Constant 1- **K1** watts/(meter squared * ster * µm)	Constant 2 - **K2** Kelvin
Landsat 7	666.09	1282.71
Landsat 5	607.76	1260.56

Once the Landsat data was processed following the above steps, LST of selected points in both the wetland area, including the points (Urban Stations) of continuous data logging were extracted from the LST map, for correlational analysis. Two sets of points were selected for both the wetlands to extract LST data, the first set were at the Upwind side of the wetland and second set of points were at the Down-wind side of the wetland based on the wind direction during Hot-Dry and Warm-Humid season in the urban area Dhaka. All the points chosen were nearer to 100m apart from each other to avoid the possibilities of them being into the same pixel, as the Landsat TIR image (Band 10 and 11 in case of Landsat 8) has a 100m resolution. Band 10 and 11 later resampled to 30m. Distance from those points to the edge of the wetlands were measured. Then Correlational analysis between the distance and LST were done using both Microsoft Excel and R programing language in R studio.

4.6 Analysis of Normalized Difference Vegetation Index

Figure 4.1. NDVI showing 500m buffer area of both the lake

Table 4.6. Percentage of vegetation based on the NDVI of Dhanmondi Lake.

Land Use	AREA (sqm)	Percentage (%)
other	7,200.00	0.20
Water	18,000.00	0.50
Vegetation small canopy	2,934,000.00	81.97
Vegetation Large canopy	620,100.00	17.32
Total area	3,579,300.00	
Total area (ha)	357.93	
Total area (sqkm)	3.58	

Table 4.7. Percentage of vegetation based on the NDVI of Hatirjheel Lake.

Land Use	AREA (sqm)	Percentage (%)
other	8,100.00	0.20
Water	547,200.00	13.30
Vegetation small canopy	3,339,000.00	81.15
Vegetation Large canopy	220,500.00	5.36
Total area	4,114,800.00	
Total area (ha)	411.48	
Total area (sqkm)	4.11	

The data of table 4.6 and 4.7 extracted from NDVI in figure 4.1 shows that in case of Dhanmondi lake, the area covered by vegetation canopy in the buffer zone is Higher (99.30%) than the Hatirjheel lake (86.51%). Moreover, large tree canopy cover is much higher in the buffer zone of Dhanmondi lake than the Hatirjheel lake. Also, in case of Dhanmondi lake, only 0.50% is exposed water in the buffer zone whereas in case of Hatirjheel lake it is 13.30%. All those analyses clearly indicate the higher riparian shading potential of the Dhanmondi lake than the other lake.

Change of Large Canopy Vegetation and water area:

In case of Dhanmondi lake large vegetation showing NDVI above 0.35 decreased almost half within a span of 25 years, whereas water area increased due to the lake development project (table 4.8).

Table 4.8: Dhanmondi Lake

Land scape category	Percentage_16DEC16	Percentage_91DEC12
Vegetation Large canopy	4.98	10.08
Water Area	9.68	6.11

In case of Hatirjheel lake large vegetation- showing NDVI above 0.35 decreased almost seven-fold within a 25 years' time span. The water area also decreased as a part of new development (table 4.9).

Table 4.9: Hatirjheel Lake

Landscape category	Percentage_16DEC16	Percentage_91DEC12
Vegetation Large canopy	0.74	5.51
Water Area	21.52	29.66

Change of Albedo:

The calculated albedo difference in between 12 December 1991 and 16 December 2016 (Fig. 4.2) clearly demonstrate that buffer zone of both the wetland area showing minimal albedo increase, whereas the water surface of the lakes is showing maximum albedo increase.

4.7 Cool Spots in The Urban Area Due to Riparian Shading

Land surface temperature (LST) of eight dates had been derived from the Landsat data obtained from USGS and Nasa. The first date to derive LST was 12 Dec 1991 (figure 4.3) which was nearer and similar (typical winter day) to the date 3rd January 1992, when Bangladesh Meteorological Department (BMD) carried out field measurement at ten locations in the city to determine Urban Heat Island effect of Dhaka.

The other dates as shown in Figure 4.4 were chosen from the year 2015 to represent the typical day of the three seasons. As consistent with the studies of BMD Land Surface Temperature derived from the Landsat data (Fig.4.3) is also showing that Dhanmondi Lake area is cooler than the rest of the spots, which acts as a cool spot in all seasons of the year. Tejgaon area which is an industrial area located beside Hatirjheel Lake is warmer than Dhanmondi area despite the presence of water body due to the difference in Riparian shading (Fig.4.3 & 4.4). Also, topographical and shading by built-form are more prominent in Dhanmondi lake than Hatirjheel lake.

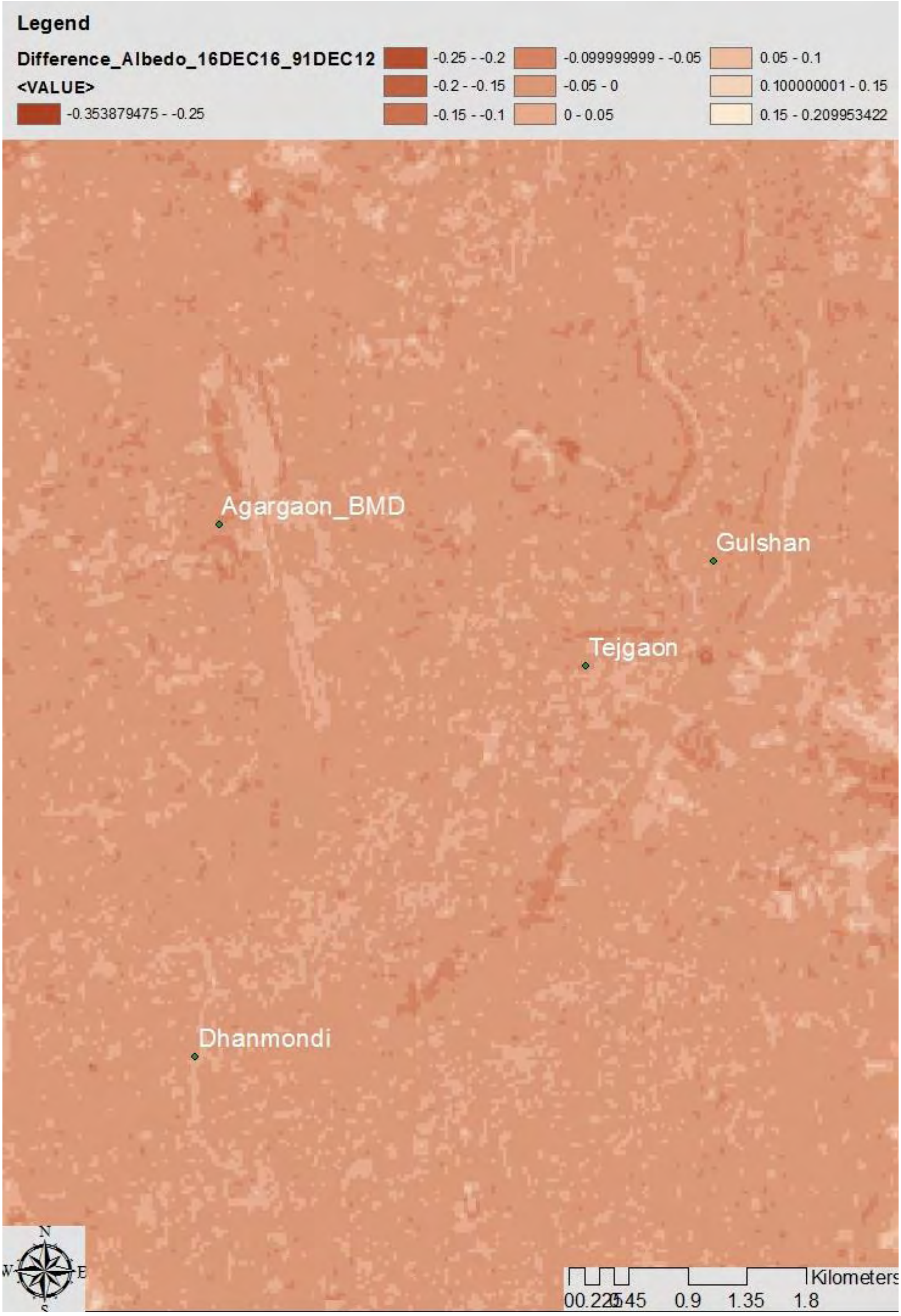

Figure 4.2: Change of Albedo within 25 years (map overlay is provided in the back of this thesis)

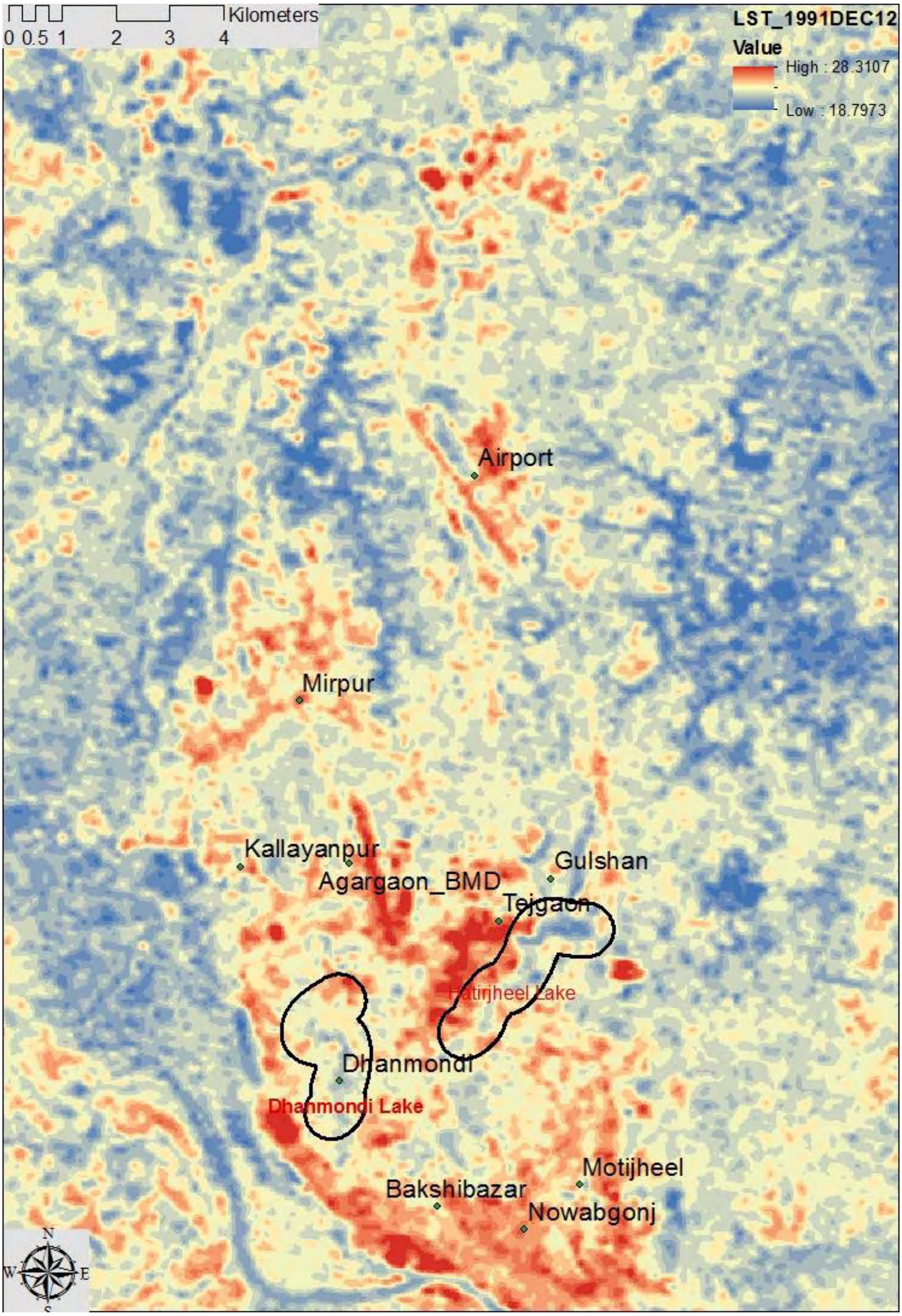

Figure 4.3: LST of Urban Dhaka12 Dec 1991 derived from Landsat data showing cool spots (map overlay is provided in the back of this thesis)

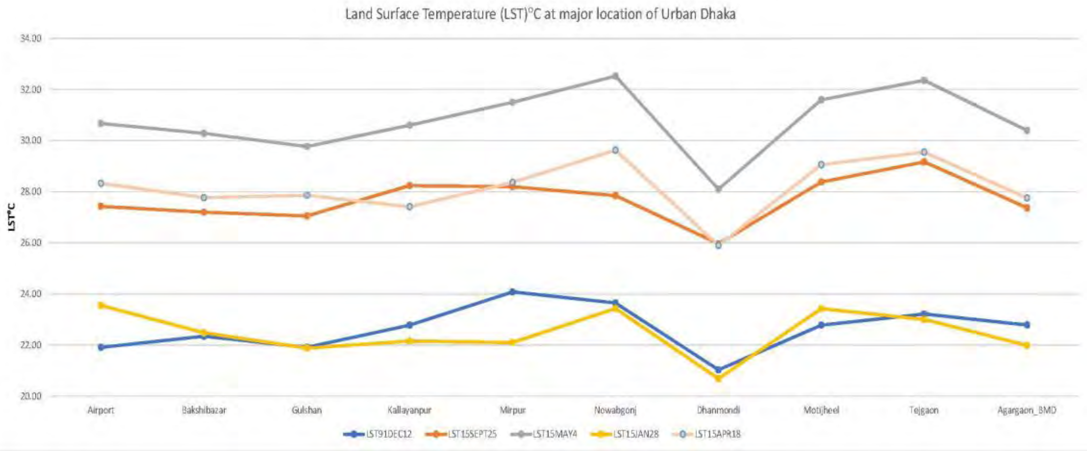

Figure 4.4: Comparison of Land Surface Temperature of different season of selected spots in Dhaka.

4.8 Relationship Between the LST and Distance from The Wetland in Different Season

Results of Correlational analysis between Land Surface Temperature (LST) at selected points and their distance from water edge for both the Dhanmondi and Hatirjheel for the selected dates (representing three seasons) of 2013 to 2017 are presented below. All the related data of this part of work are given in the Data Appendices A, B and C. in the attached computer disk with the thesis.

Land Surface Temperature 12 April 2013:

Extracted Land Surface Temperature is presented in the figure 4.5 and correlational analysis in the table 4.10

Wind flow and the cooling effect:

At this date and time, the predominant wind flow was from Southern side. The cooling effect from the lake was clearly carried towards the downwind side of both the lake through Advection process. Because the correlation between temperature at the urban station and their distance from the wetland along the line of wind direction was more at the downwind side than the upwind side.

Dhanmondi Lake:

The correlation between temperature at the urban station and their distance from the wetland along the line of wind direction was more at the downwind side than the upwind side. The cooling effect from the lake was clearly carried towards the downwind side of the lake through Advection process as the North and North-west area of the Dhanmondi lake area were surrounded by the part of the lake on its Southern side. The other part South and south-east didn’t have any part of the lake on its Southern side and hence the cooling effect of wetland was not carried through advection process to this area.

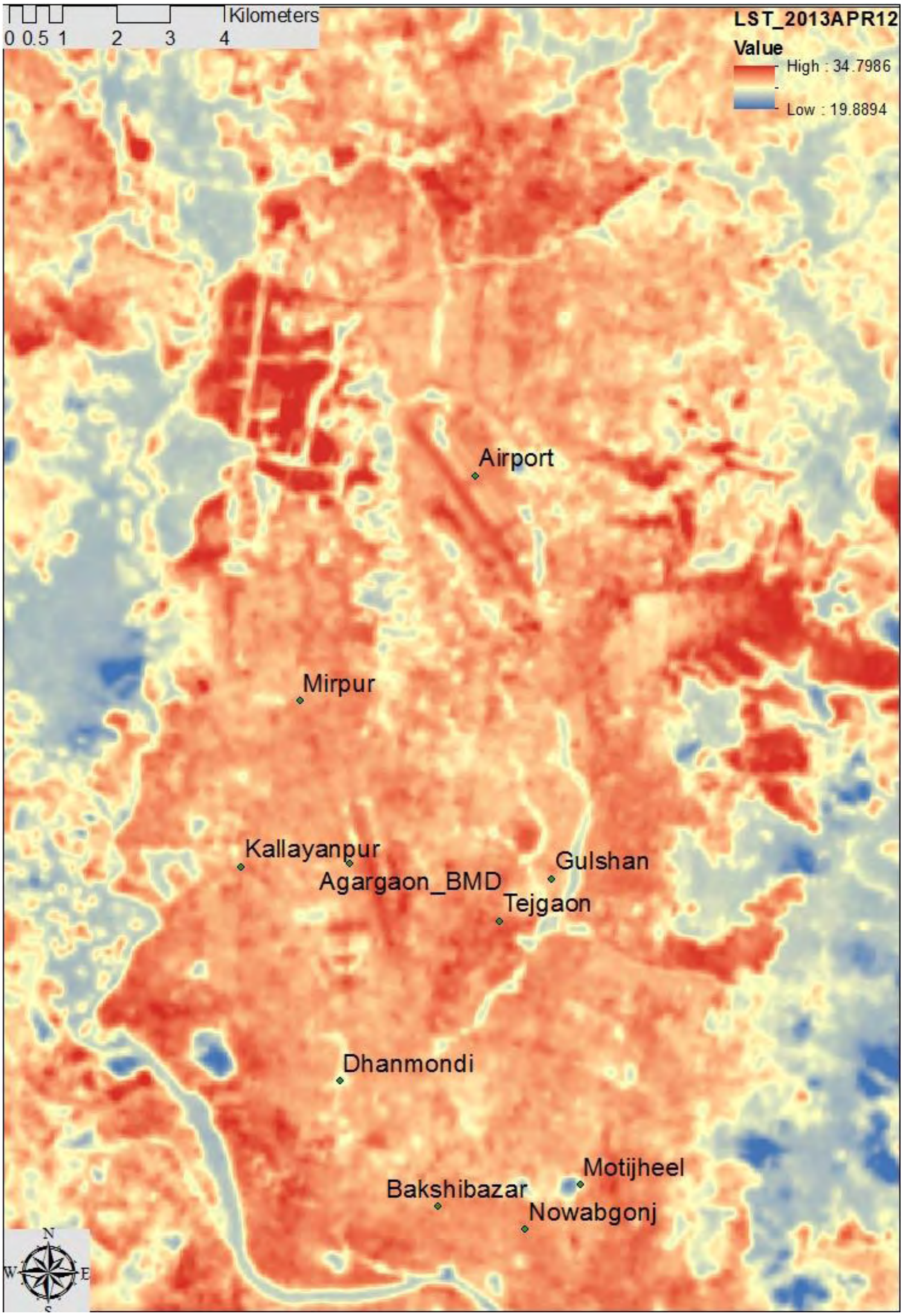

Figure 4.5: LST 12 April 2013(map overlay is provided in the back of this thesis)

Table 4.10: Correlation analysis between distance and LST on 12 April 2013

Wind Direction (WD) % {N=0 or 360, E=90, S=180, W=270}, WS means Wind Speed in m/s.

sl no	LST Date	HatirJheel_ N&NW area	HatirJheel_ S&SE area	Dhanmondi _ N&NW area	Dhanmondi _ S&SE area	WD 9am	WD 12pm	WS 9am	WS 12pm	Air Temp. 9am	Air Temp. 12pm
1	LST 12 April 2013	0.67	0.57	0.5	0.35	200	180	1.02	1.02	30.3	34.7

Hatirjheel Lake:

In case of the Hatirjheel lake, the correlation between temperature at the urban station and their distance from the wetland along the line of wind direction was slightly more at the downwind North and North-West area than the South and South-East area. In the absence of riparian shading, the lake was partly shaded by topographic shading (by the bank of the lake) due to low water level. Hence the chance of advective cooling of North and North-West area from the lake was not so great due to the minimal shading of lake water.

Land Surface Temperature 15 June 2013:

Extracted Land Surface Temperature is presented in the figure 4.6 and correlational analysis in the table 4.11

Wind flow and the cooling effect:

At this date and time, the predominant wind flow was from Eastern side.

Dhanmondi Lake:

The correlation between temperature at the urban station and their distance from the wetland along the line of wind direction was more at the downwind side than the upwind side. The cooling effect from the lake was clearly carried towards the downwind side of the lake through Advection process as the North and Northwest area of the Dhanmondi lake area were surrounded by the part of the lake on its East side. The other part South and south-east didn’t have any part of the lake on its East side and hence missed the cooling effect being carried through advection process.

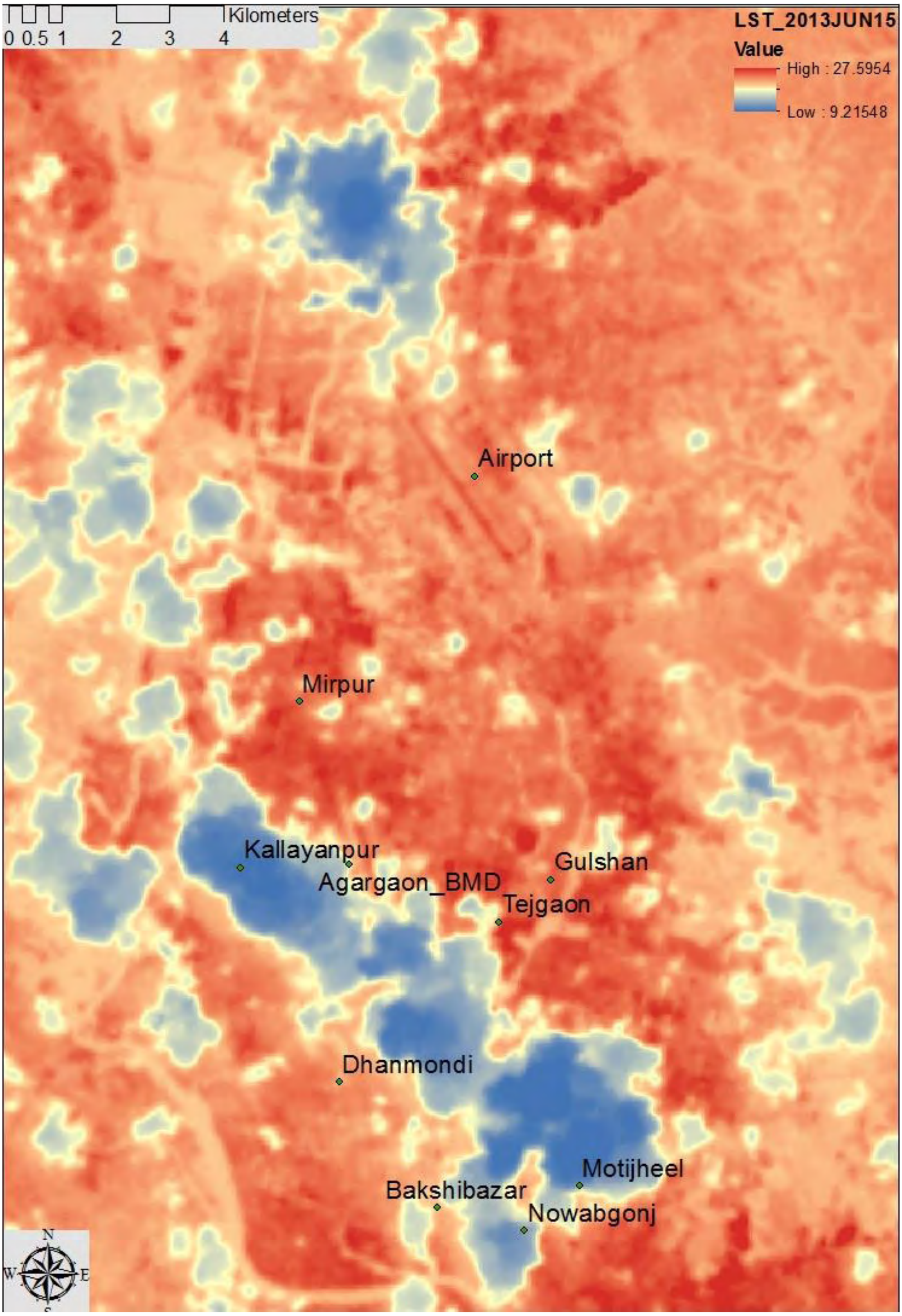

Figure 4.6: LST 15 JUNE 2013 (map overlay is provided in the back of this thesis)

Table 4.11: Correlation analysis between distance and LST on 15 June 2013

Wind Direction % {N=0 or 360, E=90, S=180, W=270}

sl no	*LST Date*	HatirJheel_ N&NW area	HatirJheel_ S&SE area	Dhanmondi _ N&NW area	Dhanmondi _ S&SE area	WD 9 am	WD 12 pm	WS 9 am	WS 12 pm	Air Temp. 9 am	Air Temp. 12 pm
1	LST 15JUNE2013	-0.46	0.50	0.26	0.18	90	90	1.02	1.02	29.80	33.40

Hatirjheel Lake:

In case of the Hatirjheel lake, the correlation between temperature at the urban station and their distance from the wetland along the line of wind direction was less at the downwind North and North-West area than the South and South-East area. Because due to the lack of riparian shading North and North-West area is getting warmer by the hot air flow from the lake. At that time of the season due to the high-water level for monsoon rain, the chance of topographic shading (by the bank of the lake) was also very low.

Land Surface Temperature 6 November 2013:

Extracted Land Surface Temperature is presented in the figure 4.7 and correlational analysis in the table 4.12.

Wind flow and the cooling effect:

At that date and time, the predominant wind flow was from North and North-east side.

Dhanmondi Lake:

The correlation between temperature at the urban station and their distance from the wetland along the line of wind direction was more at the downwind side than the upwind side. The cooling effect from the lake was clearly carried towards the downwind side of the lake through Advection process as the North and North-west area of the Dhanmondi lake area were also surrounded by the part of the lake on its North and East side. The other part South and south-east didn’t have any part of the lake on its East side and hence missed the cooling effect being carried through advection process.

Hatirjheel Lake:

In case of the Hatirjheel lake, the correlation between temperature at the urban station and their distance from the wetland along the line of wind direction was less at the downwind South and South-East area than the North and North-West area. Because due to the lack of riparian shading South and South-East area were getting warmer by the hot air flow from the lake. During this time of the season due to the high-water level for monsoon rain, the chance of topographic shading (by the bank of the lake) was also very low.

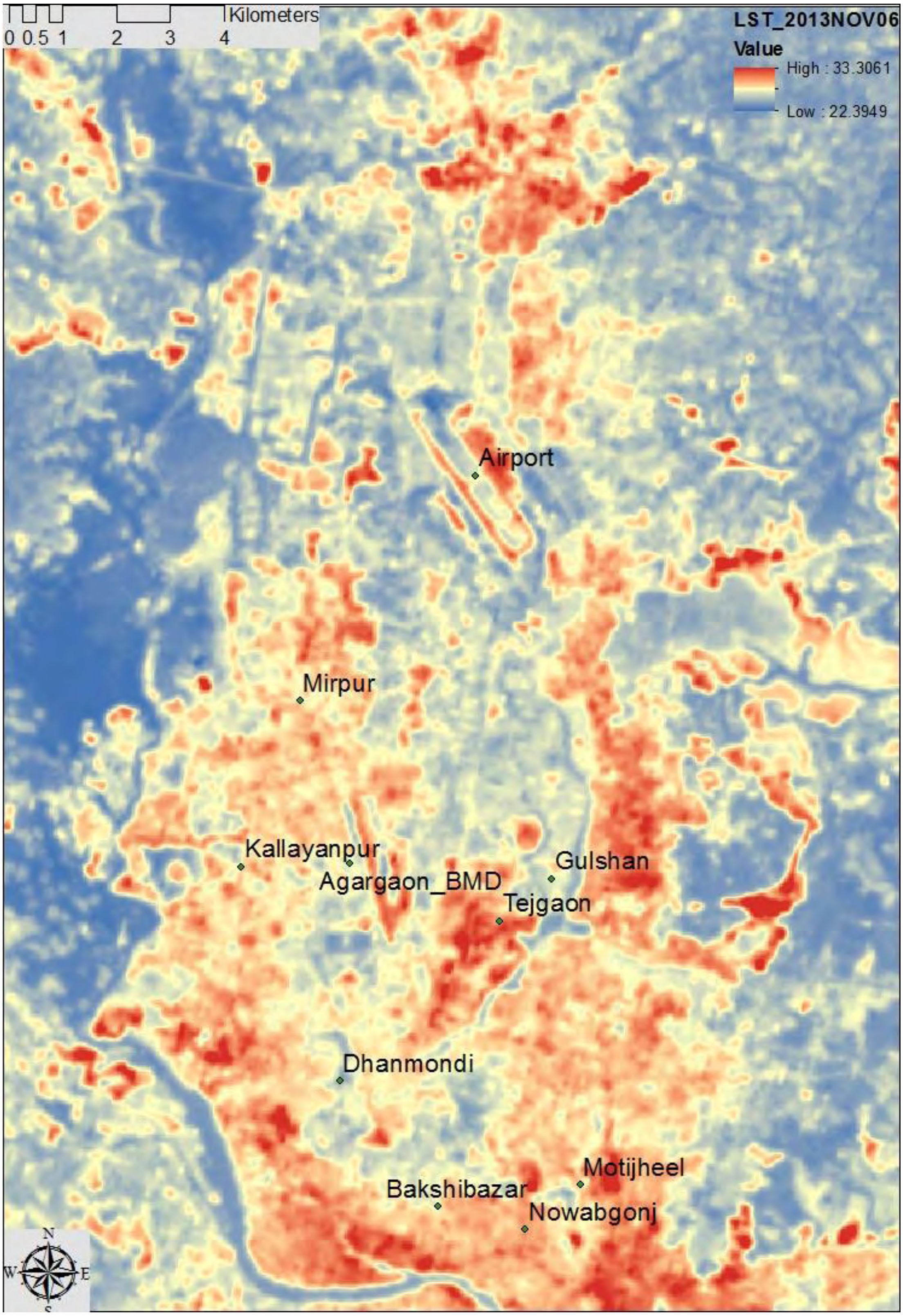

Figure 4.7: LST 6 NOV 2013 (map overlay is provided in the back of this thesis)

Table 4.12: Correlation analysis between distance and LST on 6 November 2013
Wind Direction % {N=0 or 360, E=90, S=180, W=270}

sl no	**LST Date**	Hatir Jheel _ N& NW area	Hatir Jheel _ S&SE area	Dhan mon di _ N& NW area	Dhan mon di _ S&SE area	WD 9 am	WD 12 pm	WS 9 am	WS 12 pm	Air Temp. 9 am	Air Temp. 12 pm
1	LST 6NOV2013	0.60	0.42	0.65	0.26	0	50	0	1.02	25.2	28.5

Land Surface Temperature 24 December 2013:

Extracted Land Surface Temperature is presented in the figure 4.8 and correlational analysis in the table 4.13.

Wind flow and the cooling effect:

At this date and time, the predominant wind flow was from Western side.

Dhanmondi Lake:

The correlation between temperature at the urban station and their distance from the wetland along the line of wind direction was more at the downwind side than the upwind side. The cooling effect from the lake was clearly carried towards the downwind side of the lake through Advection process because the South and South-East area of the Dhanmondi lake area was surrounded by the part of the lake on its Western side. The other part North and North-West area didn't have any part of the lake on its Western side and hence missed the cooling effect being carried through advection process.

Hatirjheel Lake:

In case of the Hatirjheel lake, the correlation between temperature at the urban station and their distance from the wetland along the line of wind direction was more at the downwind North and North-West area than the South and South-East area. Because North and North-West area was having part of the lake on its western side which the other area didn't have. Because of the lack of riparian shading, at that time of the season the topographic shading (by the bank of the lake) due to the low water level is the only option for the lake water to avoid direct solar radiation.

Table 4.13: Correlation analysis between distance and LST on 24 December 2013
Wind Direction % {N=0 or 360, E=90, S=180, W=270}

sl no	*LST Date*	HatirJheel_ N&NW area	HatirJheel_ S&SE area	Dhanmondi_ N&NW area	Dhanmondi _ S&SE area	WD 9 am	WD 12 pm	WS 9 am	WS 12 pm	Air Temp 9 am	Air Temp 12 pm
1	LST 24DEC 2013	0.78	0.50	.54	.75	270	270	1.54	1.54	20.3	25

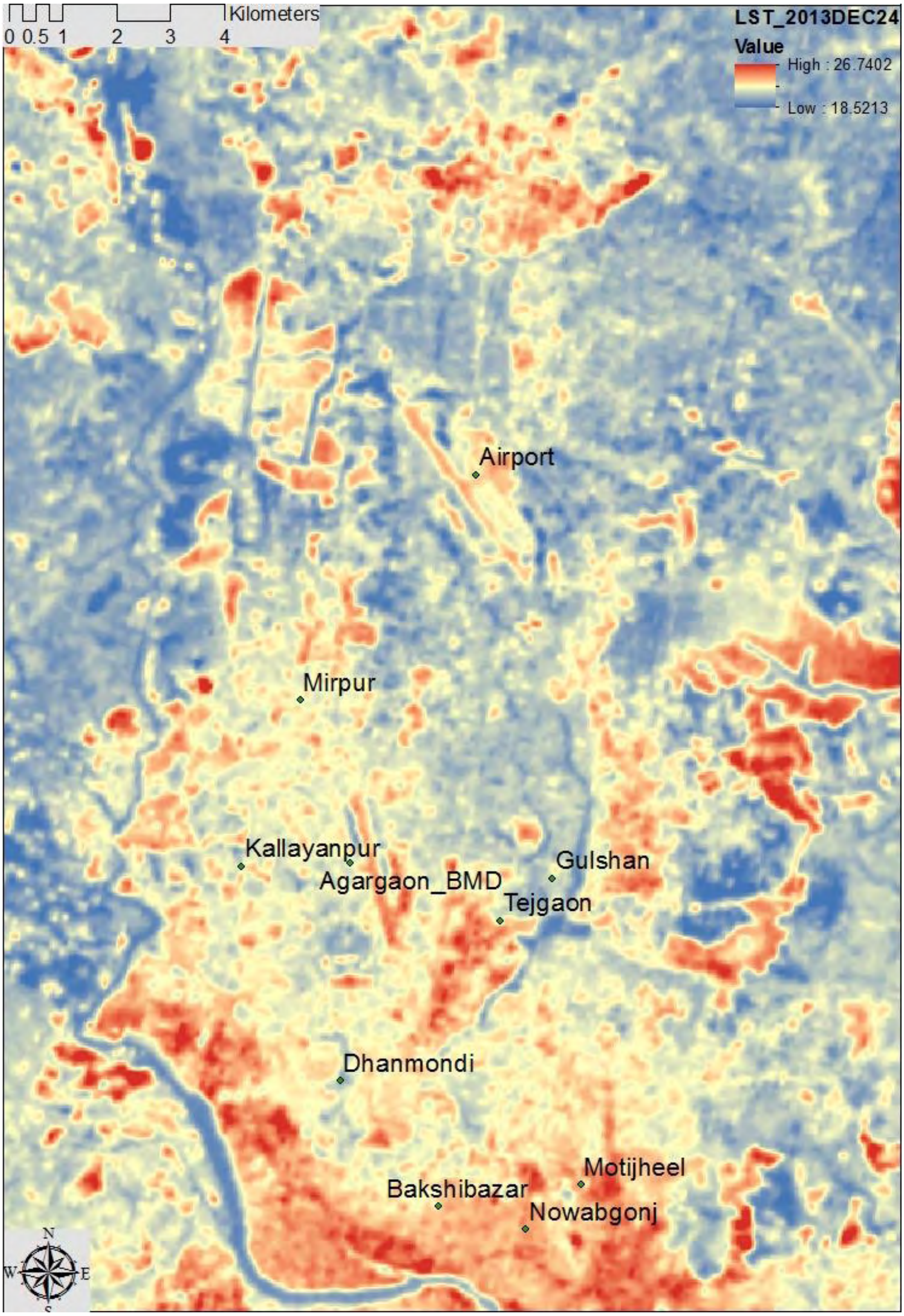

Figure 4.8: LST 24 DEC2013 (map overlay is provided in the back of this thesis)

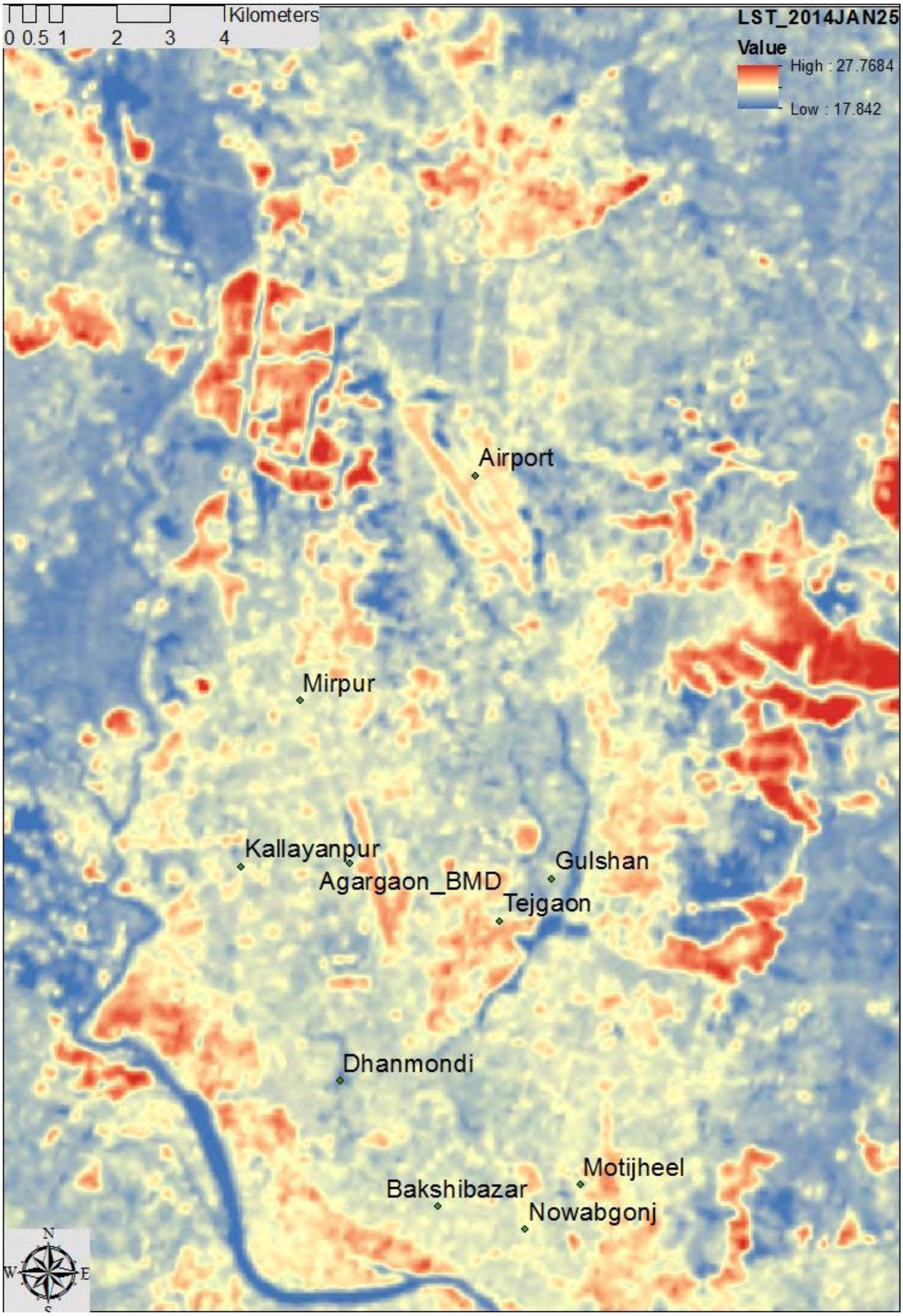

Figure 4.9: LST 25 January 2014 (map overlay is provided in the back of this thesis)

Land Surface Temperature 25 January 2014:

Table 4.14: Correlation analysis between distance and LST on 25 January 2014

Wind Direction % {N=0 or 360, E=90, S=180, W=270}

sl no	LST Date	HatirJheel_ N&NW area	HatirJheel_ S&SE area	Dhanmondi _ N&NW area	Dhanmondi _ S&SE area	WD 9 am	WD 12 pm	WS 9 am	WS 12 pm	Air Temp 9 am	Air Temp 12 pm
1	LST 25JAN 2014	0.44	0.58	.53	.18	270	0	1.02	0	19.8	25.2

Extracted Land Surface Temperature is presented in the figure 4.9 and correlational analysis in the table 4.14.

Wind flow and the cooling effect:

At this date and time, the predominant wind flow was from Northern side.

Dhanmondi Lake:

The correlation between temperature at the urban station and their distance from the wetland along the line of wind direction was more at the downwind side than the upwind side. The cooling effect from the lake is clearly carried towards the downwind side of the lake through Advection process as the North and North-West area of the Dhanmondi lake area also surrounded by the part of the lake on its Northern side. The other part South and South-East areas had very small part of the lake on its Northern side and hence missed the cooling effect being carried through advection process.

Hatirjheel Lake:

In case of the Hatirjheel lake, the correlation between temperature at the urban station and their distance from the wetland along the line of wind direction was more at the downwind South and South-East area than the North and North-West area. Because South and South-East area had part of the lake on its Northern side which the other area didn't. Because of the lack of riparian shading, at that time of the season the topographic shading (by the bank of the lake) due to the low water level was the only option for the lake water to avoid direct solar radiation.

Land Surface Temperature 10 February 2014:

Extracted Land Surface Temperature is presented in the figure 4.10 and correlational analysis in the table 4.15. At this date and time, the predominant wind flow was from the North-Eastern side.

Dhanmondi Lake:

The correlation between temperature at the urban station and their distance from the wetland along the line of wind direction was more at the downwind side than the upwind side.

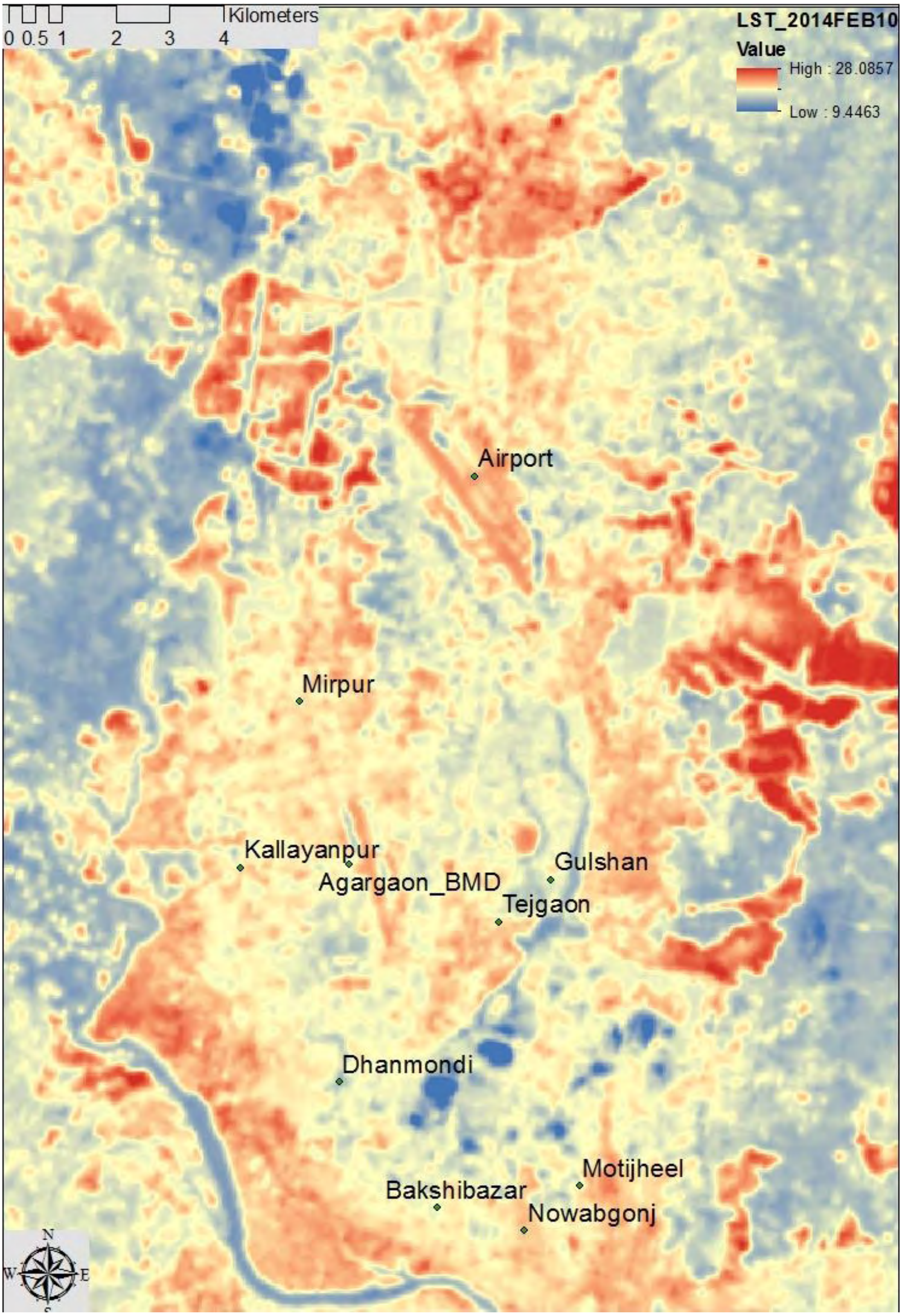

Figure 4.10: LST 10 February 2014 (map overlay is provided in the back of this thesis)

Table 4.15: Correlation analysis between distance and LST on 10 February 2014

Wind Direction % {N=0 or 360, E=90, S=180, W=270}

Sl no	LST Date	Hatir Jheel _ N&NW area	Hatir Jheel _ S&SE area	Dhanmondi _ N&NW area	Dhanmondi _ S&SE area	WD 9 am	WD 12 pm	WS 9 am	WS 12 pm	Air Temp 9 am	Air Temp. 12 pm
1	LST 10FEB2014	0.61	0.29	0.59	-0.03	360	**50**	3.08	1.54	22.2	26

The cooling effect from the lake was clearly carried towards the downwind side of the lake through Advection process, as the North and North-West area of the Dhanmondi lake area were surrounded by the part of the lake on its Northern side. The other part South and South-East area didn't have any part of the lake on its North-Eastern side and hence missed the cooling effect being carried through advection process.

Hatirjheel Lake:

In case of the Hatirjheel lake, the correlation between temperature at the urban station and their distance from the wetland along the line of wind direction was more at the downwind North and North-West area than the South and South-East area. Because North and North-West area was having part of the lake on its Northern side which the other area didn't have. Due to the lack of riparian shading at that time of the season, the topographic shading (by the bank of the lake) due to the low water level was the only option for the lake water to avoid direct solar radiation.

Land Surface Temperature 26 February 2014:

Extracted Land Surface Temperature is presented in the figure 4.11 and correlational analysis in the table 4.16.

At this date and time, the predominant wind flow was from the North-Eastern side.

Dhanmondi Lake:

The correlation between temperature at the urban station and their distance from the wetland along the line of wind direction was more at the downwind side than the upwind side. The cooling effect from the lake was clearly carried towards the downwind side of the lake through Advection process as the North and North-West area of the Dhanmondi lake area also surrounded by the part of the lake on its Northern side. The other part South and South-East area didn't have any part of the lake on its North-Eastern side and hence missed the cooling effect being carried through advection process.

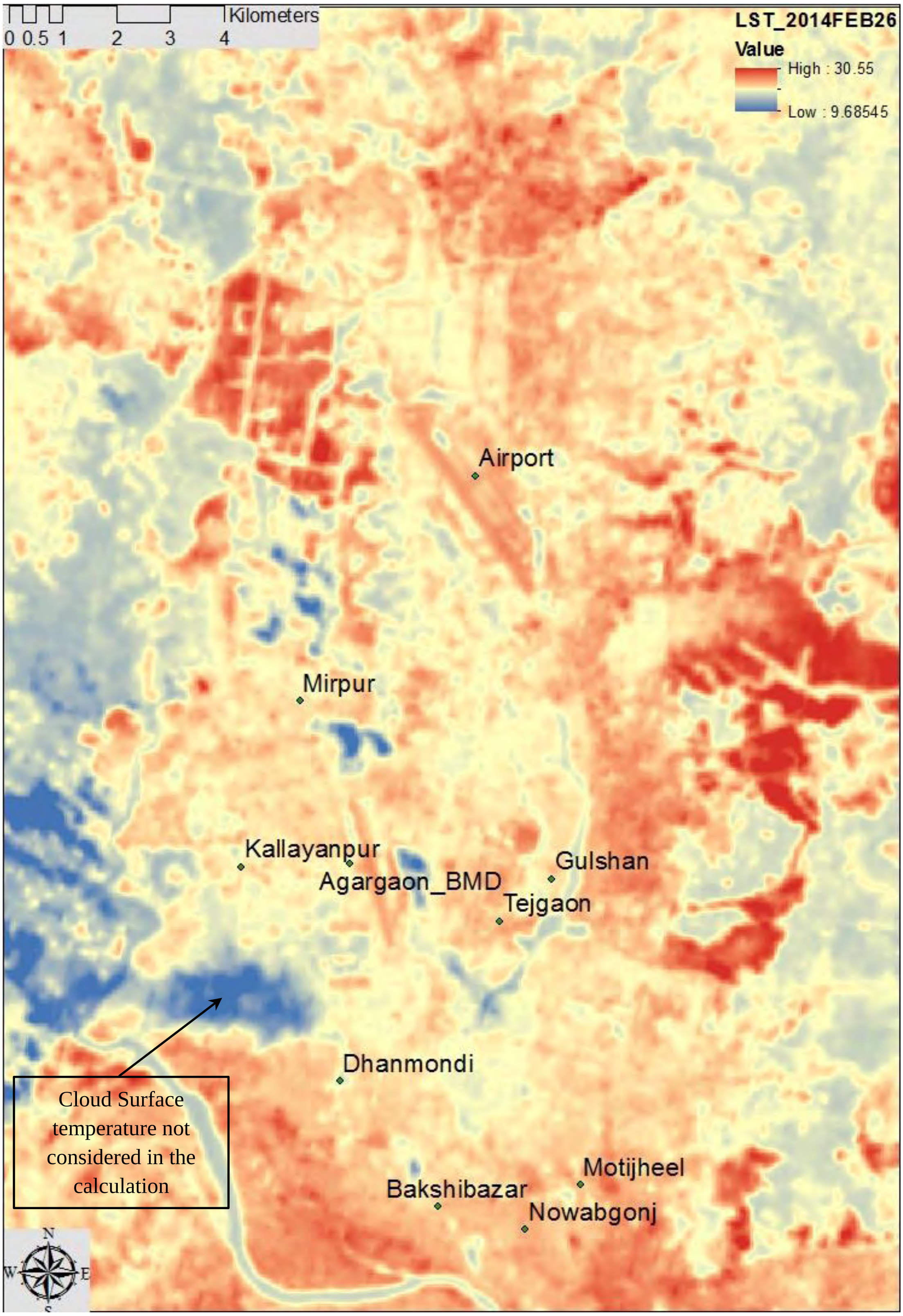

Figure 4.11: LST 26 FEBRUARY 2014 (map overlay is provided in the back of this thesis)

Table 4.16: Correlation analysis between distance and LST on 26 February 2014

Wind Direction % {N=0 or 360, E=90, S=180, W=270}

Sl no	LST Date	HatirJheel_ N&NW area	HatirJheel_ S&SE area	Dhanmondi _ N&NW area	Dhanmondi _ S&SE area	WD 9 am	WD 12 pm	WS 9 am	WS 12 pm	Air Temp. 9 am	Air Temp. 12 pm
1	LST 26FEB 2014	0.64	0.31	.54	.13	360	50	1.02	1.02	23.4	27.8

<u>Hatirjheel Lake:</u>

In case of the Hatirjheel lake, the correlation between temperature at the urban station and their distance from the wetland along the line of wind direction was more at the downwind North and North-West area than the South and South-East area. Because North and North-West area was having part of the lake on its North-eastern side but in case of the other area there was no lake on similar side. Because of the lack of riparian shading, at that time of the season the topographic shading (by the bank of the lake) due to the low water level was the only option for the lake water to avoid direct solar radiation.

<u>Land Surface Temperature 14 March 2014:</u>

Extracted Land Surface Temperature is presented in the figure 4.12 and correlational analysis in the table 4.17.

At this date and time, the predominant wind flow was from Northern side.

<u>Dhanmondi Lake:</u>

The correlation between temperature at the urban station and their distance from the wetland along the line of wind direction was more at the downwind side than the upwind side. The cooling effect from the lake was clearly carried towards the downwind side of the lake through Advection process as the North and North-West area of the Dhanmondi lake area also surrounded by the part of the lake on its Northern side. There was very small part of the lake on the Northern side of South and South-East areas and hence missed the cooling effect being carried through advection process.

<u>Hatirjheel Lake:</u>

In case of the Hatirjheel lake, the correlation between temperature at the urban station and their distance from the wetland along the line of wind direction was relatively more at the downwind South and South-East area than the North and North-West area. Because South and South-East area was having part of the lake adjacent to its Northern side which the other area didn’t have. Because of the lack of riparian shading, at that time of the season, the topographic shading (by the bank of the lake) due to low water level was the only option for the lake water to avoid direct solar radiation.

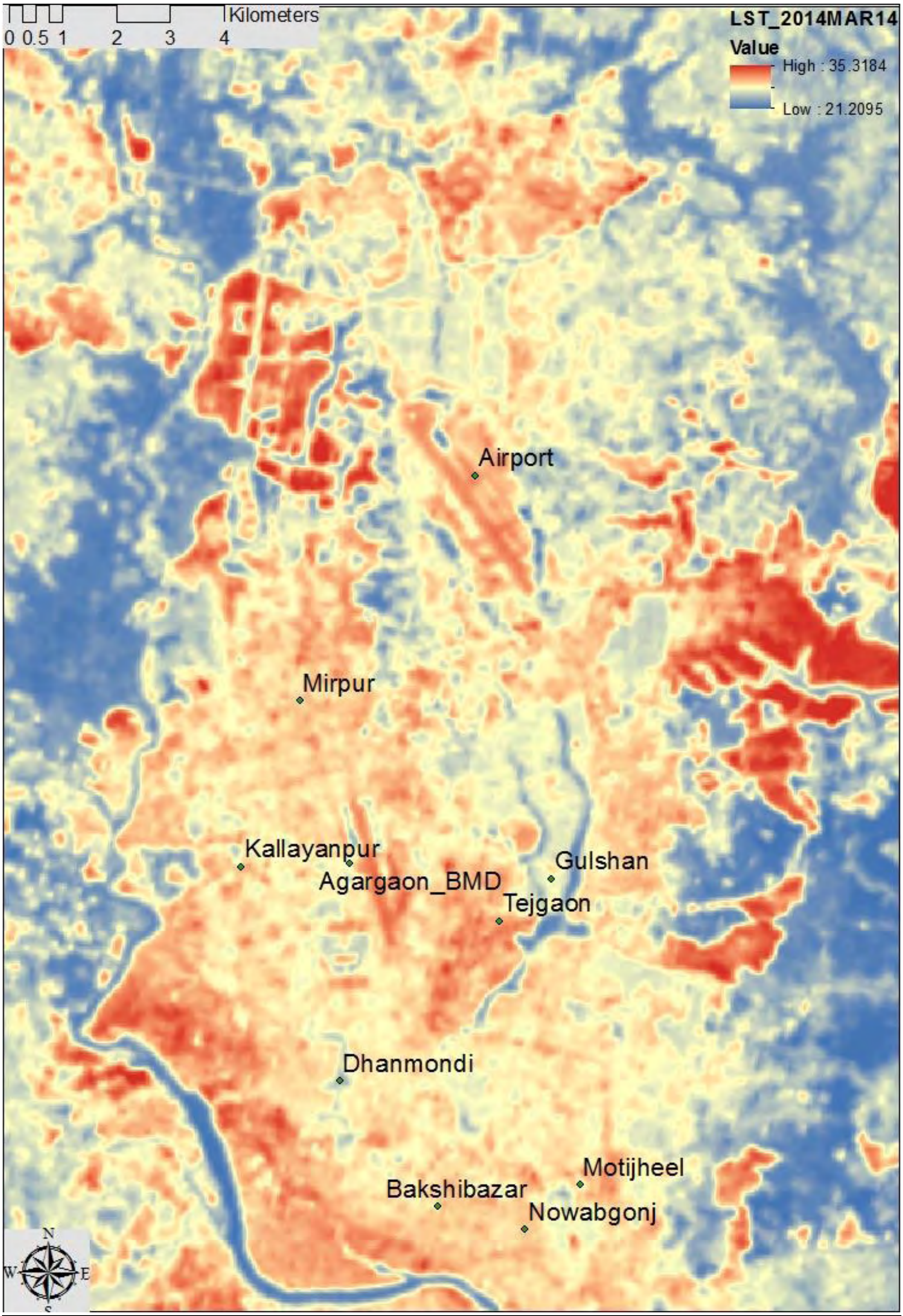

Figure 4.12: LST 14 March 2014 (map overlay is provided in the back of this thesis)

Table 4.17: Correlation analysis between distance and LST on 14 March 2014
Wind Direction % {N=0 or 360, E=90, S=180, W=270}

Sl no	LST Date	HatirJheel_ N&NW area	HatirJheel _ S&SE area	Dhanmondi _ N&NW area	Dhanmondi _ S&SE area	WD 9 am	WD 12 pm	WS 9 am	WS 12 pm	Air Temp. 9 am	Air Temp. 12 pm
1	LST 14MAR 2014	0.47	0.52	0.53	0.20	360	360	1.02	1.02	28.4	31.8

Land Surface Temperature 30 March 2014:

Extracted Land Surface Temperature is presented in the figure 4.13 and correlational analysis in the table 4.18.

Wind flow and the cooling effect:

At this date and time, the predominant wind flow was from the South-Western side.

Dhanmondi Lake:

At this direction of wind flow both the selected area around the lake had part of the lake at their upwind end. So, the correlation between temperature at the urban station and their distance from the wetland along the line of wind direction were relatively high in both the area, with North and North-Western area demonstrated slightly higher correlation. This may be due to the part of the lake at the upwind side of the North and North-West area was wider than the lake at the upwind of the other area.

Hatirjheel Lake:

In case of the Hatirjheel lake, the correlation between temperature at the urban station and their distance from the wetland along the line of wind direction was more at the downwind North and North-West area than the South and South-East area. Because North and North-West area were surrounded by part of the lake on its western and south-western side, but the other area didn't have lake on its south-western side. Because of the lack of riparian shading, at that time of the season, the topographic shading (by the bank of the lake) due to the low water level was the only option for the lake water to avoid direct solar radiation.

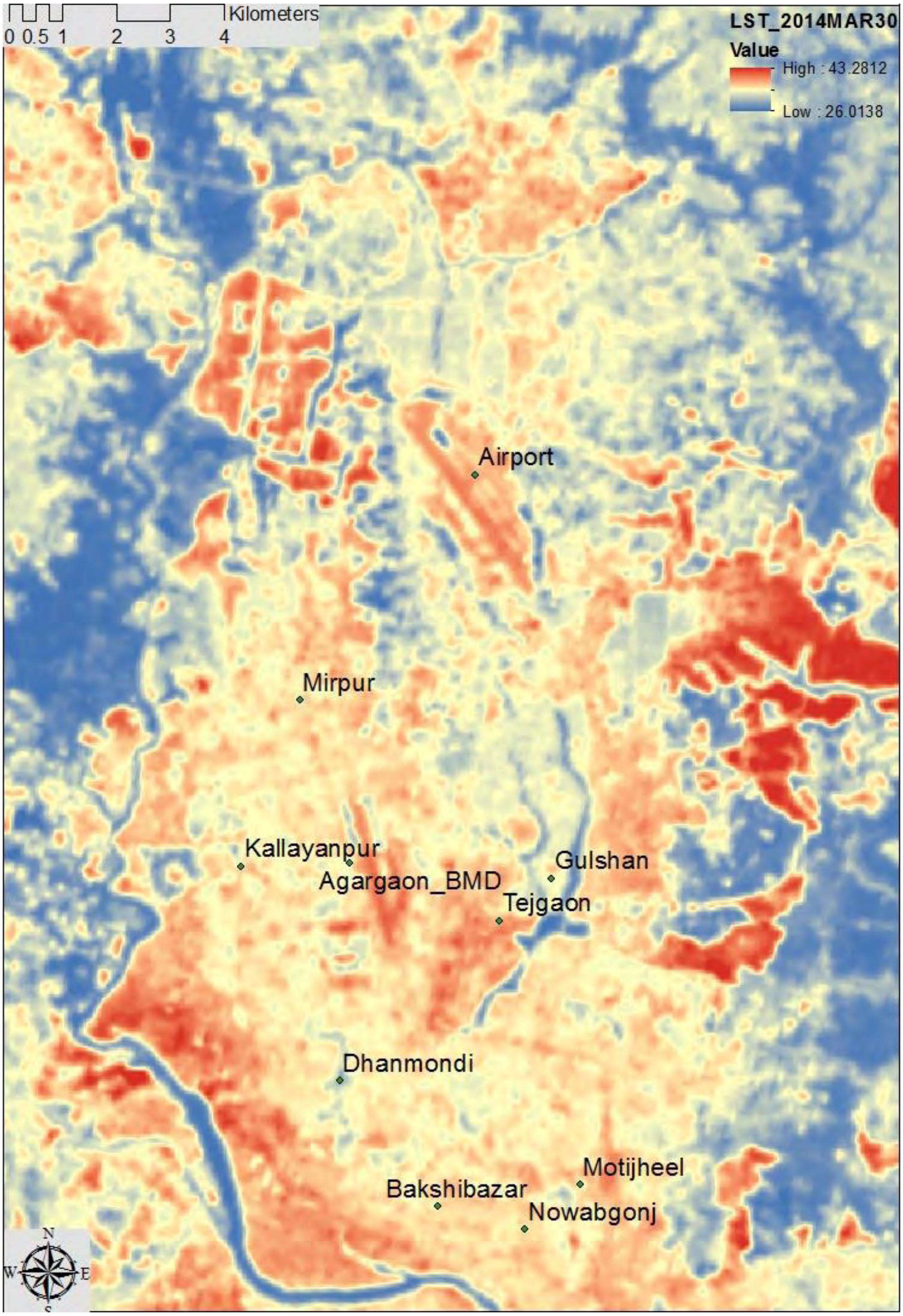

Figure 4.13: LST 30 March 2014 (map overlay is provided in the back of this thesis)

Table 4.18: Correlation analysis between distance and LST on 30 March 2014
Wind Direction % {N=0 or 360, E=90, S=180, W=270}

Sl no	LST Date	HatirJheel_ N&NW area	HatirJheel_ S&SE area	Dhanmondi _ N&NW area	Dhanmondi _ S&SE area	WD 9 am	WD 12 pm	WS 9 am	WS 12 pm	Air Temp 9 am	Air Temp. 12 pm
1	LST 30MAR 2014	0.72	0.31	0.67	0.62	240	250	1.02	1.54	30.4	36.2

Land Surface Temperature 25 November 2014:

Extracted Land Surface Temperature is presented in the figure 4.14 and correlational analysis in the table 4.19.

Wind flow and the cooling effect:

At this date and time, the predominant wind flow was from Western side.

Dhanmondi Lake:

The correlation between temperature at the urban station and their distance from the wetland along the line of wind direction was more at the downwind side than the upwind side. The cooling effect from the lake was clearly carried towards the downwind side of the lake through Advection process as the South and South-East area of the Dhanmondi lake area were surrounded by the part of the lake on its Western side. The other part North and North-West area didn't have any part of the lake on its Western side and hence missing the cooling effect being carried through advection process.

Hatirjheel Lake:

In case of the Hatirjheel lake, the correlation between temperature at the urban station and their distance from the wetland along the line of wind direction was more at the downwind North and North-West area than the South and South-East area. Because North and North-West area is having part of the lake on its western side which the other area didn't have. Riparian shading was scarce in this lake and at this time of the season due to the high-water level accumulated during the rainy season, the potential for topographic shading (by the bank of the lake) was also low for the lake water to avoid direct solar radiation. But there was shading from the built form on the part of the lake on the western side of North and North-West area, as this part was comparatively narrow, hence able to produce cooling effect.

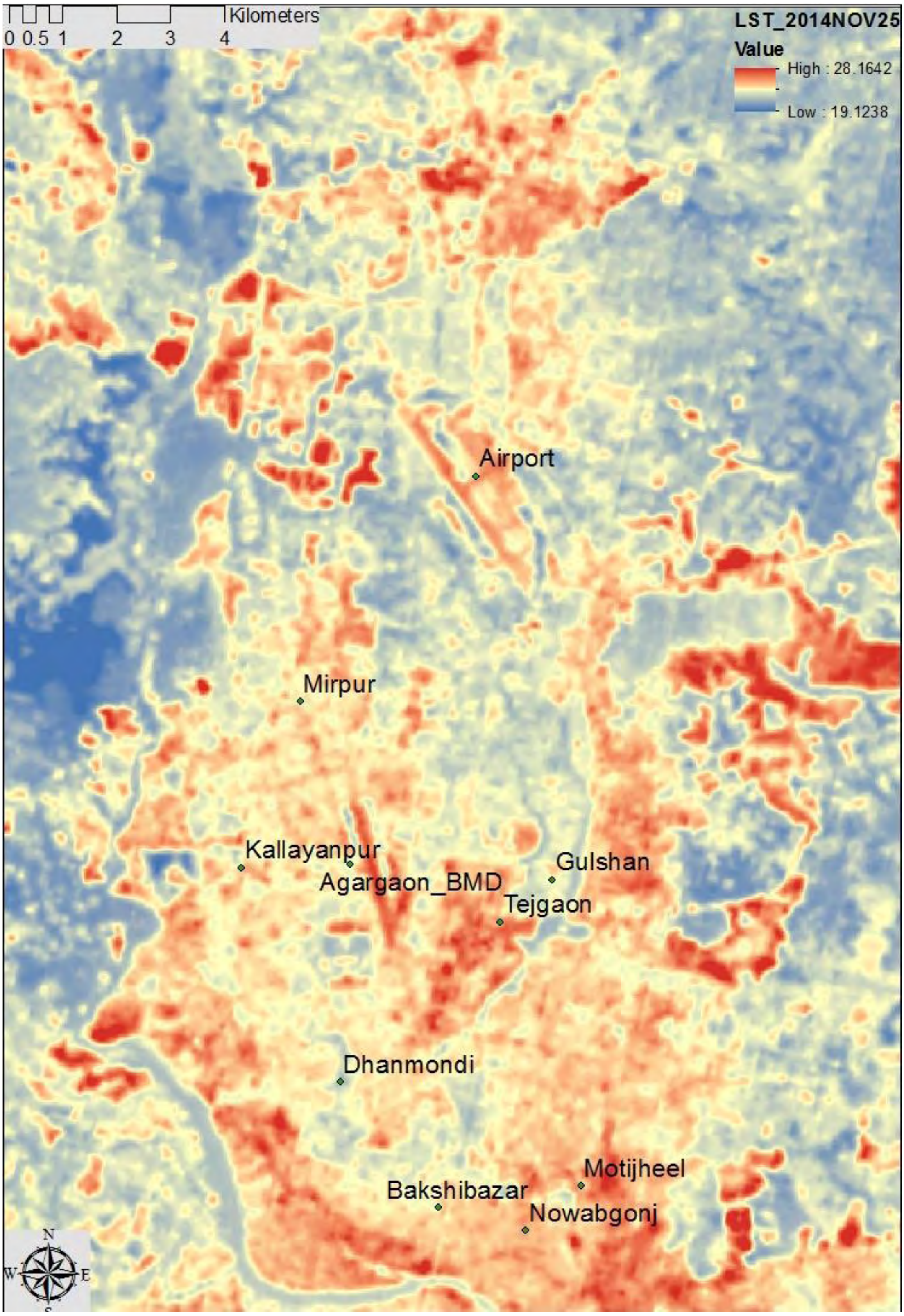

Figure 4.14: LST 25 November 2014 (map overlay is provided in the back of this thesis)

Table 4.19: Correlation analysis between distance and LST on 25 November 2014

Wind Direction % {N=0 or 360, E=90, S=180, W=270}

Sl no	LST Date	HatirJheel_ N&NW area	HatirJheel_ S&SE area	Dhanmondi _ N&NW area	Dhanmondi _ S&SE area	WD 9 am	WD 12 pm	WS 9 am	WS 12 pm	Air Temp 9 am	Air Temp. 12 pm
1	LST 25NOV2014	0.61	0.30	0.53	0.75	320	**270**	1.02	1.02	21.6	26.4

Land Surface Temperature 28 January 2015:

Extracted Land Surface Temperature is presented in the figure 4.15 and correlational analysis in the table 4.20.

Wind flow and the cooling effect:

At this date and time, the predominant wind flow was from Northern side.

Dhanmondi Lake:

The correlation between temperature at the urban station and their distance from the wetland along the line of wind direction was more at the downwind side than the upwind side. The cooling effect from the lake was clearly carried towards the downwind side of the lake through Advection process as the North and North-West area of the Dhanmondi lake area was also surrounded by the part of the lake on its Northern side. The other part South and South-East area had very small part of the lake on its Northern side and hence missed the cooling effect being carried through advection process.

Hatirjheel Lake:

In case of the Hatirjheel lake, the correlation between temperature at the urban station and their distance from the wetland along the line of wind direction was slightly more at the downwind South and South-East area than the North and North-West area. Because South and South-East area was having part of the lake on its Northern side which the other area didn't have. Due to the lack of riparian shading at that time of the season, the topographic shading (by the bank of the lake) due to the low water level was the only option for the lake water to avoid direct solar radiation.

Table 4.20: Correlation analysis between distance and LST on 28 January 2015

Wind Direction % {N=0 or 360, E=90, S=180, W=270}

Sl no	LST Date	HatirJheel_ N&NW area	HatirJheel_ S&SE area	Dhanmondi _ N&NW area	Dhanmondi _ S&SE area	WD 9 am	WD 12 pm	WS 9 am	WS 12 pm	Air Temp 9 am	Air Temp. 12 pm
1	LST28JAN 2015	0.51	0.54	0.58	0.32	0	**0**	0	0	21.2	24.5

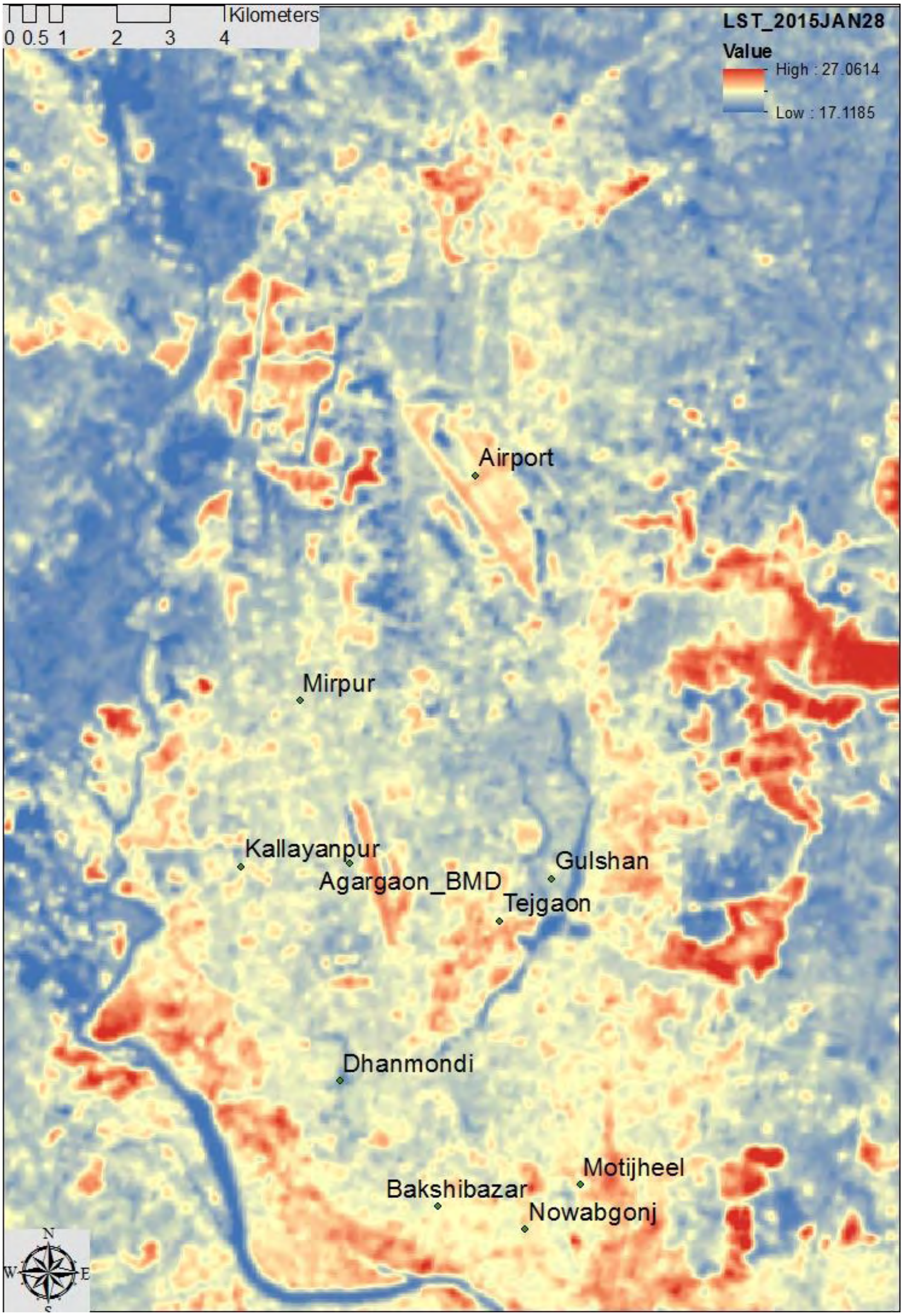

Figure 4.15: LST 28 January 2015 (map overlay is provided in the back of this thesis)

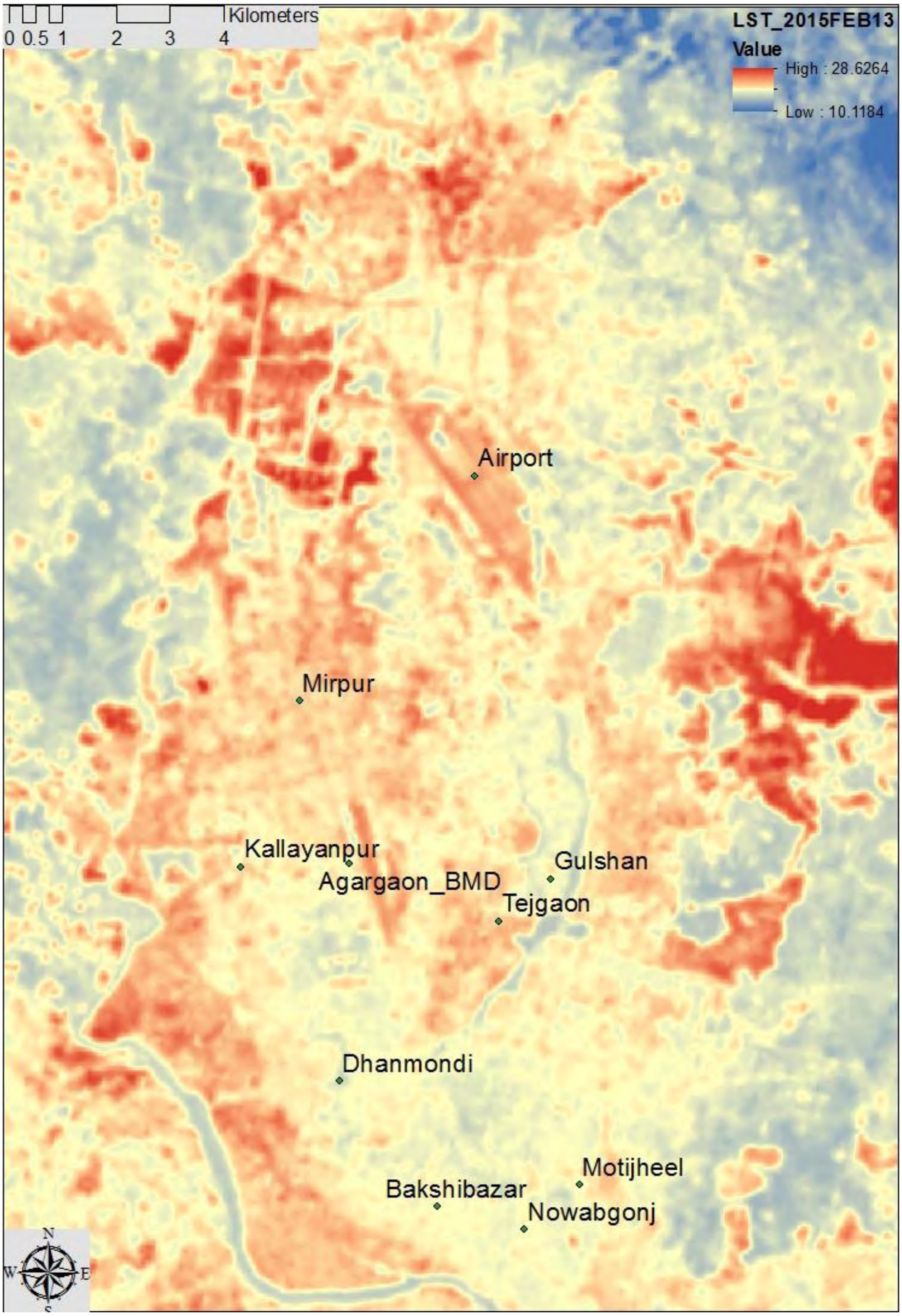

Figure 4.16: LST 13 February 2015 (map overlay is provided in the back of this thesis)

Land Surface Temperature 13 February 2015:

Extracted Land Surface Temperature is presented in the figure 4.16 and correlational analysis in the table 4.21.

Wind flow and the cooling effect:

At that date and time, the predominant wind flow was from Western side.

Table 4.21: Correlation analysis between distance and LST on 13 February 2015

Wind Direction % {N=0 or 360, E=90, S=180, W=270}

Sl no	LST Date	HatirJheel_ N&NW area	HatirJheel_ S&SE area	Dhanmondi_ N&NW area	Dhanmondi_ S&SE area	WD 9 am	WD 12 pm	WS 9 am	WS 12 pm	Air Temp 9 am	Air Temp. 12 pm
1	LST13FEB 2015	0.57	0.22	0.56	0.58	0	270	0	1.54	20.6	25.4

Dhanmondi Lake:

The correlation between temperature at the urban station and their distance from the wetland along the line of wind direction was slightly more at the downwind side than the upwind side. The cooling effect from the lake was clearly carried towards the downwind side of the lake through Advection process as the South and South-East area of the Dhanmondi lake area was also surrounded by the part of the lake on its Western side. The other part North and North-West area didn’t have any part of the lake on its Western side and hence missing the cooling effect being carried through advection process.

Hatirjheel Lake:

In case of the Hatirjheel lake, the correlation between temperature at the urban station and their distance from the wetland along the line of wind direction was more at the downwind North and North-West area than the South and South-East area. Because North and North-West area were having part of the lake on its western side which the other area didn’t have. Because of the lack of riparian shading at that time of the season, the topographic shading (by the bank of the lake) due to the low water level is the only option for the lake water to avoid direct solar radiation.

Land Surface Temperature 17 March 2015:

Extracted Land Surface Temperature is presented in the figure 4.17 and correlational analysis in the table 4.22.

Wind flow and the cooling effect:

At that date and time, the predominant wind flow was from Western side.

Dhanmondi Lake:

The correlation between temperature at the urban station and their distance from the wetland along the line of wind direction was slightly more at the downwind side than the upwind side. The cooling effect from the lake was clearly carried towards the downwind side of the lake through Advection process as the South and South-East area of the Dhanmondi lake area was also surrounded by the part of the lake on its Western side.

Table 4.22: Correlation analysis between distance and LST on 17 March 2015

Wind Direction % {N=0 or 360, E=90, S=180, W=270}

Sl no	LST Date	HatirJheel_ N&NW area	HatirJheel_ S&SE area	Dhanmondi _ N&NW area	Dhanmondi _ S&SE area	WD 9 am	WD 12 pm	WS 9 am	WS 12 pm	Air Temp 9 am	Air Temp. 12 pm
1	LST17MAR 2015	0.60	0.12	0.73	0.14	0	**270**	0	1.02	26.8	30.4

The other part North and North-West area didn't have any part of the lake on its Western side and hence missed the cooling effect being carried through advection process.

Hatirjheel Lake:

In case of the Hatirjheel lake, the correlation between temperature at the urban station and their distance from the wetland along the line of wind direction was more at the downwind North and North-West area than the South and South-East area. Because North and North-West area was having part of the lake on its western side which the other area didn't have. Because of the lack of riparian shading at that time of the season topographic shading (by the bank of the lake) due to the low water level was the only option for the lake water to avoid direct solar radiation.

Land Surface Temperature 18 April 2015:

Extracted Land Surface Temperature is presented in the figure 4.18 and correlational analysis in the table 4.23.

Wind flow and the cooling effect:

At that date and time, the predominant wind flow was from the South-Western side.

Dhanmondi Lake:

The correlation between temperature at the urban station and their distance from the wetland along the line of wind direction was more at the downwind side than the upwind side. The cooling effect from the lake was clearly carried towards the downwind side of the lake through Advection process, as the South and South-East area of the Dhanmondi lake area was surrounded by the part of the lake on its Western side. The other part North and North-West area didn't have any part of the lake on its Western side and hence missed the cooling effect being carried through advection process.

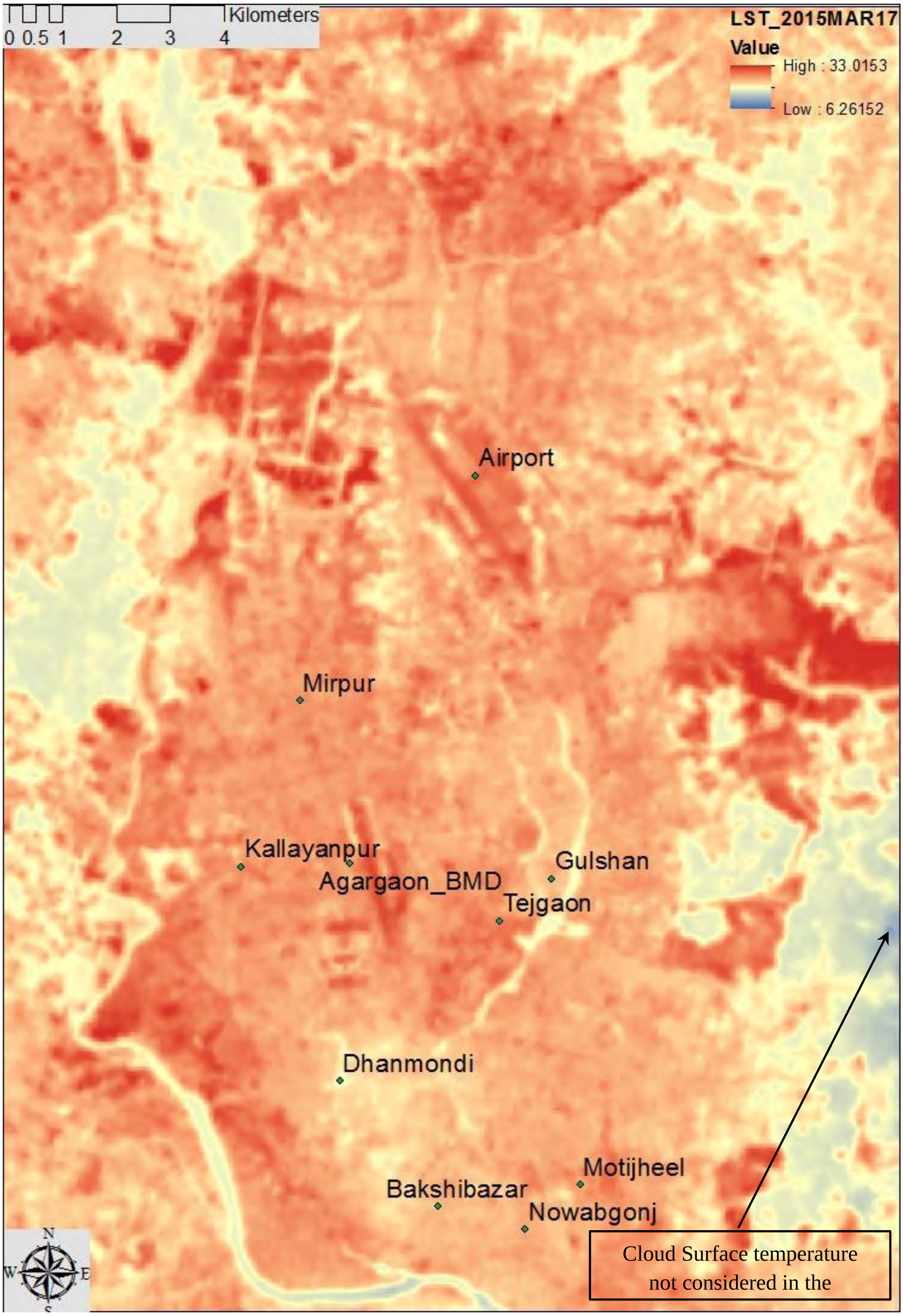

Figure 4.17: LST 17 March 2015 (map overlay is provided in the back of this thesis)

Hatirjheel Lake:

In case of the Hatirjheel lake, the correlation between temperature at the urban station and their distance from the wetland along the line of wind direction was more at the downwind North and North-West area than the South and South-East area. Because North and North-West area was having part of the lake on its western side which the other area didn't have.

Table 4.23: Correlation analysis between distance and LST on 18 April 2015

Wind Direction % {N=0 or 360, E=90, S=180, W=270}

Sl no	LST Date	HatirJheel_ N&NW area	HatirJheel_ S&SE area	Dhanmondi _ N&NW area	Dhanmondi _ S&SE area	WD 9 am	WD 12 pm	WS 9 am	WS 12 pm	Air Temp 9 am	Air Temp. 12 pm
1	LST18 APRIL 2015	0.85	0.43	0.63	0.80	260	240	1.02	5.15	28.5	31.8

Due to the lack of riparian shading at this time of the season, the topographic shading (by the bank of the lake) due to the low water level was the only option for the lake water to avoid direct solar radiation.

Land Surface Temperature 4 May 2015:

Extracted Land Surface Temperature is presented in the figure 4.19 and correlational analysis in the table 4.24.

Table 4.24: Correlation analysis between distance and LST on 4 May 2015

Wind Direction % {N=0 or 360, E=90, S=180, W=270}

Sl no	LST Date	HatirJheel_ N&NW area	HatirJheel_ S&SE area	Dhanmondi _ N&NW area	Dhanmondi _ S&SE area	WD 9 am	WD 12 pm	WS 9 am	WS 12 pm	Air Temp 9 am	Air Temp. 12 pm
1	LST4MAY 2015	0.67	0.46	0.35	0.51	180	130	1.02	1.02	29.8	33.6

Wind flow and the cooling effect:

At this date and time, the predominant wind flow was from South and South-Eastern side. The cooling effect from the lake was clearly carried towards the downwind side of both the lake through Advection process. Because the correlation between temperature at the urban station and their distance from the wetland along the line of wind direction was more at the downwind side than the upwind side.

Dhanmondi Lake:

In case of Dhanmondi lake the correlation between temperature at the urban station and their distance from the wetland along the line of wind direction was more at the downwind side than the upwind side.

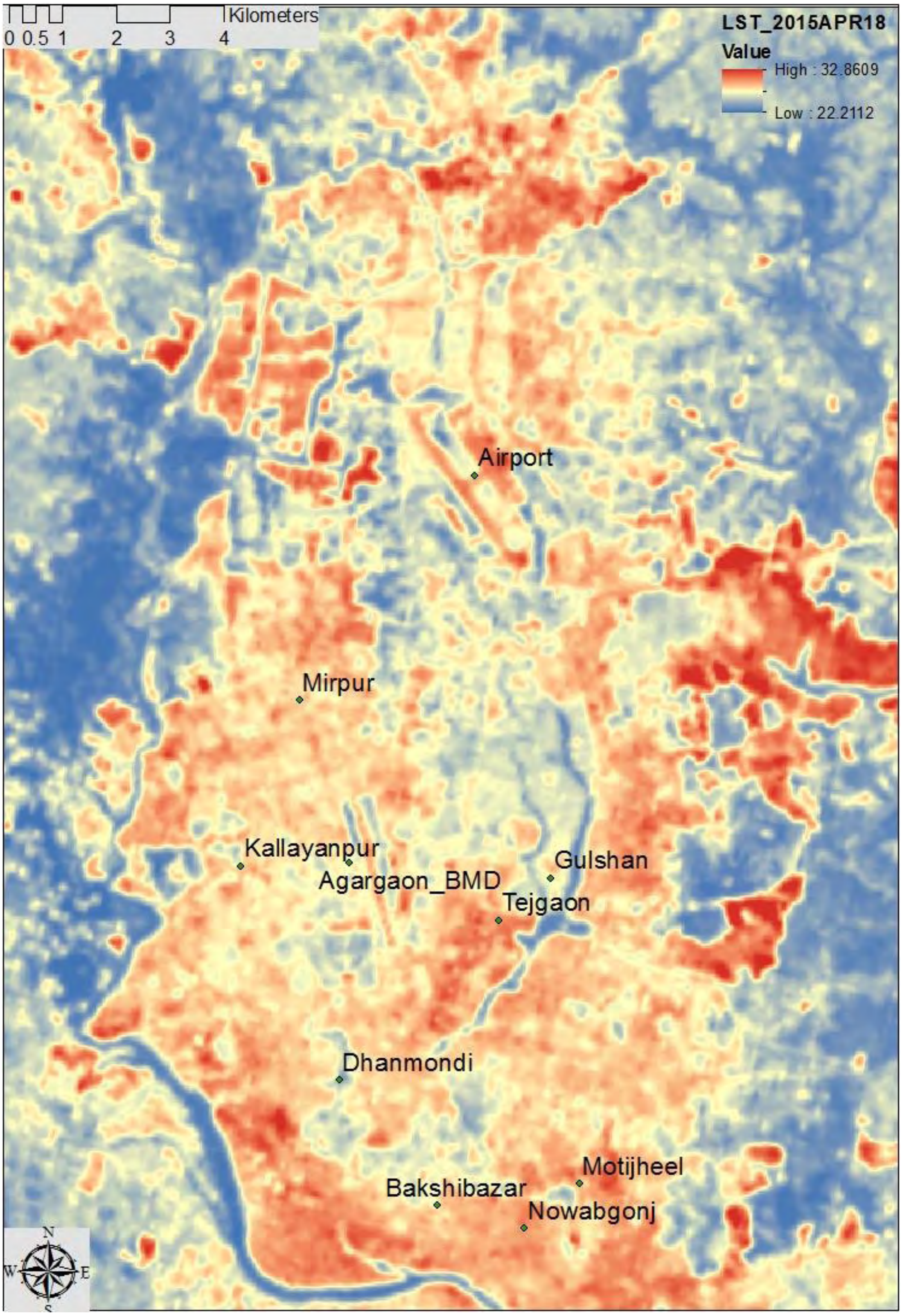

Figure 4.18: LST 18 April 2015 (map overlay is provided in the back of this thesis)

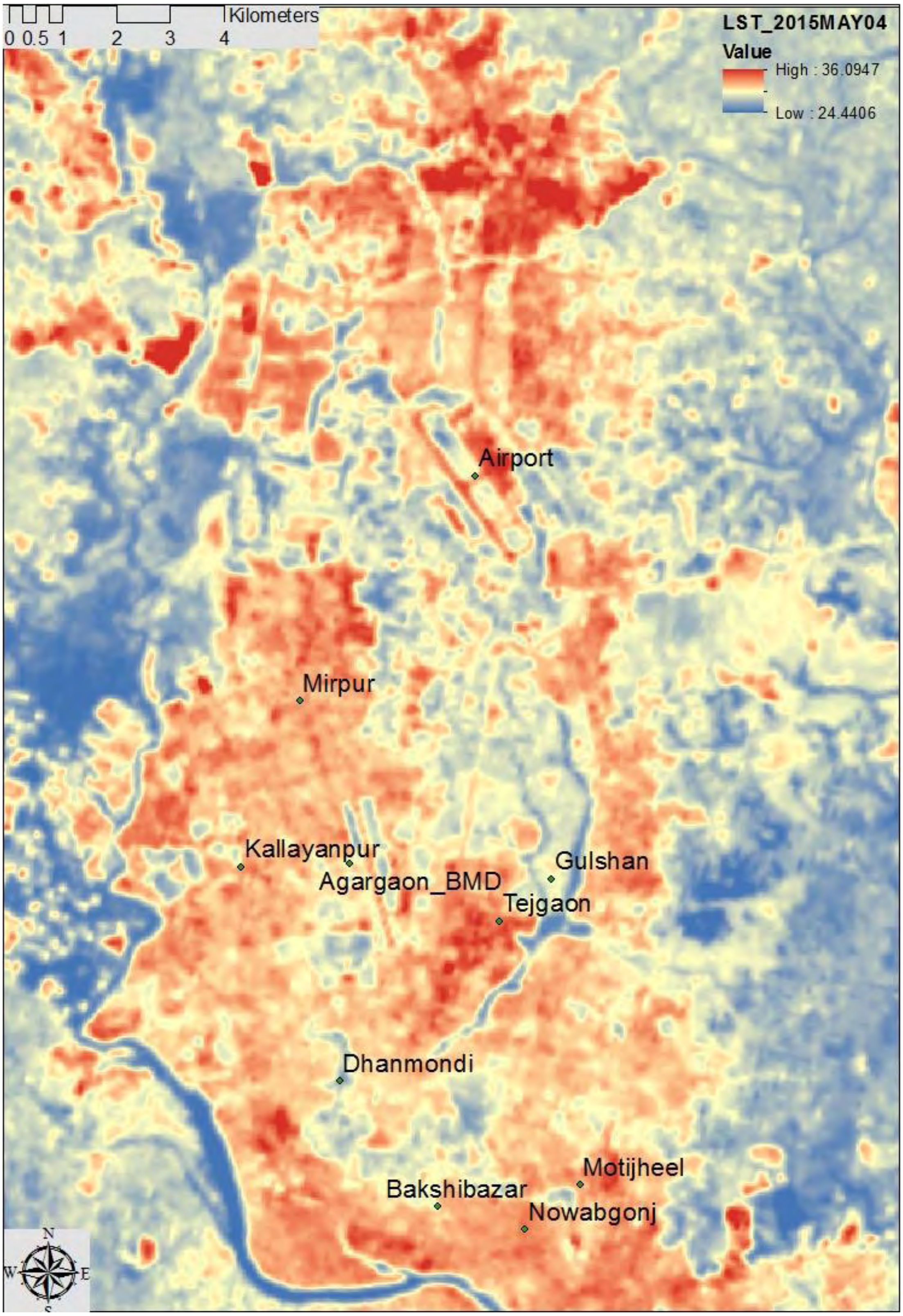

Figure 4.19: LST 4 May 2015 (map overlay is provided in the back of this thesis)

The cooling effect from the lake was clearly carried towards the downwind side of the lake through Advection process as the North and North-west area of the Dhanmondi lake area was surrounded by the part of the lake on its Southern side. The other part South and south-east didn't have any part of the lake on its Southern side and hence missed the cooling effect of wetland being carried through advection process.

Hatirjheel Lake:

In case of the Hatirjheel lake, the correlation between temperature at the urban station and their distance from the wetland along the line of wind direction was slightly more at the downwind North and North-West area than the South and South-East area. In the absence of riparian shading, the lake is partly shaded by topographic shading (by the bank of the lake) due to low water level. Hence the chance of advective cooling of North and North-West area from the lake was not so great due to the minimal shading of lake water.

Land Surface Temperature 25 September 2015:

Extracted Land Surface Temperature is presented in the figure 4.20 and correlational analysis in the table 4.25.

Wind flow and the cooling effect:

At this date and time, the predominant wind flow was from South and South-Western side. The cooling effect from the lake was clearly carried towards the downwind side of both the lake through Advection process.

Table 4.25: Correlation analysis between distance and LST on 25 September 2015

Wind Direction % {N=0 or 360, E=90, S=180, W=270}

Sl no	LST Date	HatirJheel_ N&NW area	HatirJheel_ S&SE area	Dhanmondi _ N&NW area	Dhanmondi _ S&SE area	WD 9 am	WD 12 pm	WS 9 am	WS 12 pm	Air Temp 9 am	Air Temp. 12 pm
1	LST25SEPT 2015	0.62	0.34	0.58	0.79	0	**210**	0	1.02	30	33

Because correlation between temperature at the urban station and their distance from the wetland along the line of wind direction was more at the downwind side than the upwind side.

Dhanmondi Lake:

The correlation between temperature at the urban station and their distance from the wetland along the line of wind direction was more at the downwind side than the upwind side. The cooling effect from the lake was clearly carried towards the downwind side of the lake through Advection process as the South and

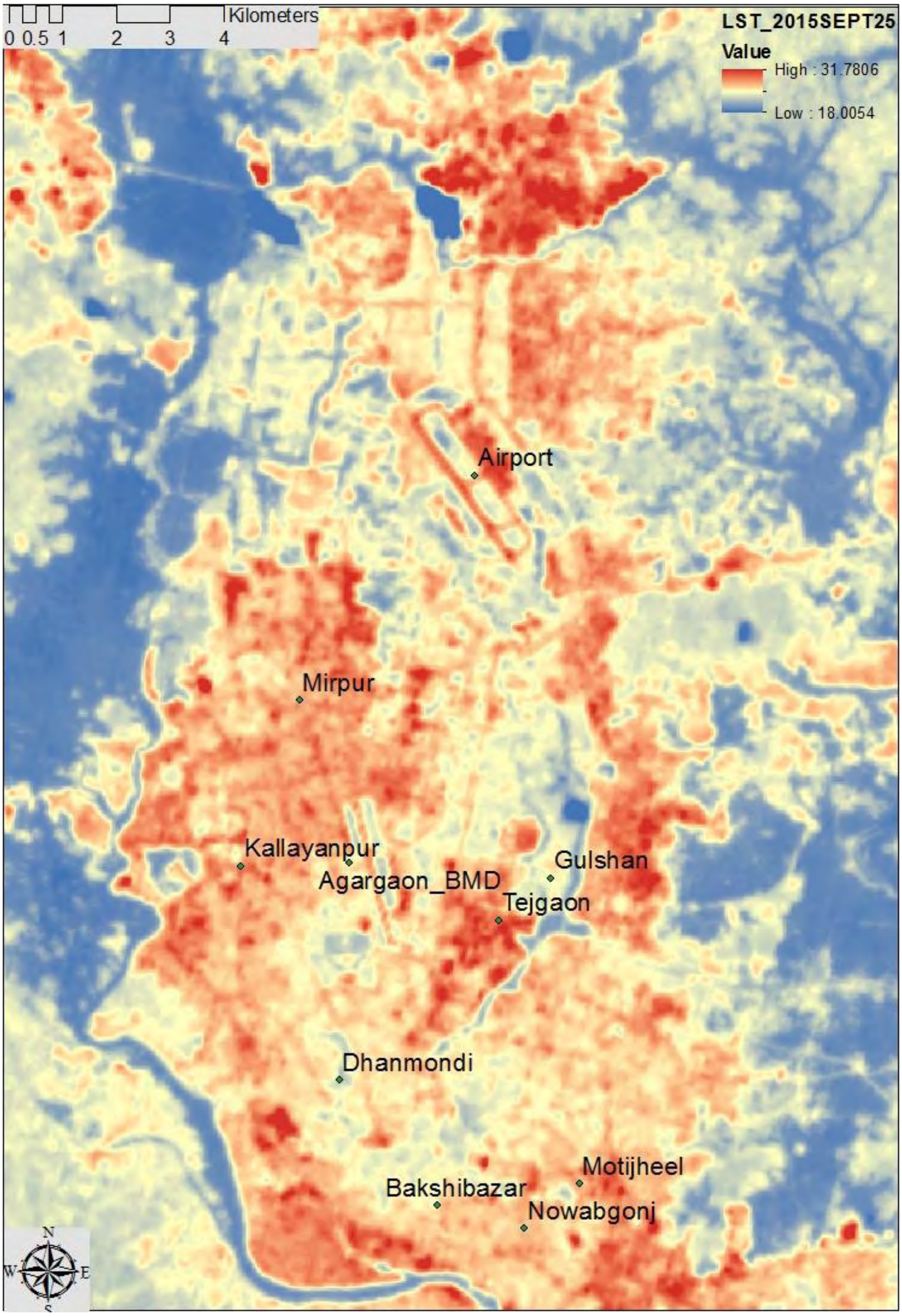

Figure 4.20: LST 25 September 2015 (map overlay is provided in the back of this thesis)

South-East area of the Dhanmondi lake was surrounded by the part of the lake on its South-Western side. The other part North and North-West had less exposure to the lake on its South-Western side and hence missed the cooling effect of wetland being carried through advection process.

Hatirjheel Lake:

In case of the Hatirjheel lake, the correlation between temperature at the urban station and their distance from the wetland along the line of wind direction was more at the downwind North and North-West area than the South and South-East area. In the absence of riparian shading, the lake was partly shaded by topographic shading (by the bank of the lake) due to low water level. Hence the chance of advective cooling of North and North-West area from the lake was not so great due to the minimal shading of lake water.

Land Surface Temperature 27 October 2015:

Extracted Land Surface Temperature is presented in the figure 4.21 and correlational analysis in the table 4.26.

Wind flow and the cooling effect:

At this date and time, the predominant wind flow was from Northern side.

Dhanmondi Lake:

The correlation between temperature at the urban station and their distance from the wetland along the line of wind direction was more at the downwind side than the upwind side. The cooling effect from the lake was clearly carried towards the downwind side of the lake through Advection process as the North and North-west area of the Dhanmondi lake area were surrounded by the part of the lake on its Northern side. The other part South and south-east had very little part of the lake on its Northern side and hence missed the cooling effect being carried through advection process.

Hatirjheel Lake:

In case of the Hatirjheel lake, the correlation between temperature at the urban station and their distance from the wetland along the line of wind direction was relatively low at the downwind South and South-East area than the North and North-West area. Because due to the lack of riparian shading South and South-East area were getting warmer by the hot air flow from the lake. At this time of the season due to the high-water level accumulated from monsoon rain, the chance of topographic shading (by the bank of the lake) was also very low.

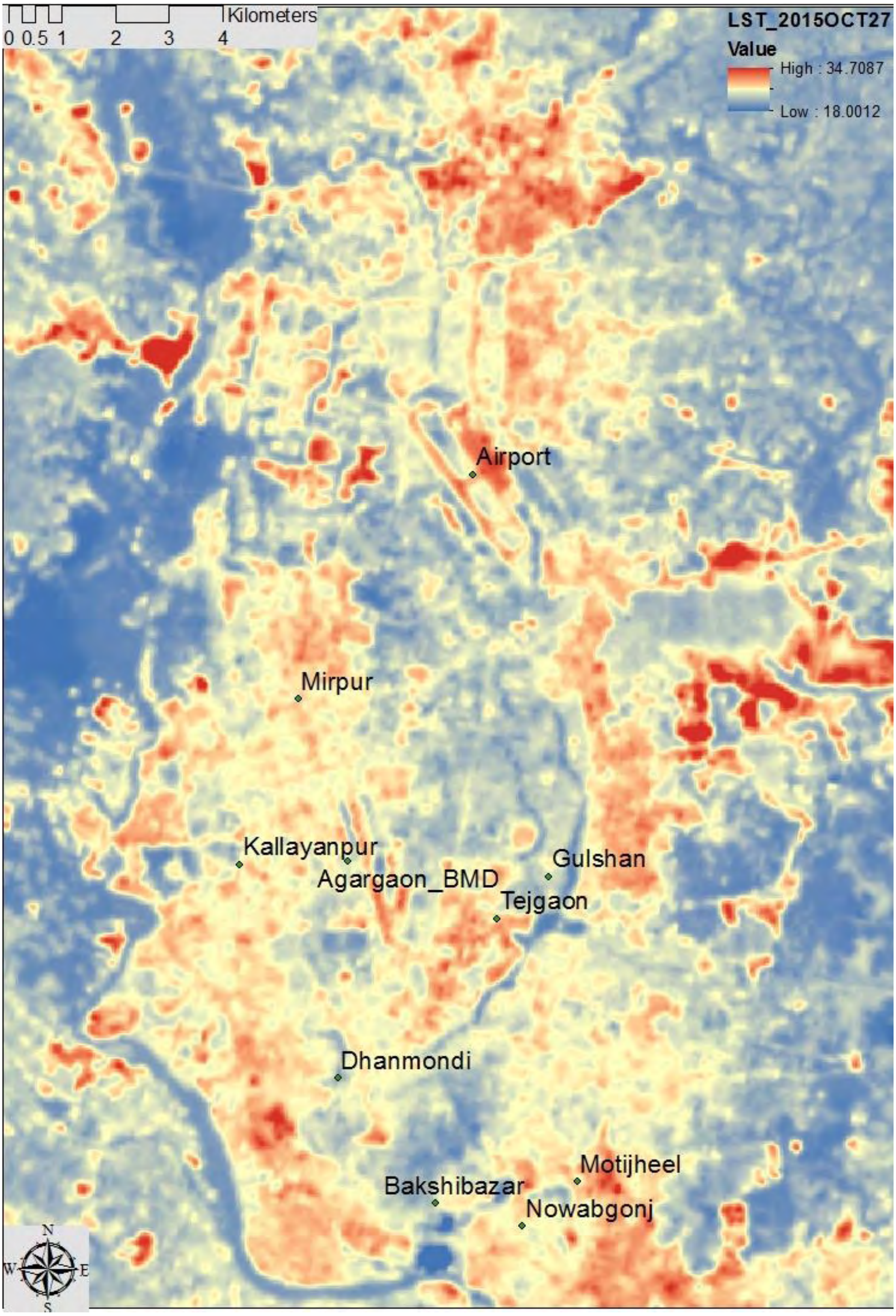

Figure 4.21: LST 27 October 2015 (map overlay is provided in the back of this thesis)

Table 4.26: Correlation analysis between distance and LST on 27 October 2015

Wind Direction % {N=0 or 360, E=90, S=180, W=270}

Sl no	LST Date	HatirJheel_ N&NW area	HatirJheel_ S&SE area	Dhanmondi_ N&NW area	Dhanmondi_ S&SE area	WD 9 am	WD 12 pm	WS 9 am	WS 12 pm	Air Temp 9 am	Air Temp. 12 pm
1	LST27OCT2015	0.58	0.54	0.63	0.19	0	**0**	0	0	28.4	31

Land Surface Temperature 12 November 2015:

Extracted Land Surface Temperature is presented in the figure 4.22 and correlational analysis in the table 4.27.

Wind flow and the cooling effect:

At this date and time, the predominant wind flow was from Northern side.

Dhanmondi Lake:

The correlation between temperature at the urban station and their distance from the wetland along the line of wind direction was more at the downwind side than the upwind side. The cooling effect from the lake was clearly carried towards the downwind side of the lake through Advection process as the North and North-west area of the Dhanmondi lake area was surrounded by the part of the lake on its Northern side. The other part South and south-east had very little part of the lake on its Northern side and hence missed the cooling effect being carried through advection process.

Hatirjheel Lake:

In case of the Hatirjheel lake, the correlation between temperature at the urban station and their distance from the wetland along the line of wind direction was relatively low at the downwind South and South-East area than the North and North-West area. Because due to the lack of riparian shading South and South-East area were getting warmer by the hot air flow from the lake. At this time of the season due to the high-water level accumulated from monsoon rain, the chance of topographic shading (by the bank of the lake) was also very low.

Table 4.27: Correlation analysis between distance and LST on 12 November 2015

Wind Direction % {N=0 or 360, E=90, S=180, W=270}

Sl no	LST Date	HatirJheel_ N&NW area	HatirJheel_ S&SE area	Dhanmondi_ N&NW area	Dhanmondi_ S&SE area	WD 9 am	WD 12 pm	WS 9 am	WS 12 pm	Air Temp 9 am	Air Temp. 12 pm
1	12NOV2015	0.58	0.57	0.55	0.11	0	**0**	0	0	27	30

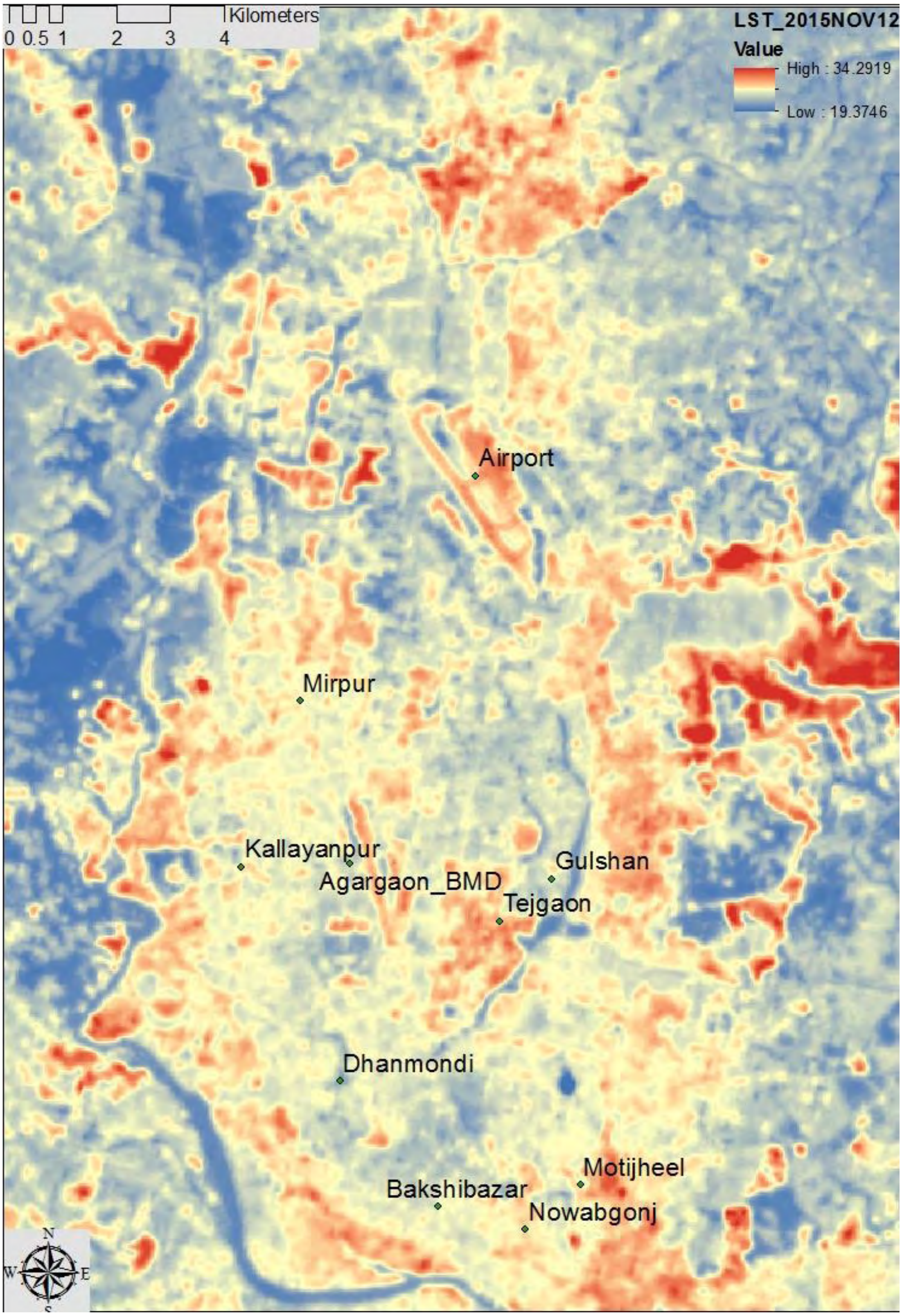

Figure 4.22: LST 12 November 2015 (map overlay is provided in the back of this thesis)

Land Surface Temperature 28 November 2015:

Extracted Land Surface Temperature is presented in the figure 4.23 and correlational analysis in the table 4.28. At this date and time, the predominant wind flow was from Northern side.

Dhanmondi Lake:

The correlation between temperature at the urban station and their distance from the wetland along the line of wind direction was more at the downwind side than the upwind side. The cooling effect from the lake was clearly carried towards the downwind side of the lake through Advection process as the North and North-west area of the Dhanmondi lake area was surrounded by the part of the lake on its Northern side. The other part South and south-east had very little part of the lake on its Northern side and hence missed the cooling effect being carried through advection process.

Hatirjheel Lake:

In case of the Hatirjheel lake, the correlation between temperature at the urban station and their distance from the wetland along the line of wind direction was relatively low at the downwind South and South-East area than the North and North-West area. Because due to the lack of riparian shading South and South-East area were getting warmer by the hot air flow from the lake. At this time of the season due to the high-water level accumulated from monsoon rain, the chance of topographic shading (by the bank of the lake) was also very low.

Table 4.28: Correlation analysis between distance and LST on 28 November 2015

Wind Direction % {N=0 or 360, E=90, S=180, W=270}

Sl no	LST Date	HatirJheel_ N&NW area	HatirJheel_ S&SE area	Dhanmondi _ N&NW area	Dhanmondi _ S&SE area	WD 9 am	WD 12 pm	WS 9 am	WS 12 pm	Air Temp 9 am	Air Temp. 12 pm
1	28 NOV 2015	0.59	0.33	0.59	0.1	0	**0**	0	0	24	27.6

Land Surface Temperature 30 December 2015:

Extracted Land Surface Temperature is presented in the figure 4.24 and correlational analysis in the table 4.29.

Table 4.29: Correlation analysis between distance and LST on 30 December 2015

Wind Direction % {N=0 or 360, E=90, S=180, W=270}

Sl no	LST Date	HatirJheel_ N&NW area	HatirJheel_ S&SE area	Dhanmondi _ N&NW area	Dhanmondi _ S&SE area	WD 9 am	WD 12 pm	WS 9 am	WS 12 pm	Air Temp 9 am	Air Temp. 12 pm
1	30 DEC 2015	0.51	0.49	0.57	0.32	0	0	0	0	18	24.2

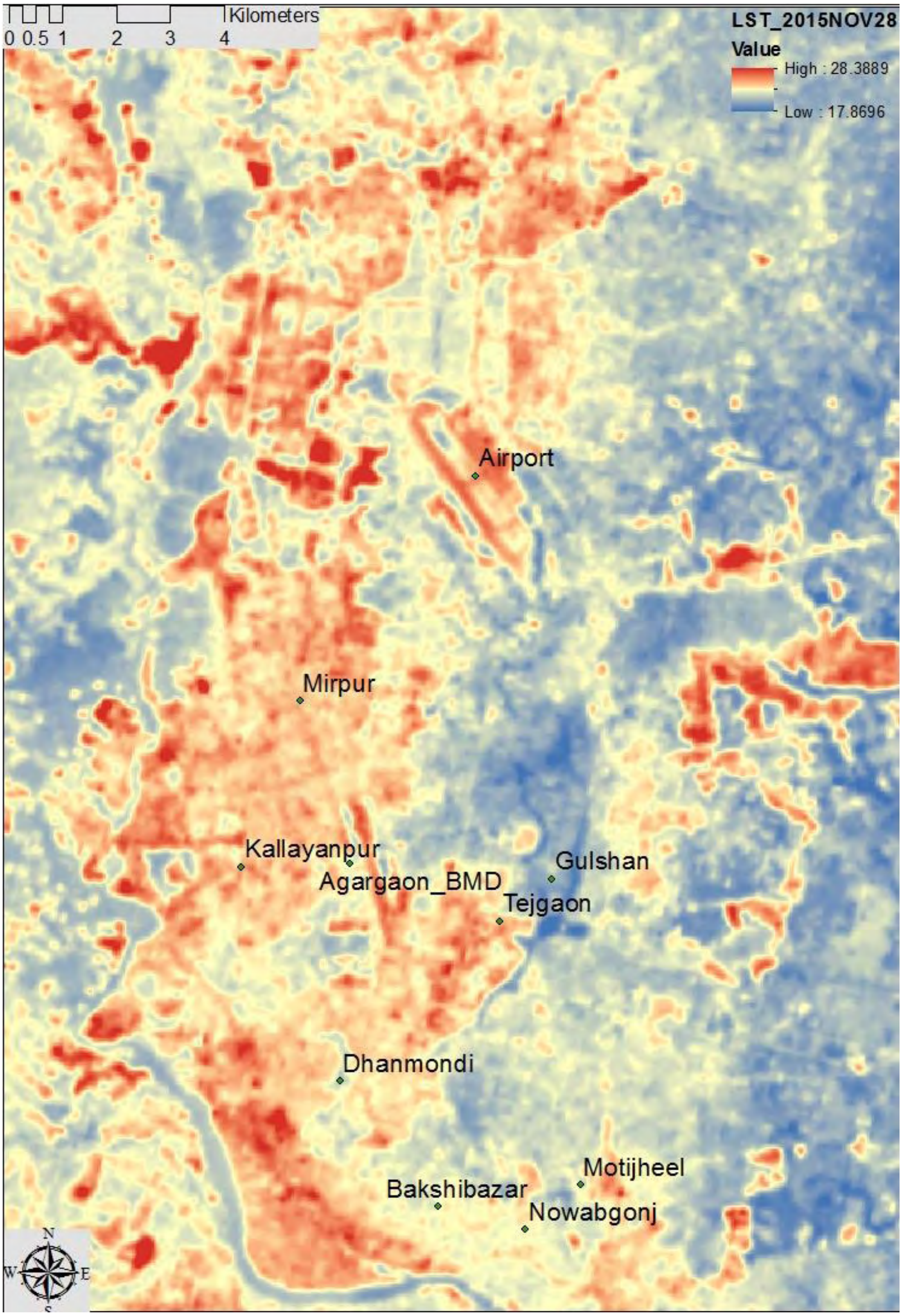

Figure 4.23: LST 28 November 2015 (map overlay is provided in the back of this thesis)

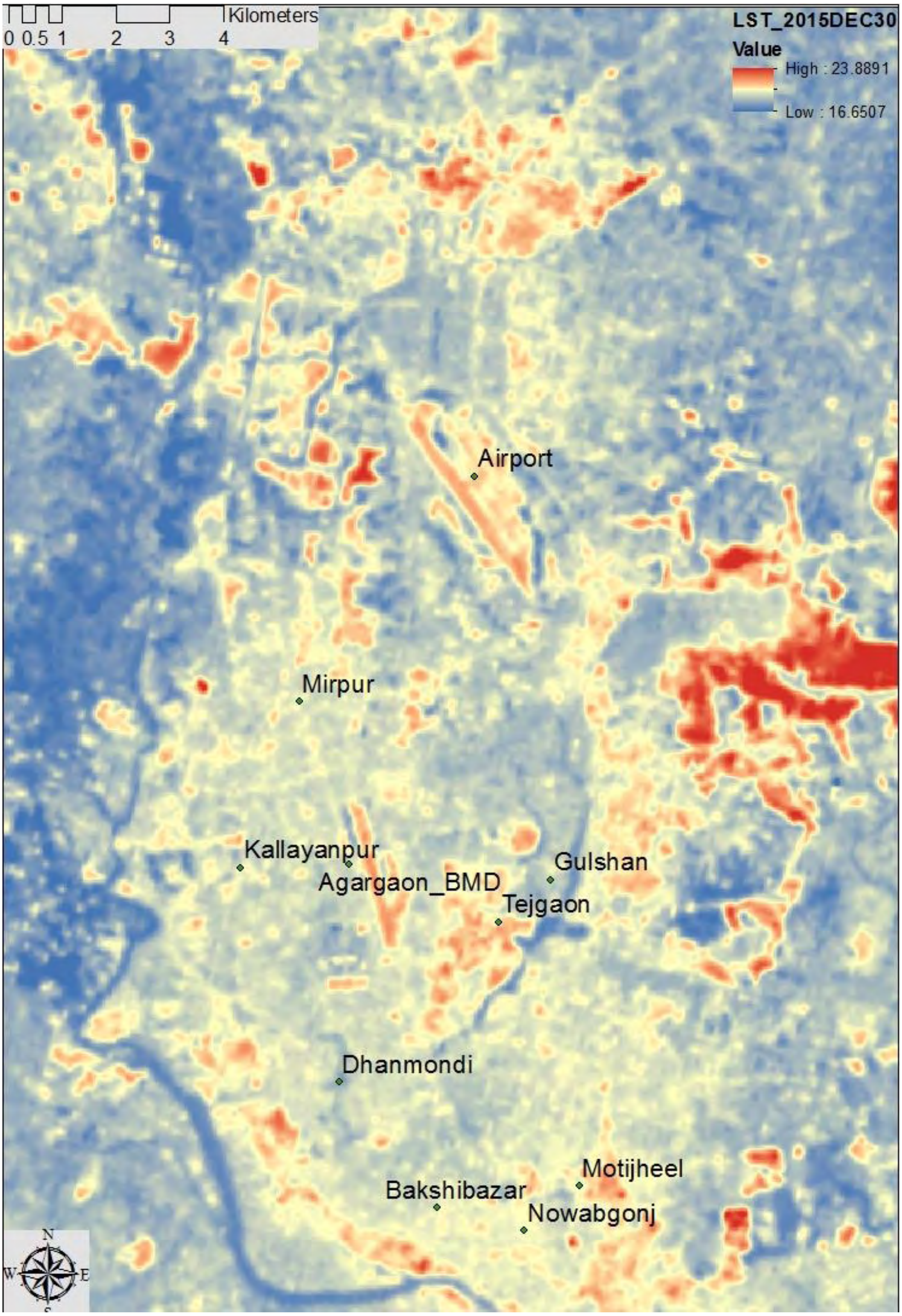

Figure 4.24: LST 30 December 2015 (map overlay is provided in the back of this thesis)

Wind flow and the cooling effect:

At this date and time, the predominant wind flow was from Northern side.

Dhanmondi Lake:

The correlation between temperature at the urban station and their distance from the wetland along the line of wind direction was more at the downwind side than the upwind side. The cooling effect from the lake was clearly carried towards the downwind side of the lake through Advection process as the North and North-west area of the Dhanmondi lake area were surrounded by the part of the lake on its Northern side. The other part South and south-east had very little part of the lake on its Northern side and hence missed the cooling effect being carried through advection process.

Hatirjheel Lake:

In case of the Hatirjheel lake, the correlation between temperature at the urban station and their distance from the wetland along the line of wind direction was relatively low at the downwind South and South-East area than the North and North-West area. Because due to the lack of riparian shading South and South-East area were getting warmer by the hot air flow from the lake. At this time of the season due to the high-water level accumulated from monsoon rain, the chance of topographic shading (by the bank of the lake) was also very low.

Land Surface Temperature 15 January 2016:

Extracted Land Surface Temperature is presented in the figure 4.25 and correlational analysis in the table 4.30. At this date and time, the predominant wind flow was from Northern side.

Table 4.30: Correlation analysis between distance and LST on 15 January 2016

Wind Direction % {N=0 or 360, E=90, S=180, W=270}

Sl no	LST Date	HatirJheel _ N&NW area	HatirJheel_ S&SE area	Dhanmondi _ N&NW area	Dhanmondi _ S&SE area	WD 9 am	WD 12 pm	WS 9 am	WS 12 pm	Air Temp 9 am	Air Temp. 12 pm
1	15 JAN 2016	0.36	0.57	0.48	0.30	0	**0**	0	0	18.2	24.2

Dhanmondi Lake:

The correlation between temperature at the urban station and their distance from the wetland along the line of wind direction was more at the downwind side than the upwind side. The cooling effect from the lake was clearly carried towards the downwind side of the lake through Advection process as the North and North-west area of the Dhanmondi lake area were surrounded by the part of the lake on its Northern side. The other part South and south-east had very little part of the lake on its Northern side and hence missed the cooling effect being carried through advection process.

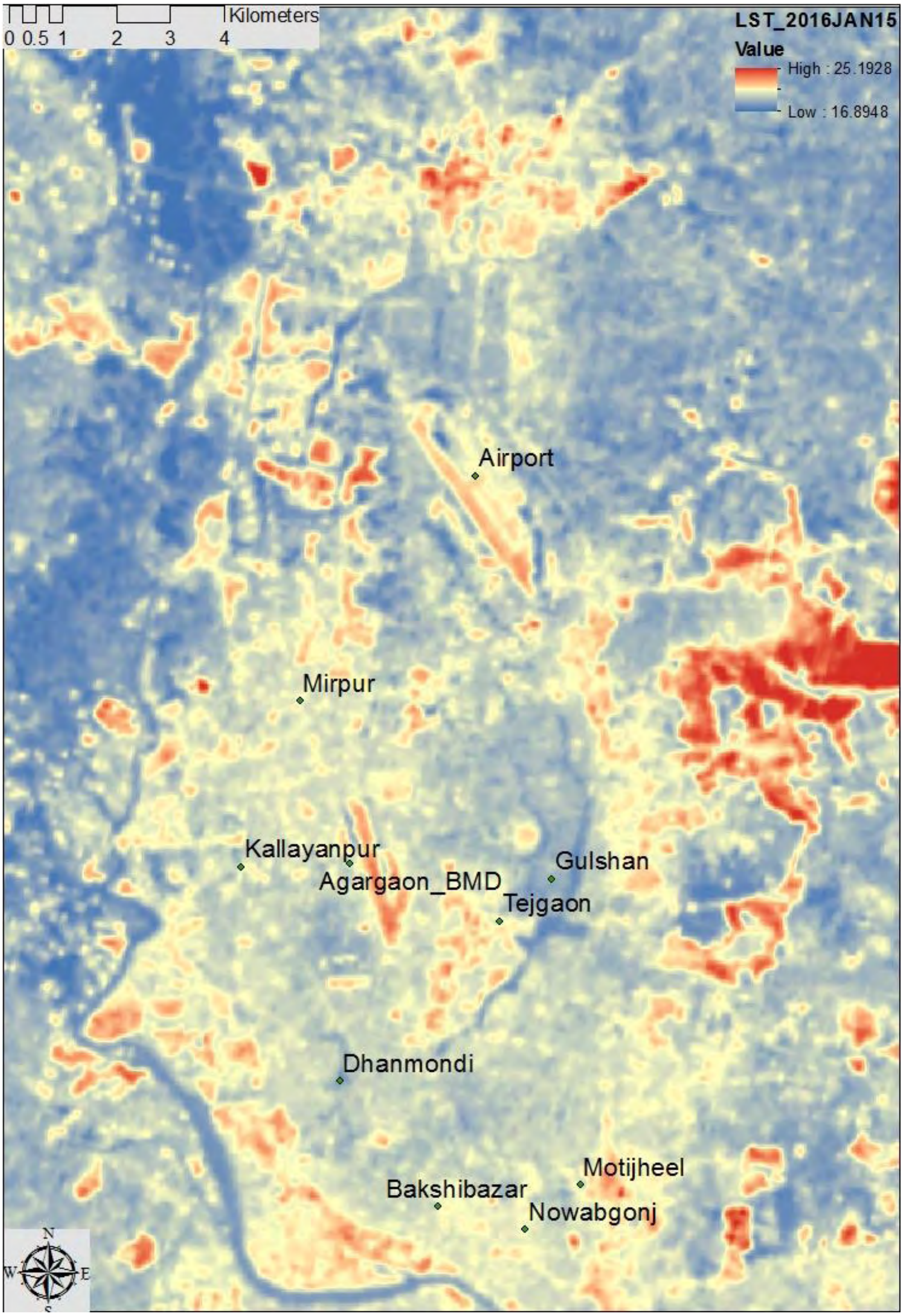

Figure 4.25: LST 15 January 2016 (map overlay is provided in the back of this thesis)

Hatirjheel Lake:

At this time of the season high-water level accumulated from monsoon rain dropped down, together with the low angle of winter sun the chance of topographic shading (by the bank of the lake) was also very high. This helps the lake water to avoid a significant amount of direct solar radiation. That is the reason in case of the Hatirjheel lake, the correlation between temperature at the urban station and their distance from the wetland along the line of wind direction was relatively high at the downwind South and South-East area than the North and North-West area. The cooling effect from the lake was clearly carried towards the downwind side of the lake through Advection process as the South and South-East area of the Hatirjheel lake were surrounded by the part of the lake on its Northern side.

Land Surface Temperature 16 February 2016:

Extracted Land Surface Temperature is presented in the figure 4.26 and correlational analysis in the table 4.31.

Wind flow and the cooling effect:

At this date and time, the predominant wind flow was from Northern side.

Dhanmondi Lake:

The correlation between temperature at the urban station and their distance from the wetland along the line of wind direction was more at the downwind side than the upwind side. The cooling effect from the lake was clearly carried towards the downwind side of the lake through Advection process as the North and North-west area of the Dhanmondi lake area were surrounded by the part of lake on its Northern side. The other part South and south east had very little part of the lake on its Northern side and hence missed the cooling effect being carried through advection process.

Table 4.31: Correlation analysis between distance and LST on 16 February 2016

Wind Direction % {N=0 or 360, E=90, S=180, W=270}

Sl no	LST Date	HatirJheel_ N&NW area	HatirJheel_ S&SE area	Dhanmondi _ N&NW area	Dhanmondi _ S&SE area	WD 9 am	WD 12 pm	WS 9 am	WS 12 pm	Air Temp 9 am	Air Temp 12 pm
1	16 FEB 2016	0.43	0.46	0.57	0.21	0	360	0	1.02	24.2	29.5

Hatirjheel Lake:

At this time of the season high-water level accumulated from monsoon rain dropped down, together with the low angle of winter sun the chance of topographic shading (by the bank of the lake) was also quite high. This helps the lake water to avoid significant amount of direct solar radiation.

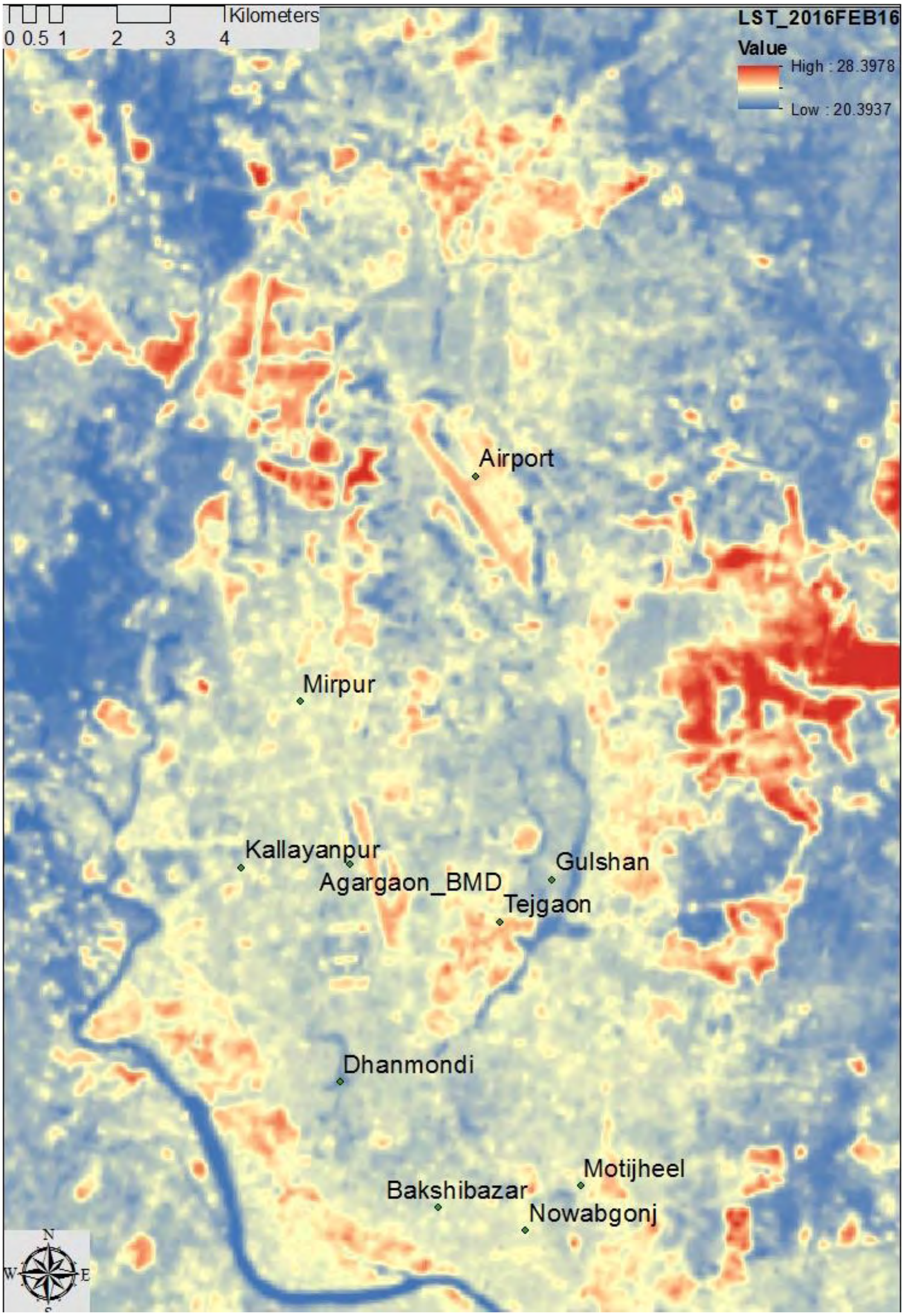

Figure 4.26: LST 16 February 2016 (map overlay is provided in the back of this thesis)

That was the reason in case of the Hatirjheel lake, the correlation between temperature at the urban station and their distance from the wetland along the line of wind direction was relatively high at the downwind South and South-East area than the North and North-West area. The cooling effect from the lake was clearly carried towards the downwind side of the lake through Advection process as the South and South-East area of the Hatirjheel lake surrounded by the part of lake on its Northern side.

Land Surface Temperature 3 March 2016:

Extracted Land Surface Temperature is presented in the figure 4.27 and correlational analysis in the table 4.32.

Wind flow and the cooling effect:

At this date and time, the predominant wind flow was from Western side.

Dhanmondi Lake:

The correlation between temperature at the urban station and their distance from the wetland along the line of wind direction was slightly more at the downwind side than the upwind side. The cooling effect from the lake was clearly carried towards the downwind side of the lake through Advection process as the South and South-East area of the Dhanmondi lake area was surrounded by the part of lake on its Western side. The other part North and North-West area didn't have any part of the lake on its Western side and hence missed the cooling effect being carried through advection process.

Hatirjheel Lake:

In case of the Hatirjheel lake, the correlation between temperature at the urban station and their distance from the wetland along the line of wind direction was more at the downwind North and North-West area than the South and South-East area. Because North and North-West area was having part of the lake on its western side which the other area didn't have. Due to the lack of riparian shading at this time of the season, the topographic shading (by the bank of the lake) due to the low water level was the only option for the lake water to avoid direct solar radiation.

Table 4.32: Correlation analysis between distance and LST on 3 March 2016

Wind Direction % {N=0 or 360, E=90, S=180, W=270}

Sl no	LST Date	HatirJheel_ N&NW area	HatirJheel_ S&SE area	Dhanmondi_ N&NW area	Dhanmondi_ S&SE area	WD 9am	WD 12pm	WS 9am	WS 12pm	Air Temp 9am	Air Temp. 12pm
1	3 MAR 2016	0.79	0.29	0.46	0.75	0	290	0	1.54	26.7	30.9

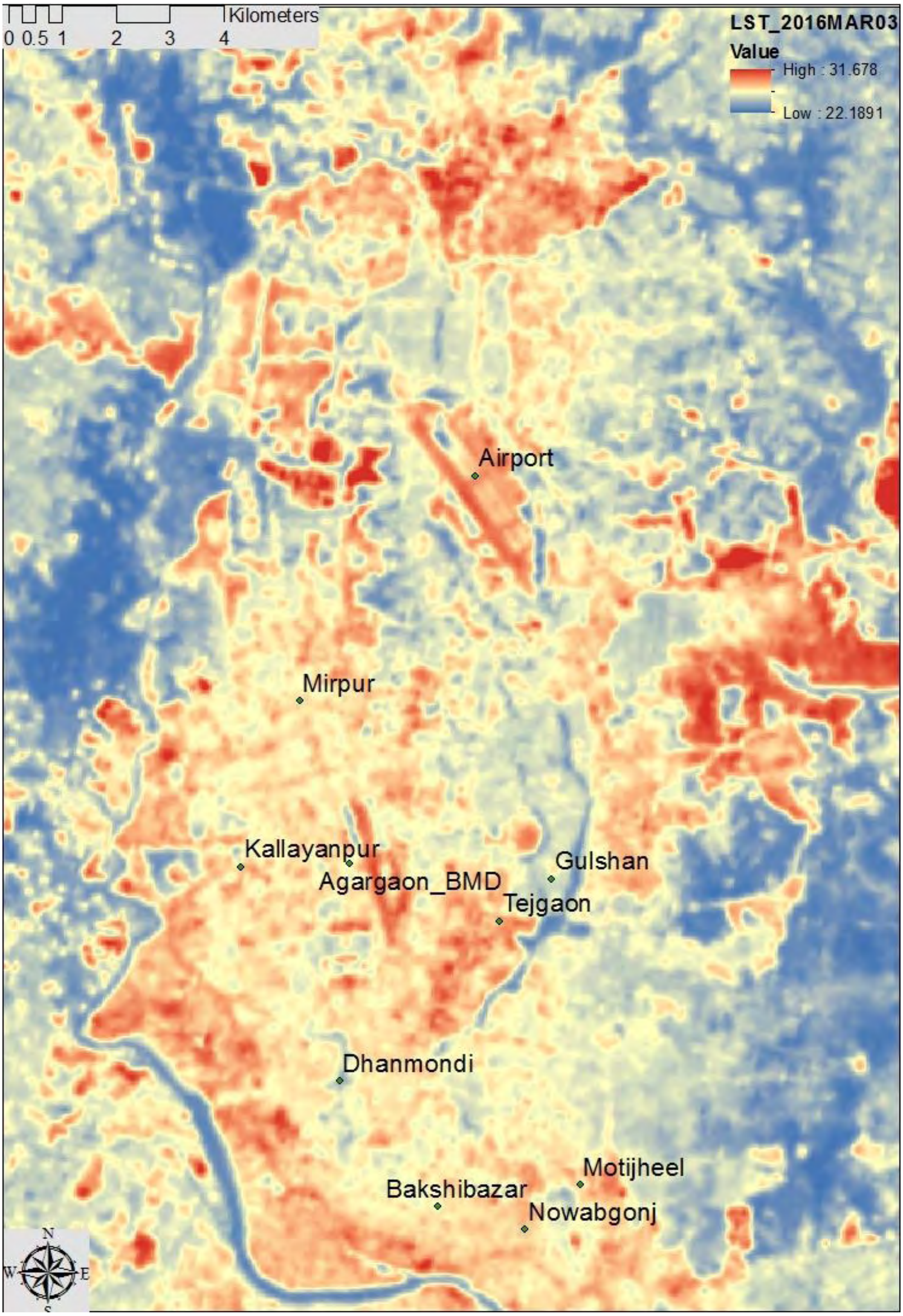

Figure 4.27: LST 3 March 2016 (map overlay is provided in the back of this thesis)

Land Surface Temperature 14 November 2016:

Extracted Land Surface Temperature is presented in the figure 4.28 and correlational analysis in the table 4.33.

Wind flow and the cooling effect:

At this date and time, the predominant wind flow was from Northern side.

Dhanmondi Lake:

The correlation between temperature at the urban station and their distance from the wetland along the line of wind direction was more at the downwind side than the upwind side. The cooling effect from the lake was clearly carried towards the downwind side of the lake through Advection process as the North and North-west area of the Dhanmondi lake area were surrounded by the part of lake on its Northern side. The other part South and south east had very little part of the lake on its Northern side and hence missed the cooling effect being carried through advection process.

Hatirjheel Lake:

In case of the Hatirjheel lake, the correlation between temperature at the urban station and their distance from the wetland along the line of wind direction was relatively low at the downwind South and South-East area than the North and North-West area. Because due to the lack of riparian shading South and South-East area were getting warmer by the hot air flow from the lake. At this time of the season due to the high-water level accumulated from monsoon rain, the chance of topographic shading (by the bank of the lake) was also quite low.

Table 4.33:Correlation analysis between distance and LST on 14 November 2016

Wind Direction % {N=0 or 360, E=90, S=180, W=270}

Sl no	LST Date	HatirJheel_ N&NW area	HatirJheel_ S&SE area	Dhanmondi_ N&NW area	Dhanmondi_ S&SE area	WD 9am	WD 12pm	WS 9am	WS 12pm	Air Temp 9am	Air Temp 12pm
1	14 NOV 2016	0.71	0.48	0.48	0.22	50	360	1.02	1.02	26.2	29.5

Land Surface Temperature 30 November 2016:

Extracted Land Surface Temperature is presented in the figure 4.29 and correlational analysis in the table 4.34.

Wind flow and the cooling effect:

At that date and time, the predominant wind flow was from Northern side.

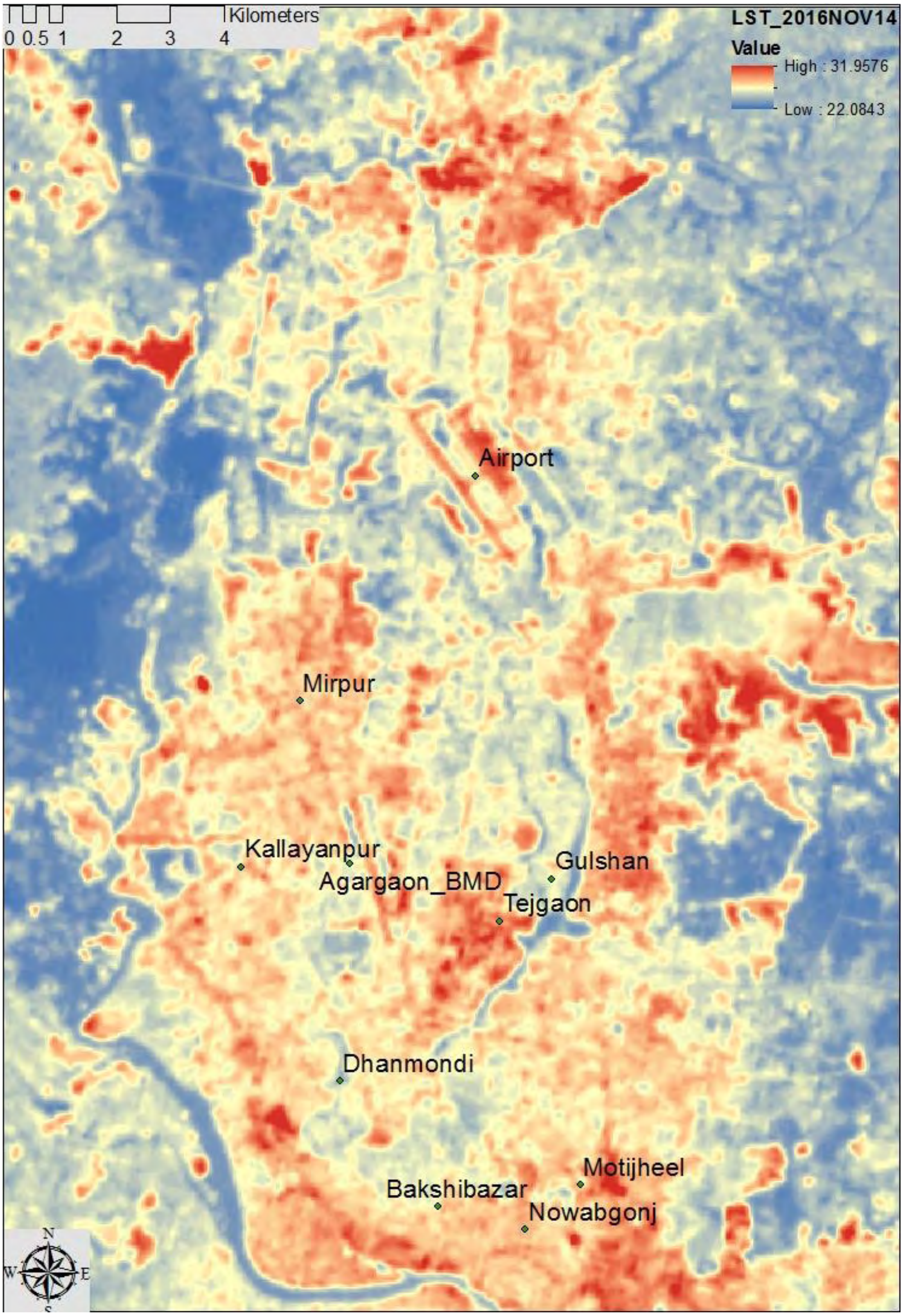

Figure 4.28: LST 14 November 2016 (map overlay is provided in the back of this thesis)

Dhanmondi Lake:

The correlation between temperature at the urban station and their distance from the wetland along the line of wind direction was more at the downwind side than the upwind side. The cooling effect from the lake was clearly carried towards the downwind side of the lake through Advection process as the North and North-west area of the Dhanmondi lake area were surrounded by the part of lake on its Northern side. The other part South and south east had very little part of the lake on its Northern side and hence missed the cooling effect being carried through advection process.

Hatirjheel Lake:

In case of the Hatirjheel lake, the correlation between temperature at the urban station and their distance from the wetland along the line of wind direction was slightly high at the downwind South and South-East area than the North and North-West area. Although located at the downwind side, due to the lack of riparian shading South and South-East area were getting warmer due to the hot air flow from the lake, hence the correlation due to the cooling effect of the lake are not that much high. At this time of the season due to the high-water level accumulated from monsoon rain, the chance of topographic shading (by the bank of the lake) was also quite low.

Table 4.34: Correlation analysis between distance and LST on 30 November 2016

Wind Direction % {N=0 or 360, E=90, S=180, W=270}

Sl no	LST Date	HatirJheel_ N&NW area	HatirJheel_ S&SE area	Dhanmondi _ N&NW area	Dhanmondi _ S&SE area	WD 9am	WD 12pm	WS 9am	WS 12pm	Air Temp 9am	Air Temp. 12pm
1	30 NOV 2016	0.54	0.56	0.63	0.26	90	0	1.02	0	24	27.5

Land Surface Temperature 18 February 2017:

Extracted Land Surface Temperature is presented in the figure 4.30 and correlational analysis in the table 4.35.

Table 4.35: Correlation analysis between distance and LST on 18 February 2017

Wind Direction % {N=0 or 360, E=90, S=180, W=270}

Sl no	LST Date	HatirJheel_ N&NW area	HatirJheel_ S&SE area	Dhanmondi _ N&NW area	Dhanmondi _ S&SE area
1	18 FEB 2017	0.71	0.60	0.70	0.66

In both case of Hatirjheel and Dhanmondi lake area correlations were strong in the downwind side, hence proved the advection process to transport the cooling effect from the lake.

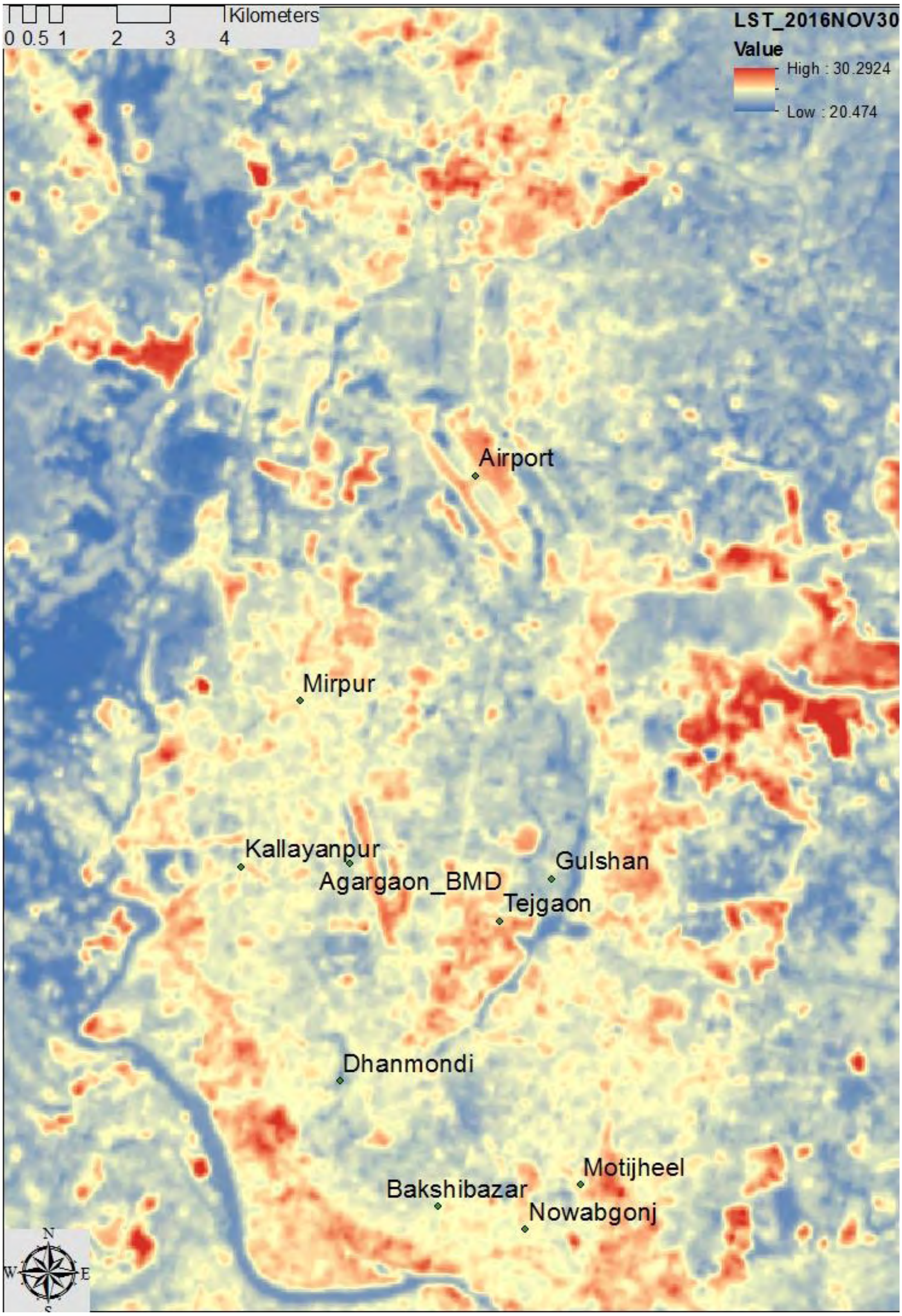

Figure 4.29: LST 30 November 2016 (map overlay is provided in the back of this thesis)

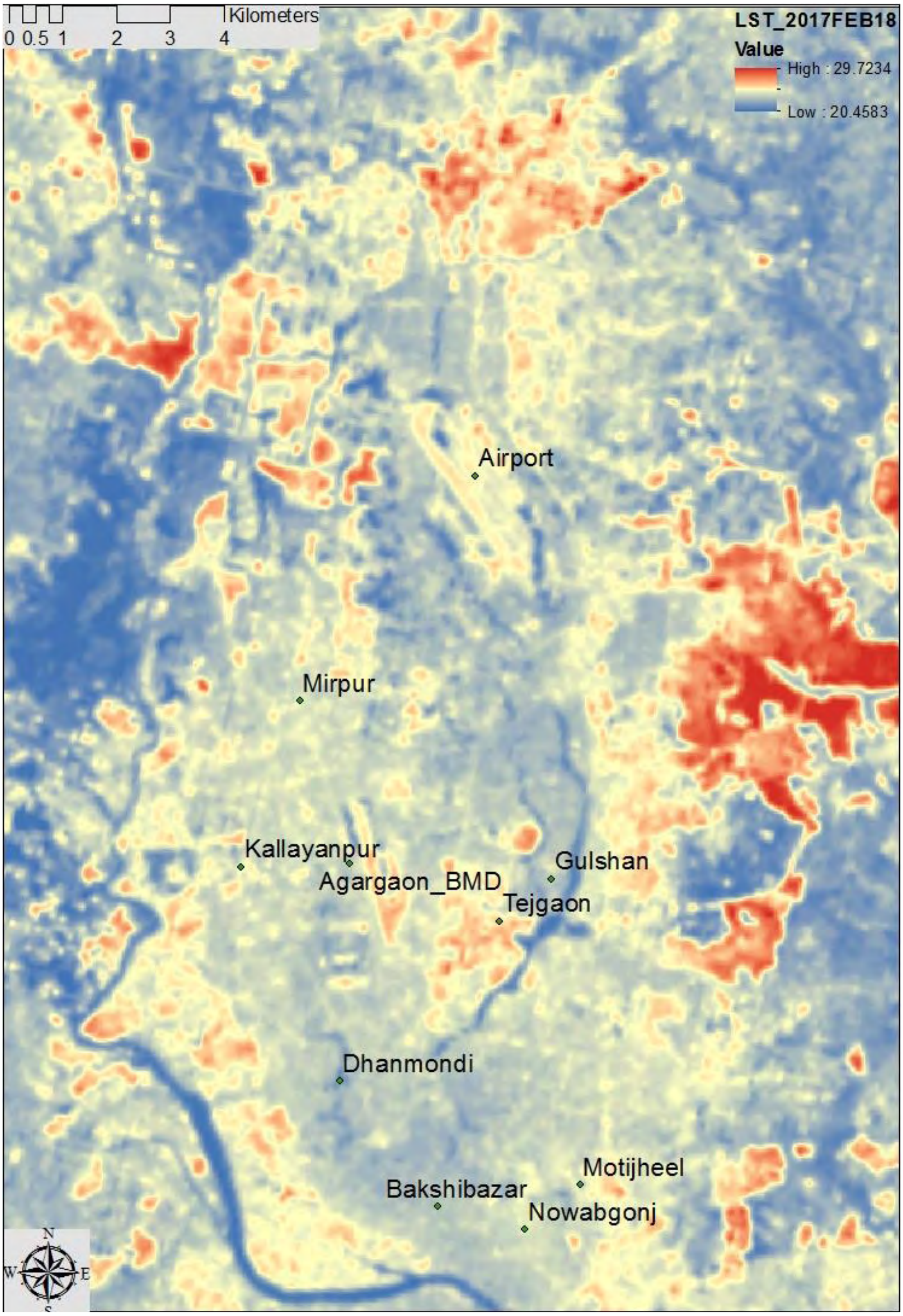

Figure 4.30: LST 18 February 2017 (map overlay is provided in the back of this thesis)

<u>Land Surface Temperature 22 March 2017:</u>

Extracted Land Surface Temperature is presented in the figure 4.31 and correlational analysis in the table 4.36.

Table 4.36: Correlation analysis between distance and LST on 22 March 2017

Wind Direction % {N=0 or 360, E=90, S=180, W=270}

Sl no	LST Date	HatirJheel_ N&NW area	HatirJheel_ S&SE area	Dhanmondi _ N&NW area	Dhanmondi _ S&SE area
1	22 MAR 2017	0.78	0.47	0.71	0.58

In both case of Hatirjheel and Dhanmondi lake area correlations were strong in the downwind side, hence showed the advection process as a means of transport coolth to the urban fabric.

Results of Correlational analysis between Land Surface Temperature (LST) at selected points and their distance from water edge for both the Dhanmondi and Hatirjheel lake for the selected dates (representing three seasons) of 2013 to 2017 are presented in table 4.37 and corresponding figure 4.32. The result of the correlation analysis (Table 4.37) shows that the LST strongly and positively correlated with distance from the edge of wetland. In case of Hatirjheel the correlation is strongest in April, which is Hot dry season and in case of Dhanmondi Lake the correlation was strongest in September which is Warm-Humid season. The possible explanation was that during the hot dry season Hatirjheel lake get more topographical shading due to low water level and hence the water temperature stays comparatively low to produce more cooling which in turn increases the difference of the cooling effect with the distance.

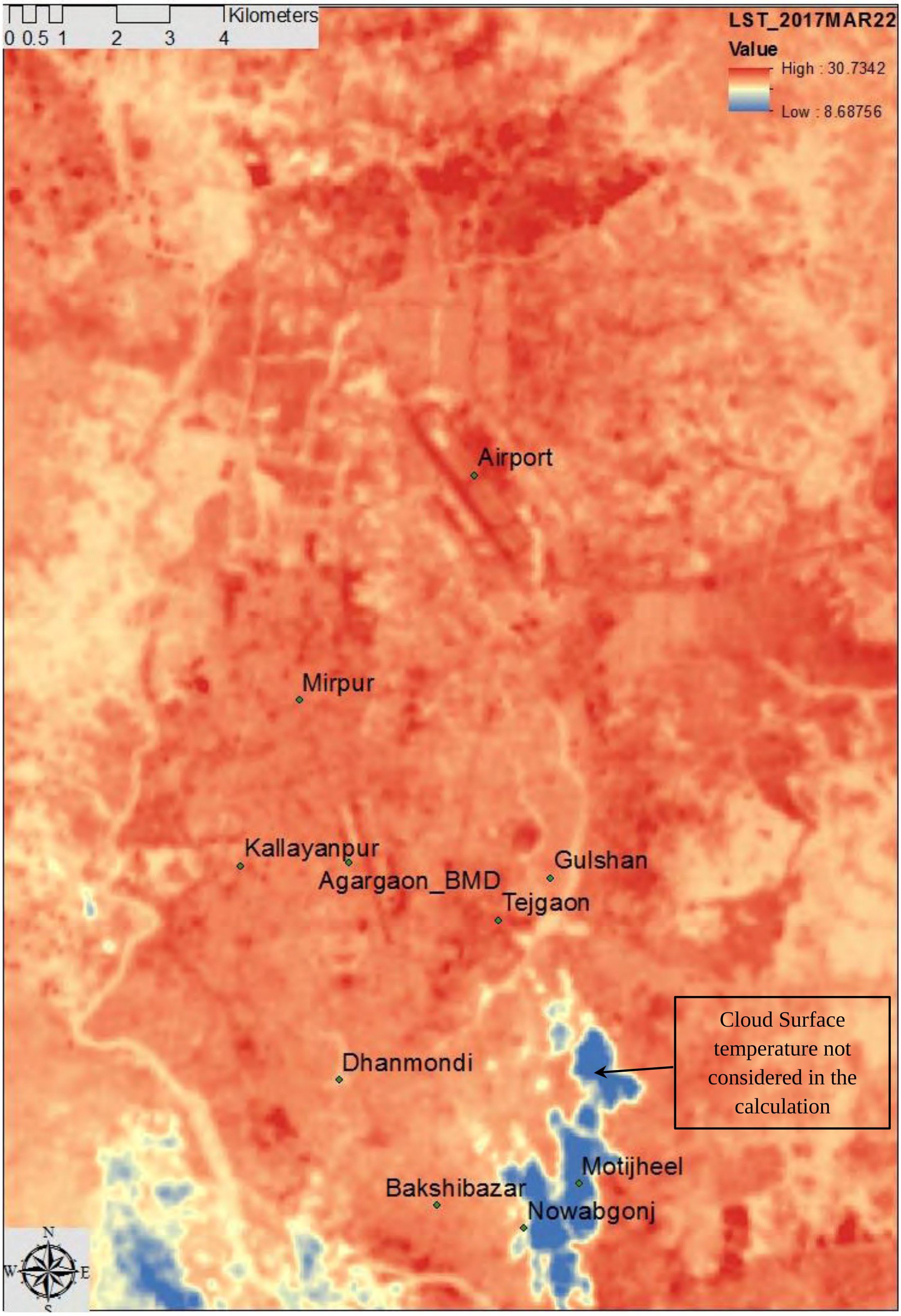

Figure 4.31: LST 22 March 2017 (map overlay is provided in the back of this thesis)

Table 4.37. Correlation coefficient (r) between LST and Distance from the edge of the wetland.

Sl no	LST Date	Hatirjheel Down Wind	Dhanmondi Down Wind	Hatirjheel Upwind	Dhanmondi Upwind	Wind Speed (ms-1) 9am	Wind Speed (ms-1) 12pm	Temp (°C) 9am	Temp (°C) 12pm
1	LST 12APRIL 2013	0.67	0.5	0.57	0.35	1.02	1.02	30.3	34.7
2	LST 15JUNE 2013	-0.46	0.26	0.5	0.18	1.02	1.02	29.8	33.4
3	LST 6NOV2013	0.42	0.65	0.6	0.26	0	1.02	25.2	28.5
4	LST 24DEC2013	0.78	0.75	0.5	0.54	1.54	1.54	20.3	25
5	LST 25JAN2014	0.58	0.53	0.44	0.18	1.02	0	19.8	25.2
6	LST 10FEB2014	0.61	0.59	0.29	-0.03	3.08	1.54	22.2	26
7	LST 26FEB2014	0.64	0.54	0.31	0.13	1.02	1.02	23.4	27.8
8	LST 14MAR 2014	0.52	0.53	0.47	0.2	1.02	1.02	28.4	31.8
9	LST 30MAR 2014	0.72	0.62	0.31	0.67	1.02	1.54	30.4	36.2
10	LST 25NOV2014	0.61	0.75	0.3	0.53	1.02	1.02	21.6	26.4
11	LST 28JAN2015	0.54	0.58	0.51	0.32	0	0	21.2	24.5
12	LST 13FEB2015	0.57	0.58	0.22	0.56	0	1.54	20.6	25.4
13	LST 17 MAR 2015	0.6	*0.14*	0.12	*0.73*	0	1.02	26.8	30.4
14	LST 18APRIL2015	0.85	0.8	0.43	0.63	1.02	5.15	28.5	31.8
15	LST 4MAY2015	0.67	0.35	0.46	0.51	1.02	1.02	29.8	33.6
16	LST 25SEPT 2015	0.62	0.79	0.34	0.58	0	1.02	30	33
17	LST 27OCT2015	0.54	0.63	0.58	0.19	0	0	28.4	31

Sl no	LST Date	Hatirjheel Down Wind	Dhanmondi Down Wind	Hatirjheel Upwind	Dhanmondi Upwind	Wind Speed (ms-1) 9am	Wind Speed (ms-1) 12pm	Temp (°C) 9am	Temp (°C) 12pm
18	LST 12NOV2015	0.57	0.55	0.58	0.11	0	0	27	30
19	LST 28NOV2015	0.33	0.59	0.59	0.1	0	0	24	27.6
20	LST 30DEC2015	0.49	0.57	0.51	0.32	0	0	18	24.2
21	LST15JAN2016	0.57	0.48	0.36	0.3	0	0	18.2	24.2
22	LST 16FEB2016	0.46	0.57	0.43	0.21	0	1.02	24.2	29.5
23	LST 3MAR2016	0.79	0.75	0.29	0.46	0	1.54	26.7	30.9
24	LST 14NOV2016	0.48	0.48	0.71	0.22	1.02	1.02	26.2	29.5
25	LST 30NOV2016	0.56	0.63	0.54	0.26	1.02	0	24	27.5
26	LST 18FEB2017	0.71	0.7	0.6	0.66				
27	LST 22MAR 2017	0.78	0.71	0.47	0.58				

4.9 Conclusion

From the analysis of land surface temperature and other parameters of the urban landcover extracted from the remotely sensed satellite data, three significant findings could be made. They are as follows:

a. The Urban Cooling Island (UCI) Intensity of urban wetland were co-related with the distance from the water edge.
b. The cooling efficiency of the urban wetland were closely moderated by riparian, topographical and built environmental shading.
c. Seasonal variation in the Urban Cooling Island (UCI) intensity were also observed through the remote sensing technique.

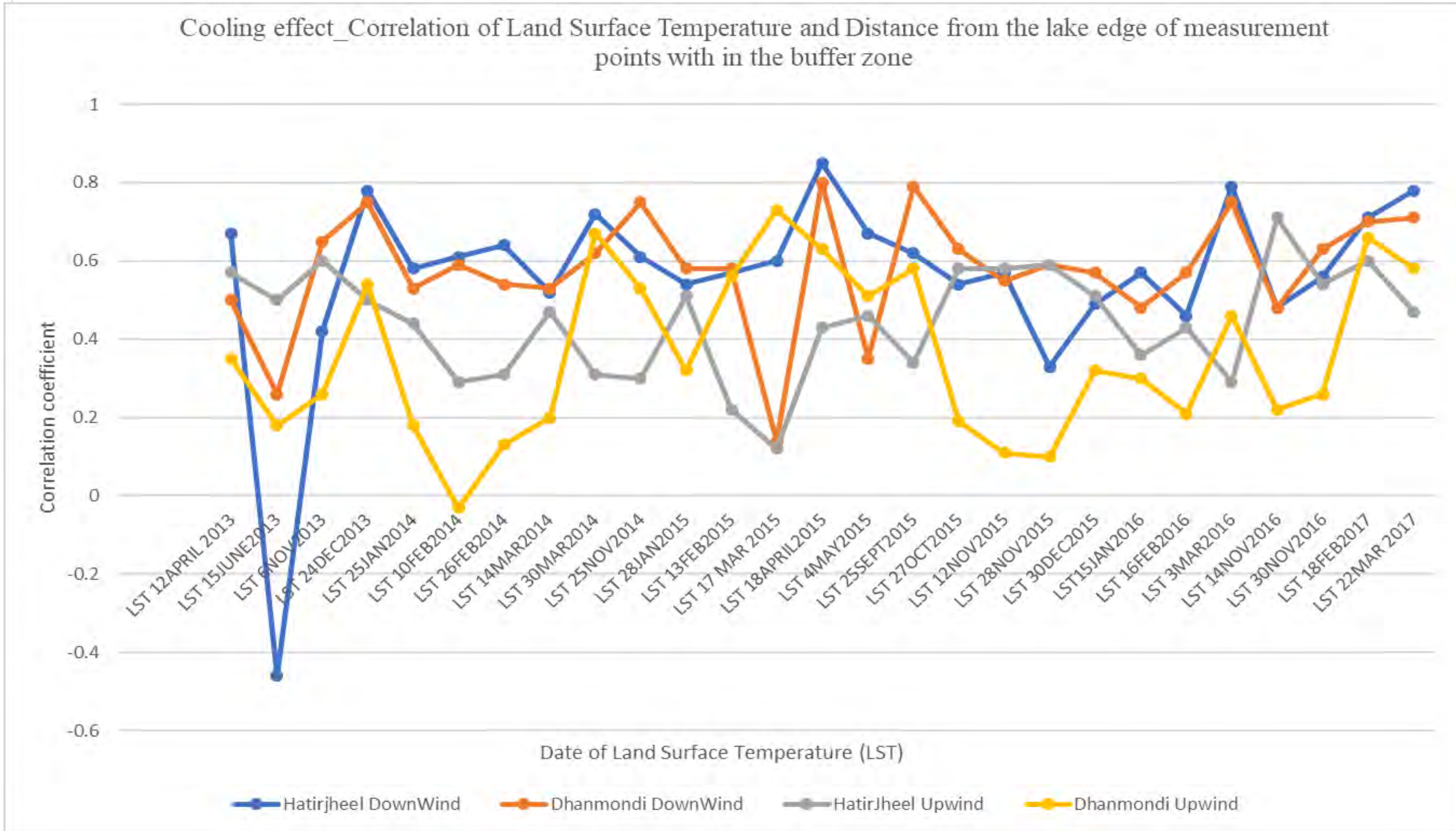

Figure 4.32: Cooling effect of the wetland

4.10 References

1. Ahmed B., Kamruzzaman M., Zhu X., Rahman S.M. and Choi K. (2013). "*Simulating Land Cover Changes and Their Impacts on Land Surface Temperature in Dhaka, Bangladesh*". *Remote Sens.*, 5, 5969-5998; doi:10.3390/rs5115969.
2. Chen X.L., Zhao H.M., Li P.X., Yin Z.Y. (2006). *"Remote sensing image-based analysis of the relationship between urban heat island and land use/cover changes".* Remote Sensing of Environment 104, 133–146.
3. Carlson T.N., Riziley D.A. (1997). "*On the Relation between NDVI, Fractional Vegetation Cover, and Leaf Area Index"*. Remote Sensing of Environment, 62, pp. 241–252.
4. Finding values for $ESUN_\lambda$
   "Remote Sensing of Environment" 113(2009) 893-903
   http://landsathandbook.gsfc.nasa.gov/pdfs/Landsat_Calibration_Summary_RSE.pdf
5. Finding the Julian day (day of the year) http://amsu.cira.colostate.edu/julian.htm
6. Finding the distance between the Sun and Earth for a Julian day:
   http://landsathandbook.gsfc.nasa.gov/data_prod/prog_sect11_3.html
7. H. Xu (2008). "*A new index for delineating built-up land features in satellite imagery*". International Journal of Remote Sensing, 29:14, 4269-4276
8. Hanqiu Xu (2006). "*Modification of normalized difference water index (NDWI) to enhance open water features in remotely sensed imagery"*, International Journal of Remote Sensing, 27:14, 3025-3033, DOI: 10.1080/01431160600589179
9. Hung T, Uchihama D, Ochi S, Yasuoka Y. (2006) "*Assessment with satellite data of the urban heat island effects in Asian mega cities"*. Int. J Appl. Earth Obs; 8:34e48.
10. Iino A., Hoyano A. *"Development of a method to predict the heat island potential using remote sensing and GIS data"*. Energy and Buildings 23 (1996) 199-205, Elsevier.
11. Kadygrov, E.N. 2006. "*Operational Aspects of Different Ground-Based Remote Sensing Observing Techniques for Vertical Profiling of Temperature, Wind, Humidity and Cloud Structure"*. IOM Report No. 89, WMO/TD No. 1309. Available from: http://www.wmo.int/web/www/IMOP/publications-IOM-series.html
12. Kato S., Yamaguchi Y (2007). "*Estimation of storage heat flux in an urban area using ASTER data"*. Remote Sensing of Environment 110, 1–17.
13. Liang, S. (2000). *"Narrowband to broadband conversions of land surface albedo I algorithms."* Remote Sensing of Environment 76, 213-238.
14. Markham B.L., Barker J.L. (1985). "*Spectral characterization of the LANDSAT Thematic Mapper sensors"*. International Journal of Remote Sensing, 6:5, 697-716.
15. Masson, V. (2006). "*Urban surface modeling and the meso-scale impact of cities"*. Theoretical and Applied Climatology, 84(1-3), 35-45.
16. Mackey C.W., Lee X., Smith R.B. (2012). "*Remotely sensing the cooling effects of city scale efforts to reduce urban heat island.* Building and Environment 49, 348-358.
17. Mcfeeters, S.K., 1996, *The use of normalized difference water index (NDWI) in the delineation of open water features*. International Journal of Remote Sensing, 17, pp. 1425–1432.
18. NASA: Landsat 7 Science Data Users Handbook (2010), http://landsathandbook.gsfc.nasa.gov/pdfs/Landsat7_Handbook.pdf

19. Purevdorj T. S., Tateishi R., Ishiyama T., & Honda, Y. (1998). "*Relationships between percent vegetation cover and vegetation indices"*. International Journal of Remote Sensing, 19(18), 3519−3535.
20. R.B. Smith; (March 2010). "*The heat budget of the earth's surface deduced from space".* Centre for earth observation, Yale University.
21. Sobrino J.A., Jimenez-Munoz J.C., Paolini L. (2004). "*Land surface temperature retrieval from LANDSAT TM 5"*. Remote Sensing of Environment, 90, pp. 434–440.
22. Voogt, J.A., & Oke, T.R. 2003. "*Thermal remote sensing of urban climates"*. Remote Sensing of Environment, 86, 370–384.
23. Weng Q. (2003). "*Fractal Analysis of Satellite-Detected Urban Heat Island Effect".* Photogrammetric Engineering & Remote Sensing Vol. 69, No. 5, May 2003, pp. 555–566.
24. Weng Q., Lu D., Schubring J. (2004). "*Estimation of land surface temperature–vegetation abundance relationship for urban heat island studies"*. Remote Sensing of Environment, 89, pp. 467–483
25. Weng Q. (2001). *"A remote sensing GIS evaluation of urban expansion and its impact on surface temperature in the Zhujiang Delta, China".* International Journal of Remote Sensing. 22:10, 1999-2014, DOI: 10.1080/713860788
26. Zha Y., Gao, J., & Ni, S. (2003). "*Use of normalized difference built-up index in automatically mapping urban areas from TM imagery"*. International Journal of Remote Sensing, 24(3), 583−594.

Chapter 5 : FIELD MEASUREMENT OF URBAN COOLING ISLAND

5.1 Introduction

The main objective of the field measurement was to determine the morphological characteristics of the Urban Cooling Island (UCI) at Urban Canopy Layer (UCL). For this reason, the measurement had been carried out in the two-study area described in the previous section at the Urban Canopy Layer (UCL) at a height of 1.5m to 2m from the ground. Some measurements were also taken on top of the water surface and its edge to determine the effect of water on the air layer above it.

5.2 Methods

5.2.1 Location of the study area

Based on the Remote sensing study of chapter four, two wetlands, Dhanmondi and Hatirjheel lake of Urban Dhaka were selected for the field study. The main rationale for selecting the wetlands sites is to enable the analysis of the effect of riparian shade as Dhanmondi Lake had been chosen for its visible riparian shade and Hatirjheel lake was chosen for its absence of visible riparian shade.

Table 5.1: Simplified classification of distinct urban forms arranged in approximate decreasing order of their ability to impact local climate [Oke, 2006]

Urban Climate Zone, UCZ[1]	*Image*	*Roughness class*[2]	*Aspect ratio*[3]	*% Built (impermeable)*[4]
1. *Intensely developed urban with detached close-set high-rise buildings with cladding, e.g downtown towers*		8	> 2	> 90
2. *Intensely developed high density urban with 2 – 5 storey, attached or very close-set buildings often of brick or stone, e.g. old city core*		7	1.0 – 2.5	> 85
3. *Highly developed, medium density urban with row or detached but close-set houses, stores & apartments e.g. urban housing*		7	0.5 – 1.5	70 - 85
4. *Highly developed, low or medium density urban with large low buildings & paved parking, e.g. shopping mall, warehouses*		5	0.05 – 0.2	70 - 95
5. *Medium development, low density suburban with 1 or 2 storey houses, e.g. suburban housing*		6	0.2 – 0.6, up to >1 with trees	35 - 65
6. *Mixed use with large buildings in open landscape, e.g. institutions such as hospital, university, airport*	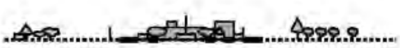	5	0.1 – 0.5, depends on trees	< 40
7. *Semi-rural development, scattered houses in natural or agricultural area, e.g. farms, estates*		4	> 0.05, depends on trees	< 10

Key to image symbols: buildings; vegetation; impervious ground; pervious ground

[1] A simplified set of classes that includes aspects of the schemes of Auer (1978) and Ellefsen (1990/91) plus physical measures relating to wind, thermal and moisture controls (columns at right). Approximate correspondence between UCZ and Ellefsen's urban terrain zones is: 1(Dc1, Dc8), 2 (A1-A4, Dc2), 3 (A5, Dc3-5, Do2), 4 (Do1, Do4, Do5), 5 (Do3), 6 (Do6), 7 (none).
[2] Effective terrain roughness according to the Davenport classification (Davenport *et al.*, 2000); see Table 2.
[3] Aspect ratio = z_H/W is the average height of the main roughness elements (buildings, trees) divided by their average spacing, in the city center this is the street canyon height/width. This measure is known to be related to flow regime types (Oke 1987) and thermal controls (solar shading and longwave screening) (Oke, 1981). Tall trees increase this measure significantly.
[4] The average proportion of ground plan covered by built features (buildings, roads, paved and other impervious areas) the rest of the area is occupied by pervious cover (green space, water, and other natural surfaces). Permeability affects the moisture status of the ground and hence humidification and evaporative cooling potential.

As per the Urban Climate Zone (UCZ) classification by Oke (Table 5.1), the surrounding urban area of the selected Urban Wetland belongs to UCZ 2. A buffer zone of 0.5 km (fig 5.1 & 1.3) from the edge of the wetland had been taken into consideration for the field measurement as well as Remote sensing.

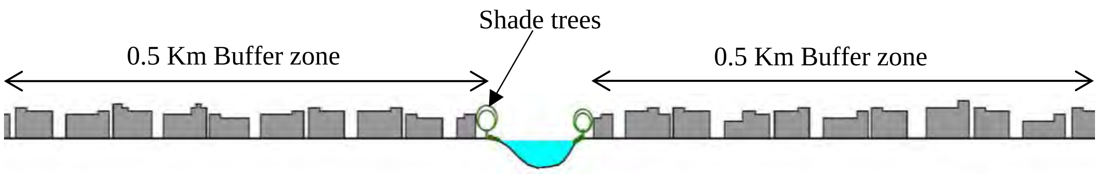

Figure 5.1: Buffer zone for field measurement

5.2.2 Physiography of the study area

The physiography of the both the wetland are same as they are located on the same physiographic regions and consequent sub regions (Brammer H., 2012). The physiographic region of the wetland is Madhupur Tract. Much of the Dhaka city lies on the Madhupur Tract, but in the map (figure 5.2), it has been shown separately. Next important locational information is that, both the lakes are located on the same overall geothermal gradient zone (Akbar M.A.,2011). From the above information it could be safely deduce that in terms of heat gain from the ground source both Dhanmondi and Hatirjheel lakes are in the same category, that means if they gain heat from the ground that will be in the same rate. In fact, they won't get any heat at all from the ground source as the geothermal potential in this location is not high enough. So, it is only the differential shading pattern, due to the big riparian shading and the built form, will create differential solar gain for both the lake.

5.2.3 Date and time of data logging

Dates for the field measurement were selected from three design seasons of Dhaka, which are Hot Dry (March-May), Warm Humid (June-November) and Cold Dry (December-February). For all the measurement, the sky was mostly free of cloud with bright sunlight. Data logging was done from morning to sunset on the following dates, at Dhanmondi Lake site on 21 Oct 2016 and 24 Feb 2017; at Hatirjheel lakeside on 11 Nov 2016 and 10 Feb 2017. One additional Data logging was done on 13 Dec 2016 at Hatirjheel lake site. On this date simultaneously one data logger was placed inside Stevenson Screen at the measurement point of Bangladesh Meteorological Department (BMD) at Agargaon together with instruments of BMD from 12 Dec 2016 11:00 am to 14 Dec 2016 11:00 am for calibration of the instrument used in the study and also as a reference measurement.

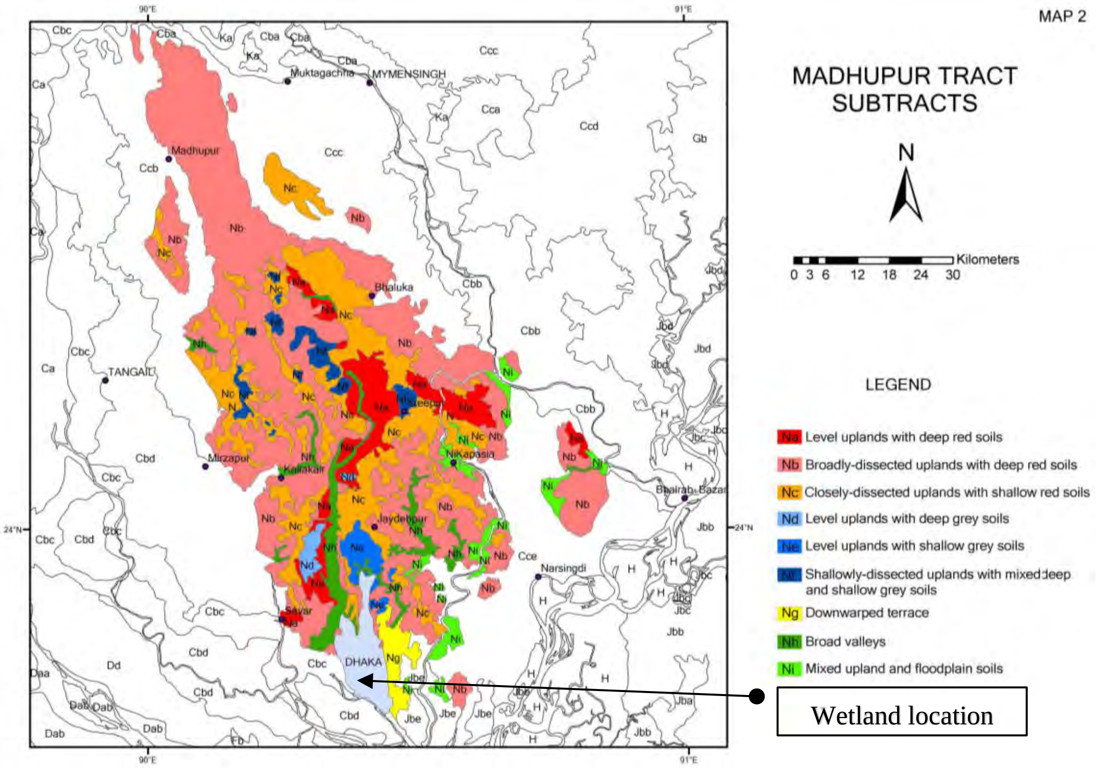

Figure 5.2: Physiographic region of the wetland area (Brammer H.,2012)

5.2.4 Characteristics of the urban stations

Dhanmondi Lake urban Stations:

The locations of the urban stations chosen for field measurement are shown on the google earth image (fig.5.3) In case of Dhanmondi lake, all the urban stations except one (UCILogger4) were installed along the path of prevailing wind direction form the lake. The urban station UCILogger4 was placed in a road deep inside the urban fabric which was perpendicular to the prevailing wind direction. One urban station UCIlogger1 was placed on a small island inside the lake.

Figure 5.3: Location of the Urban stations of field measurement at Dhanmondi Lake on 24 February 2017

Figure 5.4: View of the Dhanmondi Lake on 24 February 2017

Following three tables (5.2,5.3 and 5.4) provides detail information of each urban stations in each measurement day of the Dhanmondi Lake area.

Table 5.2: Data Logger Location at Dhanmondi Lake area_21 October 2016

Sl	Logger Name	Location and Physical Characteristics of location	Location Photo	Geographical Co-ordinates	Duration of the Data Logging
1	UCI Logger1	Island 1_near road 6A & 5A. On the edge of a small island, at the middle of the lake under tree shade		Latitude 23°44'35.84"N Longitude 90°22'38.98"E	Start: 7:50 am Finish: 5:30 pm
2	UCI Logger2	Local play ground_Rd # 4, south eastern side. Bamboo tripod mounted (at 1.8m height) in a partly grass-covered ground surface under the shade of a tree, two air corridors from the lake: 330m from the edge of the water in western direction. 327m in the northern direction 291m directly from the water edge		Latitude 23°44'28.12"N Longitude 90°22'49.25"E	Start: 9:03 am Finish: 5:30 pm
3	UCI Logger4	the crossing of Road 8A &10A. Bamboo tripod mounted (at 1.8m height) in a partly grass-covered ground surface under the shade of a tree, Deep in the urban fabric with no direct air corridor from the lake to the point. Approx.420m distance directly from the edge of the lake water in the North-Eastern direction (Heading 112 degree).		Latitude 23°44'43.11"N Longitude 90°22'29.06"E	Start: 8:27 am Finish: 5:30 pm
4	UCI Logger6	Road 8A near Rabindra Sorobor. Bamboo tripod mounted (at 1.8m height) on paved footpath under the shade of a tree, two air corridors from the lake: 157m from the edge of the water in North-Eastern direction.		Latitude 23°44'45.80"N Longitude 90°22'34.01"E	Start: 8:13 am Finish: 5:30 pm
5	UCI Logger7	Junction Road 10A & Sultana Kamal Mohila Complex. Bamboo tripod mounted (at 1.8m height) in a partly grass-covered ground surface under the shade of a tree, with a direct air corridor from the lake to the point. Approx.265m distance from the edge of the lake water along the air corridor in North-Eastern direction.		Latitude 23°44'53.71"N Longitude 90°22'32.77"E	Start: 9:41 am Finish: 5:30 pm

Table 5.3: Data Logger Location at Dhanmondi Lake area_27 January 2017

Sl.	Logger Name	Location and Physical Characteristics of location	Geographical Co-ordinates	Duration of the Data Logging
1	UCILogger1	Middle of bridge between Island and road 6A. 1.1 m from the top of water surface, suspended with the help of a rope.	Latitude 23.743354 Longitude 90.377209	Start: 9:03 am Finish: 5:00pm
2	UCILogger2	Rabindra shorobor water edge tied with the branch of a banyan tree. 0.8m from the top of water surface.	Latitude 23.744261 Longitude 90.376882	Start: 11:25 am Finish: 5:00pm
3	UCILogger3	PWD playfield. on a partly grass-covered ground surface under the shade of a tree, two air corridors from the lake: 330m from the edge of the water in western direction. 327m in the northern direction Height: 1.8m from ground surface	Latitude 23.740808 Longitude 90.380631	Start: 10:34 am Finish: 5:00pm
4	UCILogger4	the crossing of Road 8A &10A. Ventilated Box mounted (at 1.8m height) in a partly grass-covered ground surface under the shade of a tree, Deep in the urban fabric with no direct air corridor from the lake to the point. Approx.420m distance directly from the edge of the lake water in the North-Eastern direction (Heading 112 degree).	Latitude 23.747157 Longitude 90.373729	Start: 9:47 am Finish: 5:00pm
5	UCILogger5	Island in between road 6A and Sudha Sadan. On the edge of a small island, at the middle of the lake under tree shade. 1m from the ground surface, tied with a branch of shrubs	Latitude 23.743262 Longitude 90.377415	Start: 9:10am Finish: 5:00pm
6	UCILogger6	Road 8A near Rabindra Sorobor. Ventilated Box mounted (at 1.8m height) on paved footpath under the shade of a tree, two air corridors from the lake:120m from the edge of the water in North-Eastern direction.120m on South-Eastern direction.	Latitude 23.746108 Longitude 90.376076	Start: 9:20 am Finish: 5:00pm
7	UCILogger7	Junction Road 10A & Sultana Kamal Mohila Complex. Ventilated Box mounted (at 1.6m height) in a partly grass-covered ground surface under the shade of a tree, with a direct air corridor from the lake to the point. Approx.230m distance from the edge of the lake water along the air corridor in North-Eastern direction.	Latitude 23.748209 Longitude 90.375590	Start: 9:37 am Finish: 5:00pm
8	UCILogger8	Middle of bridge between Kalabagan field island and road 12A. Height .85 m from the water surface, suspended with the help of a rope.	Latitude 23.747981 Longitude 90.3784	Start: 10:09 am Finish: 5:00pm

Sl.	Logger Name	Location and Physical Characteristics of location	Geographical Co-ordinates	Duration of the Data Logging
9	UCILogger9	island behind Kalabagan field. Height 1m from ground surface	Latitude 23.747870 Longitude 90.378587	Start: 10:09 am Finish: 5:00pm

Table 5.4: Data Logger Location at Dhanmondi Lake area_2**4 February** 201**7**

Sl	Logger Name	Location and Physical Characteristics of location	Geographical Co-ordinates	Duration of the Data Logging
1	UCILogger1	Island in between road 6A and Sudha Sadan. Ventilated Box mounted. On the edge of a small island, at the middle of the lake under tree shade. 1m from the ground surface, tied with a branch of shrubs	Latitude 23.743302 Longitude 90.377449	Start 7:35 am Finish 6:00pm
2	UCILogger1_ Extech Dual Sensor	Island in between road 6A and Sudha Sadan. Handheld. On the edge of a small island, at the middle of the lake under tree shade. 1m from the ground surface, tied with a branch of shrubs	Latitude 90.377449 Longitude 23.743302	Start 7:45am Finish 6:00pm
3	UCILogger2	Rabindra Sorobor water edge tied with the branch of a banyan tree. Ventilated Box mounted. 0.8m from the top of water surface.	Latitude 23.744261 Longitude 90.376882	Start 7:55 am Finish 6:00pm
4	UCILogger2_ Extech Thermo-anemometer	Rabindra Sorobor water. Handheld. 1.5m from the top of the ground surface.	Latitude 23.744261 Longitude 90.376882	Start 11:50 am Finish 6:00pm
5	UCILogger3	Rabindra Sorobar restaurant, Junction of road 7A. Ventilated Box mounted (at 1.8m height) under the shade of a tree, exposed to direct air from the lake: 80m from the edge of the water in North-western direction.	Latitude 23.745408 Longitude90. 376686	Start 9:10 am Finish 6:00pm
6	UCILogger4	the crossing of Road 8A &10A. Ventilated Box mounted (at 1.8m height) in a partly grass-covered ground surface under the shade of a tree, Deep in the urban fabric with no direct air corridor from the lake to the point. Approx.420m distance directly from the edge of the lake water in the North-Eastern direction (Heading 112 degree).	Latitude 23.747157 Longitude 90.373729	Start 8:32 am Finish 6:00pm
7	UCILogger6	Road 8A near Rabindra Sorobor. Ventilated Box mounted (at 1.8m height) on paved footpath under the shade of a tree, two air corridors from the lake: 120m from the edge of the water in North-Eastern direction. 120m on South-Eastern direction.157m directly from the edge.	Latitude 23.745942 Longitude 90.376096	Start 9:25 am Finish 6:00pm

Sl	Logger Name	Location and Physical Characteristics of location	Geographical Co-ordinates	Duration of the Data Logging
8	UCILogger7	Junction Road 10A & Sultana Kamal Mohila Complex. Ventilated Box mounted (at 1.6m height) in a partly grass-covered ground surface under the shade of a tree, with a direct air corridor from the lake to the point. Approx.265m distance from the edge of the lake water along the air corridor in North-Eastern direction.	Latitude 23.748209 Longitude 90.375590	Start 8:25am Finish 6:00pm
9	UCILogger8	At the junction between road 9A & 11A, South-West corner of Sultana Kamal Mohila complex. Height 1.6 m from the footpath. 160m from the edge of the water in North-Western direction.	Latitude 23.747469 Longitude 90.376386	Start 8:45 am Finish 6:00pm

Hatirjheel Lake Urban Stations:

In case of Hatirjheel Lake, one urban station UCILogger1 was suspended form the middle of the Mahanagar Bridge above the water of the lake. Urban station UCILogger2 placed beside the Lake edge. Two Urban stations (UCILogger8 & 3) placed inside and the edge of the park beside the lake. Rest of the Urban stations are placed along a road parallel to the prevailing wind direction. All the location of the urban stations except UCILogger1 could be seen in the google-earth image of figure 5.5.

Figure 5.5: Location of the Urban stations of field measurement at Hatirjheel Lake on 10 February 2017

Figure 5.6: Hatirjheel Lake on 10 February 2017

Following three tables (5.5,6 and 7) provides detail information of each urban stations in each measurement day of the Hatirjheel Lake area.

Table 5.5:Data Logger Location at Hatirjheel Lake area_11 November 2016

Sl	Logger Name	Location and Physical Characteristics of location	Location Photo	Geographical Co-ordinates	Duration of the Data Logging
1	UCILogger1	Mahanagar Bridge (Bridge 2). Suspended from the middle of the bridge at the top of water surface		Latitude 23.768043 Longitude 90.413047	Start 9:25 am Finish 5:15 pm
2	UCILogger2	Gulshan 1 park, opposite of shooting club. Bamboo tripod mounted in a partly grass-covered ground surface under the shade of tree, 190m from the edge of the water in southern direction		Latitude 23.773993 Longitude 90.415802	Start 7:25 am Finish 5:15 pm

Sl	Logger Name	Location and Physical Characteristics of location	Location Photo	Geographical Co-ordinates	Duration of the Data Logging
3	UCILogger6	HatirJheel Link Road South Badda side. Bamboo tripod mounted at the edge of water		Latitude 23.770620 Longitude 90.420367	Start 8:25 am Finish 5:15 pm
4	UCILogger7	Roundabout, South Badda road. Bamboo tripod mounted on bare ground, 100 m from the edge of water		Latitude 23.772746 Longitude 90.418953	Start 8:40 am Finish 5:15 pm
5	UCILogger8	At the junction of Road 2 and Road 4 of Gulshan 1. Bamboo tripod mounted on roadside paved footpath, 425 m from the lake in southern direction and 110 m from the lake edge in western direction.		Latitude 23.776434 Longitude 90.414946	Start 9:03 am Finish 5:15 pm

Table 5.6: Data Logger Location at Hatirjheel Lake area_13 December 2016

Sl	Logger Name	Location and Physical Characteristics of location	Location Photo	Geographical Co-ordinate	Duration of the Data Logging
1	UCILogger1	Mahanagar Bridge (Bridge 2). Handheld Suspended from the middle of the bridge at 6m_above the top of water surface		Latitude 23.768043 Longitude 90.413047	Start 10:10 am Finish 5:00 pm
2	UCILogger2	Gulshan 1 park, opposite of shooting club. Cased inside ventilated Hard Paper box and tied to the branch of shrub, in a partly grass-covered ground surface under the shade of tree, 190m from the edge of the water in southern direction		Latitude 23.773993 Longitude 90.415802	Start 8:15 am Finish 5:00 pm

Sl	Logger Name	Location and Physical Characteristics of location	Location Photo	Geographical Co-ordinate	Duration of the Data Logging
3	UCILogger6	4.49m downwards from the top of Mahanagar Bridge (Bridge 2). Cased inside ventilated Hard Paper box, Suspended from the middle of the bridge at 1.63m_above the top of water surface		Latitude 23.768043 Longitude 90.413047	Start 8:49 am Finish 5:00 pm
4	UCILogger7	2m downwards from the top of Mahanagar Bridge (Bridge 2). Cased inside ventilated Hard Paper box, Suspended from the middle of the bridge at 4.12m_above the top of water surface.		Latitude 23.768043 Longitude 90.413047	Start 8:55 am Finish 5:00 pm
5	UCILogger8	Bangladesh Meteorological Department, Agargaon Dhaka. Placed inside the Stevenson screen of the BMD beside the office instrument (Thermometer and Hygrometer) used to collect meteorological data.		Latitude 23.779854 Longitude 90.378410	Start 12:00 pm at 13/12/2016. Finish 11:00 am at 14/12/2016

Table 5.7: Data Logger Location at Hatirjheel Lake area_10 February 2017

Sl	Logger Name	Location and Physical Characteristics of location	Location Photo	Geographical Co-ordinate	Duration of the Data Logging
1	UCILogger 1	Mahanagar Bridge (Bridge 2). Suspended from the middle of the bridge at 6m_above the top of water surface		Latitude 23.768043 Longitude 90.413047	Start 8:19 am Finish5: 50pm
2	UCILogger 1_Extech Dual Sensor	Mahanagar Bridge (Bridge 2). Suspended from the middle of the bridge at 6m_above the top of water surface		Latitude 23.768043 Longitude 90.413047	Start 8:25 am Finish5: 50 pm
3	UCILogger 2	Opposite of Police Plaza Concord. Cased inside ventilated Particle board box and tied to the branch of shrub, 1.8m above a grass-covered ground surface under the shade of tree, at the edge of the water of HatirJheel Lake.		Latitude 23.772448 Longitude 90.415489	Start 8:35 am Finish 5:50 pm
4	UCILogger 2_Extech Thermo anemometer	Opposite of police plaza Concord. Hand Held_1.2m above a grass-covered ground surface under the shade of tree, at the edge of the water of HatirJheel Lake.		Latitude 23.772448 Longitude 90.415489	Start 8:50 am Finish 5:50pm

Sl	Logger Name	Location and Physical Characteristics of location	Location Photo	Geographical Co-ordinate	Duration of the Data Logging
5	UCILogger 3	Gulshan 1 park, opposite of shooting club. Cased inside ventilated Particle board box and tied to the branch of shrub, 1.5m above a partly grass-covered ground surface under the shade of tree, 190m (155m towards east) away from the edge of the water on southern direction		Latitude 23.774313 Longitude 90.415876	Start 7:50 am Finish5: 50 pm
6	UCILogger 4	Junction between road 2 & 4. Cased inside ventilated Particle board box and tied to the trunk of the tree, 1.5m above the paved surface, approx. 425m (105m towards NW) away from the edge of the water in the southern direction and 110 m from the lake edge in the western direction.		Latitude 23.776312 Longitude 90.414983	Start 9:06 am Finish 5:50 pm
7	UCILogger 6	Junction between road 2 & 6. Cased inside ventilated Particle board box and tied to the trunk of the tree, 1.5m above the paved surface, approx. 550m (164m towards NW) away from the edge of the water in the southern direction		Latitude 23.777164 Longitude 90.415349	Start 9:17 am Finish5: 50 pm
8	UCILogger 7	Junction between road 8 & 2. Cased inside ventilated Particle board box and tied to the trunk of the tree, 1.5m above the paved surface, approx. 660m (243m towards NW) away from the edge of the water in the southern direction		Latitude 23.777975 Longitude 90.415434	Start 9:25 am Finish5: 50 pm
9	UCILogger 8	Gulshan-1 park, police plaza complex corner. Cased inside ventilated Particle board box and tied to the branch of shrub, 1.5m above a partly grass-covered ground surface under the shade of tree, approximately 120m away from the edge of the water in southern direction	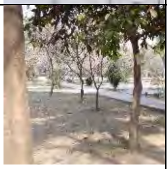	Latitude 23.773342 Longitude 90.415418	Start 9:45 am Finish5: 50 pm
10	UCILogger 8_Davis	Gulshan-1 park, police plaza complex corner. 2m above a partly grass-covered ground surface under the shade of a tree, approximately 120m away from the edge of the water in the southern direction		Latitude 23.773342 Longitude 90.415418	Start 11:30 am Finish 5:50 pm

5.2.5 Climatic variables measured

Air Temperature (Ta), Relative Humidity (RH) and wind speed (ws) inside and around the selected Urban Wetlands had been measured at selected Urban Stations (Data logging points) by continuous data logging using Fixed data logger.

5.2.6 Instruments

The instruments used for data collections are EL-USB-2-LCD Temp & RH Data Logger of Lascar Electronics, Extech 445713: Big Digit Indoor/Outdoor Hygro-Thermometer and Extech AN400 Rotating Cup Thermo-Anemometer. All the measurements were done at pedestrian level in between a height of 1.5m-2m. During the first two measurements in both the study area, the Lascar instruments were Bamboo tripod mounted in a partly grass-covered ground or paved surface under the shade of a tree. In The second two measurements, Lascar instruments were Ventilated Box mounted under the shade of a tree. In case of both the wetland all the data logging stations were selected on the downwind side of the wetland except Dhanmondi lake, where one station is chosen on the upwind side. Detail specification of the instruments are on the appendix 2.

5.3 Results from The Urban Station

All the related data from the field measurement are given in the Appendices D, E and F.

5.3.1 Reference measurement at Bangladesh Meteorological Department

As stated earlier one data logger was placed inside the Stevenson screen of the Bangladesh Meteorological department’s (BMD) measurement site at Agargaon together with the BMD’s instrument. The duration of the measurement was from 11:00 am 12 December 2016 to 11:00 am 14 December 2016. The air temperature and relative humidity data from 6:00 pm 12 December to 6:00 am 14 December 2016 of this urban station were analyzed. For the correlational analysis the data was divided into three chunks, first one was 6:00 pm 12 December to 6:00 am 13 December 2016 (Night), the second one was 6:00 am 13 December to 6:00 pm 13 December 2016 (day) and the third one was 6:00 pm 13 December to 6:00 am 14 December 2016 (Night).

The Air temperature and relative humidity showed a typical diurnal pattern (Figure 5.7). At the beginning of the day, air temperature started to rise with a pick in between 13:00 pm to 15:30 pm than started to decline again. Relative Humidity shows the opposite trend with highest at the beginning of the day and continues to decline as the day progress with the lowest in between 13:00 pm to 15:30 pm than started to rise again. Air temperature continues to decline after the sunset throughout the night with the lowest in between 05:33 am to 07:15 am. Again, relative Humidity showed the opposite trend which continued rising after sunset throughout the night with the highest in between 05:34 am to 07:15 am.

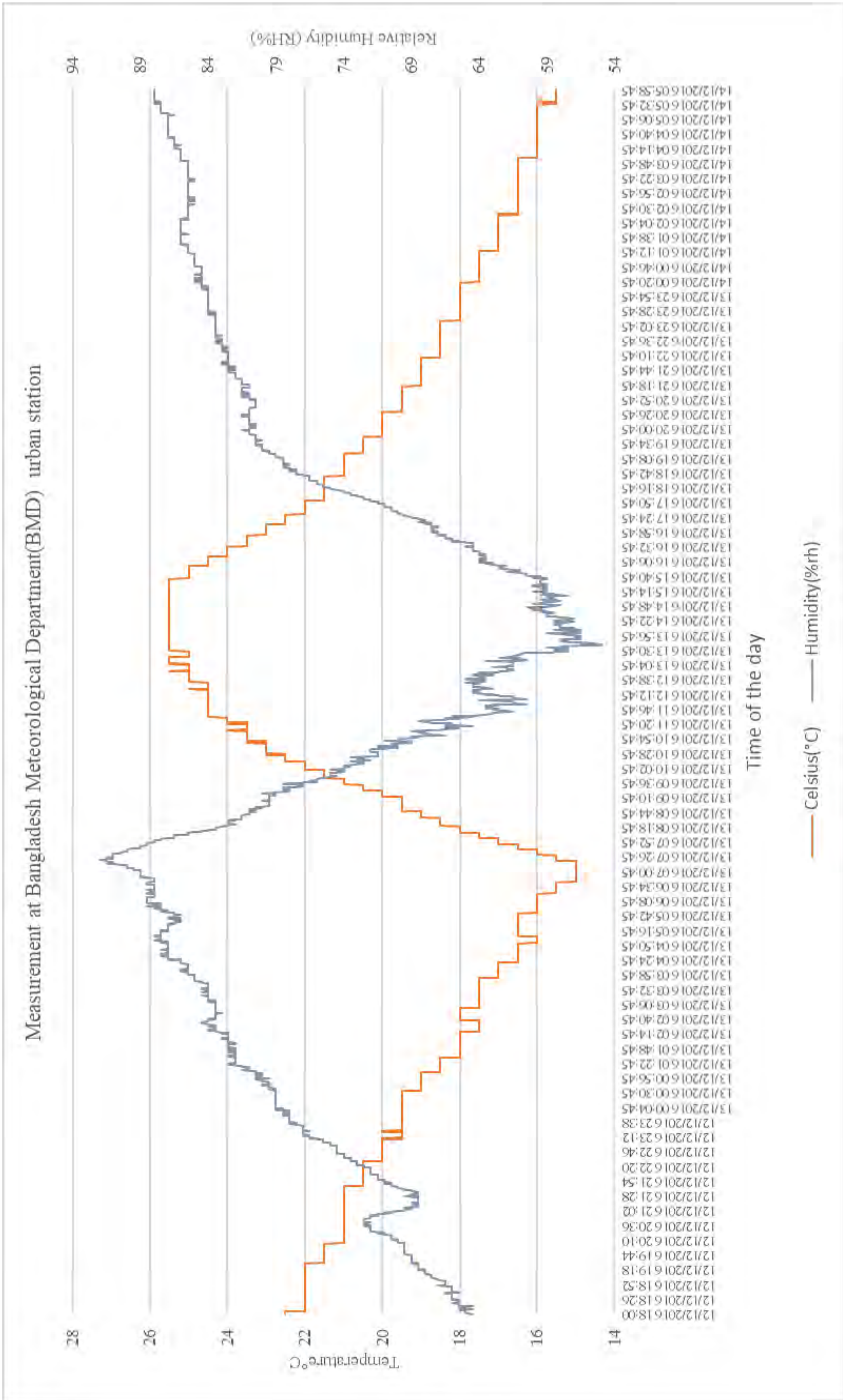

Figure 5.7: Air Temperature and Relative Humidity measurement at Bangladesh Meteorological Urban Station (BMD)

Table 5.8: Correlation coefficient of Air temperature and Relative humidity at the Bangladesh Meteorological Department urban station

Variables	6:00 pm 12 December to 6:00 am (Night)	6:00 am 13 December to 6:00 pm 13 December 2016 (Day)	6:00 pm 13 December to 6:00 am 14 December 2016 (Night)
Air Temperature (Ta)	-0.9917444	0.7866812	-0.9848626
Relative Humidity (RH)	0.9834432	-0.8062279	0.9341942

The correlation analysis had been done separately by dividing the data into the day (6:00 am to 6:00 pm) and night (6:00 pm to 6:00 am) part (table 7-8). Both the air temperature and relative humidity had shown strong correlation with cumulative time, but the correlation is opposite for air temperature and relative humidity. At the day air temperature showed strong positive correlation with cumulative time and relative humidity showed strong negative correlation with cumulative time. At the night the phenomenon changed to opposite where air temperature showed an almost negative linear relationship with cumulative time and relative humidity showed an almost positive linear relationship with cumulative time. The positive correlation of air temperature with cumulative time indicates heat gain from solar radiation whereas the negative correlation of air temperature with cumulative time indicates heat loss through longwave radiation to the sky and advection through wind flow.

When considered as a continuous independent variable rather than a categorical value Time has a cumulative effect throughout the day and night on dependent variables like Air Temperature and Relative Humidity(RH) in terms of solar influx. The strong positive correlational value in between cumulative time and air temperature showed that the rate of change in the solar influx is always positive during the daytime. Although the rate of solar influx varies throughout the day. At the beginning of the day, the solar influx started to increase as the sunrises which continue till afternoon. After that solar influx started to decrease towards zero at the sunset. The overall rate of change of solar influx throughout the day is positive. At night with the absence of sun, there is no solar influx and urban rate of heat loss from the urban fabric is constant till the sunrise.

5.3.2 Calibration of the instrument

One of the objective to place an automatic air temperature and relative humidity data logger used in this study, with the instrument of Bangladesh meteorological department (BMD) for 3 days of measurement was to calibrate the instrument. Figure 5.8 presents the results of the calibration data. The air temperature data collected by the instrument exactly matches the reading from the instrument of BMD. In case of relative humidity (RH) during the time of maximum humidity spell both the reading from the UCIL8 and BMD instrument almost same.

As the RH goes down BMD reading for RH always stays less than UCIL8 and the difference is maximum at the lowest RH spell, which is as high as 24.5 percentage point.

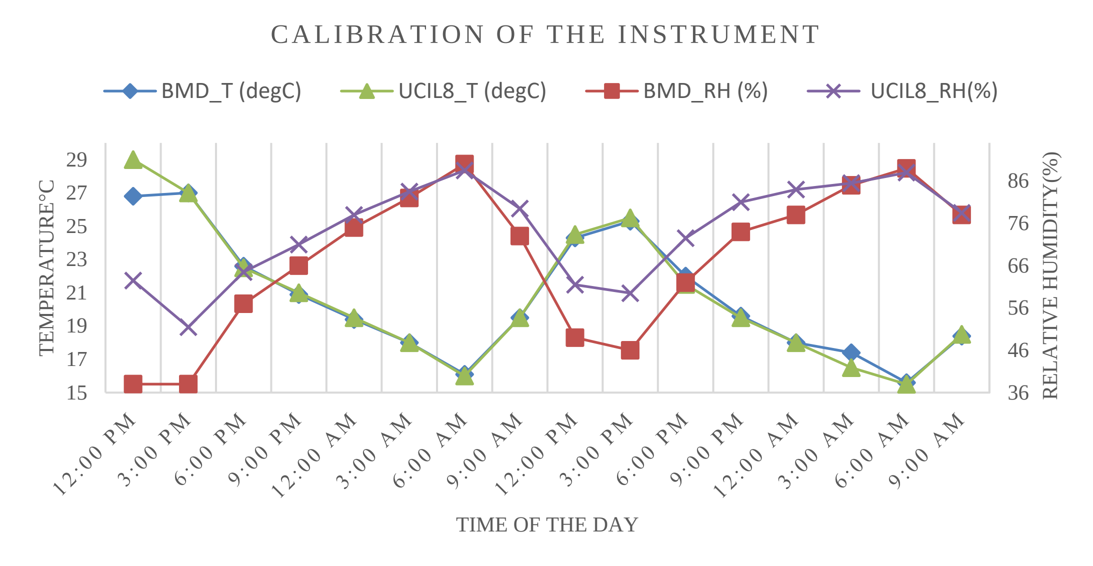

Figure 5.8: Calibration of the instrument

5.3.3 Dhanmondi Lake temperature

On 21st October 2016 during the maximum hot spell of the day (figure 5.9) which is at 3:25 pm UCILogger4 showed the maximum temperature of 35.5°C as it is in a road perpendicular to the wind direction from the lake. Among the urban stations placed in the road parallel to the wind direction UCILogger6 showed the highest temperature of 34.0°C as it was located further away from the lake edge. But being the furthest station in the wind corridor UCILogger7 was showing significantly lower temperature 32.5°C. Because this station was receiving unhindered wind flow from the lake due to wide and unobstructed road whereas wind flow to UCILoggere6 is reduced by trees, small road width and other small man-made structure. The maximum temperature of the urban station at the island UCILogger1 was 32.9°C, which was almost equal to UCILogger7. In general, UCILogger4 showed greater temperature throughout the day.

Form table 5.9 urban station UCIL1 which was on the island showed the strongest correlation in between air temperature and cumulative time. Urban stations UCIL7 showed the least correlation followed by Urban stations UCIL2 with second lowest correlational value, which indicates less heat gain in this two points or heat was being advected away. Overall all the urban stations showed a positive correlation between air temperature and cumulative time.

Table 5.9: correlation coefficient between air temperature and cumulative time of the urban stations of Dhanmondi lake on 21 October 2016

Urban stations	correlation coefficient
UCIL1(°C)	0.7287369
UCIL2(°C)	0.3943478
UCIL4(°C)	0.5682237
UCIL6(°C)	0.7629839
UCIL7(°C)	0.06319901

Figure 5.10 showing the temperature of the urban stations during measurement campaign on 27th January 2017. Urban stations UCILogger9 located on an island with no riparian shading inside the lake showing maximum temperature throughout the day. Due to the sky became cloudy from 11:00 am onwards on this measurement day the temperature difference between the different urban stations reduced with respect to previous measurement day. Even though urban station UCIL9 located in the island middle of the lake had shown a higher temperature than the other station throughout the day.

Form table 5.10 urban station UCIL9 which is on the island is showing the strongest correlation in between air temperature and cumulative time. But one important thing to observe is that the correlation between air temperature and cumulative time has been significantly changed due to the cloudy sky. The value decreased in case of Urban station UCIL4, 6 and increased in case of UCIL7. Some urban stations UCIL2,3,5 and 8 showed negative correlation, which means the state of heat loss due to the absence of sun.

Table 5.10: correlation coefficient between air temperature and cumulative time of the urban stations of Dhanmondi lake on 27 January 2017

urban stations	correlation coefficient
UCIL1(°C)	0.3637763
UCIL2(°C)	-0.7791296
UCIL3(°C)	-0.259729
UCIL4(°C)	0.4463227
UCIL5_Hh(°C)	-0.02484631
UCIL6(°C)	0.4421808
UCIL7(°C)	0.3723458
UCIL8(°C)	-0.7303561
UCIL9_Hh(°C)	0.4710534

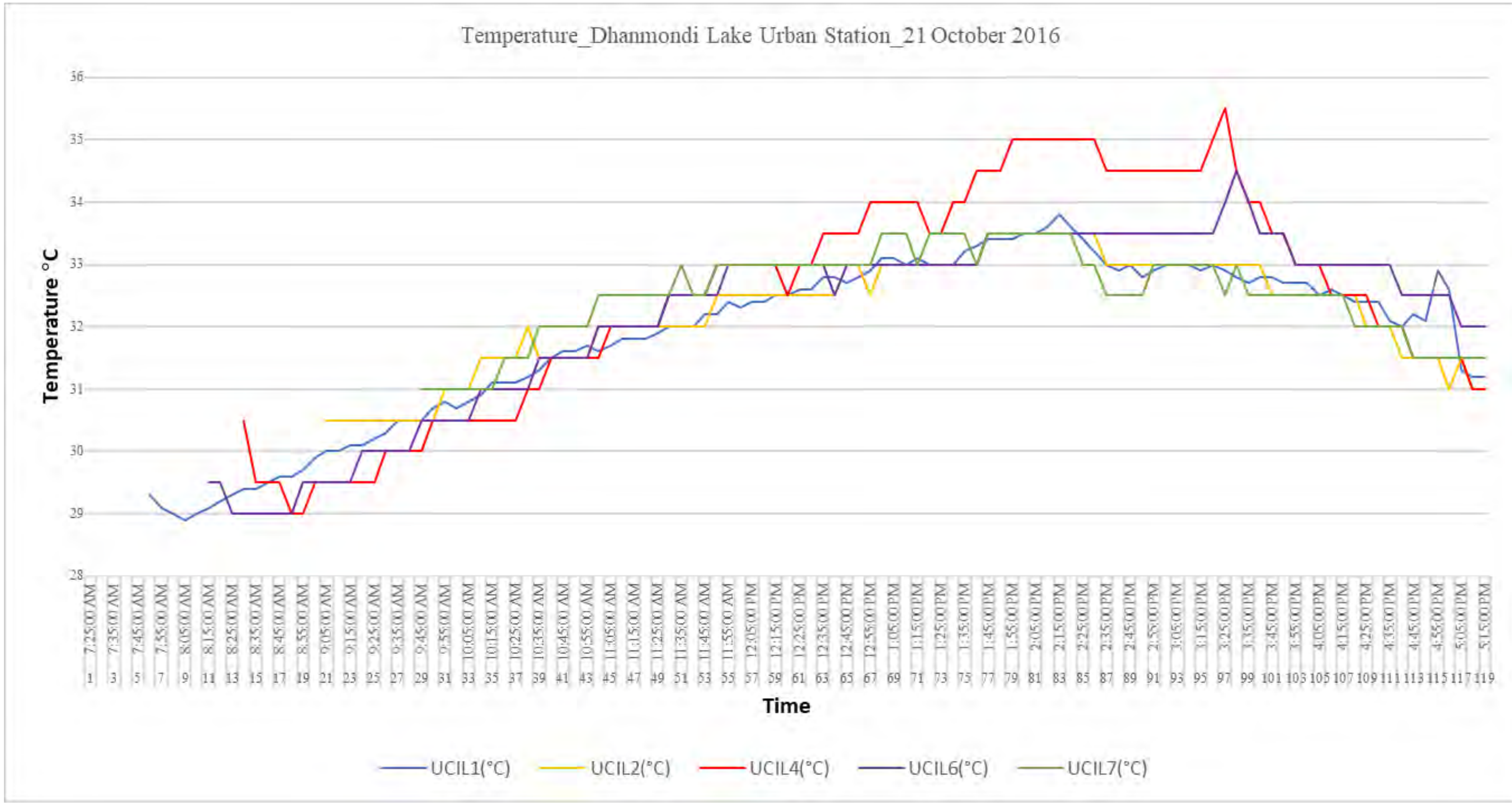

Figure 5.9: Air Temperature at Dhanmondi lake Urban stations on 21 October 2016

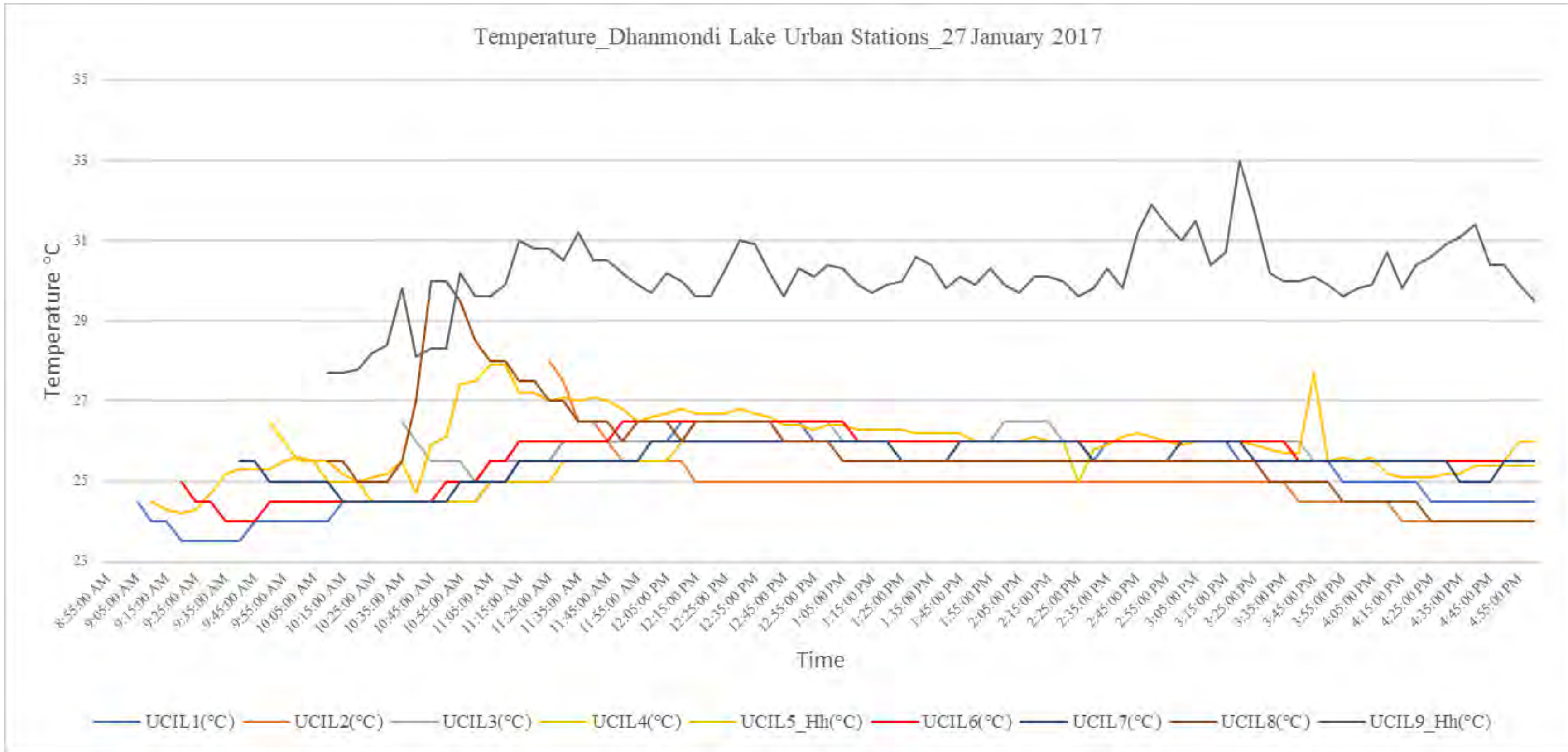

Figure 5.10: Air Temperature at Dhanmondi lake Urban stations on 27 January 2017

Figure 5.11 is showing the temperature of the urban stations during measurement campaign on 24th February 2017. On this day, during the maximum hot spell of the day which was in between 3:35 pm to 4:20 pm UCILogger4 showed the maximum temperature of 30.5°C as it is in a road perpendicular to the wind direction from the lake. Urban station UCILogger2 showed lower temperature throughout the day. Among the urban stations placed in the road parallel to the wind direction UCILogger7 and 8 exhibited the higher temperature of 28.5°C as they were located further away from the lake edge. The maximum temperature of the urban station at the island UCILogger1 is 29°C which is 0.5°C more than UCILogger7. In general, UCILogger4 showed greater temperature throughout the day.

The correlation analysis in (table 5.11 and fig. 5.12) between air temperature and cumulative time throughout the day, shows heat gain with time for all the urban station. It is important to note that urban station at the small island and water edge was on the higher side in terms of heat gain.

Table 5.11: correlation coefficient between air temperature and cumulative time of the urban stations of Dhanmondi lake on 24th February 2017

Urban Stations	Distance from the water edge	Correlation coefficient
UCIL1(°C)	0, middle	0.8550726
UCIL2(°C)	0, edge	0.8893085
UCIL3(°C)	80m	0.8769852
UCIL4(°C)	420m	0.873383
UCIL6(°C)	157m	0.7462933
UCIL7(°C)	230m	0.8052079
UCIL8(°C)	206m	0.695779

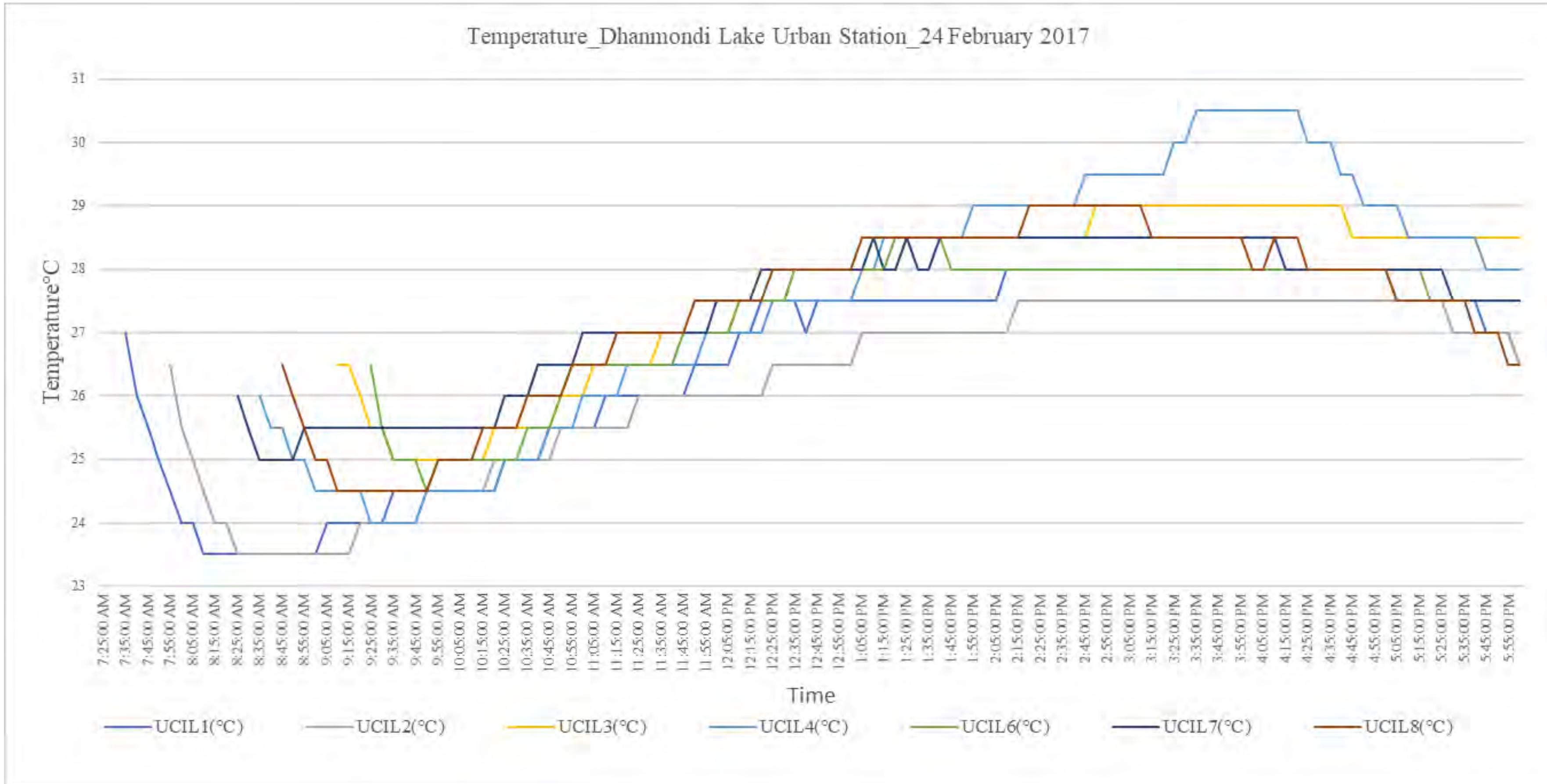

Figure 5.11: Air Temperature at Dhanmondi lake Urban stations on 24 February 2017

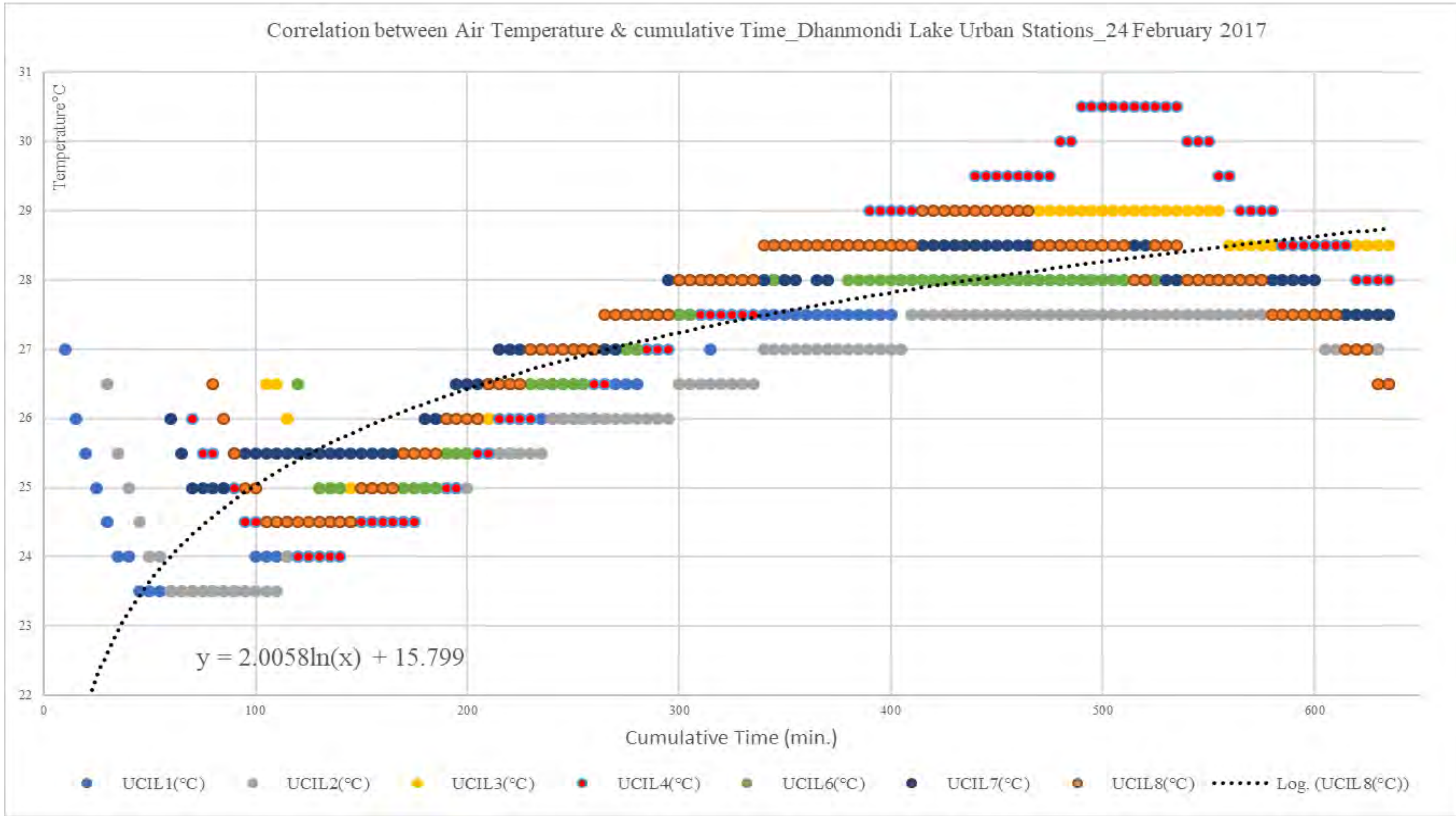

Figure 5.12: Correlation between Air Temperature & cumulative Time at Dhanmondi lake Urban stations on 24 February

5.3.4 Dhanmondi Lake relative humidity

On this measurement day of 21st October (fig. 5.13), 2016 the minimum humidity was observed throughout the day at the Urban station UCILogger1 at the island inside the lake, which was contrary to the current assumption that humidity near and over the lake should be maximum. The maximum humidity observed throughout the day are at the urban station UCILogger6 and 7. The urban station at UCILogger4 showed relatively less humidity than UCILogger6 and 7.

The correlation calculated from the observation on 21 October 2016 between cumulative time and observed relative humidity (RH) (Table 5.12) indicates negative correlation which is consistent with the reference observation made at BMD site. This negative correlation indicates the positive rate of change in the solar influx throughout the day which is opposite to the air temperature. For a particular point in the UCL the more the heat gains due to the solar radiation the less will be the RH. But this positive solar gain could be affected by other factors such as advection and shading from trees or built fabric, which is evident from the observation. From the correlation coefficient, it is evident that the highest solar gain is at the Urban station UCIL1, 4 & 6. The least solar heat gain is on the urban station UCIL7.

Table 5.12: correlation coefficient between Relative Humidity and cumulative time of the urban stations of Dhanmondi lake on 21 October 2016

Urban stations	correlation coefficient
UCIL1(%rh)	-0.5848008
UCIL2(%rh)	-0.3303872
UCIL4(%rh)	-0.5752285
UCIL6(%rh)	-0.6392395
UCIL7(%rh)	-0.08758491

Figure 5.14 showing the Relative Humidity (RH) of the urban stations during measurement campaign on 27th January 2017. As the sky becomes overcast from 11:00 am onwards the Relative Humidity (RH) measurement shows little difference. The correlation coefficient in between cumulative time and RH calculated from the observation made on 27 January 2017 is presented in table 5.13. The result in table 5.13 clearly indicates the heat loss due to the absence of solar influx as the sky became overcast. Usually, at the daytime, the RH is negatively correlated with the cumulative time due to solar influx although variable. But as the sun disappears behind the cloud direct solar gain stops immediately and net radiative loss increase immediately, which is the case in all the urban stations except UCIL4 and 6. UCIL4 and 6 were deep in the fabric and devoid of airflow from the lake. But due to heat storage by the fabric they were still gaining heat although much slower rate than before.

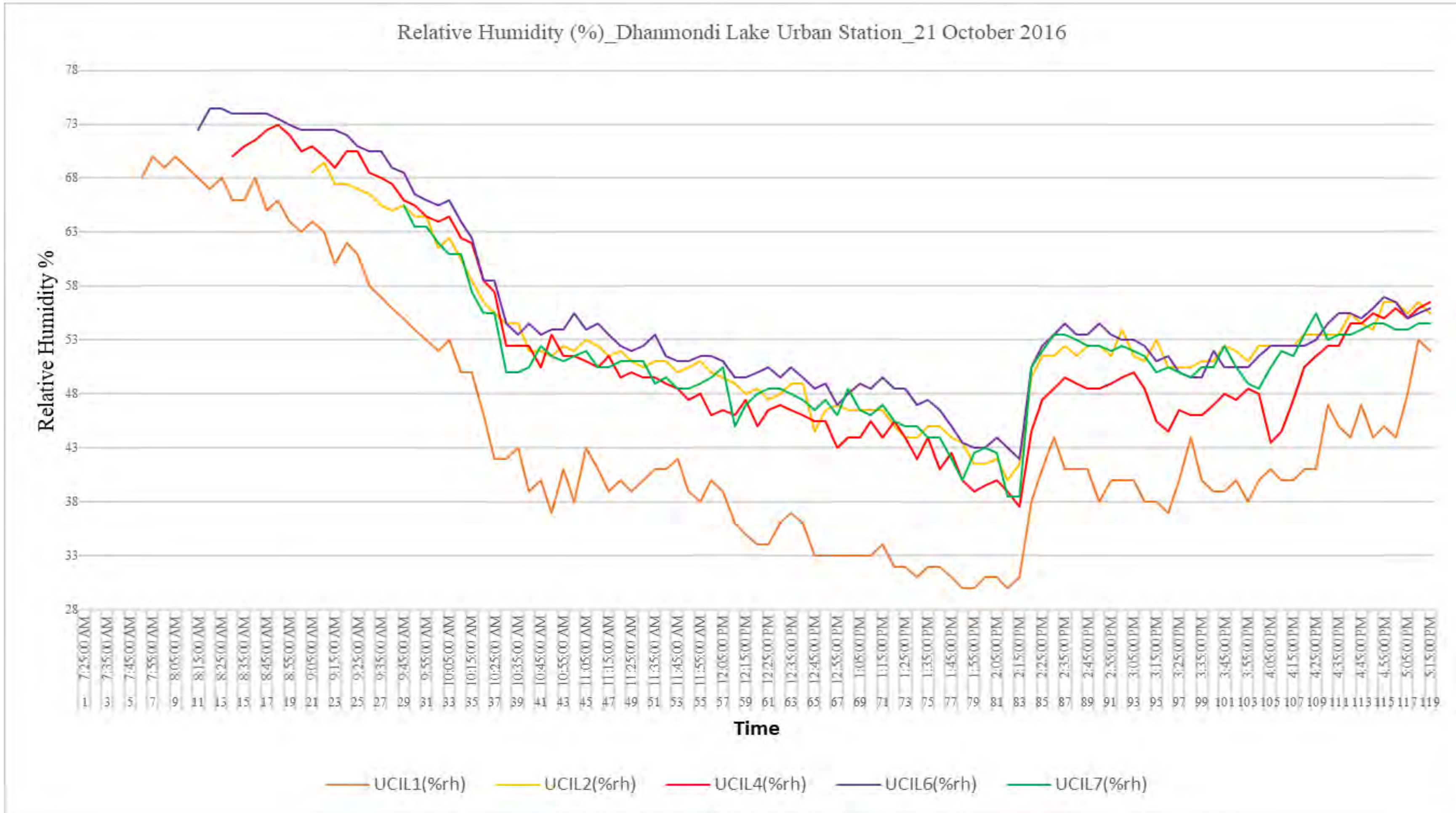

Figure 5.13: Relative Humidity at Dhanmondi lake Urban stations on 21 October 2016

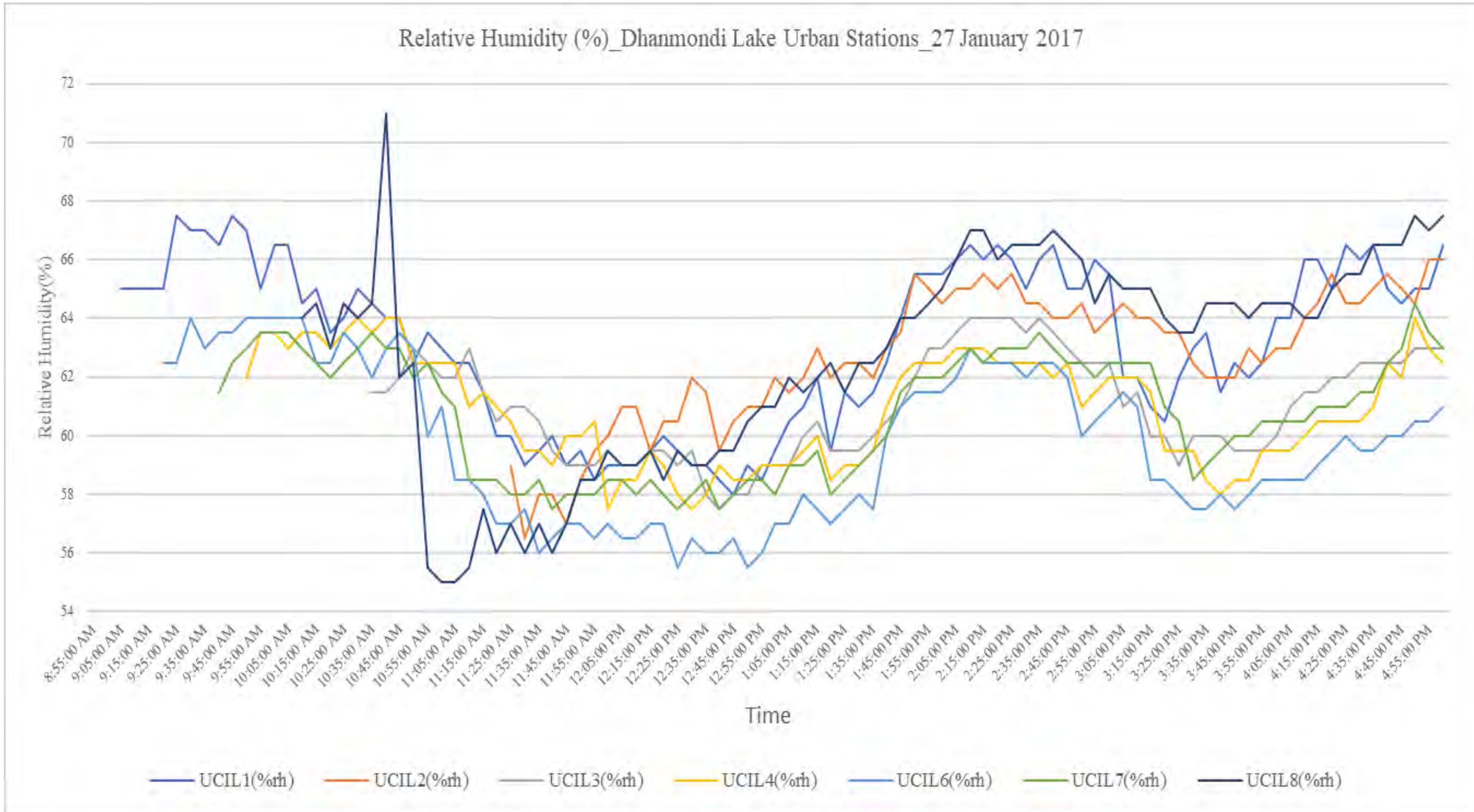

Figure 5.14: Relative Humidity at Dhanmondi lake Urban stations on 27 January 2017

Table 5.13: correlation coefficient between Relative Humidity and cumulative time of the urban stations of Dhanmondi lake on 27 January 2017

urban stations	correlation coefficient
UCIL1(%rh)	0.06428339
UCIL2(%rh)	0.7835108
UCIL3(%rh)	0.2770792
UCIL4(%rh)	-0.1739092
UCIL6(%rh)	-0.2526658
UCIL7(%rh)	0.1213577
UCIL8(%rh)	0.6251589

The observations at the urban stations made on 24 February 2017 are presented in fig.5.15 & 16. In the all the urban station relative humidity stays in its highest value at the starting of the day which decreased as the day progress. The rate of decrease ceased out in the late afternoon approximately around 03:00 pm. After 04:00 pm it started slow increase till the sunset. The lowest humidity observed is 30.5 % at 3:50 pm at the urban station 4 which is the furthest inside the urban fabric.

From the correlation coefficient calculated from the 24 February 2014 (Table 5.14) observation of the urban stations, all the urban stations are showing a negative correlation with humidity change with cumulative time. This indicates heat gain due to solar influx throughout the day and thus the drop in RH. Maximum heat gain and thus increased rate of RH drop identified at the Urban stations UCIL4 deep in the urban fabric. The second highest rate of RH drop was observed at the island urban station UCIL1. The UCIL 6, 7 and 8 are showing comparatively less RH drop as they were getting moist air directly from the lake and the RH drop increased with the distance.

Table 5.14: correlation coefficient between Relative Humidity and cumulative time of the urban stations of Dhanmondi lake on 24th February 2017

Urban Stations	Distance from the water edge	Correlation coefficient
UCIL1(%rh)	0, middle	-0.7073007
UCIL2(%rh)	0, edge	-0.5923311
UCIL3(%rh)	80m	-0.5166587
UCIL4(%rh)	420m	-0.7891712
UCIL6(%rh)	157m	-0.2328342
UCIL7(%rh)	230m	-0.6613266
UCIL8(%rh)	206m	-0.4341711

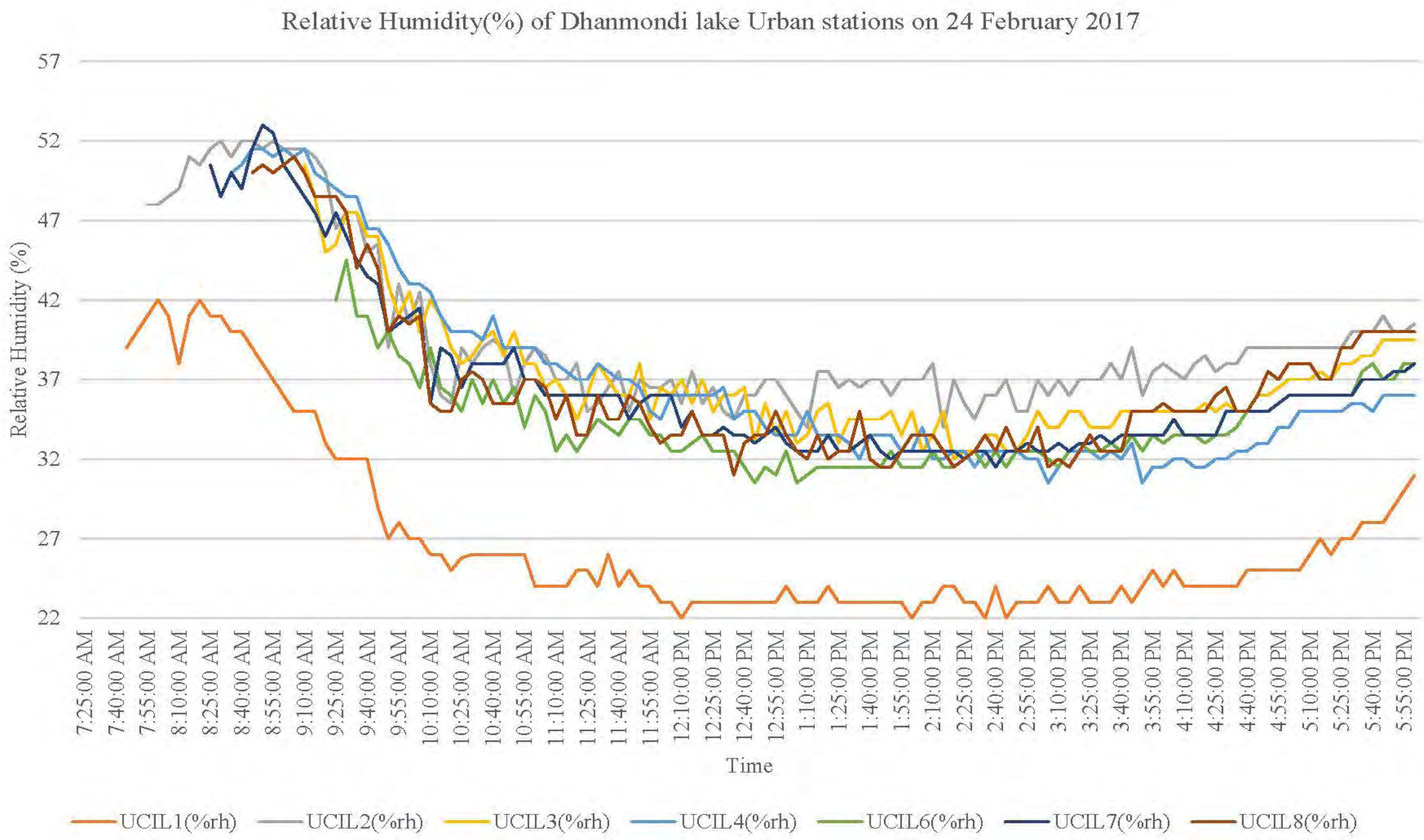

Figure 5.15: Relative Humidity at Dhanmondi lake Urban stations on 24 February 2017

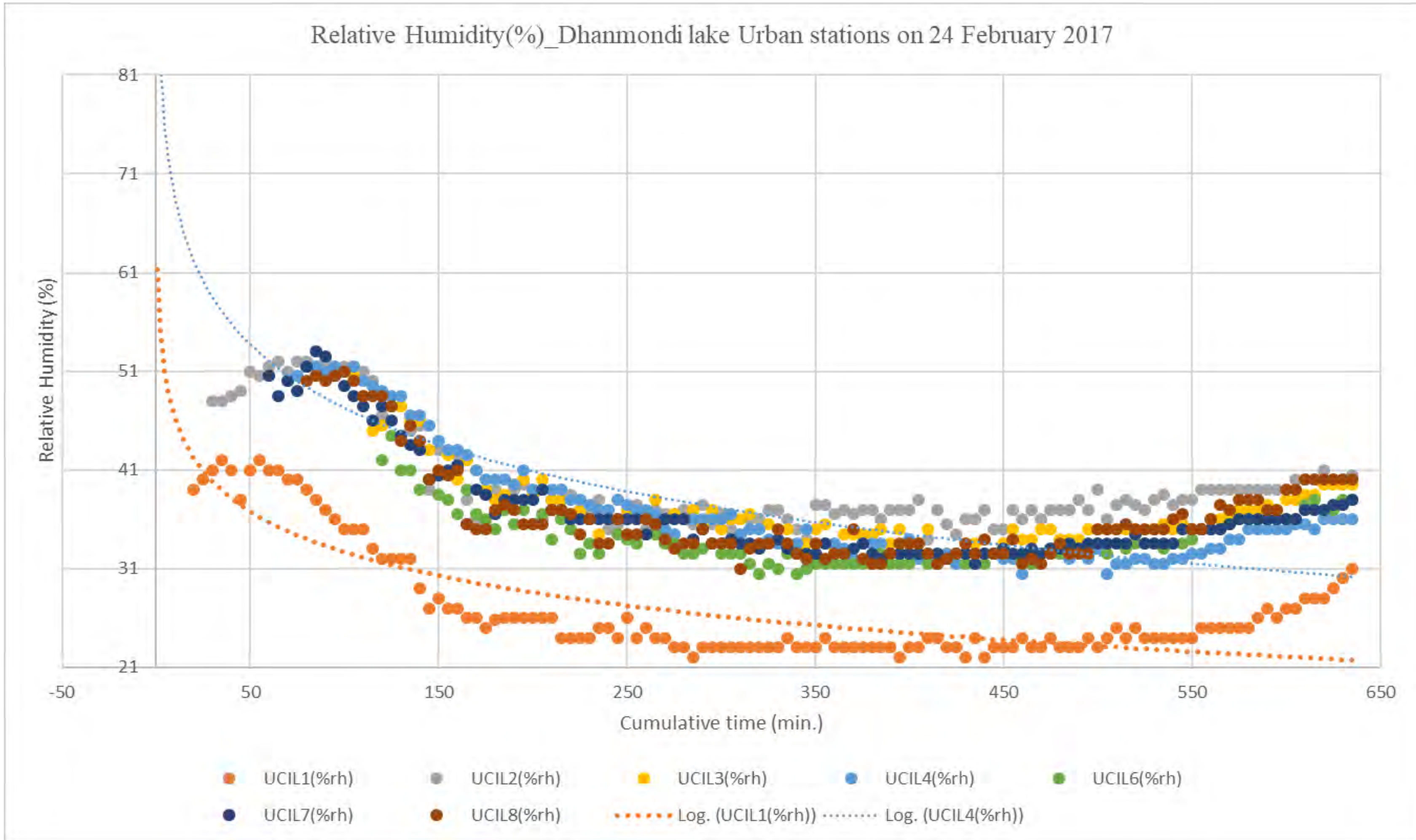

Figure 5.16: Correlation between Relative Humidity & cumulative Time at Dhanmondi lake Urban stations on 24 February 2017

5.3.5 Hatirjheel Lake temperature

The observation result (figure 5.17) on 11 November 2016 at the Hatirjheel lake Urban stations demonstrated one of the advective effect named “Oasis effect” in an urban area due to the presence of an urban park. The trees in the park reduced solar gain through shading and evapotranspiration. Otherwise, Hatirjheel lake area is mostly devoid of significantly large trees for evapotranspiration and shading at UCL. The Urban station UCIL2 located at the edge of the park on the downwind side showed overall lower temperature than the others. The urban station UCIL1 showed higher temperature with some unusual high peak due to the location was on the top of the water of the lake on a bridge without any shading. Also, the passing vehicle was also contributing to sudden peak in temperature. But overall UCIL1 is showing higher temperature. Although being inside the fabric and without significant tree shading UCIL8 showed comparatively lower temperature due to the canyon shading at the UCL.

The correlation analysis (Table 5.15) in between cumulative time and air temperature for all the urban stations on 11 November 2016 showed moderately positive correlation except for the urban station UCIL8. Being the furthest from the water edge its showed almost zero correlation which indicates neither heat gain nor heat loss. One reason is that due to its location on an Urban canopy of the north-south elongated road at this time of the year, it stays mostly in shade throughout the day. The urban stations in the middle of the lake and water edge showed moderate correlation, which indicates solar gain throughout the day.

Table 5.15: correlation coefficient between air temperature and cumulative time of the urban stations of Hatirjheel lake on 11th November 2016

Urban Statins	Distance from the water edge	correlation coefficient
UCIL1(°C)	0m, middle	0.560289187
UCIL2(°C)	190m, park	0.546136277
UCIL6(°C)	0m, edge	0.52784335
UCIL7(°C)	100m	0.386346895
UCIL8(°C)	425m	-0.035748094

On 13 December 2016 (fig 5.18), one of the urban station UCIL8 was at the Bangladesh meteorological department site with their instrument. This was done to consider it as a reference point and also for calibration purpose. Among the four Urban stations at Hatirjheel lake area three stations UCIL1,6 & 7 are hanged from a bridge in the middle of the lake at a different level from the top of the water surface. UCIL2 was placed at the edge of the park like before on the downwind side of the park. At the urban stations at Hatirjheel lake area, UCIL2 showed maximum temperature during the hottest spell of the day. The urban stations in the middle of the water behaved in a similar manner.

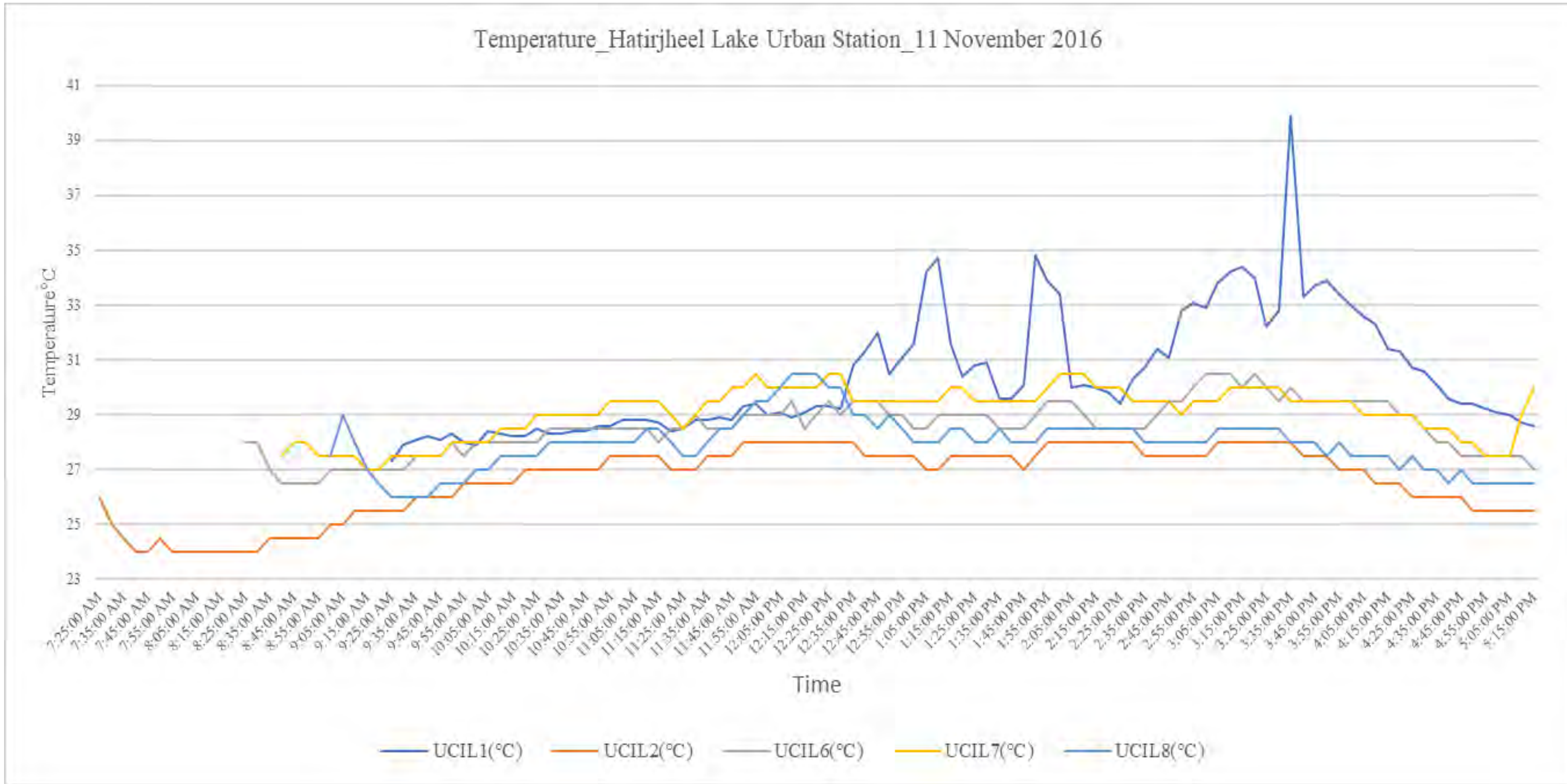

Figure 5.17: Temperature at Hatirjheel lake Urban stations on 11 November 2016

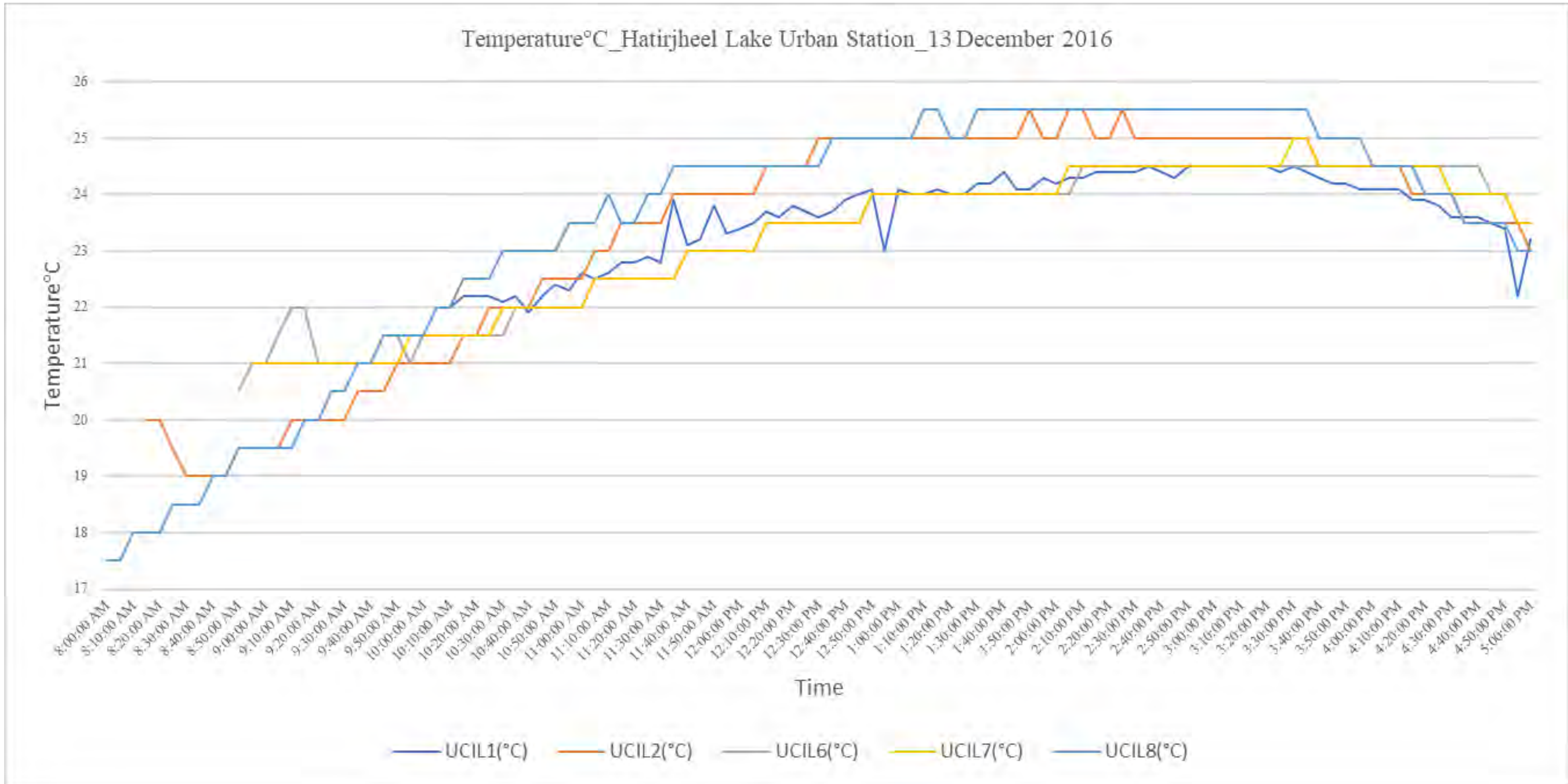

Figure 5.18: Temperature at Hatirjheel lake Urban stations on 13 December 2016

The correlation analysis (table 5.16) from the data of 13 December 2016 showed a strong relationship between cumulative time and air temperature in case of the two urban stations nearest to the top of the surface of the lake water which indicates positive solar gain. The urban stations at the park also showing positive solar gain although less the former two.

Table 5.16: correlation coefficient between air temperature and cumulative time of the urban stations of Hatirjheel lake on 13th December 2016

Urban stations	correlation coefficient
UCIL1(°C)	0.648584
UCIL2(°C)	0.7980454
UCIL6(°C)	0.9158919
UCIL7(°C)	0.9083694
UCIL8(°C)	0.7867869

The air temperature data from the observation of the urban stations at Hatirjheel lake on 10 February 2017 are presented in figure 5.19. The minimum temperature at the time of hot spell was 27.5 °C at the urban station UCIL6 and the maximum were 30°C at the urban station UCIL7. Urban station UCIL1 in the middle of the lake hanging on the top of water showed a consistent increase in air temperature although the temperature stayed below the urban station on the land inside the urban fabric till afternoon. But it didn't decrease like the other urban station on the land inside the urban fabric in the late afternoon. Urban station UCIL2 at the water edge also followed the pattern like UCIL1.

The correlational analysis of the air temperature data and cumulative time of Hatirjheel Lake urban stations on 10 February 2017 are given at table 5.17. The urban stations on the top of the water UCIL1 and at the edge of the water UCIL2 showing a strongest positive correlation of air temperature with cumulative time, which means strong heat gain throughout the day due to the solar influx. This could be explained by the heat capacity of the water which is larger than the land and air temperature near the water surface are regulated by the temperature of the water surface. Water can contain large amount of heat and it has very low albedo. So, with the beginning of the day, it absorbs heat without increasing the temperature quickly like the urban hard surface. But in the late afternoon when urban hard surface started losing heat and thus decrease its temperature water surface doesn't exhibit temperature decrease so quickly. It stays relatively warmer till late in the evening than the land, so does the air layer near the water surface. That's why air temperature at the urban station1 and 2 are strongly positively correlated with cumulative time which indicates strong solar gain. The two urban stations at the middle and edge of the urban park UCIL8 & 3 also exhibited strong positive correlation between air temperature and cumulative time and thus indicated strong heat gain due to the solar influx.

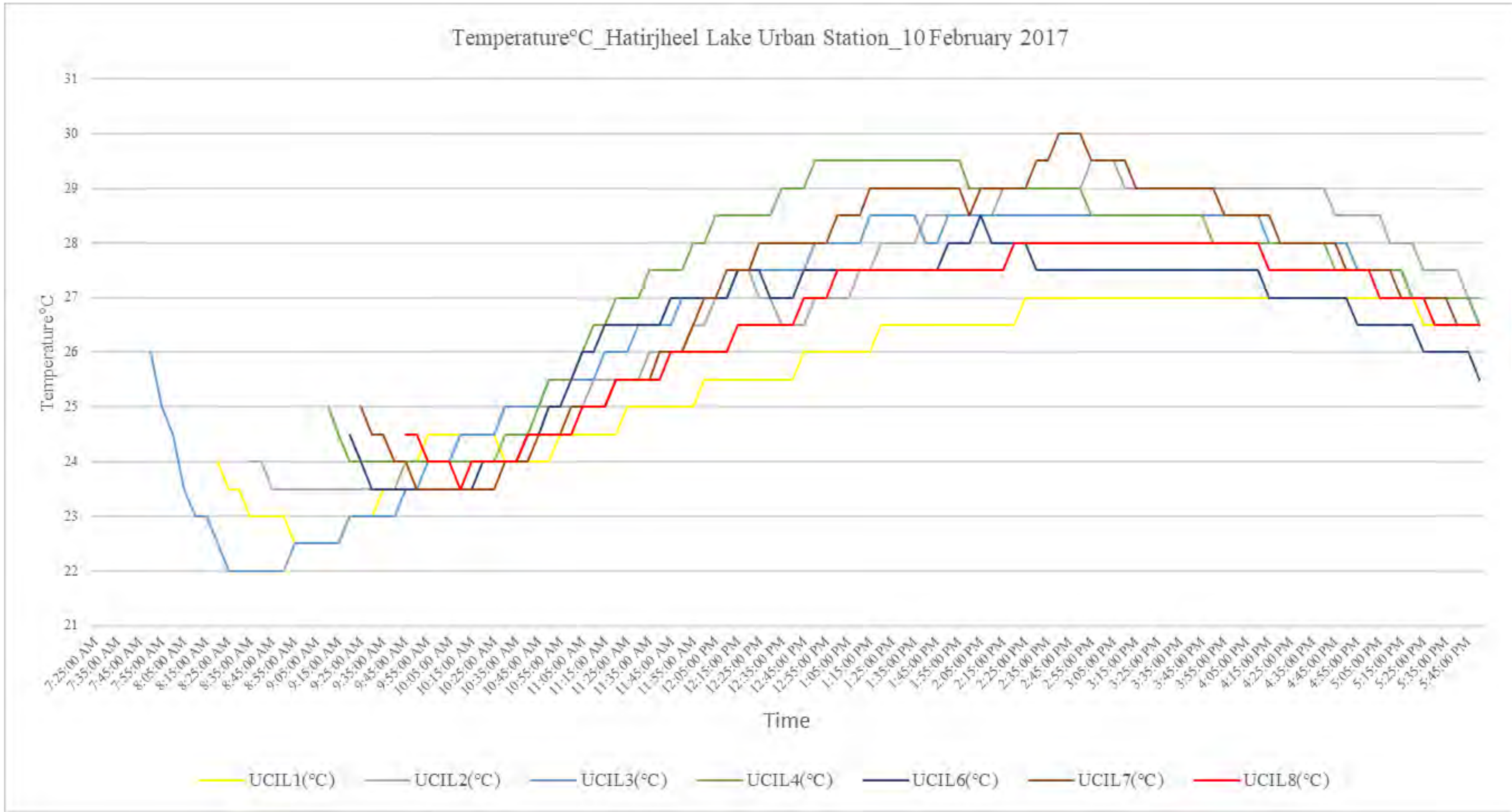

Figure 5.19: Temperature at Hatirjheel lake Urban stations on 10 February 2017

The other three urban station inside the urban fabric UCIL4, 6 and 7 exhibited moderate positive correlation and thus indicated moderate heat gain due to the solar influx. Among these urban stations heat gain increased with their distance from the water edge.

Table 5.17: correlation coefficient between air temperature and cumulative time of the urban stations of Hatirjheel lake on 10th February 2017

Urban Stations	Distance from the water edge	correlation coefficient
UCIL1(°C)	0m	0.9234208
UCIL2(°C)	0m water Edge	0.8790585
UCIL8(°C)	120m, middle of the park	0.7683875
UCIL3(°C)	190m, edge of the park	0.8194174
UCIL4(°C)	425m	0.5792301
UCIL6(°C)	550m	0.5944549
UCIL7(°C)	660m	0.6755592

5.3.6 Hatirjheel Lake relative humidity

From the Relative Humidity (RH) data (figure 5.20) of the measurement at Urban stations at Hatirjheel lake on 11 November 2016, the overall lowest RH was observed at urban station UCIL1 throughout the day. Overall higher RH was observed by the UCIL2 located at the edge of the urban park on downwind side. Urban station UCIL6 at the water edge also showed overall lower RH throughout the day.

The correlation analysis (table 5.18) between RH and the cumulative time of the data from the urban stations at Hatirjheel lake on 11 November 2016 showed the urban stations at the water edge, top of the water and the park were negatively correlated with the correlation strength is moderate. The other two stations in the urban fabric are also showing a negative correlation. UCIL8 showed the least negative correlation for RH which indicates least heat gain throughout the day.

Table 5.18: correlation coefficient between Relative Humidity and cumulative time of the urban stations of Hatirjheel lake on 11th November 2016

Urban Statins	correlation coefficient
UCIL1(%rh)	-0.4922671
UCIL2(%rh)	-0.5230172
UCIL6(%rh)	-0.4645949
UCIL7(%rh)	-0.3971748
UCIL8(%rh)	-0.1057552

Figure 5.21 showing the Relative humidity data from the urban stations at Hatirjheel lake on 13 December 2016. Overall the topmost Urban stations on the top of the water surface showed low relative humidity throughout the day

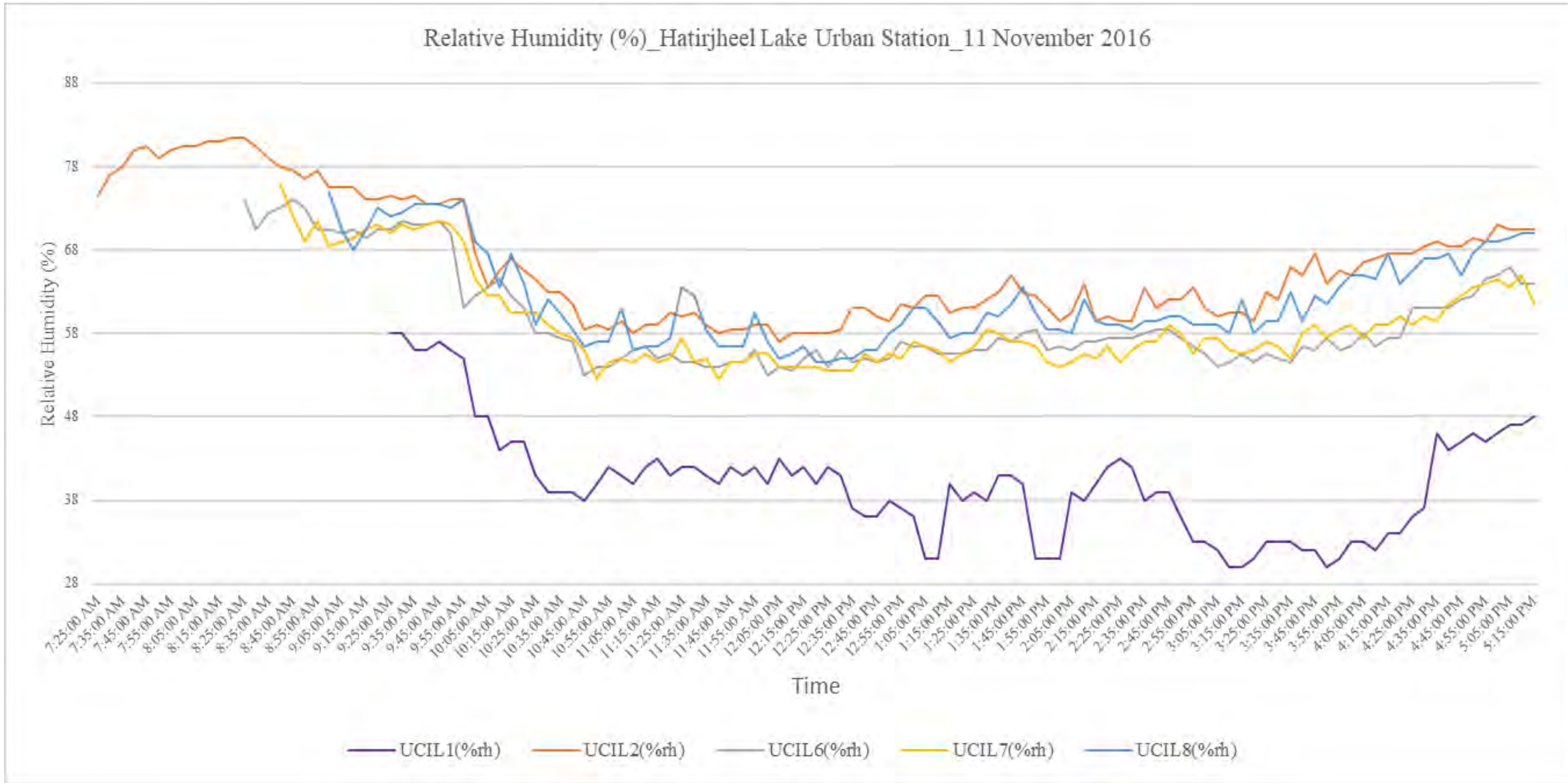

Figure 5.20: Relative Humidity at Hatirjheel lake Urban stations on 11 November 2016

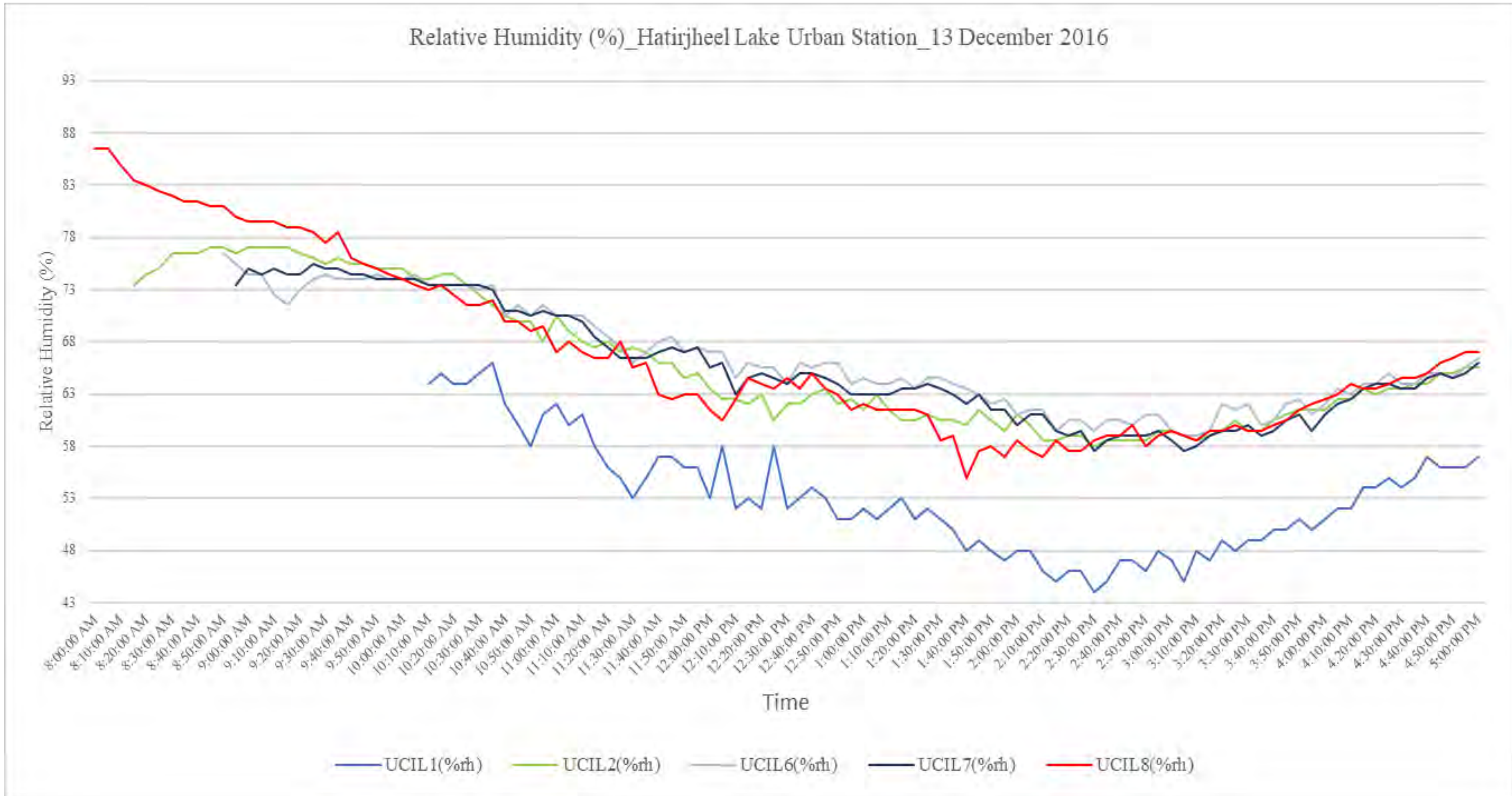

Figure 5.21: Relative Humidity at Hatirjheel lake Urban stations on 13 December 2016

The correlational analysis (Table 5.19) in between cumulative time and Relative humidity data from the urban stations at Hatirjheel lake on 13 December 2016 showed negative correlation throughout the day for all the stations, which is in correspondence with the reference urban station at BMD site. The negative correlation is strong at the urban stations nearer to water surface UCIL6 and 7. The urban station at the edge of park UCIL2 is also showing strong negative correlation which indicates strong positive heat gain by air due to solar influx throughout the day.

Table 5.19: correlation coefficient between Relative Humidity and cumulative time of the urban stations of Hatirjheel lake on 13th December 2016

Urban stations	correlation coefficient
UCIL1(%rh)	-0.5896493
UCIL2(%rh)	-0.8396173
UCIL6(%rh)	-0.8576293
UCIL7(%rh)	-0.848607
UCIL8(%rh)	-0.8210089

Figure 5.22 showing the relative humidity data from the urban stations at Hatirjheel lake on 10 February 2017. Overall all the urban stations showed a decline of relative humidity as the day progress which flattens from the afternoon to late afternoon. Relative humidity again continued to increase slowly in the late afternoon. Urban station UCIL2 at the edge of water surface started showing lower relative humidity than the other stations starting from the afternoon till sunset. The humidity at the urban station UCIL1 on top of the water surface declined relative to other urban stations on the ground from afternoon till sunset.

The correlational analysis (Table 5.20) between cumulative time and relative humidity data of the urban stations of Hatirjheel lake on 10 February 2017 are presented in table 5.20 indicates overall negative correlation at all urban stations. This correlational analysis clearly showed the strongest negative correlation between cumulative time and relative humidity at the urban station on top of the water UCIL1 and at the water edge UCIL2, which indicates a decrease in relative humidity due to the high heat gain of water due to solar influx throughout the day. The urban stations at the middle of park UCIL8 and at the edge of the park UCIL3 also showed strong negative correlation. The other three urban stations inside the urban fabric UCIL4,6 &7 also showed strong negative correlation although to some lesser extent than the previous four stations at the top of the water and at the park near the water edge.

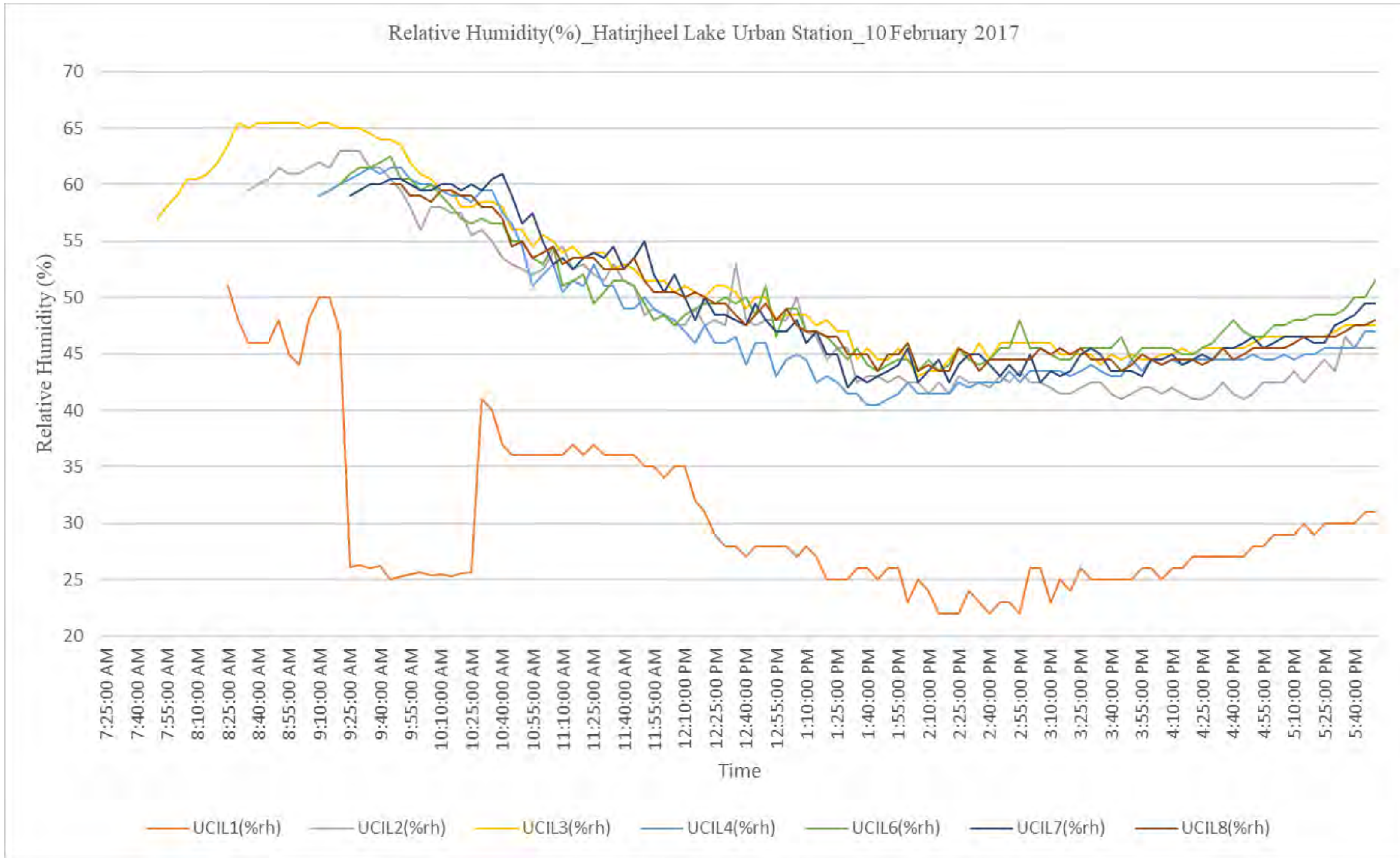

Figure 5.22: Relative Humidity at Hatirjheel lake Urban stations on 10 February 2017

Table 5.20: correlation coefficient between Relative Humidity and cumulative time of the urban stations of Hatirjheel lake on 10th February 2017

Urban Stations	Distance from the water edge	correlation coefficient
UCIL1(%rh)	0m	-0.9025281
UCIL2(%rh)	0m water Edge	-0.9010745
UCIL8(%rh)	120m, middle of the park	-0.8260548
UCIL3(%rh)	190m, edge of the park	-0.8866804
UCIL4(%rh)	425m	-0.7792143
UCIL6(%rh)	550m	-0.7394349
UCIL7(%rh)	660m	-0.7949549

5.4 Determining Morphology of Urban Cooling Island from Field Measurement

Several important observations could be made from the analyzed field measurement data obtained from the selected urban stations on both the wetland in the previous section.

5.4.1 Effect of cumulative time on the rate of change of air temperature and relative humidity

The study shows that Time if considered as an increasing quantity rather than a categorical value, has a cumulative effect on the rate of change of air temperature and relative humidity in terms of solar influx. At the night due to the absence of solar influx air temperature has an almost negative linear relationship with cumulative time and relative humidity (RH) has an almost positive linear relationship with cumulative time. During the day with the presence of solar influx, although variable, the time cumulative effect is reversed. At day air temperature has a strong positive correlation with cumulative time and Relative Humidity has a strong negative correlation with cumulative time.

5.4.2 Effect of riparian shading on the cumulative time effect

In case of urban wetland devoid of riparian shading, the cumulative effect of time is strongest at the top and near the edge of the wetland, which is evident from the analysis of the field data measured at Hatirjheel lake urban stations. In case of Dhanmondi lake area cumulative effect of time relatively lower than that of Hatirjheel lake area.

5.4.3 Influence of the distance from the edge of the wetland on temperature

Air temperature drops in those urban stations which are located on the road parallel to the wind flow from the wetland and the wind flow are not obstructed by the built from or natural feature. This effect is more pronounced in case of Dhanmondi lake then Hatirjheel lake. The temperature on the urban station increases with distance from the lake edge. The urban station located on the road perpendicular to the prevailing wind direction from the lake exhibits higher temperature.

5.4.4 Effect of the location of the park on temperature

The existence of urban park creates “oasis effect” by moderating temperature and increasing humidity, which is the case in Hatirjheel Lake area. Hatirjheel lake is mostly devoid of large vegetation on its surrounding. But the existence of the urban park creates a small “oasis effect”.

5.4.5 Effect of shading in the urban canyon

Urban stations which are located in the urban canyon shaded most of the time by canyon itself showed decreased temperature.

5.4.6 Humidity and distance from the lake edge

Relative humidity (RH) near the edge of the water and over the water is lower than the park and vegetated area, which is consistent with the findings of Geiger R. (2009).

5.4.7 Evaporative cooling potential

Another important observation is, with the progress of the day relative humidity decreases which dip significantly from the mid-day to late afternoon. This phenomenon of the relative humidity increases the evaporative cooling potential.

5.5 References

1. Brammer H. (2012). "*The physical geography of Bangladesh*". First edition, The University press limited, Dhaka.
2. Geiger R., Aron R.H., Todhunter P. (March 16, 2009). "*The Climate Near the Ground"*. Rowman & Littlefield Publishers; 7th edition.
3. Oke T.R. "*Boundary Layer Climates*" (January 30, 1988). Routledge; 2nd edition
4. Oke, T.R. 2006. "*Initial Guidance to Obtain Representative Meteorological Observations at Urban Site". World Meteorological Organization, Instruments and Observing Methods*, IOM Report No. 81, WMO/TD-No. 1250 Available from: http://www.wmo.int/web/www/IMOP/publications-IOM-series.html

Chapter 6 : SIMULATION AND MODELING

6.1 Introduction

The main objective of the simulation work was to determine the morphological characteristics of the Urban Cooling Island (UCI) at Urban Canopy Layer (UCL). The principal assumption which has been tested in the simulation model is that the water in the wetland will be cooled down with the help of continuous riparian shading to act as UCI, this cooling effect will then be transferred to the urban fabric through the advective process. For this reason, the simulation work was conducted in one of the study area described in the previous section at the Urban Canopy Layer (UCL) recording the result at a height of 1.5m to 2m from the ground. Some measurements were also recorded on top of the water surface and edge of the lake to determine the effect of water on the air layer above it.

6.2 Preparation of The Model

6.2.1 Location of the modeling area

An area (approx. 750m length) adjacent to the Dhanmondi Lake bounded by road 12A on North-west, Satmasjid road on South-west and road 6A on the south-east was selected for the simulation study as all the data logger except one in one occasion, were placed in this zone to collect microclimatic data.

6.2.2 Morphology of the modeling the area

Due to the limited computational power of the computer available for simulation study, this area was scaled down at a scale of 1: 50. Data obtained from the field measurement of this wetlands were used as an initial condition into the COMSOL–Multiphysics software as a part of problem modeling study. Water and Air temperature, Relative humidity and Wind speed are primary inputs for the simulation besides types of ground cover and the built form. Although all the buildings in each block are the detached type, the gaps between the buildings in most of the case, is not more than 2 m. So, for the simplicity of the model, all the buildings in a single block were safely considered as a single building mass. Average building height of the area approximately 24 m. Also, only the part of the lake in the line of prevailing wind direction was modeled. One of the days of field measurement in this area, 24 Feb 2017 was used for the position of the sun in the simulation model. The simulation time was fixed from 9 AM to 16:00 PM on that day. The whole simulation study was conducted for four cases depicting four types of ambient condition:

i. Case 1: First simulation study was conducted with the water of the lake completely under solar radiation and inlet temperature equal to maximum temperature of the day obtained from the field measurement.

ii. Case 2: Second simulation study was conducted with the water of the lake completely under solar radiation and inlet temperature equal to minimum temperature of the day obtained from the field measurement.

iii. Case 3: Third simulation study was conducted with the water body completely shaded from solar radiation and inlet temperature equal to maximum temperature of the day obtained from the field measurement.

iv. Case 4: Fourth simulation study was conducted with the water body completely shaded from solar radiation and inlet temperature equal to minimum temperature of the day obtained from the field measurement.

In all the four cases relative humidity(RH), which is equal to starting RH at 9:00 am was obtained from the field measurement on 24 Feb 2017.

6.2.3 Computational domain

Only the bottom of the computational domain represents an actual physical boundary. The side faces and top of the model are non-physical boundaries. These non-physical boundaries should be located far enough from the urban model to avoid too strong artificial acceleration of the flow. This artificial acceleration happens due to too strong contraction of the flow by these boundaries. There are three types of guidelines have been established to determine the size of the computational domain. (Franke, J. et al. 2004). They are

Type-1: guidelines that impose minimum distances between the urban or building model and the boundaries of the domain;

Type-2: guidelines that impose a maximum allowed blockage ratio; and

Type-3: guidelines that are a combination of Types 1 and 2.

The blockage ratio is defined as in wind-tunnel testing: it is the ratio of the projected frontal (windward) area of the obstacles to the cross-section of the computational domain [Fig.6.1(e)] and in CFD it is generally required to be less than 3%.

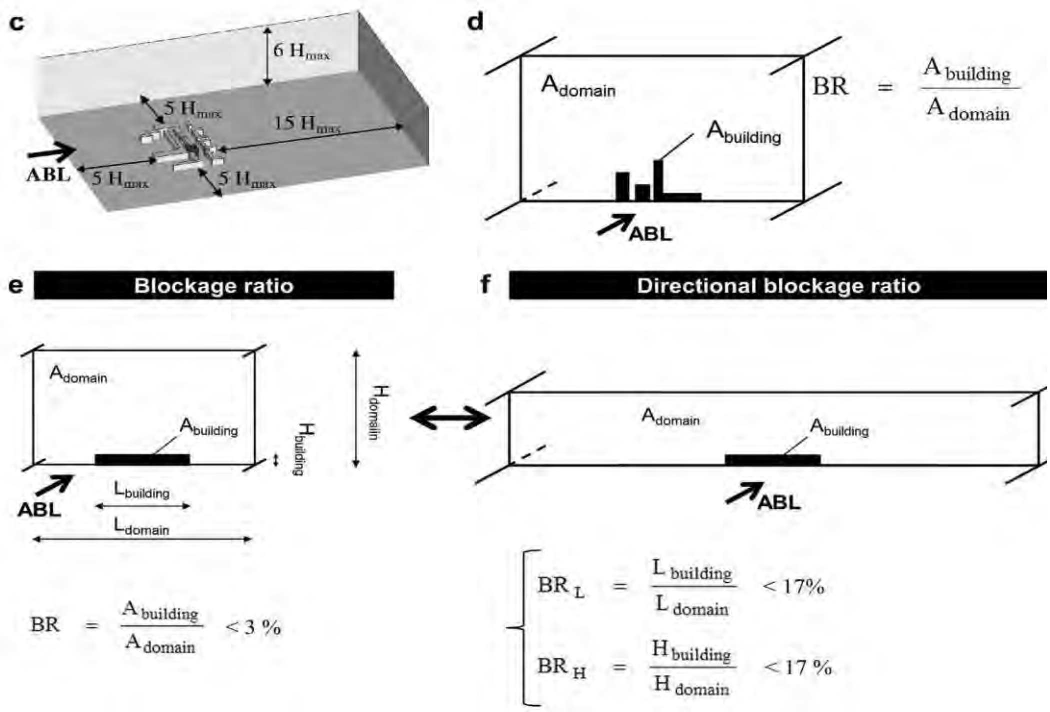

Figure 6.1: Computational Domain (Blocken B., 2007)

Figure 6.1 illustrates (c) Type 1 guidelines by Franke et al for the size of computational domain (d) View in streamwise direction of building models in computational domain and definition of blockage ratio. (e) Low-rise wide building in a computational domain that satisfies existing best practice guidelines but that will give rise to artificial acceleration on lateral sides. (f) Same building in a computational domain defined based on the new concept of directional blockage ratio.

6.2.4 Computational grid (mesh)

High-quality computational grids are important to reduce discretization errors besides allowing convergence of the iterative process with the minimum required second-order discretization schemes. Blocken B. (2015) described two characteristics of the high-quality computational grid. They are:

1.Sufficient overall grid resolution

2. Quality of the computational cells in terms of shape (including skewness) orientation and stretching ratio.

For urban and building model Franke et al (2007) suggested to use at least 10 cells per cube root of the building volume, and 10 cells in between every two buildings. For studies of pedestrian-level wind speed, the focus height of the 1.5-2m should coincide with the 3rd and 4th cell above ground level. Computational grid of control domain is given in figure 6.2.

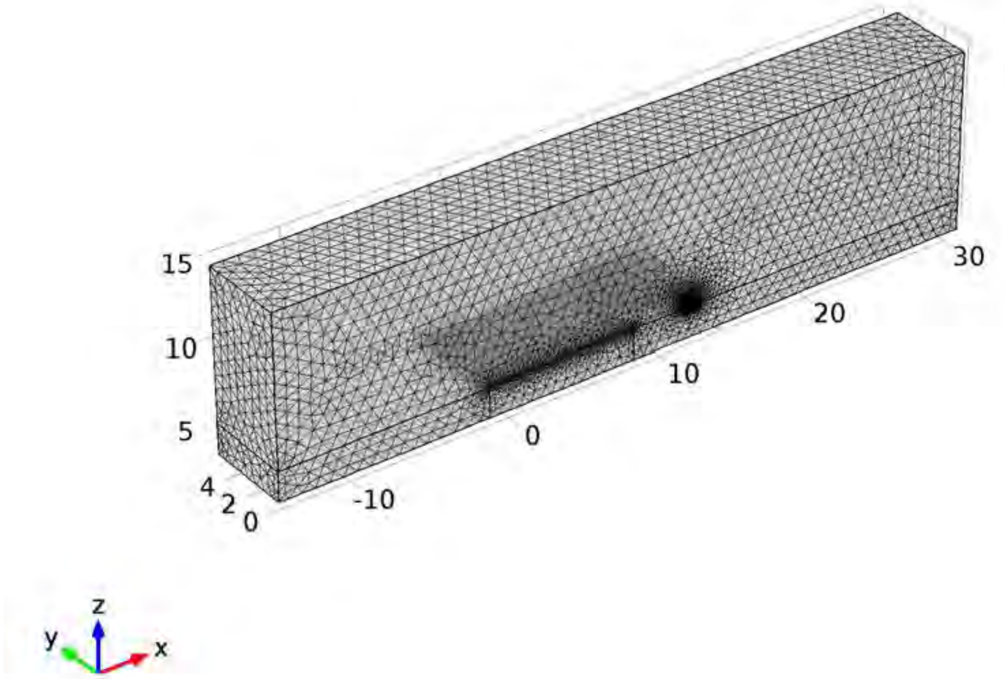

Figure 6.2: computational grid of control domain

Form figure 6.3 computational grid of the model with its different area could be seen.

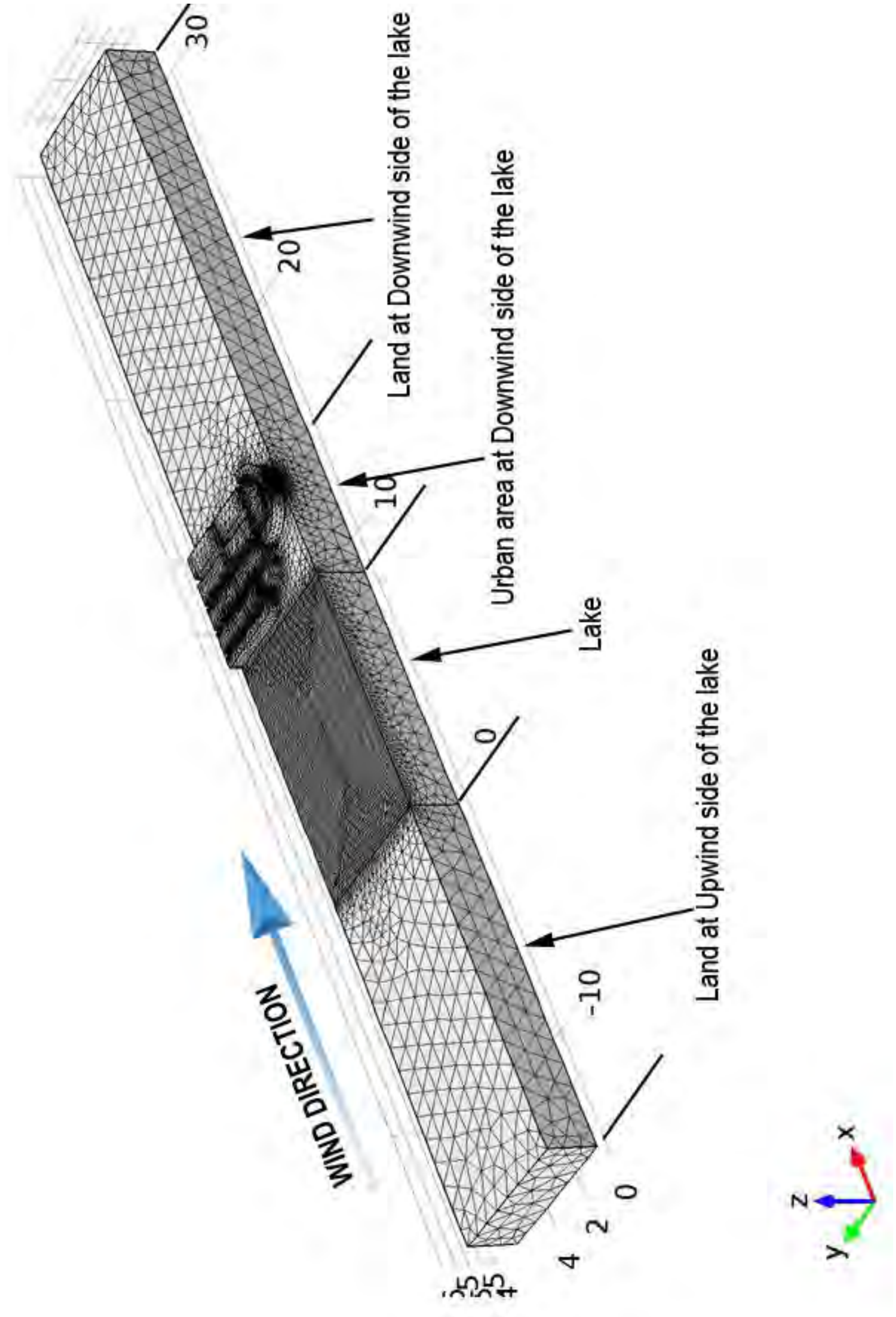

Figure 6.3: computational grid of the model

6.2.5 Roughness parameters

Hargreaves (2006) stated that there are two aspects of the real flow situation that are not amenable to direct representation in the CFD and that must, therefore, be modeled in some way. Firstly, "the atmospheric boundary layer (ABL) extends for a considerable distance above the earth's surface relative to the average building height: a CFD model can only represent a smaller, finite distance because of hardware limitations and the complexity of including a meteorological model". Secondly, smaller-scale features such as vegetation and small buildings cannot be included in the computational grid and are therefore represented by a roughness model. He further stated that most of the modeling irrespective of modeling process have been conducted with buildings embedded in a neutral ABL because buoyancy-induced turbulence need not be modeled.

Roughness parameters had been specified for five spatial areas inside the computational domain as suggested by blocken (2015). Area one is upstream of the computational domain. Area two is the area inside the computational domain and upstream of the explicitly modeled building. Area three inside the computational domain representing the ground surface amidst the explicitly modeled buildings and other obstacles. Area four is the surface of the explicitly modeled buildings (façade, roofs) and structures inside the computational domain. Area five is the area inside the computational domain and downstream of the explicitly modeled buildings. Also, two types of roughness specification had been made (blocken,2015):

i. Aerodynamic roughness length z_0: used for area one, two, three and five
ii. Equivalent sand-grain roughness length k_s: used in area four

6.2.6 Discretization scheme

By default, "COMSOL uses second-order elements for most physics, the two exceptions are problems involving chemical species transport and when solving for a fluid flow field. (Since those types of problems are convection dominated, the governing equations are better solved with first-order elements.) Higher order elements are also available, but the default second-order elements usually represent a good compromise between accuracy and computational requirements".

6.2.7 Simulation categories

Two main categories of equations used in CFD are steady RANS (Reynolds-average Navier-Strokes) and Large Eddy Simulation (LES). In addition, hybrid RANS/LES approaches are sometimes used. "The RANS equations are derived by averaging the NS equations (time-averaging if the flow is statistically steady or ensemble averaging for time-dependent flows). With the RANS equations, only the mean flow is solved while all scales of the turbulence are modelled (i.e. approximated). The averaging process generates additional unknowns and as a result, the RANS equations do not form a closed set" (COMSOL). Therefore, approximations must be made to achieve closure. These approximations are called turbulence models. Up to now, RANS had been the most commonly used approach in CFD for urban physics.

In the LES approach, the NS equations are filtered in space, which consists of removing only the small turbulent eddies (that are smaller than the size of a filter that is often taken as the mesh size). The large-scale motions of the flow are solved, while the small-scale motions are modeled: "the filtering process generates additional unknowns that must be modeled in order to obtain closure" (COMSOL). This is done with a sub-filter turbulence model. LES generally shows superior performance compared to RANS and URANS, because a large part of the unsteady turbulent flow is actually resolved. However, the required computational resources increase significantly, the inlet boundary condition requires time and space resolved data and a larger amount of output data is generated.

6.2.8 Model definition

The modules of the COMSOL-Multiphysics that were combined to model the Urban Cooling Island Effect of the urban wetland were (1) CFD module: Fluid Flow-Single phase flow, Turbulent Flow, k-ω. (2) Heat Transfer Module: Heat Transfer in Fluids and Heat Transfer with Surface to Surface Radiation (ht). (3) Chemical Species Transport: Transport of Diluted species (tds)

i. Turbulent Flow:

The flow was modeled using Wilcox *k*-ω turbulence model. The main reason for using the *k*-ω model over the *k*-ε model is that former is, in general, more reliable when it comes to predicting the spreading rate of jets (Wilcox,1998). The *k*-ω model uses wall functions which is quite all right in this case since all walls are almost insulated and there would not be much benefit from using the more expensive low-Re *k*-ε model.

Further, it is assumed that the velocity and pressure field is independent of the air temperature and moisture content. This allows to calculate the flow field in advance and then use it as input for the heat transfer and species transport equation. Mathematical model of the *k*-ω by Wilcox has been given in the Appendix 1.

ii. Heat Transfer:

The primary source of heat in this model was the solar irradiation, which was included using the External Radiation Source feature. This feature uses the longitude, latitude, time zone, time of year, and time of day to compute the direction of the incident solar radiation over the simulation time. Assuming no cloud cover, the solar flux at the surface was about 1000 W/m2. "All of the ambient surfaces of the model were included in the solar loading calculation, and shadowing effects were included. The temperature of the sun is about 5800 K, and it emits primarily short-wavelength infrared and visible light at wavelengths shorter than 2.5 microns" (COMSOL). The fraction of this short-wavelength solar radiation that is absorbed by the various materials is quantified by the solar absorptivity. Because the surfaces are at a much lower temperature, they reradiate in the long-wavelength infrared band, at wavelengths above 2.5 microns, and the fraction of reradiated energy is quantified by the surface emissivity. "The solar and ambient wavelength dependence of emissivity model was used to account for differing emissivities in different wavelength bands" (COMSOL).

The heat transfer between the lake and land is due to conduction only. For the air, convection dominates the heat transfer and the turbulent flow field is required. The material properties were determined by the moist air theory. During evaporation, latent heat was released from the water surface which cools down the water in addition to convective and conductive cooling by the surrounding. This means that the fraction of convective and diffusive flux normal to the water surface contributes to the evaporative heat flux (Incropera F.P. et al, 2006).

$$-n.(-k\nabla T) = H_{vap} n.(-D\nabla c + uc)$$

The latent heat of vaporization H_{vap} is given in kj/mol.

iii. Transport of water vapor:

To obtain the correct amount of water evaporated from the lake into the air, the Transport of Diluted Species interface was used in the air domain. The initial concentration was chosen to keep the initial relative humidity (RH) equal to the RH at 9 am in the morning obtain from the field measurement. The source term for water vapor at the water surface is given by the ideal gas law at saturation pressure (Monteith J. et al, 2013):

$$c_{vap} = \frac{p_{sat}}{R_g T}$$

The transport equation again uses the turbulent flow field as input. Turbulent has been considered for the diffusion coefficient, by adding the following turbulent diffusivity to the diffusion tensor:

$$D_T = \frac{v_T}{Sc_T} I$$

Where v_T is the turbulent kinematic viscosity, Sc_T is the turbulent Schmidt number and I the unit matrix.

6.2.9 Measurement points in the model

Two sets of measurement points had been taken in the model. The first set of seven measurement points at the downwind side of the lake had been chosen to keep similarity with the actual urban stations (data logging point) in the field measurement around Dhanmondi lake area, started from over the water of the lake, then edge of the lake gradually shifting deep inside the urban fabric. The second set of twenty-two measurement points were taken starting from the land -lake boundary at the upwind side of the lake to the land-lake boundary of the downwind side of the lake. Most of those points in the second set are at equal distance along the length of the lake. All those points are given in fig.6.4.

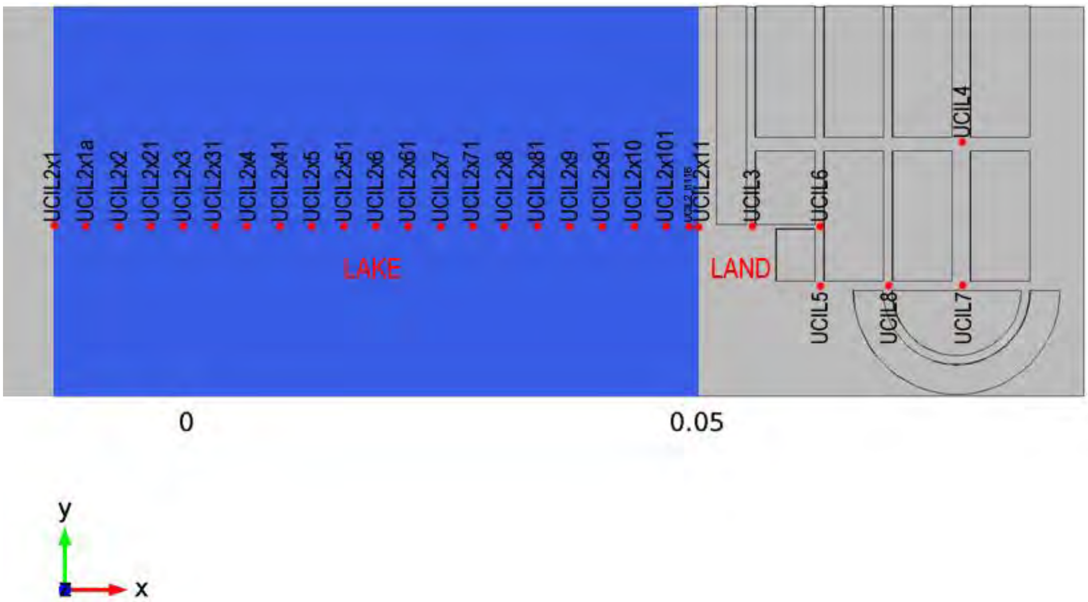

Figure 6.4: measurement points of the model

6.3 Simulation Results and Analysis

All the related data for the simulation results and analysis are given in the appendix G.

6.3.1 Effect of cumulative time on the rate of change of air temperature and relative humidity

when the time is considered as a continuous variable rather than the categorical value we get the cumulative effect of time on the rate of change of air temperature and relative humidity.

Case 1: In the first case water of the whole lake was under complete under solar radiation with inlet temperature equals the maximum temperature of the day. Temperature and Relative humidity(RH) data at the first set of seven points extracted and correlation analysis done in the R-studio using R programming language considering time as a continuous independent variable to see its cumulative effect. (Table 6.1)

Table 6.1: Case 1 Correlation analysis of Air Temperature, Relative Humidity and Time

Measurement point	Pearson's product-moment correlation coefficient for air temperature	Pearson's product-moment correlation coefficient for Relative Humidity
UCIL2	0.8956205	0.8866912
UCIL3	0.9110763	0.5179765
UCIL4	0.9209397	-0.8439007
UCIL5	0.9156383	0.6140438
UCIL6	0.8544383	0.1261469
UCIL7	0.9219397	-0.8535848
UCIL8	0.8226153	-0.06217233

Case 2: In the second case water of the whole lake was under complete under solar radiation with inlet temperature equals the minimum temperature of the day. Temperature and Relative humidity(RH) data at the first set of seven points extracted and correlation analysis done in the R-studio using R programming language considering time as a continuous independent variable to see its cumulative effect. (Table 6.2)

Table 6.2: Case 2 Correlation analysis of Air Temperature, Relative Humidity and Time

Measurement point	Pearson's product-moment correlation coefficient for air temperature	Pearson's product-moment correlation coefficient for Relative Humidity
UCIL2	0.9820582	0.734411
UCIL3	0.9386021	0.4670124
UCIL4	0.9383335	-0.8390386
UCIL5	0.9498092	0.5335272
UCIL6	0.8731839	0.1466815
UCIL7	0.9344495	-0.8475209
UCIL8	0.8438288	-0.05475282

Case 3: In the third case water of the whole lake was completely shaded from solar radiation with inlet temperature equals the maximum temperature of the day. Temperature and Relative humidity(RH) data at the first set of seven points extracted and correlation analysis done in the R-studio using R programming language considering time as a continuous independent variable to see its cumulative effect (Table 6.3).

Table 6.3: Case 3 Correlation analysis of Air Temperature, Relative Humidity and Time

Measurement point	Pearson's product-moment correlation coefficient for Air Temperature	Pearson's product-moment correlation coefficient for Relative Humidity
UCIL2	0.8161152	0.3497697
UCIL3	0.8424691	-0.3760967
UCIL4	0.9087311	-0.8948763
UCIL5	0.842523	-0.3727366
UCIL6	0.7835263	-0.5478617
UCIL7	0.9143121	-0.8936088
UCIL8	0.7327484	-0.5152106

Case 4: In the fourth case water of the whole lake was completely shaded from solar radiation with inlet temperature equals the minimum temperature of the day. Temperature and Relative humidity(RH) data at the first set of seven points extracted and correlation analysis done in the R-studio using R programming language considering time as a continuous independent variable to see its cumulative effect (Table 6.4).

Table 6.4: Case 4 Correlation analysis of Air Temperature, Relative Humidity and Time

Measurement point	Pearson's product-moment correlation coefficient for Air Temperature	Pearson's product-moment correlation coefficient for Relative Humidity
UCIL2	0.9747011	0.1416486
UCIL3	0.8970227	-0.3672817
UCIL4	0.9285554	-0.8920262
UCIL5	0.912889	-0.3555603
UCIL6	0.8104017	-0.5294822
UCIL7	0.9276761	-0.8903609
UCIL8	0.7581881	-0.4985059

The correlation analysis of the four cases strongly corresponds with the result of field measurement at the two-lake areas and reference measurement at Bangladesh Meteorological Department (BMD). It has been observed from the field study that the time, if considered as a continuous variable (an increasing quantity rather than a categorical value), has a cumulative effect on the rate of change of air temperature and relative humidity in terms of solar influx. In all the four cases rate of change of air temperature strongly and positively correlated with time. In case of Relative Humidity, it is mostly negatively correlated, with the measurement point deep inside the urban fabric (UCIL4 and UCIL7) showing the strongest negative correlation. The measurement points near and over the water of the lake showing weak negative or weak positive correlation with time, which corresponds to the field measurement of both the lake area.

6.3.2 Development of inversion layer

Fraedrich K. (1972) observed a shallow stably stratified layer over the water of the lake which he named as "inversion layer". This layer produced by a negative downward flux over a water surface, when the air is blowing from the warmer land. Also, if the advected air is relatively dry, evaporative cooling amplifies the stable inversion layer. The inversion can also happen even if the air temperature of the environment is equal or less compared with the temperature of the water surface at the shore. The reason is interaction between the air and the water varies (decreases) the water surface temperature along the air trajectory. Inversion layer also increasingly suppresses the evaporation from the lake which increases with the travel distance of the air over the lake by creating a "Vapor blanket".

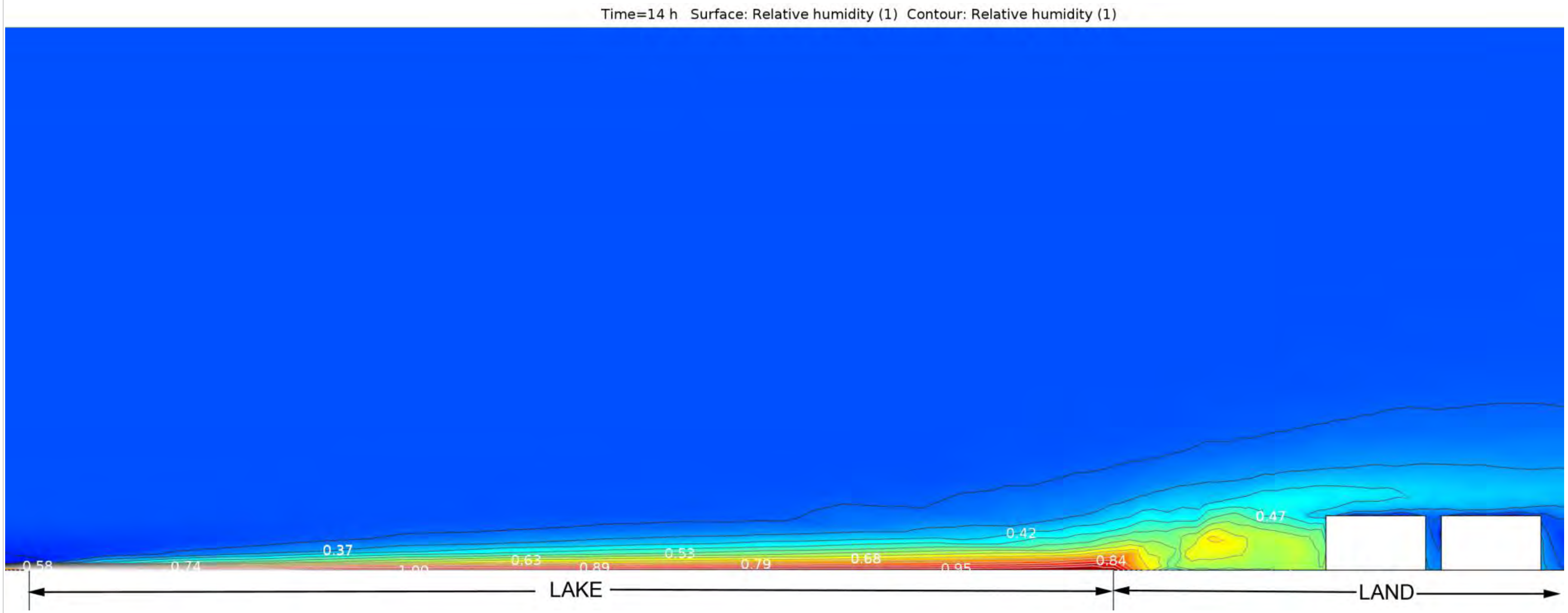

Figure 6.5: Case 1_Inversion layer above the lake

All this above-mentioned phenomenon observed by Fraedrich clearly demonstrated in the four cases of the simulation study. All the conditions of the creation of “inversion layer” has been covered by the four cases of the simulation study.

Case 1: In the first case water of the whole lake was under complete under solar radiation with inlet temperature equals the maximum temperature of the day. The starting Relative Humidity (RH) of the simulation was set equal to the RH observed at 9:00 am on 24th February in the Dhanmondi lake area. The simulation showed (fig. 6.5) a clear inversion layer above the water surface of the lake. The inversion layer is slightly advected towards the downwind side of the lake above the ground.

Case 2: In the second case water of the whole lake was under complete solar radiation with inlet temperature equals the minimum temperature of the day and the starting Relative Humidity (RH) of the simulation was set equal to the RH observed at 9:00 am on 24th February in the Dhanmondi lake area. The simulation showed (fig. 6.6) a clear inversion layer above the water surface of the lake. The inversion layer is slightly advected towards the downwind side of the lake above the ground.

Case 3: In the Third case water of the whole lake was completely shaded from solar radiation with inlet temperature equals the maximum temperature of the day and the starting Relative Humidity (RH) of the simulation was set equal to the RH observed at 9:00 am on 24th February in the Dhanmondi lake area. The simulation showed (fig. 6.7) a clear inversion layer above the water surface of the lake. The inversion layer is slightly advected towards the downwind side of the lake above the ground, although this advection is less than case 1 and 2. Also, the thickness of the inversion layer is less than case 1 and 2.

Case 4: In the Third case water of the whole lake was completely shaded from solar radiation with inlet temperature equals the minimum temperature of the day and the starting Relative Humidity (RH) of the simulation was set equal to the RH observed at 9:00 am on 24th February in the Dhanmondi lake area. The simulation showed (fig.6.8) a clear inversion layer above the water surface of the lake. The inversion layer is slightly advected towards the downwind side of the lake above the ground, although this advection is less than case 1 and 2. Also, the thickness of the inversion layer is less than case 1,2 & 3

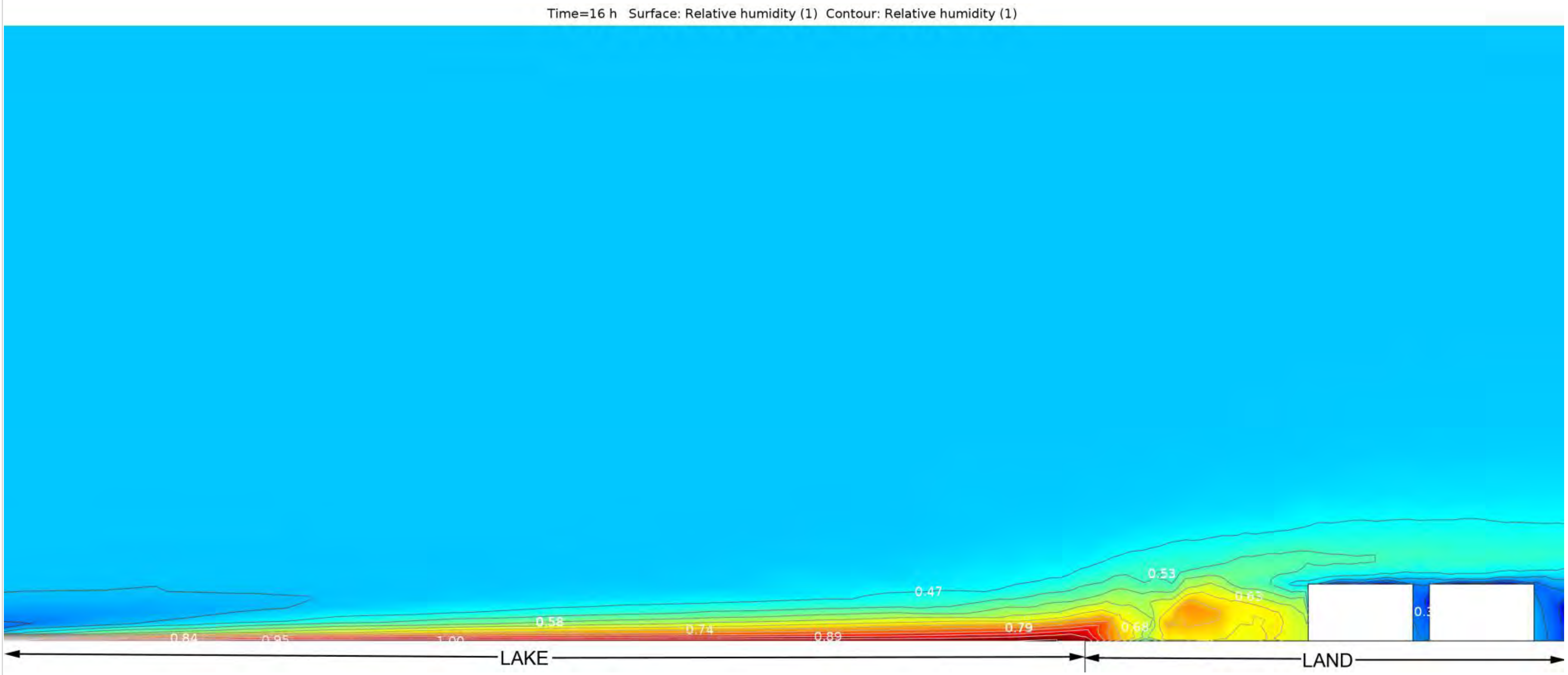

Figure 6.6: Case 2_Inversion layer above the lake

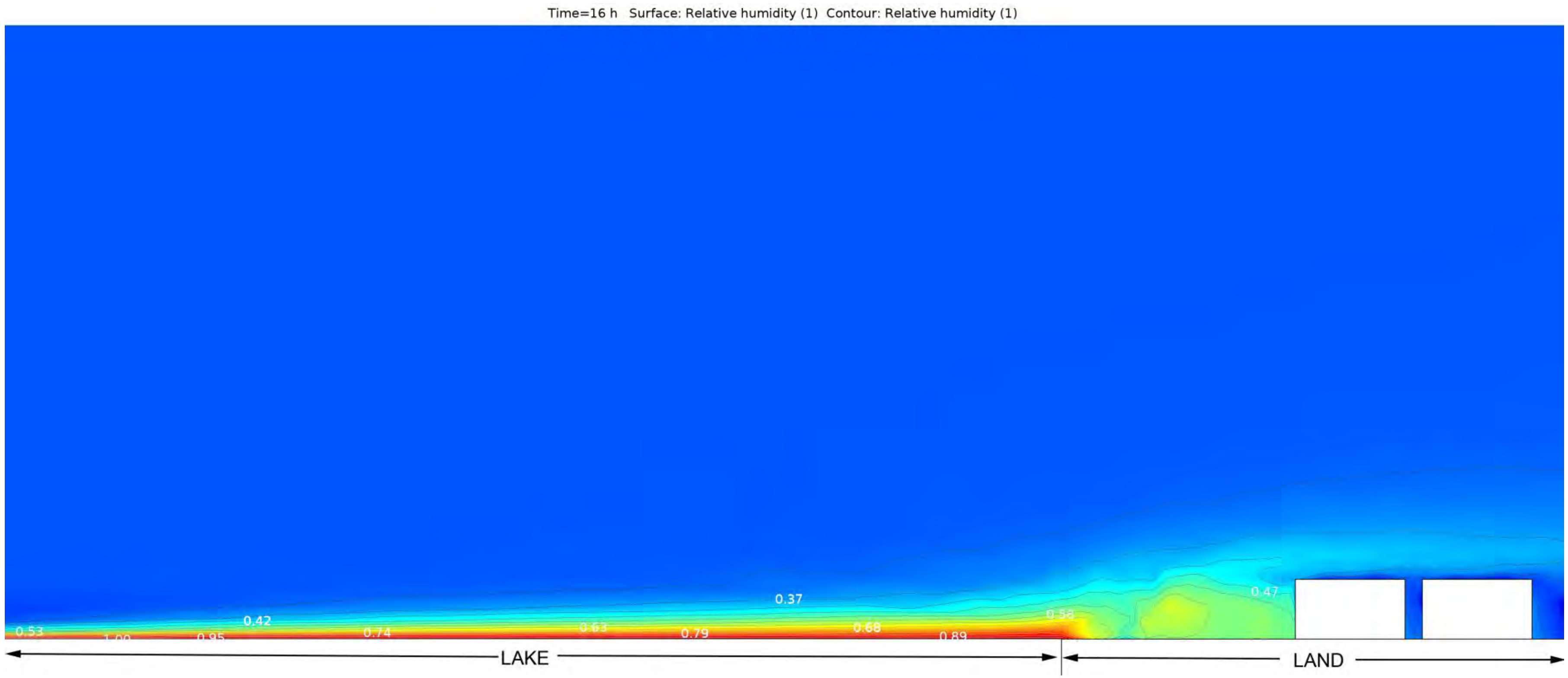

Figure 6.7: Case 3_Inversion layer above the lake

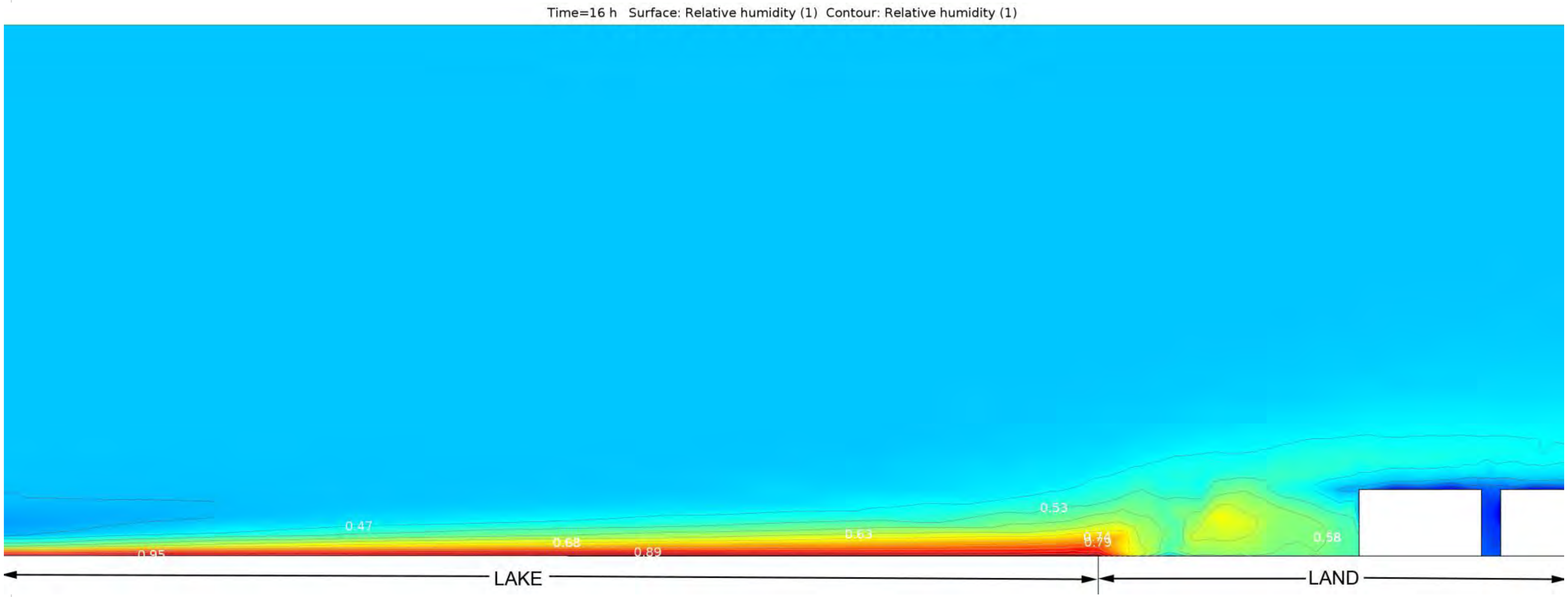

Figure 6.8: Case 4_Inversion layer above the lake

6.3.3 Effect of the fetch on the inversion height

A strong relationship between the inversion height and the fetch had been observed in all the four cases. Fetch is the distance starting from the land-lake boundary of the downwind side of the lake to the upwind side towards wind flow direction. Inversion height is the maximum thickness of the inversion layer (fully saturated with water vapor) at a particular point over the lake.

Case 1: In the first case water of the whole lake was under complete under solar radiation with inlet temperature equals the maximum temperature of the day. In this case, the inversion layer increases in height with the increasing fetch (fig.6.9).

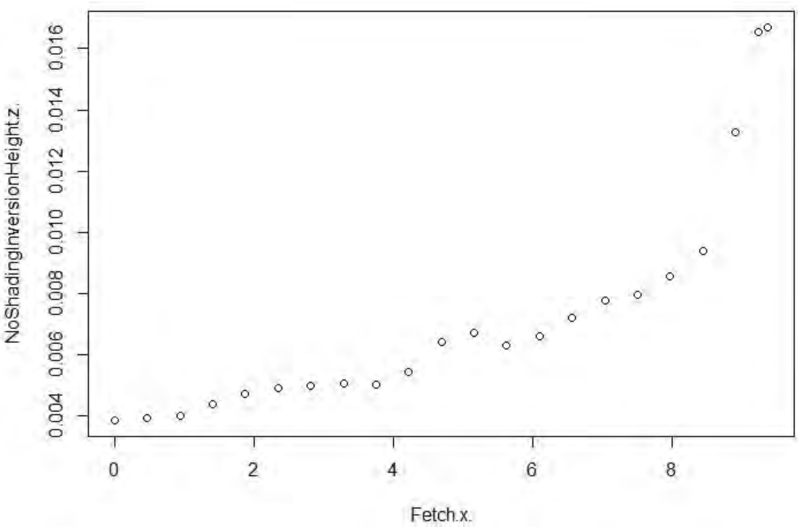

Figure 6.9: Case 1_Inversion height z versus fetch x

Case 2: In the second case water of the whole lake was under complete solar radiation with inlet temperature equals the minimum temperature of the day. In this case, the inversion layer increases in height with the increasing fetch (fig6.10), although this increase is less than case 1.

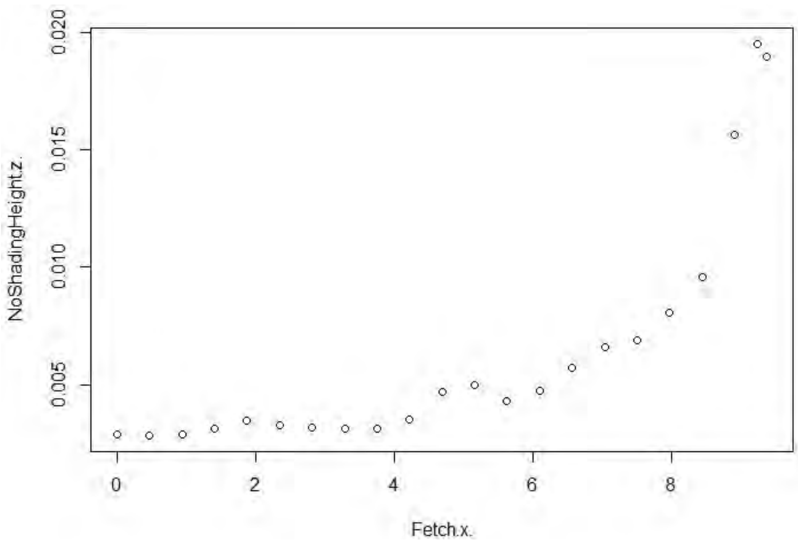

Figure 6.10: Case 2_Inversion height z versus fetch x

Case 3: In the third case water of the whole lake was completely shaded from solar radiation with inlet temperature equals the maximum temperature of the day. In this case, the inversion layer decreases in height with the increasing fetch (fig. 6.11).

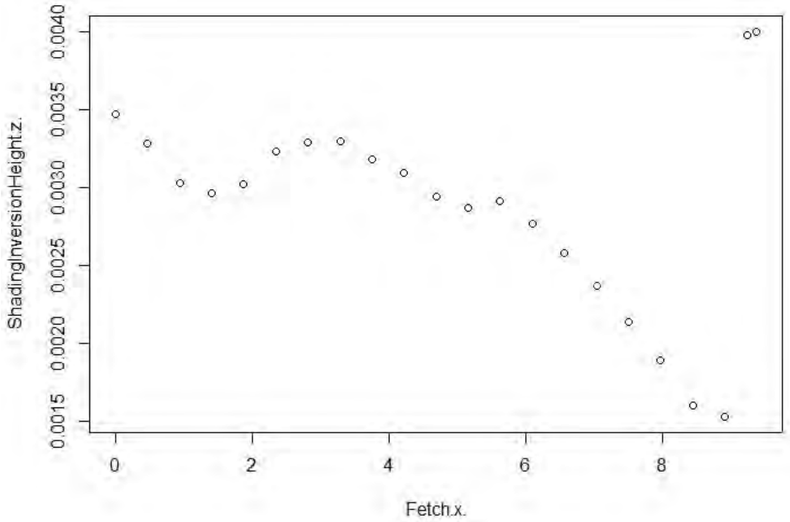

Figure 6.11: Case 3_Inversion height z versus fetch x

Case 4: In the fourth case water of the whole lake was completely shaded from solar radiation with inlet temperature equals the minimum temperature of the day. In this case, the inversion layer decreases in height with the increasing fetch (fig6.12).

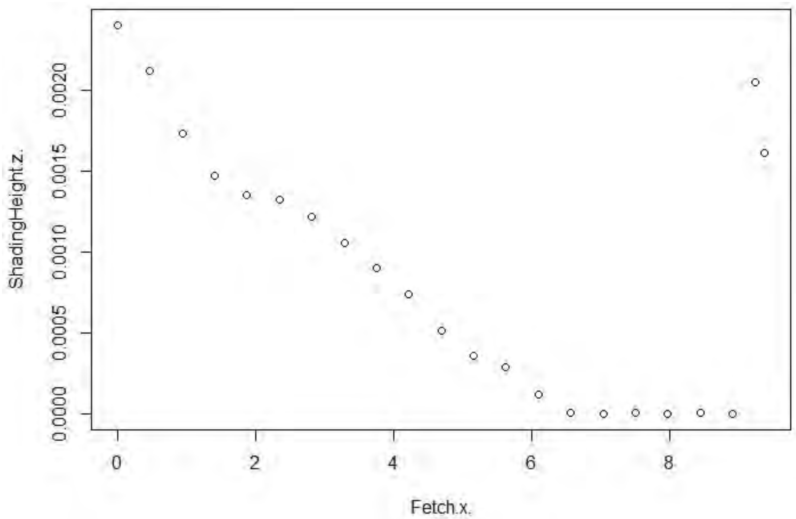

Figure 6.12: Case 4_Inversion height z versus fetch x

Correlation between the Inversion height and Fetch:

Table 6.5 shows the correlation between the inversion height and fetch. In case of case 1 and 2 inversion height has a strong positive correlation with fetch with the case1 has the strongest positive correlation. Whereas in case of case 3 and 4 correlation is negative with the case 4 is having the strongest negative correlation.

Table 6.5: Correlation between inversion height and fetch

	Pearson's product-moment correlation between Inversion height z and fetch x
Case 1	0.8494861
Case 2	0.7983775
Case 3	-0.3815254
Case 4	-0.5927785

This correlational analysis clearly demonstrates the effect of riparian shading on the water temperature of the lake and hence the thickness of the inversion layer. It is clear from the study that Urban wetland with shade and less warm wind flow from the upwind will have thinner inversion layer than the wetland with no shading and warmer inflow.

Also, relative humidity(RH) above the inversion layer of the lake will be less even comparing with the land. This is the reason in the field study the urban station over the water of the lake and edge of the lake showed lower Relative Humidity(RH) compared to the urban station deep inside the fabric. Because in average urban station above the water surface and edge of the lake were approximately 6m above the water. So those urban stations were above the inversion layer and hence showed lower RH.

6.3.4 Inversion model

A linear regression model has been built based on the simulation model to test the relation between fetch, inversion layer thickness, temperature and horizontal component of total energy flux in the inversion layer. All the four cases described in the chapter 6 are considered in the regression analysis. The variables included are:

Independent variable: Fetch (x)

Dependent variable: Inversion height (z), Air temperature (T), Relative humidity (RH), horizontal component of the total energy flux (*f*).

From the simulation data, all the values of the variables are selected for the fully saturated air i.e. 100% relative humidity. The regression analysis is done on the R-studio using “R” programming language. Following are the regression models that describe the relationship:

Case 1:

For the case one the regression model is:

$$x = 39.42 + 868.6928z - 1.319T + .003547f$$

From the model it is obvious that if the T and *f* are unchanged increasing fetch will increase the inversion layer thickness.

Case 2:

For the case two the regression model is:

$$x = 43.02 + 740.7z - 1.321T + .00004596f$$

From the model it is obvious that if the T and *f* are unchanged increasing fetch will increase the inversion layer thickness, although the increase will be less than case 1.

From these two models, it is clear that we have to reduce fetch to reduce the thickness of the inversion layer and thus promote heat exchange between water and the air blowing above it. To reduce fetch longer direction or length of the wetland should be perpendicular to the prevailing wind direction.

Case 3:

For the case three the regression model is:

$$x = 3.317 - 491.1z - .3212T + .00004596f$$

From this model it is obvious that if the T and *f* are unchanged increasing fetch will decrease the inversion layer thickness.

Case 4:

For the case four the regression model is:

$$x = -17.74 - 305.93952z + 1.0244T - .01463f$$

From the model it is obvious that if the T and *f* are unchanged increasing fetch will decrease the inversion layer thickness. This reduction will be greater than case 3.

Form these four models it is obvious that in an unshaded wetland increasing fetch will increase the depth of the inversion layer, whereas in a shaded wetland increasing fetch will decrease the depth of the inversion layer. As the inversion layer decreases with increasing fetch and thus promote heat exchange between water and the air blowing above it.

6.3.5 Effect of the relative humidity on the inversion layer thickness

To test the relationship between the inversion height and the relative humidity two additional scenarios of relative humidity had been considered both with the case 1 and case 3 described before.

Case 1: In the first case water of the whole lake was under complete under solar radiation with inlet temperature equals the maximum temperature of the day. Relative humidity (RH) was equal to the starting RH obtained from the field measurement at 9:00 am which was 51.5%. In the first scenario of case1 initial RH is set to 1.5 times of RH of the field measurement, which is 77.25%. In the second scenario of case1 initial RH is set 0.5 times of RH of the field measurement, which is 25.75%. The results of case 1 with 2 scenarios are plotted below in figure 6.13.The results clearly indicate the increase of the inversion layer thickness with increasing humidity from the upwind flow.

Case 3: In the third case water of the whole lake was completely shaded from solar radiation with inlet temperature equals the maximum temperature of the day. Relative humidity (RH) was equal to the starting RH obtained from the field measurement at 9:00 am which is 51.5%. In the first scenario of case3 initial RH is set to 1.5 times of RH of the field measurement, which is 77.25%. In the second scenario of case3 initial RH is set 0.5 times of RH of the field measurement, which is 25.75%. The results of case 3 with 2 scenarios are plotted below in figure 6.14.

The results clearly indicate the increase of the inversion layer thickness with increasing humidity from the upwind flow although the water surface is under completely shading.

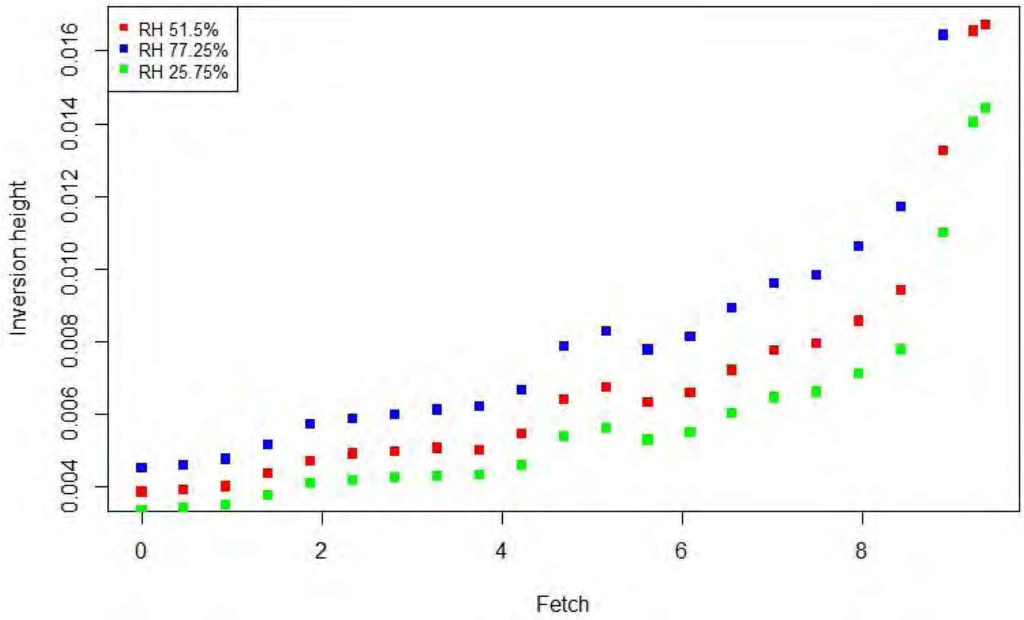

Figure 6.13: Case1_Effect of relative humidity (RH) on inversion height

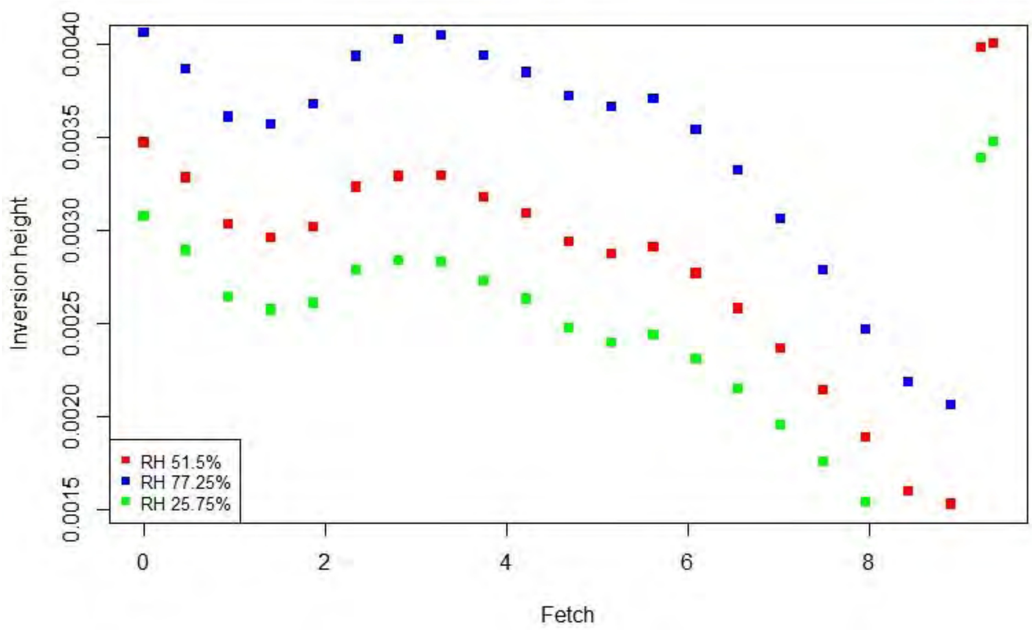

Figure 6.14: Case3_Effect of relative humidity (RH) on inversion height

6.3.6 Effect of the orientation and riparian shading height of the wetland on the water temperature

The effect of orientation and shading height on the water surface temperature was simulated. The simulation time was 9:00 hours in the morning to 16:00 hours in the afternoon. The date of the simulation was considered as 24th February to keep consistency with the field measurement date of the Dhanmondi lake area. For this simulation a hypothetical wetland of linear shape with shading on it's both side was considered. Four ratios between the shading height (H) and wetland water surface width (W) was considered in conjunction with three orientations of the wetland. The ratios were H/W=1, H/W=2, H/W=3 and H/W=4. The three orientations of the long axis of the wetland considered were East-West (90°), North/East-South/West (45°) and North-South (0°). The result of the simulations is given on the following figure 6.15.

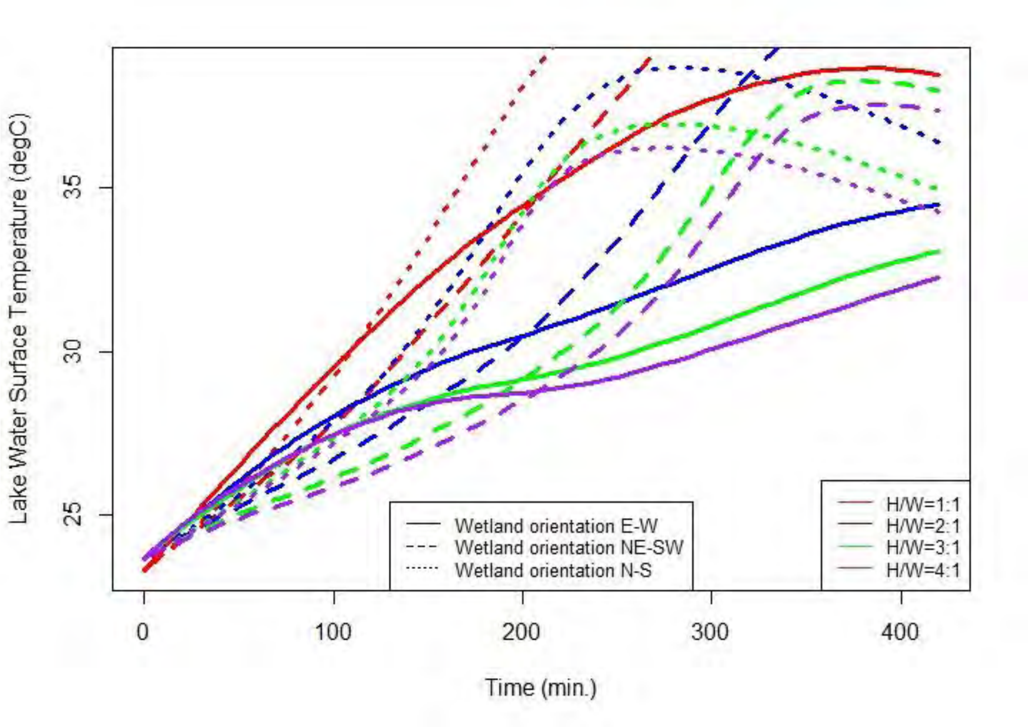

Figure 6.15: Effect of wetland orientation and ratio of shading height (H) vs water surface width (W) on the temperature of water surface.

It could be concluded from figure 6.15 that for the same amount of shading if the long axis of the wetland is oriented towards East-west (i.e. wetland is more elongated towards East-West than North-South), it will be shielded more from the direct solar radiation, hence heat gain will be less. Wetland with long North-South axis is less desirable in terms of shading from direct shortwave radiation from sun. Although Increase in H/W ratio will provide better shielding against the direct solar radiation, but together with the correct orientation this high H/W ratio will create optimal shading for the water of the wetland. Also, beyond H/W ratio 2, further increase in shading height won't bring significant benefit in terms of controlling the temperature of the water surface.

6.4 References

1. Bert Blocken. (2015). "*Computational Fluid Dynamics for urban physics: Importance, scales, possibilities, limitations and ten tips and tricks towards accurate and reliable simulations"*. Building and Environment 91, 219-245.
2. Blocken B, Stathopoulos T, Carmeliet J. "*CFD simulation of the atmospheric boundary layer: wall function problems"*. Atmos. Environ 2007;41(2): 238-52.
3. Blocken B, Carmeliet J, Stathopoulos T. "*CFD evaluation of wind speed conditions in passages between parallel buildings effect of wall-function roughness modifications for the atmospheric boundary layer flow"*. J Wind Eng. Ind. Aerodyn. 2007;95(9e11):941-62.
4. Di Sabatino S, Buccolieri R, Pulvirtenti B, Britter R. "*Simulations of pollutant dispersion within idealised urban-type geometries with CFD and integral models"*. Atmos. Environ 2007; 41:8316-29.
5. Fraedrich K. (1972). "*On the evaporation of a lake in warm and dry environment*". Tellus, 24: 116–121. doi:10.1111/j.2153-3490. 1972.tb01538.x
6. Franke J, Hellsten A, Schlünzen H, Carissimo B. (2007). "*Best practice guideline for the CFD simulation of flows in the urban environment"*. Brussels: COST Office; 2007, ISBN 3-00-018312-4.
7. Gorl_e C, van Beeck J, Rambaud P, Van Tendeloo G. "*CFD modelling of small particle dispersion: the influence of the turbulence kinetic energy in the atmospheric boundary layer"*. Atmos. Environ 2009;43(3):673-81.
8. Hargreaves DM, Wright NG. "*On the use of the k-ε model in commercial CFD software to model the neutral atmospheric boundary layer"*. J Wind Eng. Ind. Aerodyn 2007;95(5):355e69.
9. Incropera F.P., DeWitt D.P., Bergman T.L., and Lavine A.S. (2006). "*Fundamentals of Heat and Mass Transfer"*, 6th ed., John Wiley & Sons.
10. Monteith J. L. & Unsworth M. H. (2013). "*Principles of environmental physics"*. 4th edition, Academic Press
11. Parente A, Gorl_e C, van Beeck J, Benocci C. "*Improved k-ε model and wall function formulation for the RANS simulation of ABL flows"*. J Wind Eng Ind Aerodyn 2011;99(4):267-78.
12. Richards PJ, Hoxey RP. *"Appropriate boundary conditions for computational wind engineering models using the k-ε turbulence model".* J Wind Eng Ind Aerodyn 1993;46&47:145-53.
13. Richards PJ, Norris SE. "*Appropriate boundary conditions for computational wind engineering models revisited"*. J Wind Eng. Ind. Aerodyn 2011;99(4): 257-66.
14. Tucker PG, Mosquera A. "*NAFEMS introduction to grid and mesh generation for CFD"*. NAFEMS CFD Working Group; 2001. p. 56. R0079.
15. Tominaga Y, Mochida A, Yoshie R, Kataoka H, Nozu T, Yoshikawa M, et al. "*AIJ guidelines for practical applications of CFD to pedestrian wind environment around buildings"*. J Wind Eng. Ind. Aerodyn. 2008;96(10-11):1749-61.
16. van Hooff T., Blocken B. "*Coupled urban wind flow and indoor natural ventilation modelling on a high-resolution grid: a case study for the Amsterdam ArenA stadium"*. Environ Model Softw 2010;25(1):51-65.
17. Wilcox D.C. (1998) *"Turbulence modeling for CFD*". DCW industries Inc. La Canada, California.
18. Yang Y, Gu M, Chen S, Jin X. "*New inflow boundary conditions for modelling the neutral equilibrium atmospheric boundary layer in computational wind engineering"*. J Wind Eng. Ind. Aerodyn 2009;97(2):88-95.
19. COMSOL Documentation. (n.d.). Retrieved February 01, 2018, from https://www.comsol.com/documentation

Chapter 7 : TRANSFORMING URBAN WETLAND INTO URBAN COOLING ISLANDS

7.1 Significant Findings of Urban Cooling Islands

Throughout the research, reasons effecting Urban wetland to their ability to act as an adaptation strategy against Urban heat island (UHI) has been identified. Those reasons are summarized below:

7.1.1 Change of surface Urban Heat Island

Landsat estimated UHIsurf for Dhaka in 12 December 1991 is 5.18°C and 16 December 2016 is 7.07°C. within the span of 25 years Landsat estimated Surface Urban Heat Island (UHIsurf) increased around 2°C. Newly developed urban area has exhibited highest change in UHIsurf. Urban canyon with shading exhibited decreased Land surface temperature (LST) due to increased shading from tall building. These findings have been based on the Urban Heat Island study of chapter two.

7.1.2 Rate of change of temperature and relative humidity in terms of solar influx

Time if considered as a continuous independent variable rather than a categorical value has a cumulative effect throughout the day and night on independent variables like Air Temperature and Relative Humidity (RH) in terms of solar influx. During the day at the land rate of change of air temperature are strongly positively correlated with cumulative time in terms of solar influx which is strongly negative at night. On the other hand, at the land during the day rate of change of RH has strong negative correlation with cumulative time in terms of solar influx, which is strongly positively correlated at night. These findings have been detailed on the field measurement of chapter five.

7.1.3 Shading impact on rate of change of temperature and relative humidity

In case of the urban wetland devoid of riparian shading this cumulative effect of time on Air temperature and RH becomes stronger near the edge and at the top of wetland. Whereas, in case of the urban wetland with significant riparian shading this cumulative effect of time on Air temperature and RH becomes weaker near the edge and at the top of the water surface of wetland. But in both the case cumulative effect of time on Air temperature and RH still maintains the same trend.

7.1.4 Humidity distribution

Contrary to the common assumption, Relative Humidity (RH) near the edge of wetland and at the top of water surface of the wetland are lower than the park and the vegetated area.

7.1.5 Day time evaporative cooling potential

With the progress of the day relative humidity decreases, which dips significantly from the mid-day to late afternoon, which increase evaporative cooling potential of urban environment.

7.1.6 Inversion layer development

When relatively dry and warm air from a warmer land advected at the top of the water surface of the wetland a shallow stably stratified layer of fully saturated air develops over the surface of the wetland known as “inversion layer”. Although the inversion layer can develop even air temperature of the surroundings environment is less than or equal to the temperature of the wetland it is most amplified if the advected air is warmer and relatively dry.

7.1.7 Evaporation suppression

Inversion layer at the top of the water surface act as a “vapor blanket” and suppress the evaporation from the lake which increases with travelling distance of the air from the land-lake boundary to the downwind direction.

7.1.8 Humidity over wetland

Relative Humidity (RH) above the inversion layer is relatively low and air temperature is higher, that is why wetland devoid of riparian shading exhibits low RH and higher air temperature above its water surface in the middle and at the edge of wetland.

7.1.9 Fetch and the inversion height

Fetch or leading edge is the distance from the land-lake boundary at the upwind side to the downwind side towards the wind direction. In case of wetland without shading inversion height of the inversion layer increases with increasing fetch. In case of wetland with significant shading inversion height of the inversion layer decreases with increasing fetch.

7.2 Measures to Create Urban Cooling Islands

Form the research some important measures have been identified to convert urban wetlands as Urban Cooling Island. They are given below:

7.2.1 Shading measure

Riparian shading provides thermal and ecological benefit by moderating the water temperature of the wetland. At least 30m wide riparian shading needed to protect the physical, chemical and biological integrity of wetland. Riparian Shading the urban wetlands alone can significantly improves the water quality by lowering water temperature. Shading of urban wetland by topography and built form also positively modify Urban thermal environment. Also Shading in the urban canyon can decrease air temperature.

7.2.2 Orientation measure

E-W elongation of the wetland can produce greatest shielding from the direct solar influx. Complex wetland shape with major east-west axis have the greatest shading potential beside other ecological potential.

7.2.3 Advection measure

The cooling effect produced in the wetland by exchanging heat between air and water would carried to the land at upwind through advection known as "leading-edge or fetch effect".

7.2.4 Proximity measure

Urban Cooling Intensity of the urban wetland are correlated with the distance from the edge of the wetland. UCI intensity in generally more prominent within 500 m from the edge of the wetland. This correlation is generally more at the downwind side of the wetland than the upwind side. UCI intensity also vary seasonally and closely moderated by riparian, topographical and build form shading.

7.2.5 Air corridor from the wetland measure

The point on the urban fabric located on the road parallel to the wind direction from the wetland can benefit from the cooling effect through advection of air from the wetland (Figure 7.1).

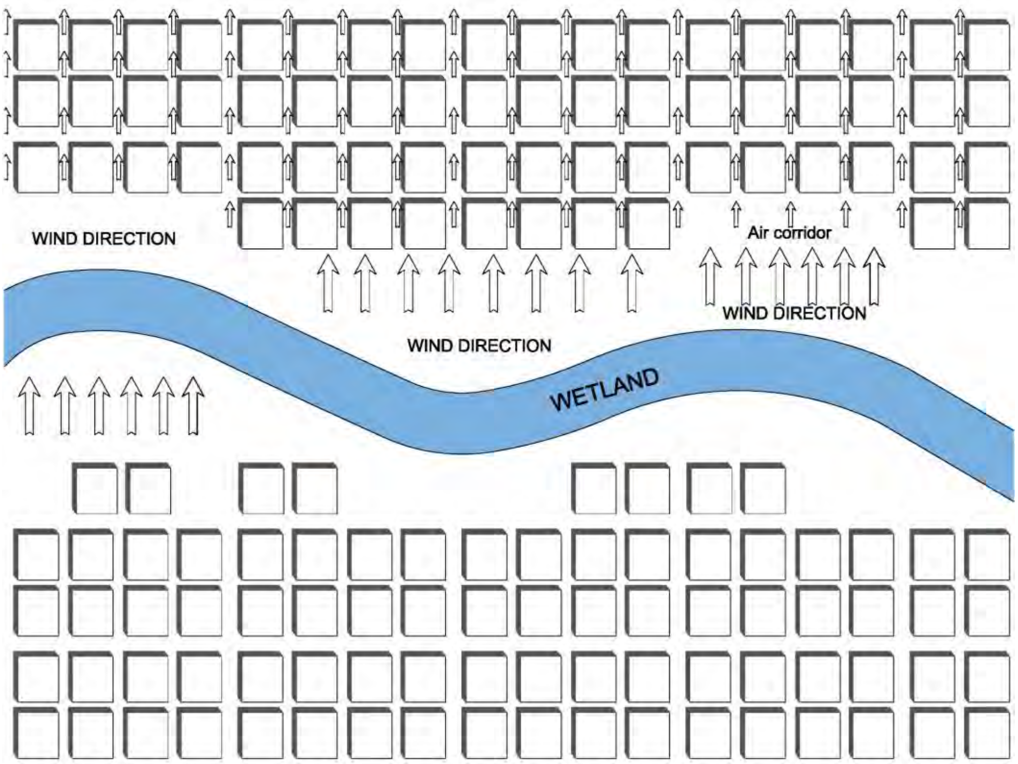

Figure 7.1: Air corridor inside the Urban fabric

7.2.6 Oasis effect measure

Existence of urban park creates oasis effect in otherwise dry urban surroundings. Because due to the more surface area present in the leaves of plant they can evaporate more water to cool down the air surrounding them by removing latent heat from the air. Among the artificial measures to create oasis effect, fountains and sprinkler will also have positive impact as they break down the water into smaller particles which promote rapid evaporation and thus cooling.

7.3 Wetland as An Urban Cooling Islands in Urban Design

To effectively use urban wetland as an urban cooling islands several strategies might need in existing urban area and new design. One of the most important strategies found from the research is delineated in the following section.

7.3.1 Controlling the "inversion layer" over the water surface of urban wetlands

One of the consideration in the urban area for the wetland should be strategy to keep "Inversion layer" over the surface of wetland weak. Because inversion layer suppresses the evaporation from the water surface and also act as barrier between heat exchange in between the water surface and air above it to cool down. There are several ways to weaken the inversion layer above the water surface.

Preventing solar gain of the urban wetland:

As the inversion layer thickens with the heat supplied from sun following measures should be taken to prevent direct solar gain from the sun:

a. **Riparian shading:**

Shading is one of the most important parameter to keep the water of the urban wetland from gaining heat. The 30m buffer of riparian shading should be maintained around the edge of the wetland to gain optimum thermal performance. Where the riparian shading is not possible, built structure could be oriented to shed the water of the lake. If the wetland is wider emergent macrophytes and other water born local trees could be introduced to keep the water of the wetland under shading. Wetland plant species also helps to improve the quality of water besides shading.

b. **Topographical shading through orientation:**

If the wetland could be oriented in a correct orientation (figure: 7.2) it can utilize the benefit of shading from the natural feature like hills or high land. Also in case of low water level, which often happens in the dry season wetland can shade itself by its bank. For this reason, E-W orientation will be most beneficial for reducing solar gain though out the day.

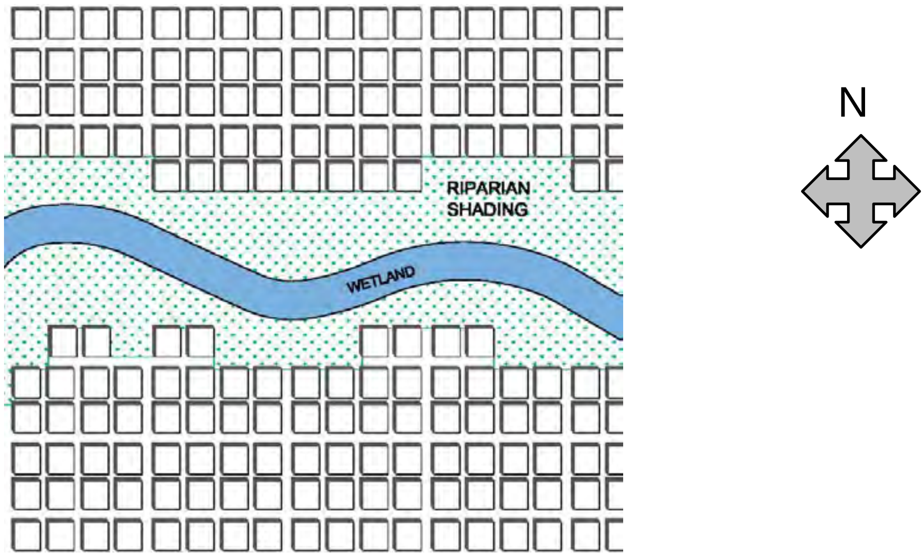

Figure 7.2: Correctly oriented (E-W axis) Wetland for both topographical and riparian shading

Controlling "Fetch" to reduce the thickness of inversion layer:

Controlling of "Fetch" could be effective strategy to reduce inversion layer in case of Urban wetland. Four linear regression models were built based on the simulation model to test the effect of fetch on inversion layer in chapter 6. Based on those models following are the strategies for fetch control.

a. **Wetland without shading "reduce fetch":**

Urban areas like case one and case two of the simulation study need to follow similar strategy for fetch control. For an unshaded urban wetland, we have to reduce fetch to reduce the thickness of the inversion layer and thus promote heat exchange between water and the air blowing above it. Thus, the warm air cooled down by the wetland could be supplied to the urban area at the downwind side for urban cooling. To reduce fetch longer direction or length of the wetland should be perpendicular to the prevailing wind direction (Fig 7.3).

b. **Wetland with shading "increase fetch":**

Urban areas like case two and case three of the simulation study need to follow similar strategy for fetch control. For a shaded urban wetland, we must increase fetch to reduce the depth of the inversion layer as the inversion layer decreases with increasing fetch and thus promote heat exchange between water and the air blowing above it. Thus, the warm air cooled down by the shaded wetland could be supplied to the urban area at the downwind side for urban cooling. For this reason, wetland should be oriented with its longer dimension parallel to the prevailing wind, to increase contact between wind and the water surface (Figure 7.4).

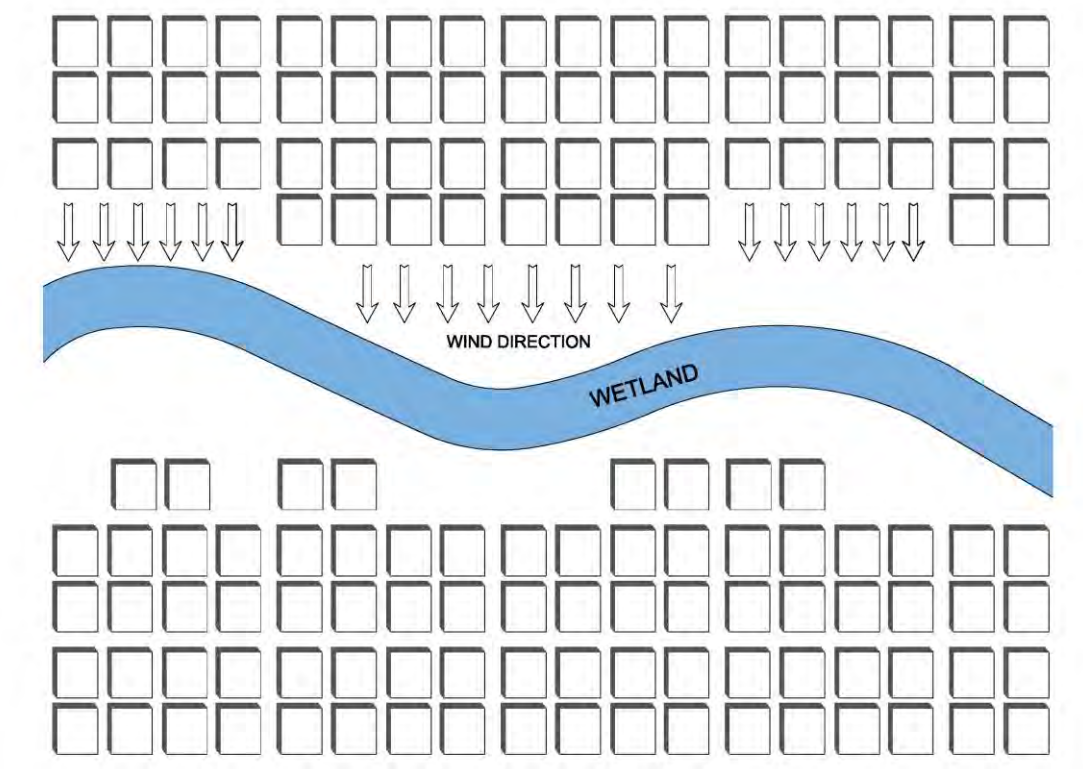

Figure 7.3: Wind flow direction in Wetland with no shading

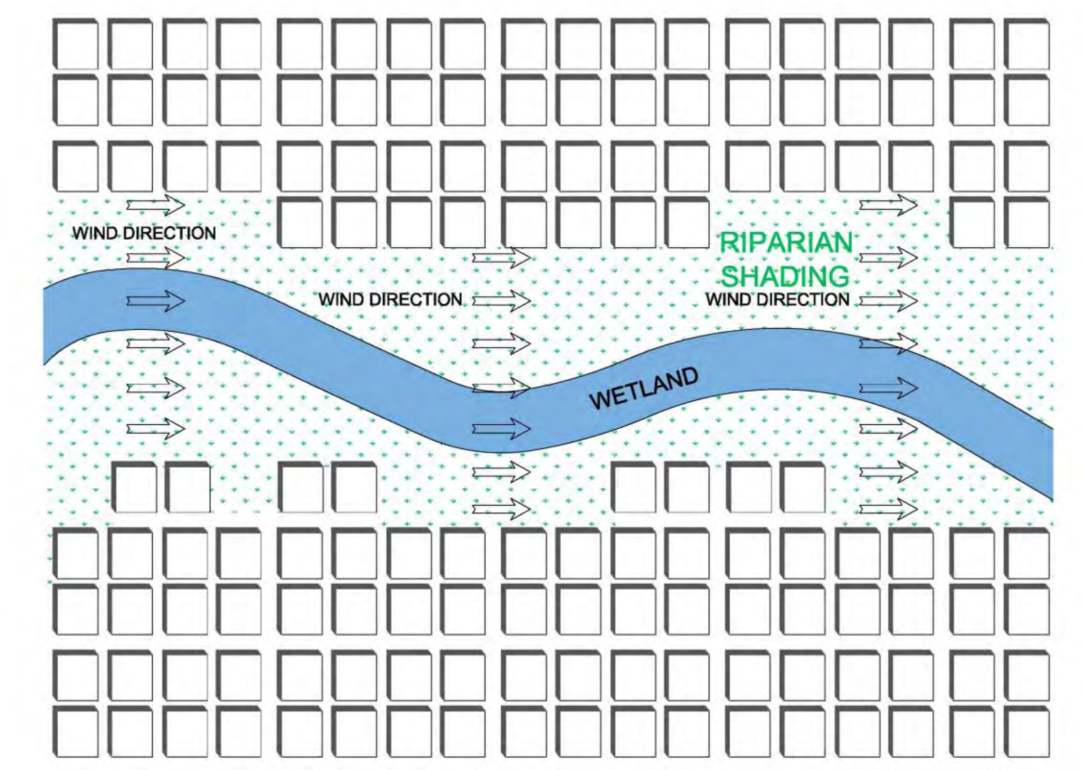

Figure 7.4: Wind flow direction in Wetland with riparian shading

7.4 Urban Design Guidelines for Urban Wetland

Urban wetlands are paramount for their environmental functions besides their role in improving the aesthetic characteristics of urban places. They also have significant social and economic functions besides its primary environmental functions. To use the wetland in the urban fabric without considering its wide range of physical and morphological characteristics might create unfavorable urban environment or may result in a loss of opportunity. However shading is essential for the urban environment in the tropics. Without necessary shading urban wetland will cease to play its role as a source of coolth for the urban fabric. Shading of the urban wetland could be achieved through topography, urban built form, and riparian shading. Although built form and topographical shading potentially shield the urban wetland from the direct solar radiation to prevent temperature increase of the wetland water, they don't have any other ecological, economical, and social functions pertaining to the wetland. On the other hand, riparian shading of urban wetlands both by the shade trees and macrophytes have multiple economic and social functions besides their multiple primary environmental functions. Beside preventing the temperature increase of wetland water, shade trees and macrophytes included in riparian shading further cools down the urban environment through evapotranspiration. While floating and emergent macrophytes contribute in improving water quality, large shade trees can trap airborne pollutants to improve air quality. Carbon sequestration is an important function by large shade trees and macrophytes besides creating habitat for urban wild life. Space under the large shade beside the wetland can act as emergency evacuation spaces in times of major urban disaster like earthquakes or fire subject to their accessibility. The shade trees and wetland plants (macrophytes) can transforms the urban wetland into a leisure space in the form of a wetland park which is an immense social service. So, urban wetland with riparian shading can render several environmental, economic, and social functions besides its essential role as "Urban Cooling Island (UCI)". The application of the urban design guidelines for urban wetlands provided in the design matrix in figure 7.5 can provide a thermally desirable micro climate which is essential in the warm-humid conditions of Bangladesh as an adaptation measure against climate change. The effectiveness of the urban design guidelines for urban wetlands can be improved significantly if they are adopted as a part of overall urban design scheme.

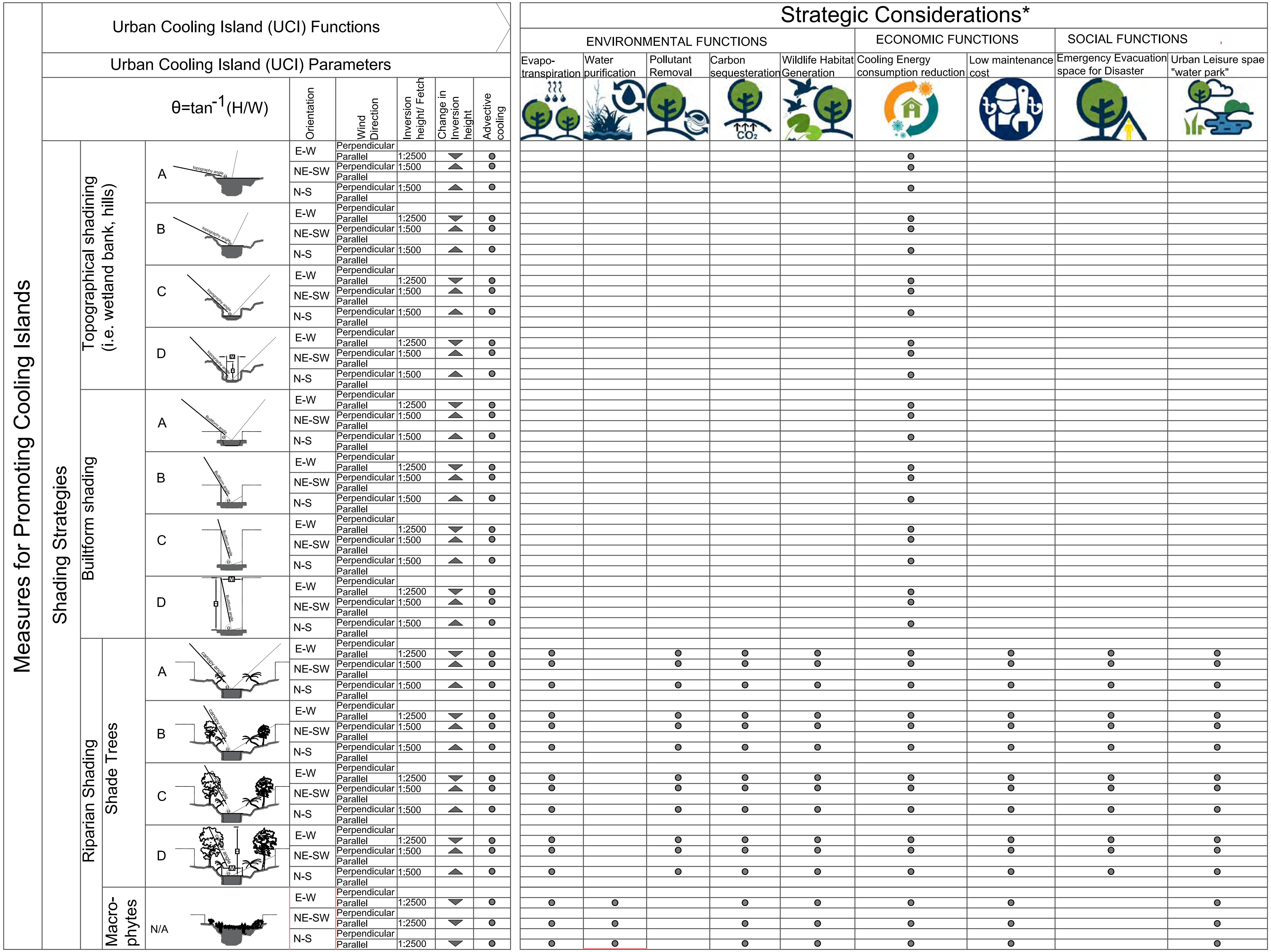

H/W ratio category: A< 1, B=1, C=2, D=3 or more ▼ Lower value ▲ Higher value • Affirmative Ө=Shadow angle

*Strategic Considerations were derived from secondary data

Figure 7.5: Urban design matrix for urban wetlands

7.5 Suggestions for Further Work

Further works are required to investigate the behavior of urban wetland in terms of its heat exchange with the atmosphere and with the land. This works required specially in two forms:

Field measurement:

Field measurement at multiple points both at horizontal and vertical direction to capture the characteristic of the inversion layer in detail. This measurement need to be carried out both diurnal basis and throughout the whole year in different season. Because in this study the measurement point was only one or two points at the top and edge of the water with no robust measurement to capture the vertical profile of the variables.

Simulation work:

Due to the limited computational resources, the simulation model of the urban area was scaled down to 1:50 and also simplified. So, to get accurate understanding of the heat exchange mechanism of the urban wetland with its surroundings and atmosphere full scale model simulation with possible detail is required. Also, evapo-transpiration of tree has not been included in the simulation model, which must be included to get accurate scenario of urban environment.

Appendix 1 Wilcox *K*-Ω Turbulence Model

With the *k*-ω model (Wilcox, 1993,1998) the major difference from the standard k– ε model is that the second turbulence property solved is the specific dissipation:

$$\omega = \frac{\varepsilon}{k\beta'}$$

The constant β' is equivalent to C_μ and also has a value of 0.09.

The conservation equations are:

$$\frac{D(\rho k)}{Dt} = \tau_{ij}\frac{\partial U_i}{\partial X_j} - \beta'\rho k\omega + \frac{\partial}{\partial X_j}(\left(\mu_l + \frac{\mu_T}{\partial_{kw}}\right)\frac{\partial k}{\partial X_j})$$

$$\frac{D(\rho\omega)}{Dt} = \alpha\frac{\omega}{k}\tau_{ij}\frac{\partial U_i}{\partial X_j} - \beta\rho\omega^2\frac{\partial}{\partial X_j}(\left(\mu_l + \frac{\mu_T}{\partial_\omega}\right)\frac{\partial\omega}{\partial X_j})$$

with the supplementary equation:

$$\mu_T = \rho\frac{k}{\omega}$$

Solution of these equations for the atmospheric surface layer as a horizontally homogeneous turbulent surface layer (HHTSL) is essentially the same as for the k–ε model and yields essentially the same U and k; however, with the standard constants α=5/9, β=0.075, $\sigma_{kw} = 2$, $\sigma_\omega = 2$ the effective Von Kármán's constant is given by:

$$k_{k-\omega} = \sqrt{\frac{(\beta - \alpha\beta')\sigma_\omega}{\sqrt{\beta'}}} = 0.408$$

Wilcox (1993, p.94) explains that the value was chosen in order to be consistent with a Von Kármán's constant of 0.41.

The profile of the specific dissipation is given by:

$$\omega = \frac{u_*}{\sqrt{\beta'}k_{k-\omega}z}$$

To implement the model similar boundary conditions are imposed at the upper boundary, with the flux of ω being prescribed as:

$$\frac{\mu_T}{\sigma_\omega}\frac{d\omega}{dz} = -\frac{\rho {u_*}^2}{\sqrt{\beta'}\sigma_\omega z}$$

Appendix 2 Instrumentation

Appendix 2.1 Temperature and humidity data logger

EL-USB-2-LCD

Temperature, Humidity and Dew Point Data Logger with LCD Screen.

1. -35 to +80°C (-31 to +176°F) and 0 to 100%RH measurement range
2. Stores over 16,000 readings for both temperature and humidity
3. Easy Log software available as a free download
4. High contrast LCD, with two-and-a-half-digit temperature and humidity display function
5. Logging rates between 10 seconds and 12 hours
6. Immediate, delayed and push-to-start logging
7. User-programmable alarm thresholds for both temperature and humidity
8. Status indication via red/green LEDs
9. Environmental protection to IP67

Specification:

Temperature	**Measurement range**	-35 to +80°C (-31 to +176°F)
	Internal resolution	0.5°C (1°F)
	Accuracy (overall error)	±0.3°C (±0.7°F) typical (see page 3)
	Repeatability	±0.1°C (±0.2°F)
	Long term stability	<0.02°C (0.04°F)/year
Relative Humidity	**Measurement range**	0 to 100%RH (see page 3)
	Internal resolution	0.5%RH
	Accuracy (overall error)	±2%RH typical (see page 3)
	Repeatability	±0.1%RH
	Long term stability	<0.25%RH/year
Dew Point	**Accuracy (overall error)**	±1.1°C (±2°F)
Logging rate		User selectable between 10 seconds & 12 hours
Operating temperature range		-35 to +80°C (-31 to +176°F)
Battery life		2 years (at 25°C and 1 minute logging rate, LCD on)
Readings		16,382 temperature, 16,382 relative humidity
Dimensions		126 x 25 x 22mm (4.96 x 0.98 x 0.86")

Appendix 2.2 Temperature and humidity data logger
Extech Big Digit Indoor/Outdoor Hygro-Thermometer

1. Max/Min with "reset" function
2. Humidity: 10 to 99% RH
3. Temperature: 14 to 140°F or -10 to 60°C
4. Accuracy: ±5%RH; ±1.8°F, ±1°C
5. Dimensions: 4.3 x 3.9 x 0.78" (109 x 99 x 20mm)
6. Weight: 6oz (169g)
7. Complete with built-in stand, wall mounting bracket, outdoor sensor with 35" (89cm) cable, and 01.5V AAA battery

Appendix 2.3 Dial stem thermometers
Extech Penetration Stem Thermometer For use in liquids, semi-solids and solids

Penetration Stem (Model 392050):
Temperature range: -58 to 302°F (-50 to 150°C)
Basic Accuracy of 2°F or 1°C
0.1° resolution to 199.9; 1° over 200°

Appendix 2.4 Temperature and wind speed logger
Extech Cup Thermo-Anemometer AN400

The AN400 measures air velocity in five units of measure: feet per minute (ft/min), meters per second (m/sec), miles per hour (MPH), kilometers per hour (km/hr), & nautical miles per hour (knots). The low-friction cup vane freely rotates in response to air flow. An internal thermistor allows the AN400 to measure air temperature in Centigrade or Fahrenheit units. This meter is shipped fully tested and calibrated and with proper use will provide years of reliable service

Specification:

Circuit description: Custom LSI microprocessor design
Display: Dual function 9999 count LCD display
Measurement units: m/s, km/h, ft/min, knots, mph, Temperature oC/oF
Data hold: Freezes reading on the display
Sensor Structure: Air velocity sensor: Cup vane arm with low-friction ball bearing design. Temperature sensor: Precision thermistor
Memory Recall: Record and Recall Maximum (MAX) and Minimum (MIN) readings
Data Logger: Manual store/recall of up to 100 data points
Auto Power off: After 10 minutes
Sampling Time: Approx. 1 second
Water Resistance: IP65
Operating Temperature: 32 °F to 122 °F (0 °C to 50 °C)
Operating Humidity: Max. 80% RH
Power Supply: 4 x 1.5V AAA batteries
Power Consumption: Approx. 6.8mA DC (typical battery life: approx. 150 hrs)
Weight: 0.4 lbs. (181g)
Dimensions: Main instrument: 7.5 x 1.6 x1.3” (190 x 40 x 32mm)
Cup Vane: 5.3” (135mm) diameter

Appendix 2.5 Weather station

Davis Vantage Vue® wireless weather station

Specification:

Operating Temperature .... -40° to +150°F (-40° to +65°C)
Non-operating (Storage) Temperature......................... -40° to +158°F (-40° to +70°C)
Current Draw ....0.20 mA (average), 30 mA (peak) at 3.3 VDC
Solar Power Panel ....0.5 Watts
Battery ....CR-123 3-Volt Lithium cell
Battery Life (3-Volt Lithium cell) ....8 months without sunlight - greater than 2 years depending on solar charging
Wind Speed Sensor ....Wind cups with magnetic detection
Wind Direction Sensor ....Wind vane with magnetic encoder
Rain Collector Type ....Tipping spoon, 0.01" per tip (0.2 mm with metric rain cartridge, Part No. 7345.319), 18.0 in2 (116 cm2) collection area
Temperature Sensor Type ....PN Junction Silicon Diode
Relative Humidity Sensor Type ....Film capacitor element
Housing Material ....UV-resistant ABS & ASA plastic
ISS Dimensions ....12.95" x 5.75" x 13.40" (329 mm x 146 mm x 340 mm)
Package weight: ....5.44 lbs (2.47 kg)

Appendix A: Data from the field measurement and Remote Sensing

Dhanmondi Lake Area: Land Surface Temperature and Distance from Lake edge_2013-17

Name	LST13APR12	Distance WD (9am-200, 12pm-180)
UCILogger_KI	27.55899239	0
UCILogger_KIB	27.51291466	0
UCILogger2	28.26181602	0
UCILogger1	26.89401627	0
UCILogger8	29.3281517	485
UCILogger7	29.20265007	619
UCILogger6	29.37782478	328
UCILogger4	29.16551018	397
UCILogger3	29.12707901	249
DP41	29.824646	374
DP40	29.35160255	280
DP39	28.78481483	256
DP38	28.11304283	88
DP37	28.10058594	76
DP36	27.91230965	322
DP35	28.75405884	33
DP34	29.42637825	848
DP33	29.60425568	181
DP32	29.87803459	221
DP31	30.33423996	1280
DP30	28.96141624	101
DP29	29.65961456	172
DP28	30.0568409	1162
DP27	29.12354279	1066
DP26	29.93835449	1038
DP25	28.94070244	985
DP24	29.88695717	958
DP23	29.45984077	905
DP22	28.82393265	883
DP21	29.33380699	793
DP20	30.02137756	742
DP19	29.8374176	637
DP18	29.22636223	677
DP17	29.20448685	750
DP16	27.81456566	760
DP15	28.82081223	689
DP14	27.58621025	156
DP13	29.19809532	549
DP12	30.1885643	514
DP11	29.63791847	465
DP10	29.95774269	403
DP9	29.76374054	286
DP8	29.66111755	345
DP7	29.10132027	355
DP6	29.177248	70
DP5	28.75335121	83
DP4	27.80923843	91
DP3	29.32538795	177
DP2	29.63889694	212
DP1	28.96811104	226

	LST13APR12	*Distance WD (9am-200, 12pm-180)*
LST13APR12	1	
Distance WD (9am-200, 12pm-180)	0.501809462	1

Name	LST13DEC24	Distance WD (9am-270, 12pm-270)
UCILogger_KI	20.5145359	0
UCILogger_KIB	20.57286072	0
UCILogger2	21.18546104	0
UCILogger1	20.35394287	0
UCILogger8	21.9434967	178
UCILogger7	21.87019348	283
UCILogger6	22.10237694	150
UCILogger4	21.79226494	438
UCILogger3	21.92160416	63
DP41	21.55378723	711
DP40	22.02470016	105
DP39	21.90082169	49
DP38	21.50691414	29
DP37	21.1554451	31
DP36	20.78884506	60
DP35	21.34121132	107
DP34	21.69859123	463
DP33	21.50734329	48
DP32	21.90434265	245
DP31	22.18977737	373
DP30	21.26730347	54
DP29	21.67851257	123
DP28	22.23493004	366
DP27	21.62276459	71
DP26	22.06394959	928
DP25	21.90188026	74
DP24	22.34445572	896
DP23	21.70721054	636
DP22	21.18813896	193
DP21	21.79416275	595
DP20	21.79439926	799
DP19	22.13556099	702
DP18	21.71347618	541
DP17	21.99071121	309
DP16	20.93001938	131
DP15	21.80297279	198
DP14	20.73634338	43
DP13	21.50531006	152
DP12	22.17165947	605
DP11	22.30623817	349
DP10	22.21884346	517
DP9	22.26106644	472
DP8	22.10262871	256
DP7	21.95052528	77
DP6	21.64117622	131
DP5	21.55214882	138
DP4	20.7632122	41
DP3	21.98130226	349
DP2	22.16476059	213
DP1	21.79588127	74

	LST13DEC24	*Distance WD (9am-270, 12pm-270)*
LST13DEC24	1	
Distance WD (9am-270, 12pm-270)	0.540160694	1

Name	LST13JUN15	Distance WD (9am-90, 12pm-90)
UCILogger_KI	19.95090675	0
UCILogger_KIB	19.95290375	0
UCILogger2	21.62176895	0
UCILogger1	20.94186783	0
UCILogger8	21.57720947	178
UCILogger7	21.50227356	283
UCILogger6	21.50240898	150
UCILogger4	21.24580002	438
UCILogger3	21.61228371	63
DP41	20.52697945	711
DP40	21.58065033	105
DP39	21.39236069	49
DP38	21.26144028	29
DP37	20.82192421	31
DP36	19.82249832	60
DP35	19.25704193	107
DP34	20.37498856	463
DP33	15.48937035	48
DP32	19.6421032	245
DP31	21.62387848	373
DP30	16.29462051	54
DP29	19.10718727	123
DP28	21.28384781	366
DP27	18.54211617	71
DP26	21.11183548	928
DP25	18.55875206	74
DP24	21.11968231	896
DP23	19.33279228	636
DP22	20.29029655	193
DP21	19.68258667	595
DP20	21.72526932	799
DP19	21.95998192	702
DP18	20.38695145	541
DP17	21.26153564	309
DP16	20.06114769	131
DP15	20.89827347	198
DP14	20.04605675	43
DP13	20.82775116	152
DP12	22.59066582	605
DP11	22.07172203	349
DP10	22.91754723	517
DP9	23.00911713	472
DP8	22.03660202	256
DP7	21.37984657	77
DP6	22.56264496	131
DP5	22.00109863	138
DP4	21.16813278	41
DP3	22.58888626	349
DP2	22.43638992	213
DP1	21.73933411	74

	LST13JUN15	*Distance WD (9am-90, 12pm-90)*
LST13JUN15	1	
Distance WD (9am-90, 12pm-90)	0.26	1

Name	LST13NOV6	Distance WD (9am-0, 12pm-0)
UCILogger_KI	24.76684189	0
UCILogger_KIB	24.88622284	0
UCILogger2	25.34615135	0
UCILogger1	24.7461338	0
UCILogger8	26.49707413	367
UCILogger7	26.13654327	282
UCILogger6	26.55716705	540
UCILogger4	26.48220825	397
UCILogger3	26.09937668	601
DP41	25.87960815	374
DP40	26.35326386	579
DP39	26.04003143	572
DP38	26.17629242	513
DP37	25.49721718	339
DP36	24.9011898	140
DP35	25.74861717	33
DP34	26.35626984	139
DP33	26.38489723	181
DP32	26.94606018	221
DP31	27.56030464	1280
DP30	26.18153763	101
DP29	26.66465569	172
DP28	27.4478302	1162
DP27	26.13755226	1066
DP26	27.1965847	1038
DP25	26.2934227	135
DP24	26.84923172	958
DP23	25.84303474	123
DP22	25.60301209	65
DP21	26.18989182	206
DP20	26.53853798	742
DP19	27.13204384	637
DP18	25.97982407	297
DP17	26.49277687	160
DP16	24.99811745	77
DP15	25.87457085	183
DP14	25.11519241	209
DP13	25.94434929	281
DP12	27.18758774	514
DP11	26.68123817	503
DP10	27.38622475	624
DP9	27.22078705	716
DP8	26.73107719	590
DP7	26.32740402	469
DP6	26.34084702	929
DP5	26.16503143	792
DP4	25.50988197	721
DP3	26.42168045	826
DP2	26.7124958	686
DP1	26.03126144	621

	LST13NOV6	*Distance WD (9am-0, 12pm-0)*
LST13NOV6	1	
Distance WD (9am-0, 12pm-0)	0.650396603	1

Name	LST14FEB10	Distance WD (12pm-50)
UCILogger_KI	20.24439812	0
UCILogger_KIB	20.41776466	0
UCILogger2	20.7977829	0
UCILogger1	19.35940933	0
UCILogger8	21.65517044	367
UCILogger7	21.65634537	282
UCILogger6	21.94299698	540
UCILogger4	21.66063309	397
UCILogger3	21.52023697	601
DP41	21.69752121	374
DP40	21.88226509	579
DP39	21.43734932	572
DP38	21.32493401	513
DP37	20.9973526	339
DP36	20.35373878	140
DP35	20.76519394	33
DP34	21.41280365	139
DP33	21.52464104	181
DP32	22.14418411	221
DP31	22.36668968	1280
DP30	21.2413311	101
DP29	22.04558182	172
DP28	22.28333473	1162
DP27	21.23915863	1066
DP26	22.14478302	1038
DP25	21.20534325	135
DP24	22.18023872	958
DP23	21.35279846	123
DP22	20.68870163	65
DP21	21.59988022	206
DP20	22.12188339	742
DP19	22.22383118	637
DP18	21.53271866	297
DP17	21.62555695	160
DP16	20.16108513	77
DP15	21.48195267	183
DP14	20.55070496	209
DP13	21.59807205	281
DP12	22.36610222	514
DP11	22.08889961	503
DP10	22.49728012	624
DP9	22.3533802	716
DP8	22.0577774	590
DP7	21.76104546	469
DP6	21.56440735	929
DP5	21.39062309	792
DP4	20.26312256	721
DP3	22.02249146	826
DP2	22.01908684	686
DP1	21.52023697	621

	LST14FEB10	*Distance WD (12pm-50)*
LST14FEB10	1	
Distance WD (12pı	0.59	1

Name	LST14FEB26	Distance WD (12pm-50)_PR
UCILogger_KI	21.64054108	0
UCILogger_KIB	21.82856941	0
UCILogger2	22.58848953	0
UCILogger1	21.12413406	0
UCILogger8	23.60874367	367
UCILogger7	23.51888084	282
UCILogger6	23.53924751	540
UCILogger4	23.28371048	397
UCILogger3	23.20077705	601
DP41	23.41959953	374
DP40	23.52061462	579
DP39	23.06609154	572
DP38	22.97356415	513
DP37	22.41320419	339
DP36	21.88452148	140
DP35	21.90950012	33
DP34	22.58494186	139
DP33	18.55518723	181
DP32	16.77632713	221
DP30	18.49469376	101
DP29	18.17883301	172
DP25	21.92731667	135
DP24	23.06128311	958
DP23	22.50924492	123
DP22	21.78736687	65
DP21	22.9498291	206
DP20	23.75411224	742
DP19	24.03909302	637
DP18	22.97211456	297
DP17	23.15160751	160
DP16	21.26787186	77
DP15	23.13250542	183
DP14	22.03943253	209
DP13	23.35758972	281
DP12	24.22351265	514
DP11	23.9290123	503
DP10	24.28420448	624
DP9	24.2821064	716
DP8	23.78886604	590
DP7	23.43303299	469
DP6	23.60534477	929
DP5	23.1961689	792
DP4	22.00958633	721
DP3	23.94886971	826
DP2	23.79486847	686
DP1	23.20077705	621

	LST14FEB26	*Distance WD (12pm-50)_PR*
LST14FEB26	1	
Distance WD (12pı	0.54	1

Name	LST14JAN25	Distance WD (12pm-0)
UCILogger_KI	20.21820641	0
UCILogger_KIB	20.32680511	0
UCILogger2	20.65257454	0
UCILogger1	19.45575523	0
UCILogger8	21.71073341	367
UCILogger7	21.85265732	282
UCILogger6	21.69313049	540
UCILogger4	21.76649857	397
UCILogger3	21.27594376	601
DP41	21.5848484	374
DP40	21.62275696	579
DP39	21.18209457	572
DP38	21.04570389	513
DP37	20.6521225	339
DP36	20.44461441	140
DP35	20.9475975	33
DP34	21.41365242	139
DP33	21.46100044	181
DP32	21.88524055	221
DP31	22.17446709	1280
DP30	21.12317467	101
DP29	21.83937263	172
DP28	22.0778904	1162
DP27	21.26120949	1066
DP26	21.96772957	1038
DP25	21.32205391	135
DP24	22.30065918	958
DP23	21.34868622	123
DP22	20.73423576	65
DP21	21.6091404	206
DP20	21.88978577	742
DP19	22.04043388	637
DP18	21.53465843	297
DP17	21.83582878	160
DP16	20.39679909	77
DP15	21.82293129	183
DP14	20.5554142	209
DP13	21.76334763	281
DP12	22.18224525	514
DP11	22.07774544	503
DP10	22.43768883	624
DP9	22.34618187	716
DP8	21.87335205	590
DP7	21.53217125	469
DP6	21.49992752	929
DP5	21.33441353	792
DP4	20.12130737	721
DP3	21.95657921	826
DP2	21.98667336	686
DP1	21.27594376	621

	LST14JAN25	*Distance WD (12pm-0)*
LST14JAN25	1	
Distance WD (12pı	0.53	1

Name	LST14MAR14	Distance WD (12pm-360)
UCILogger_KI	26.41306686	0
UCILogger_KIB	26.54836845	0
UCILogger2	27.09721184	0
UCILogger1	25.45395088	0
UCILogger8	28.60222054	367
UCILogger7	28.61509895	282
UCILogger6	28.56582451	540
UCILogger4	28.54867554	397
UCILogger3	28.33023071	601
DP41	28.83337784	374
DP40	28.5647068	579
DP39	27.89804459	572
DP38	27.14112854	513
DP37	27.11016464	339
DP36	27.30084801	140
DP35	27.39703941	33
DP34	28.24647713	139
DP33	28.30628014	181
DP32	28.66745186	221
DP31	29.16180611	1280
DP30	27.6301384	101
DP29	28.57455063	172
DP28	29.11633682	1162
DP27	27.8465519	1066
DP26	29.07578659	1038
DP25	27.88796806	135
DP24	29.12275696	958
DP23	28.60268211	123
DP22	27.17525864	65
DP21	28.24173355	206
DP20	29.21717072	742
DP19	29.117342	637
DP18	28.37799263	297
DP17	28.44901276	160
DP16	26.5786438	77
DP15	28.72974396	183
DP14	26.5304184	209
DP13	28.72603798	281
DP12	29.43102646	514
DP11	28.70651817	503
DP10	29.41175652	624
DP9	29.13299179	716
DP8	28.65461349	590
DP7	28.58897209	469
DP6	28.19287682	929
DP5	28.2579689	792
DP4	26.46896172	721
DP3	28.67796516	826
DP2	28.86034584	686
DP1	28.33023071	621

	LST14MAR14	*Distance WD (12pm-360)*
LST14MAR14	1	
Distance WD (12pm-360)	0.53	1

Name	LST14MAR30	Distance WD (9am-240, 12pm-250)
UCILogger_KI	31.94124794	0
UCILogger_KIB	32.32409668	0
UCILogger2	33.03062058	0
UCILogger1	30.66671944	0
UCILogger8	35.15718842	178
UCILogger7	34.95095062	283
UCILogger6	34.50928879	150
UCILogger4	34.30347443	438
UCILogger3	34.07836914	63
DP41	35.23468781	711
DP40	34.47000504	105
DP39	33.70753098	49
DP38	33.34250641	29
DP37	33.28330612	31
DP36	32.72219849	60
DP35	33.77443695	107
DP34	34.27917099	463
DP33	34.10957336	48
DP32	34.98778915	245
DP31	35.38929749	373
DP30	33.36483383	54
DP29	34.45339584	123
DP28	34.94655609	366
DP27	33.75304413	71
DP26	35.20031738	928
DP25	33.99977875	74
DP24	35.76265335	896
DP23	34.42549133	636
DP22	33.25687027	193
DP21	34.59024811	595
DP20	35.83687592	799
DP19	35.33322144	702
DP18	34.34708405	541
DP17	34.93606567	309
DP16	32.56393814	131
DP15	35.04942322	198
DP14	32.8991394	43
DP13	35.33551407	152
DP12	35.54343414	605
DP11	34.96499634	349
DP10	35.51331329	517
DP9	35.36540222	472
DP8	34.97321701	256
DP7	34.27005386	77
DP6	34.41926193	131
DP5	33.86035538	138
DP4	31.90798569	41
DP3	34.73984909	349
DP2	34.9459877	213
DP1	34.07836914	74

	LST14MAR30	*Distance WD (9am-240, 12pm-250)*
LST14MAR30	1	
Distance WD (9am-240, 12pm-250)	0.67	1

Name	LST14NOV25	Distance WD (12pm-270)
UCILogger_KI	21.88544846	0
UCILogger_KIB	21.88653564	0
UCILogger2	22.34484291	0
UCILogger1	21.78601074	0
UCILogger8	23.12737656	178
UCILogger7	22.98659515	283
UCILogger6	23.31984711	150
UCILogger4	23.0518322	438
UCILogger3	23.07877541	63
DP41	22.86313248	711
DP40	23.29360962	105
DP39	22.84338379	49
DP38	22.50882721	29
DP37	22.27090454	31
DP36	22.11588287	60
DP35	22.50589561	107
DP34	22.94690132	463
DP33	23.07299614	48
DP32	23.27829933	245
DP31	23.49144173	373
DP30	22.66136551	54
DP29	23.05804253	123
DP28	23.62441063	366
DP27	22.76399612	71
DP26	23.3764019	928
DP25	22.71155739	74
DP24	23.32036781	896
DP23	22.87493134	636
DP22	22.29171753	193
DP21	22.79299736	595
DP20	23.09386444	799
DP19	23.25490189	702
DP18	22.85340309	541
DP17	23.11191559	309
DP16	21.74361038	131
DP15	22.61801338	198
DP14	21.86744499	43
DP13	22.68364716	152
DP12	23.58968925	605
DP11	23.60182762	349
DP10	23.75366402	517
DP9	23.7410202	472
DP8	23.44302177	256
DP7	23.2538414	77
DP6	22.88213348	131
DP5	22.99320602	138
DP4	22.05893898	41
DP3	23.32438087	349
DP2	23.33640671	213
DP1	23.07877541	74

	LST14NOV25	*Distance WD (12pm-270)*
LST14NOV25	1	
Distance WD (12pm-270)	0.53	1

Name	LST15APR18	Distance WD (12pm-240)
UCILogger_KI	24.94127274	0
UCILogger_KIB	24.97157478	0
UCILogger8	27.05012131	0
UCILogger7	26.60859871	0
UCILogger6	27.02362251	178
UCILogger4	26.64056587	283
UCILogger3	26.50679016	150
UCILogger2	26.4468174	438
UCILogger1	24.91942596	63
DP41	27.48780441	711
DP40	26.88678551	105
DP39	26.31933975	49
DP38	26.05332375	29
DP37	25.87170601	31
DP36	25.59609604	60
DP35	26.49096489	107
DP34	27.00353622	463
DP33	27.36369133	48
DP32	27.34659195	245
DP31	27.84961128	373
DP30	26.65947914	54
DP29	27.22490311	123
DP28	27.74847031	366
DP27	26.74550819	71
DP26	27.62053871	928
DP25	26.74916458	74
DP24	27.60276031	896
DP23	27.4497242	636
DP22	26.06333923	193
DP21	26.92636108	595
DP20	27.36926842	799
DP19	27.67188644	702
DP18	26.6884594	541
DP17	26.95894241	309
DP16	25.31918526	131
DP15	26.21961212	198
DP14	25.31868935	43
DP13	26.33035469	152
DP12	27.73249435	605
DP11	27.11400604	349
DP10	27.70153999	517
DP9	27.77252769	472
DP8	27.28151131	256
DP7	26.70643616	77
DP6	26.83194542	131
DP5	26.9708786	138
DP4	25.92165375	41
DP3	27.09246635	349
DP2	27.43297958	213
DP1	26.78681755	74

	LST15APR18	*Distance WD (12pm-240)*
LST15APR18	1	
Distance WD (12pm-240)	0.63	1

Name	LST15DEC30	Distance WD (12pm-0)
UCILogger_KI	18.54937172	0
UCILogger_KIB	18.64752388	0
UCILogger2	18.94364166	0
UCILogger1	18.50945663	0
UCILogger8	19.61043358	367
UCILogger7	19.52008629	282
UCILogger6	19.46564484	540
UCILogger4	19.5640831	397
UCILogger3	19.36130333	601
DP41	19.55333519	374
DP40	19.4410305	579
DP39	19.23167419	572
DP38	18.95183373	513
DP37	18.97763443	339
DP36	18.96571159	140
DP35	19.23621178	33
DP34	19.43015862	139
DP33	19.34487343	181
DP32	19.5720768	221
DP31	19.77958107	1280
DP30	19.19052887	101
DP29	19.42188263	172
DP28	19.90254593	1162
DP27	19.27513695	1066
DP26	19.80483818	1038
DP25	19.2416172	135
DP24	19.81464958	958
DP23	19.4954834	123
DP22	18.97209167	65
DP21	19.37314415	206
DP20	19.42993164	742
DP19	19.56952858	637
DP18	19.51886749	297
DP17	19.476017	160
DP16	18.83122253	77
DP15	19.44608498	183
DP14	18.75587463	209
DP13	19.19863892	281
DP12	19.79589272	514
DP11	19.66027832	503
DP10	20.12000465	624
DP9	20.03688812	716
DP8	19.53086853	590
DP7	19.64523888	469
DP6	19.47207069	929
DP5	19.28346443	792
DP4	18.76573563	721
DP3	19.78164101	826
DP2	19.60366249	686
DP1	19.36130333	621

	LST15DEC30	*Distance WD (12pm-0)*
LST15DEC30	1	
Distance WD (12pm-0)	0.57	1

Name	LST15FEB13	Distance WD (12pm-270)
UCILogger_KI	19.30706215	0
UCILogger_KIB	19.367342	0
UCILogger2	19.90709686	0
UCILogger1	18.96791267	0
UCILogger8	20.96928024	178
UCILogger7	20.88335037	283
UCILogger6	20.80402374	150
UCILogger4	20.62944031	438
UCILogger3	20.54317856	63
DP41	20.6289196	711
DP40	20.75356865	105
DP39	20.32355881	49
DP38	19.83369446	29
DP37	20.07940674	31
DP36	19.82494545	60
DP35	19.95335007	107
DP34	20.34241295	463
DP33	20.60959435	48
DP32	20.77904129	245
DP31	21.27729034	373
DP30	20.21826744	54
DP29	20.73724937	123
DP28	21.3730526	366
DP27	20.30407906	71
DP26	21.07284737	928
DP25	20.3279953	74
DP24	21.03385925	896
DP23	20.70531654	636
DP22	19.76270485	193
DP21	20.30497742	595
DP20	20.79804611	799
DP19	21.04580116	702
DP18	20.40491676	541
DP17	20.61475945	309
DP16	19.27139473	131
DP15	20.56617737	198
DP14	19.52913094	43
DP13	20.65500832	152
DP12	21.2549572	605
DP11	21.03134155	349
DP10	21.46902466	517
DP9	21.4381752	472
DP8	20.85310364	256
DP7	20.93863869	77
DP6	20.770401	131
DP5	20.6055603	138
DP4	19.5292511	41
DP3	21.06798172	349
DP2	20.76491165	213
DP1	20.54317856	74

	LST15FEB13	*Distance WD (12pm-270)*
LST15FEB13	1	
Distance WD (12pm-270)	0.56	1

Name	LST15JAN28	Distance WD (12pm-0)
UCILogger_KI	19.94853973	0
UCILogger_KIB	19.8859005	0
UCILogger2	20.81212425	0
UCILogger1	19.699543	0
UCILogger8	21.30670738	367
UCILogger7	21.40082359	282
UCILogger6	21.52838135	540
UCILogger4	21.46484375	397
UCILogger3	21.07804108	601
DP41	21.46632957	374
DP40	21.44095612	579
DP39	20.86271286	572
DP38	20.92133522	513
DP37	20.58213234	339
DP36	20.55900764	140
DP35	20.49017715	33
DP34	21.20211792	139
DP33	21.25830078	181
DP32	21.30590057	221
DP31	21.74995422	1280
DP30	21.07233238	101
DP29	21.46544456	172
DP28	22.02182579	1162
DP27	21.01214218	1066
DP26	21.88498688	1038
DP25	21.40457916	135
DP24	21.89233398	958
DP23	21.95951653	123
DP22	20.3180809	65
DP21	21.27350044	206
DP20	21.49612045	742
DP19	21.63026619	637
DP18	21.1041851	297
DP17	21.25249672	160
DP16	19.85071182	77
DP15	21.01806068	183
DP14	20.2569828	209
DP13	21.39074707	281
DP12	21.77539635	514
DP11	21.79972839	503
DP10	22.1655407	624
DP9	22.08949471	716
DP8	21.66020584	590
DP7	21.20491982	469
DP6	21.35679817	929
DP5	21.28787422	792
DP4	20.42910576	721
DP3	21.65449905	826
DP2	21.69479179	686
DP1	21.40836716	621

	LST15JAN28	*Distance WD (12pm-0)*
LST15JAN28	1	
Distance WD (12pm-0)	0.58	1

Name	LST15MAR17	Distance WD (12pm-270)
UCILogger_KI	23.01456833	0
UCILogger_KIB	23.29629135	0
UCILogger2	24.35463905	0
UCILogger1	23.10140991	0
UCILogger8	25.33636093	178
UCILogger7	25.6012001	283
UCILogger6	25.25854301	150
UCILogger4	25.62698936	438
UCILogger3	24.86424255	63
DP41	26.55724525	711
DP40	25.16665459	105
DP39	24.55076218	49
DP38	24.21345901	29
DP37	23.83267403	31
DP36	24.16709328	60
DP35	25.39282608	107
DP34	25.91882706	463
DP33	26.18945503	48
DP32	26.5876236	245
DP31	27.19805336	373
DP30	25.73166084	54
DP29	26.2498188	123
DP28	26.93418884	366
DP27	25.87014389	71
DP26	26.68669128	928
DP25	25.86968994	74
DP24	26.88722801	896
DP23	26.27582932	636
DP22	24.78824043	193
DP21	26.05925179	595
DP20	26.67726898	799
DP19	26.65724373	702
DP18	25.71229744	541
DP17	25.66685104	309
DP16	24.24734688	131
DP15	25.22394943	198
DP14	23.55499458	43
DP13	25.01010704	152
DP12	26.85995293	605
DP11	25.70321465	349
DP10	26.61964226	517
DP9	26.27028275	472
DP8	25.49564934	256
DP7	25.19951439	77
DP6	25.26398659	131
DP5	25.09684944	138
DP4	23.94216537	41
DP3	25.87918854	349
DP2	25.34685326	213
DP1	24.86424255	74

	LST15MAR17	*Distance WD (12pm-270)*
LST15MAR17	1	
Distance WD (12pm-270)	0.73	1

Name	LST15MAY4	Distance WD (12pm-130)
UCILogger_KI	27.28395653	0
UCILogger_KIB	27.36493874	0
UCILogger8	29.47881317	0
UCILogger7	29.19140053	0
UCILogger6	29.2914238	485
UCILogger4	29.34162712	619
UCILogger3	28.72475433	328
UCILogger2	28.46801376	397
UCILogger1	27.12102699	249
DP41	29.52919197	374
DP40	29.11878204	280
DP39	28.43891144	256
DP38	28.35732651	88
DP37	28.01373863	76
DP36	27.70403099	322
DP35	28.7406559	33
DP34	29.37358284	848
DP33	29.72714043	181
DP32	29.72139931	221
DP31	30.29904175	1280
DP30	28.87541389	101
DP29	29.53899193	172
DP28	30.22474098	1162
DP27	29.1693573	1066
DP26	29.81516647	1038
DP25	28.90762138	985
DP24	29.72934341	958
DP23	29.36598396	905
DP22	28.19911194	883
DP21	29.29626274	793
DP20	29.62049675	742
DP19	29.83184624	637
DP18	29.22905922	677
DP17	29.39987946	750
DP16	27.46296501	760
DP15	28.48926735	689
DP14	27.68124962	156
DP13	28.97784233	549
DP12	30.03294182	514
DP11	29.81424522	465
DP10	30.22495842	403
DP9	30.15446472	286
DP8	29.77375412	345
DP7	29.08500099	355
DP6	29.10317421	70
DP5	29.30441666	83
DP4	27.96052742	91
DP3	29.60575867	177
DP2	29.81461906	212
DP1	29.07491875	226

	LST15MAY4	*Distance WD (12pm-130)*
LST15MAY4	1	
Distance WD (12pı	0.35	1

Name	LST15NOV12	Distance WD (12pm-0)
UCILogger_KI	25.59336472	0
UCILogger_KIB	25.70890999	0
UCILogger2	26.32953644	0
UCILogger1	25.46924782	0
UCILogger8	27.55172539	367
UCILogger7	27.65784073	282
UCILogger6	27.58842659	540
UCILogger4	27.71347427	397
UCILogger3	27.26453018	601
DP41	27.25551414	374
DP40	27.53576088	579
DP39	26.99832535	572
DP38	26.71020126	513
DP37	26.40507507	339
DP36	26.15367699	140
DP35	26.57845879	33
DP34	27.24671364	139
DP33	27.21031189	181
DP32	27.24048042	221
DP31	27.85450554	1280
DP30	26.6531105	101
DP29	27.33625984	172
DP28	27.85964203	1162
DP27	26.7237606	1066
DP26	27.50414276	1038
DP25	26.76075363	135
DP24	27.62366104	958
DP23	27.19772148	123
DP22	26.5073204	65
DP21	27.16242981	206
DP20	27.31723213	742
DP19	27.72520638	637
DP18	27.13462448	297
DP17	27.58589363	160
DP16	25.71379852	77
DP15	27.15186882	183
DP14	25.87380028	209
DP13	27.1230278	281
DP12	27.919487	514
DP11	27.88973618	503
DP10	28.09835243	624
DP9	28.18984032	716
DP8	27.83319664	590
DP7	27.55734253	469
DP6	27.09501266	929
DP5	26.96175385	792
DP4	26.20131111	721
DP3	27.56323242	826
DP2	27.72185707	686
DP1	27.26453018	621

	LST15NOV12	*Distance WD (12pm-0)*
LST15NOV12	1	
Distance WD (12pm-0)	0.55	1

Name	LST15NOV28	Distance WD (12pm-0)
UCILogger_KI	21.63009262	0
UCILogger_KIB	21.74761391	0
UCILogger2	22.28561401	0
UCILogger1	21.5662632	0
UCILogger8	23.24843979	367
UCILogger7	22.91410446	282
UCILogger6	23.15269279	540
UCILogger4	23.27471542	397
UCILogger3	22.94863701	601
DP41	23.13188362	374
DP40	23.11302948	579
DP39	23.00980377	572
DP38	22.6929512	513
DP37	22.39918327	339
DP36	21.93152046	140
DP35	22.82050323	33
DP34	22.92630768	139
DP33	23.05930328	181
DP32	23.16127014	221
DP31	23.64034462	1280
DP30	22.63469505	101
DP29	23.03627205	172
DP28	23.65540314	1162
DP27	22.81009865	1066
DP26	23.41309547	1038
DP25	22.85031509	135
DP24	23.50796318	958
DP23	22.94170189	123
DP22	22.4470253	65
DP21	23.11096191	206
DP20	23.23603821	742
DP19	23.37687874	637
DP18	23.03684235	297
DP17	23.08113861	160
DP16	22.00945091	77
DP15	22.87983322	183
DP14	21.9121685	209
DP13	22.77598381	281
DP12	23.59365082	514
DP11	23.49217224	503
DP10	23.63064766	624
DP9	23.79916763	716
DP8	23.19146156	590
DP7	23.12510872	469
DP6	22.96954155	929
DP5	22.81890297	792
DP4	21.93353844	721
DP3	23.33790207	826
DP2	23.18900108	686
DP1	22.94863701	621

	LST15NOV28	*Distance WD (12pm-0)*
LST15NOV28	1	
Distance WD (12pm-0)	0.59	1

Name	LST15OCT27	Distance WD (12pm-0)
UCILogger_KI	25.90423393	0
UCILogger_KIB	25.94477844	0
UCILogger2	27.02303123	0
UCILogger1	25.83488846	0
UCILogger8	27.96661949	367
UCILogger7	27.52586937	282
UCILogger6	27.81725311	540
UCILogger4	28.00553131	397
UCILogger3	27.5649128	601
DP41	27.70175362	374
DP40	27.76361847	579
DP39	27.5041008	572
DP38	27.20890236	513
DP37	26.71101761	339
DP36	25.95157242	140
DP35	27.36364174	33
DP34	27.71842194	139
DP33	27.77272987	181
DP32	28.1105423	221
DP31	28.72278214	1280
DP30	27.20928764	101
DP29	27.91887665	172
DP28	28.86738396	1162
DP27	27.52939987	1066
DP26	28.69121361	1038
DP25	27.28120041	135
DP24	28.64123344	958
DP23	27.43820572	123
DP22	26.82836723	65
DP21	27.85104179	206
DP20	28.24673843	742
DP19	28.56832504	637
DP18	27.77705574	297
DP17	27.77989388	160
DP16	26.0342083	77
DP15	27.2078495	183
DP14	26.02125931	209
DP13	26.87330437	281
DP12	28.89750671	514
DP11	28.41512108	503
DP10	28.93136024	624
DP9	28.94553757	716
DP8	28.1710434	590
DP7	27.76783943	469
DP6	27.68710136	929
DP5	27.71287346	792
DP4	26.41771126	721
DP3	28.25793457	826
DP2	28.12141228	686
DP1	27.5649128	621

	LST15OCT27	*Distance WD (12pm-0)*
LST15OCT27	1	
Distance WD (12pm-0)	0.63	1

Name	LST15SEPT25	Distance WD (12pm-210)
UCILogger_KI	24.99556732	0
UCILogger_KIB	25.07178497	0
UCILogger8	26.51268005	0
UCILogger7	26.03376007	0
UCILogger6	26.07391548	178
UCILogger4	26.23056221	283
UCILogger3	25.76970673	150
UCILogger2	26.0718689	438
UCILogger1	24.98154259	63
DP41	26.32443619	711
DP40	25.94344711	105
DP39	25.71636009	49
DP38	25.77305222	29
DP37	25.59649277	31
DP36	25.29000092	60
DP35	25.89530182	107
DP34	26.1004467	463
DP33	26.51526642	48
DP32	26.55491638	245
DP31	27.09239578	373
DP30	26.04083252	54
DP29	26.41222954	123
DP28	27.09516335	366
DP27	26.14433861	71
DP26	26.73960876	928
DP25	25.98805046	74
DP24	26.76395416	896
DP23	25.95827103	636
DP22	25.77359772	193
DP21	26.04800415	595
DP20	26.59969139	799
DP19	26.83258057	702
DP18	26.10860443	541
DP17	26.12829208	309
DP16	25.09835815	131
DP15	25.88916206	198
DP14	25.39480972	43
DP13	26.33059883	152
DP12	26.81440544	605
DP11	26.55830765	349
DP10	26.9229393	517
DP9	27.05386925	472
DP8	26.42269135	256
DP7	25.9597702	77
DP6	26.43149757	131
DP5	26.25091553	138
DP4	25.63817978	41
DP3	26.5071106	349
DP2	26.32857704	213
DP1	25.93506813	74

	LST15SEPT25	*Distance WD (12pm-210)*
LST15SEPT25	1	
Distance WD (12pm-210)	0.58	1

Name	LST16FEB16	Distance WD (12pm-360)
UCILogger_KI	22.15961838	0
UCILogger_KIB	22.1741066	0
UCILogger2	22.47871208	0
UCILogger1	21.92053986	0
UCILogger8	23.30681419	367
UCILogger7	23.30292702	282
UCILogger6	23.27261353	540
UCILogger4	23.30373955	397
UCILogger3	23.21545219	601
DP41	23.47742271	374
DP40	23.27415848	579
DP39	23.00675011	572
DP38	22.51990509	513
DP37	22.43805122	339
DP36	22.37311745	140
DP35	22.77059174	33
DP34	23.19329453	139
DP33	23.23851585	181
DP32	23.40394783	221
DP31	23.81472588	1280
DP30	22.99324989	101
DP29	23.36915779	172
DP28	23.85360336	1162
DP27	23.09151649	1066
DP26	23.52403069	1038
DP25	22.91843605	135
DP24	23.63060379	958
DP23	23.18855476	123
DP22	22.52530479	65
DP21	23.18861961	206
DP20	23.35618973	742
DP19	23.49160385	637
DP18	23.18294144	297
DP17	23.2742939	160
DP16	22.26248741	77
DP15	23.2477417	183
DP14	22.33090591	209
DP13	23.09077072	281
DP12	23.52087784	514
DP11	23.36085701	503
DP10	23.59209061	624
DP9	23.62317657	716
DP8	23.33384895	590
DP7	23.26542854	469
DP6	23.07593536	929
DP5	23.02584076	792
DP4	22.14673805	721
DP3	23.36934471	826
DP2	23.3605423	686
DP1	23.21545219	621

	LST16FEB16	*Distance WD (12pm-360)*
LST16FEB16	1	
Distance WD (12pm-360)	0.57	1

Name	LST16JAN15	Distance WD (12pm-0)
UCILogger_KI	18.74083328	0
UCILogger_KIB	18.84362602	0
UCILogger8	20.0084362	0
UCILogger7	19.76615524	0
UCILogger6	19.87608147	367
UCILogger4	19.7941227	282
UCILogger3	19.68351746	540
UCILogger2	19.25710869	397
UCILogger1	18.55200386	601
DP41	19.70663643	374
DP40	19.83482742	579
DP39	19.64854622	572
DP38	19.47627258	513
DP37	19.33452034	339
DP36	19.02214623	140
DP35	19.45546913	33
DP34	19.57364845	139
DP33	19.78629303	181
DP32	20.06110764	221
DP31	20.36043549	1280
DP30	19.5863781	101
DP29	19.89291	172
DP28	20.47771263	1162
DP27	19.58579826	1066
DP26	20.1698761	1038
DP25	19.60767746	135
DP24	20.27838135	958
DP23	19.65192413	123
DP22	19.1245842	65
DP21	19.72211266	206
DP20	19.80314255	742
DP19	19.98461151	637
DP18	19.69923019	297
DP17	19.83362961	160
DP16	18.99092865	77
DP15	19.7401371	183
DP14	19.02994919	209
DP13	19.7130127	281
DP12	20.07063484	514
DP11	19.98012924	503
DP10	20.1638546	624
DP9	20.30907249	716
DP8	19.93962669	590
DP7	19.84564209	469
DP6	19.83210182	929
DP5	19.56759644	792
DP4	18.92821503	721
DP3	20.12582397	826
DP2	19.89691734	686
DP1	19.68351746	621

	LST16JAN15	*Distance WD (12pm-0)*
LST16JAN15	1	
Distance WD (12pm-0)	0.48	1

Name	LST16MAR3	Distance WD (12pm-290)
UCILogger_KI	24.77837372	0
UCILogger_KIB	25.05787659	0
UCILogger8	26.56407547	0
UCILogger7	26.45191002	0
UCILogger6	26.43847084	178
UCILogger4	26.2964344	283
UCILogger3	26.25210381	150
UCILogger2	25.69402504	438
UCILogger1	24.50333023	63
DP41	26.58964157	711
DP40	26.38586235	105
DP39	26.09647942	49
DP38	25.76172638	29
DP37	25.77726173	31
DP36	25.34503365	60
DP35	25.56712341	107
DP34	26.03742981	463
DP33	26.36139679	48
DP32	26.24639702	245
DP31	26.72821999	373
DP30	25.89201927	54
DP29	26.20056343	123
DP28	26.60197639	366
DP27	26.06071663	71
DP26	26.36354065	928
DP25	26.03495979	74
DP24	26.48718071	896
DP23	26.42458916	636
DP22	25.42116928	193
DP21	26.10953331	595
DP20	26.40062904	799
DP19	26.53442574	702
DP18	25.98200226	541
DP17	26.51109886	309
DP16	24.98506165	131
DP15	26.34998894	198
DP14	25.241745	43
DP13	26.46155357	152
DP12	26.71559906	605
DP11	26.59600067	349
DP10	26.81097412	517
DP9	26.91358757	472
DP8	26.49457359	256
DP7	26.36897469	77
DP6	26.22481155	131
DP5	26.15012169	138
DP4	25.37694168	41
DP3	26.5899601	349
DP2	26.64041519	213
DP1	26.25210381	74

	LST16MAR3	*Distance WD (12pm-290)*
LST16MAR3	1	
Distance WD (12pm-290)	0.46	1

Name	LST16NOV14	Distance WD (12pm-360)
UCILogger_KI	24.18758583	0
UCILogger_KIB	24.18758583	0
UCILogger8	25.76178932	0
UCILogger7	25.56616974	0
UCILogger6	25.69049072	367
UCILogger4	26.01422882	282
UCILogger3	25.26690483	540
UCILogger2	24.7007637	397
UCILogger1	24.22936249	601
DP41	25.56958771	374
DP40	25.69405556	579
DP39	25.39904785	572
DP38	24.83474159	513
DP37	24.70333481	339
DP36	24.62117577	140
DP35	25.06873131	33
DP34	25.56108093	139
DP33	25.95536232	181
DP32	26.01483536	221
DP31	26.70137024	1280
DP30	25.4889946	101
DP29	25.84190941	172
DP28	26.52998734	1162
DP27	25.58164215	1066
DP26	26.33446503	1038
DP25	25.54001045	135
DP24	26.33153152	958
DP23	25.69163322	123
DP22	25.33251572	65
DP21	25.6631813	206
DP20	25.99007607	742
DP19	26.52311897	637
DP18	25.67915726	297
DP17	25.77395058	160
DP16	24.58778191	77
DP15	25.22923088	183
DP14	24.41128349	209
DP13	25.17917442	281
DP12	26.67565537	514
DP11	26.07141113	503
DP10	26.6119175	624
DP9	26.61827278	716
DP8	25.9393692	590
DP7	25.45814514	469
DP6	25.82240868	929
DP5	25.29128456	792
DP4	24.48386192	721
DP3	26.05405235	826
DP2	25.71559715	686
DP1	25.53160477	621

	LST16NOV14	*Distance WD (12pm-360)*
LST16NOV14	1	
Distance WD (12pm-360)	0.48	1

Name	LST16NOV30	Distance WD (12pm-0)
UCILogger_KI	22.58520889	0
UCILogger_KIB	22.62083626	0
UCILogger2	23.33563042	0
UCILogger1	22.42624283	0
UCILogger8	24.40879822	367
UCILogger7	24.07154655	282
UCILogger6	24.33375359	540
UCILogger4	24.25638962	397
UCILogger3	24.04073524	601
DP41	23.9858532	374
DP40	24.28215408	579
DP39	23.95067787	572
DP38	23.61395454	513
DP37	23.32476616	339
DP36	22.66961098	140
DP35	23.55568123	33
DP34	23.86967659	139
DP33	23.88651657	181
DP32	24.24012947	221
DP31	24.81686592	1280
DP30	23.60579681	101
DP29	24.2095108	172
DP28	24.88736343	1162
DP27	23.92747879	1066
DP26	24.59565544	1038
DP25	23.60059929	135
DP24	24.67635155	958
DP23	23.84066391	123
DP22	23.29746437	65
DP21	24.01224136	206
DP20	24.1348629	742
DP19	24.46587563	637
DP18	23.92476082	297
DP17	24.26247025	160
DP16	22.8860302	77
DP15	23.91324615	183
DP14	22.76467705	209
DP13	23.81148148	281
DP12	24.8172245	514
DP11	24.46084976	503
DP10	24.97382927	624
DP9	25.02753258	716
DP8	24.35298538	590
DP7	24.15691566	469
DP6	24.01189423	929
DP5	23.91671562	792
DP4	22.75994682	721
DP3	24.52214241	826
DP2	24.35403252	686
DP1	24.04073524	621

	LST16NOV30	*Distance WD (12pm-0)*
LST16NOV30	1	
Distance WD (12pm-360)	0.63	1

Name	LST17FEB18	Distance
UCILogger_KI	22.24634743	0
UCILogger_KIB	22.30157852	0
UCILogger8	23.65303993	160
UCILogger7	23.42924881	265
UCILogger6	23.44867706	157
UCILogger4	23.64612579	420
UCILogger3	23.24389648	80
UCILogger2	22.60085106	0
UCILogger1	21.94315338	0
DP41	23.40809631	284
DP40	23.43651962	108
DP39	23.30550766	53
DP38	23.12462425	37
DP37	22.75092125	32
DP36	22.64050484	54
DP35	23.06549454	27
DP34	23.42974281	130
DP33	23.5180645	41
DP32	23.86180878	219
DP31	24.26826286	381
DP30	23.19261742	52
DP29	23.74727058	123
DP28	24.1926918	337
DP27	23.42321014	73
DP26	23.98384285	312
DP25	23.36884117	72
DP24	23.93370628	304
DP23	23.40904045	115
DP22	23.09582329	65
DP21	23.52274323	197
DP20	23.71075249	381
DP19	23.68988991	445
DP18	23.51947021	293
DP17	23.59653854	150
DP16	22.54181862	70
DP15	23.46080971	170
DP14	22.62553787	40
DP13	23.46196365	154
DP12	23.69329834	591
DP11	23.69577217	340
DP10	23.85445976	522
DP9	23.8921566	472
DP8	23.44219589	262
DP7	23.52713203	73
DP6	23.34137917	81
DP5	23.0481205	84
DP4	22.07772827	44
DP3	23.66414452	188
DP2	23.30095673	218
DP1	23.24389648	78

	LST17FEB18	*Distance*
LST17FEB18	1	
Distance	0.699624844	1

Name	LST17MAR22	Distance
UCILogger_KI	21.92351913	0
UCILogger_KIB	21.94105339	0
UCILogger8	23.53137589	160
UCILogger7	23.09280014	265
UCILogger6	23.19987679	157
UCILogger4	23.19150925	420
UCILogger3	23.02290344	80
UCILogger2	22.59947586	0
UCILogger1	21.79406548	0
DP41	23.12265396	284
DP40	23.17647552	108
DP39	23.01342583	53
DP38	22.67833138	37
DP37	22.32533455	32
DP36	22.06396103	54
DP35	22.70689774	27
DP34	23.06121254	130
DP33	23.45934677	41
DP32	23.49821091	219
DP31	23.96851921	381
DP30	22.97460365	52
DP29	23.49461937	123
DP28	24.08452988	337
DP27	22.98265648	73
DP26	23.72892952	312
DP25	22.80956268	72
DP24	23.61465645	304
DP23	22.90384293	115
DP22	22.85455704	65
DP21	22.96403503	197
DP20	23.5430603	381
DP19	23.5814209	445
DP18	22.97453308	293
DP17	23.13466072	150
DP16	22.08281708	70
DP15	22.89976692	170
DP14	22.06343269	40
DP13	22.97865295	154
DP12	23.49751854	591
DP11	23.37978554	340
DP10	23.79037094	522
DP9	23.77598572	472
DP8	23.35434341	262
DP7	23.30615234	73
DP6	23.34026337	81
DP5	22.97974586	84
DP4	22.05021286	44
DP3	23.34622765	188
DP2	23.20217705	218
DP1	23.02290344	78

	LST17MAR22	*Distance*
LST17MAR22	1	
Distance	0.706436221	1

Name	LST13APR12	Distance WD (9am-200, 12pm-180)
DW_DP1	28.95789719	509
DW_DP2	27.33084297	65
DW_DP3	28.86349297	94
DW_DP4	28.8585968	336
DW_DP5	29.33179665	396
DW_DP6	29.24243736	150
DW_DP7	29.29669762	235
DW_DP8	29.38947868	346
DW_DP9	29.08367729	98
DW_DP10	29.42903519	265
DW_DP11	28.71652222	396
DW_DP12	29.62737274	455
DW_DP13	28.87569809	50
DW_DP14	29.36657524	517
DW_DP15	29.04884148	511
DW_DP16	29.01838303	424
DW_DP17	29.16185379	536
DW_DP18	29.16013527	580
DW_DP19	29.36651039	483
DW_DP20	29.49435234	318
DW_DP21	29.66441536	387
DW_DP22	29.65711021	222
DW_DP23	29.68217087	326
DW_DP24	29.57777023	187
DW_DP25	29.70368958	509
DW_DP26	29.22967911	41
DW_DP27	29.58985519	360
DW_DP28	30.24546814	374
DW_DP29	29.73584557	137
DW_DP30	30.0081501	303
DW_DP31	29.73766518	238
DW_DP32	29.54528236	218
DW_DP33	28.69837189	167
DW_DP34	28.65053177	150
DW_DP35	29.67712021	261
DW_DP36	29.78377151	323
DW_DP37	28.37061691	353
DW_DP38	29.75048065	405
DW_DP39	27.13711548	44
UCILogger_PWD	29.14830399	324

	LST13APR12	*Distance WD (9am-200, 12pm-180)*
LST13APR12	1	
Distance WD (9am-200, 12pm-180)	0.352005805	1

Name	LST13DEC24	Distance WD (9am-270, 12pm-270)
DW_DP1	21.29298973	89
DW_DP2	20.70066452	31
DW_DP3	21.33873558	53
DW_DP4	21.58759117	197
DW_DP5	21.85621071	291
DW_DP6	21.446064	68
DW_DP7	21.73889542	176
DW_DP8	21.9292202	288
DW_DP9	21.5987606	92
DW_DP10	21.9323101	212
DW_DP11	21.66807365	320
DW_DP12	21.70804596	136
DW_DP13	21.12359619	23
DW_DP14	21.70065498	249
DW_DP15	21.63105202	343
DW_DP16	21.88271904	449
DW_DP17	21.81839752	464
DW_DP18	21.99981689	591
DW_DP19	22.091959	577
DW_DP20	22.1260128	426
DW_DP21	22.16114998	555
DW_DP22	21.984375	426
DW_DP23	21.96464348	529
DW_DP24	21.89547539	201
DW_DP25	21.99246407	280
DW_DP26	21.37599373	137
DW_DP27	21.62949562	273
DW_DP28	22.26100349	389
DW_DP29	21.63367844	188
DW_DP30	21.65518379	377
DW_DP31	21.80960274	269
DW_DP32	21.69814873	149
DW_DP33	21.21478844	47
DW_DP34	20.98441887	43
DW_DP35	21.89363861	204
DW_DP36	22.06850815	292
DW_DP37	21.17105865	73
DW_DP38	22.02111053	148
DW_DP39	20.65110397	58
UCILogger_PWD	21.86992455	314

	LST13DEC24	*Distance WD (9am-270, 12pm-270)*
LST13DEC24	1	
Distance WD (9am-270, 12pm-270)	0.75	1

Name	LST13JUN15	Distance WD (9am-90, 12pm-90)
DW_DP1	21.95865631	89
DW_DP2	21.40783882	31
DW_DP3	22.24785042	53
DW_DP4	22.07725716	197
DW_DP5	22.08502579	291
DW_DP6	22.15506172	68
DW_DP7	22.07564163	176
DW_DP8	21.97249985	288
DW_DP9	22.2494278	92
DW_DP10	21.94813728	212
DW_DP11	21.82358551	320
DW_DP12	22.3814373	136
DW_DP13	22.19264793	23
DW_DP14	22.06041336	249
DW_DP15	21.90695953	343
DW_DP16	22.07889366	449
DW_DP17	22.03710175	464
DW_DP18	21.62785912	591
DW_DP19	21.74951744	577
DW_DP20	22.18923187	426
DW_DP21	22.14189911	555
DW_DP22	22.11787033	426
DW_DP23	21.92404747	529
DW_DP24	22.00873375	201
DW_DP25	21.71125793	280
DW_DP26	21.78738213	137
DW_DP27	21.82344437	273
DW_DP28	21.65685081	389
DW_DP29	21.94270515	188
DW_DP30	21.48171425	377
DW_DP31	21.55597687	269
DW_DP32	21.6872673	149
DW_DP33	21.60241699	47
DW_DP34	21.20609856	43
DW_DP35	21.54617691	204
DW_DP36	21.19468308	292
DW_DP37	20.97101593	73
DW_DP38	20.86477852	148
DW_DP39	20.96318626	58
UCILogger_PWD	21.8606205	314

	LST13JUN15	*Distance WD (9am-90, 12pm-90)*
LST13JUN15	1	
Distance WD (9am-9	0.187292013	1

Name	LST13NOV6	Distance WD (9am-0, 12pm-0)
DW_DP1	25.88509369	509
DW_DP2	24.98672867	27
DW_DP3	25.82793808	173
DW_DP4	25.79135895	170
DW_DP5	26.21168709	170
DW_DP6	25.96434212	287
DW_DP7	26.07874298	266
DW_DP8	26.19717216	279
DW_DP9	26.20536041	399
DW_DP10	26.18810463	400
DW_DP11	26.00242424	396
DW_DP12	26.0589962	455
DW_DP13	25.76803207	50
DW_DP14	26.19096565	517
DW_DP15	26.199543	511
DW_DP16	26.3412056	424
DW_DP17	26.70082664	536
DW_DP18	26.703022	580
DW_DP19	27.07055855	483
DW_DP20	26.67780685	318
DW_DP21	27.11974525	387
DW_DP22	26.92887306	222
DW_DP23	26.83304977	326
DW_DP24	26.45812035	187
DW_DP25	26.78967667	509
DW_DP26	25.65303802	261
DW_DP27	26.33108902	360
DW_DP28	27.11719513	374
DW_DP29	26.22660637	256
DW_DP30	26.5171032	278
DW_DP31	26.25800323	196
DW_DP32	26.26640892	181
DW_DP33	25.27684784	238
DW_DP34	25.32729912	78
DW_DP35	26.35152626	141
DW_DP36	26.6471653	167
DW_DP37	25.34019661	52
DW_DP38	26.92116165	80
DW_DP39	24.76049232	577
UCILogger_PWD	26.00055313	324

	LST13NOV6	*Distance WD (9am-0, 12pm-0)*
LST13NOV6	1	
Distance WD (9am-0, 12pm-0)	0.264311946	1

Name	LST14FEB10	Distance WD (12pm-50)
DW_DP1	21.2500267	509
DW_DP2	19.80583191	27
DW_DP3	21.26882362	173
DW_DP4	21.23693657	170
DW_DP5	21.50837708	170
DW_DP6	21.30121613	287
DW_DP7	21.43424416	266
DW_DP8	21.46463585	279
DW_DP9	21.38700294	399
DW_DP10	21.60222244	400
DW_DP11	21.16921234	396
DW_DP12	21.57628822	455
DW_DP13	20.82612038	50
DW_DP14	21.61466599	517
DW_DP15	21.35234833	511
DW_DP16	21.2308197	424
DW_DP17	21.07157516	536
DW_DP18	20.08674431	580
DW_DP19	21.71539307	483
DW_DP20	21.61661148	318
DW_DP21	21.63564873	387
DW_DP22	21.50771713	222
DW_DP23	21.29188919	326
DW_DP24	21.69521904	187
DW_DP25	21.4795723	509
DW_DP26	21.33053398	261
DW_DP27	21.3535099	360
DW_DP28	22.029953	374
DW_DP29	21.50939751	256
DW_DP30	21.79060173	278
DW_DP31	21.63393211	196
DW_DP32	21.67822075	181
DW_DP33	21.18661499	238
DW_DP34	20.71076775	78
DW_DP35	21.63150978	141
DW_DP36	21.8997879	167
DW_DP37	20.65870857	52
DW_DP38	22.11941719	80
DW_DP39	20.05394554	577
UCILogger_PWD	21.37178802	324

	LST14FEB10	*Distance WD (12pm-50)*
LST14FEB10	1	
Distance WD (12pm-50)	-0.03	1

Name	LST14FEB26	Distance WD (12pm-50)
DW_DP1	22.71440506	509
DW_DP2	21.52771759	27
DW_DP3	23.11514854	173
DW_DP4	22.81243324	170
DW_DP5	23.07728767	170
DW_DP6	23.23098755	287
DW_DP7	23.14871216	266
DW_DP8	23.28301811	279
DW_DP9	23.13466072	399
DW_DP10	23.23606491	400
DW_DP11	22.85917473	396
DW_DP12	23.36474419	455
DW_DP13	22.71306038	50
DW_DP14	23.270298	517
DW_DP15	22.79227448	511
DW_DP16	23.13870239	424
DW_DP17	22.94420242	536
DW_DP18	23.07791328	580
DW_DP19	23.77965546	483
DW_DP20	23.48591042	318
DW_DP21	23.80456924	387
DW_DP22	23.38222504	222
DW_DP23	23.38828087	326
DW_DP24	23.38771057	187
DW_DP25	23.47502708	509
DW_DP26	22.91074181	261
DW_DP27	22.99011803	360
DW_DP28	23.89157486	374
DW_DP29	23.2381382	256
DW_DP30	23.44663048	278
DW_DP31	23.40936661	196
DW_DP32	23.47001648	181
DW_DP33	22.70137787	238
DW_DP34	22.34452057	78
DW_DP35	23.41417694	141
DW_DP36	23.44741249	167
DW_DP37	22.10783005	52
DW_DP38	23.57925606	80
DW_DP39	21.40253639	577
UCILogger_PWD	23.12308693	324

	LST14FEB26	*Distance WD (12pm-50)*
LST14FEB26	1	
Distance WD (12pm-50)	0.13	1

Name	LST14JAN25	Distance WD (9am-270)
DW_DP1	21.18372154	89
DW_DP2	19.86787605	31
DW_DP3	21.14456749	53
DW_DP4	21.14901161	197
DW_DP5	21.47565079	291
DW_DP6	21.17416	68
DW_DP7	21.36197853	176
DW_DP8	21.50717163	288
DW_DP9	21.38810921	92
DW_DP10	21.57784843	212
DW_DP11	21.05452538	320
DW_DP12	21.40512276	136
DW_DP13	20.52709007	23
DW_DP14	21.43259621	249
DW_DP15	21.16544914	343
DW_DP16	21.53602028	449
DW_DP17	21.48896217	464
DW_DP18	21.56572533	591
DW_DP19	21.95142365	577
DW_DP20	22.02389908	426
DW_DP21	21.99402428	555
DW_DP22	21.7484417	426
DW_DP23	21.53311729	529
DW_DP24	21.65283775	201
DW_DP25	21.72779846	280
DW_DP26	21.13618088	137
DW_DP27	21.34688568	273
DW_DP28	22.0639782	389
DW_DP29	21.67780495	188
DW_DP30	21.73455238	377
DW_DP31	21.95353889	269
DW_DP32	21.78641891	149
DW_DP33	21.11351776	47
DW_DP34	20.51395798	43
DW_DP35	21.9037571	204
DW_DP36	21.8372364	292
DW_DP37	20.55254555	73
DW_DP38	21.8641777	148
DW_DP39	19.90518379	58
UCILogger_PWD	21.37257004	314

	LST14JAN25	*Distance WD (9am-270)*
LST14JAN25	1	
Distance WD (9am-270)	0.62	1

Name	LST14MAR14	Distance WD (12pm-360)
DW_DP1	27.83653069	509
DW_DP2	25.92771339	27
DW_DP3	27.53509331	173
DW_DP4	27.77313614	170
DW_DP5	28.19771576	170
DW_DP6	28.09882927	287
DW_DP7	28.08064079	266
DW_DP8	28.35075378	279
DW_DP9	27.96924782	399
DW_DP10	28.4114151	400
DW_DP11	27.99795341	396
DW_DP12	27.94600296	455
DW_DP13	27.23954201	50
DW_DP14	28.55514908	517
DW_DP15	27.87121582	511
DW_DP16	28.35575294	424
DW_DP17	28.24697876	536
DW_DP18	28.65777397	580
DW_DP19	28.66233253	483
DW_DP20	28.78842163	318
DW_DP21	28.84275818	387
DW_DP22	28.50135231	222
DW_DP23	28.20978737	326
DW_DP24	28.43980789	187
DW_DP25	28.42363739	509
DW_DP26	28.01243401	261
DW_DP27	28.25651741	360
DW_DP28	28.9236412	374
DW_DP29	28.59032059	256
DW_DP30	28.81522751	278
DW_DP31	28.58806419	196
DW_DP32	28.38840866	181
DW_DP33	27.59379578	238
DW_DP34	27.46425629	78
DW_DP35	28.44775391	141
DW_DP36	28.73087692	167
DW_DP37	26.79078102	52
DW_DP38	28.62261391	80
DW_DP39	25.82839966	577
UCILogger_PWD	28.33613205	324

	LST14MAR14	*Distance WD (12pm-360)*
LST14MAR14	1	
Distance WD (12pm-360)	0.20	1

Name	LST14MAR30	Distance WD (9am-240, 12pm-250)
DW_DP1	33.61787033	89
DW_DP2	31.38440895	31
DW_DP3	33.72140121	53
DW_DP4	33.77561188	197
DW_DP5	34.2911644	291
DW_DP6	33.72712326	68
DW_DP7	34.21504211	176
DW_DP8	34.61620712	288
DW_DP9	33.98496246	92
DW_DP10	34.47325897	212
DW_DP11	34.13871384	320
DW_DP12	34.39377213	136
DW_DP13	32.89753723	23
DW_DP14	34.42948151	249
DW_DP15	34.00094986	343
DW_DP16	34.2823143	449
DW_DP17	34.37247086	464
DW_DP18	34.69065475	591
DW_DP19	35.04236984	577
DW_DP20	35.06632614	426
DW_DP21	35.0761261	555
DW_DP22	34.87301254	426
DW_DP23	34.26702118	529
DW_DP24	34.52825165	201
DW_DP25	34.46055222	280
DW_DP26	34.06145477	137
DW_DP27	34.00384521	273
DW_DP28	35.2827034	389
DW_DP29	34.94768906	188
DW_DP30	35.26515579	377
DW_DP31	35.18164825	269
DW_DP32	34.98906326	149
DW_DP33	33.48957062	47
DW_DP34	32.88623428	43
DW_DP35	34.78432846	204
DW_DP36	34.85029602	292
DW_DP37	32.96969223	73
DW_DP38	34.79711533	148
DW_DP39	31.40942383	58
UCILogger_PWD	34.50806046	314

	LST14MAR30	*Distance WD (9am-240, 12pm-250)*
LST14MAR30	1	
Distance WD (9am-270, 12pm-270)	0.62	1

Name	LST14NOV25	Distance WD (12pm-270)
DW_DP1	22.91063499	89
DW_DP2	21.94418335	31
DW_DP3	22.559021	53
DW_DP4	22.77630043	197
DW_DP5	23.1698761	291
DW_DP6	22.92641068	68
DW_DP7	22.97971153	176
DW_DP8	23.26277924	288
DW_DP9	22.82282066	92
DW_DP10	23.09713554	212
DW_DP11	22.51706123	320
DW_DP12	22.78500366	136
DW_DP13	22.52007675	23
DW_DP14	23.09863853	249
DW_DP15	22.73962021	343
DW_DP16	23.3199749	449
DW_DP17	23.17499733	464
DW_DP18	23.39904785	591
DW_DP19	23.5225544	577
DW_DP20	23.4677372	426
DW_DP21	23.83959389	555
DW_DP22	23.19160271	426
DW_DP23	23.39322662	529
DW_DP24	23.29368782	201
DW_DP25	23.27226639	280
DW_DP26	22.72547913	137
DW_DP27	22.97504234	273
DW_DP28	23.59886169	389
DW_DP29	23.00102615	188
DW_DP30	23.22255325	377
DW_DP31	23.11132622	269
DW_DP32	22.99685097	149
DW_DP33	22.58162117	47
DW_DP34	22.3573513	43
DW_DP35	23.18387222	204
DW_DP36	23.50171852	292
DW_DP37	22.2955246	73
DW_DP38	23.23373413	148
DW_DP39	21.86547661	58
UCILogger_PWD	23.04258728	314

	LST14NOV25	*Distance WD (12pm-270)*
LST14NOV25	1	
Distance WD (12pm-270)	0.75	1

Name	LST15APRIL18	Distance WD (12pm-240)
DW_DP1	26.12661934	89
DW_DP2	24.78730392	31
DW_DP3	25.78170204	53
DW_DP4	26.15192604	197
DW_DP5	26.74104881	291
DW_DP6	26.5711174	68
DW_DP7	26.77507591	176
DW_DP8	27.13092804	288
DW_DP9	26.46225929	92
DW_DP10	26.99249268	212
DW_DP11	26.81687355	320
DW_DP12	26.77795219	136
DW_DP13	26.08176613	23
DW_DP14	26.97561836	249
DW_DP15	26.80854797	343
DW_DP16	27.03079987	449
DW_DP17	27.19995689	464
DW_DP18	27.53151512	591
DW_DP19	27.45005226	577
DW_DP20	27.46313095	426
DW_DP21	27.75742722	555
DW_DP22	27.50187302	426
DW_DP23	27.23493004	529
DW_DP24	27.08253288	201
DW_DP25	27.40272522	280
DW_DP26	26.47068596	137
DW_DP27	26.8672142	273
DW_DP28	27.59274864	389
DW_DP29	26.97686768	188
DW_DP30	27.18815994	377
DW_DP31	26.92538452	269
DW_DP32	26.43162346	149
DW_DP33	25.47333527	47
DW_DP34	25.71751213	43
DW_DP35	26.52779961	204
DW_DP36	26.77441788	292
DW_DP37	25.16032982	73
DW_DP38	26.61255264	148
DW_DP39	24.54416275	58
UCILogger_PWD	27.07656288	314

	LST15APRIL18	*Distance WD (12pm-240)*
LST15APRIL18	1	
Distance WD (12pm-240)	0.80	1

Name	LST15DEC30	Distance WD (12pm-0)
DW_DP1	19.35626793	509
DW_DP2	18.66500854	27
DW_DP3	19.14376259	173
DW_DP4	19.35754395	170
DW_DP5	19.5530014	170
DW_DP6	19.32640076	287
DW_DP7	19.5069294	266
DW_DP8	19.46137047	279
DW_DP9	19.31986046	399
DW_DP10	19.46277618	400
DW_DP11	19.27908134	396
DW_DP12	19.40044212	455
DW_DP13	19.02845001	50
DW_DP14	19.54455948	517
DW_DP15	19.36566544	511
DW_DP16	19.59525871	424
DW_DP17	19.48278809	536
DW_DP18	19.69050598	580
DW_DP19	19.63117599	483
DW_DP20	19.80012703	318
DW_DP21	19.82977104	387
DW_DP22	19.54107094	222
DW_DP23	19.46565247	326
DW_DP24	19.54812813	187
DW_DP25	19.58579254	509
DW_DP26	19.12573624	261
DW_DP27	19.29234123	360
DW_DP28	19.65416908	374
DW_DP29	19.21351242	256
DW_DP30	19.49595833	278
DW_DP31	19.21767616	196
DW_DP32	19.23844719	181
DW_DP33	19.0489502	238
DW_DP34	19.00073242	78
DW_DP35	19.28347206	141
DW_DP36	19.58980179	167
DW_DP37	18.83094597	52
DW_DP38	19.54800606	80
DW_DP39	18.46168327	577
UCILogger_PWD	19.45927429	324

	LST15DEC30	*Distance WD (12pm-0)*
LST15DEC30	1	
Distance WD (12pm-0)	0.32	1

Name	LST15FEB13	Distance WD (12pm-270)
DW_DP1	20.2234211	89
DW_DP2	19.19548416	31
DW_DP3	20.23931122	53
DW_DP4	20.31364059	197
DW_DP5	20.61742592	291
DW_DP6	20.46596146	68
DW_DP7	20.40509987	176
DW_DP8	20.51019478	288
DW_DP9	20.28354263	92
DW_DP10	20.43811035	212
DW_DP11	20.08980179	320
DW_DP12	20.24690628	136
DW_DP13	19.97310638	23
DW_DP14	20.53719521	249
DW_DP15	20.14632225	343
DW_DP16	20.27072906	449
DW_DP17	20.35370064	464
DW_DP18	20.61628723	591
DW_DP19	20.68200874	577
DW_DP20	20.60539818	426
DW_DP21	20.76353645	555
DW_DP22	20.51915932	426
DW_DP23	20.38508224	529
DW_DP24	20.50251579	201
DW_DP25	20.47980309	280
DW_DP26	20.09845161	137
DW_DP27	20.26345062	273
DW_DP28	20.85294914	389
DW_DP29	20.44223785	188
DW_DP30	20.60732079	377
DW_DP31	20.50539207	269
DW_DP32	20.37861061	149
DW_DP33	19.90446854	47
DW_DP34	19.90838432	43
DW_DP35	20.41363335	204
DW_DP36	20.55574799	292
DW_DP37	19.56109238	73
DW_DP38	20.66790962	148
DW_DP39	18.84983635	58
UCILogger_PWD	20.2814312	314

	LST15FEB13	*Distance WD (12pm-270)*
LST15FEB13	1	
Distance WD (12pm-270)	0.58	1

Name	LST15JAN28	Distance WD (12pm-0)
DW_DP1	20.346365	509
DW_DP2	19.4479637	27
DW_DP3	20.282526	173
DW_DP4	20.734581	170
DW_DP5	21.0186138	170
DW_DP6	20.8332424	287
DW_DP7	20.9462776	266
DW_DP8	21.1995392	279
DW_DP9	20.5092545	399
DW_DP10	21.2783146	400
DW_DP11	21.0728321	396
DW_DP12	20.9106827	455
DW_DP13	20.1872368	50
DW_DP14	21.2647438	517
DW_DP15	20.9023724	511
DW_DP16	21.1464272	424
DW_DP17	21.1482258	536
DW_DP18	21.552393	580
DW_DP19	21.5458298	483
DW_DP20	21.3266869	318
DW_DP21	21.5651169	387
DW_DP22	21.1637745	222
DW_DP23	21.1158581	326
DW_DP24	21.0112953	187
DW_DP25	21.3190193	509
DW_DP26	20.5976944	261
DW_DP27	20.6666794	360
DW_DP28	21.1700268	374
DW_DP29	20.9793797	256
DW_DP30	20.9960175	278
DW_DP31	21.0247936	196
DW_DP32	20.8159027	181
DW_DP33	19.9398365	238
DW_DP34	20.4763527	78
DW_DP35	21.072958	141
DW_DP36	21.3640823	167
DW_DP37	19.8019257	52
DW_DP38	20.9768562	80
DW_DP39	19.2791634	577
UCILogger_PWD	21.1616707	324

	LST15JAN28	*Distance WD (12pm-0)*
LST15JAN28	1	
Distance WD (12pm-0)	0.32	1

Name	LST15MAR17	Distance WD (12pm-270)
DW_DP1	24.23814011	89
DW_DP2	23.52156067	31
DW_DP3	24.61844063	53
DW_DP4	24.63724899	197
DW_DP5	24.67419243	291
DW_DP6	24.95020294	68
DW_DP7	24.9009819	176
DW_DP8	24.83939552	288
DW_DP9	24.84752655	92
DW_DP10	24.98726273	212
DW_DP11	24.30470657	320
DW_DP12	24.83336258	136
DW_DP13	24.77239037	23
DW_DP14	25.02953339	249
DW_DP15	24.6521244	343
DW_DP16	24.55590057	449
DW_DP17	24.65556335	464
DW_DP18	24.56152534	591
DW_DP19	24.43317986	577
DW_DP20	24.58563614	426
DW_DP21	24.42487144	555
DW_DP22	24.22609711	426
DW_DP23	24.10147476	529
DW_DP24	24.52497101	201
DW_DP25	24.38453865	280
DW_DP26	24.33739281	137
DW_DP27	24.58007813	273
DW_DP28	25.07480812	389
DW_DP29	24.97159386	188
DW_DP30	24.91139221	377
DW_DP31	24.86240578	269
DW_DP32	24.97024155	149
DW_DP33	24.52710915	47
DW_DP34	24.09539604	43
DW_DP35	24.64081955	204
DW_DP36	24.67180824	292
DW_DP37	23.70837402	73
DW_DP38	24.59415245	148
DW_DP39	23.30380058	58
UCILogger_PWD	24.60948181	314

	LST15MAR17	*Distance WD (12pm-270)*
LST15MAR17	1	
Distance WD (12pm-270)	0.14	1

Name	LST15MAY4	Distance WD (12pm-130)
DW_DP1	28.48204422	509
DW_DP2	27.16413879	65
DW_DP3	28.25348282	94
DW_DP4	28.52547836	336
DW_DP5	29.06589317	396
DW_DP6	28.97064781	150
DW_DP7	29.1020546	235
DW_DP8	29.34956741	346
DW_DP9	28.73234177	98
DW_DP10	29.24014282	265
DW_DP11	29.08397102	396
DW_DP12	28.78626442	455
DW_DP13	28.35130501	50
DW_DP14	29.23067665	517
DW_DP15	29.0873642	511
DW_DP16	29.06129837	424
DW_DP17	29.31108284	536
DW_DP18	29.60822105	580
DW_DP19	29.58245659	483
DW_DP20	29.4757328	318
DW_DP21	29.86571121	387
DW_DP22	29.58629227	222
DW_DP23	29.52508545	326
DW_DP24	29.42101288	187
DW_DP25	29.56125069	509
DW_DP26	28.75180244	41
DW_DP27	29.24999046	360
DW_DP28	30.02316284	374
DW_DP29	29.36109924	137
DW_DP30	29.62166595	303
DW_DP31	29.3553772	238
DW_DP32	28.90378761	218
DW_DP33	27.89078712	167
DW_DP34	28.1772747	150
DW_DP35	29.10059547	261
DW_DP36	29.34770203	323
DW_DP37	27.7547226	353
DW_DP38	29.14797592	405
DW_DP39	26.98035049	44
UCILogger_PWD	29.22504997	324

	LST15MAY4	*Distance WD (12pm-130)*
LST15MAY4	1	
Distance WD (12pm-130)	0.51	1

Name	LST15NOV12	Distance WD (12pm-0)
DW_DP1	26.99564743	509
DW_DP2	25.76623917	27
DW_DP3	27.02079773	173
DW_DP4	27.05706024	170
DW_DP5	27.55653	170
DW_DP6	27.30381775	287
DW_DP7	27.15375137	266
DW_DP8	27.23791313	279
DW_DP9	27.11696434	399
DW_DP10	27.36795616	400
DW_DP11	26.79493713	396
DW_DP12	26.83356476	455
DW_DP13	26.54713631	50
DW_DP14	27.31122971	517
DW_DP15	26.89057732	511
DW_DP16	27.26222038	424
DW_DP17	27.19685936	536
DW_DP18	27.36183167	580
DW_DP19	27.82008171	483
DW_DP20	27.91252327	318
DW_DP21	27.86175156	387
DW_DP22	27.65021896	222
DW_DP23	27.52059364	326
DW_DP24	27.41145706	187
DW_DP25	27.51071739	509
DW_DP26	26.95630264	261
DW_DP27	27.23538589	360
DW_DP28	27.82404327	374
DW_DP29	27.25528717	256
DW_DP30	27.29313469	278
DW_DP31	27.70151711	196
DW_DP32	27.53235817	181
DW_DP33	26.5887661	238
DW_DP34	26.46166229	78
DW_DP35	27.73377609	141
DW_DP36	27.64635277	167
DW_DP37	26.16446114	52
DW_DP38	27.72153282	80
DW_DP39	25.65202522	577
UCILogger_PWD	27.10024261	324

	LST15NOV12	*Distance WD (12pm-0)*
LST15NOV12	1	
Distance WD (12pm-0)	0.11	1

Name	LST15NOV28	Distance WD (12pm-0)
DW_DP1	22.89214706	509
DW_DP2	21.92383194	27
DW_DP3	22.68466759	173
DW_DP4	22.76096344	170
DW_DP5	23.2090416	170
DW_DP6	22.72232056	287
DW_DP7	23.05101395	266
DW_DP8	23.01645088	279
DW_DP9	22.94252586	399
DW_DP10	23.00752449	400
DW_DP11	22.60483933	396
DW_DP12	22.82714462	455
DW_DP13	22.3304615	50
DW_DP14	22.83135223	517
DW_DP15	22.65512657	511
DW_DP16	22.97522163	424
DW_DP17	22.84397697	536
DW_DP18	22.88188362	580
DW_DP19	23.16125107	483
DW_DP20	23.19325829	318
DW_DP21	23.26364326	387
DW_DP22	23.08029366	222
DW_DP23	22.84887314	326
DW_DP24	23.08205986	187
DW_DP25	22.74458122	509
DW_DP26	22.71378899	261
DW_DP27	22.86055946	360
DW_DP28	23.12124062	374
DW_DP29	22.73813057	256
DW_DP30	22.82238197	278
DW_DP31	22.91499329	196
DW_DP32	22.91944504	181
DW_DP33	22.80861282	238
DW_DP34	22.16419029	78
DW_DP35	22.97924042	141
DW_DP36	23.13259697	167
DW_DP37	22.33650589	52
DW_DP38	23.47323418	80
DW_DP39	21.81532097	577
UCILogger_PWD	22.83078003	324

	LST15NOV28	*Distance WD (12pm-0)*
LST15NOV28	1	
Distance WD (12pm-0)	0.10	1

Name	LST15OCT27	Distance WD (12pm-0)
DW_DP1	27.59517097	509
DW_DP2	26.41083717	27
DW_DP3	27.49738693	173
DW_DP4	27.45519447	170
DW_DP5	28.01793289	170
DW_DP6	27.72128677	287
DW_DP7	27.83703804	266
DW_DP8	27.90311432	279
DW_DP9	27.77222443	399
DW_DP10	27.79910469	400
DW_DP11	27.46105576	396
DW_DP12	27.6458931	455
DW_DP13	27.2083683	50
DW_DP14	27.71976852	517
DW_DP15	27.70387077	511
DW_DP16	27.97961807	424
DW_DP17	27.96711922	536
DW_DP18	27.75621033	580
DW_DP19	28.09443665	483
DW_DP20	28.27488709	318
DW_DP21	28.55330467	387
DW_DP22	28.2942028	222
DW_DP23	28.08028603	326
DW_DP24	28.11181259	187
DW_DP25	28.16804314	509
DW_DP26	27.29574394	261
DW_DP27	27.83889961	360
DW_DP28	28.53358841	374
DW_DP29	27.73115158	256
DW_DP30	27.81933594	278
DW_DP31	27.85658455	196
DW_DP32	27.7136631	181
DW_DP33	27.37025452	238
DW_DP34	26.65791893	78
DW_DP35	27.82586861	141
DW_DP36	27.92582512	167
DW_DP37	26.95811462	52
DW_DP38	28.39833832	80
DW_DP39	26.14357948	577
UCILogger_PWD	27.72051048	324

	LST15OCT27	*Distance WD (12pm-0)*
LST15OCT27	1	
Distance WD (12pm-0)	0.19	1

Name	LST15SEPT25	Distance WD (12pm-210)
DW_DP1	25.87734985	89
DW_DP2	25.10789108	31
DW_DP3	25.69908142	53
DW_DP4	25.69713974	197
DW_DP5	26.26877594	291
DW_DP6	25.84822655	68
DW_DP7	26.20968437	176
DW_DP8	26.3771553	288
DW_DP9	25.94521523	92
DW_DP10	26.12932205	212
DW_DP11	26.09974861	320
DW_DP12	26.1930294	136
DW_DP13	25.66591835	23
DW_DP14	26.24375725	249
DW_DP15	26.1010704	343
DW_DP16	26.16704178	449
DW_DP17	26.41378403	464
DW_DP18	26.48934746	591
DW_DP19	26.96621132	577
DW_DP20	26.49056053	426
DW_DP21	26.66942215	555
DW_DP22	26.5107975	426
DW_DP23	26.41272736	529
DW_DP24	26.30874443	201
DW_DP25	26.63069153	280
DW_DP26	25.93961716	137
DW_DP27	26.18717003	273
DW_DP28	26.73727608	389
DW_DP29	26.26908684	188
DW_DP30	26.46072197	377
DW_DP31	26.37009811	269
DW_DP32	25.93209648	149
DW_DP33	25.48414993	47
DW_DP34	25.35270309	43
DW_DP35	26.08110046	204
DW_DP36	26.41309547	292
DW_DP37	25.29710197	73
DW_DP38	26.43455124	148
DW_DP39	25.01698112	58
UCILogger_PWD	26.2511692	314

	LST15SEPT25	*Distance WD (12pm-210)*
LST15SEPT25	1	
Distance WD (12pm-210)	0.79	1

Name	LST16FEB16	Distance WD (12pm-360)
DW_DP1	22.9659653	509
DW_DP2	22.3499317	27
DW_DP3	22.8296604	173
DW_DP4	23.0152798	170
DW_DP5	23.2716904	170
DW_DP6	23.0335999	287
DW_DP7	23.2703571	266
DW_DP8	23.1370659	279
DW_DP9	23.1321125	399
DW_DP10	23.1873264	400
DW_DP11	22.9752426	396
DW_DP12	22.9355202	455
DW_DP13	22.8152065	50
DW_DP14	23.1983452	517
DW_DP15	23.018795	511
DW_DP16	23.3811302	424
DW_DP17	23.251543	536
DW_DP18	23.4205589	580
DW_DP19	23.3717613	483
DW_DP20	23.5147114	318
DW_DP21	23.6134453	387
DW_DP22	23.315361	222
DW_DP23	23.2127781	326
DW_DP24	23.2181396	187
DW_DP25	23.225769	509
DW_DP26	22.8267899	261
DW_DP27	23.018795	360
DW_DP28	23.4337349	374
DW_DP29	22.9792042	256
DW_DP30	23.2514801	278
DW_DP31	22.982069	196
DW_DP32	23.0030022	181
DW_DP33	22.8218555	238
DW_DP34	22.7508144	78
DW_DP35	23.0705585	141
DW_DP36	23.3953857	167
DW_DP37	22.6375427	52
DW_DP38	23.3166885	80
DW_DP39	22.0030174	577
UCILogger_PWD	23.1418953	324

	LST16FEB16	*Distance WD (12pm-360)*
LST16FEB16	1	
Distance WD (12pm-0)	0.21	1

Name	LST16JAN15	Distance WD (12pm-0)
DW_DP1	19.54755974	509
DW_DP2	18.78773308	27
DW_DP3	19.49594307	173
DW_DP4	19.40645599	170
DW_DP5	19.70943832	170
DW_DP6	19.5801506	287
DW_DP7	19.59175491	266
DW_DP8	19.72471046	279
DW_DP9	19.74416351	399
DW_DP10	19.75791359	400
DW_DP11	19.43231583	396
DW_DP12	19.58768654	455
DW_DP13	19.24011993	50
DW_DP14	19.68405533	517
DW_DP15	19.55937576	511
DW_DP16	19.79035378	424
DW_DP17	19.78415489	536
DW_DP18	19.76636124	580
DW_DP19	20.16456985	483
DW_DP20	19.98581505	318
DW_DP21	20.16997528	387
DW_DP22	19.75101852	222
DW_DP23	19.68135071	326
DW_DP24	19.75090027	187
DW_DP25	19.69728851	509
DW_DP26	19.45874596	261
DW_DP27	19.53759766	360
DW_DP28	19.97435188	374
DW_DP29	19.40283394	256
DW_DP30	19.44735718	278
DW_DP31	19.34631157	196
DW_DP32	19.59301758	181
DW_DP33	19.42128372	238
DW_DP34	19.05543327	78
DW_DP35	19.54220772	141
DW_DP36	19.86590004	167
DW_DP37	19.19069672	52
DW_DP38	19.92498589	80
DW_DP39	18.68899536	577
UCILogger_PWD	19.64006615	324

	LST16JAN15	*Distance WD (12pm-0)*
LST16JAN15	1	
Distance WD (12pm-0)	0.30	1

Name	LST16MAR3	Distance WD (12pm-290)
DW_DP1	25.60401344	89
DW_DP2	24.5760231	31
DW_DP3	25.60490608	53
DW_DP4	25.71974373	197
DW_DP5	26.09534073	291
DW_DP6	25.85120583	68
DW_DP7	25.94301033	176
DW_DP8	26.20421791	288
DW_DP9	25.72389984	92
DW_DP10	26.12114143	212
DW_DP11	25.71653175	320
DW_DP12	25.9078083	136
DW_DP13	25.35528564	23
DW_DP14	26.08679581	249
DW_DP15	25.83785057	343
DW_DP16	26.03648949	449
DW_DP17	25.92667198	464
DW_DP18	26.54208565	591
DW_DP19	26.78783226	577
DW_DP20	26.47003937	426
DW_DP21	26.73921585	555
DW_DP22	26.41044807	426
DW_DP23	26.38256073	529
DW_DP24	26.2890892	201
DW_DP25	26.29076386	280
DW_DP26	25.78597641	137
DW_DP27	25.95303535	273
DW_DP28	26.65179443	389
DW_DP29	26.17185211	188
DW_DP30	26.16172409	377
DW_DP31	26.08288956	269
DW_DP32	25.96019745	149
DW_DP33	25.06103325	47
DW_DP34	25.36260223	43
DW_DP35	26.04450989	204
DW_DP36	26.40891075	292
DW_DP37	24.87702179	73
DW_DP38	26.21779823	148
DW_DP39	24.45985222	58
UCILogger_PWD	26.03869247	314

	LST16MAR3	*Distance WD (12pm-290)*
LST16MAR3	1	
Distance WD (12pm-290)	0.75	1

Name	LST16NOV14	Distance WD (12pm-360)
DW_DP1	25.79252052	509
DW_DP2	24.88327408	27
DW_DP3	25.31123352	173
DW_DP4	25.66493988	170
DW_DP5	26.00790596	170
DW_DP6	25.69445038	287
DW_DP7	25.82601357	266
DW_DP8	25.67070961	279
DW_DP9	25.58016396	399
DW_DP10	25.69584465	400
DW_DP11	25.37179375	396
DW_DP12	25.54035378	455
DW_DP13	25.26965141	50
DW_DP14	25.72055244	517
DW_DP15	25.49753189	511
DW_DP16	26.18613815	424
DW_DP17	26.19094086	536
DW_DP18	26.19497108	580
DW_DP19	26.10109138	483
DW_DP20	26.09954643	318
DW_DP21	26.61589241	387
DW_DP22	26.01885414	222
DW_DP23	26.02293777	326
DW_DP24	26.0143528	187
DW_DP25	25.70922661	509
DW_DP26	25.42188072	261
DW_DP27	25.71876526	360
DW_DP28	26.05063629	374
DW_DP29	25.54872513	256
DW_DP30	25.76552582	278
DW_DP31	25.4477272	196
DW_DP32	25.51685333	181
DW_DP33	25.1620121	238
DW_DP34	25.09357071	78
DW_DP35	25.8102417	141
DW_DP36	26.02336121	167
DW_DP37	25.01140022	52
DW_DP38	26.2298851	80
DW_DP39	24.42117882	577
UCILogger_PWD	25.47258568	324

	LST16NOV14	*Distance WD (12pm-360)*
LST16NOV14	1	
Distance WD (12pm-360)	0.22	1

Name	LST16NOV30	Distance WD (12pm-0)
DW_DP1	24.07687	509
DW_DP2	22.8798618	27
DW_DP3	23.7846165	173
DW_DP4	23.8896961	170
DW_DP5	24.4401207	170
DW_DP6	23.8584385	287
DW_DP7	24.1500778	266
DW_DP8	24.2489662	279
DW_DP9	24.2431717	399
DW_DP10	24.1547222	400
DW_DP11	23.9472656	396
DW_DP12	24.0212555	455
DW_DP13	23.4316235	50
DW_DP14	23.9988079	517
DW_DP15	23.9300156	511
DW_DP16	24.2978611	424
DW_DP17	24.0933723	536
DW_DP18	23.9654694	580
DW_DP19	24.6258316	483
DW_DP20	24.6188431	318
DW_DP21	24.8482246	387
DW_DP22	24.4862576	222
DW_DP23	24.2852917	326
DW_DP24	24.295433	187
DW_DP25	24.1945915	509
DW_DP26	23.6100597	261
DW_DP27	24.0906887	360
DW_DP28	24.5111427	374
DW_DP29	23.7888145	256
DW_DP30	23.9993973	278
DW_DP31	23.9122562	196
DW_DP32	23.89361	181
DW_DP33	23.6762905	238
DW_DP34	22.9521408	78
DW_DP35	23.9358902	141
DW_DP36	24.2113438	167
DW_DP37	23.4095268	52
DW_DP38	24.4982224	80
DW_DP39	22.8139019	577
UCILogger_PWD	24.0939789	324

	LST16NOV30	*Distance WD (12pm-0)*
LST16NOV30	1	
Distance WD (12pm-0)	0.26	1

Name	LST17FEB18	Distance
DW_DP1	23.21567535	60
DW_DP2	22.37114716	17
DW_DP3	23.02347565	52
DW_DP4	23.12710762	90
DW_DP5	23.45149994	134
DW_DP6	22.9605484	52
DW_DP7	23.2528553	168
DW_DP8	23.36077881	280
DW_DP9	23.22277451	85
DW_DP10	23.33471107	207
DW_DP11	23.12059784	314
DW_DP12	23.19663811	124
DW_DP13	22.50556374	31
DW_DP14	23.40527153	230
DW_DP15	23.3057251	334
DW_DP16	23.62306786	438
DW_DP17	23.62955475	456
DW_DP18	23.43490791	579
DW_DP19	23.72403717	570
DW_DP20	23.72907448	412
DW_DP21	23.96988487	533
DW_DP22	23.64112282	414
DW_DP23	23.45601082	533
DW_DP24	23.52626801	173
DW_DP25	23.53326607	286
DW_DP26	23.20909882	50
DW_DP27	23.33840561	169
DW_DP28	23.67893791	284
DW_DP29	23.1371212	160
DW_DP30	23.51711082	290
DW_DP31	23.2289238	253
DW_DP32	23.34571648	138
DW_DP33	23.10275459	36
DW_DP34	22.80254555	36
DW_DP35	23.37903023	148
DW_DP36	23.61139297	169
DW_DP37	22.79532242	46
DW_DP38	23.79169846	56
DW_DP39	22.27600288	40
UCILogger_PWD	23.35278702	291

	LST17FEB18	*Distance*
LST17FEB18	1	
Distance	0.662680768	1

Name	LST17MAR22	Distance
DW_DP1	23.13405609	60
DW_DP2	22.17937851	17
DW_DP3	22.89559174	52
DW_DP4	22.94605827	90
DW_DP5	23.35374641	134
DW_DP6	22.91369629	52
DW_DP7	23.16709328	168
DW_DP8	23.16497993	280
DW_DP9	23.18932152	85
DW_DP10	23.04842949	207
DW_DP11	22.93556595	314
DW_DP12	23.20923042	124
DW_DP13	22.59936905	31
DW_DP14	23.22274017	230
DW_DP15	22.98255348	334
DW_DP16	23.42764091	438
DW_DP17	23.52613258	456
DW_DP18	23.34090996	579
DW_DP19	23.25079346	570
DW_DP20	23.44652939	412
DW_DP21	23.56288528	533
DW_DP22	23.48319244	414
DW_DP23	23.31802559	533
DW_DP24	23.46072578	173
DW_DP25	23.37316513	286
DW_DP26	23.07016563	50
DW_DP27	23.17916489	169
DW_DP28	23.43778419	284
DW_DP29	23.11474609	160
DW_DP30	23.38406181	290
DW_DP31	23.30942345	253
DW_DP32	23.0478363	138
DW_DP33	22.79834938	36
DW_DP34	22.50889015	36
DW_DP35	23.22893524	148
DW_DP36	23.46387863	169
DW_DP37	22.57331467	46
DW_DP38	23.49269104	56
DW_DP39	21.879776	40
UCILogger_PWD	23.09191132	291

	LST17MAR22	*Distance*
LST17MAR22	1	
Distance	0.584719528	1

Appendix B: Data from the field measurement and Remote Sensing

Hatirjheel Lake Area: Land Surface Temperature and Distance from Lake edge_2013-17

Name	LST14FEB10	Distance WD (12pm-50)
UCILogger7_BPP	21.07230759	175
UCILogger6_Ledge	20.6345005	0
UCILogger8	21.1095314	121
UCILogger7	21.2079792	633
UCILogger6	20.90851784	542
UCILogger4	20.68213081	448
UCILogger3	21.70109558	218
UCILogger2	21.28859138	0
UCILogger1	18.86213303	0
HP44	21.53298187	156
HP43	21.72225952	215
HP42	21.41362762	344
HP41	21.02770042	492
HP40	21.27186394	639
HP39	21.47010994	686
HP38	22.04853249	777
HP37	22.35439873	779
HP36	22.31563568	844
HP35	22.26340675	877
HP34	22.30940628	824
HP33	21.58469582	431
HP32	21.43399811	333
HP31	21.14166069	277
HP30	21.5201149	361
HP29	20.4717083	134
HP28	20.78372192	208
HP27	20.87615967	261
HP26	21.12074471	281
HP25	22.05729866	467
HP24	21.7533741	674
HP23	21.5300312	690
HP22	21.39256096	670
HP21	20.49172783	88
HP20	20.69186211	126
HP19	20.79345512	190
HP18	20.89327812	134
HP17	20.55488777	75
HP16	21.31156349	640
HP15	21.28512955	561
HP14	21.09729576	597
HP13	20.82268715	502
HP12	20.98593521	442
HP11	20.87289619	491
HP10	20.77215004	457
HP9	20.5180645	331
HP8	20.50951195	254
HP7	21.15731239	345
HP6	20.7497673	349
HP5	20.88903618	273
HP4	21.0162468	200
HP3	20.98771286	146
HP2	21.32868958	100
HP1	21.39116478	32

	LST14FEB10	*Distance WD (12pm-50)*
LST14FEB10	1	
Distance WD (12pm-50)	0.61	1

Name	LST13APR12	Distance WD (12pm-180)	LST13APR12	Distance WD (12pm-50)
UCILogger7_BPP	29.46073151	206	29.46073151	175
UCILogger6_Ledge	28.2534008	0	28.2534008	0
UCILogger8	29.14341927	118	29.14341927	121
UCILogger7	29.33443642	631	29.33443642	633
UCILogger6	28.92001724	545	28.92001724	542
UCILogger4	28.67988205	445	28.67988205	448
UCILogger3	29.59271431	221	29.59271431	218
UCILogger2	28.34359169	19	28.34359169	0
UCILogger1	27.13567162	0	27.13567162	0
HP44	29.52172661	162	29.52172661	156
HP43	29.59271431	220	29.59271431	215
HP42	29.62142181	347	29.62142181	344
HP41	28.92027473	493	28.92027473	492
HP40	29.18147469	639	29.18147469	639
HP39	29.41089821	677	29.41089821	686
HP38	29.60534859	768	29.60534859	777
HP37	30.46299171	784	30.46299171	779
HP36	29.92575264	838	29.92575264	844
HP35	29.99979019	875	29.99979019	877
HP34	30.19892693	853	30.19892693	824
HP33	29.62206078	427	29.62206078	431
HP32	29.44628906	335	29.44628906	333
HP31	29.22922516	275	29.22922516	277
HP30	29.29692078	355	29.29692078	361
HP29	28.29449081	138	28.29449081	134
HP28	28.61473846	204	28.61473846	208
HP27	28.77193832	270	28.77193832	261
HP26	28.91108704	316	28.91108704	281
HP25	30.14922905	795	30.14922905	467
HP24	29.35223389	762	29.35223389	674
HP23	29.66654968	688	29.66654968	690
HP22	29.08654404	703	29.08654404	670
HP21	28.21660423	81	28.21660423	88
HP20	28.65283966	125	28.65283966	126
HP19	28.71460533	196	28.71460533	190
HP18	28.52591705	147	28.52591705	134
HP17	28.24023247	84	28.24023247	75
HP16	29.3775177	643	29.3775177	640
HP15	29.02226257	666	29.02226257	561
HP14	29.18309402	592	29.18309402	597
HP13	28.80867195	502	28.80867195	502
HP12	28.67992592	567	28.67992592	442
HP11	28.89151192	489	28.89151192	491
HP10	28.84324646	461	28.84324646	457
HP9	28.44547081	334	28.44547081	331
HP8	28.32659149	256	28.32659149	254
HP7	29.43701553	346	29.43701553	345
HP6	28.69723129	348	28.69723129	349
HP5	28.73150063	291	28.73150063	273
HP4	28.77635384	231	28.77635384	200
HP3	28.82321739	170	28.82321739	146
HP2	29.24698257	100	29.24698257	100
HP1	28.80643845	31	28.80643845	32

	LST13APR12	*Distance WD (12pm-180)*
LST13APR12	1	
Distance WD (12pm-180)	0.666589857	1

	LST13APR12	*Distance WD (12pm-50)*
LST13APR12	1	
Distance WD (12pm-50)	0.651680407	1

Name	LST15NOV12	Distance WD (12pm-0)
UCILogger7_BPP	27.15605545	175
UCILogger6_Ledge	27.12168121	0
UCILogger8	26.97395134	121
UCILogger7	27.42021179	633
UCILogger6	27.11036682	542
UCILogger4	26.63853264	448
UCILogger3	27.53449249	218
UCILogger2	27.52316666	0
UCILogger1	24.80630875	0
HP44	27.25712967	156
HP43	27.53513908	215
HP42	27.20445442	344
HP41	26.56753349	492
HP40	27.21420479	639
HP39	27.31880379	686
HP38	27.90166664	777
HP37	28.49149132	779
HP36	28.17803955	844
HP35	28.21446037	877
HP34	28.31011581	824
HP33	27.23286057	431
HP32	26.86507225	333
HP31	26.71022034	277
HP30	27.11558533	361
HP29	26.3151207	134
HP28	26.6894474	208
HP27	26.75402832	261
HP26	26.85586166	281
HP25	27.80771255	467
HP24	27.36309242	674
HP23	27.6247673	690
HP22	27.17517662	670
HP21	26.74407768	88
HP20	26.96616364	126
HP19	26.88204575	190
HP18	27.18756485	134
HP17	26.81817436	75
HP16	27.506073	640
HP15	27.25934219	561
HP14	27.27319527	597
HP13	26.97576141	502
HP12	27.03520775	442
HP11	26.66609573	491
HP10	26.88597107	457
HP9	26.54092979	331
HP8	26.6062851	254
HP7	27.01080322	345
HP6	26.74283409	349
HP5	26.77933502	273
HP4	26.95269394	200
HP3	26.73205566	146
HP2	27.0583992	100
HP1	27.6027298	32

	LST15NOV12	*Distance WD (12pm-0)*
LST15NOV12	1	
Distance WD (12pm-0)	0.58	1

Name	LST15FEB13	Distance WD (12pm-270)
UCILogger7_BPP	20.79406166	103
UCILogger6_Ledge	20.47874832	0
UCILogger8	20.51211548	92
UCILogger7	20.53376198	316
UCILogger6	20.3239212	242
UCILogger4	20.19808197	109
UCILogger3	20.97784424	217
UCILogger2	20.373209	0
UCILogger1	18.49598312	0
HP44	20.80133247	174
HP43	20.92317963	205
HP42	20.62364769	197
HP41	20.18852806	295
HP40	20.40408516	427
HP39	20.57087326	450
HP38	20.66794777	482
HP37	21.39030647	389
HP36	20.94328499	485
HP35	21.04570961	399
HP34	21.13852501	297
HP33	20.41479492	202
HP32	20.21188927	121
HP31	20.06822205	100
HP30	20.29291916	192
HP29	19.87661362	41
HP28	20.00642395	97
HP27	20.10101128	173
HP26	20.22165489	187
HP25	21.15290642	296
HP24	20.73171997	291
HP23	20.70261192	376
HP22	20.26388741	272
HP21	19.84162903	49
HP20	20.11547852	91
HP19	20.01145172	154
HP18	19.94824982	126
HP17	19.87950325	74
HP16	20.59018898	370
HP15	20.29610634	258
HP14	20.47254372	278
HP13	20.26290894	187
HP12	20.11558151	166
HP11	20.2089119	249
HP10	20.23365402	146
HP9	20.12722015	63
HP8	20.01312828	42
HP7	20.4469986	145
HP6	20.18217659	90
HP5	20.26764679	76
HP4	20.58701324	127
HP3	20.66246796	83
HP2	20.53054619	91
HP1	20.38797951	91

	LST15FEB13	*Distance WD (12pm-270)*
LST15FEB13	1	
Distance WD (12pm-270)	0.57	1

Name	LST14MAR14	Distance WD (12pm-360)
UCILogger7_BPP	27.94954491	175
UCILogger6_Ledge	27.68795013	0
UCILogger8	28.13482094	121
UCILogger7	27.771101	633
UCILogger6	27.7604599	542
UCILogger4	27.47467041	448
UCILogger3	28.48416901	218
UCILogger2	27.51570129	0
UCILogger1	23.80748367	0
HP44	28.46842384	156
HP43	28.52576065	215
HP42	28.18871117	344
HP41	27.40358543	492
HP40	27.69121361	639
HP39	27.926651	686
HP38	28.26803589	777
HP37	28.72854805	779
HP36	28.34062576	844
HP35	28.34745216	877
HP34	28.85622025	824
HP33	27.74995232	431
HP32	27.5989399	333
HP31	27.29238892	277
HP30	27.77012634	361
HP29	26.50600052	134
HP28	26.83983421	208
HP27	27.23128891	261
HP26	27.35196114	281
HP25	28.40432358	467
HP24	28.11750031	674
HP23	28.1697998	690
HP22	27.60183525	670
HP21	26.65025139	88
HP20	27.1409874	126
HP19	27.31709671	190
HP18	27.28466225	134
HP17	26.73791313	75
HP16	28.00605965	640
HP15	27.56803513	561
HP14	27.70231438	597
HP13	27.67179108	502
HP12	27.37496376	442
HP11	27.39204216	491
HP10	27.5930481	457
HP9	27.12653542	331
HP8	26.92314529	254
HP7	27.82127953	345
HP6	27.24435425	349
HP5	27.29252815	273
HP4	27.63938713	200
HP3	27.85238266	146
HP2	28.27581215	100
HP1	27.68746376	32

	LST14MAR14	*Distance WD (12pm-360)*
LST14MAR14	1	
Distance WD (12pm-360)	0.47	1

Name	LST16NOV14	Distance WD (12pm-360)
UCILogger7_BPP	25.82184029	175
UCILogger6_Ledge	24.7926712	0
UCILogger8	25.29207611	121
UCILogger7	25.56406975	633
UCILogger6	25.38982391	542
UCILogger4	25.06285477	448
UCILogger3	25.68849564	218
UCILogger2	24.85932159	0
UCILogger1	23.64270973	0
HP44	25.59459305	156
HP43	25.68849564	215
HP42	25.59062004	344
HP41	25.2292881	492
HP40	25.69399261	639
HP39	25.70706749	686
HP38	26.17664719	777
HP37	26.18170166	779
HP36	26.44609261	844
HP35	26.44644737	877
HP34	26.15156937	824
HP33	25.50872421	431
HP32	25.19106293	333
HP31	24.97076988	277
HP30	25.16460419	361
HP29	24.91012001	134
HP28	24.98046494	208
HP27	25.00960732	261
HP26	25.02531624	281
HP25	25.47791481	467
HP24	25.22333336	674
HP23	25.82554817	690
HP22	25.19196892	670
HP21	25.03242874	88
HP20	25.16607285	126
HP19	25.17434311	190
HP18	25.18213844	134
HP17	24.94488716	75
HP16	25.73656845	640
HP15	25.24456215	561
HP14	25.52124214	597
HP13	25.25086212	502
HP12	25.22710991	442
HP11	25.40670013	491
HP10	25.1662159	457
HP9	24.9151001	331
HP8	25.00475883	254
HP7	25.55723763	345
HP6	25.19080162	349
HP5	25.18157768	273
HP4	25.10355568	200
HP3	25.0282402	146
HP2	25.32138443	100
HP1	25.04345131	32

	LST16NOV14	*Distance WD (12pm-360)*
LST16NOV14	1	
Distance WD (12pm-360)	0.71	1

Name	LST16JAN15	Distance WD (12pm-0)
UCILogger7_BPP	19.07183075	175
UCILogger6_Ledge	19.33108711	0
UCILogger8	19.0801487	121
UCILogger7	18.98269081	633
UCILogger6	18.79936409	542
UCILogger4	18.83381462	448
UCILogger3	19.47894859	218
UCILogger2	19.04063416	0
UCILogger1	18.31298637	0
HP44	19.21132469	156
HP43	19.38129425	215
HP42	19.08283615	344
HP41	18.83766365	492
HP40	18.96848297	639
HP39	19.01892662	686
HP38	19.19230652	777
HP37	19.33231544	779
HP36	19.50908089	844
HP35	19.59891319	877
HP34	19.62900352	824
HP33	19.27972603	431
HP32	19.05504417	333
HP31	18.85508919	277
HP30	19.08786964	361
HP29	18.78672409	134
HP28	18.95668602	208
HP27	19.12065887	261
HP26	19.04606438	281
HP25	19.4929924	467
HP24	19.38434601	674
HP23	19.11749458	690
HP22	19.0886898	670
HP21	18.88972282	88
HP20	18.97978401	126
HP19	19.04405403	190
HP18	18.99302101	134
HP17	19.00650024	75
HP16	19.06202507	640
HP15	19.05108261	561
HP14	18.90949631	597
HP13	18.79974556	502
HP12	18.95976067	442
HP11	18.80115891	491
HP10	18.80750847	457
HP9	18.83258247	331
HP8	18.82459259	254
HP7	19.03435898	345
HP6	18.92688179	349
HP5	19.00702286	273
HP4	19.0401783	200
HP3	19.00849342	146
HP2	19.1265316	100
HP1	19.07617188	32

	LST16JAN15	*Distance WD (12pm-0)*
LST16JAN15	1	
Distance WD (12pm-0)	0.36	1

Name	LST13JUN15	Distance WD (9am-90, 12pm-90)
UCILogger7_BPP	23.93180656	106
UCILogger6_Ledge	22.1544857	0
UCILogger8	22.96927643	201
UCILogger7	23.34112549	371
UCILogger6	23.19211197	348
UCILogger4	22.95661354	343
UCILogger3	23.60252571	168
UCILogger2	21.99586105	0
UCILogger1	21.16384125	0
HP44	23.37701988	157
HP43	23.60252571	146
HP42	23.92206383	188
HP41	23.4552269	223
HP40	23.61211205	269
HP39	23.59896278	256
HP38	23.55892754	222
HP37	23.67510605	316
HP36	24.03573608	212
HP35	23.30280685	315
HP34	21.92207909	405
HP33	20.39698601	512
HP32	20.9056797	609
HP31	20.78723526	599
HP30	20.57614136	505
HP29	21.56859779	658
HP28	21.68314743	601
HP27	22.24157333	528
HP26	21.7761364	518
HP25	22.31038094	409
HP24	22.32104301	412
HP23	23.62656975	332
HP22	23.00244713	437
HP21	22.32743645	652
HP20	22.50178528	613
HP19	22.72885895	548
HP18	22.69246483	540
HP17	22.49726677	526
HP16	23.50728035	322
HP15	23.13615608	440
HP14	23.27477455	370
HP13	23.05747223	339
HP12	22.86995697	426
HP11	23.26029587	280
HP10	23.08198929	330
HP9	22.87660599	369
HP8	22.84291458	355
HP7	23.58625984	248
HP6	23.07641983	305
HP5	23.06982231	280
HP4	22.78297997	266
HP3	22.73212242	246
HP2	23.06731796	177
HP1	22.46200371	117

	LST13JUN15	*Distance WD (9am-90, 12pm-90)*
LST13JUN15	1	
Distance WD (9am-90, 12pm-90)	-0.46	1

Name	LST16FEB16	Distance WD (12pm-360)
UCILogger7_BPP	23.37106705	175
UCILogger6_Ledge	23.15265274	0
UCILogger8	23.36294746	121
UCILogger7	23.05738068	633
UCILogger6	22.95835876	542
UCILogger4	22.85134125	448
UCILogger3	23.5176506	218
UCILogger2	23.04958153	0
UCILogger1	21.63009262	0
HP44	23.65060806	156
HP43	23.56675339	215
HP42	23.2786293	344
HP41	23.02569199	492
HP40	23.13209915	639
HP39	23.24872208	686
HP38	23.42477226	777
HP37	23.67208481	779
HP36	23.58030319	844
HP35	23.7215538	877
HP34	23.55810738	824
HP33	23.28470993	431
HP32	22.90591621	333
HP31	22.76063156	277
HP30	23.0272522	361
HP29	22.6551075	134
HP28	22.73008919	208
HP27	22.8173008	261
HP26	22.85767174	281
HP25	23.37517548	467
HP24	23.24409676	674
HP23	23.29935265	690
HP22	23.03320313	670
HP21	22.69702148	88
HP20	22.82099342	126
HP19	22.86659622	190
HP18	22.87950325	134
HP17	22.67462158	75
HP16	23.189888	640
HP15	22.99657631	561
HP14	23.04029083	597
HP13	22.9105854	502
HP12	22.83026695	442
HP11	23.01052284	491
HP10	22.89562607	457
HP9	22.80861664	331
HP8	22.86965942	254
HP7	23.29594994	345
HP6	23.05623245	349
HP5	23.09649658	273
HP4	23.18051529	200
HP3	23.16274643	146
HP2	23.45853996	100
HP1	23.10497856	32

	LST16FEB16	*Distance WD (12pm-360)*
LST16FEB16	1	
Distance WD (12pm-0)	0.43	1

Name	LST15MAR17	Distance WD (12pm-270)
UCILogger7_BPP	26.27622604	103
UCILogger6_Ledge	25.81309319	0
UCILogger8	26.30768394	92
UCILogger7	26.07144547	316
UCILogger6	25.972229	242
UCILogger4	25.66913223	109
UCILogger3	26.49465752	217
UCILogger2	25.49404716	0
UCILogger1	23.23783112	0
HP44	26.53184319	174
HP43	26.53148842	205
HP42	26.08693886	197
HP41	25.70582199	295
HP40	25.97935104	427
HP39	26.09911919	450
HP38	26.32005501	482
HP37	26.90071297	389
HP36	26.61017036	485
HP35	26.81735992	399
HP34	27.08653641	297
HP33	26.14045334	202
HP32	25.84095573	121
HP31	25.47408676	100
HP30	25.94413567	192
HP29	25.17154503	41
HP28	25.43055153	97
HP27	25.74020195	173
HP26	25.83507538	187
HP25	26.75675201	296
HP24	26.50920486	291
HP23	26.38492966	376
HP22	26.0246563	272
HP21	25.33504105	49
HP20	25.61192322	91
HP19	25.65363503	154
HP18	25.6185894	126
HP17	25.34121132	74
HP16	26.21055985	370
HP15	25.93422699	258
HP14	26.03841782	278
HP13	25.87887764	187
HP12	25.66901588	166
HP11	25.77933121	249
HP10	25.80139542	146
HP9	25.58497047	63
HP8	25.53936195	42
HP7	25.98299026	145
HP6	25.69823456	90
HP5	25.79959488	76
HP4	26.15699577	127
HP3	26.32522774	83
HP2	26.20252037	91
HP1	25.56925201	91

	LST15MAR17	*Distance WD (12pm-270)*
LST15MAR17	1	
Distance WD (12pm-270)	0.60	1

Name	LST15APR18	Distance WD (12pm-240)
UCILogger7_BPP	26.57172966	103
UCILogger6_Ledge	25.81293678	0
UCILogger8	25.75804138	92
UCILogger7	26.88162804	316
UCILogger6	26.48834991	242
UCILogger4	26.08683395	109
UCILogger3	26.74811935	217
UCILogger2	25.68483543	0
UCILogger1	24.05893326	0
HP44	26.51528931	174
HP43	26.58886719	205
HP42	27.06299973	197
HP41	26.57369232	295
HP40	26.985672	427
HP39	27.12794876	450
HP38	27.49543571	482
HP37	28.0514679	389
HP36	27.77061462	485
HP35	27.31213188	399
HP34	27.58166122	297
HP33	26.89657021	202
HP32	26.40122032	121
HP31	26.26978683	100
HP30	26.87231827	192
HP29	25.31271553	41
HP28	25.84670639	97
HP27	26.29046822	173
HP26	26.56332779	187
HP25	27.53996468	296
HP24	27.38579369	291
HP23	27.1180172	376
HP22	26.58259201	272
HP21	25.47660446	49
HP20	26.10006714	91
HP19	26.32619476	154
HP18	26.15903282	126
HP17	25.78968048	74
HP16	26.99032021	370
HP15	26.58293915	258
HP14	26.74772835	278
HP13	26.3421402	187
HP12	26.29966927	166
HP11	26.51373863	249
HP10	26.26922798	146
HP9	25.88063431	63
HP8	25.4749279	42
HP7	26.68274117	145
HP6	25.94312477	90
HP5	25.82193565	76
HP4	25.56550407	127
HP3	25.50411987	83
HP2	26.17965698	91
HP1	25.68886566	91

	LST15APR18	*Distance WD (12pm-240)*
LST15APR18	1	
Distance WD (12pm-240)	0.85	1

Name	LST17FEB18	Distance
UCILogger7_BPP	23.5841732	100
UCILogger6_Ledge	23.2454052	0
UCILogger8	23.4272995	120
UCILogger7	23.61764717	243
UCILogger6	23.48441315	164
UCILogger4	23.24731255	105
UCILogger3	23.70653152	190
UCILogger2	23.39885521	0
UCILogger1	21.65570831	0
HP44	23.69408798	155
HP43	23.67469597	142
HP42	23.69244957	167
HP41	23.2275219	213
HP40	23.43977547	259
HP39	23.51747131	262
HP38	23.80945396	227
HP37	24.14282417	312
HP36	24.14878464	212
HP35	24.2604599	321
HP34	24.41351128	299
HP33	23.86772919	190
HP32	23.44189453	105
HP31	23.31803703	92
HP30	23.69003677	186
HP29	22.86031532	39
HP28	23.25292778	96
HP27	23.16110039	168
HP26	23.27483559	181
HP25	24.0486927	292
HP24	23.86910629	285
HP23	23.67245293	314
HP22	23.56069183	240
HP21	23.17205429	47
HP20	23.17729759	88
HP19	23.2178421	133
HP18	23.32437515	93
HP17	23.07699013	52
HP16	23.60766411	287
HP15	23.54382896	204
HP14	23.57044601	211
HP13	23.42941475	136
HP12	23.35468674	120
HP11	23.32341766	186
HP10	23.36119461	117
HP9	23.10823059	56
HP8	23.10085297	36
HP7	23.6088829	140
HP6	23.30452538	84
HP5	23.37441063	74
HP4	23.3508091	98
HP3	23.30908775	74
HP2	23.55201149	75
HP1	23.34331131	32

	LST17FEB18	*Distance*
LST17FEB18	1	
Distance	0.705426567	1

Name	LST17MAR22	Distance
UCILogger7_BPP	23.5358696	100
UCILogger6_Ledge	22.97171974	0
UCILogger8	22.93670273	120
UCILogger7	23.36762619	243
UCILogger6	23.18298912	164
UCILogger4	22.93900871	105
UCILogger3	23.77362251	190
UCILogger2	22.82412148	0
UCILogger1	21.50562859	0
HP44	23.50478363	155
HP43	23.70474815	142
HP42	23.51466942	167
HP41	23.41859436	213
HP40	23.4015522	259
HP39	23.4321022	262
HP38	23.62701797	227
HP37	23.97257233	312
HP36	24.03278351	212
HP35	24.09917068	321
HP34	24.11761284	299
HP33	23.71288109	190
HP32	23.20607948	105
HP31	23.07490158	92
HP30	23.61170769	186
HP29	22.65313721	39
HP28	22.87290573	96
HP27	23.05835724	168
HP26	23.20522118	181
HP25	23.8409214	292
HP24	23.6990242	285
HP23	23.46853828	314
HP22	23.31288528	240
HP21	22.74554062	47
HP20	22.99796104	88
HP19	23.12335777	133
HP18	23.26485825	93
HP17	23.0658741	52
HP16	23.43987083	287
HP15	23.28385162	204
HP14	23.32465172	211
HP13	23.11021423	136
HP12	23.29222679	120
HP11	23.37325859	186
HP10	23.05405045	117
HP9	22.83187866	56
HP8	22.87304688	36
HP7	23.40191841	140
HP6	23.06468964	84
HP5	23.1841507	74
HP4	23.15065765	98
HP3	22.91320229	74
HP2	23.08378983	75
HP1	22.79793549	32

	LST17MAR22	*Distance*
LST17MAR22	1	
Distance	0.77623663	1

Name	LST13DEC24	Distance WD (9am-270, 12pm-270)
UCILogger7_BPP	21.26242447	103
UCILogger6_Ledge	20.83275604	0
UCILogger8	20.94756126	92
UCILogger7	21.22313309	316
UCILogger6	21.06760025	242
UCILogger4	20.91688728	109
UCILogger3	21.38843536	217
UCILogger2	20.81262016	0
UCILogger1	20.14089394	0
HP44	21.16176987	174
HP43	21.47331429	205
HP42	21.23695755	197
HP41	21.05365562	295
HP40	21.06734848	427
HP39	21.26918602	450
HP38	21.7040596	482
HP37	21.9253788	389
HP36	21.69044685	485
HP35	21.70932198	399
HP34	21.42047691	297
HP33	21.03223038	202
HP32	20.83589172	121
HP31	20.64804459	100
HP30	20.76399231	192
HP29	20.46231651	41
HP28	20.65077972	97
HP27	20.83893013	173
HP26	20.78135681	187
HP25	21.36691475	296
HP24	21.37496185	291
HP23	21.50702858	376
HP22	21.19879532	272
HP21	20.57034683	49
HP20	20.66215897	91
HP19	20.87566376	154
HP18	20.92423058	126
HP17	20.8990593	74
HP16	21.21534157	370
HP15	21.14988899	258
HP14	21.14647484	278
HP13	20.93514442	187
HP12	20.95647621	166
HP11	21.03850365	249
HP10	20.91688728	146
HP9	20.8333931	63
HP8	20.62134743	42
HP7	21.19049454	145
HP6	20.94005013	90
HP5	21.00184822	76
HP4	21.11817169	127
HP3	21.19030762	83
HP2	20.84682846	91
HP1	20.82767296	91

	LST13DEC24	*Distance WD (9am-270, 12pm-270)*
LST13DEC24	1	
Distance WD (9am-270, 12pm-270)	0.78	1

Name	LST14JAN25	Distance WD (12pm-0)
UCILogger7_BPP	21.49466515	175
UCILogger6_Ledge	21.90737534	0
UCILogger8	21.45809364	121
UCILogger7	21.29961586	633
UCILogger6	21.1517086	542
UCILogger4	20.97349548	448
UCILogger3	22.10553932	218
UCILogger2	21.55820274	0
UCILogger1	19.44239044	0
HP44	21.7869873	156
HP43	22.1163559	215
HP42	21.70196533	344
HP41	21.13199615	492
HP40	21.31366158	639
HP39	21.54538727	686
HP38	22.02885628	777
HP37	22.40271568	779
HP36	22.04606438	844
HP35	22.0500946	877
HP34	22.34000015	824
HP33	21.47486496	431
HP32	21.24405479	333
HP31	20.91884041	277
HP30	21.45860291	361
HP29	20.28230858	134
HP28	20.85175133	208
HP27	21.07244301	261
HP26	21.12755203	281
HP25	22.07287216	467
HP24	21.83557129	674
HP23	21.72295189	690
HP22	21.46675301	670
HP21	20.92414856	88
HP20	21.08358383	126
HP19	21.15678597	190
HP18	21.23991776	134
HP17	20.93435287	75
HP16	21.492239	640
HP15	21.39118195	561
HP14	21.22564507	597
HP13	21.06907463	502
HP12	21.34064865	442
HP11	21.0458355	491
HP10	21.0670433	457
HP9	20.77516365	331
HP8	20.70344925	254
HP7	21.35359764	345
HP6	20.90496254	349
HP5	21.09776115	273
HP4	21.45303917	200
HP3	21.47636986	146
HP2	21.51189613	100
HP1	21.59087753	32

	LST14JAN25	*Distance WD (12pm-0)*
LST14JAN25	1	
Distance WD (12pm-0)	0.44	1

Name	LST14NOV25	Distance WD (12pm-270)
UCILogger7_BPP	23.22732925	103
UCILogger6_Ledge	23.28960419	0
UCILogger8	23.03052902	92
UCILogger7	23.11923599	316
UCILogger6	22.93547249	242
UCILogger4	22.55843353	109
UCILogger3	23.43976021	217
UCILogger2	23.0160408	0
UCILogger1	21.68705177	0
HP44	23.2540493	174
HP43	23.37767029	205
HP42	23.08154297	197
HP41	22.74255371	295
HP40	22.96858788	427
HP39	23.1223278	450
HP38	23.42792892	482
HP37	23.78170967	389
HP36	23.61406899	485
HP35	23.65307236	399
HP34	23.65745735	297
HP33	23.00034523	202
HP32	22.98601723	121
HP31	22.590271	100
HP30	22.81768799	192
HP29	22.34248924	41
HP28	22.55102921	97
HP27	22.69230652	173
HP26	22.69972229	187
HP25	23.42913246	296
HP24	23.13489342	291
HP23	23.30532265	376
HP22	22.94505501	272
HP21	22.56883621	49
HP20	22.79003525	91
HP19	22.71879578	154
HP18	22.76464081	126
HP17	22.59175873	74
HP16	23.1438942	370
HP15	22.97109413	258
HP14	23.1081028	278
HP13	22.78711891	187
HP12	22.758564	166
HP11	22.76490784	249
HP10	22.69818878	146
HP9	22.59370613	63
HP8	22.70471573	42
HP7	22.97600555	145
HP6	22.7978363	90
HP5	22.87504578	76
HP4	22.94185448	127
HP3	22.83265495	83
HP2	23.19713783	91
HP1	23.12840843	91

	LST14NOV25	*Distance WD (12pm-270)*
LST14NOV25	1	
Distance WD (12pm-270)	0.61	1

Name	**LST15SEPT25**	**Distance WD (12pm-210)**
UCILogger7_BPP	26.06269646	175
UCILogger6_Ledge	26.04868698	0
UCILogger8	25.67826653	121
UCILogger7	26.06468391	633
UCILogger6	25.94261551	542
UCILogger4	25.66576958	448
UCILogger3	26.14492798	218
UCILogger2	25.85544014	0
UCILogger1	24.7744503	0
HP44	26.20664024	156
HP43	26.18918991	215
HP42	26.23283958	344
HP41	25.97000504	492
HP40	26.25380898	639
HP39	26.24875641	686
HP38	26.29050446	777
HP37	26.4523983	779
HP36	26.67171288	844
HP35	26.47999763	877
HP34	26.55895996	824
HP33	26.08937263	431
HP32	25.96933556	333
HP31	25.81488991	277
HP30	26.04143524	361
HP29	25.25344658	134
HP28	25.50073433	208
HP27	25.79215431	261
HP26	25.74792862	281
HP25	26.42631149	467
HP24	26.13761711	674
HP23	26.17854881	690
HP22	25.82258987	670
HP21	25.60242844	88
HP20	25.82529449	126
HP19	25.86455727	190
HP18	25.93040657	134
HP17	25.82859802	75
HP16	26.15225792	640
HP15	25.85001755	561
HP14	25.9732666	597
HP13	25.86625099	502
HP12	25.80669022	442
HP11	25.99902916	491
HP10	25.80174255	457
HP9	25.58578682	331
HP8	25.27457428	254
HP7	26.03689957	345
HP6	25.61285973	349
HP5	25.5133152	273
HP4	25.44864082	200
HP3	25.45622635	146
HP2	25.91085625	100
HP1	25.87038612	32

	LST15SEPT25	*Distance WD (12pm-210)*
LST15SEPT25	1	
Distance WD (12pm-210)	0.62	1

Name	LST14FEB26	Distance WD (12pm-50)
UCILogger7_BPP	23.38903618	175
UCILogger6_Ledge	23.15207481	0
UCILogger8	22.80521774	121
UCILogger7	23.12043762	633
UCILogger6	22.84405899	542
UCILogger4	22.67425156	448
UCILogger3	23.44403458	218
UCILogger2	22.91437912	0
UCILogger1	20.63393021	0
HP44	23.24328613	156
HP43	23.40651131	215
HP42	23.20483971	344
HP41	23.02166557	492
HP40	23.15850067	639
HP39	23.46854401	686
HP38	23.82757759	777
HP37	24.29417992	779
HP36	24.01568985	844
HP35	23.89422989	877
HP34	23.97485542	824
HP33	23.04163933	431
HP32	23.05189133	333
HP31	22.83713913	277
HP30	23.04876518	361
HP29	22.26615143	134
HP28	22.59585381	208
HP27	22.63333511	261
HP26	22.85276985	281
HP25	23.82745171	467
HP24	23.44503784	674
HP23	23.59150124	690
HP22	23.05888557	670
HP21	22.38687515	88
HP20	22.59596443	126
HP19	22.59942055	190
HP18	22.71290588	134
HP17	22.53177261	75
HP16	23.39238358	640
HP15	23.05643272	561
HP14	23.00768089	597
HP13	22.77872086	502
HP12	22.78923416	442
HP11	22.85696602	491
HP10	22.74389839	457
HP9	22.5098381	331
HP8	22.35346794	254
HP7	23.00957108	345
HP6	22.61042976	349
HP5	22.73989677	273
HP4	22.941185	200
HP3	22.84540939	146
HP2	22.93061829	100
HP1	22.95107651	32

	LST14FEB26	*Distance WD (12pm-50)*
LST14FEB26	1	
Distance WD (12pm-50)	0.64	1

Name	LST15OCT27	Distance WD (12pm-0)
UCILogger7_BPP	27.32489204	175
UCILogger6_Ledge	27.01925087	0
UCILogger8	27.05891418	121
UCILogger7	27.22872162	633
UCILogger6	27.00713348	542
UCILogger4	26.65093613	448
UCILogger3	27.89116287	218
UCILogger2	26.97361374	0
UCILogger1	25.30589294	0
HP44	27.61241913	156
HP43	27.77291298	215
HP42	27.34220123	344
HP41	26.86693001	492
HP40	27.15732574	639
HP39	27.24657822	686
HP38	27.56876373	777
HP37	28.06633377	779
HP36	28.17333412	844
HP35	28.32903481	877
HP34	28.06925964	824
HP33	27.57361603	431
HP32	27.06820488	333
HP31	26.8353672	277
HP30	27.19085312	361
HP29	26.33025742	134
HP28	26.77922821	208
HP27	26.7234726	261
HP26	26.92598343	281
HP25	27.75618935	467
HP24	27.52977943	674
HP23	27.50702667	690
HP22	27.0968399	670
HP21	26.6374855	88
HP20	26.78946877	126
HP19	26.80549812	190
HP18	26.9247303	134
HP17	26.66233635	75
HP16	27.33636856	640
HP15	27.0779705	561
HP14	27.17359161	597
HP13	26.85646248	502
HP12	26.87939072	442
HP11	26.8380127	491
HP10	26.74784279	457
HP9	26.53923988	331
HP8	26.57835388	254
HP7	27.28279495	345
HP6	26.83999634	349
HP5	26.93173409	273
HP4	26.74633217	200
HP3	26.49097252	146
HP2	27.41436386	100
HP1	27.09051323	32

	LST15OCT27	*Distance WD (12pm-0)*
LST15OCT27	1	
Distance WD (12pm-0)	0.58	1

Name	LST15JAN28	Distance WD (12pm-0)
UCILogger7_BPP	21.16945648	175
UCILogger6_Ledge	21.01707268	0
UCILogger8	20.84356499	121
UCILogger7	20.89387894	633
UCILogger6	20.76651192	542
UCILogger4	20.40363884	448
UCILogger3	21.36205292	218
UCILogger2	21.01212883	0
UCILogger1	19.16513824	0
HP44	21.27124596	156
HP43	21.39034271	215
HP42	21.08154106	344
HP41	20.42520905	492
HP40	20.96952057	639
HP39	21.14836502	686
HP38	21.52693558	777
HP37	22.06480408	779
HP36	21.49258804	844
HP35	21.11684418	877
HP34	21.61092949	824
HP33	20.54746628	431
HP32	20.63926125	333
HP31	20.34357834	277
HP30	20.51543236	361
HP29	19.81254959	134
HP28	20.0783596	208
HP27	20.48817635	261
HP26	20.42707825	281
HP25	21.56497955	467
HP24	21.34069824	674
HP23	21.16057777	690
HP22	20.75184441	670
HP21	19.96879959	88
HP20	20.40994835	126
HP19	20.55646896	190
HP18	20.57364845	134
HP17	20.41183853	75
HP16	21.00003624	640
HP15	20.7564888	561
HP14	20.87418175	597
HP13	20.65613747	502
HP12	20.76735687	442
HP11	20.51714897	491
HP10	20.58631516	457
HP9	20.28721237	331
HP8	19.94091415	254
HP7	20.7554512	345
HP6	20.25925064	349
HP5	20.29967117	273
HP4	20.54027939	200
HP3	20.79812431	146
HP2	20.8301487	100
HP1	20.92370605	32

	LST15JAN28	*Distance WD (12pm-0)*
LST15JAN28	1	
Distance WD (12pm-0)	0.51	1

Name	LST15NOV28	Distance WD (12pm-0)
UCILogger7_BPP	21.17711449	175
UCILogger6_Ledge	21.19530106	0
UCILogger8	20.80040169	121
UCILogger7	21.1532917	633
UCILogger6	20.8741951	542
UCILogger4	20.62255096	448
UCILogger3	21.49179459	218
UCILogger2	20.88084984	0
UCILogger1	20.34848213	0
HP44	21.15449142	156
HP43	21.32202911	215
HP42	20.99163055	344
HP41	20.76774788	492
HP40	21.13900757	639
HP39	21.25928879	686
HP38	21.34944916	777
HP37	21.90465164	779
HP36	21.69314194	844
HP35	21.8101387	877
HP34	21.85848999	824
HP33	21.50634575	431
HP32	21.22705841	333
HP31	21.00233459	277
HP30	21.24003601	361
HP29	20.81513405	134
HP28	20.8650856	208
HP27	20.84766197	261
HP26	21.02795601	281
HP25	21.78006554	467
HP24	21.5635643	674
HP23	21.41204643	690
HP22	21.12428665	670
HP21	20.92835045	88
HP20	20.88097	126
HP19	20.86179543	190
HP18	20.85398102	134
HP17	20.75234222	75
HP16	21.29238129	640
HP15	21.06319809	561
HP14	21.07945633	597
HP13	20.74056625	502
HP12	20.71482277	442
HP11	20.76840591	491
HP10	20.67447472	457
HP9	20.54433632	331
HP8	20.55283546	254
HP7	20.96923637	345
HP6	20.74905014	349
HP5	20.89129257	273
HP4	20.8700943	200
HP3	20.75808525	146
HP2	20.91423035	100
HP1	20.91909599	32

	LST15NOV28	*Distance WD (12pm-0)*
LST15NOV28	1	
Distance WD (12pm-0)	0.59	1

Name	LST15DEC30	Distance WD (12pm-0)
UCILogger7_BPP	19.42455482	175
UCILogger6_Ledge	19.28300285	0
UCILogger8	19.26221085	121
UCILogger7	19.41624641	633
UCILogger6	19.19215393	542
UCILogger4	19.11730003	448
UCILogger3	19.60018349	218
UCILogger2	19.24983597	0
UCILogger1	17.90820503	0
HP44	19.60253716	156
HP43	19.56262589	215
HP42	19.45670891	344
HP41	19.01222801	492
HP40	19.1938324	639
HP39	19.3120842	686
HP38	19.55950928	777
HP37	19.91077423	779
HP36	19.7922821	844
HP35	19.79182625	877
HP34	19.75739479	824
HP33	19.43153572	431
HP32	19.20160294	333
HP31	18.99643326	277
HP30	19.19616699	361
HP29	19.02893829	134
HP28	18.99755478	208
HP27	19.13591576	261
HP26	19.14553642	281
HP25	19.72252083	467
HP24	19.57087135	674
HP23	19.4692173	690
HP22	19.35463142	670
HP21	18.97175789	88
HP20	19.16286087	126
HP19	19.16620445	190
HP18	19.13850975	134
HP17	19.05377197	75
HP16	19.33700562	640
HP15	19.31666565	561
HP14	19.34790993	597
HP13	19.12319756	502
HP12	19.15447807	442
HP11	18.99761581	491
HP10	19.08905029	457
HP9	19.08891296	331
HP8	19.03136444	254
HP7	19.26349068	345
HP6	19.12524414	349
HP5	19.17915726	273
HP4	19.18423843	200
HP3	19.13722038	146
HP2	19.41876984	100
HP1	19.39881134	32

	LST15DEC30	*Distance WD (12pm-0)*
LST15DEC30	1	
Distance WD (12pm-0)	0.51	1

Name	LST14MAR30	Distance WD (12pm-250)
UCILogger7_BPP	33.99338531	103
UCILogger6_Ledge	32.7760582	0
UCILogger8	33.84411621	92
UCILogger7	34.48681641	316
UCILogger6	34.09265137	242
UCILogger4	33.61750412	109
UCILogger3	34.74507523	217
UCILogger2	33.26016235	0
UCILogger1	28.82238388	0
HP44	34.41184616	174
HP43	34.7117424	205
HP42	34.52597809	197
HP41	33.88198853	295
HP40	34.36735916	427
HP39	34.61366272	450
HP38	35.11930847	482
HP37	36.16002655	389
HP36	35.34640121	485
HP35	35.26332855	399
HP34	35.80652618	297
HP33	34.09277344	202
HP32	33.80453873	121
HP31	33.55791473	100
HP30	34.19335938	192
HP29	32.54400635	41
HP28	33.37517166	97
HP27	33.81441116	173
HP26	34.10700607	187
HP25	35.82312393	296
HP24	35.26276398	291
HP23	34.97893524	376
HP22	34.62430954	272
HP21	33.24638367	49
HP20	33.66254807	91
HP19	33.87744141	154
HP18	33.74160385	126
HP17	33.00733566	74
HP16	34.69761658	370
HP15	34.53031921	258
HP14	34.30764771	278
HP13	33.90799713	187
HP12	33.96429443	166
HP11	33.70808792	249
HP10	33.78313828	146
HP9	33.2112236	63
HP8	32.84631729	42
HP7	34.36439514	145
HP6	33.42469788	90
HP5	33.61641312	76
HP4	34.10564041	127
HP3	33.9604454	83
HP2	33.72693634	91
HP1	33.18045044	91

	LST14MAR30	*Distance WD (12pm-250)*
LST14MAR30	1	
Distance WD (12pm-250)	0.72	1

Name	LST16NOV30	Distance WD (12pm-0)
UCILogger7_BPP	23.63318253	175
UCILogger6_Ledge	23.69040298	0
UCILogger8	23.43926048	121
UCILogger7	23.47665596	633
UCILogger6	23.24538612	542
UCILogger4	23.05434227	448
UCILogger3	23.8248806	218
UCILogger2	23.3180294	0
UCILogger1	22.13399696	0
HP44	23.50309372	156
HP43	23.69398499	215
HP42	23.65930176	344
HP41	23.12071228	492
HP40	23.34708405	639
HP39	23.4292469	686
HP38	23.67424202	777
HP37	24.13190079	779
HP36	24.13282013	844
HP35	24.21331406	877
HP34	24.13865471	824
HP33	23.77714729	431
HP32	23.37059784	333
HP31	23.09701347	277
HP30	23.39222908	361
HP29	22.84087563	134
HP28	23.14076614	208
HP27	23.10626411	261
HP26	23.1935997	281
HP25	24.04987907	467
HP24	23.81186295	674
HP23	23.67629242	690
HP22	23.52745056	670
HP21	23.15006828	88
HP20	23.23537636	126
HP19	23.21476364	190
HP18	23.39316559	134
HP17	23.22538757	75
HP16	23.55216599	640
HP15	23.49404716	561
HP14	23.3857975	597
HP13	23.17073441	502
HP12	23.2088604	442
HP11	23.10440254	491
HP10	23.10401344	457
HP9	23.12528801	331
HP8	23.21068954	254
HP7	23.54395294	345
HP6	23.30480957	349
HP5	23.38845444	273
HP4	23.34255219	200
HP3	23.23418999	146
HP2	23.4000206	100
HP1	23.328125	32

	LST16NOV30	*Distance WD (12pm-0)*
LST16NOV30	1	
Distance WD (12pm-360)	0.54	1

Name	LST16MAR3	Distance WD (12pm-290)
UCILogger7_BPP	25.28881645	103
UCILogger6_Ledge	25.09617615	0
UCILogger8	25.17972183	92
UCILogger7	25.5265522	316
UCILogger6	25.22647476	242
UCILogger4	24.99818802	109
UCILogger3	25.76316834	217
UCILogger2	24.95301628	0
UCILogger1	23.77632904	0
HP44	25.57648659	174
HP43	25.6962738	205
HP42	25.56160545	197
HP41	25.12624741	295
HP40	25.4224968	427
HP39	25.72982407	450
HP38	26.12590599	482
HP37	26.50536919	389
HP36	26.29140282	485
HP35	26.37527657	399
HP34	26.11663437	297
HP33	25.60143089	202
HP32	25.42423439	121
HP31	25.17447662	100
HP30	25.38278198	192
HP29	24.91356468	41
HP28	25.03911972	97
HP27	25.15198517	173
HP26	25.26900101	187
HP25	25.97395325	296
HP24	25.60739517	291
HP23	25.82971191	376
HP22	25.36832237	272
HP21	24.83077049	49
HP20	25.11407089	91
HP19	25.0660305	154
HP18	24.97472572	126
HP17	24.78189278	74
HP16	25.63216782	370
HP15	25.35858727	258
HP14	25.44265747	278
HP13	25.10823822	187
HP12	25.02998543	166
HP11	25.12273979	249
HP10	25.04369164	146
HP9	24.90055084	63
HP8	24.79742241	42
HP7	25.43016243	145
HP6	25.05229568	90
HP5	25.102314	76
HP4	25.14946747	127
HP3	25.09781647	83
HP2	25.33371925	91
HP1	24.94029045	91

	LST16MAR3	*Distance WD (12pm-290)*
LST16MAR3	1	
Distance WD (12pm-290)	0.79	1

Name	LST15MAY4	Distance WD (12pm-130)
UCILogger7_BPP	29.04849434	175
UCILogger6_Ledge	28.29521942	0
UCILogger8	28.35543442	121
UCILogger7	28.79200554	633
UCILogger6	28.67600632	542
UCILogger4	28.43808365	448
UCILogger3	29.24754524	218
UCILogger2	28.08401108	0
UCILogger1	26.67748833	0
HP44	29.06051445	156
HP43	29.1142025	215
HP42	29.20979309	344
HP41	28.78223419	492
HP40	28.94613838	639
HP39	28.98505211	686
HP38	29.23022461	777
HP37	29.45655251	779
HP36	29.663517	844
HP35	29.37565041	877
HP34	29.3689785	824
HP33	29.03306961	431
HP32	29.00050163	333
HP31	28.60785866	277
HP30	28.74896812	361
HP29	27.76655579	134
HP28	28.17707253	208
HP27	28.5624485	261
HP26	28.57616806	281
HP25	29.18716621	467
HP24	29.09330559	674
HP23	28.92006302	690
HP22	28.74577904	670
HP21	27.8939476	88
HP20	28.42313576	126
HP19	28.60237312	190
HP18	28.44766998	134
HP17	28.05592155	75
HP16	28.8535614	640
HP15	28.71004677	561
HP14	28.7906456	597
HP13	28.55931282	502
HP12	28.5243969	442
HP11	28.6611042	491
HP10	28.51028442	457
HP9	28.33509445	331
HP8	28.13102341	254
HP7	28.94100571	345
HP6	28.45793533	349
HP5	28.34266853	273
HP4	28.09895897	200
HP3	28.01004982	146
HP2	28.82140541	100
HP1	28.24211884	32

	LST15MAY4	*Distance WD (12pm-130)*
LST15MAY4	1	
Distance WD (12pm-130)	0.67	1

Name	LST13NOV6	Distance WD (9am-0, 12pm-50)
UCILogger7_BPP	26.67201233	175
UCILogger6_Ledge	26.17141342	0
UCILogger8	25.93484116	121
UCILogger7	25.95052528	633
UCILogger6	25.83473778	542
UCILogger4	25.60040665	448
UCILogger3	26.38063622	218
UCILogger2	25.94286919	0
UCILogger1	25.15662766	0
HP44	25.89102554	156
HP43	26.61367035	215
HP42	26.46184921	344
HP41	26.04480934	492
HP40	26.14921951	639
HP39	26.26958466	686
HP38	27.07745552	777
HP37	27.0282917	779
HP36	27.14072418	844
HP35	27.01286888	877
HP34	26.72686958	824
HP33	26.25460625	431
HP32	25.94471931	333
HP31	25.40377998	277
HP30	25.7065239	361
HP29	25.13117027	134
HP28	25.326437	208
HP27	25.38538933	261
HP26	25.42951393	281
HP25	26.21204758	467
HP24	26.09692574	674
HP23	26.46566772	690
HP22	26.02592087	670
HP21	25.43236542	88
HP20	25.4352684	126
HP19	25.51422882	190
HP18	25.61478424	134
HP17	25.52272034	75
HP16	26.09393883	640
HP15	26.00540161	561
HP14	25.91767311	597
HP13	25.72919655	502
HP12	25.82447052	442
HP11	25.82273483	491
HP10	25.66433144	457
HP9	25.53342819	331
HP8	25.42944336	254
HP7	26.22228622	345
HP6	25.72438622	349
HP5	25.63288689	273
HP4	25.45620728	200
HP3	25.28273201	146
HP2	25.93484116	100
HP1	26.30605316	32

	LST15JAN28	*Distance WD (9am-0, 12pm-50)*
LST15JAN28	1	
Distance WD (9am-0, 12pm-50)	0.601089032	1

Name	LST14FEB10	Distance WD (12pm-50)
HP_UW50	21.560215	230
HP_UW49	21.08701324	473
HP_UW48	21.30892944	338
HP_UW47	20.90348816	310
HP_UW46	21.30145454	281
HP_UW45	21.37646484	427
HP_UW44	21.40200424	456
HP_UW43	21.54867935	520
HP_UW42	21.13157463	347
HP_UW41	20.55293274	189
HP_UW40	20.27675629	114
HP_UW39	19.75155449	53
HP_UW38	20.63752365	221
HP_UW37	22.37640381	209
HP_UW36	20.73784637	595
HP_UW35	21.40611076	516
HP_UW34	21.16398621	455
HP_UW33	20.9272995	364
HP_UW32	21.40858078	554
HP_UW31	21.49405289	381
HP_UW30	20.86114311	252
HP_UW29	20.40727615	153
HP_UW28	19.6024189	40
HP_UW27	21.34845734	257
HP_UW26	20.92603302	179
HP_UW25	20.88078308	116
HP_UW24	20.06185722	30
HP_UW23	21.56773186	184
HP_UW22	21.28560066	516
HP_UW21	21.02701569	450
HP_UW20	21.61410332	345
HP_UW19	22.04118156	227
HP_UW18	20.16909027	27
HP_UW17	21.41192245	115
HP_UW16	20.58666611	28
HP_UW15	21.56590652	121
HP_UW14	21.82072639	167
HP_UW13	21.83697319	155
HP_UW12	21.41562653	128
HP_UW11	21.25909615	107
HP_UW10	20.5628109	32
HP_UW9	21.76467323	95
HP_UW8	20.88552666	26
HP_UW7	20.95277214	27
HP_UW6	22.01826668	122
HP_UW5	21.34529877	64
HP_UW4	21.97210121	143
HP_UW3	21.91047668	150
HP_UW2	20.5830307	33
HP_UW1	20.6081543	34

	LST14FEB10	*Distance WD (12pm-50)*
LST14FEB10	1	
Distance WD (12pm-50)	0.29	1

Name	LST13APR12	Distance WD (12pm-180)
HP_UW50	30.5234375	230
HP_UW49	30.35430717	473
HP_UW48	30.4441452	338
HP_UW47	30.40014648	310
HP_UW46	30.30260658	281
HP_UW45	30.20253754	427
HP_UW44	30.52522469	456
HP_UW43	30.29545593	520
HP_UW42	29.95039177	347
HP_UW41	29.67269707	189
HP_UW40	29.91170692	114
HP_UW39	29.68024063	53
HP_UW38	29.91683197	221
HP_UW37	30.52573013	209
HP_UW36	30.49089813	595
HP_UW35	30.67596436	516
HP_UW34	30.62539864	455
HP_UW33	30.44368172	364
HP_UW32	30.66832161	554
HP_UW31	30.33048439	381
HP_UW30	30.03769112	252
HP_UW29	30.21306419	153
HP_UW28	29.65826607	40
HP_UW27	30.38701439	257
HP_UW26	30.29842758	179
HP_UW25	30.34285164	116
HP_UW24	29.56113434	30
HP_UW23	30.44835091	184
HP_UW22	29.96423912	516
HP_UW21	30.40815926	450
HP_UW20	30.5592804	345
HP_UW19	30.62620735	227
HP_UW18	29.47291183	27
HP_UW17	30.37901688	115
HP_UW16	30.04814148	28
HP_UW15	30.49747658	121
HP_UW14	30.5206871	167
HP_UW13	30.35235786	155
HP_UW12	30.4540863	128
HP_UW11	30.29405403	107
HP_UW10	29.83460236	32
HP_UW9	30.15557289	95
HP_UW8	29.41970825	26
HP_UW7	29.64756966	27
HP_UW6	30.29867935	122
HP_UW5	30.09592628	64
HP_UW4	30.29872704	143
HP_UW3	30.30464554	150
HP_UW2	29.57120895	33
HP_UW1	30.05172348	34

	LST13APR12	*Distance WD (12pm-180)*
LST13APR12	1	
Distance WD (12pm-180)	0.57	1

Name	LST15NOV12	Distance WD (12pm-0)
HP_UW50	27.81661034	230
HP_UW49	27.51746559	473
HP_UW48	27.77463722	338
HP_UW47	27.81694603	310
HP_UW46	27.58391571	281
HP_UW45	27.33657074	427
HP_UW44	27.41083145	456
HP_UW43	27.58077049	520
HP_UW42	27.01295662	347
HP_UW41	26.6827507	189
HP_UW40	26.83410645	114
HP_UW39	26.40926933	53
HP_UW38	27.03457451	221
HP_UW37	28.22821236	209
HP_UW36	27.73148918	595
HP_UW35	27.50029945	516
HP_UW34	27.90869141	455
HP_UW33	27.9528656	364
HP_UW32	27.84020805	554
HP_UW31	27.5467701	381
HP_UW30	27.22641373	252
HP_UW29	27.37789536	153
HP_UW28	26.31409645	40
HP_UW27	27.75619125	257
HP_UW26	27.62351608	179
HP_UW25	27.57030296	116
HP_UW24	26.60501099	30
HP_UW23	27.82586861	184
HP_UW22	27.35560417	516
HP_UW21	27.55815887	450
HP_UW20	28.16889572	345
HP_UW19	28.06022453	227
HP_UW18	26.29561424	27
HP_UW17	27.82856941	115
HP_UW16	26.63482857	28
HP_UW15	27.71316338	121
HP_UW14	27.85223579	167
HP_UW13	27.83293533	155
HP_UW12	27.47317314	128
HP_UW11	27.17095184	107
HP_UW10	26.38665962	32
HP_UW9	27.12378693	95
HP_UW8	26.39157867	26
HP_UW7	26.37793732	27
HP_UW6	27.44576836	122
HP_UW5	26.65861321	64
HP_UW4	27.72286415	143
HP_UW3	27.79644585	150
HP_UW2	26.25109673	33
HP_UW1	26.1570549	34

	LST15NOV12	*Distance WD (12pm-0)*
LST15NOV12	1	
Distance WD (12pm-0)	0.57	1

Name	LST15FEB13	Distance WD (12pm-270)
HP_UW50	20.91737556	444
HP_UW49	20.69038963	595
HP_UW48	20.96579742	404
HP_UW47	21.07767868	432
HP_UW46	20.9849453	349
HP_UW45	20.36721992	354
HP_UW44	20.58738709	392
HP_UW43	20.62434578	382
HP_UW42	20.19952011	324
HP_UW41	20.20246696	198
HP_UW40	20.3913517	139
HP_UW39	19.77941513	69
HP_UW38	20.51505661	252
HP_UW37	21.47016907	602
HP_UW36	20.70531273	559
HP_UW35	20.74963379	492
HP_UW34	20.91801643	525
HP_UW33	21.03312874	476
HP_UW32	20.95731926	430
HP_UW31	20.51000404	368
HP_UW30	20.6848793	290
HP_UW29	20.81717491	191
HP_UW28	19.74069214	57
HP_UW27	21.05225182	389
HP_UW26	21.2432785	257
HP_UW25	21.15932274	180
HP_UW24	19.91627121	47
HP_UW23	21.21949196	327
HP_UW22	20.5620327	679
HP_UW21	20.7744503	631
HP_UW20	21.33719254	570
HP_UW19	21.1560154	508
HP_UW18	19.78696251	82
HP_UW17	21.18522644	212
HP_UW16	20.21693802	232
HP_UW15	20.86137199	326
HP_UW14	20.98034668	442
HP_UW13	21.05745888	502
HP_UW12	20.74873543	392
HP_UW11	20.61820602	430
HP_UW10	20.02379799	323
HP_UW9	20.15722466	732
HP_UW8	19.251194	623
HP_UW7	19.62974739	549
HP_UW6	20.80700111	670
HP_UW5	20.07138443	613
HP_UW4	21.02523994	569
HP_UW3	21.04501343	534
HP_UW2	19.77114677	390
HP_UW1	19.61315346	428

	LST15FEB13	*Distance WD (12pm-270)*
LST15FEB13	1	
Distance WD (12pm-270)	0.22	1

Name	LST14MAR14	Distance WD (12pm-360)
HP_UW50	29.12005615	230
HP_UW49	28.62580681	473
HP_UW48	28.69167328	338
HP_UW47	28.85860825	310
HP_UW46	28.69526863	281
HP_UW45	28.24146843	427
HP_UW44	28.29532814	456
HP_UW43	28.42389679	520
HP_UW42	27.99497604	347
HP_UW41	27.91999054	189
HP_UW40	28.04402542	114
HP_UW39	26.95621872	53
HP_UW38	28.30172539	221
HP_UW37	29.48025322	209
HP_UW36	28.71255493	595
HP_UW35	28.5237999	516
HP_UW34	29.07255554	455
HP_UW33	29.01301765	364
HP_UW32	28.94301987	554
HP_UW31	28.34850502	381
HP_UW30	28.47288322	252
HP_UW29	28.67195511	153
HP_UW28	26.77088356	40
HP_UW27	28.98357773	257
HP_UW26	28.88277054	179
HP_UW25	28.89640236	116
HP_UW24	27.02073288	30
HP_UW23	29.11816216	184
HP_UW22	28.30139732	516
HP_UW21	28.71894455	450
HP_UW20	29.43656158	345
HP_UW19	29.39007568	227
HP_UW18	26.70230865	27
HP_UW17	29.11358643	115
HP_UW16	27.09404564	28
HP_UW15	28.94576645	121
HP_UW14	29.15843391	167
HP_UW13	28.94929886	155
HP_UW12	28.67026901	128
HP_UW11	28.05352592	107
HP_UW10	26.87128448	32
HP_UW9	28.04616737	95
HP_UW8	26.73916054	26
HP_UW7	27.03547478	27
HP_UW6	28.57233047	122
HP_UW5	27.64584732	64
HP_UW4	28.7224617	143
HP_UW3	28.80782509	150
HP_UW2	26.53564453	33
HP_UW1	26.38143158	34

	LST14MAR14	*Distance WD (12pm-360)*
LST14MAR14	1	
Distance WD (12pm-360)	0.52	1

Name	LST16NOV14	Distance WD (12pm-360)
HP_UW50	26.6008625	230
HP_UW49	26.10102654	473
HP_UW48	26.81863594	338
HP_UW47	26.6565361	310
HP_UW46	26.23962402	281
HP_UW45	25.83028984	427
HP_UW44	26.01461983	456
HP_UW43	26.13633728	520
HP_UW42	25.91032028	347
HP_UW41	25.34496498	189
HP_UW40	25.01429939	114
HP_UW39	24.7970829	53
HP_UW38	25.61348534	221
HP_UW37	27.11166954	209
HP_UW36	26.21030808	595
HP_UW35	26.21969032	516
HP_UW34	26.30341721	455
HP_UW33	26.84522247	364
HP_UW32	26.28533745	554
HP_UW31	26.10458565	381
HP_UW30	25.75245857	252
HP_UW29	25.52051353	153
HP_UW28	24.97732353	40
HP_UW27	26.43343163	257
HP_UW26	25.93763351	179
HP_UW25	26.06348228	116
HP_UW24	25.03639412	30
HP_UW23	26.53822899	184
HP_UW22	25.97561455	516
HP_UW21	26.12195778	450
HP_UW20	26.826231	345
HP_UW19	26.86743927	227
HP_UW18	24.86363411	27
HP_UW17	26.22201538	115
HP_UW16	25.28203774	28
HP_UW15	26.41646767	121
HP_UW14	26.54900932	167
HP_UW13	26.8983345	155
HP_UW12	26.40809059	128
HP_UW11	26.25944519	107
HP_UW10	24.8492794	32
HP_UW9	25.80027199	95
HP_UW8	24.96345329	26
HP_UW7	24.47452736	27
HP_UW6	26.13055992	122
HP_UW5	25.47760773	64
HP_UW4	26.67827606	143
HP_UW3	26.83229637	150
HP_UW2	25.13944817	33
HP_UW1	24.94248581	34

	LST16NOV14	*Distance WD (12pm-360)*
LST16NOV14	1	
Distance WD (12pm-360)	0.48	1

Name	LST16JAN15	Distance WD (12pm-0)
HP_UW50	19.77915955	230
HP_UW49	19.76191139	473
HP_UW48	19.77037621	338
HP_UW47	19.73586082	310
HP_UW46	19.59053421	281
HP_UW45	19.29536247	427
HP_UW44	19.49855042	456
HP_UW43	19.53100777	520
HP_UW42	19.2497406	347
HP_UW41	19.11880684	189
HP_UW40	19.07179451	114
HP_UW39	18.78491783	53
HP_UW38	19.33901787	221
HP_UW37	19.96790123	209
HP_UW36	19.73476219	595
HP_UW35	19.59607315	516
HP_UW34	19.70921707	455
HP_UW33	19.87605667	364
HP_UW32	19.57377052	554
HP_UW31	19.61392975	381
HP_UW30	19.4424839	252
HP_UW29	19.37991714	153
HP_UW28	18.89831924	40
HP_UW27	19.67506027	257
HP_UW26	19.74794197	179
HP_UW25	19.66954994	116
HP_UW24	18.94604492	30
HP_UW23	19.81000328	184
HP_UW22	19.55827332	516
HP_UW21	19.78962898	450
HP_UW20	20.0710144	345
HP_UW19	19.90806961	227
HP_UW18	18.93990135	27
HP_UW17	19.74541473	115
HP_UW16	18.89783096	28
HP_UW15	19.62612915	121
HP_UW14	19.70318413	167
HP_UW13	19.695961	155
HP_UW12	19.55887032	128
HP_UW11	19.47732162	107
HP_UW10	18.9663372	32
HP_UW9	19.30698586	95
HP_UW8	18.86569977	26
HP_UW7	18.89190865	27
HP_UW6	19.49083138	122
HP_UW5	19.13602638	64
HP_UW4	19.70633698	143
HP_UW3	19.7066021	150
HP_UW2	18.89554214	33
HP_UW1	18.81199455	34

	LST16JAN15	*Distance WD (12pm-0)*
LST16JAN15	1	
Distance WD (12pm-0)	0.57	1

Name	LST13JUN15	Distance WD (12pm-90)
HP_UW50	24.50431252	444
HP_UW49	24.27438736	595
HP_UW48	24.28182411	404
HP_UW47	24.32299995	432
HP_UW46	24.18887138	349
HP_UW45	23.97188377	354
HP_UW44	24.19052124	392
HP_UW43	24.27911949	382
HP_UW42	23.92583466	324
HP_UW41	23.57961845	198
HP_UW40	23.54046631	139
HP_UW39	23.21581268	69
HP_UW38	23.86239433	252
HP_UW37	24.73604012	602
HP_UW36	24.53941536	559
HP_UW35	24.6397686	492
HP_UW34	24.48365021	525
HP_UW33	24.51708603	476
HP_UW32	24.52363777	430
HP_UW31	24.19261742	368
HP_UW30	23.96925735	290
HP_UW29	23.6750145	191
HP_UW28	22.63206863	57
HP_UW27	24.25197983	389
HP_UW26	23.97408295	257
HP_UW25	23.86550713	180
HP_UW24	22.77412224	47
HP_UW23	24.48772049	327
HP_UW22	23.93221855	679
HP_UW21	24.33058739	631
HP_UW20	24.63251305	570
HP_UW19	24.72264862	508
HP_UW18	23.07849693	82
HP_UW17	24.27685547	212
HP_UW16	23.72294235	232
HP_UW15	24.59144211	326
HP_UW14	24.64752579	442
HP_UW13	24.60464096	502
HP_UW12	24.53403664	392
HP_UW11	24.45255089	430
HP_UW10	22.9666996	323
HP_UW9	24.12062836	732
HP_UW8	22.92551231	623
HP_UW7	23.05950356	549
HP_UW6	24.51874542	670
HP_UW5	23.75879097	613
HP_UW4	24.57538795	569
HP_UW3	24.58598137	534
HP_UW2	22.82421303	390
HP_UW1	23.45598221	428

	LST13JUN15	*Distance WD (12pm-90)*
LST13JUN15	1	
Distance WD (12pm-90)	0.50	1

Name	LST16FEB16	Distance WD (12pm-360)
HP_UW50	23.71189499	230
HP_UW49	23.45067787	473
HP_UW48	23.70815659	338
HP_UW47	23.67988777	310
HP_UW46	23.5285778	281
HP_UW45	23.20406151	427
HP_UW44	23.37168694	456
HP_UW43	23.37965584	520
HP_UW42	23.20386124	347
HP_UW41	23.13448524	189
HP_UW40	23.19429398	114
HP_UW39	22.80682564	53
HP_UW38	23.32974052	221
HP_UW37	24.02151299	209
HP_UW36	23.63198471	595
HP_UW35	23.54974365	516
HP_UW34	23.55237389	455
HP_UW33	23.79582024	364
HP_UW32	23.54267693	554
HP_UW31	23.4547863	381
HP_UW30	23.41320229	252
HP_UW29	23.46339798	153
HP_UW28	22.88970947	40
HP_UW27	23.63773155	257
HP_UW26	23.73647308	179
HP_UW25	23.66144943	116
HP_UW24	22.82207298	30
HP_UW23	23.78050423	184
HP_UW22	23.31753159	516
HP_UW21	23.54125595	450
HP_UW20	23.97932816	345
HP_UW19	23.81092072	227
HP_UW18	22.85326767	27
HP_UW17	23.75856781	115
HP_UW16	22.73586845	28
HP_UW15	23.63568687	121
HP_UW14	23.67535019	167
HP_UW13	23.79950714	155
HP_UW12	23.57590675	128
HP_UW11	23.46050453	107
HP_UW10	22.76583672	32
HP_UW9	23.36472511	95
HP_UW8	22.6179924	26
HP_UW7	22.6492157	27
HP_UW6	23.53131485	122
HP_UW5	23.03481674	64
HP_UW4	23.72464752	143
HP_UW3	23.78984833	150
HP_UW2	22.53971863	33
HP_UW1	22.41057396	34

	LST16FEB16	*Distance WD (12pm-360)*
LST16FEB16	1	
Distance WD (12pm-360)	0.46	1

Name	LST15MAR17	Distance WD (12pm-270)
HP_UW50	26.84909058	444
HP_UW49	26.61771965	595
HP_UW48	27.063591	404
HP_UW47	26.96011353	432
HP_UW46	26.97304726	349
HP_UW45	26.58063698	354
HP_UW44	26.74604034	392
HP_UW43	26.88067627	382
HP_UW42	26.48315239	324
HP_UW41	26.4010601	198
HP_UW40	26.42663956	139
HP_UW39	25.59250259	69
HP_UW38	26.87304115	252
HP_UW37	27.06912613	602
HP_UW36	26.77884293	559
HP_UW35	26.73172188	492
HP_UW34	26.78637886	525
HP_UW33	27.07279396	476
HP_UW32	26.92955971	430
HP_UW31	26.79687881	368
HP_UW30	27.01252174	290
HP_UW29	27.10097313	191
HP_UW28	25.61823463	57
HP_UW27	26.92025948	389
HP_UW26	27.15328598	257
HP_UW25	26.979496	180
HP_UW24	25.64563942	47
HP_UW23	26.98784637	327
HP_UW22	26.47361374	679
HP_UW21	26.73233795	631
HP_UW20	27.28928947	570
HP_UW19	27.09458542	508
HP_UW18	25.49770355	82
HP_UW17	26.92671585	212
HP_UW16	25.3735733	232
HP_UW15	26.87273598	326
HP_UW14	26.8880043	442
HP_UW13	26.93526649	502
HP_UW12	26.75706673	392
HP_UW11	26.4353199	430
HP_UW10	25.22512054	323
HP_UW9	26.01132202	732
HP_UW8	24.90502167	623
HP_UW7	24.95769501	549
HP_UW6	26.56581879	670
HP_UW5	25.59491539	613
HP_UW4	26.798172	569
HP_UW3	26.86141205	534
HP_UW2	24.99906731	390
HP_UW1	24.80977821	428

	LST15MAR17	*Distance WD (12pm-270)*
LST15MAR17	1	
Distance WD (12pm-270)	0.12	1

Name	LST15APRIL18	Distance WD (12pm-240)
HP_UW50	27.86079216	444
HP_UW49	27.62883949	595
HP_UW48	27.88176155	404
HP_UW47	27.82115746	432
HP_UW46	27.84192848	349
HP_UW45	27.55628395	354
HP_UW44	27.64958191	392
HP_UW43	27.78630638	382
HP_UW42	27.51085281	324
HP_UW41	27.1218071	198
HP_UW40	26.88558006	139
HP_UW39	26.02633476	69
HP_UW38	27.43659401	252
HP_UW37	28.20325279	602
HP_UW36	28.02186394	559
HP_UW35	27.76828003	492
HP_UW34	27.70195198	525
HP_UW33	27.75707436	476
HP_UW32	27.81095696	430
HP_UW31	27.60195351	368
HP_UW30	27.59710693	290
HP_UW29	27.59717178	191
HP_UW28	25.81502342	57
HP_UW27	27.92191505	389
HP_UW26	27.95158958	257
HP_UW25	27.71068954	180
HP_UW24	25.86078453	47
HP_UW23	28.14195251	327
HP_UW22	27.41560745	679
HP_UW21	27.7017498	631
HP_UW20	28.04304504	570
HP_UW19	27.98880768	508
HP_UW18	26.03438568	82
HP_UW17	28.00156784	212
HP_UW16	26.7993927	232
HP_UW15	27.94119072	326
HP_UW14	27.96672821	442
HP_UW13	28.00855064	502
HP_UW12	27.95894241	392
HP_UW11	27.89922142	430
HP_UW10	27.02291298	323
HP_UW9	27.38363266	732
HP_UW8	25.93332672	623
HP_UW7	26.49946976	549
HP_UW6	27.96959305	670
HP_UW5	27.26135826	613
HP_UW4	28.03472137	569
HP_UW3	28.02478027	534
HP_UW2	26.72406387	390
HP_UW1	26.24505806	428

	LST15APRIL18	*Distance WD (12pm-240)*
LST15APRIL18	1	
Distance WD (12pm-270)	0.43	1

Name	LST17FEB18	Distance
HP_UW50	24.31643295	223
HP_UW49	24.26260757	450
HP_UW48	24.27282333	301
HP_UW47	24.31129646	302
HP_UW46	24.26959991	248
HP_UW45	23.64860916	318
HP_UW44	23.89373398	350
HP_UW43	23.93725395	370
HP_UW42	23.62171936	279
HP_UW41	23.44055939	154
HP_UW40	23.60063934	91
HP_UW39	23.11918259	40
HP_UW38	23.82999229	187
HP_UW37	24.6875515	205
HP_UW36	24.18091965	528
HP_UW35	24.3136692	445
HP_UW34	24.49780655	427
HP_UW33	24.45879364	350
HP_UW32	24.12798309	402
HP_UW31	23.9954071	312
HP_UW30	24.04850578	207
HP_UW29	24.04244614	128
HP_UW28	23.04268265	35
HP_UW27	24.26522446	252
HP_UW26	24.34332657	155
HP_UW25	24.30348587	102
HP_UW24	23.10945892	25
HP_UW23	24.3457737	182
HP_UW22	23.92131615	508
HP_UW21	24.208004	424
HP_UW20	24.58328247	323
HP_UW19	24.39139175	220
HP_UW18	22.9902916	23
HP_UW17	24.48591995	110
HP_UW16	23.18119049	25
HP_UW15	24.26725578	115
HP_UW14	24.30371666	152
HP_UW13	24.29421043	152
HP_UW12	23.98694801	106
HP_UW11	23.80527115	106
HP_UW10	23.10764313	30
HP_UW9	23.63613129	93
HP_UW8	22.95876312	24
HP_UW7	23.02038193	26
HP_UW6	23.95833778	120
HP_UW5	23.37424469	60
HP_UW4	24.26602745	140
HP_UW3	24.31890869	147
HP_UW2	23.02694702	32
HP_UW1	22.94577217	32

	LST17FEB18	*Distance*
LST17FEB18	1	
Distance	0.595180675	1

Name	LST17MAR22	Distance
HP_UW50	24.224617	223
HP_UW49	23.96577644	450
HP_UW48	23.79745102	301
HP_UW47	24.09764862	302
HP_UW46	23.65782928	248
HP_UW45	23.04035759	318
HP_UW44	23.33227348	350
HP_UW43	23.38224602	370
HP_UW42	22.9678421	279
HP_UW41	22.5896492	154
HP_UW40	22.9109993	91
HP_UW39	22.74027443	40
HP_UW38	22.97459221	187
HP_UW37	24.43915939	205
HP_UW36	24.02250862	528
HP_UW35	24.13367844	445
HP_UW34	24.29132271	427
HP_UW33	24.31274223	350
HP_UW32	23.70922661	402
HP_UW31	23.49674797	312
HP_UW30	23.18379211	207
HP_UW29	23.20236397	128
HP_UW28	22.76481247	35
HP_UW27	24.04959488	252
HP_UW26	23.60692406	155
HP_UW25	23.85113907	102
HP_UW24	22.90848732	25
HP_UW23	24.18031693	182
HP_UW22	23.64055252	508
HP_UW21	23.90744591	424
HP_UW20	24.48064613	323
HP_UW19	24.31625938	220
HP_UW18	22.92375374	23
HP_UW17	24.22430801	110
HP_UW16	23.30771255	25
HP_UW15	24.1810627	115
HP_UW14	24.17009354	152
HP_UW13	24.06878281	152
HP_UW12	23.95613861	106
HP_UW11	23.70344734	106
HP_UW10	23.21721458	30
HP_UW9	23.66165543	93
HP_UW8	22.89413071	24
HP_UW7	22.98500252	26
HP_UW6	23.70765114	120
HP_UW5	23.40265274	60
HP_UW4	23.88784409	140
HP_UW3	23.98085976	147
HP_UW2	22.92052841	32
HP_UW1	22.67741203	32

	LST17MAR22	*Distance*
LST17MAR22	1	
Distance	0.465227317	1

Name	LST13DEC24	Distance WD (9am-270, 12pm-270)
HP_UW50	21.4891243	444
HP_UW49	21.05958748	595
HP_UW48	21.47496796	404
HP_UW47	21.36790276	432
HP_UW46	21.29309464	349
HP_UW45	21.06009674	354
HP_UW44	21.13881874	392
HP_UW43	21.47757339	382
HP_UW42	20.96465492	324
HP_UW41	20.66912079	198
HP_UW40	20.52885818	139
HP_UW39	20.38691139	69
HP_UW38	20.85477257	252
HP_UW37	21.78848648	602
HP_UW36	21.39883614	559
HP_UW35	21.27978897	492
HP_UW34	21.45232201	525
HP_UW33	21.6627636	476
HP_UW32	21.47301483	430
HP_UW31	21.13230133	368
HP_UW30	21.1043911	290
HP_UW29	20.73945808	191
HP_UW28	20.27619553	57
HP_UW27	21.28476143	389
HP_UW26	21.14752579	257
HP_UW25	20.90747833	180
HP_UW24	20.245924	47
HP_UW23	21.47756004	327
HP_UW22	21.13045311	679
HP_UW21	21.2366581	631
HP_UW20	21.75676155	570
HP_UW19	21.5968399	508
HP_UW18	20.3679924	82
HP_UW17	21.22096443	212
HP_UW16	20.71325874	232
HP_UW15	21.37241745	326
HP_UW14	21.41449547	442
HP_UW13	21.30920792	502
HP_UW12	21.24298477	392
HP_UW11	21.18869972	430
HP_UW10	20.38316727	323
HP_UW9	21.14688301	732
HP_UW8	20.32489014	623
HP_UW7	20.38545036	549
HP_UW6	21.23769569	670
HP_UW5	20.68129349	613
HP_UW4	21.46991348	569
HP_UW3	21.424366	534
HP_UW2	20.31315422	390
HP_UW1	20.61464882	428

	LST13DEC24	*Distance WD (9am-270, 12pm-270)*
LST13DEC24	1	
Distance WD (9am-270, 12pm-270)	0.50	1

Name	LST14JAN25	Distance WD (12pm-0)
HP_UW50	22.44334984	230
HP_UW49	22.0218792	473
HP_UW48	22.25964165	338
HP_UW47	22.28164291	310
HP_UW46	22.15021133	281
HP_UW45	21.65964127	427
HP_UW44	21.90369797	456
HP_UW43	21.86094475	520
HP_UW42	21.55295181	347
HP_UW41	21.21100998	189
HP_UW40	21.33937454	114
HP_UW39	20.72034836	53
HP_UW38	21.59792137	221
HP_UW37	22.69602585	209
HP_UW36	22.15952683	595
HP_UW35	22.19029617	516
HP_UW34	22.62804985	455
HP_UW33	22.61117744	364
HP_UW32	22.05620003	554
HP_UW31	22.10732269	381
HP_UW30	21.8278656	252
HP_UW29	22.02865791	153
HP_UW28	20.69620514	40
HP_UW27	22.36317253	257
HP_UW26	22.36348724	179
HP_UW25	22.06860542	116
HP_UW24	20.86749077	30
HP_UW23	22.41141319	184
HP_UW22	21.77977562	516
HP_UW21	22.10112572	450
HP_UW20	22.60539246	345
HP_UW19	22.50767899	227
HP_UW18	20.67486763	27
HP_UW17	22.29153442	115
HP_UW16	20.95377541	28
HP_UW15	22.12500763	121
HP_UW14	22.1708889	167
HP_UW13	22.00968742	155
HP_UW12	21.68775368	128
HP_UW11	21.32815552	107
HP_UW10	20.51081848	32
HP_UW9	21.54809761	95
HP_UW8	20.76245689	26
HP_UW7	20.78437042	27
HP_UW6	21.87317657	122
HP_UW5	21.16887856	64
HP_UW4	22.17705154	143
HP_UW3	22.12024689	150
HP_UW2	20.47958946	33
HP_UW1	20.44000435	34

	LST14JAN25	Distance WD (12pm-0)
LST14JAN25	1	
Distance WD (12pm-0)	0.58	1

Name	LST14NOV25	Distance WD (12pm-270)
HP_UW50	23.84895325	444
HP_UW49	23.4069767	595
HP_UW48	23.89774132	404
HP_UW47	23.81472969	432
HP_UW46	23.62731934	349
HP_UW45	23.18412209	354
HP_UW44	23.39468575	392
HP_UW43	23.46357155	382
HP_UW42	23.08212662	324
HP_UW41	22.89794731	198
HP_UW40	22.90218163	139
HP_UW39	22.5894146	69
HP_UW38	23.22046852	252
HP_UW37	24.1696682	602
HP_UW36	23.45673752	559
HP_UW35	23.42458344	492
HP_UW34	23.59455681	525
HP_UW33	23.96513748	476
HP_UW32	23.60871315	430
HP_UW31	23.49156761	368
HP_UW30	23.38066673	290
HP_UW29	23.34127998	191
HP_UW28	22.65615463	57
HP_UW27	23.82427788	389
HP_UW26	23.82670403	257
HP_UW25	23.57896423	180
HP_UW24	22.71681404	47
HP_UW23	23.98191261	327
HP_UW22	23.25380135	679
HP_UW21	23.56121254	631
HP_UW20	24.26880455	570
HP_UW19	24.0796299	508
HP_UW18	22.67028427	82
HP_UW17	23.70905685	212
HP_UW16	22.73629761	232
HP_UW15	23.69127274	326
HP_UW14	23.86164284	442
HP_UW13	23.78031731	502
HP_UW12	23.61637878	392
HP_UW11	23.25077629	430
HP_UW10	22.59767532	323
HP_UW9	23.1609745	732
HP_UW8	22.38499451	623
HP_UW7	22.38772964	549
HP_UW6	23.55399323	670
HP_UW5	22.84262657	613
HP_UW4	23.68502998	569
HP_UW3	23.71522713	534
HP_UW2	22.44401169	390
HP_UW1	22.32711792	428

	LST14NOV25	*Distance WD (12pm-270)*
LST14NOV25	1	
Distance WD (12pm-270)	0.30	1

Name	LST15SEPT25	Distance WD (12pm-210)
HP_UW50	26.95055008	230
HP_UW49	26.81550217	473
HP_UW48	26.52653885	338
HP_UW47	26.74288559	310
HP_UW46	26.44454193	281
HP_UW45	26.19943619	427
HP_UW44	26.31713104	456
HP_UW43	26.47873497	520
HP_UW42	26.18148804	347
HP_UW41	25.9523983	189
HP_UW40	25.88803673	114
HP_UW39	25.53695488	53
HP_UW38	26.00526237	221
HP_UW37	27.3447361	209
HP_UW36	26.99497414	595
HP_UW35	26.72788048	516
HP_UW34	26.91526794	455
HP_UW33	26.76907349	364
HP_UW32	26.62437439	554
HP_UW31	26.34284592	381
HP_UW30	26.17683792	252
HP_UW29	26.30203247	153
HP_UW28	25.41989708	40
HP_UW27	26.76294136	257
HP_UW26	26.65468216	179
HP_UW25	26.74031448	116
HP_UW24	25.7233448	30
HP_UW23	27.00197983	184
HP_UW22	26.47673416	516
HP_UW21	26.91610909	450
HP_UW20	27.28843117	345
HP_UW19	27.14267921	227
HP_UW18	25.67175484	27
HP_UW17	27.26457596	115
HP_UW16	25.94781494	28
HP_UW15	27.02788353	121
HP_UW14	27.11538887	167
HP_UW13	27.16201401	155
HP_UW12	26.97110176	128
HP_UW11	26.93966293	107
HP_UW10	26.38271904	32
HP_UW9	26.46552086	95
HP_UW8	25.63759422	26
HP_UW7	25.92014885	27
HP_UW6	26.86458397	122
HP_UW5	26.26934052	64
HP_UW4	27.07849121	143
HP_UW3	27.1518364	150
HP_UW2	26.26642227	33
HP_UW1	25.78245544	34

	LST15SEPT25	*Distance WD (12pm-210)*
LST15SEPT25	1	
Distance WD (12pm-210)	0.34	1

Name	LST14FEB26	Distance WD (12pm-50)
HP_UW50	23.5644722	230
HP_UW49	23.08900642	473
HP_UW48	23.23388672	338
HP_UW47	23.32100296	310
HP_UW46	23.34160423	281
HP_UW45	22.55536652	427
HP_UW44	22.92047882	456
HP_UW43	22.90999031	520
HP_UW42	22.50982475	347
HP_UW41	22.47676468	189
HP_UW40	22.68343544	114
HP_UW39	22.10223961	53
HP_UW38	22.83026695	221
HP_UW37	23.89462662	209
HP_UW36	23.07637215	595
HP_UW35	22.99292946	516
HP_UW34	23.22824669	455
HP_UW33	23.26398087	364
HP_UW32	23.15175819	554
HP_UW31	22.93372536	381
HP_UW30	23.01687241	252
HP_UW29	23.10318756	153
HP_UW28	21.93189812	40
HP_UW27	23.49044991	257
HP_UW26	23.46775627	179
HP_UW25	23.33366013	116
HP_UW24	22.10105324	30
HP_UW23	23.65400696	184
HP_UW22	22.79915619	516
HP_UW21	23.20395851	450
HP_UW20	23.76669884	345
HP_UW19	23.80390358	227
HP_UW18	22.20454979	27
HP_UW17	23.64078331	115
HP_UW16	22.73323441	28
HP_UW15	23.55468941	121
HP_UW14	23.58731079	167
HP_UW13	23.42503548	155
HP_UW12	23.28251076	128
HP_UW11	22.98125649	107
HP_UW10	22.38834381	32
HP_UW9	23.14559174	95
HP_UW8	22.11636543	26
HP_UW7	22.24192238	27
HP_UW6	23.32174873	122
HP_UW5	22.73204803	64
HP_UW4	23.45059395	143
HP_UW3	23.43123436	150
HP_UW2	22.21002007	33
HP_UW1	22.07181931	34

	LST14FEB26	*Distance WD (12pm-50)*
LST14FEB26	1	
Distance WD (12pm-50)	0.31	1

Name	LST15OCT27	Distance WD (12pm-0)
HP_UW50	28.10982895	230
HP_UW49	27.75059319	473
HP_UW48	28.04508018	338
HP_UW47	27.98088837	310
HP_UW46	27.70166588	281
HP_UW45	27.63537025	427
HP_UW44	27.72080803	456
HP_UW43	27.79028511	520
HP_UW42	27.54210854	347
HP_UW41	27.12280655	189
HP_UW40	26.9830513	114
HP_UW39	26.48350334	53
HP_UW38	27.31038094	221
HP_UW37	28.48789597	209
HP_UW36	27.93976784	595
HP_UW35	27.78606606	516
HP_UW34	27.84445953	455
HP_UW33	28.25654411	364
HP_UW32	27.83287811	554
HP_UW31	27.92142677	381
HP_UW30	27.49713707	252
HP_UW29	27.31344223	153
HP_UW28	26.53717422	40
HP_UW27	27.90921211	257
HP_UW26	27.93199539	179
HP_UW25	27.82012939	116
HP_UW24	26.54043961	30
HP_UW23	28.15218163	184
HP_UW22	27.67657852	516
HP_UW21	27.94608307	450
HP_UW20	28.37766266	345
HP_UW19	28.27333641	227
HP_UW18	26.77346802	27
HP_UW17	28.02799034	115
HP_UW16	26.77159119	28
HP_UW15	28.01725388	121
HP_UW14	28.15814018	167
HP_UW13	28.15821838	155
HP_UW12	27.9059124	128
HP_UW11	27.76773453	107
HP_UW10	26.73560715	32
HP_UW9	27.40111542	95
HP_UW8	26.31832504	26
HP_UW7	26.29353714	27
HP_UW6	27.81220245	122
HP_UW5	26.92951202	64
HP_UW4	28.20691299	143
HP_UW3	28.22517776	150
HP_UW2	26.54266167	33
HP_UW1	26.34500313	34

	LST15OCT27	*Distance WD (12pm-0)*
LST15OCT27	1	
Distance WD (12pm-0)	0.54	1

Name	LST15JAN28	Distance WD (12pm-0)
HP_UW50	21.73438644	230
HP_UW49	21.51975632	473
HP_UW48	21.68424606	338
HP_UW47	21.77161407	310
HP_UW46	21.55907822	281
HP_UW45	21.10740471	427
HP_UW44	21.24761772	456
HP_UW43	21.50248146	520
HP_UW42	20.98696899	347
HP_UW41	20.57119751	189
HP_UW40	20.48106384	114
HP_UW39	19.95233345	53
HP_UW38	20.94169044	221
HP_UW37	22.43829155	209
HP_UW36	21.78042412	595
HP_UW35	21.47949982	516
HP_UW34	21.80526733	455
HP_UW33	21.82128334	364
HP_UW32	21.71955299	554
HP_UW31	21.18081474	381
HP_UW30	21.16807938	252
HP_UW29	21.15689278	153
HP_UW28	19.72389603	40
HP_UW27	21.75510979	257
HP_UW26	21.6678524	179
HP_UW25	21.3641758	116
HP_UW24	19.96974182	30
HP_UW23	21.86327744	184
HP_UW22	21.26124763	516
HP_UW21	21.59796715	450
HP_UW20	22.04836273	345
HP_UW19	21.94943047	227
HP_UW18	19.9067173	27
HP_UW17	21.72195625	115
HP_UW16	20.52537537	28
HP_UW15	21.72364616	121
HP_UW14	21.83020782	167
HP_UW13	21.79456139	155
HP_UW12	21.60316849	128
HP_UW11	21.24231911	107
HP_UW10	20.65457916	32
HP_UW9	20.9301815	95
HP_UW8	20.08335876	26
HP_UW7	20.29477501	27
HP_UW6	21.58452034	122
HP_UW5	20.69372749	64
HP_UW4	21.71170616	143
HP_UW3	21.70555687	150
HP_UW2	20.35396576	33
HP_UW1	20.10568047	34

	LST15JAN28	*Distance WD (12pm-0)*
LST15JAN28	1	
Distance WD (12pm-0)	0.54	1

Name	LST15NOV28	Distance WD (12pm-0)
HP_UW50	21.81775665	230
HP_UW49	21.60148811	473
HP_UW48	21.62450218	338
HP_UW47	21.6727047	310
HP_UW46	21.5221138	281
HP_UW45	21.25500107	427
HP_UW44	21.27064323	456
HP_UW43	21.54697227	520
HP_UW42	21.16994858	347
HP_UW41	21.05049896	189
HP_UW40	21.10054398	114
HP_UW39	20.82413864	53
HP_UW38	21.20444489	221
HP_UW37	22.23842239	209
HP_UW36	21.55198097	595
HP_UW35	21.50768662	516
HP_UW34	21.60785675	455
HP_UW33	21.88951874	364
HP_UW32	21.53218842	554
HP_UW31	21.34719658	381
HP_UW30	21.33714867	252
HP_UW29	21.24023628	153
HP_UW28	20.80448341	40
HP_UW27	21.60067177	257
HP_UW26	21.68915749	179
HP_UW25	21.71698761	116
HP_UW24	20.72751045	30
HP_UW23	21.91177177	184
HP_UW22	21.34788322	516
HP_UW21	21.65168381	450
HP_UW20	22.15915108	345
HP_UW19	22.08646393	227
HP_UW18	20.95741081	27
HP_UW17	21.9077549	115
HP_UW16	21.21167374	28
HP_UW15	21.85766983	121
HP_UW14	21.89153099	167
HP_UW13	21.87910652	155
HP_UW12	21.69778061	128
HP_UW11	21.59220505	107
HP_UW10	21.01412773	32
HP_UW9	21.47642899	95
HP_UW8	20.72503853	26
HP_UW7	20.79985046	27
HP_UW6	21.6831646	122
HP_UW5	21.19387245	64
HP_UW4	21.98755836	143
HP_UW3	21.96192551	150
HP_UW2	20.89315033	33
HP_UW1	20.7826252	34

	LST15NOV28	*Distance WD (12pm-0)*
LST15NOV28	1	
Distance WD (12pm-0)	0.33	1

Name	LST15DEC30	Distance WD (12pm-0)
HP_UW50	19.7638588	230
HP_UW49	19.45110893	473
HP_UW48	19.86441612	338
HP_UW47	19.84436226	310
HP_UW46	19.65920258	281
HP_UW45	19.13644981	427
HP_UW44	19.40419197	456
HP_UW43	19.5465126	520
HP_UW42	19.21716881	347
HP_UW41	19.18282127	189
HP_UW40	19.20337105	114
HP_UW39	18.84999275	53
HP_UW38	19.37253952	221
HP_UW37	20.12726402	209
HP_UW36	19.74118233	595
HP_UW35	19.68907928	516
HP_UW34	19.62298012	455
HP_UW33	19.88511467	364
HP_UW32	19.7110424	554
HP_UW31	19.44751549	381
HP_UW30	19.47505951	252
HP_UW29	19.44921684	153
HP_UW28	18.98310089	40
HP_UW27	19.71806335	257
HP_UW26	19.75100327	179
HP_UW25	19.75063896	116
HP_UW24	18.95685577	30
HP_UW23	19.82805824	184
HP_UW22	19.39683723	516
HP_UW21	19.53375626	450
HP_UW20	20.10969543	345
HP_UW19	19.94860268	227
HP_UW18	18.86837196	27
HP_UW17	19.74689102	115
HP_UW16	18.96438789	28
HP_UW15	19.62651443	121
HP_UW14	19.70332527	167
HP_UW13	19.78298187	155
HP_UW12	19.60616684	128
HP_UW11	19.39451981	107
HP_UW10	18.92668724	32
HP_UW9	19.17713737	95
HP_UW8	18.62438774	26
HP_UW7	18.6516304	27
HP_UW6	19.54706001	122
HP_UW5	19.01856613	64
HP_UW4	19.71012115	143
HP_UW3	19.76537895	150
HP_UW2	18.69758224	33
HP_UW1	18.59353828	34

	LST15DEC30	*Distance WD (12pm-0)*
LST15DEC30	1	
Distance WD (12pm-0)	0.49	1

Name	LST14MAR30	Distance WD (12pm-250)
HP_UW50	35.41059494	444
HP_UW49	34.59390259	595
HP_UW48	34.97451782	404
HP_UW47	35.05498123	432
HP_UW46	35.23092651	349
HP_UW45	34.51668549	354
HP_UW44	34.54154205	392
HP_UW43	34.92593384	382
HP_UW42	34.29933929	324
HP_UW41	34.23593903	198
HP_UW40	34.49620056	139
HP_UW39	32.83964539	69
HP_UW38	34.72631454	252
HP_UW37	35.62037659	602
HP_UW36	34.99520111	559
HP_UW35	34.8365593	492
HP_UW34	34.80919266	525
HP_UW33	34.86292267	476
HP_UW32	34.96484756	430
HP_UW31	34.67930603	368
HP_UW30	34.94822693	290
HP_UW29	34.96285248	191
HP_UW28	32.36601257	57
HP_UW27	35.38477325	389
HP_UW26	35.44711304	257
HP_UW25	35.13874054	180
HP_UW24	32.62581635	47
HP_UW23	35.66892624	327
HP_UW22	34.53803635	679
HP_UW21	34.76237106	631
HP_UW20	35.44299316	570
HP_UW19	35.57802963	508
HP_UW18	32.57541656	82
HP_UW17	35.52333832	212
HP_UW16	33.34925461	232
HP_UW15	35.32771683	326
HP_UW14	35.34283447	442
HP_UW13	35.08055496	502
HP_UW12	34.81642151	392
HP_UW11	34.31983185	430
HP_UW10	32.81469345	323
HP_UW9	34.63487244	732
HP_UW8	32.59328079	623
HP_UW7	32.87669373	549
HP_UW6	34.97012329	670
HP_UW5	33.99000931	613
HP_UW4	35.1500206	569
HP_UW3	35.13262939	534
HP_UW2	32.60424042	390
HP_UW1	32.27597809	428

	LST14MAR30	*Distance WD (12pm-250)*
LST14MAR30	1	
Distance WD (12pm-250)	0.31	1

Name	LST16NOV30	Distance WD (12pm-0)
HP_UW50	24.69256592	230
HP_UW49	24.50520515	473
HP_UW48	24.77346611	338
HP_UW47	24.59464645	310
HP_UW46	24.46829033	281
HP_UW45	23.8806324	427
HP_UW44	24.04779625	456
HP_UW43	24.19262314	520
HP_UW42	23.81505585	347
HP_UW41	23.58721924	189
HP_UW40	23.51502991	114
HP_UW39	23.04439354	53
HP_UW38	23.91208076	221
HP_UW37	25.17662239	209
HP_UW36	24.6117115	595
HP_UW35	24.50380707	516
HP_UW34	24.64850616	455
HP_UW33	24.83438492	364
HP_UW32	24.27416611	554
HP_UW31	24.37114906	381
HP_UW30	24.18213654	252
HP_UW29	23.98618507	153
HP_UW28	23.15935516	40
HP_UW27	24.49119949	257
HP_UW26	24.48492813	179
HP_UW25	24.28541756	116
HP_UW24	23.23856163	30
HP_UW23	24.70054817	184
HP_UW22	24.28953934	516
HP_UW21	24.51570129	450
HP_UW20	25.03688431	345
HP_UW19	24.86547661	227
HP_UW18	23.34662437	27
HP_UW17	24.51919746	115
HP_UW16	23.39686966	28
HP_UW15	24.52156258	121
HP_UW14	24.61415863	167
HP_UW13	24.58355141	155
HP_UW12	24.33218193	128
HP_UW11	24.12489319	107
HP_UW10	23.25645256	32
HP_UW9	23.79753876	95
HP_UW8	22.87465858	26
HP_UW7	22.91378593	27
HP_UW6	24.17533112	122
HP_UW5	23.37221909	64
HP_UW4	24.59849167	143
HP_UW3	24.62824059	150
HP_UW2	23.09910202	33
HP_UW1	22.88074112	34

	LST16NOV30	*Distance WD (12pm-0)*
LST16NOV30	1	
Distance WD (12pm-0)	0.56	1

Name	LST16MAR3	Distance WD (12pm-290)
HP_UW50	26.12771988	444
HP_UW49	25.74199104	595
HP_UW48	26.09409142	404
HP_UW47	26.06204987	432
HP_UW46	25.86433983	349
HP_UW45	25.69513702	354
HP_UW44	25.77595329	392
HP_UW43	26.02541161	382
HP_UW42	25.56254768	324
HP_UW41	25.38105774	198
HP_UW40	25.29888153	139
HP_UW39	24.742939	69
HP_UW38	25.56568718	252
HP_UW37	26.31900024	602
HP_UW36	26.09508514	559
HP_UW35	25.91873741	492
HP_UW34	25.91857338	525
HP_UW33	26.28914261	476
HP_UW32	25.96237946	430
HP_UW31	25.78567314	368
HP_UW30	25.6806736	290
HP_UW29	25.7041378	191
HP_UW28	24.79715729	57
HP_UW27	26.00021553	389
HP_UW26	26.20525932	257
HP_UW25	26.13583565	180
HP_UW24	25.0261116	47
HP_UW23	26.31634331	327
HP_UW22	25.55557823	679
HP_UW21	25.80740547	631
HP_UW20	26.29529572	570
HP_UW19	26.27838135	508
HP_UW18	25.10665321	82
HP_UW17	26.24592018	212
HP_UW16	25.31789398	232
HP_UW15	26.35004997	326
HP_UW14	26.29319572	442
HP_UW13	26.11727142	502
HP_UW12	26.32736588	392
HP_UW11	25.97378159	430
HP_UW10	25.27708626	323
HP_UW9	25.52430725	732
HP_UW8	24.68471336	623
HP_UW7	24.88557816	549
HP_UW6	25.9569931	670
HP_UW5	25.35776901	613
HP_UW4	26.10134506	569
HP_UW3	26.07979584	534
HP_UW2	24.99782372	390
HP_UW1	24.84340477	428

	LST16MAR3	*Distance WD (12pm-290)*
LST16MAR3	1	
Distance WD (12pm-290)	0.29	1

Name	LST15MAY4	Distance WD (12pm-130)
HP_UW50	30.12346458	230
HP_UW49	29.96056175	473
HP_UW48	29.85290337	338
HP_UW47	29.95142555	310
HP_UW46	29.65921402	281
HP_UW45	29.49341583	427
HP_UW44	29.71884537	456
HP_UW43	29.84348488	520
HP_UW42	29.40135193	347
HP_UW41	29.1397419	189
HP_UW40	28.79077148	114
HP_UW39	28.13479424	53
HP_UW38	29.38591003	221
HP_UW37	30.76463318	209
HP_UW36	30.56443977	595
HP_UW35	30.17009163	516
HP_UW34	29.95178795	455
HP_UW33	30.08270836	364
HP_UW32	29.99190331	554
HP_UW31	29.55920219	381
HP_UW30	29.5019989	252
HP_UW29	29.45025253	153
HP_UW28	28.01029205	40
HP_UW27	29.85260582	257
HP_UW26	29.8402977	179
HP_UW25	29.56099129	116
HP_UW24	28.07156181	30
HP_UW23	30.13689613	184
HP_UW22	29.87441254	516
HP_UW21	30.05376625	450
HP_UW20	30.48532867	345
HP_UW19	30.47376633	227
HP_UW18	28.44830513	27
HP_UW17	29.90200424	115
HP_UW16	28.68468857	28
HP_UW15	30.36439514	121
HP_UW14	30.51862144	167
HP_UW13	30.44018555	155
HP_UW12	30.49723816	128
HP_UW11	30.30900574	107
HP_UW10	29.27239037	32
HP_UW9	29.79889107	95
HP_UW8	28.29524422	26
HP_UW7	28.66526413	27
HP_UW6	30.55130005	122
HP_UW5	29.53233147	64
HP_UW4	30.56617165	143
HP_UW3	30.46533775	150
HP_UW2	29.02650261	33
HP_UW1	28.46346092	34

	LST15MAY4	*Distance WD (12pm-130)*
LST15MAY4	1	
Distance WD (12pm-0)	0.46	1

Name	LST13NOV6	Distance WD (9am-0, 12pm-50)
HP_UW50	27.43475151	230
HP_UW49	26.86514664	473
HP_UW48	27.17402649	338
HP_UW47	27.13775635	310
HP_UW46	26.83324242	281
HP_UW45	26.83057976	427
HP_UW44	26.86397552	456
HP_UW43	27.13028526	520
HP_UW42	26.70049095	347
HP_UW41	26.15581894	189
HP_UW40	26.13817024	114
HP_UW39	25.86006546	53
HP_UW38	26.29422379	221
HP_UW37	27.9243679	209
HP_UW36	27.44838333	595
HP_UW35	27.2724762	516
HP_UW34	27.20902634	455
HP_UW33	27.37090874	364
HP_UW32	27.14720917	554
HP_UW31	26.9388237	381
HP_UW30	26.59797668	252
HP_UW29	26.29381561	153
HP_UW28	25.98705101	40
HP_UW27	26.90934563	257
HP_UW26	26.81923866	179
HP_UW25	26.79558754	116
HP_UW24	25.94518852	30
HP_UW23	27.19934082	184
HP_UW22	26.80956078	516
HP_UW21	26.98597145	450
HP_UW20	27.6490097	345
HP_UW19	27.59474182	227
HP_UW18	25.93326759	27
HP_UW17	27.25302696	115
HP_UW16	26.31463623	28
HP_UW15	27.2918644	121
HP_UW14	27.37414551	167
HP_UW13	27.46487427	155
HP_UW12	27.20580292	128
HP_UW11	27.17685699	107
HP_UW10	26.05885696	32
HP_UW9	27.24908066	95
HP_UW8	26.11788559	26
HP_UW7	26.15808678	27
HP_UW6	27.46391678	122
HP_UW5	27.02859497	64
HP_UW4	27.7112999	143
HP_UW3	27.57791901	150
HP_UW2	26.37590408	33
HP_UW1	26.35897827	34

	LST13NOV6	*Distance WD (9am-0, 12pm-50)*
LST13NOV6	1	
Distance WD (9am-0, 12pm-50)	0.42	1

Appendix C: Data from the field measurement and Remote Sensing

Solar angle and time of the day of Landsat pass_2013-17

Name	LST91DEC12	LST13APR12	LST13JUN15	LST13NOV6	LST13DEC24	LST14JAN25
SUN_ELEVATION	35.00505087	63.63618502	68.85373393	46.8600317	37.36177871	40.861972
SUN_AZIMUTH	144.9518863	118.960079	84.52699309	152.950763	153.5645038	146.511122
Time of the day	9:54:00 AM	10:28:00 AM	10:27:00 AM	10:35:00 AM	10:22:00 AM	10:31:00 AM
Wind Direction9am	N	200.00	90.00	0	270	270
Wind Direction12pm		180.00	90.00	50	270	0
Wind Speed 9am		1.02	1.02	0	1.54	1.02
Wind Speed 12pm		1.02	1.02	1.02	1.54	0

- Monthly Wind Direction % {N=0 or 360,E=90,S=180,W=270}

	Jan	Feb	Mar	Apr	May	Jun
North	**98**	**67**	**56**	38	37	24
NorthEast	1	4	2	3	5	0
East	0	3	3	1	16	4
SouthEast	0	0	5	6	10	20
South	0	8	17	**49**	23	**42**
SouthWest	0	11	6	1	4	10
West	0	4	4	0	4	0
NorthWest	0	4	6	2	0	0

LST14FEB10	LST14FEB26	LST14MAR14	LST14MAR30	LST14NOV25	LST15JAN28	LST15FEB13	LST15MAR17
44.39224208	49.04143798	54.27717614	59.47781141	42.12883676	41.23130251	44.98517176	55.05047594
142.4320455	137.7935396	132.3075142	125.4700419	154.3612878	145.5582843	141.4052045	130.9843444
10:30:00 AM	10:30:00 AM	10:28:00 AM	10:27:00 AM	10:34:00 AM	10:30:00 AM	10:29:00 AM	10:27:00 AM
360	360	360	240	320	0	0	0
50	50	360	250	270	0	270	270
3.08	1.02	1.02	1.02	1.02	0	0	0
1.54	1.02	1.02	1.54	1.02	0	1.54	1.02

Jul	Aug	Sep	Oct	Nov	Dec
57	**59**	**58**	**84**	**96**	**83**
0	1	1	2	0	8
4	9	3	4	1	1
16	19	2	2	0	0
17	10	29	4	0	0
6	1	7	0	1	0
0	2	1	3	0	3
0	0	1	1	2	5

LST15APR18	LST15MAY4	LST15SEP25	LST15OCT27	LST15NOV12	LST15NOV28	LST15DEC30	LST16JAN15
64.47193416	67.30699394	58.38129521	49.52284282	45.10495132	41.44353568	38.19196082	39.10028096
114.8193699	104.5042733	135.9828252	150.1262121	153.3742885	154.4511084	151.6960992	148.6668196
10:25:00 AM	10:24:00 AM	10:29:00 AM	10:31:00 AM	10:32:00 AM	10:32:00 AM	10:31:00 AM	10:30:00 AM
260	180	0	0	0	0	0	0
240	130	210	0	0	0	0	0
1.02	1.02	0	0	0	0	0	0
5.15	1.02	1.02	0	0	0	0	0

LST16FEB16	LST16MAR3	LST16NOV14	LST16NOV30	LST17FEB18	LST17MAR22
45.66159944	50.59388956	44.42461594	40.94110416	46.45721396	56.80888777
140.7578886	135.9226066	153.7597953	154.4870957	139.9780613	128.943383
10:28:00 AM	10:30:00 AM	10:30:00 AM	10:31:00 AM	10:30:00 AM	10:27:00 AM
0	0	50	90		
360	290	360	0		
0	0	1.02	1.02		
1.02	1.54	1.02	0		

Appendix D: Data from the field measurement

Bangladesh Meteorological Department (BMD)_Field measurement data

Timecum	Temperature (12T)	Relative Humidity(12RH)	Dew Point (12DP)	Variables	Correlation coefficent
0.0	22.5	64.5	15.5	12T	-0.9917444
1.0	22.5	64.5	15.5	12RH	0.9834432
2.0	22.5	65.0	15.6	12DP	-0.7602334
3.0	22.5	65.0	15.6		
4.0	22.5	65.0	15.6		
5.0	22.5	65.0	15.6		
6.0	22.0	65.0	15.1		
7.0	22.0	65.0	15.1		
8.0	22.0	65.5	15.2		
9.0	22.0	64.5	15.0		
10.0	22.0	65.0	15.1		
11.0	22.0	65.5	15.2		
12.0	22.0	65.0	15.1		
13.0	22.0	65.0	15.1		
14.0	22.0	64.5	15.0		
15.0	22.0	65.5	15.2		
16.0	22.0	65.5	15.2		
17.0	22.0	65.5	15.2		
18.0	22.0	65.5	15.2		
19.0	22.0	65.5	15.2		
20.0	22.0	66.0	15.4		
21.0	22.0	65.5	15.2		
22.0	22.0	65.5	15.2		
23.0	22.0	65.5	15.2		
24.0	22.0	65.5	15.2		
25.0	22.0	66.0	15.4		
26.0	22.0	65.5	15.2		
27.0	22.0	66.0	15.4		
28.0	22.0	66.0	15.4		
29.0	22.0	66.0	15.4		
30.0	22.0	66.0	15.4		
31.0	22.0	66.0	15.4		
32.0	22.0	66.0	15.4		
33.0	22.0	66.0	15.4		
34.0	22.0	66.0	15.4		
35.0	22.0	66.0	15.4		
36.0	22.0	66.0	15.4		
37.0	22.0	66.5	15.5		
38.0	22.0	66.5	15.5		
39.0	22.0	65.5	15.2		
40.0	22.0	66.0	15.4		
41.0	22.0	66.0	15.4		
42.0	22.0	66.0	15.4		
43.0	22.0	66.0	15.4		
44.0	22.0	66.0	15.4		
45.0	22.0	66.0	15.4		
46.0	22.0	66.0	15.4		
47.0	22.0	66.0	15.4		

48.0	22.0	66.0	15.4		
49.0	22.0	66.0	15.4		
50.0	22.0	66.5	15.5		
51.0	22.0	67.0	15.6		
52.0	22.0	66.5	15.5		
53.0	22.0	66.5	15.5		
54.0	22.0	66.5	15.5		
55.0	22.0	66.5	15.5		
56.0	22.0	66.5	15.5		
57.0	22.0	66.5	15.5		
58.0	22.0	66.5	15.5		
59.0	22.0	66.5	15.5		
60.0	22.0	67.0	15.6		
61.0	22.0	67.0	15.6		
62.0	22.0	67.0	15.6		
63.0	22.0	67.0	15.6		
64.0	22.0	67.5	15.7		
65.0	22.0	67.5	15.7		
66.0	22.0	67.5	15.7		
67.0	22.0	67.5	15.7		
68.0	22.0	67.5	15.7		
69.0	22.0	67.5	15.7		
70.0	22.0	67.5	15.7		
71.0	22.0	68.0	15.8		
72.0	22.0	68.0	15.8		
73.0	22.0	68.0	15.8		
74.0	22.0	68.0	15.8		
75.0	22.0	68.0	15.8		
76.0	22.0	68.0	15.8		
77.0	22.0	68.0	15.8		
78.0	22.0	68.5	15.9		
79.0	22.0	68.0	15.8		
80.0	22.0	68.5	15.9		
81.0	22.0	68.5	15.9		
82.0	22.0	68.5	15.9		
83.0	22.0	68.5	15.9		
84.0	22.0	68.5	15.9		
85.0	22.0	68.5	15.9		
86.0	22.0	68.5	15.9		
87.0	22.0	68.5	15.9		
88.0	22.0	68.5	15.9		
89.0	22.0	69.0	16.1		
90.0	22.0	69.0	16.1		
91.0	21.5	68.5	15.5		
92.0	21.5	69.0	15.6		
93.0	21.5	69.0	15.6		
94.0	21.5	69.0	15.6		
95.0	21.5	69.0	15.6		
96.0	21.5	69.0	15.6		
97.0	21.5	69.0	15.6		

98.0	21.5	69.0	15.6		
99.0	21.5	69.0	15.6		
100.0	21.5	69.0	15.6		
101.0	21.5	69.0	15.6		
102.0	21.5	69.0	15.6		
103.0	21.5	69.0	15.6		
104.0	21.5	69.0	15.6		
105.0	21.5	69.0	15.6		
106.0	21.5	69.5	15.7		
107.0	21.5	69.5	15.7		
108.0	21.5	69.5	15.7		
109.0	21.5	69.5	15.7		
110.0	21.5	69.5	15.7		
111.0	21.5	69.5	15.7		
112.0	21.5	69.5	15.7		
113.0	21.5	69.5	15.7		
114.0	21.5	69.5	15.7		
115.0	21.5	69.5	15.7		
116.0	21.5	69.5	15.7		
117.0	21.5	69.5	15.7		
118.0	21.5	69.5	15.7		
119.0	21.5	69.5	15.7		
120.0	21.5	69.5	15.7		
121.0	21.5	69.5	15.7		
122.0	21.5	69.5	15.7		
123.0	21.5	69.5	15.7		
124.0	21.5	69.5	15.7		
125.0	21.5	69.5	15.7		
126.0	21.0	69.5	15.2		
127.0	21.0	70.0	15.3		
128.0	21.0	70.0	15.3		
129.0	21.0	70.0	15.3		
130.0	21.0	70.0	15.3		
131.0	21.0	70.5	15.4		
132.0	21.0	70.0	15.3		
133.0	21.0	70.5	15.4		
134.0	21.0	70.5	15.4		
135.0	21.0	70.5	15.4		
136.0	21.0	70.5	15.4		
137.0	21.0	70.5	15.4		
138.0	21.0	70.5	15.4		
139.0	21.0	70.5	15.4		
140.0	21.0	71.0	15.5		
141.0	21.0	71.0	15.5		
142.0	21.0	71.0	15.5		
143.0	21.0	71.5	15.7		
144.0	21.0	71.5	15.7		
145.0	21.0	71.0	15.5		
146.0	21.0	72.0	15.8		
147.0	21.0	72.0	15.8		

148.0	21.0	72.0	15.8		
149.0	21.0	72.0	15.8		
150.0	21.0	72.0	15.8		
151.0	21.0	72.0	15.8		
152.0	21.0	72.0	15.8		
153.0	21.0	72.0	15.8		
154.0	21.0	72.0	15.8		
155.0	21.0	72.5	15.9		
156.0	21.0	72.0	15.8		
157.0	21.0	72.0	15.8		
158.0	21.0	72.0	15.8		
159.0	21.0	72.5	15.9		
160.0	21.0	72.5	15.9		
161.0	21.0	72.5	15.9		
162.0	21.0	72.0	15.8		
163.0	21.0	72.5	15.9		
164.0	21.0	72.5	15.9		
165.0	21.0	72.5	15.9		
166.0	21.0	72.5	15.9		
167.0	21.0	72.5	15.9		
168.0	21.0	72.5	15.9		
169.0	21.0	72.5	15.9		
170.0	21.0	72.0	15.8		
171.0	21.0	72.0	15.8		
172.0	21.0	72.0	15.8		
173.0	21.0	72.0	15.8		
174.0	21.0	71.5	15.7		
175.0	21.0	72.0	15.8		
176.0	21.0	71.5	15.7		
177.0	21.0	71.5	15.7		
178.0	21.0	71.0	15.5		
179.0	21.0	70.5	15.4		
180.0	**21.0**	**71.0**	15.5		
181.0	21.0	70.5	15.4		
182.0	21.0	70.0	15.3		
183.0	21.0	69.5	15.2		
184.0	21.0	69.5	15.2		
185.0	21.0	69.5	15.2		
186.0	21.0	69.0	15.1		
187.0	21.0	69.5	15.2		
188.0	21.0	69.5	15.2		
189.0	21.0	69.0	15.1		
190.0	21.0	68.5	15.0		
191.0	21.0	69.0	15.1		
192.0	21.0	69.0	15.1		
193.0	21.0	68.5	15.0		
194.0	21.0	68.5	15.0		
195.0	21.0	68.5	15.0		
196.0	21.0	68.5	15.0		
197.0	21.0	69.0	15.1		

198.0	21.0	68.5	15.0		
199.0	21.0	68.5	15.0		
200.0	21.0	68.5	15.0		
201.0	21.0	68.5	15.0		
202.0	21.0	68.5	15.0		
203.0	21.0	68.5	15.0		
204.0	21.0	68.5	15.0		
205.0	21.0	68.5	15.0		
206.0	21.0	68.5	15.0		
207.0	21.0	69.0	15.1		
208.0	21.0	69.0	15.1		
209.0	21.0	69.5	15.2		
210.0	21.0	68.5	15.0		
211.0	21.0	68.5	15.0		
212.0	21.0	69.0	15.1		
213.0	21.0	68.5	15.0		
214.0	21.0	68.5	15.0		
215.0	21.0	68.5	15.0		
216.0	21.0	68.5	15.0		
217.0	21.0	69.0	15.1		
218.0	21.0	69.0	15.1		
219.0	21.0	69.0	15.1		
220.0	21.0	69.5	15.2		
221.0	21.0	69.5	15.2		
222.0	21.0	69.5	15.2		
223.0	21.0	70.0	15.3		
224.0	21.0	70.0	15.3		
225.0	21.0	70.0	15.3		
226.0	21.0	70.5	15.4		
227.0	20.5	70.5	15.0		
228.0	20.5	70.5	15.0		
229.0	20.5	70.5	15.0		
230.0	20.5	70.5	15.0		
231.0	20.5	71.0	15.1		
232.0	20.5	70.5	15.0		
233.0	20.5	71.0	15.1		
234.0	20.5	71.0	15.1		
235.0	20.5	71.0	15.1		
236.0	20.5	71.0	15.1		
237.0	20.5	71.0	15.1		
238.0	20.5	71.5	15.2		
239.0	20.5	71.5	15.2		
240.0	20.5	71.5	15.2		
241.0	20.5	71.5	15.2		
242.0	20.5	71.5	15.2		
243.0	20.5	71.5	15.2		
244.0	20.5	71.5	15.2		
245.0	20.5	71.5	15.2		
246.0	20.5	71.5	15.2		
247.0	20.5	72.0	15.3		

248.0	20.5	72.0	15.3		
249.0	20.5	72.0	15.3		
250.0	20.5	72.0	15.3		
251.0	20.5	72.0	15.3		
252.0	20.5	72.0	15.3		
253.0	20.5	72.0	15.3		
254.0	20.5	72.0	15.3		
255.0	20.5	72.0	15.3		
256.0	20.5	72.0	15.3		
257.0	20.5	72.0	15.3		
258.0	20.5	72.0	15.3		
259.0	20.5	72.0	15.3		
260.0	20.5	72.5	15.4		
261.0	20.5	72.5	15.4		
262.0	20.5	72.5	15.4		
263.0	20.5	72.5	15.4		
264.0	20.5	73.0	15.5		
265.0	20.5	73.0	15.5		
266.0	20.5	73.0	15.5		
267.0	20.5	73.0	15.5		
268.0	20.5	73.0	15.5		
269.0	20.5	73.0	15.5		
270.0	20.5	73.0	15.5		
271.0	20.0	73.5	15.1		
272.0	20.0	73.5	15.1		
273.0	20.0	73.5	15.1		
274.0	20.0	73.5	15.1		
275.0	20.0	73.5	15.1		
276.0	20.0	74.0	15.2		
277.0	20.0	74.0	15.2		
278.0	20.0	74.0	15.2		
279.0	20.0	74.0	15.2		
280.0	20.0	74.0	15.2		
281.0	20.0	74.0	15.2		
282.0	20.0	74.0	15.2		
283.0	20.0	74.0	15.2		
284.0	20.0	74.5	15.3		
285.0	20.0	74.5	15.3		
286.0	20.0	74.5	15.3		
287.0	20.0	74.5	15.3		
288.0	20.0	74.5	15.3		
289.0	20.0	74.5	15.3		
290.0	20.0	74.5	15.3		
291.0	20.0	74.5	15.3		
292.0	20.0	74.5	15.3		
293.0	20.0	74.5	15.3		
294.0	20.0	74.5	15.3		
295.0	20.0	74.5	15.3		
296.0	20.0	74.5	15.3		
297.0	20.0	74.5	15.3		

298.0	20.0	75.0	15.4		
299.0	20.0	75.0	15.4		
300.0	20.0	75.0	15.4		
301.0	20.0	75.0	15.4		
302.0	20.0	75.0	15.4		
303.0	20.0	75.0	15.4		
304.0	20.0	75.5	15.5		
305.0	20.0	75.5	15.5		
306.0	20.0	75.5	15.5		
307.0	20.0	75.5	15.5		
308.0	20.0	75.5	15.5		
309.0	19.5	76.0	15.2		
310.0	19.5	76.5	15.3		
311.0	20.0	76.0	15.6		
312.0	19.5	76.5	15.3		
313.0	19.5	76.5	15.3		
314.0	19.5	76.5	15.3		
315.0	19.5	77.0	15.4		
316.0	19.5	76.5	15.3		
317.0	19.5	77.0	15.4		
318.0	19.5	77.0	15.4		
319.0	19.5	77.0	15.4		
320.0	19.5	77.0	15.4		
321.0	19.5	77.0	15.4		
322.0	20.0	77.0	15.8		
323.0	20.0	77.0	15.8		
324.0	20.0	76.5	15.7		
325.0	19.5	77.0	15.4		
326.0	19.5	77.0	15.4		
327.0	19.5	77.0	15.4		
328.0	19.5	77.0	15.4		
329.0	19.5	77.0	15.4		
330.0	19.5	77.0	15.4		
331.0	19.5	77.0	15.4		
332.0	19.5	77.0	15.4		
333.0	19.5	77.0	15.4		
334.0	19.5	77.5	15.5		
335.0	19.5	77.5	15.5		
336.0	19.5	78.0	15.6		
337.0	19.5	78.0	15.6		
338.0	19.5	77.5	15.5		
339.0	19.5	78.0	15.6		
340.0	19.5	78.0	15.6		
341.0	19.5	78.0	15.6		
342.0	19.5	78.0	15.6		
343.0	19.5	78.0	15.6		
344.0	19.5	78.0	15.6		
345.0	19.5	78.0	15.6		
346.0	19.5	78.0	15.6		
347.0	19.5	78.0	15.6		

348.0	19.5	78.0	15.6		
349.0	19.5	78.0	15.6		
350.0	19.5	78.0	15.6		
351.0	19.5	78.5	15.7		
352.0	19.5	78.5	15.7		
353.0	19.5	78.5	15.7		
354.0	19.5	78.0	15.6		
355.0	19.5	78.5	15.7		
356.0	19.5	78.5	15.7		
357.0	19.5	78.0	15.6		
358.0	19.5	78.0	15.6		
359.0	**19.5**	**78.0**	15.6		
360.0	19.5	79.0	15.8		
361.0	19.5	79.0	15.8		
362.0	19.5	79.0	15.8		
363.0	19.5	78.5	15.7		
364.0	19.5	79.0	15.8		
365.0	19.5	79.0	15.8		
366.0	19.5	79.0	15.8		
367.0	19.5	79.0	15.8		
368.0	19.5	79.0	15.8		
369.0	19.5	79.0	15.8		
370.0	19.5	79.0	15.8		
371.0	19.5	79.0	15.8		
372.0	19.5	79.0	15.8		
373.0	19.5	79.0	15.8		
374.0	19.5	79.0	15.8		
375.0	19.5	79.0	15.8		
376.0	19.5	79.0	15.8		
377.0	19.5	79.0	15.8		
378.0	19.5	79.0	15.8		
379.0	19.5	79.0	15.8		
380.0	19.5	79.0	15.8		
381.0	19.5	79.0	15.8		
382.0	19.5	79.0	15.8		
383.0	19.5	79.0	15.8		
384.0	19.5	79.0	15.8		
385.0	19.5	79.0	15.8		
386.0	19.5	79.0	15.8		
387.0	19.5	79.0	15.8		
388.0	19.5	79.0	15.8		
389.0	19.5	79.0	15.8		
390.0	19.5	79.0	15.8		
391.0	19.5	79.0	15.8		
392.0	19.5	79.0	15.8		
393.0	19.5	79.0	15.8		
394.0	19.5	79.0	15.8		
395.0	19.0	79.0	15.3		
396.0	19.0	79.5	15.4		
397.0	19.0	79.5	15.4		

398.0	19.0	79.5	15.4		
399.0	19.0	79.0	15.3		
400.0	19.0	79.5	15.4		
401.0	19.0	79.5	15.4		
402.0	19.0	79.5	15.4		
403.0	19.0	80.0	15.5		
404.0	19.0	80.0	15.5		
405.0	19.0	80.0	15.5		
406.0	19.0	79.5	15.4		
407.0	19.0	79.5	15.4		
408.0	19.0	79.5	15.4		
409.0	19.0	79.5	15.4		
410.0	19.0	80.0	15.5		
411.0	19.0	80.0	15.5		
412.0	19.0	80.0	15.5		
413.0	19.0	80.0	15.5		
414.0	19.0	80.5	15.6		
415.0	19.0	80.0	15.5		
416.0	19.0	79.5	15.4		
417.0	19.0	80.5	15.6		
418.0	19.0	80.0	15.5		
419.0	19.0	80.5	15.6		
420.0	19.0	80.0	15.5		
421.0	19.0	80.0	15.5		
422.0	19.0	80.5	15.6		
423.0	19.0	80.5	15.6		
424.0	19.0	80.0	15.5		
425.0	19.0	80.0	15.5		
426.0	19.0	80.5	15.6		
427.0	19.0	80.5	15.6		
428.0	18.5	80.5	15.1		
429.0	18.5	80.5	15.1		
430.0	18.5	81.0	15.2		
431.0	18.5	81.5	15.3		
432.0	18.5	81.0	15.2		
433.0	18.5	81.0	15.2		
434.0	18.5	81.0	15.2		
435.0	18.5	81.0	15.2		
436.0	18.5	81.0	15.2		
437.0	18.5	81.5	15.3		
438.0	18.5	81.5	15.3		
439.0	18.5	82.0	15.4		
440.0	18.5	82.0	15.4		
441.0	18.5	82.5	15.5		
442.0	18.5	82.5	15.5		
443.0	18.5	82.0	15.4		
444.0	18.5	82.0	15.4		
445.0	18.5	82.0	15.4		
446.0	18.5	82.0	15.4		
447.0	18.5	82.0	15.4		

448.0	18.5	82.0	15.4		
449.0	18.5	82.0	15.4		
450.0	18.5	82.0	15.4		
451.0	18.5	82.0	15.4		
452.0	18.5	82.0	15.4		
453.0	18.0	82.0	14.9		
454.0	18.0	82.5	15.0		
455.0	18.0	82.0	14.9		
456.0	18.0	82.5	15.0		
457.0	18.0	82.0	14.9		
458.0	18.0	82.0	14.9		
459.0	18.0	82.0	14.9		
460.0	18.0	82.0	14.9		
461.0	18.0	82.0	14.9		
462.0	18.0	82.5	15.0		
463.0	18.0	82.0	14.9		
464.0	18.0	82.0	14.9		
465.0	18.0	82.0	14.9		
466.0	18.0	82.5	15.0		
467.0	18.0	82.5	15.0		
468.0	18.0	82.0	14.9		
469.0	18.0	82.0	14.9		
470.0	18.0	82.0	14.9		
471.0	18.0	82.5	15.0		
472.0	18.0	82.5	15.0		
473.0	18.0	82.5	15.0		
474.0	18.0	82.5	15.0		
475.0	18.0	82.5	15.0		
476.0	18.0	82.5	15.0		
477.0	18.0	82.0	14.9		
478.0	18.0	82.0	14.9		
479.0	18.0	82.0	14.9		
480.0	18.0	82.5	15.0		
481.0	18.0	82.5	15.0		
482.0	18.0	82.5	15.0		
483.0	18.0	82.5	15.0		
484.0	18.0	82.5	15.0		
485.0	18.0	82.5	15.0		
486.0	18.0	83.0	15.1		
487.0	18.0	83.0	15.1		
488.0	18.0	82.5	15.0		
489.0	18.0	82.5	15.0		
490.0	18.0	82.5	15.0		
491.0	18.0	82.5	15.0		
492.0	18.0	82.5	15.0		
493.0	18.0	82.5	15.0		
494.0	18.0	82.5	15.0		
495.0	18.0	83.0	15.1		
496.0	18.0	82.5	15.0		
497.0	18.0	83.0	15.1		

498.0	18.0	83.5	15.2		
499.0	17.5	83.5	14.7		
500.0	17.5	83.5	14.7		
501.0	17.5	84.0	14.8		
502.0	17.5	84.0	14.8		
503.0	17.5	84.0	14.8		
504.0	17.5	83.5	14.7		
505.0	17.5	83.5	14.7		
506.0	17.5	83.5	14.7		
507.0	17.5	83.5	14.7		
508.0	17.5	84.0	14.8		
509.0	17.5	83.5	14.7		
510.0	17.5	83.5	14.7		
511.0	17.5	84.0	14.8		
512.0	17.5	84.0	14.8		
513.0	17.5	84.5	14.9		
514.0	17.5	84.5	14.9		
515.0	17.5	84.5	14.9		
516.0	17.5	84.0	14.8		
517.0	17.5	84.0	14.8		
518.0	17.5	84.0	14.8		
519.0	18.0	84.0	15.3		
520.0	18.0	83.5	15.2		
521.0	18.0	84.0	15.3		
522.0	18.0	83.5	15.2		
523.0	18.0	83.5	15.2		
524.0	18.0	83.5	15.2		
525.0	18.0	83.5	15.2		
526.0	18.0	83.5	15.2		
527.0	18.0	83.5	15.2		
528.0	18.0	83.5	15.2		
529.0	18.0	83.5	15.2		
530.0	18.0	83.5	15.2		
531.0	18.0	83.0	15.1		
532.0	18.0	83.5	15.2		
533.0	18.0	83.5	15.2		
534.0	18.0	83.5	15.2		
535.0	18.0	83.5	15.2		
536.0	18.0	83.5	15.2		
537.0	18.0	83.5	15.2		
538.0	18.0	83.5	15.2		
539.0	18.0	83.5	15.2		
540.0	**18.0**	**83.5**	15.2		
541.0	17.5	83.5	14.7		
542.0	17.5	83.5	14.7		
543.0	17.5	83.5	14.7		
544.0	17.5	83.5	14.7		
545.0	17.5	83.5	14.7		
546.0	17.5	83.5	14.7		
547.0	17.5	83.5	14.7		

548.0	17.5	83.5	14.7		
549.0	17.5	83.5	14.7		
550.0	17.5	83.5	14.7		
551.0	17.5	84.0	14.8		
552.0	17.5	83.5	14.7		
553.0	17.5	84.0	14.8		
554.0	17.5	83.5	14.7		
555.0	17.5	84.0	14.8		
556.0	17.5	84.0	14.8		
557.0	17.5	84.0	14.8		
558.0	17.5	84.0	14.8		
559.0	17.5	84.0	14.8		
560.0	17.5	84.0	14.8		
561.0	17.5	84.0	14.8		
562.0	17.5	84.5	14.9		
563.0	17.5	84.0	14.8		
564.0	17.5	84.0	14.8		
565.0	17.5	84.0	14.8		
566.0	17.5	84.0	14.8		
567.0	17.5	84.0	14.8		
568.0	17.5	84.5	14.9		
569.0	17.5	84.0	14.8		
570.0	17.5	84.0	14.8		
571.0	17.5	84.0	14.8		
572.0	17.5	84.0	14.8		
573.0	17.5	84.5	14.9		
574.0	17.5	84.0	14.8		
575.0	17.5	84.5	14.9		
576.0	17.5	84.0	14.8		
577.0	17.5	84.0	14.8		
578.0	17.5	84.0	14.8		
579.0	17.5	84.0	14.8		
580.0	17.5	84.0	14.8		
581.0	17.5	84.0	14.8		
582.0	17.5	84.0	14.8		
583.0	17.5	84.0	14.8		
584.0	17.5	84.0	14.8		
585.0	17.5	84.5	14.9		
586.0	17.5	84.5	14.9		
587.0	17.5	84.5	14.9		
588.0	17.5	85.0	15.0		
589.0	17.5	85.0	15.0		
590.0	17.5	85.0	15.0		
591.0	17.5	85.0	15.0		
592.0	17.5	85.0	15.0		
593.0	17.5	85.0	15.0		
594.0	17.0	85.0	14.5		
595.0	17.0	85.0	14.5		
596.0	17.0	85.0	14.5		
597.0	17.0	85.0	14.5		

598.0	17.0	85.0	14.5		
599.0	17.0	85.5	14.6		
600.0	17.0	85.5	14.6		
601.0	17.0	85.5	14.6		
602.0	17.0	85.5	14.6		
603.0	17.0	85.5	14.6		
604.0	17.0	86.0	14.6		
605.0	17.0	86.0	14.6		
606.0	17.0	86.0	14.6		
607.0	17.0	85.5	14.6		
608.0	17.0	86.0	14.6		
609.0	17.0	85.5	14.6		
610.0	17.0	85.5	14.6		
611.0	17.0	85.5	14.6		
612.0	17.0	85.5	14.6		
613.0	17.0	85.5	14.6		
614.0	17.0	85.5	14.6		
615.0	17.0	85.5	14.6		
616.0	17.0	85.5	14.6		
617.0	17.0	85.5	14.6		
618.0	17.0	85.5	14.6		
619.0	17.0	86.0	14.6		
620.0	17.0	86.0	14.6		
621.0	16.5	86.0	14.2		
622.0	16.5	86.0	14.2		
623.0	16.5	86.0	14.2		
624.0	16.5	86.0	14.2		
625.0	16.5	87.0	14.3		
626.0	16.5	86.0	14.2		
627.0	16.5	87.0	14.3		
628.0	16.5	87.0	14.3		
629.0	16.5	87.0	14.3		
630.0	16.5	87.0	14.3		
631.0	16.5	87.5	14.4		
632.0	16.5	87.5	14.4		
633.0	16.5	87.0	14.3		
634.0	16.5	87.0	14.3		
635.0	16.5	87.5	14.4		
636.0	16.5	87.5	14.4		
637.0	16.5	87.0	14.3		
638.0	16.5	87.0	14.3		
639.0	16.5	87.0	14.3		
640.0	16.5	87.0	14.3		
641.0	16.5	87.0	14.3		
642.0	16.5	87.0	14.3		
643.0	16.5	87.5	14.4		
644.0	16.5	87.0	14.3		
645.0	16.5	87.0	14.3		
646.0	16.5	87.0	14.3		
647.0	16.5	87.0	14.3		

648.0	16.5	87.0	14.3		
649.0	16.5	87.0	14.3		
650.0	16.5	87.0	14.3		
651.0	16.5	87.0	14.3		
652.0	16.5	87.0	14.3		
653.0	16.5	87.0	14.3		
654.0	16.5	87.0	14.3		
655.0	16.0	87.5	13.9		
656.0	16.0	87.5	13.9		
657.0	16.0	87.0	13.8		
658.0	16.0	87.0	13.8		
659.0	16.0	88.0	14.0		
660.0	16.0	88.0	14.0		
661.0	16.0	87.5	13.9		
662.0	16.0	87.5	13.9		
663.0	16.0	87.5	13.9		
664.0	16.0	87.5	13.9		
665.0	16.0	87.5	13.9		
666.0	16.0	88.0	14.0		
667.0	16.5	87.5	14.4		
668.0	16.5	88.0	14.5		
669.0	16.5	87.5	14.4		
670.0	16.5	87.5	14.4		
671.0	16.5	87.5	14.4		
672.0	16.5	87.5	14.4		
673.0	16.5	87.5	14.4		
674.0	16.5	87.5	14.4		
675.0	16.5	87.5	14.4		
676.0	16.5	87.0	14.3		
677.0	16.5	87.5	14.4		
678.0	16.5	87.0	14.3		
679.0	16.5	87.0	14.3		
680.0	16.5	87.0	14.3		
681.0	16.5	87.0	14.3		
682.0	16.5	87.0	14.3		
683.0	16.5	87.0	14.3		
684.0	16.5	87.0	14.3		
685.0	16.5	87.0	14.3		
686.0	16.5	87.0	14.3		
687.0	16.5	87.0	14.3		
688.0	16.5	86.5	14.2		
689.0	16.5	87.0	14.3		
690.0	16.5	86.5	14.2		
691.0	16.5	86.5	14.2		
692.0	16.5	86.0	14.2		
693.0	16.5	86.5	14.2		
694.0	16.5	86.0	14.2		
695.0	16.5	86.0	14.2		
696.0	16.5	86.0	14.2		
697.0	16.5	87.0	14.3		

698.0	16.5	86.0	14.2		
699.0	16.5	86.0	14.2		
700.0	16.5	87.0	14.3		
701.0	16.5	86.5	14.2		
702.0	16.5	86.5	14.2		
703.0	16.5	86.5	14.2		
704.0	16.5	86.0	14.2		
705.0	16.5	86.5	14.2		
706.0	16.5	86.5	14.2		
707.0	16.5	86.5	14.2		
708.0	16.0	86.5	13.7		
709.0	16.0	87.0	13.8		
710.0	16.0	87.5	13.9		
711.0	16.0	87.5	13.9		
712.0	16.0	87.0	13.8		
713.0	16.0	87.5	13.9		
714.0	16.0	87.5	13.9		
715.0	16.0	88.0	14.0		
716.0	16.0	88.0	14.0		
717.0	16.0	87.5	13.9		
718.0	16.0	87.5	13.9		
719.0	16.0	87.5	13.9		

Timecum	Temperature (13T)	Relative Humidity (13RH)	Dew Point (13DP)	Variables	Correlation coefficent
0.0	16.0	88.5	14.1	13T	0.7866812
1.0	16.0	87.5	13.9	13RH	-0.8062279
2.0	16.0	88.0	14.0	13DP	0.6506874
3.0	16.0	88.0	14.0		
4.0	16.0	87.5	13.9		
5.0	16.0	88.5	14.1		
6.0	16.0	88.5	14.1		
7.0	16.0	88.5	14.1		
8.0	16.0	88.5	14.1		
9.0	16.0	88.5	14.1		
10.0	16.0	88.5	14.1		
11.0	16.0	88.5	14.1		
12.0	16.0	88.5	14.1		
13.0	16.0	88.5	14.1		
14.0	16.0	88.5	14.1		
15.0	16.0	88.5	14.1		
16.0	16.0	88.0	14.0		
17.0	16.0	88.0	14.0		
18.0	16.0	88.0	14.0		
19.0	16.0	88.0	14.0		
20.0	16.0	88.0	14.0		
21.0	16.0	88.0	14.0		
22.0	16.0	88.5	14.1		
23.0	15.5	88.5	13.6		
24.0	15.5	88.0	13.5		
25.0	15.5	88.0	13.5		
26.0	15.5	88.0	13.5		
27.0	15.5	88.0	13.5		
28.0	15.5	88.5	13.6		
29.0	15.5	88.0	13.5		
30.0	15.5	88.0	13.5		
31.0	15.5	88.0	13.5		
32.0	15.5	88.0	13.5		
33.0	15.5	88.0	13.5		
34.0	15.5	88.0	13.5		
35.0	15.5	88.0	13.5		
36.0	15.5	88.0	13.5		
37.0	15.5	88.0	13.5		
38.0	15.5	88.5	13.6		
39.0	15.5	88.5	13.6		
40.0	15.5	88.5	13.6		
41.0	15.5	88.5	13.6		
42.0	15.5	88.5	13.6		
43.0	15.0	88.0	13.0		
44.0	15.0	88.0	13.0		
45.0	15.0	88.0	13.0		
46.0	15.0	88.0	13.0		
47.0	15.0	88.0	13.0		

48.0	15.0	88.0	13.0		
49.0	15.0	88.0	13.0		
50.0	15.0	89.0	13.2		
51.0	15.0	88.5	13.1		
52.0	15.0	89.0	13.2		
53.0	15.0	89.0	13.2		
54.0	15.0	89.0	13.2		
55.0	15.0	89.0	13.2		
56.0	15.0	89.0	13.2		
57.0	15.0	89.0	13.2		
58.0	15.0	89.0	13.2		
59.0	15.0	89.0	13.2		
60.0	15.0	89.0	13.2		
61.0	15.0	89.0	13.2		
62.0	15.0	89.0	13.2		
63.0	15.0	89.0	13.2		
64.0	15.0	89.5	13.3		
65.0	15.0	89.5	13.3		
66.0	15.0	89.5	13.3		
67.0	15.0	90.0	13.4		
68.0	15.0	90.0	13.4		
69.0	15.0	90.0	13.4		
70.0	15.0	90.0	13.4		
71.0	15.0	90.0	13.4		
72.0	15.0	90.0	13.4		
73.0	15.0	90.5	13.5		
74.0	15.0	91.0	13.5		
75.0	15.0	91.5	13.6		
76.0	15.0	91.0	13.5		
77.0	15.0	91.0	13.5		
78.0	15.0	91.5	13.6		
79.0	15.0	91.5	13.6		
80.0	15.5	91.5	14.1		
81.0	15.5	92.0	14.2		
82.0	15.5	91.5	14.1		
83.0	15.5	91.5	14.1		
84.0	15.5	91.0	14.0		
85.0	15.5	91.0	14.0		
86.0	15.5	91.5	14.1		
87.0	15.5	91.0	14.0		
88.0	15.5	91.0	14.0		
89.0	15.5	91.0	14.0		
90.0	16.0	91.0	14.5		
91.0	16.0	91.0	14.5		
92.0	16.0	91.0	14.5		
93.0	16.0	90.5	14.4		
94.0	16.0	90.5	14.4		
95.0	16.0	90.5	14.4		
96.0	16.0	90.0	14.4		
97.0	16.0	90.0	14.4		
98.0	16.0	90.0	14.4		

99.0	16.0	90.0	14.4		
100.0	16.5	90.0	14.9		
101.0	16.5	89.5	14.8		
102.0	16.5	89.0	14.7		
103.0	16.5	89.0	14.7		
104.0	16.5	89.0	14.7		
105.0	16.5	89.0	14.7		
106.0	16.5	89.0	14.7		
107.0	16.5	88.5	14.6		
108.0	16.5	88.5	14.6		
109.0	17.0	88.5	15.1		
110.0	17.0	88.5	15.1		
111.0	17.0	88.5	15.1		
112.0	17.0	88.0	15.0		
113.0	17.0	88.0	15.0		
114.0	17.0	88.0	15.0		
115.0	17.0	88.0	15.0		
116.0	17.0	88.0	15.0		
117.0	17.0	87.5	14.9		
118.0	17.0	87.5	14.9		
119.0	17.0	87.0	14.8		
120.0	17.5	86.5	15.2		
121.0	17.5	86.5	15.2		
122.0	17.5	86.5	15.2		
123.0	17.5	86.5	15.2		
124.0	17.5	86.5	15.2		
125.0	17.5	86.5	15.2		
126.0	17.5	85.5	15.0		
127.0	17.5	85.5	15.0		
128.0	17.5	85.5	15.0		
129.0	18.0	85.5	15.5		
130.0	18.0	85.0	15.4		
131.0	18.0	84.5	15.3		
132.0	18.0	84.5	15.3		
133.0	18.0	84.0	15.3		
134.0	18.0	84.0	15.3		
135.0	18.0	83.5	15.2		
136.0	18.0	83.5	15.2		
137.0	18.0	83.5	15.2		
138.0	18.0	83.5	15.2		
139.0	18.0	83.0	15.1		
140.0	18.0	83.0	15.1		
141.0	18.5	82.5	15.5		
142.0	18.5	82.5	15.5		
143.0	18.5	82.5	15.5		
144.0	18.5	82.0	15.4		
145.0	18.5	82.5	15.5		
146.0	18.5	82.5	15.5		
147.0	18.5	82.5	15.5		
148.0	18.5	82.5	15.5		
149.0	18.5	82.5	15.5		

150.0	18.5	82.0	15.4		
151.0	18.5	82.5	15.5		
152.0	18.5	82.0	15.4		
153.0	18.5	81.5	15.3		
154.0	18.5	81.5	15.3		
155.0	18.5	81.5	15.3		
156.0	19.0	81.5	15.8		
157.0	19.0	81.5	15.8		
158.0	19.0	81.5	15.8		
159.0	19.0	81.5	15.8		
160.0	19.0	81.5	15.8		
161.0	19.0	81.0	15.7		
162.0	19.0	81.0	15.7		
163.0	19.0	81.0	15.7		
164.0	19.0	81.0	15.7		
165.0	19.0	81.0	15.7		
166.0	19.0	80.5	15.6		
167.0	19.0	81.0	15.7		
168.0	19.5	80.5	16.1		
169.0	19.5	80.5	16.1		
170.0	19.5	81.0	16.2		
171.0	19.5	80.5	16.1		
172.0	19.5	80.0	16.0		
173.0	19.5	80.0	16.0		
174.0	19.5	80.5	16.1		
175.0	19.5	80.0	16.0		
176.0	19.5	79.5	15.9		
177.0	19.5	79.5	15.9		
178.0	19.5	79.5	15.9		
179.0	19.5	79.5	15.9		
180.0	**19.5**	**79.5**	15.9		
181.0	19.5	79.5	15.9		
182.0	19.5	79.5	15.9		
183.0	19.5	79.5	15.9		
184.0	19.5	79.5	15.9		
185.0	19.5	79.5	15.9		
186.0	19.5	80.0	16.0		
187.0	19.5	79.5	15.9		
188.0	19.5	79.5	15.9		
189.0	19.5	79.5	15.9		
190.0	19.5	79.5	15.9		
191.0	19.5	79.5	15.9		
192.0	19.5	79.5	15.9		
193.0	20.0	79.5	16.3		
194.0	20.0	79.5	16.3		
195.0	20.0	79.0	16.2		
196.0	20.0	79.0	16.2		
197.0	20.0	79.5	16.3		
198.0	20.0	79.5	16.3		
199.0	20.0	80.0	16.4		

200.0	20.0	79.0	16.2		
201.0	20.0	78.0	16.0		
202.0	20.0	78.0	16.0		
203.0	20.0	78.0	16.0		
204.0	20.5	78.0	16.5		
205.0	20.5	78.5	16.6		
206.0	20.5	78.0	16.5		
207.0	20.5	78.5	16.6		
208.0	20.5	78.0	16.5		
209.0	20.5	78.5	16.6		
210.0	20.5	77.5	16.4		
211.0	20.5	77.0	16.3		
212.0	20.5	77.5	16.4		
213.0	20.5	77.0	16.3		
214.0	21.0	77.5	16.9		
215.0	21.0	78.5	17.1		
216.0	21.0	78.0	17.0		
217.0	21.0	77.0	16.8		
218.0	21.0	77.0	16.8		
219.0	21.0	76.0	16.6		
220.0	21.0	76.0	16.6		
221.0	21.0	76.5	16.7		
222.0	21.0	76.0	16.6		
223.0	21.0	76.0	16.6		
224.0	21.0	76.0	16.6		
225.0	21.5	75.5	17.0		
226.0	21.5	75.5	17.0		
227.0	21.5	75.0	16.9		
228.0	21.5	75.0	16.9		
229.0	21.5	74.5	16.8		
230.0	21.5	75.0	16.9		
231.0	21.5	75.0	16.9		
232.0	21.5	75.0	16.9		
233.0	21.5	75.0	16.9		
234.0	21.5	75.0	16.9		
235.0	21.5	74.5	16.8		
236.0	21.5	74.0	16.7		
237.0	21.5	74.0	16.7		
238.0	21.5	74.0	16.7		
239.0	21.5	74.5	16.8		
240.0	21.5	74.0	16.7		
241.0	22.0	75.0	17.4		
242.0	22.0	74.0	17.2		
243.0	22.0	74.0	17.2		
244.0	22.0	74.0	17.2		
245.0	22.0	73.5	17.0		
246.0	22.0	74.0	17.2		
247.0	22.0	74.0	17.2		
248.0	22.0	74.0	17.2		
249.0	22.0	73.0	16.9		
250.0	22.0	73.0	16.9		

251.0	22.0	72.5	16.8		
252.0	22.0	73.0	16.9		
253.0	22.0	72.5	16.8		
254.0	22.0	73.0	16.9		
255.0	22.5	73.5	17.5		
256.0	22.5	72.5	17.3		
257.0	22.5	72.0	17.2		
258.0	22.5	73.0	17.4		
259.0	22.5	72.5	17.3		
260.0	22.5	72.5	17.3		
261.0	22.5	72.5	17.3		
262.0	22.5	72.5	17.3		
263.0	22.5	73.5	17.5		
264.0	22.5	71.5	17.1		
265.0	22.5	71.5	17.1		
266.0	23.0	71.5	17.6		
267.0	23.0	71.5	17.6		
268.0	22.5	71.5	17.1		
269.0	23.0	71.5	17.6		
270.0	23.0	71.5	17.6		
271.0	23.0	71.5	17.6		
272.0	23.0	72.0	17.7		
273.0	23.0	72.0	17.7		
274.0	23.0	72.0	17.7		
275.0	23.0	72.0	17.7		
276.0	23.0	72.0	17.7		
277.0	23.0	71.0	17.5		
278.0	23.0	70.5	17.3		
279.0	23.0	70.0	17.2		
280.0	23.0	70.0	17.2		
281.0	23.0	71.5	17.6		
282.0	23.0	71.5	17.6		
283.0	23.0	70.0	17.2		
284.0	23.0	70.5	17.3		
285.0	23.0	70.0	17.2		
286.0	23.0	70.5	17.3		
287.0	23.5	69.0	17.5		
288.0	23.5	69.5	17.6		
289.0	23.0	69.5	17.1		
290.0	23.0	69.0	17.0		
291.0	23.0	71.0	17.5		
292.0	23.5	70.0	17.7		
293.0	23.5	70.0	17.7		
294.0	23.5	70.0	17.7		
295.0	23.5	69.5	17.6		
296.0	23.5	68.5	17.4		
297.0	23.5	69.0	17.5		
298.0	23.5	68.5	17.4		
299.0	23.5	69.0	17.5		
300.0	23.5	67.0	17.0		
301.0	23.5	66.5	16.9		

302.0	23.5	68.0	17.3		
303.0	23.5	67.5	17.1		
304.0	23.5	68.0	17.3		
305.0	23.5	68.0	17.3		
306.0	23.5	68.5	17.4		
307.0	23.5	68.0	17.3		
308.0	23.5	69.0	17.5		
309.0	24.0	68.0	17.7		
310.0	24.0	67.0	17.5		
311.0	23.5	66.5	16.9		
312.0	23.5	66.5	16.9		
313.0	23.5	65.5	16.7		
314.0	23.5	66.5	16.9		
315.0	23.5	66.5	16.9		
316.0	23.5	66.0	16.8		
317.0	23.5	64.5	16.4		
318.0	23.5	66.0	16.8		
319.0	23.5	66.5	16.9		
320.0	23.5	66.5	16.9		
321.0	24.0	66.0	17.3		
322.0	23.5	66.0	16.8		
323.0	23.5	67.5	17.1		
324.0	23.5	68.0	17.3		
325.0	24.0	68.0	17.7		
326.0	24.0	68.5	17.8		
327.0	24.0	67.0	17.5		
328.0	24.0	66.5	17.4		
329.0	24.0	66.5	17.4		
330.0	24.0	65.5	17.1		
331.0	24.0	66.5	17.4		
332.0	24.0	65.5	17.1		
333.0	24.5	64.5	17.4		
334.0	24.5	64.5	17.4		
335.0	24.5	66.0	17.7		
336.0	24.5	64.5	17.4		
337.0	24.5	63.5	17.1		
338.0	24.5	63.0	17.0		
339.0	24.5	63.0	17.0		
340.0	24.5	63.0	17.0		
341.0	24.5	62.5	16.9		
342.0	24.5	62.0	16.7		
343.0	24.5	61.5	16.6		
344.0	24.5	62.0	16.7		
345.0	24.5	62.5	16.9		
346.0	24.5	63.0	17.0		
347.0	24.5	62.5	16.9		
348.0	24.5	63.5	17.1		
349.0	24.5	63.0	17.0		
350.0	24.5	63.0	17.0		
351.0	24.5	63.5	17.1		
352.0	24.5	63.5	17.1		

353.0	24.5	63.5	17.1		
354.0	24.5	62.5	16.9		
355.0	24.5	63.0	17.0		
356.0	24.5	60.5	16.4		
357.0	24.5	61.5	16.6		
358.0	24.5	61.5	16.6		
359.0	24.5	61.5	16.6		
360.0	**24.5**	**61.5**	16.6		
361.0	24.5	62.0	16.7		
362.0	24.5	63.5	17.1		
363.0	24.5	64.0	17.2		
364.0	24.5	60.5	16.4		
365.0	24.5	60.5	16.4		
366.0	24.5	61.5	16.6		
367.0	24.5	61.5	16.6		
368.0	24.5	61.5	16.6		
369.0	24.5	61.5	16.6		
370.0	24.5	62.5	16.9		
371.0	24.5	62.5	16.9		
372.0	24.5	63.5	17.1		
373.0	24.5	63.0	17.0		
374.0	24.5	63.5	17.1		
375.0	24.5	64.5	17.4		
376.0	24.5	64.0	17.2		
377.0	24.5	64.0	17.2		
378.0	24.5	64.5	17.4		
379.0	24.5	64.5	17.4		
380.0	24.5	64.0	17.2		
381.0	24.5	64.5	17.4		
382.0	25.0	63.5	17.6		
383.0	24.5	63.0	17.0		
384.0	24.5	63.5	17.1		
385.0	24.5	63.5	17.1		
386.0	24.5	64.0	17.2		
387.0	24.5	64.5	17.4		
388.0	24.5	64.5	17.4		
389.0	24.5	64.5	17.4		
390.0	24.5	64.5	17.4		
391.0	24.5	64.5	17.4		
392.0	24.5	64.0	17.2		
393.0	24.5	64.0	17.2		
394.0	24.5	65.0	17.5		
395.0	25.0	63.5	17.6		
396.0	25.0	63.5	17.6		
397.0	25.0	63.5	17.6		
398.0	25.0	64.0	17.7		
399.0	25.0	65.0	18.0		
400.0	25.0	65.0	18.0		
401.0	25.0	63.5	17.6		
402.0	25.0	63.5	17.6		

403.0	25.0	64.0	17.7		
404.0	25.0	63.5	17.6		
405.0	25.0	63.5	17.6		
406.0	25.0	64.5	17.8		
407.0	25.0	63.0	17.5		
408.0	25.0	63.0	17.5		
409.0	25.0	64.5	17.8		
410.0	25.0	63.0	17.5		
411.0	25.0	64.0	17.7		
412.0	25.0	62.5	17.3		
413.0	25.0	62.5	17.3		
414.0	25.5	62.0	17.7		
415.0	25.0	61.5	17.1		
416.0	25.0	61.5	17.1		
417.0	25.0	61.5	17.1		
418.0	25.0	62.0	17.2		
419.0	25.0	62.0	17.2		
420.0	25.0	62.0	17.2		
421.0	25.0	63.0	17.5		
422.0	25.0	61.5	17.1		
423.0	25.0	62.0	17.2		
424.0	25.0	61.5	17.1		
425.0	25.0	61.5	17.1		
426.0	25.5	61.5	17.6		
427.0	25.0	61.5	17.1		
428.0	25.5	61.5	17.6		
429.0	25.5	61.5	17.6		
430.0	25.5	61.5	17.6		
431.0	25.5	63.5	18.1		
432.0	25.5	61.0	17.4		
433.0	25.5	60.5	17.3		
434.0	25.5	60.5	17.3		
435.0	25.5	61.5	17.6		
436.0	25.5	61.0	17.4		
437.0	25.5	62.5	17.8		
438.0	25.5	61.0	17.4		
439.0	25.5	62.0	17.7		
440.0	25.0	61.5	17.1		
441.0	25.0	61.5	17.1		
442.0	25.0	61.0	17.0		
443.0	25.0	61.0	17.0		
444.0	25.0	61.0	17.0		
445.0	25.0	61.0	17.0		
446.0	25.0	60.5	16.8		
447.0	25.0	58.5	16.3		
448.0	25.0	58.5	16.3		
449.0	25.0	57.5	16.0		
450.0	25.5	58.5	16.8		
451.0	25.5	58.0	16.6		
452.0	25.5	57.5	16.5		
453.0	25.5	58.5	16.8		

454.0	25.5	57.5	16.5		
455.0	25.5	59.0	16.9		
456.0	25.5	57.5	16.5		
457.0	25.5	57.5	16.5		
458.0	25.5	58.0	16.6		
459.0	25.5	56.0	16.1		
460.0	25.5	55.0	15.8		
461.0	25.5	55.0	15.8		
462.0	25.5	56.5	16.2		
463.0	25.5	55.5	15.9		
464.0	25.5	56.5	16.2		
465.0	25.5	57.5	16.5		
466.0	25.5	58.0	16.6		
467.0	25.5	57.5	16.5		
468.0	25.5	57.5	16.5		
469.0	25.5	57.5	16.5		
470.0	25.5	58.0	16.6		
471.0	25.5	56.5	16.2		
472.0	25.5	56.5	16.2		
473.0	25.5	56.5	16.2		
474.0	25.5	57.0	16.4		
475.0	25.5	57.0	16.4		
476.0	25.5	56.5	16.2		
477.0	25.5	57.0	16.4		
478.0	25.5	57.5	16.5		
479.0	25.5	58.0	16.6		
480.0	25.5	58.5	16.8		
481.0	25.5	59.0	16.9		
482.0	25.5	56.5	16.2		
483.0	25.5	56.5	16.2		
484.0	25.5	57.5	16.5		
485.0	25.5	57.5	16.5		
486.0	25.5	58.5	16.8		
487.0	25.5	56.5	16.2		
488.0	25.5	57.5	16.5		
489.0	25.5	58.0	16.6		
490.0	25.5	57.0	16.4		
491.0	25.5	58.0	16.6		
492.0	25.5	58.0	16.6		
493.0	25.5	58.0	16.6		
494.0	25.5	58.0	16.6		
495.0	25.5	58.5	16.8		
496.0	25.5	58.0	16.6		
497.0	25.5	58.5	16.8		
498.0	25.5	58.5	16.8		
499.0	25.5	57.5	16.5		
500.0	25.5	57.5	16.5		
501.0	25.5	58.5	16.8		
502.0	25.5	57.0	16.4		
503.0	25.5	58.5	16.8		
504.0	25.5	57.5	16.5		

505.0	25.5	57.5	16.5		
506.0	25.5	57.0	16.4		
507.0	25.5	57.5	16.5		
508.0	25.5	57.5	16.5		
509.0	25.5	58.0	16.6		
510.0	25.5	58.5	16.8		
511.0	25.5	59.0	16.9		
512.0	25.5	59.0	16.9		
513.0	25.5	59.0	16.9		
514.0	25.5	59.0	16.9		
515.0	25.5	59.0	16.9		
516.0	25.5	58.5	16.8		
517.0	25.5	58.5	16.8		
518.0	25.5	59.5	17.0		
519.0	25.5	59.0	16.9		
520.0	25.5	59.0	16.9		
521.0	25.5	59.5	17.0		
522.0	25.5	60.0	17.2		
523.0	25.5	59.5	17.0		
524.0	25.5	59.5	17.0		
525.0	25.5	60.0	17.2		
526.0	25.5	60.5	17.3		
527.0	25.5	59.0	16.9		
528.0	25.5	58.5	16.8		
529.0	25.5	58.5	16.8		
530.0	25.5	58.0	16.6		
531.0	25.5	58.5	16.8		
532.0	25.5	59.5	17.0		
533.0	25.5	60.0	17.2		
534.0	25.5	59.5	17.0		
535.0	25.5	59.0	16.9		
536.0	25.5	58.5	16.8		
537.0	25.5	58.0	16.6		
538.0	25.5	58.0	16.6		
539.0	25.5	58.5	16.8		
540.0	**25.5**	**59.5**	17.0		
541.0	25.5	58.5	16.8		
542.0	25.5	58.5	16.8		
543.0	25.5	58.5	16.8		
544.0	25.5	58.5	16.8		
545.0	25.5	59.0	16.9		
546.0	25.5	58.5	16.8		
547.0	25.5	57.5	16.5		
548.0	25.5	58.5	16.8		
549.0	25.5	59.5	17.0		
550.0	25.5	58.5	16.8		
551.0	25.5	59.0	16.9		
552.0	25.5	59.0	16.9		
553.0	25.5	59.0	16.9		
554.0	25.5	60.0	17.2		

555.0	25.5	59.5	17.0		
556.0	25.5	59.0	16.9		
557.0	25.5	59.0	16.9		
558.0	25.5	59.0	16.9		
559.0	25.5	59.5	17.0		
560.0	25.5	59.5	17.0		
561.0	25.5	59.5	17.0		
562.0	25.5	59.0	16.9		
563.0	25.5	59.0	16.9		
564.0	25.5	60.0	17.2		
565.0	25.5	60.0	17.2		
566.0	25.5	59.5	17.0		
567.0	25.5	59.0	16.9		
568.0	25.5	59.5	17.0		
569.0	25.5	59.5	17.0		
570.0	25.5	59.5	17.0		
571.0	25.5	59.5	17.0		
572.0	25.5	59.5	17.0		
573.0	25.5	59.5	17.0		
574.0	25.5	59.5	17.0		
575.0	25.5	59.5	17.0		
576.0	25.5	59.0	16.9		
577.0	25.0	59.0	16.4		
578.0	25.0	60.0	16.7		
579.0	25.0	60.0	16.7		
580.0	25.0	60.0	16.7		
581.0	25.0	59.5	16.6		
582.0	25.0	60.5	16.8		
583.0	25.0	60.5	16.8		
584.0	25.0	60.5	16.8		
585.0	25.0	60.5	16.8		
586.0	25.0	60.5	16.8		
587.0	25.0	61.0	17.0		
588.0	25.0	62.0	17.2		
589.0	25.0	61.0	17.0		
590.0	25.0	61.5	17.1		
591.0	25.0	61.0	17.0		
592.0	25.0	61.0	17.0		
593.0	25.0	61.5	17.1		
594.0	25.0	62.5	17.3		
595.0	25.0	62.0	17.2		
596.0	25.0	62.5	17.3		
597.0	25.0	62.5	17.3		
598.0	25.0	62.5	17.3		
599.0	25.0	62.0	17.2		
600.0	24.5	62.5	16.9		
601.0	24.5	63.0	17.0		
602.0	24.5	63.0	17.0		
603.0	24.5	63.5	17.1		
604.0	24.5	63.5	17.1		
605.0	24.5	63.0	17.0		

606.0	24.5	64.0	17.2		
607.0	24.5	64.0	17.2		
608.0	24.5	63.5	17.1		
609.0	24.5	63.5	17.1		
610.0	24.5	64.0	17.2		
611.0	24.5	63.5	17.1		
612.0	24.5	64.0	17.2		
613.0	24.5	63.5	17.1		
614.0	24.5	63.5	17.1		
615.0	24.5	63.5	17.1		
616.0	24.5	63.5	17.1		
617.0	24.0	63.5	16.6		
618.0	24.0	64.0	16.8		
619.0	24.0	64.0	16.8		
620.0	24.0	63.5	16.6		
621.0	24.0	64.0	16.8		
622.0	24.0	64.0	16.8		
623.0	24.0	64.0	16.8		
624.0	24.0	64.0	16.8		
625.0	24.0	64.0	16.8		
626.0	24.0	64.5	16.9		
627.0	24.0	64.5	16.9		
628.0	24.0	64.5	16.9		
629.0	24.0	64.5	16.9		
630.0	24.0	64.5	16.9		
631.0	24.0	64.5	16.9		
632.0	24.0	64.5	16.9		
633.0	24.0	65.0	17.0		
634.0	23.5	65.0	16.5		
635.0	23.5	64.5	16.4		
636.0	23.5	64.5	16.4		
637.0	23.5	64.5	16.4		
638.0	23.5	64.5	16.4		
639.0	23.5	64.5	16.4		
640.0	23.5	65.0	16.5		
641.0	23.5	65.0	16.5		
642.0	23.5	66.0	16.8		
643.0	23.5	65.5	16.7		
644.0	23.5	66.0	16.8		
645.0	23.5	66.0	16.8		
646.0	23.5	66.0	16.8		
647.0	23.5	66.5	16.9		
648.0	23.5	66.0	16.8		
649.0	23.5	66.5	16.9		
650.0	23.5	66.5	16.9		
651.0	23.5	66.5	16.9		
652.0	23.5	66.5	16.9		
653.0	23.5	67.0	17.0		
654.0	23.0	66.5	16.4		
655.0	23.0	67.0	16.5		
656.0	23.0	67.0	16.5		

657.0	23.0	67.0	16.5		
658.0	23.0	67.0	16.5		
659.0	23.0	67.5	16.7		
660.0	23.0	67.0	16.5		
661.0	23.0	67.5	16.7		
662.0	23.0	67.5	16.7		
663.0	23.0	67.5	16.7		
664.0	23.0	67.5	16.7		
665.0	23.0	67.5	16.7		
666.0	23.0	67.5	16.7		
667.0	23.0	67.0	16.5		
668.0	23.0	67.5	16.7		
669.0	23.0	67.0	16.5		
670.0	23.0	67.5	16.7		
671.0	23.0	67.5	16.7		
672.0	23.0	67.5	16.7		
673.0	22.5	68.0	16.3		
674.0	22.5	68.0	16.3		
675.0	22.5	67.5	16.2		
676.0	22.5	68.0	16.3		
677.0	22.5	68.5	16.4		
678.0	22.5	68.0	16.3		
679.0	22.5	68.0	16.3		
680.0	22.5	68.0	16.3		
681.0	22.5	68.5	16.4		
682.0	22.5	68.5	16.4		
683.0	22.5	68.5	16.4		
684.0	22.5	69.0	16.5		
685.0	22.5	69.0	16.5		
686.0	22.5	69.0	16.5		
687.0	22.5	69.5	16.6		
688.0	22.5	69.5	16.6		
689.0	22.5	69.5	16.6		
690.0	22.5	69.5	16.6		
691.0	22.0	70.0	16.3		
692.0	22.0	70.0	16.3		
693.0	22.0	70.0	16.3		
694.0	22.0	70.0	16.3		
695.0	22.0	70.0	16.3		
696.0	22.0	70.5	16.4		
697.0	22.0	70.5	16.4		
698.0	22.0	70.5	16.4		
699.0	22.0	70.5	16.4		
700.0	22.0	70.5	16.4		
701.0	22.0	70.5	16.4		
702.0	22.0	70.5	16.4		
703.0	22.0	71.0	16.5		
704.0	22.0	71.0	16.5		
705.0	22.0	71.0	16.5		
706.0	22.0	71.0	16.5		
707.0	22.0	71.0	16.5		

708.0	22.0	71.0	16.5		
709.0	22.0	71.0	16.5		
710.0	22.0	71.5	16.6		
711.0	22.0	71.5	16.6		
712.0	22.0	71.5	16.6		
713.0	22.0	72.0	16.7		
714.0	22.0	72.0	16.7		
715.0	21.5	72.0	16.2		
716.0	21.5	72.0	16.2		
717.0	21.5	72.5	16.3		
718.0	21.5	72.5	16.3		
719.0	21.5	72.5	16.3		

Timecum	Temperature (14T)	Relative Humidity (14RH)	Dew Point (14DP)	Variables	Correlation coefficent
0	21.5	72.5	16.3	14T	-0.9848626
1	21.5	72.5	16.3	14RH	0.9341942
2	21.5	73	16.5	14DP	-0.984206
3	21.5	73	16.5		
4	21.5	73.5	16.6		
5	21.5	73.5	16.6		
6	21.5	73.5	16.6		
7	21.5	73.5	16.6		
8	21.5	73.5	16.6		
9	21.5	74	16.7		
10	21.5	74	16.7		
11	21.5	74	16.7		
12	21.5	74	16.7		
13	21.5	74.5	16.8		
14	21.5	75	16.9		
15	21.5	75	16.9		
16	21.5	75	16.9		
17	21.5	75	16.9		
18	21.5	75.5	17		
19	21.5	75.5	17		
20	21.5	75.5	17		
21	21.5	75.5	17		
22	21.5	75.5	17		
23	21.5	75.5	17		
24	21.5	76	17.1		
25	21.5	76	17.1		
26	21.5	76	17.1		
27	21.5	76	17.1		
28	21.5	76	17.1		
29	21.5	76	17.1		
30	21.5	76.5	17.2		
31	21.5	76.5	17.2		
32	21.5	76.5	17.2		
33	21.5	76.5	17.2		
34	21.5	76.5	17.2		
35	21.5	76.5	17.2		
36	21.5	76.5	17.2		
37	21.5	76.5	17.2		
38	21	76.5	16.7		
39	21	77	16.8		
40	21	77	16.8		
41	21	77.5	16.9		
42	21	77.5	16.9		
43	21	77.5	16.9		
44	21	77.5	16.9		
45	21	77.5	16.9		
46	21	78	17		

47	21	77.5	16.9		
48	21	78	17		
49	21	77.5	16.9		
50	21	78	17		
51	21	78	17		
52	21	78	17		
53	21	78.5	17.1		
54	21	78.5	17.1		
55	21	78.5	17.1		
56	21	78	17		
57	21	78	17		
58	21	78.5	17.1		
59	21	78	17		
60	21	78.5	17.1		
61	21	78.5	17.1		
62	21	78.5	17.1		
63	21	78.5	17.1		
64	21	78.5	17.1		
65	21	78.5	17.1		
66	21	78.5	17.1		
67	21	78.5	17.1		
68	21	78.5	17.1		
69	21	78.5	17.1		
70	21	78.5	17.1		
71	21	79	17.2		
72	21	79	17.2		
73	21	79	17.2		
74	21	79	17.2		
75	21	79	17.2		
76	21	79	17.2		
77	21	79.5	17.3		
78	20.5	79.5	16.8		
79	20.5	79.5	16.8		
80	20.5	79.5	16.8		
81	20.5	79.5	16.8		
82	20.5	80	16.9		
83	20.5	79.5	16.8		
84	20.5	80	16.9		
85	20.5	80	16.9		
86	20.5	80	16.9		
87	20.5	80	16.9		
88	20.5	80	16.9		
89	20.5	80	16.9		
90	20.5	80	16.9		
91	20.5	80.5	17		
92	20.5	80	16.9		
93	20.5	80	16.9		
94	20.5	80.5	17		
95	20.5	80.5	17		
96	20.5	80.5	17		

97	20.5	80.5	17		
98	20.5	80.5	17		
99	20.5	80.5	17		
100	20.5	80	16.9		
101	20.5	80	16.9		
102	20.5	80.5	17		
103	20.5	80.5	17		
104	20.5	80.5	17		
105	20.5	80.5	17		
106	20.5	80.5	17		
107	20	80.5	16.5		
108	20	80.5	16.5		
109	20	80.5	16.5		
110	20	80.5	16.5		
111	20	81	16.6		
112	20	81	16.6		
113	20	81	16.6		
114	20	81	16.6		
115	20	81	16.6		
116	20	81	16.6		
117	20	81	16.6		
118	20	81.5	16.7		
119	20	81	16.6		
120	20	81	16.6		
121	20	81	16.6		
122	20	81	16.6		
123	20	80.5	16.5		
124	20	80.5	16.5		
125	20	80.5	16.5		
126	20	80.5	16.5		
127	20	81	16.6		
128	20	81	16.6		
129	20	80.5	16.5		
130	20	81	16.6		
131	20	81	16.6		
132	20	81	16.6		
133	20	81	16.6		
134	20	81	16.6		
135	20	81	16.6		
136	20	81	16.6		
137	20	81	16.6		
138	20	81	16.6		
139	20	81	16.6		
140	20	81	16.6		
141	20	81	16.6		
142	20	81	16.6		
143	20	81.5	16.7		
144	20	81.5	16.7		
145	20	81.5	16.7		
146	20	81.5	16.7		

147	20	81	16.6		
148	20	81	16.6		
149	20	81	16.6		
150	20	81	16.6		
151	19.5	81	16.2		
152	19.5	81	16.2		
153	19.5	81	16.2		
154	19.5	81	16.2		
155	19.5	81	16.2		
156	19.5	81	16.2		
157	19.5	81	16.2		
158	19.5	81	16.2		
159	19.5	80.5	16.1		
160	19.5	80.5	16.1		
161	19.5	80.5	16.1		
162	19.5	80.5	16.1		
163	19.5	80.5	16.1		
164	19.5	80.5	16.1		
165	19.5	80.5	16.1		
166	19.5	80.5	16.1		
167	19.5	80.5	16.1		
168	19.5	80.5	16.1		
169	19.5	80.5	16.1		
170	19.5	80.5	16.1		
171	19.5	80.5	16.1		
172	19.5	81	16.2		
173	19.5	80.5	16.1		
174	19.5	81	16.2		
175	19.5	81	16.2		
176	19.5	81	16.2		
177	19.5	81	16.2		
178	19.5	81.5	16.2		
179	19.5	81.5	16.2		
180	**19.5**	**81**	16.2		
181	19.5	81.5	16.2		
182	19.5	81.5	16.2		
183	19.5	81.5	16.2		
184	19.5	81	16.2		
185	19.5	81	16.2		
186	19.5	81.5	16.2		
187	19.5	81.5	16.2		
188	19.5	81.5	16.2		
189	19.5	81.5	16.2		
190	19.5	81.5	16.2		
191	19.5	81.5	16.2		
192	19.5	81.5	16.2		
193	19.5	81.5	16.2		
194	19.5	81	16.2		
195	19.5	81	16.2		
196	19.5	81	16.2		

197	19	81	15.7		
198	19	81	15.7		
199	19	81	15.7		
200	19	81.5	15.8		
201	19	81.5	15.8		
202	19	81.5	15.8		
203	19	81.5	15.8		
204	19	81.5	15.8		
205	19	81.5	15.8		
206	19	81.5	15.8		
207	19	81.5	15.8		
208	19	81.5	15.8		
209	19	81.5	15.8		
210	19	82	15.9		
211	19	82	15.9		
212	19	82	15.9		
213	19	82	15.9		
214	19	82	15.9		
215	19	82	15.9		
216	19	82	15.9		
217	19	82	15.9		
218	19	82	15.9		
219	19	82	15.9		
220	19	82	15.9		
221	19	82.5	16		
222	19	82.5	16		
223	19	82.5	16		
224	19	82.5	16		
225	19	82	15.9		
226	19	82.5	16		
227	19	82.5	16		
228	19	82	15.9		
229	19	82.5	16		
230	19	82.5	16		
231	19	82	15.9		
232	19	82.5	16		
233	19	82.5	16		
234	19	83	16		
235	19	82.5	16		
236	19	82.5	16		
237	19	83	16		
238	19	83	16		
239	19	83	16		
240	19	82.5	16		
241	19	82.5	16		
242	19	82.5	16		
243	19	82.5	16		
244	19	82.5	16		
245	19	82.5	16		
246	19	82.5	16		

247	18.5	82.5	15.5		
248	18.5	82.5	15.5		
249	18.5	82.5	15.5		
250	18.5	82.5	15.5		
251	18.5	82.5	15.5		
252	18.5	82.5	15.5		
253	18.5	82.5	15.5		
254	18.5	82.5	15.5		
255	18.5	82.5	15.5		
256	18.5	82.5	15.5		
257	18.5	83	15.6		
258	18.5	82.5	15.5		
259	18.5	83	15.6		
260	18.5	83	15.6		
261	18.5	83	15.6		
262	18.5	83	15.6		
263	18.5	82.5	15.5		
264	18.5	83	15.6		
265	18.5	82.5	15.5		
266	18.5	83	15.6		
267	18.5	83	15.6		
268	18.5	83	15.6		
269	18.5	83	15.6		
270	18.5	83	15.6		
271	18.5	83	15.6		
272	18.5	83.5	15.7		
273	18.5	83	15.6		
274	18.5	83.5	15.7		
275	18.5	83	15.6		
276	18.5	83.5	15.7		
277	18.5	83	15.6		
278	18.5	83	15.6		
279	18.5	83	15.6		
280	18.5	83	15.6		
281	18.5	83.5	15.7		
282	18.5	83.5	15.7		
283	18.5	83.5	15.7		
284	18.5	83.5	15.7		
285	18.5	83	15.6		
286	18.5	83.5	15.7		
287	18.5	83.5	15.7		
288	18.5	83.5	15.7		
289	18.5	83.5	15.7		
290	18.5	83.5	15.7		
291	18.5	83.5	15.7		
292	18.5	83.5	15.7		
293	18.5	83.5	15.7		
294	18.5	83.5	15.7		
295	18.5	83.5	15.7		
296	18.5	83.5	15.7		

297	18.5	83.5	15.7		
298	18.5	83.5	15.7		
299	18.5	83.5	15.7		
300	18.5	83.5	15.7		
301	18.5	83.5	15.7		
302	18.5	83.5	15.7		
303	18.5	83.5	15.7		
304	18.5	83.5	15.7		
305	18.5	83.5	15.7		
306	18.5	83.5	15.7		
307	18.5	83.5	15.7		
308	18.5	83.5	15.7		
309	18.5	83.5	15.7		
310	18.5	83.5	15.7		
311	18.5	83.5	15.7		
312	18	83.5	15.2		
313	18	83.5	15.2		
314	18	83.5	15.2		
315	18	83.5	15.2		
316	18	83.5	15.2		
317	18	83.5	15.2		
318	18	83.5	15.2		
319	18	83.5	15.2		
320	18	83.5	15.2		
321	18	83.5	15.2		
322	18	84	15.3		
323	18	84	15.3		
324	18	83.5	15.2		
325	18	84	15.3		
326	18	84	15.3		
327	18	83.5	15.2		
328	18	84	15.3		
329	18	84	15.3		
330	18	84	15.3		
331	18	84	15.3		
332	18	84	15.3		
333	18	84	15.3		
334	18	84	15.3		
335	18	84	15.3		
336	18	84	15.3		
337	18	84	15.3		
338	18	84	15.3		
339	18	84	15.3		
340	18	84	15.3		
341	18	84	15.3		
342	18	84	15.3		
343	18	84	15.3		
344	18	84	15.3		
345	18	84	15.3		
346	18	84	15.3		

347	18	84	15.3		
348	18	84	15.3		
349	18	84	15.3		
350	18	84	15.3		
351	18	84	15.3		
352	18	84	15.3		
353	18	84	15.3		
354	18	84	15.3		
355	18	84	15.3		
356	18	84	15.3		
357	18	84	15.3		
358	18	84	15.3		
359	18	84	15.3		
360	**18**	**84**	15.3		
361	18	84	15.3		
362	18	84	15.3		
363	18	84	15.3		
364	18	84	15.3		
365	18	84	15.3		
366	18	84	15.3		
367	18	84.5	15.3		
368	18	84	15.3		
369	18	84.5	15.3		
370	18	84.5	15.3		
371	18	84.5	15.3		
372	18	84	15.3		
373	18	84.5	15.3		
374	18	84.5	15.3		
375	18	84.5	15.3		
376	18	84.5	15.3		
377	18	84.5	15.3		
378	18	84.5	15.3		
379	17.5	85	15		
380	17.5	84.5	14.9		
381	17.5	84.5	14.9		
382	17.5	84.5	14.9		
383	17.5	85	15		
384	17.5	84.5	14.9		
385	17.5	84.5	14.9		
386	17.5	84.5	14.9		
387	17.5	85	15		
388	17.5	84.5	14.9		
389	17.5	84.5	14.9		
390	17.5	84.5	14.9		
391	17.5	84.5	14.9		
392	17.5	84.5	14.9		
393	17.5	85	15		
394	17.5	84.5	14.9		
395	17.5	84.5	14.9		
396	17.5	84.5	14.9		

397	17.5	84.5	14.9		
398	17.5	84.5	14.9		
399	17.5	84.5	14.9		
400	17.5	84.5	14.9		
401	17.5	84.5	14.9		
402	17.5	84.5	14.9		
403	17.5	84.5	14.9		
404	17.5	84.5	14.9		
405	17.5	84.5	14.9		
406	17.5	84.5	14.9		
407	17.5	84.5	14.9		
408	17.5	85	15		
409	17.5	85	15		
410	17.5	85	15		
411	17.5	85	15		
412	17.5	85	15		
413	17.5	85	15		
414	17.5	85	15		
415	17.5	85	15		
416	17.5	85	15		
417	17.5	85	15		
418	17.5	85	15		
419	17.5	85	15		
420	17.5	85	15		
421	17.5	85	15		
422	17.5	85	15		
423	17.5	85	15		
424	17.5	85	15		
425	17.5	85	15		
426	17.5	85	15		
427	17.5	85	15		
428	17.5	85	15		
429	17.5	85	15		
430	17.5	85.5	15		
431	17.5	85.5	15		
432	17.5	85.5	15		
433	17.5	85.5	15		
434	17.5	85.5	15		
435	17	85.5	14.6		
436	17	85.5	14.6		
437	17	85.5	14.6		
438	17	85.5	14.6		
439	17	85.5	14.6		
440	17	85.5	14.6		
441	17	85.5	14.6		
442	17	85.5	14.6		
443	17	85.5	14.6		
444	17	85.5	14.6		
445	17	86	14.6		
446	17	85.5	14.6		

447	17	86	14.6		
448	17	86	14.6		
449	17	86	14.6		
450	17	86	14.6		
451	17	86	14.6		
452	17	86	14.6		
453	17	86	14.6		
454	17	86	14.6		
455	17	86	14.6		
456	17	86	14.6		
457	17	86	14.6		
458	17	86	14.6		
459	17	86	14.6		
460	17	86	14.6		
461	17	86	14.6		
462	17	86	14.6		
463	17	86	14.6		
464	17	85.5	14.6		
465	17	86	14.6		
466	17	86	14.6		
467	17	86	14.6		
468	17	86	14.6		
469	17	86	14.6		
470	17	86	14.6		
471	17	86	14.6		
472	17	86	14.6		
473	17	86	14.6		
474	17	86	14.6		
475	17	86	14.6		
476	17	86	14.6		
477	17	86	14.6		
478	17	86	14.6		
479	17	86	14.6		
480	17	86	14.6		
481	17	86	14.6		
482	17	86	14.6		
483	17	86	14.6		
484	17	86	14.6		
485	17	86	14.6		
486	17	86	14.6		
487	17	86	14.6		
488	17	86	14.6		
489	17	86	14.6		
490	17	85.5	14.6		
491	17	85.5	14.6		
492	17	86	14.6		
493	17	85.5	14.6		
494	17	85.5	14.6		
495	17	85.5	14.6		
496	17	85.5	14.6		

497	17	85.5	14.6		
498	16.5	85.5	14.1		
499	16.5	85.5	14.1		
500	17	85.5	14.6		
501	16.5	85.5	14.1		
502	16.5	85.5	14.1		
503	16.5	85.5	14.1		
504	16.5	85.5	14.1		
505	16.5	85.5	14.1		
506	16.5	85.5	14.1		
507	16.5	85.5	14.1		
508	16.5	85.5	14.1		
509	16.5	85.5	14.1		
510	16.5	85.5	14.1		
511	16.5	85.5	14.1		
512	16.5	85.5	14.1		
513	16.5	85.5	14.1		
514	16.5	85.5	14.1		
515	16.5	85.5	14.1		
516	16.5	85	14		
517	16.5	85.5	14.1		
518	16.5	85.5	14.1		
519	16.5	85.5	14.1		
520	16.5	85.5	14.1		
521	16.5	85.5	14.1		
522	16.5	85.5	14.1		
523	16.5	85	14		
524	16.5	85	14		
525	16.5	85	14		
526	16.5	85.5	14.1		
527	16.5	85.5	14.1		
528	16.5	85	14		
529	16.5	85	14		
530	16.5	85.5	14.1		
531	16.5	85.5	14.1		
532	16.5	85.5	14.1		
533	16.5	85.5	14.1		
534	16.5	85.5	14.1		
535	16.5	85.5	14.1		
536	16.5	85.5	14.1		
537	16.5	85.5	14.1		
538	16.5	85.5	14.1		
539	16.5	85.5	14.1		
540	**16.5**	**85.5**	14.1		
541	16.5	85.5	14.1		
542	16.5	85.5	14.1		
543	16.5	85.5	14.1		
544	16.5	85.5	14.1		
545	16.5	85.5	14.1		
546	16.5	85.5	14.1		

547	16.5	85.5	14.1		
548	16.5	85.5	14.1		
549	16.5	85.5	14.1		
550	16.5	85.5	14.1		
551	16.5	85.5	14.1		
552	16.5	85.5	14.1		
553	16.5	85.5	14.1		
554	16.5	85.5	14.1		
555	16.5	85.5	14.1		
556	16.5	85.5	14.1		
557	16.5	85	14		
558	16.5	85	14		
559	16.5	85.5	14.1		
560	16.5	85	14		
561	16.5	85	14		
562	16.5	85.5	14.1		
563	16.5	85.5	14.1		
564	16.5	85.5	14.1		
565	16.5	85.5	14.1		
566	16.5	85.5	14.1		
567	16.5	85.5	14.1		
568	16.5	85.5	14.1		
569	16.5	85.5	14.1		
570	16.5	85.5	14.1		
571	16.5	85.5	14.1		
572	16.5	85.5	14.1		
573	16.5	85.5	14.1		
574	16.5	85.5	14.1		
575	16.5	85.5	14.1		
576	16.5	85.5	14.1		
577	16.5	85.5	14.1		
578	16.5	85.5	14.1		
579	16.5	85.5	14.1		
580	16.5	85.5	14.1		
581	16.5	85.5	14.1		
582	16.5	85.5	14.1		
583	16.5	85.5	14.1		
584	16.5	85.5	14.1		
585	16.5	85.5	14.1		
586	16.5	85.5	14.1		
587	16.5	85.5	14.1		
588	16.5	85.5	14.1		
589	16.5	85.5	14.1		
590	16.5	85.5	14.1		
591	16.5	85.5	14.1		
592	16.5	85.5	14.1		
593	16.5	85.5	14.1		
594	16.5	86	14.2		
595	16.5	86	14.2		
596	16.5	86	14.2		

597	16.5	86	14.2		
598	16.5	86	14.2		
599	16	86	13.7		
600	16	86	13.7		
601	16	86	13.7		
602	16	86	13.7		
603	16	86	13.7		
604	16	86	13.7		
605	16	86	13.7		
606	16	86	13.7		
607	16	86	13.7		
608	16	86	13.7		
609	16	86	13.7		
610	16	86	13.7		
611	16	86	13.7		
612	16	86	13.7		
613	16	86	13.7		
614	16	86	13.7		
615	16	86.5	13.7		
616	16	86.5	13.7		
617	16	86.5	13.7		
618	16	86.5	13.7		
619	16	86.5	13.7		
620	16	86	13.7		
621	16	86	13.7		
622	16	86.5	13.7		
623	16	86.5	13.7		
624	16	86.5	13.7		
625	16	86.5	13.7		
626	16	86.5	13.7		
627	16	86.5	13.7		
628	16	86.5	13.7		
629	16	86.5	13.7		
630	16	86.5	13.7		
631	16	86.5	13.7		
632	16	86.5	13.7		
633	16	86.5	13.7		
634	16	87	13.8		
635	16	86.5	13.7		
636	16	87	13.8		
637	16	87	13.8		
638	16	87	13.8		
639	16	87	13.8		
640	16	87	13.8		
641	16	87	13.8		
642	16	87	13.8		
643	16	87	13.8		
644	16	87	13.8		
645	16	87	13.8		
646	16	87	13.8		

647	16	87	13.8		
648	16	87	13.8		
649	16	87	13.8		
650	16	87	13.8		
651	16	87	13.8		
652	16	87	13.8		
653	16	87	13.8		
654	16	87	13.8		
655	16	87	13.8		
656	16	87	13.8		
657	16	87	13.8		
658	16	87	13.8		
659	16	87	13.8		
660	16	87	13.8		
661	16	87	13.8		
662	16	87	13.8		
663	16	87	13.8		
664	16	87	13.8		
665	16	87	13.8		
666	16	87	13.8		
667	16	87	13.8		
668	16	87	13.8		
669	16	87	13.8		
670	16	87	13.8		
671	16	87	13.8		
672	16	87	13.8		
673	16	87	13.8		
674	16	86.5	13.7		
675	16	87	13.8		
676	16	87	13.8		
677	16	87	13.8		
678	16	87.5	13.9		
679	16	87.5	13.9		
680	16	87.5	13.9		
681	16	87.5	13.9		
682	16	87.5	13.9		
683	16	87.5	13.9		
684	16	87.5	13.9		
685	16	87.5	13.9		
686	16	87.5	13.9		
687	16	87.5	13.9		
688	16	87.5	13.9		
689	16	87.5	13.9		
690	16	87.5	13.9		
691	16	87.5	13.9		
692	16	87.5	13.9		
693	15.5	87.5	13.4		
694	15.5	88	13.5		
695	15.5	88	13.5		
696	16	88	14		

697	16	88	14		
698	15.5	87.5	13.4		
699	15.5	88	13.5		
700	15.5	88	13.5		
701	15.5	88	13.5		
702	15.5	88	13.5		
703	15.5	88	13.5		
704	15.5	88	13.5		
705	15.5	88	13.5		
706	15.5	88	13.5		
707	15.5	88	13.5		
708	15.5	88	13.5		
709	15.5	88	13.5		
710	15.5	88	13.5		
711	15.5	88	13.5		
712	15.5	88	13.5		
713	15.5	88	13.5		
714	15.5	88	13.5		
715	15.5	88	13.5		
716	15.5	88	13.5		
717	15.5	88	13.5		
718	15.5	88	13.5		
719	15.5	88	13.5		

Appendix E: Data from the field measurement

Dhanmondi Lake_Field measurement data

Timecum	UCIL1 degC	UCIL2 degC	UCIL4 degC	UCIL6 degC	UCIL7 degC
0.0					
5.0					
10.0					
15.0					
20.0					
25.0	29.3				
30.0	29.1				
35.0	29.0				
40.0	28.9				
45.0	29.0				
50.0	29.1			29.5	
55.0	29.2			29.5	
60.0	29.3			29.0	
65.0	29.4		30.5	29.0	
70.0	29.4		29.5	29.0	
75.0	29.5		29.5	29.0	
80.0	29.6		29.5	29.0	
85.0	29.6		29.0	29.0	
90.0	29.7		29.0	29.5	
95.0	29.9		29.5	29.5	
100.0	30.0	30.5	29.5	29.5	
105.0	30.0	30.5	29.5	29.5	
110.0	30.1	30.5	29.5	29.5	
115.0	30.1	30.5	29.5	30.0	
120.0	30.2	30.5	29.5	30.0	
125.0	30.3	30.5	30.0	30.0	
130.0	30.5	30.5	30.0	30.0	
135.0	30.5	30.5	30.0	30.0	
140.0	30.5	30.5	30.0	30.5	31.0
145.0	30.7	30.5	30.5	30.5	31.0
150.0	30.8	31.0	30.5	30.5	31.0
155.0	30.7	31.0	30.5	30.5	31.0
160.0	30.8	31.0	30.5	30.5	31.0
165.0	30.9	31.5	30.5	31.0	31.0
170.0	31.1	31.5	30.5	31.0	31.0
175.0	31.1	31.5	30.5	31.0	31.5
180.0	31.1	31.5	30.5	31.0	31.5
185.0	31.2	32.0	31.0	31.0	31.5
190.0	31.3	31.5	31.0	31.5	32.0
195.0	31.5	31.5	31.5	31.5	32.0
200.0	31.6	31.5	31.5	31.5	32.0
205.0	31.6	31.5	31.5	31.5	32.0
210.0	31.7	31.5	31.5	31.5	32.0
215.0	31.6	32.0	31.5	32.0	32.5
220.0	31.7	32.0	32.0	32.0	32.5
225.0	31.8	32.0	32.0	32.0	32.5
230.0	31.8	32.0	32.0	32.0	32.5
235.0	31.8	32.0	32.0	32.0	32.5

240.0	31.9	32.0	32.0	32.0	32.5
245.0	32.0	32.0	32.5	32.5	32.5
250.0	32.0	32.0	32.5	32.5	33.0
255.0	32.0	32.0	32.5	32.5	32.5
260.0	32.2	32.0	32.5	32.5	32.5
265.0	32.2	32.5	33.0	32.5	33.0
270.0	32.4	32.5	33.0	33.0	33.0
275.0	32.3	32.5	33.0	33.0	33.0
280.0	32.4	32.5	33.0	33.0	33.0
285.0	32.4	32.5	33.0	33.0	33.0
290.0	32.5	32.5	33.0	33.0	33.0
295.0	32.5	32.5	32.5	33.0	33.0
300.0	32.6	32.5	33.0	33.0	33.0
305.0	32.6	32.5	33.0	33.0	33.0
310.0	32.8	32.5	33.5	33.0	33.0
315.0	32.8	32.5	33.5	32.5	33.0
320.0	32.7	33.0	33.5	33.0	33.0
325.0	32.8	33.0	33.5	33.0	33.0
330.0	32.9	32.5	34.0	33.0	33.0
335.0	33.1	33.0	34.0	33.0	33.5
340.0	33.1	33.0	34.0	33.0	33.5
345.0	33.0	33.0	34.0	33.0	33.5
350.0	33.1	33.0	34.0	33.0	33.0
355.0	33.0	33.0	33.5	33.0	33.5
360.0	33.0	33.0	33.5	33.0	33.5
365.0	33.0	33.0	34.0	33.0	33.5
370.0	33.2	33.0	34.0	33.0	33.5
375.0	33.3	33.0	34.5	33.0	33.0
380.0	33.4	33.5	34.5	33.5	33.5
385.0	33.4	33.5	34.5	33.5	33.5
390.0	33.4	33.5	35.0	33.5	33.5
395.0	33.5	33.5	35.0	33.5	33.5
400.0	33.5	33.5	35.0	33.5	33.5
405.0	33.6	33.5	35.0	33.5	33.5
410.0	33.8	33.5	35.0	33.5	33.5
415.0	33.6	33.5	35.0	33.5	33.5
420.0	33.4	33.5	35.0	33.5	33.0
425.0	33.2	33.5	35.0	33.5	33.0
430.0	33.0	33.0	34.5	33.5	32.5
435.0	32.9	33.0	34.5	33.5	32.5
440.0	33.0	33.0	34.5	33.5	32.5
445.0	32.8	33.0	34.5	33.5	32.5
450.0	32.9	33.0	34.5	33.5	33.0
455.0	33.0	33.0	34.5	33.5	33.0
460.0	33.0	33.0	34.5	33.5	33.0
465.0	33.0	33.0	34.5	33.5	33.0
470.0	32.9	33.0	34.5	33.5	33.0
475.0	33.0	33.0	35.0	33.5	33.0
480.0	32.9	33.0	35.5	34.0	32.5
485.0	32.8	33.0	34.5	34.5	33.0

490.0	32.7	33.0	34.0	34.0	32.5
495.0	32.8	33.0	34.0	33.5	32.5
500.0	32.8	32.5	33.5	33.5	32.5
505.0	32.7	32.5	33.5	33.5	32.5
510.0	32.7	32.5	33.0	33.0	32.5
515.0	32.7	32.5	33.0	33.0	32.5
520.0	32.5	32.5	33.0	33.0	32.5
525.0	32.6	32.5	32.5	33.0	32.5
530.0	32.5	32.5	32.5	33.0	32.5
535.0	32.4	32.5	32.5	33.0	32.0
540.0	32.4	32.0	32.5	33.0	32.0
545.0	32.4	32.0	32.0	33.0	32.0
550.0	32.1	32.0	32.0	33.0	32.0
555.0	32.0	31.5	32.0	32.5	32.0
560.0	32.2	31.5	31.5	32.5	31.5
565.0	32.1	31.5	31.5	32.5	31.5
570.0	32.9	31.5	31.5	32.5	31.5
575.0	32.6	31.0	31.5	32.5	31.5
580.0	31.3	31.5	31.5	32.0	31.5
585.0	31.2	31.0	31.0	32.0	31.5
590.0	31.2	31.0	31.0	32.0	31.5
595.0	31.1	31.0	31.0	32.0	31.5
600.0	31.1	31.0	31.0	31.5	31.5
605.0	31.1	31.0	31.0	31.5	31.5

Timecum	UCIL1 (%)	UCIL2 (%)	UCIL4 (%)	UCIL6 (%)	UCIL7 (%)
0.0					
5.0					
10.0					
15.0					
20.0					
25.0	68.0				
30.0	70.0				
35.0	69.0				
40.0	70.0				
45.0	69.0				
50.0	68.0			72.5	
55.0	67.0			74.5	
60.0	68.0			74.5	
65.0	66.0		70.0	74.0	
70.0	66.0		71.0	74.0	
75.0	68.0		71.5	74.0	
80.0	65.0		72.5	74.0	
85.0	66.0		73.0	73.5	
90.0	64.0		72.0	73.0	
95.0	63.0		70.5	72.5	
100.0	64.0	68.5	71.0	72.5	
105.0	63.0	69.5	70.0	72.5	
110.0	60.0	67.5	69.0	72.5	
115.0	62.0	67.5	70.5	72.0	
120.0	61.0	67.0	70.5	71.0	
125.0	58.0	66.5	68.5	70.5	
130.0	57.0	65.5	68.0	70.5	
135.0	56.0	65.0	67.5	69.0	
140.0	55.0	65.5	66.0	68.5	65.5
145.0	54.0	64.5	65.5	66.5	63.5
150.0	53.0	64.5	64.5	66.0	63.5
155.0	52.0	61.5	64.0	65.5	62.0
160.0	53.0	62.5	64.5	66.0	61.0
165.0	50.0	60.5	62.5	64.0	61.0
170.0	50.0	58.5	62.0	62.5	57.5
175.0	46.0	56.5	58.5	58.5	55.5
180.0	42.0	55.5	57.5	58.5	55.5
185.0	42.0	54.5	52.5	54.5	50.0
190.0	43.0	54.5	52.5	53.5	50.0
195.0	39.0	52.0	52.5	54.5	50.5
200.0	40.0	52.0	50.5	53.5	52.5
205.0	37.0	51.5	53.5	54.0	51.5
210.0	41.0	52.5	51.5	54.0	51.0
215.0	38.0	52.0	51.5	55.5	51.5
220.0	43.0	53.0	51.0	54.0	52.0
225.0	41.0	52.5	50.5	54.5	50.5
230.0	39.0	51.5	51.5	53.5	50.5
235.0	40.0	52.0	49.5	52.5	51.0
240.0	39.0	51.0	50.0	52.0	51.0

245.0	40.0	50.5	49.5	52.5	51.0
250.0	41.0	51.0	49.5	53.5	49.0
255.0	41.0	51.0	49.0	51.5	49.5
260.0	42.0	50.0	48.5	51.0	48.5
265.0	39.0	50.5	47.5	51.0	48.5
270.0	38.0	51.0	48.0	51.5	49.0
275.0	40.0	50.0	46.0	51.5	49.5
280.0	39.0	49.5	46.5	51.0	50.5
285.0	36.0	49.0	46.0	49.5	45.0
290.0	35.0	48.0	47.5	49.5	47.0
295.0	34.0	48.5	45.0	50.0	48.0
300.0	34.0	47.5	46.5	50.5	48.5
305.0	36.0	48.0	47.0	49.5	48.5
310.0	37.0	49.0	46.5	50.5	48.0
315.0	36.0	49.0	46.0	49.5	47.5
320.0	33.0	44.5	45.5	48.5	46.5
325.0	33.0	46.5	45.5	49.0	47.5
330.0	33.0	47.0	43.0	47.0	46.0
335.0	33.0	46.5	44.0	48.0	48.5
340.0	33.0	46.5	44.0	49.0	46.5
345.0	33.0	46.5	45.5	48.5	46.0
350.0	34.0	46.5	44.0	49.5	47.0
355.0	32.0	45.0	45.5	48.5	45.5
360.0	32.0	44.0	44.0	48.5	45.0
365.0	31.0	44.0	42.0	47.0	45.0
370.0	32.0	45.0	44.0	47.5	44.0
375.0	32.0	45.0	41.0	46.5	44.0
380.0	31.0	44.0	42.5	45.0	42.0
385.0	30.0	43.5	40.0	43.5	40.0
390.0	30.0	41.5	39.0	43.0	42.5
395.0	31.0	41.5	39.5	43.0	43.0
400.0	31.0	42.0	40.0	44.0	42.5
405.0	30.0	40.0	39.0	43.0	38.5
410.0	31.0	41.5	37.5	42.0	38.5
415.0	38.0	49.5	44.5	50.5	50.5
420.0	41.0	51.5	47.5	52.5	52.0
425.0	44.0	51.5	48.5	53.5	53.5
430.0	41.0	52.5	49.5	54.5	53.5
435.0	41.0	51.5	49.0	53.5	53.0
440.0	41.0	52.5	48.5	53.5	52.5
445.0	38.0	52.5	48.5	54.5	52.5
450.0	40.0	51.5	49.0	53.5	52.0
455.0	40.0	54.0	49.5	53.0	52.5
460.0	40.0	51.5	50.0	53.0	52.0
465.0	38.0	51.0	48.5	52.5	51.5
470.0	38.0	53.0	45.5	51.0	50.0
475.0	37.0	50.5	44.5	51.5	50.5
480.0	40.0	50.5	46.5	50.0	50.0
485.0	44.0	50.5	46.0	49.5	49.5
490.0	40.0	51.0	46.0	49.5	50.5
495.0	39.0	51.0	47.0	52.0	50.5

500.0	39.0	52.5	48.0	50.5	52.5
505.0	40.0	52.0	47.5	50.5	50.5
510.0	38.0	51.0	48.5	50.5	49.0
515.0	40.0	52.5	48.0	51.5	48.5
520.0	41.0	52.5	43.5	52.5	50.5
525.0	40.0	52.5	44.5	52.5	52.0
530.0	40.0	52.5	47.5	52.5	51.5
535.0	41.0	53.5	50.5	52.5	53.5
540.0	41.0	53.5	51.5	53.0	55.5
545.0	47.0	53.5	52.5	54.5	53.0
550.0	45.0	53.5	52.5	55.5	53.5
555.0	44.0	55.5	54.5	55.5	53.5
560.0	47.0	54.5	54.5	55.0	54.0
565.0	44.0	54.0	55.5	56.0	54.5
570.0	45.0	56.5	55.0	57.0	54.5
575.0	44.0	56.5	56.0	56.5	54.0
580.0	48.0	55.5	55.0	55.0	54.0
585.0	53.0	56.5	56.0	55.5	54.5
590.0	52.0	55.5	56.5	56.0	54.5
595.0	53.0	57.5	56.0	56.0	54.5
600.0	51.0	58.5	56.5	56.5	55.5
605.0	52.0	66.0	57.5	58.0	56.5

Timecum	UCIL1 degC	UCIL2 degC	UCIL3 degC	UCIL4 degC	UCIL5_Hh degC	UCIL6 degC	UCIL7 degC	UCIL8 degC	UCIL9_Hh degC
0.0	24.5								
5.0	24.0				24.5				
10.0	24.0				24.3				
15.0	23.5				24.2	25.0			
20.0	23.5				24.3	24.5			
25.0	23.5				24.7	24.5			
30.0	23.5				25.2	24.0			
35.0	23.5				25.3	24.0	25.5		
40.0	24.0				25.3	24.0	25.5		
45.0	24.0			26.5	25.3	24.5	25.0		
50.0	24.0			26.0	25.5	24.5	25.0		
55.0	24.0			25.5	25.6	24.5	25.0		
60.0	24.0			25.5	25.5	24.5	25.0		
65.0	24.0			25.0	25.5	24.5	25.0	25.5	27.7
70.0	24.5			25.0	25.2	24.5	24.5	25.5	27.7
75.0	24.5			25.0	25.0	24.5	24.5	25.0	27.8
80.0	24.5			24.5	25.1	24.5	24.5	25.0	28.2
85.0	24.5			24.5	25.2	24.5	24.5	25.0	28.4
90.0	24.5		26.5	24.5	25.5	24.5	24.5	25.5	29.8
95.0	24.5		26.0	24.5	24.7	24.5	24.5	27.0	28.1
100.0	24.5		25.5	24.5	25.9	24.5	24.5	30.0	28.3
105.0	24.5		25.5	24.5	26.1	25.0	24.5	30.0	28.3
110.0	24.5		25.5	24.5	27.4	25.0	25.0	29.5	30.2
115.0	24.5		25.0	24.5	27.5	25.0	25.0	28.5	29.6
120.0	25.0		25.5	25.0	27.9	25.5	25.0	28.0	29.6
125.0	25.0		25.5	25.0	27.9	25.5	25.0	28.0	29.9
130.0	25.5		25.5	25.0	27.2	26.0	25.5	27.5	31.0
135.0	25.5		25.5	25.0	27.2	26.0	25.5	27.5	30.8
140.0	25.5	28.0	25.5	25.0	27.0	26.0	25.5	27.0	30.8
145.0	26.0	27.5	26.0	25.5	27.1	26.0	25.5	27.0	30.5
150.0	26.0	26.5	26.0	25.5	27.0	26.0	25.5	26.5	31.2
155.0	26.0	26.5	26.0	25.5	27.1	26.0	25.5	26.5	30.5
160.0	26.0	26.0	26.0	25.5	27.0	26.0	25.5	26.5	30.5
165.0	26.0	25.5	26.0	25.5	26.8	26.5	25.5	26.0	30.2
170.0	26.0	25.5	26.0	25.5	26.5	26.5	25.5	26.5	29.9
175.0	26.0	25.5	26.0	25.5	26.6	26.5	26.0	26.5	29.7
180.0	26.0	25.5	26.0	25.5	26.7	26.5	26.0	26.5	30.2
185.0	26.5	25.5	26.0	26.0	26.8	26.5	26.0	26.0	30.0
190.0	26.5	25.0	26.5	26.0	26.7	26.5	26.0	26.5	29.6
195.0	26.5	25.0	26.5	26.0	26.7	26.5	26.0	26.5	29.6
200.0	26.5	25.0	26.5	26.0	26.7	26.5	26.0	26.5	30.3
205.0	26.5	25.0	26.5	26.0	26.8	26.5	26.0	26.5	31.0
210.0	26.5	25.0	26.5	26.0	26.7	26.5	26.0	26.5	30.9
215.0	26.5	25.0	26.5	26.0	26.6	26.5	26.0	26.5	30.2
220.0	26.5	25.0	26.5	26.0	26.4	26.5	26.0	26.0	29.6
225.0	26.5	25.0	26.5	26.0	26.4	26.5	26.0	26.0	30.3
230.0	26.0	25.0	26.5	26.0	26.3	26.5	26.0	26.0	30.1

235.0	26.0	25.0	26.5	26.0	26.4	26.5	26.0	26.0	30.4
240.0	26.0	25.0	26.0	26.0	26.4	26.5	26.0	25.5	30.3
245.0	26.0	25.0	26.0	26.0	26.3	26.0	26.0	25.5	29.9
250.0	26.0	25.0	26.0	26.0	26.3	26.0	26.0	25.5	29.7
255.0	26.0	25.0	26.0	26.0	26.3	26.0	26.0	25.5	29.9
260.0	26.0	25.0	26.0	26.0	26.3	26.0	25.5	25.5	30.0
265.0	26.0	25.0	26.0	26.0	26.2	26.0	25.5	25.5	30.6
270.0	26.0	25.0	26.0	26.0	26.2	26.0	25.5	25.5	30.4
275.0	26.0	25.0	26.0	26.0	26.2	26.0	25.5	25.5	29.8
280.0	26.0	25.0	26.0	26.0	26.2	26.0	26.0	25.5	30.1
285.0	26.0	25.0	26.0	26.0	26.0	26.0	26.0	25.5	29.9
290.0	26.0	25.0	26.0	26.0	26.0	26.0	26.0	25.5	30.3
295.0	26.0	25.0	26.5	26.0	26.0	26.0	26.0	25.5	29.9
300.0	26.0	25.0	26.5	26.0	26.0	26.0	26.0	25.5	29.7
305.0	26.0	25.0	26.5	26.0	26.1	26.0	26.0	25.5	30.1
310.0	26.0	25.0	26.5	26.0	26.0	26.0	26.0	25.5	30.1
315.0	26.0	25.0	26.0	26.0	26.0	26.0	26.0	25.5	30.0
320.0	26.0	25.0	26.0	26.0	25.0	26.0	26.0	25.5	29.6
325.0	25.5	25.0	26.0	26.0	25.8	26.0	25.5	25.5	29.8
330.0	26.0	25.0	26.0	26.0	25.9	26.0	25.5	25.5	30.3
335.0	26.0	25.0	26.0	26.0	26.1	26.0	25.5	25.5	29.8
340.0	26.0	25.0	26.0	26.0	26.2	26.0	25.5	25.5	31.2
345.0	26.0	25.0	26.0	26.0	26.1	26.0	25.5	25.5	31.9
350.0	26.0	25.0	26.0	26.0	26.0	26.0	25.5	25.5	31.4
355.0	26.0	25.0	26.0	26.0	25.9	26.0	26.0	25.5	31.0
360.0	26.0	25.0	26.0	26.0	26.0	26.0	26.0	25.5	31.5
365.0	26.0	25.0	26.0	26.0	26.0	26.0	26.0	25.5	30.4
370.0	26.0	25.0	26.0	26.0	26.0	26.0	26.0	25.5	30.7
375.0	25.5	25.0	26.0	26.0	26.0	26.0	26.0	25.5	33.0
380.0	25.5	25.0	26.0	26.0	25.9	26.0	25.5	25.5	31.7
385.0	25.5	25.0	26.0	26.0	25.8	26.0	25.5	25.0	30.2
390.0	25.5	25.0	26.0	26.0	25.7	26.0	25.5	25.0	30.0
395.0	25.5	24.5	26.0	25.5	25.7	25.5	25.5	25.0	30.0
400.0	25.5	24.5	25.5	25.5	27.7	25.5	25.5	25.0	30.1
405.0	25.5	24.5	25.5	25.5	25.5	25.5	25.5	25.0	29.9
410.0	25.0	24.5	25.5	25.5	25.6	25.5	25.5	24.5	29.6
415.0	25.0	24.5	25.5	25.5	25.5	25.5	25.5	24.5	29.8
420.0	25.0	24.5	25.5	25.5	25.6	25.5	25.5	24.5	29.9
425.0	25.0	24.5	25.5	25.5	25.2	25.5	25.5	24.5	30.7
430.0	25.0	24.0	25.5	25.5	25.1	25.5	25.5	24.5	29.8
435.0	25.0	24.0	25.5	25.5	25.1	25.5	25.5	24.5	30.4
440.0	24.5	24.0	25.5	25.5	25.1	25.5	25.5	24.0	30.6
445.0	24.5	24.0	25.5	25.5	25.2	25.5	25.5	24.0	30.9
450.0	24.5	24.0	25.5	25.5	25.2	25.5	25.0	24.0	31.1
455.0	24.5	24.0	25.5	25.5	25.4	25.5	25.0	24.0	31.4
460.0	24.5	24.0	25.5	25.5	25.4	25.5	25.0	24.0	30.4
465.0	24.5	24.0	25.5	25.5	25.4	25.5	25.5	24.0	30.4
470.0	24.5	24.0	25.5	26.0	25.4	25.5	25.5	24.0	29.9
475.0	24.5	24.0	25.5	26.0	25.4	25.5	25.5	24.0	29.5

Timecum	UCIL1 (%)	UCIL2 (%)	UCIL3 (%)	UCIL4 (%)	UCIL6 (%)	UCIL7 (%)	UCIL8 (%)
0.0	65.0						
5.0	65.0						
10.0	65.0						
15.0	65.0				62.5		
20.0	67.5				62.5		
25.0	67.0				64.0		
30.0	67.0				63.0		
35.0	66.5				63.5	61.5	
40.0	67.5				63.5	62.5	
45.0	67.0			62.0	64.0	63.0	
50.0	65.0			63.5	64.0	63.5	
55.0	66.5			63.5	64.0	63.5	
60.0	66.5			63.0	64.0	63.5	
65.0	64.5			63.5	64.0	63.0	64.0
70.0	65.0			63.5	62.5	62.5	64.5
75.0	63.5			63.0	62.5	62.0	63.0
80.0	64.0			63.5	63.5	62.5	64.5
85.0	65.0			64.0	63.0	63.0	64.0
90.0	64.5		61.5	63.5	62.0	63.5	64.5
95.0	64.0		61.5	64.0	63.0	63.0	71.0
100.0	64.0		62.0	64.0	63.5	63.0	62.0
105.0	62.5		63.0	62.5	63.0	62.0	62.5
110.0	63.5		62.5	62.5	60.0	62.5	55.5
115.0	63.0		62.0	62.5	61.0	61.5	55.0
120.0	62.5		62.0	62.5	58.5	61.0	55.0
125.0	62.5		63.0	61.0	58.5	58.5	55.5
130.0	61.5		61.5	61.5	58.0	58.5	57.5
135.0	60.0		60.5	61.0	57.0	58.5	56.0
140.0	60.0	59.0	61.0	60.5	57.0	58.0	57.0
145.0	59.0	56.5	61.0	59.5	57.5	58.0	56.0
150.0	59.5	58.0	60.5	59.5	56.0	58.5	57.0
155.0	60.0	58.0	59.5	59.0	56.5	57.5	56.0
160.0	59.0	57.0	59.0	60.0	57.0	58.0	57.0
165.0	59.5	58.5	59.0	60.0	57.0	58.0	58.5
170.0	58.5	59.5	59.0	60.5	56.5	58.0	58.5
175.0	59.0	60.0	59.5	57.5	57.0	58.5	59.5
180.0	59.0	61.0	59.0	58.5	56.5	58.5	59.0
185.0	59.0	61.0	59.0	58.5	56.5	58.0	59.0
190.0	59.5	59.5	59.5	59.5	57.0	58.5	59.5
195.0	60.0	60.5	59.5	59.0	57.0	58.0	58.5
200.0	59.5	60.5	59.0	58.0	55.5	57.5	59.5
205.0	59.0	62.0	59.5	57.5	56.5	58.0	59.0
210.0	59.0	61.5	58.0	58.0	56.0	58.5	59.0
215.0	58.5	59.5	57.5	59.0	56.0	57.5	59.5
220.0	58.0	60.5	58.0	58.5	56.5	58.0	59.5
225.0	59.0	61.0	58.0	58.5	55.5	58.5	60.5
230.0	58.5	61.0	59.0	59.0	56.0	58.5	61.0
235.0	59.5	62.0	59.0	59.0	57.0	58.0	61.0

240.0	60.5	61.5	59.0	59.0	57.0	59.0	62.0
245.0	61.0	62.0	60.0	59.5	58.0	59.0	61.5
250.0	62.0	63.0	60.5	60.0	57.5	59.5	62.0
255.0	59.5	62.0	59.5	58.5	57.0	58.0	62.5
260.0	61.5	62.5	59.5	59.0	57.5	58.5	61.5
265.0	61.0	62.5	59.5	59.0	58.0	59.0	62.5
270.0	61.5	62.0	60.0	59.5	57.5	59.5	62.5
275.0	62.5	63.0	60.5	61.0	60.0	60.0	63.0
280.0	64.0	63.5	61.0	62.0	61.0	61.5	64.0
285.0	65.5	65.5	62.0	62.5	61.5	62.0	64.0
290.0	65.5	65.0	63.0	62.5	61.5	62.0	64.5
295.0	65.5	64.5	63.0	62.5	61.5	62.0	65.0
300.0	66.0	65.0	63.5	63.0	62.0	62.5	66.0
305.0	66.5	65.0	64.0	63.0	63.0	63.0	67.0
310.0	66.0	65.5	64.0	63.0	62.5	62.5	67.0
315.0	66.5	65.0	64.0	62.5	62.5	63.0	66.0
320.0	66.0	65.5	64.0	62.5	62.5	63.0	66.5
325.0	65.0	64.5	63.5	62.5	62.0	63.0	66.5
330.0	66.0	64.5	64.0	62.5	62.5	63.5	66.5
335.0	66.5	64.0	63.5	62.0	62.5	63.0	67.0
340.0	65.0	64.0	63.0	62.5	62.0	62.5	66.5
345.0	65.0	64.5	62.5	61.0	60.0	62.5	66.0
350.0	66.0	63.5	62.5	61.5	60.5	62.0	64.5
355.0	65.5	64.0	62.5	62.0	61.0	62.5	65.5
360.0	62.0	64.5	61.0	62.0	61.5	62.5	65.0
365.0	62.0	64.0	61.5	62.0	61.0	62.5	65.0
370.0	61.0	64.0	60.0	61.5	58.5	62.5	65.0
375.0	60.5	63.5	60.0	59.5	58.5	61.0	64.0
380.0	62.0	63.5	59.0	59.5	58.0	60.5	63.5
385.0	63.0	62.5	60.0	59.5	57.5	58.5	63.5
390.0	63.5	62.0	60.0	58.5	57.5	59.0	64.5
395.0	61.5	62.0	60.0	58.0	58.0	59.5	64.5
400.0	62.5	62.0	59.5	58.5	57.5	60.0	64.5
405.0	62.0	63.0	59.5	58.5	58.0	60.0	64.0
410.0	62.5	62.5	59.5	59.5	58.5	60.5	64.5
415.0	64.0	63.0	60.0	59.5	58.5	60.5	64.5
420.0	64.0	63.0	61.0	59.5	58.5	60.5	64.5
425.0	66.0	64.0	61.5	60.0	58.5	60.5	64.0
430.0	66.0	64.5	61.5	60.5	59.0	61.0	64.0
435.0	65.0	65.5	62.0	60.5	59.5	61.0	65.0
440.0	66.5	64.5	62.0	60.5	60.0	61.0	65.5
445.0	66.0	64.5	62.5	60.5	59.5	61.5	65.5
450.0	66.5	65.0	62.5	61.0	59.5	61.5	66.5
455.0	65.0	65.5	62.5	62.5	60.0	62.5	66.5
460.0	64.5	65.0	62.5	62.0	60.0	63.0	66.5
465.0	65.0	64.5	63.0	64.0	60.5	64.5	67.5
470.0	65.0	66.0	63.0	63.0	60.5	63.5	67.0
475.0	66.5	66.0	63.0	62.5	61.0	63.0	67.5

Timecum	UCIL1 degC	UCIL1_Hh degC	UCIL2 degC	UCIL3 degC	UCIL4 degC	UCIL6 degC	UCIL7 degC	UCIL8 degC
0.0	27.0							
5.0	26.0							
10.0	25.5	23.6						
15.0	25.0	23.2						
20.0	24.5	23.3	26.5					
25.0	24.0	23.6	25.5					
30.0	24.0	23.5	25.0					
35.0	23.5	23.8	24.5					
40.0	23.5	23.7	24.0					
45.0	23.5	23.9	24.0					
50.0	23.5	24.1	23.5				26.0	
55.0	23.5	24.1	23.5				25.5	
60.0	23.5	24.3	23.5		26.0		25.0	
65.0	23.5	24.5	23.5		25.5		25.0	
70.0	23.5	24.6	23.5		25.5		25.0	26.5
75.0	23.5	24.7	23.5		25.0		25.0	26.0
80.0	23.5	24.8	23.5		25.0		25.5	25.5
85.0	23.5	25.0	23.5		24.5		25.5	25.0
90.0	24.0	25.1	23.5		24.5		25.5	25.0
95.0	24.0	25.1	23.5	26.5	24.5		25.5	24.5
100.0	24.0	25.4	23.5	26.5	24.5		25.5	24.5
105.0	24.0	25.4	24.0	26.0	24.5		25.5	24.5
110.0	24.0	25.5	24.0	25.5	24.0	26.5	25.5	24.5
115.0	24.0	25.7	24.0	25.5	24.0	25.5	25.5	24.5
120.0	24.5	25.7	24.0	25.0	24.0	25.0	25.5	24.5
125.0	24.5	25.7	24.0	25.0	24.0	25.0	25.5	24.5
130.0	24.5	26.1	24.0	25.0	24.0	25.0	25.5	24.5
135.0	24.5	25.9	24.5	25.0	24.5	24.5	25.5	24.5
140.0	24.5	26.1	24.5	25.0	24.5	25.0	25.5	25.0
145.0	24.5	26.1	24.5	25.0	24.5	25.0	25.5	25.0
150.0	24.5	26.4	24.5	25.0	24.5	25.0	25.5	25.0
155.0	24.5	26.2	24.5	25.0	24.5	25.0	25.5	25.0
160.0	24.5	26.1	24.5	25.0	24.5	25.0	25.5	25.5
165.0	24.5	26.4	25.0	25.5	24.5	25.0	25.5	25.5
170.0	25.0	26.5	25.0	25.5	25.0	25.0	26.0	25.5
175.0	25.0	26.8	25.0	25.5	25.0	25.0	26.0	25.5
180.0	25.0	27.0	25.0	25.5	25.0	25.5	26.0	26.0
185.0	25.0	26.6	25.0	25.5	25.0	25.5	26.5	26.0
190.0	25.5	26.9	25.0	25.5	25.5	25.5	26.5	26.0
195.0	25.5	27.1	25.5	26.0	25.5	26.0	26.5	26.0
200.0	25.5	27.2	25.5	26.0	25.5	26.5	26.5	26.5
205.0	25.5	27.2	25.5	26.0	26.0	26.5	27.0	26.5
210.0	25.5	27.3	25.5	26.5	26.0	26.5	27.0	26.5
215.0	26.0	27.5	25.5	26.5	26.0	26.5	27.0	26.5
220.0	26.0	27.1	25.5	26.5	26.0	26.5	27.0	27.0
225.0	26.0	27.1	25.5	26.5	26.5	26.5	27.0	27.0
230.0	26.0	27.3	26.0	26.5	26.5	26.5	27.0	27.0
235.0	26.0	27.0	26.0	26.5	26.5	26.5	27.0	27.0

240.0	26.0	27.7	26.0	27.0	26.5	26.5	27.0	27.0
245.0	26.0	27.0	26.0	27.0	26.5	26.5	27.0	27.0
250.0	26.0	27.4	26.0	27.0	26.5	27.0	27.0	27.0
255.0	26.5	28.5	26.0	27.0	26.5	27.0	27.0	27.5
260.0	26.5	27.9	26.0	27.0	27.0	27.0	27.0	27.5
265.0	26.5	28.4	26.0	27.0	27.0	27.0	27.5	27.5
270.0	26.5	29.0	26.0	27.0	27.0	27.0	27.5	27.5
275.0	27.0	29.5	26.0	27.5	27.0	27.5	27.5	27.5
280.0	27.0	28.4	26.0	27.5	27.0	27.5	27.5	27.5
285.0	27.5	28.4	26.0	27.5	27.0	27.5	28.0	27.5
290.0	27.5	28.3	26.5	27.5	27.5	27.5	28.0	28.0
295.0	27.5	28.8	26.5	27.5	27.5	27.5	28.0	28.0
300.0	27.5	27.4	26.5	28.0	27.5	28.0	28.0	28.0
305.0	27.0	28.1	26.5	28.0	27.5	28.0	28.0	28.0
310.0	27.5	28.6	26.5	28.0	27.5	28.0	28.0	28.0
315.0	27.5	28.5	26.5	28.0	27.5	28.0	28.0	28.0
320.0	27.5	28.4	26.5	28.0	27.5	28.0	28.0	28.0
325.0	27.5	27.8	26.5	28.0	27.5	28.0	28.0	28.0
330.0	27.5	28.2	27.0	28.0	28.0	28.0	28.0	28.5
335.0	27.5	28.3	27.0	28.0	28.0	28.0	28.5	28.5
340.0	27.5	28.4	27.0	28.0	28.5	28.0	28.0	28.5
345.0	27.5	28.4	27.0	28.0	28.5	28.5	28.0	28.5
350.0	27.5	28.2	27.0	28.5	28.5	28.5	28.5	28.5
355.0	27.5	28.7	27.0	28.5	28.5	28.5	28.0	28.5
360.0	27.5	28.6	27.0	28.5	28.5	28.5	28.0	28.5
365.0	27.5	28.3	27.0	28.5	28.5	28.5	28.5	28.5
370.0	27.5	28.7	27.0	28.5	28.5	28.0	28.5	28.5
375.0	27.5	28.8	27.0	28.5	28.5	28.0	28.5	28.5
380.0	27.5	29.3	27.0	28.5	29.0	28.0	28.5	28.5
385.0	27.5	28.8	27.0	28.5	29.0	28.0	28.5	28.5
390.0	27.5	28.6	27.0	28.5	29.0	28.0	28.5	28.5
395.0	28.0	29.0	27.0	28.5	29.0	28.0	28.5	28.5
400.0	28.0	28.8	27.5	28.5	29.0	28.0	28.5	28.5
405.0	28.0	28.9	27.5	28.5	29.0	28.0	28.5	29.0
410.0	28.0	28.7	27.5	28.5	29.0	28.0	28.5	29.0
415.0	28.0	28.9	27.5	28.5	29.0	28.0	28.5	29.0
420.0	28.0	29.1	27.5	28.5	29.0	28.0	28.5	29.0
425.0	28.0	**29.8**	27.5	28.5	29.0	28.0	28.5	29.0
430.0	28.0	29.2	27.5	28.5	29.5	28.0	28.5	29.0
435.0	28.0	28.9	27.5	29.0	29.5	28.0	28.5	29.0
440.0	28.0	28.7	27.5	29.0	29.5	28.0	28.5	29.0
445.0	28.0	28.7	27.5	29.0	29.5	28.0	28.5	29.0
450.0	28.0	28.8	27.5	29.0	29.5	28.0	28.5	29.0
455.0	28.0	28.7	27.5	29.0	29.5	28.0	28.5	29.0
460.0	28.0	28.8	27.5	29.0	29.5	28.0	28.5	28.5
465.0	28.0	28.9	27.5	29.0	29.5	28.0	28.5	28.5
470.0	28.0	28.7	27.5	29.0	30.0	28.0	28.5	28.5
475.0	28.0	29.0	27.5	29.0	30.0	28.0	28.5	28.5
480.0	28.0	28.9	27.5	29.0	30.5	28.0	28.5	28.5
485.0	28.0	28.8	27.5	29.0	30.5	28.0	28.5	28.5

490.0	28.0	28.8	27.5	29.0	30.5	28.0	28.5	28.5
495.0	28.0	29.0	27.5	29.0	30.5	28.0	28.5	28.5
500.0	28.0	28.7	27.5	29.0	30.5	28.0	28.5	28.5
505.0	28.0	28.8	27.5	29.0	30.5	28.0	28.5	28.0
510.0	28.0	28.8	27.5	29.0	30.5	28.0	28.5	28.0
515.0	28.0	28.7	27.5	29.0	30.5	28.0	28.5	28.5
520.0	28.0	28.7	27.5	29.0	30.5	28.0	28.0	28.5
525.0	28.0	28.6	27.5	29.0	30.5	28.0	28.0	28.5
530.0	28.0	28.7	27.5	29.0	30.0	28.0	28.0	28.0
535.0	28.0	28.6	27.5	29.0	30.0	28.0	28.0	28.0
540.0	28.0	28.6	27.5	29.0	30.0	28.0	28.0	28.0
545.0	28.0	28.5	27.5	29.0	29.5	28.0	28.0	28.0
550.0	28.0	28.5	27.5	28.5	29.5	28.0	28.0	28.0
555.0	28.0	28.4	27.5	28.5	29.0	28.0	28.0	28.0
560.0	28.0	28.4	27.5	28.5	29.0	28.0	28.0	28.0
565.0	28.0	28.3	27.5	28.5	29.0	28.0	28.0	28.0
570.0	27.5	28.2	27.5	28.5	29.0	28.0	28.0	27.5
575.0	27.5	28.0	27.5	28.5	28.5	28.0	28.0	27.5
580.0	27.5	27.9	27.5	28.5	28.5	28.0	28.0	27.5
585.0	27.5	27.7	27.5	28.5	28.5	27.5	28.0	27.5
590.0	27.5	27.5	27.5	28.5	28.5	27.5	28.0	27.5
595.0	27.5	27.3	27.0	28.5	28.5	27.5	27.5	27.5
600.0	27.5	26.9	27.0	28.5	28.5	27.5	27.5	27.5
605.0	27.5	26.6	27.0	28.5	28.5	27.5	27.5	27.0
610.0	27.0	26.3	27.0	28.5	28.0	27.5	27.5	27.0
615.0	27.0	26.1	27.0	28.5	28.0	27.5	27.5	27.0
620.0	27.0	25.9	27.0	28.5	28.0	27.5	27.5	26.5
625.0	26.5	25.8	26.5	28.5	28.0	27.5	27.5	26.5

Timecum	UCIL1 (%)	UCIL1_Hh (%)	UCIL2 (%)	UCIL3 (%)	UCIL4 (%)	UCIL6 (%)	UCIL7 (%)	UCIL8 (%)
0.0	52.0							
5.0	51.5							
10.0	51.5	39.0						
15.0	52.5	40.0						
20.0	52.5	41.0	48.0					
25.0	53.5	42.0	48.0					
30.0	54.0	41.0	48.5					
35.0	53.5	38.0	49.0					
40.0	54.5	41.0	51.0					
45.0	55.5	42.0	50.5					
50.0	55.5	41.0	51.5				50.5	
55.0	56.5	41.0	52.0				48.5	
60.0	56.0	40.0	51.0		50.0		50.0	
65.0	56.0	40.0	52.0		50.5		49.0	
70.0	55.5	39.0	52.0		51.5		51.5	50.0
75.0	54.5	38.0	51.5		51.5		53.0	50.5
80.0	53.0	37.0	52.0		51.0		52.5	50.0
85.0	53.0	36.0	51.5		51.5		50.5	50.5
90.0	51.5	35.0	51.5		51.0		49.5	51.0
95.0	51.5	35.0	51.5	50.5	51.5		48.5	50.0
100.0	52.5	35.0	51.0	48.5	50.0		47.5	48.5
105.0	50.5	33.0	50.0	45.0	49.5		46.0	48.5
110.0	48.5	32.0	46.5	45.5	49.0	42.0	47.5	48.5
115.0	48.0	32.0	47.5	47.5	48.5	44.5	46.0	47.5
120.0	48.5	32.0	47.5	47.5	48.5	41.0	44.5	44.0
125.0	47.5	32.0	45.0	46.0	46.5	41.0	43.5	45.5
130.0	43.5	29.0	45.5	46.0	46.5	39.0	43.0	44.0
135.0	40.5	27.0	39.0	43.0	45.5	40.0	40.0	40.0
140.0	43.0	28.0	43.0	41.0	44.0	38.5	40.5	41.0
145.0	43.0	27.0	40.5	42.5	43.0	38.0	41.0	40.5
150.0	43.0	27.0	42.5	40.0	43.0	36.5	41.5	41.0
155.0	39.0	26.0	38.0	42.0	42.5	39.0	35.5	35.5
160.0	39.0	26.0	36.0	41.0	41.0	36.5	39.0	35.0
165.0	39.0	25.0	35.5	39.0	40.0	36.0	38.5	35.0
170.0	37.5	25.8	39.0	38.0	40.0	35.0	36.5	37.0
175.0	40.5	26.0	38.0	38.5	40.0	37.0	38.0	37.5
180.0	39.0	26.0	39.0	39.5	39.5	35.5	38.0	37.0
185.0	38.5	26.0	39.5	40.0	41.0	37.0	38.0	35.5
190.0	42.0	26.0	39.0	38.5	39.0	35.5	38.0	35.5
195.0	41.0	26.0	36.0	40.0	39.0	36.5	39.0	35.5
200.0	40.0	26.0	38.0	38.0	39.0	34.0	37.0	37.0
205.0	41.0	24.0	39.0	38.0	39.0	36.0	37.0	37.0
210.0	38.0	24.0	38.5	36.5	38.0	35.0	36.0	36.5
215.0	39.0	24.0	37.0	37.0	38.0	32.5	36.0	34.5
220.0	37.0	24.0	37.0	36.0	37.5	33.5	36.0	36.0
225.0	38.0	25.0	38.0	34.5	37.0	32.5	36.0	33.5
230.0	39.5	25.0	35.0	36.0	37.0	33.5	36.0	33.5
235.0	39.0	24.0	35.5	38.0	38.0	34.5	36.0	36.0

240.0	38.0	26.0	36.5	37.0	37.5	34.0	36.0	34.5
245.0	37.5	24.0	37.5	36.0	37.0	33.5	36.0	34.5
250.0	39.5	25.0	35.0	36.0	37.0	34.5	34.5	36.0
255.0	38.0	24.0	37.0	38.0	36.5	34.5	35.5	35.5
260.0	38.0	24.0	36.5	34.5	35.0	33.5	36.0	34.0
265.0	38.0	23.0	36.5	36.5	34.5	33.5	36.0	33.0
270.0	39.0	23.0	37.0	36.0	36.0	32.5	36.0	33.5
275.0	36.0	22.0	35.5	37.0	36.0	32.5	34.0	33.5
280.0	36.0	23.0	37.5	35.5	36.0	33.0	35.0	35.0
285.0	37.0	23.0	35.5	37.0	36.0	33.5	33.5	33.5
290.0	36.0	23.0	36.5	35.0	36.0	32.5	33.5	33.5
295.0	35.0	23.0	35.0	36.0	36.5	32.5	34.0	33.5
300.0	34.0	23.0	34.5	36.0	34.5	32.5	33.5	31.0
305.0	38.0	23.0	36.0	36.5	35.0	31.5	33.5	33.0
310.0	37.5	23.0	36.0	33.0	35.0	30.5	33.0	33.5
315.0	36.0	23.0	37.0	35.5	34.0	31.5	33.5	33.5
320.0	36.0	23.0	37.0	33.5	33.5	31.0	34.0	35.0
325.0	36.0	24.0	36.0	35.0	33.5	32.5	33.0	33.5
330.0	36.0	23.0	35.0	33.0	33.5	30.5	32.5	32.5
335.0	37.0	23.0	34.0	33.5	35.0	31.0	32.5	32.0
340.0	36.0	23.0	37.5	35.0	33.5	31.5	32.5	33.5
345.0	37.0	24.0	37.5	35.5	33.5	31.5	33.5	32.0
350.0	36.5	23.0	36.5	33.0	33.5	31.5	32.5	32.5
355.0	36.0	23.0	37.0	34.5	33.0	31.5	32.5	32.5
360.0	37.0	23.0	36.5	34.5	32.0	31.5	33.0	35.0
365.0	36.0	23.0	37.0	34.5	33.5	31.5	33.5	32.0
370.0	36.0	23.0	37.0	34.5	33.5	31.5	32.5	31.5
375.0	36.0	23.0	36.0	35.0	33.5	32.5	32.0	31.5
380.0	37.0	23.0	37.0	33.5	32.5	31.5	32.5	32.5
385.0	35.0	22.0	37.0	35.0	32.5	31.5	32.5	33.5
390.0	36.0	23.0	37.0	32.5	34.0	31.5	32.5	33.5
395.0	36.5	23.0	38.0	33.5	32.0	32.5	32.5	33.5
400.0	37.0	24.0	34.0	35.0	32.0	31.5	32.5	32.5
405.0	36.0	24.0	37.0	32.0	32.5	31.5	32.5	31.5
410.0	37.0	23.0	35.5	32.5	32.5	32.0	32.0	32.0
415.0	35.0	23.0	34.5	32.5	31.5	32.5	32.5	32.5
420.0	35.5	22.0	36.0	33.5	32.5	31.5	32.5	33.5
425.0	37.0	24.0	36.0	33.5	32.5	32.5	31.5	32.5
430.0	36.0	22.0	37.0	32.5	32.5	31.5	32.5	34.0
435.0	36.0	23.0	35.0	32.5	32.5	32.5	32.5	32.5
440.0	36.0	23.0	35.0	33.5	32.0	32.5	33.0	32.5
445.0	35.0	23.0	37.0	35.0	32.0	32.5	32.5	34.0
450.0	36.5	24.0	36.0	34.0	30.5	32.0	32.5	31.5
455.0	35.0	23.0	37.0	34.0	31.5	31.5	33.0	32.0
460.0	35.0	23.0	36.0	35.0	32.5	32.5	32.5	31.5
465.0	36.0	24.0	37.0	35.0	32.5	33.0	33.0	32.5
470.0	36.5	23.0	37.0	34.0	32.5	32.5	33.0	33.5
475.0	37.0	23.0	37.0	34.0	32.0	32.5	33.5	32.5
480.0	36.5	23.0	38.0	34.0	32.5	33.0	33.0	32.5
485.0	35.0	24.0	37.0	35.0	32.0	32.5	33.5	32.5

490.0	35.5	23.0	39.0	35.0	33.0	33.5	33.5	35.0
495.0	37.0	24.0	36.0	35.0	30.5	32.5	33.5	35.0
500.0	37.5	25.0	37.5	35.0	31.5	33.5	33.5	35.0
505.0	37.0	24.0	38.0	35.0	31.5	33.0	33.5	35.5
510.0	38.0	25.0	37.5	35.0	32.0	33.5	34.5	35.0
515.0	37.0	24.0	37.0	35.0	32.0	33.5	33.5	35.0
520.0	37.0	24.0	38.0	35.0	31.5	33.5	33.5	35.0
525.0	37.0	24.0	38.5	35.5	31.5	33.0	33.5	35.0
530.0	38.0	24.0	37.5	35.0	32.0	33.5	33.5	36.0
535.0	37.0	24.0	38.0	35.5	32.0	33.5	35.0	36.5
540.0	37.0	24.0	38.0	35.0	32.5	34.0	35.0	35.0
545.0	38.0	25.0	39.0	35.0	32.5	35.0	35.0	35.0
550.0	37.5	25.0	39.0	36.0	33.0	35.0	35.0	36.0
555.0	38.0	25.0	39.0	36.0	33.0	35.0	35.0	37.5
560.0	39.0	25.0	39.0	36.5	34.0	35.5	35.5	37.0
565.0	39.0	25.0	39.0	37.0	34.0	36.0	36.0	38.0
570.0	39.0	25.0	39.0	37.0	35.0	36.0	36.0	38.0
575.0	40.5	26.0	39.0	37.0	35.0	36.0	36.0	38.0
580.0	39.5	27.0	39.0	37.5	35.0	36.0	36.0	37.0
585.0	39.5	26.0	39.0	37.0	35.0	36.0	36.0	37.0
590.0	40.5	27.0	39.0	38.0	35.0	36.0	36.0	39.0
595.0	40.5	27.0	40.0	38.0	35.5	36.0	36.0	39.0
600.0	40.5	28.0	40.0	38.5	35.5	37.5	37.0	40.0
605.0	40.0	28.0	40.0	38.5	35.0	38.0	37.0	40.0
610.0	40.0	28.0	41.0	39.5	36.0	37.0	37.0	40.0
615.0	40.0	29.0	40.0	39.5	36.0	37.0	37.5	40.0
620.0	40.5	30.0	40.0	39.5	36.0	38.0	37.5	40.0
625.0	40.0	31.0	40.5	39.5	36.0	38.0	38.0	40.0

Appendix F: Data from the field measurement

Hatirjheel Lake_Field measurement data

Timecum	UCIL1 degC	UCIL2 degC	UCIL6 degC	UCIL7 degC	UCIL8 degC
0		26			
5		25			
10		24.5			
15		24			
20		24			
25		24.5			
30		24			
35		24			
40		24			
45		24			
50		24			
55		24			
60		24	28		
65		24	28		
70		24.5	27		
75		24.5	26.5	27.5	
80		24.5	26.5	28	
85		24.5	26.5	28	
90		24.5	26.5	27.5	
95		25	27	27.5	27.5
100		25	27	27.5	29
105		25.5	27	27.5	28
110		25.5	27	27	27
115		25.5	27	27	26.5
120	27.3	25.5	27	27.5	26
125	27.9	25.5	27	27.5	26
130	28.1	26	27.5	27.5	26
135	28.2	26	27.5	27.5	26
140	28.1	26	27.5	27.5	26.5
145	28.3	26	28	28	26.5
150	28	26.5	27.5	28	26.5
155	27.9	26.5	28	28	27
160	28.4	26.5	28	28	27
165	28.3	26.5	28	28.5	27.5
170	28.2	26.5	28	28.5	27.5
175	28.2	27	28	28.5	27.5
180	28.5	27	28	29	27.5
185	28.3	27	28.5	29	28
190	28.3	27	28.5	29	28
195	28.4	27	28.5	29	28
200	28.4	27	28.5	29	28
205	28.6	27	28.5	29	28
210	28.6	27.5	28.5	29.5	28
215	28.8	27.5	28.5	29.5	28
220	28.8	27.5	28.5	29.5	28
225	28.8	27.5	28.5	29.5	28.5
230	28.7	27.5	28	29.5	28.5
235	28.4	27	28.5	29	28

240	28.5	27	28.5	28.5	27.5
245	28.8	27	29	29	27.5
250	28.8	27.5	28.5	29.5	28
255	28.9	27.5	28.5	29.5	28.5
260	28.8	27.5	28.5	30	28.5
265	29.3	28	29	30	29
270	29.4	28	29	30.5	29.5
275	29	28	29	30	29.5
280	29.1	28	29	30	30
285	28.9	28	29.5	30	30.5
290	29.1	28	28.5	30	30.5
295	29.3	28	29	30	30.5
300	29.3	28	29.5	30.5	30
305	29.2	28	29	30.5	30
310	30.8	28	29.5	29.5	29
315	31.3	27.5	29.5	29.5	29
320	32	27.5	29.5	29.5	28.5
325	30.5	27.5	29	29.5	29
330	31.1	27.5	29	29.5	28.5
335	31.6	27.5	28.5	29.5	28
340	34.2	27	28.5	29.5	28
345	34.7	27	29	29.5	28
350	31.6	27.5	29	30	28.5
355	30.4	27.5	29	30	28.5
360	30.8	27.5	29	29.5	28
365	30.9	27.5	29	29.5	28
370	29.6	27.5	28.5	29.5	28.5
375	29.6	27.5	28.5	29.5	28
380	30.1	27	28.5	29.5	28
385	34.8	27.5	29	29.5	28
390	33.9	28	29.5	30	28.5
395	33.4	28	29.5	30.5	28.5
400	30	28	29.5	30.5	28.5
405	30.1	28	29	30.5	28.5
410	30	28	28.5	30	28.5
415	29.8	28	28.5	30	28.5
420	29.4	28	28.5	30	28.5
425	30.3	28	28.5	29.5	28.5
430	30.7	27.5	28.5	29.5	28
435	31.4	27.5	29	29.5	28
440	31.1	27.5	29.5	29.5	28
445	32.8	27.5	29.5	29	28
450	33.1	27.5	30	29.5	28
455	32.9	27.5	30.5	29.5	28
460	33.8	28	30.5	29.5	28.5
465	34.2	28	30.5	30	28.5
470	34.4	28	30	30	28.5
475	34	28	30.5	30	28.5
480	32.2	28	30	30	28.5
485	32.8	28	29.5	30	28.5

490	**39.9**	28	30	29.5	28
495	33.3	27.5	29.5	29.5	28
500	33.7	27.5	29.5	29.5	28
505	33.9	27.5	29.5	29.5	27.5
510	33.4	27	29.5	29.5	28
515	33	27	29.5	29.5	27.5
520	32.6	27	29.5	29	27.5
525	32.3	26.5	29.5	29	27.5
530	31.4	26.5	29.5	29	27.5
535	31.3	26.5	29	29	27
540	30.7	26	29	29	27.5
545	30.6	26	28.5	28.5	27
550	30.1	26	28	28.5	27
555	29.6	26	28	28.5	26.5
560	29.4	26	27.5	28	27
565	29.4	25.5	27.5	28	26.5
570	29.2	25.5	27.5	27.5	26.5
575	29.1	25.5	27.5	27.5	26.5
580	29	25.5	27.5	27.5	26.5
585	28.7	25.5	27.5	29	26.5
590	28.6	25.5	27	30	26.5

Timecum	UCIL1 (%)	UCIL2 (%)	UCIL6 (%)	UCIL7 (%)	UCIL8 (%)
0.0		74.5			
5.0		77.0			
10.0		78.0			
15.0		80.0			
20.0		80.5			
25.0		79.0			
30.0		80.0			
35.0		80.5			
40.0		80.5			
45.0		81.0			
50.0		81.0			
55.0		81.5			
60.0		81.5	74.0		
65.0		80.5	70.5		
70.0		79.0	72.5		
75.0		78.0	73.0	76.0	
80.0		77.5	74.0	72.0	
85.0		76.5	73.0	69.0	
90.0		77.5	70.5	71.5	
95.0		75.5	70.5	68.5	75.0
100.0		75.5	70.0	69.0	70.5
105.0		75.5	70.5	69.5	68.0
110.0		74.0	69.5	70.5	70.5
115.0		74.0	70.5	71.0	73.0
120.0	58.0	74.5	70.5	70.0	72.0
125.0	58.0	74.0	71.5	71.0	72.5
130.0	56.0	74.5	71.0	70.5	73.5
135.0	56.0	73.5	71.0	71.0	73.5
140.0	57.0	73.5	71.5	71.5	73.5
145.0	56.0	74.0	70.0	71.0	73.0
150.0	55.0	74.0	61.0	69.0	74.0
155.0	48.0	67.5	62.5	64.5	69.0
160.0	48.0	63.5	63.5	62.5	67.5
165.0	44.0	65.5	64.5	62.5	63.5
170.0	45.0	67.0	62.5	60.5	67.5
175.0	45.0	65.5	61.0	60.5	64.0
180.0	41.0	64.5	58.0	60.5	59.0
185.0	39.0	63.0	58.0	59.0	62.0
190.0	39.0	63.0	57.5	58.0	60.5
195.0	39.0	61.5	57.0	57.5	58.5
200.0	38.0	58.5	53.0	56.0	56.5
205.0	40.0	59.0	54.0	52.5	57.0
210.0	42.0	58.5	54.0	54.5	57.0
215.0	41.0	59.5	55.0	55.0	61.0
220.0	40.0	58.0	56.0	54.5	56.0
225.0	42.0	59.0	56.5	55.5	56.5
230.0	43.0	59.0	55.0	54.5	56.5
235.0	41.0	60.5	55.5	55.0	57.5
240.0	42.0	60.0	54.5	57.5	63.5

245.0	42.0	60.5	54.5	54.5	62.5
250.0	41.0	59.0	54.0	55.0	58.5
255.0	40.0	58.0	54.0	52.5	56.5
260.0	42.0	58.5	54.5	54.5	56.5
265.0	41.0	58.5	54.5	54.5	56.5
270.0	42.0	59.0	56.0	55.5	60.5
275.0	40.0	59.0	53.0	55.5	57.0
280.0	43.0	57.0	54.0	54.0	55.0
285.0	41.0	58.0	53.5	54.0	55.5
290.0	42.0	58.0	55.0	54.0	56.5
295.0	40.0	58.0	56.0	54.0	54.5
300.0	42.0	58.0	54.0	53.5	54.5
305.0	41.0	58.5	56.0	53.5	55.0
310.0	37.0	61.0	54.5	53.5	55.0
315.0	36.0	61.0	55.0	55.5	56.0
320.0	36.0	60.0	54.5	54.5	56.0
325.0	38.0	59.5	55.0	55.5	58.0
330.0	37.0	61.5	57.0	55.0	59.0
335.0	36.0	61.0	56.5	57.0	61.0
340.0	31.0	62.5	56.5	56.5	61.0
345.0	31.0	62.5	55.5	56.0	59.5
350.0	40.0	60.5	55.5	54.5	57.5
355.0	38.0	61.0	55.5	55.5	58.0
360.0	39.0	61.0	56.0	56.5	58.0
365.0	38.0	62.0	56.0	58.5	60.5
370.0	41.0	63.0	57.5	58.0	60.0
375.0	41.0	65.0	57.0	57.0	61.5
380.0	40.0	63.0	58.0	57.0	63.5
385.0	31.0	62.5	58.5	56.5	60.5
390.0	31.0	61.0	56.0	54.5	58.5
395.0	31.0	59.5	56.5	54.0	58.5
400.0	39.0	60.5	56.0	54.5	58.0
405.0	38.0	64.0	57.0	55.5	62.0
410.0	40.0	59.5	57.0	55.0	59.5
415.0	42.0	60.0	57.5	56.5	59.0
420.0	43.0	59.5	57.5	54.5	59.0
425.0	42.0	59.5	57.5	56.0	58.5
430.0	38.0	63.5	58.0	57.0	59.5
435.0	39.0	61.0	58.5	57.0	59.5
440.0	39.0	62.0	58.5	59.0	60.0
445.0	36.0	62.0	57.5	58.0	60.0
450.0	33.0	63.5	56.5	55.5	59.0
455.0	33.0	61.0	55.5	57.5	59.0
460.0	32.0	60.0	54.0	57.5	59.0
465.0	30.0	60.5	54.5	56.0	58.0
470.0	30.0	60.5	55.5	55.5	62.0
475.0	31.0	59.5	54.5	56.0	58.0
480.0	33.0	63.0	55.5	57.0	59.5
485.0	33.0	62.0	55.0	56.5	59.5
490.0	**33.0**	66.0	54.5	55.0	63.0

495.0	32.0	65.0	56.5	58.0	59.5
500.0	32.0	67.5	56.0	59.0	62.5
505.0	30.0	64.0	57.5	57.5	61.5
510.0	31.0	65.5	56.0	58.5	63.5
515.0	33.0	65.0	56.5	59.0	65.0
520.0	33.0	66.5	58.0	57.5	65.0
525.0	32.0	67.0	56.5	59.0	64.5
530.0	34.0	67.5	57.5	59.0	67.5
535.0	34.0	67.5	57.5	60.0	64.0
540.0	36.0	67.5	61.0	59.0	65.5
545.0	37.0	68.5	61.0	60.0	67.0
550.0	46.0	69.0	61.0	59.5	67.0
555.0	44.0	68.5	61.0	61.5	67.5
560.0	45.0	68.5	62.0	62.5	65.0
565.0	46.0	69.5	62.5	63.5	67.5
570.0	45.0	69.0	64.5	64.0	69.0
575.0	46.0	71.0	65.0	64.5	69.0
580.0	47.0	70.5	66.0	63.5	69.5
585.0	47.0	70.5	64.0	65.0	70.0
590.0	48.0	70.5	64.0	61.5	70.0

Timecum	UCIL1 degC	UCIL2 degC	UCIL6 degC	UCIL7 degC	UCIL8 degC
0.0					17.5
5.0					17.5
10.0					18.0
15.0		20.0			18.0
20.0		20.0			18.0
25.0		19.5			18.5
30.0		19.0			18.5
35.0		19.0			18.5
40.0		19.0			19.0
45.0		19.0			19.0
50.0		19.5	20.5		19.5
55.0		19.5	21.0	21.0	19.5
60.0		19.5	21.0	21.0	19.5
65.0		19.5	21.5	21.0	19.5
70.0		20.0	22.0	21.0	19.5
75.0		20.0	22.0	21.0	20.0
80.0		20.0	21.0	21.0	20.0
85.0		20.0	21.0	21.0	20.5
90.0		20.0	21.0	21.0	20.5
95.0		20.5	21.0	21.0	21.0
100.0		20.5	21.0	21.0	21.0
105.0		20.5	21.5	21.0	21.5
110.0		21.0	21.5	21.0	21.5
115.0		21.0	21.0	21.5	21.5
120.0		21.0	21.5	21.5	21.5
125.0		21.0	21.5	21.5	22.0
130.0	22.0	21.0	21.5	21.5	22.0
135.0	22.2	21.5	21.5	21.5	22.5
140.0	22.2	21.5	21.5	21.5	22.5
145.0	22.2	22.0	21.5	21.5	22.5
150.0	22.1	22.0	21.5	22.0	23.0
155.0	22.2	22.0	22.0	22.0	23.0
160.0	21.9	22.0	22.0	22.0	23.0
165.0	22.2	22.5	22.0	22.0	23.0
170.0	22.4	22.5	22.0	22.0	23.0
175.0	22.3	22.5	22.0	22.0	23.5
180.0	22.6	22.5	22.0	22.0	23.5
185.0	22.5	23.0	22.5	22.5	23.5
190.0	22.6	23.0	22.5	22.5	24.0
195.0	22.8	23.5	22.5	22.5	23.5
200.0	22.8	23.5	22.5	22.5	23.5
205.0	22.9	23.5	22.5	22.5	24.0
210.0	22.8	23.5	22.5	22.5	24.0
215.0	23.9	24.0	22.5	22.5	24.5
220.0	23.1	24.0	23.0	23.0	24.5
225.0	23.2	24.0	23.0	23.0	24.5
230.0	23.8	24.0	23.0	23.0	24.5
235.0	23.3	24.0	23.0	23.0	24.5
240.0	23.4	24.0	23.0	23.0	24.5

245.0	23.5	24.0	23.0	23.0	24.5
250.0	23.7	24.5	23.5	23.5	24.5
255.0	23.6	24.5	23.5	23.5	24.5
260.0	23.8	24.5	23.5	23.5	24.5
265.0	23.7	24.5	23.5	23.5	24.5
270.0	23.6	25.0	23.5	23.5	24.5
275.0	23.7	25.0	23.5	23.5	25.0
280.0	23.9	25.0	23.5	23.5	25.0
285.0	24.0	25.0	23.5	23.5	25.0
290.0	24.1	25.0	24.0	24.0	25.0
295.0	23.0	25.0	24.0	24.0	25.0
300.0	24.1	25.0	24.0	24.0	25.0
305.0	24.0	25.0	24.0	24.0	25.0
310.0	24.0	25.0	24.0	24.0	25.5
315.0	24.1	25.0	24.0	24.0	25.5
320.0	24.0	25.0	24.0	24.0	25.0
325.0	24.0	25.0	24.0	24.0	25.0
330.0	24.2	25.0	24.0	24.0	25.5
335.0	24.2	25.0	24.0	24.0	25.5
340.0	24.4	25.0	24.0	24.0	25.5
345.0	24.1	25.0	24.0	24.0	25.5
350.0	24.1	25.5	24.0	24.0	25.5
355.0	24.3	25.0	24.0	24.0	25.5
360.0	24.2	25.0	24.0	24.0	25.5
365.0	24.3	25.5	24.0	24.5	25.5
370.0	24.3	25.5	24.5	24.5	25.5
375.0	24.4	25.0	24.5	24.5	25.5
380.0	24.4	25.0	24.5	24.5	25.5
385.0	24.4	25.5	24.5	24.5	25.5
390.0	24.4	25.0	24.5	24.5	25.5
395.0	24.5	25.0	24.5	24.5	25.5
400.0	24.4	25.0	24.5	24.5	25.5
405.0	24.3	25.0	24.5	24.5	25.5
410.0	24.5	25.0	24.5	24.5	25.5
415.0	24.5	25.0	24.5	24.5	25.5
420.0	24.5	25.0	24.5	24.5	25.5
425.0	24.5	25.0	24.5	24.5	25.5
430.0	24.5	25.0	24.5	24.5	25.5
435.0	24.5	25.0	24.5	24.5	25.5
440.0	24.5	25.0	24.5	24.5	25.5
445.0	24.4	25.0	24.5	24.5	25.5
450.0	24.5	25.0	24.5	25.0	25.5
455.0	24.4	25.0	24.5	25.0	25.5
460.0	24.3	24.5	24.5	24.5	25.0
465.0	24.2	24.5	24.5	24.5	25.0
470.0	24.2	24.5	24.5	24.5	25.0
475.0	24.1	24.5	24.5	24.5	25.0
480.0	24.1	24.5	24.5	24.5	24.5
485.0	24.1	24.5	24.5	24.5	24.5
490.0	24.1	24.5	24.5	24.5	24.5
495.0	23.9	24.0	24.5	24.5	24.5

500.0	23.9	24.0	24.5	24.5	24.0
505.0	23.8	24.0	24.5	24.5	24.0
510.0	23.6	24.0	24.5	24.0	24.0
515.0	23.6	23.5	24.5	24.0	23.5
520.0	23.6	23.5	24.5	24.0	23.5
525.0	23.5	23.5	24.0	24.0	23.5
530.0	23.4	23.5	24.0	24.0	23.5
535.0	22.2	23.5	23.5	23.5	23.0
540.0	23.2	23.0	23.5	23.5	23.0

Timecum	UCIL1 (%)	UCIL2 (%)	UCIL6 (%)	UCIL7 (%)	UCIL8 (%)
0.0					86.5
5.0					86.5
10.0					85.0
15.0		73.5			83.5
20.0		74.5			83.0
25.0		75.0			82.5
30.0		76.5			82.0
35.0		76.5			81.5
40.0		76.5			81.5
45.0		77.0			81.0
50.0		77.0	76.5		81.0
55.0		76.5	75.5	73.5	80.0
60.0		77.0	74.5	75.0	79.5
65.0		77.0	74.5	74.5	79.5
70.0		77.0	72.5	75.0	79.5
75.0		77.0	71.5	74.5	79.0
80.0		76.5	73.0	74.5	79.0
85.0		76.0	74.0	75.5	78.5
90.0		75.5	74.5	75.0	77.5
95.0		76.0	74.0	75.0	78.5
100.0		75.5	74.0	74.5	76.0
105.0		75.5	74.0	74.5	75.5
110.0		75.0	74.5	74.0	75.0
115.0		75.0	74.0	74.0	74.5
120.0		75.0	74.0	74.0	74.0
125.0		74.0	74.5	74.0	73.5
130.0	64.0	74.0	73.5	73.5	73.0
135.0	65.0	74.5	73.5	73.5	73.5
140.0	64.0	74.5	73.5	73.5	72.5
145.0	64.0	73.5	73.5	73.5	71.5
150.0	65.0	72.5	73.0	73.5	71.5
155.0	66.0	71.5	73.5	73.0	72.0
160.0	62.0	70.5	70.5	71.0	70.0
165.0	60.0	70.0	71.5	71.0	70.0
170.0	58.0	70.0	70.5	70.5	69.0
175.0	61.0	68.0	71.5	71.0	69.5
180.0	62.0	70.5	70.5	70.5	67.0
185.0	60.0	69.0	70.5	70.5	68.0
190.0	61.0	68.0	70.5	70.0	67.0
195.0	58.0	67.5	69.5	68.5	66.5
200.0	56.0	68.0	68.5	67.5	66.5
205.0	55.0	67.0	67.5	66.5	68.0
210.0	53.0	67.5	66.0	66.5	65.5
215.0	55.0	67.0	67.0	66.5	66.0
220.0	57.0	66.0	68.0	67.0	63.0
225.0	57.0	66.0	68.5	67.5	62.5
230.0	56.0	64.5	67.0	67.0	63.0
235.0	56.0	65.0	67.5	67.5	63.0
240.0	53.0	63.5	67.0	65.5	61.5

245.0	58.0	62.5	67.0	66.0	60.5
250.0	52.0	62.5	64.5	63.0	62.5
255.0	53.0	62.0	66.0	64.5	64.5
260.0	52.0	63.0	65.5	65.0	64.0
265.0	58.0	60.5	65.5	64.5	63.5
270.0	52.0	62.0	64.0	64.0	64.5
275.0	53.0	62.0	66.0	65.0	63.5
280.0	54.0	63.0	65.5	65.0	65.0
285.0	53.0	63.5	66.0	64.5	63.5
290.0	51.0	62.0	66.0	64.0	63.0
295.0	51.0	62.5	64.0	63.0	61.5
300.0	52.0	61.5	64.5	63.0	62.0
305.0	51.0	63.0	64.0	63.0	61.5
310.0	52.0	61.5	64.0	63.0	61.5
315.0	53.0	60.5	64.5	63.5	61.5
320.0	51.0	60.5	63.5	63.5	61.5
325.0	52.0	61.0	64.5	64.0	61.0
330.0	51.0	60.5	64.5	63.5	58.5
335.0	50.0	60.5	64.0	63.0	59.0
340.0	48.0	60.0	63.5	62.0	55.0
345.0	49.0	61.5	63.0	63.0	57.5
350.0	48.0	60.5	62.0	61.5	58.0
355.0	47.0	59.5	62.5	61.5	57.0
360.0	48.0	61.0	61.0	60.0	58.5
365.0	48.0	60.0	61.5	61.0	57.5
370.0	46.0	58.5	61.5	61.0	57.0
375.0	45.0	58.5	59.5	59.5	58.5
380.0	46.0	59.0	60.5	59.0	57.5
385.0	46.0	59.0	60.5	59.5	57.5
390.0	44.0	58.0	59.5	57.5	58.5
395.0	45.0	58.5	60.5	58.5	59.0
400.0	47.0	58.5	60.5	59.0	59.0
405.0	47.0	58.5	60.0	59.0	60.0
410.0	46.0	58.5	61.0	59.0	58.0
415.0	48.0	59.5	61.0	59.5	59.0
420.0	47.0	59.5	59.5	58.5	59.5
425.0	45.0	59.0	59.0	57.5	59.0
430.0	48.0	58.5	59.0	58.0	58.5
435.0	47.0	59.0	59.5	59.0	59.5
440.0	49.0	59.5	62.0	59.5	59.5
445.0	48.0	60.5	61.5	59.5	60.0
450.0	49.0	59.5	62.0	60.0	59.5
455.0	49.0	59.5	60.0	59.0	59.5
460.0	50.0	60.5	60.5	59.5	60.0
465.0	50.0	61.0	62.0	60.5	60.5
470.0	51.0	61.5	62.5	61.0	61.5
475.0	50.0	61.5	61.0	59.5	62.0
480.0	51.0	61.5	62.0	61.0	62.5
485.0	52.0	62.5	63.5	62.0	63.0
490.0	52.0	62.5	63.0	62.5	64.0
495.0	54.0	63.5	64.0	63.5	63.5

500.0	54.0	63.0	64.0	64.0	63.5
505.0	55.0	63.5	65.0	64.0	64.0
510.0	54.0	63.5	64.0	63.5	64.5
515.0	55.0	64.0	64.0	63.5	64.5
520.0	57.0	64.0	65.0	64.5	65.0
525.0	56.0	65.0	65.0	65.0	66.0
530.0	56.0	65.0	64.5	64.5	66.5
535.0	56.0	65.5	65.5	65.0	67.0
540.0	57.0	65.5	66.5	66.0	67.0

Timecum	UCIL1 degC	UCIL1Hh degC	UCIL2 degC	UCIL2Hh degC	UCIL3 degC	UCIL4 degC	UCIL6 degC	UCIL7 degC	UCIL8 degC	UCIL8_D degC
0.0										
5.0										
10.0										
15.0										
20.0										
25.0					26.0					
30.0					25.0					
35.0					24.5					
40.0					23.5					
45.0					23.0					
50.0					23.0					
55.0	24.0				22.5					
60.0	23.5	24.3			22.0					
65.0	23.5	25.1			22.0					
70.0	23.0	25.8	24.0		22.0					
75.0	23.0	25.7	24.0		22.0					
80.0	23.0	26.7	23.5		22.0					
85.0	23.0	25.5	23.5	25.8	22.0					
90.0	22.5	26.0	23.5	25.6	22.5					
95.0	22.5	26.3	23.5	26.7	22.5					
100.0	22.5	25.3	23.5	27.3	22.5					
105.0	22.5	25.2	23.5	28.8	22.5	25.0				
110.0	22.5	25.3	23.5	29.4	22.5	24.5				
115.0	23.0	25.8	23.5	29.2	23.0	24.0	24.5			
120.0	23.0	26.1	23.5	28.9	23.0	24.0	24.0	25.0		
125.0	23.0	26.3	23.5	28.5	23.0	24.0	23.5	24.5		
130.0	23.5	26.0	23.5	28.1	23.0	24.0	23.5	24.5		
135.0	23.5	26.2	23.5	27.6	23.0	24.0	23.5	24.0		
140.0	24.0	25.0	24.0	27.5	23.5	24.0	23.5	24.0	24.5	
145.0	24.0	25.3	24.0	27.6	23.5	24.0	23.5	23.5	24.5	
150.0	24.5	25.5	24.0	27.1	24.0	24.0	23.5	23.5	24.0	
155.0	24.5	25.7	24.0	27.2	24.0	24.0	23.5	23.5	24.0	
160.0	24.5	25.4	24.0	27.4	24.0	24.0	23.5	23.5	24.0	
165.0	24.5	25.5	24.5	28.1	24.5	24.0	23.5	23.5	23.5	
170.0	24.5	25.3	24.5	29.2	24.5	24.0	23.5	23.5	24.0	
175.0	24.5	25.6	24.5	29.1	24.5	24.0	24.0	23.5	24.0	
180.0	24.5	25.7	24.5	30.7	24.5	24.0	24.0	23.5	24.0	
185.0	24.0	25.6	25.0	29.4	25.0	24.5	24.0	24.0	24.0	
190.0	24.0	25.7	25.0	28.4	25.0	24.5	24.0	24.0	24.0	
195.0	24.0	25.7	25.0	28.7	25.0	24.5	24.5	24.0	24.5	
200.0	24.0	26.0	25.0	28.6	25.0	25.0	24.5	24.5	24.5	
205.0	24.0	26.0	25.0	29.2	25.5	25.5	25.0	24.5	24.5	
210.0	24.5	25.1	25.0	30.1	25.5	25.5	25.0	24.5	24.5	
215.0	24.5	26.1	25.0	29.7	25.5	25.5	25.5	25.0	24.5	
220.0	24.5	26.2	25.0	29.8	25.5	26.0	26.0	25.0	25.0	
225.0	24.5	26.4	25.5	30.0	25.5	26.5	26.0	25.0	25.0	
230.0	24.5	26.6	25.5	31.3	26.0	26.5	26.5	25.0	25.0	
235.0	24.5	26.4	25.5	31.6	26.0	27.0	26.5	25.5	25.5	

240.0	25.0	26.1	25.5	29.8	26.0	27.0	26.5	25.5	25.5	
245.0	25.0	26.4	25.5	29.5	26.5	27.0	26.5	25.5	25.5	27.0
250.0	25.0	26.6	26.0	30.8	26.5	27.5	26.5	25.5	25.5	27.0
255.0	25.0	26.5	26.0	31.4	26.5	27.5	26.5	26.0	25.5	27.0
260.0	25.0	26.5	26.0	31.4	26.5	27.5	27.0	26.0	26.0	27.0
265.0	25.0	26.5	26.0	31.4	27.0	27.5	27.0	26.0	26.0	27.0
270.0	25.0	26.6	26.5	31.5	27.0	28.0	27.0	26.5	26.0	27.0
275.0	25.5	26.7	26.5	31.5	27.0	28.0	27.0	27.0	26.0	27.0
280.0	25.5	26.7	27.0	32.8	27.0	28.5	27.0	27.0	26.0	28.0
285.0	25.5	26.8	27.0	32.7	27.0	28.5	27.0	27.5	26.0	28.0
290.0	25.5	29.6	27.5	32.5	27.5	28.5	27.5	27.5	26.5	27.0
295.0	25.5	29.2	27.5	33.1	27.5	28.5	27.5	27.5	26.5	27.0
300.0	25.5	30.4	27.0	32.1	27.5	28.5	27.5	28.0	26.5	28.0
305.0	25.5	30.9	27.0	33.0	27.5	28.5	27.0	28.0	26.5	27.0
310.0	25.5	31.5	26.5	31.5	27.5	29.0	27.0	28.0	26.5	28.0
315.0	25.5	32.2	26.5	32.5	27.5	29.0	27.0	28.0	26.5	27.0
320.0	26.0	30.6	26.5	33.6	27.5	29.0	27.5	28.0	27.0	28.0
325.0	26.0	30.4	27.0	32.4	28.0	29.5	27.5	28.0	27.0	28.0
330.0	26.0	31.4	27.0	31.5	28.0	29.5	27.5	28.0	27.0	28.0
335.0	26.0	31.3	27.0	32.1	28.0	29.5	27.5	28.5	27.5	28.0
340.0	26.0	31.5	27.0	33.3	28.0	29.5	27.5	28.5	27.5	28.0
345.0	26.0	30.4	27.5	32.9	28.0	29.5	27.5	28.5	27.5	28.0
350.0	26.0	31.7	27.5	33.7	28.5	29.5	27.5	29.0	27.5	28.0
355.0	26.5	33.2	28.0	32.2	28.5	29.5	27.5	29.0	27.5	29.0
360.0	26.5	32.2	28.0	33.4	28.5	29.5	27.5	29.0	27.5	29.0
365.0	26.5	32.0	28.0	33.1	28.5	29.5	27.5	29.0	27.5	29.0
370.0	26.5	30.9	28.0	32.3	28.5	29.5	27.5	29.0	27.5	29.0
375.0	26.5	32.8	28.5	32.9	28.0	29.5	27.5	29.0	27.5	29.0
380.0	26.5	32.5	28.5	32.5	28.0	29.5	27.5	29.0	27.5	29.0
385.0	26.5	31.5	28.5	32.2	28.5	29.5	28.0	29.0	27.5	29.0
390.0	26.5	31.8	28.5	32.7	28.5	29.5	28.0	29.0	27.5	29.0
395.0	26.5	33.7	28.5	32.7	28.5	29.0	28.0	28.5	27.5	29.0
400.0	26.5	31.6	28.5	32.0	28.5	29.0	28.5	29.0	27.5	29.0
405.0	26.5	32.8	28.5	31.7	28.5	29.0	28.0	29.0	27.5	29.0
410.0	26.5	35.5	29.0	32.5	28.5	29.0	28.0	29.0	27.5	29.0
415.0	26.5	34.8	29.0	31.6	28.5	29.0	28.0	29.0	28.0	29.0
420.0	27.0	33.9	29.0	32.0	28.5	29.0	28.0	29.0	28.0	29.0
425.0	27.0	32.5	29.0	32.5	28.5	29.0	27.5	29.5	28.0	29.0
430.0	27.0	33.0	29.0	32.2	28.5	29.0	27.5	29.5	28.0	29.0
435.0	27.0	34.9	29.0	32.4	28.5	29.0	27.5	30.0	28.0	29.0
440.0	27.0	33.5	29.0	32.3	28.5	29.0	27.5	30.0	28.0	29.0
445.0	27.0	34.5	29.0	32.9	28.5	29.0	27.5	30.0	28.0	29.0
450.0	27.0	34.2	29.5	31.9	28.5	28.5	27.5	29.5	28.0	29.0
455.0	27.0	30.5	29.5	31.3	28.5	28.5	27.5	29.5	28.0	29.0
460.0	27.0	30.4	29.5	32.7	28.5	28.5	27.5	29.5	28.0	29.0
465.0	27.0	33.2	29.0	32.8	28.5	28.5	27.5	29.5	28.0	29.0
470.0	27.0	30.1	29.0	32.9	28.5	28.5	27.5	29.0	28.0	29.0
475.0	27.0	32.8	29.0	33.9	28.5	28.5	27.5	29.0	28.0	29.0
480.0	27.0	30.2	29.0	33.2	28.5	28.5	27.5	29.0	28.0	29.0
485.0	27.0	31.8	29.0	32.9	28.5	28.5	27.5	29.0	28.0	30.0

490.0	27.0	31.6	29.0	32.9	28.5	28.5	27.5	29.0	28.0	29.0
495.0	27.0	31.2	29.0	33.5	28.5	28.5	27.5	29.0	28.0	29.0
500.0	27.0	30.9	29.0	32.5	28.5	28.5	27.5	29.0	28.0	29.0
505.0	27.0	31.5	29.0	33.0	28.5	28.0	27.5	29.0	28.0	29.0
510.0	27.0	30.4	29.0	33.5	28.5	28.0	27.5	28.5	28.0	29.0
515.0	27.0	30.2	29.0	34.2	28.5	28.0	27.5	28.5	28.0	29.0
520.0	27.0	30.5	29.0	33.0	28.5	28.0	27.5	28.5	28.0	29.0
525.0	27.0	30.6	29.0	33.3	28.5	28.0	27.5	28.5	28.0	29.0
530.0	27.0	30.8	29.0	32.2	28.0	28.0	27.0	28.5	27.5	29.0
535.0	27.0	29.3	29.0	32.2	28.0	28.0	27.0	28.0	27.5	28.0
540.0	27.0	29.4	29.0	30.9	28.0	28.0	27.0	28.0	27.5	28.0
545.0	27.0	29.8	29.0	32.6	28.0	28.0	27.0	28.0	27.5	28.0
550.0	27.0	29.5	29.0	32.8	28.0	28.0	27.0	28.0	27.5	28.0
555.0	27.0	29.1	29.0	31.3	28.0	28.0	27.0	28.0	27.5	28.0
560.0	27.0	29.0	28.5	31.9	28.0	27.5	27.0	28.0	27.5	28.0
565.0	27.0	28.9	28.5	32.1	28.0	27.5	27.0	27.5	27.5	28.0
570.0	27.0	28.7	28.5	30.2	27.5	27.5	26.5	27.5	27.5	28.0
575.0	27.0	28.7	28.5	29.6	27.5	27.5	26.5	27.5	27.5	28.0
580.0	27.0	28.5	28.5	29.5	27.5	27.5	26.5	27.5	27.0	27.0
585.0	27.0	28.4	28.0	30.1	27.5	27.5	26.5	27.5	27.0	27.0
590.0	27.0	28.1	28.0	29.0	27.5	27.5	26.5	27.0	27.0	27.0
595.0	27.0	28.2	28.0	28.9	27.0	27.0	26.5	27.0	27.0	27.0
600.0	26.5	27.8	27.5	28.4	27.0	27.0	26.0	27.0	27.0	27.0
605.0	26.5	27.7	27.5	28.4	27.0	27.0	26.0	27.0	26.5	27.0
610.0	26.5	27.5	27.5	27.7	27.0	27.0	26.0	27.0	26.5	27.0
615.0	26.5	27.3	27.5	28.2	27.0	27.0	26.0	26.5	26.5	26.0
620.0	26.5	27.2	27.0	27.2	27.0	27.0	26.0	26.5	26.5	26.0
625.0	26.5	27.1	27.0	27.5	26.5	26.5	25.5	26.5	26.5	26.0

Timecum	UCIL1 (%)	UCIL1Hh (%)	UCIL2 (%)	UCIL3 (%)	UCIL4 (%)	UCIL6 (%)	UCIL7 (%)	UCIL8 (%)	UCIL8_D (%)
0.0									
5.0									
10.0									
15.0									
20.0									
25.0				57.0					
30.0				58.0					
35.0				59.0					
40.0				60.5					
45.0				60.5					
50.0				61.0					
55.0	62.5			62.0					
60.0	62.5	51.0		63.5					
65.0	62.5	48.0		65.5					
70.0	63.5	46.0	59.5	65.0					
75.0	65.0	46.0	60.0	65.5					
80.0	64.5	46.0	60.5	65.5					
85.0	65.5	48.0	61.5	65.5					
90.0	66.5	45.0	61.0	65.5					
95.0	66.5	44.0	61.0	65.5					
100.0	67.0	48.0	61.5	65.0					
105.0	67.5	50.0	62.0	65.5	59.0				
110.0	67.5	50.0	61.5	65.5	59.5				
115.0	67.0	47.0	63.0	65.0	60.0	60.0			
120.0	67.0	26.1	63.0	65.0	60.5	61.0	59.0		
125.0	63.0	26.3	63.0	65.0	61.0	61.5	59.5		
130.0	63.0	26.0	61.5	64.5	61.5	61.5	60.0		
135.0	63.0	26.2	61.5	64.0	61.0	62.0	60.0		
140.0	62.0	25.0	60.5	64.0	61.5	62.5	60.5	60.0	
145.0	61.0	25.3	59.5	63.5	61.5	60.5	60.5	60.0	
150.0	61.0	25.5	58.0	62.0	60.5	60.5	60.0	59.0	
155.0	60.5	25.7	56.0	61.0	60.0	59.5	59.5	59.0	
160.0	60.5	25.4	58.0	60.5	60.0	60.0	59.5	58.5	
165.0	59.0	25.5	58.0	59.5	59.5	59.0	60.0	59.5	
170.0	60.0	25.3	57.5	59.5	59.0	58.0	60.0	59.5	
175.0	59.5	25.6	57.5	58.0	59.0	57.0	59.5	59.0	
180.0	58.5	25.7	55.5	58.0	58.5	56.5	60.0	59.0	
185.0	58.0	41.0	56.0	58.5	59.5	57.0	59.5	58.0	
190.0	57.0	40.0	55.0	58.5	59.5	56.5	60.5	58.0	
195.0	54.5	37.0	53.5	58.0	57.5	56.5	61.0	57.0	
200.0	55.0	36.0	53.0	56.0	56.5	55.0	59.0	54.5	
205.0	55.5	36.0	52.5	56.0	54.5	55.0	56.5	55.0	
210.0	56.5	36.0	52.0	54.5	51.0	53.5	57.5	53.5	
215.0	53.5	36.0	52.5	55.5	52.0	53.0	55.0	54.0	
220.0	54.5	36.0	54.0	55.0	53.0	54.5	53.0	54.5	
225.0	55.0	36.0	54.5	54.0	50.5	51.0	53.5	53.0	
230.0	56.5	37.0	52.5	54.5	51.5	51.5	52.5	53.5	
235.0	54.5	36.0	53.0	53.5	51.0	52.0	53.5	53.5	

240.0	54.5	37.0	52.0	54.0	53.0	49.5	54.0	53.5	
245.0	54.5	36.0	51.5	54.0	51.0	50.5	53.5	52.5	44.0
250.0	54.5	36.0	53.0	52.5	51.0	51.5	54.5	52.5	44.0
255.0	54.0	36.0	51.5	53.0	49.0	51.5	52.5	52.5	44.0
260.0	52.5	36.0	51.0	52.5	49.0	51.0	53.5	53.5	46.0
265.0	53.0	35.0	48.5	51.5	50.0	49.5	55.0	51.5	42.0
270.0	52.5	35.0	49.0	51.5	49.0	48.0	52.0	50.5	42.0
275.0	51.5	34.0	48.5	51.5	48.5	48.5	50.5	50.5	41.0
280.0	52.5	35.0	47.5	50.5	48.0	47.5	52.0	50.5	42.0
285.0	53.0	35.0	47.5	51.0	47.0	48.5	50.0	50.0	41.0
290.0	53.5	32.0	49.0	50.5	46.0	49.0	48.0	50.5	43.0
295.0	52.0	31.0	47.5	50.0	47.5	49.5	50.0	50.0	42.0
300.0	50.5	29.0	48.0	51.0	46.0	49.5	48.5	49.5	44.0
305.0	51.5	28.0	47.5	51.0	46.0	50.0	48.5	49.5	42.0
310.0	51.5	28.0	53.0	50.5	46.5	49.5	48.0	48.5	42.0
315.0	51.0	27.0	48.0	49.0	44.0	50.0	47.5	47.5	42.0
320.0	51.0	28.0	47.5	50.0	46.0	48.5	49.5	48.5	42.0
325.0	50.5	28.0	48.0	50.0	46.0	51.0	48.0	49.5	41.0
330.0	50.5	28.0	48.0	48.0	43.0	46.5	47.0	48.0	40.0
335.0	50.0	28.0	48.0	48.5	44.5	49.0	47.0	49.0	40.0
340.0	49.5	27.0	50.0	48.5	45.0	49.0	48.0	47.5	41.0
345.0	48.5	28.0	47.0	48.5	44.5	47.0	46.0	47.0	40.0
350.0	48.5	27.0	46.5	47.5	42.5	47.0	47.0	47.0	39.0
355.0	49.5	25.0	44.5	48.0	43.0	46.5	45.0	46.5	39.0
360.0	48.0	25.0	45.5	47.0	42.5	45.5	45.0	46.5	38.0
365.0	47.5	25.0	45.5	47.0	41.5	44.5	42.0	45.0	36.0
370.0	48.0	26.0	42.5	44.5	41.5	45.5	43.0	45.0	36.0
375.0	48.5	26.0	43.0	45.5	40.5	44.0	42.5	45.0	38.0
380.0	48.5	25.0	43.0	44.5	40.5	43.5	43.0	43.5	36.0
385.0	48.5	26.0	42.5	44.5	41.0	44.0	43.5	45.0	36.0
390.0	48.5	26.0	43.0	45.5	41.5	44.5	44.0	45.0	38.0
395.0	47.5	23.0	42.5	44.5	42.5	44.5	45.5	46.0	37.0
400.0	45.5	25.0	42.5	43.0	41.5	43.5	42.5	43.5	36.0
405.0	45.5	24.0	41.5	43.5	41.5	44.5	43.5	44.0	35.0
410.0	45.5	22.0	42.5	43.5	41.5	43.5	44.5	43.5	36.0
415.0	48.0	22.0	41.5	44.5	41.5	44.0	42.5	43.5	36.0
420.0	47.5	22.0	43.0	45.5	42.5	45.5	44.0	45.5	37.0
425.0	47.5	24.0	42.5	44.5	42.0	44.5	45.0	45.0	36.0
430.0	47.5	23.0	42.5	46.0	42.5	44.0	45.0	43.5	36.0
435.0	47.5	22.0	42.0	44.5	42.5	44.5	44.0	44.5	37.0
440.0	48.0	23.0	43.0	46.0	42.5	45.5	43.0	44.5	38.0
445.0	48.5	23.0	42.5	46.0	43.5	45.5	44.0	44.5	38.0
450.0	47.5	22.0	43.5	46.0	42.5	48.0	43.0	44.5	38.0
455.0	48.0	26.0	42.5	46.0	43.5	45.5	45.0	44.5	38.0
460.0	47.5	26.0	42.5	46.0	43.5	45.5	42.5	45.5	38.0
465.0	46.5	23.0	42.0	46.0	43.5	45.0	43.5	45.0	37.0
470.0	47.0	25.0	41.5	45.0	43.5	44.5	43.0	45.5	37.0
475.0	46.5	24.0	41.5	45.0	43.0	44.5	43.5	45.0	37.0
480.0	46.5	26.0	42.0	45.0	43.5	45.5	45.0	45.5	37.0
485.0	47.5	25.0	42.5	45.0	44.0	45.5	45.5	44.5	36.0

490.0	46.5	25.0	42.5	44.0	43.5	45.5	45.0	44.5	36.0
495.0	45.5	25.0	41.5	45.0	43.0	45.5	43.5	44.5	37.0
500.0	47.5	25.0	41.0	44.5	43.0	46.5	43.5	43.5	37.0
505.0	46.5	25.0	41.5	45.0	44.5	44.5	43.5	44.0	37.0
510.0	47.0	26.0	42.0	44.5	43.5	45.5	43.0	45.0	38.0
515.0	47.0	26.0	42.0	44.5	44.5	45.5	44.5	44.5	38.0
520.0	45.5	25.0	41.5	45.0	44.0	45.5	44.5	44.0	38.0
525.0	46.5	26.0	42.0	45.0	44.5	45.5	45.0	44.5	39.0
530.0	46.5	26.0	41.5	45.5	44.0	45.0	44.0	44.5	37.0
535.0	46.0	27.0	41.0	45.0	44.5	45.0	44.5	44.5	38.0
540.0	45.5	27.0	41.0	45.5	44.5	45.5	45.0	44.0	38.0
545.0	46.5	27.0	41.5	45.5	44.5	46.0	44.5	44.5	38.0
550.0	46.0	27.0	42.5	45.5	44.5	47.0	45.5	45.5	40.0
555.0	46.5	27.0	41.5	45.5	44.5	48.0	45.5	44.5	39.0
560.0	47.0	27.0	41.0	45.5	44.5	47.0	46.0	45.0	39.0
565.0	47.0	28.0	41.5	46.0	45.0	46.5	46.5	45.5	39.0
570.0	46.5	28.0	42.5	46.5	44.5	46.5	45.5	45.5	39.0
575.0	47.0	29.0	42.5	46.5	44.5	47.5	46.0	45.5	40.0
580.0	47.0	29.0	42.5	46.5	45.0	47.5	46.5	45.5	41.0
585.0	47.5	29.0	43.5	46.5	44.5	48.0	46.5	46.0	40.0
590.0	48.5	30.0	42.5	46.5	45.0	48.0	46.5	46.5	42.0
595.0	47.5	29.0	43.5	46.5	45.0	48.5	46.0	46.5	42.0
600.0	47.5	30.0	44.5	46.5	45.5	48.5	46.0	46.5	43.0
605.0	48.0	30.0	43.5	47.0	45.5	48.5	47.5	46.5	44.0
610.0	47.5	30.0	46.5	47.5	45.5	49.0	48.0	47.0	44.0
615.0	47.0	30.0	45.5	47.5	45.5	50.0	48.5	47.5	45.0
620.0	47.0	31.0	45.5	47.5	47.0	50.0	49.5	47.5	45.0
625.0	48.0	31.0	45.5	47.5	47.0	51.5	49.5	48.0	46.0

Date	Time	BMD_T (degC)	BMD_RH (%)	UCIL8_T (degC)	UCIL8_RH(%)
12-Dec-16	12:00 PM	26.8	38	29	62.5
12-Dec-16	3:00 PM	27	38	27	51.5
12-Dec-16	6:00 PM	22.6	57	22.5	64.5
12-Dec-16	9:00 PM	20.9	66	21	71
13-Dec-16	12:00 AM	19.4	75	19.5	78
13-Dec-16	3:00 AM	18	82	18	83.5
13-Dec-16	6:00 AM	16.1	90	16	88.5
13-Dec-16	9:00 AM	19.5	73	19.5	79.5
13-Dec-16	12:00 PM	24.3	49	24.5	61.5
13-Dec-16	3:00 PM	25.3	46	25.5	59.5
13-Dec-16	6:00 PM	22	62	21.5	72.5
13-Dec-16	9:00 PM	19.6	74	19.5	81
14-Dec-16	12:00 AM	18	78	18	84
14-Dec-16	3:00 AM	17.4	85	16.5	85.5
14-Dec-16	6:00 AM	15.6	89	15.5	88
14-Dec-16	9:00 AM	18.4	78	18.5	78.5

Appendix G: Data from the Simulation and modeling

Simulated data_Dhanmondi Lake

Timecum	UCIL8 degC	UCIL7 degC	UCIL6 degC	UCIL5 degC	UCIL4 degC	UCIL3 degC	UCIL2 degC	UCIL2_a degC	UCIL2_b degC
0.00	23.20	23.20	23.20	23.20	23.20	23.20	23.20	23.20	23.20
5.00	26.83	25.26	26.71	27.69	26.11	27.51	28.52	28.92	29.04
10.00	28.09	27.05	27.84	28.59	27.86	28.46	29.06	29.38	29.46
15.00	28.67	27.72	28.30	28.84	28.42	28.77	29.14	29.42	29.49
20.00	29.22	28.18	28.73	29.09	28.82	29.04	29.21	29.44	29.48
25.00	29.71	28.58	29.12	29.29	29.17	29.31	29.27	29.48	29.51
30.00	30.18	28.97	29.50	29.49	29.52	29.56	29.33	29.51	29.53
35.00	30.62	29.34	29.86	29.68	29.85	29.80	29.40	29.54	29.54
40.00	31.05	29.71	30.22	29.87	30.18	30.04	29.46	29.57	29.55
45.00	31.46	30.07	30.56	30.06	30.50	30.27	29.53	29.60	29.57
50.00	31.85	30.43	30.90	30.24	30.81	30.50	29.59	29.63	29.58
55.00	32.23	30.77	31.23	30.42	31.12	30.72	29.66	29.66	29.59
60.00	32.61	31.11	31.55	30.58	31.42	30.94	29.73	29.70	29.61
65.00	32.92	31.44	31.87	30.80	31.71	31.15	29.79	29.73	29.62
70.00	33.35	31.76	32.10	30.79	32.00	31.38	29.90	29.76	29.63
75.00	33.63	32.08	32.44	31.09	32.27	31.56	29.94	29.79	29.65
80.00	33.96	32.39	32.74	31.27	32.54	31.76	30.01	29.82	29.66
85.00	34.26	32.68	33.02	31.43	32.81	31.96	30.09	29.85	29.67
90.00	34.56	32.97	33.29	31.60	33.07	32.16	30.17	29.88	29.68
95.00	34.85	33.26	33.56	31.76	33.32	32.35	30.24	29.91	29.70
100.00	35.13	33.54	33.82	31.91	33.56	32.54	30.32	29.94	29.71
105.00	35.41	33.81	34.07	32.07	33.80	32.73	30.40	29.97	29.72
110.00	35.67	34.07	34.32	32.22	34.04	32.91	30.47	30.00	29.73
115.00	35.93	34.33	34.56	32.37	34.26	33.09	30.54	30.03	29.75
120.00	36.18	34.59	34.79	32.51	34.49	33.26	30.61	30.06	29.76
125.00	36.41	34.83	35.01	32.66	34.71	33.44	30.69	30.09	29.77
130.00	36.64	35.08	35.23	32.80	34.92	33.61	30.76	30.12	29.78
135.00	36.86	35.31	35.44	32.94	35.13	33.77	30.83	30.15	29.80
140.00	37.07	35.55	35.65	33.07	35.33	33.93	30.90	30.18	29.81
145.00	37.28	35.77	35.85	33.20	35.53	34.09	30.97	30.21	29.82
150.00	37.47	35.99	36.04	33.33	35.73	34.25	31.04	30.23	29.83
155.00	37.66	36.21	36.22	33.46	35.91	34.39	31.11	30.26	29.85
160.00	37.84	36.42	36.40	33.58	36.10	34.54	31.18	30.29	29.86
165.00	38.00	36.63	36.57	33.71	36.28	34.68	31.24	30.32	29.87
170.00	38.16	36.83	36.73	33.82	36.45	34.82	31.31	30.35	29.88
175.00	38.31	37.02	36.88	33.93	36.62	34.95	31.37	30.37	29.89
180.00	38.46	37.20	37.03	34.04	36.78	35.08	31.44	30.40	29.90
185.00	38.59	37.38	37.17	34.15	36.94	35.20	31.50	30.43	29.92
190.00	38.72	37.56	37.31	34.25	37.09	35.32	31.57	30.45	29.93
195.00	38.85	37.73	37.44	34.36	37.24	35.44	31.63	30.48	29.94
200.00	38.96	37.89	37.57	34.46	37.39	35.55	31.69	30.50	29.95
205.00	39.06	38.05	37.68	34.56	37.53	35.67	31.75	30.53	29.96
210.00	39.16	38.21	37.78	34.66	37.67	35.78	31.81	30.55	29.97
215.00	39.24	38.36	37.87	34.75	37.80	35.88	31.87	30.58	29.98
220.00	39.32	38.50	37.95	34.84	37.93	35.99	31.92	30.60	29.99
225.00	39.40	38.64	38.02	34.93	38.06	36.09	31.98	30.62	30.00
230.00	39.47	38.78	38.09	35.01	38.18	36.18	32.03	30.65	30.01
235.00	39.55	38.90	38.16	35.09	38.30	36.28	32.09	30.67	30.02

240.00	39.61	39.02	38.23	35.18	38.42	36.37	32.14	30.69	30.02
245.00	39.68	39.14	38.29	35.25	38.53	36.45	32.19	30.71	30.03
250.00	39.73	39.25	38.35	35.33	38.63	36.54	32.24	30.73	30.04
255.00	39.78	39.35	38.40	35.40	38.73	36.62	32.29	30.75	30.05
260.00	39.83	39.45	38.45	35.47	38.83	36.69	32.33	30.77	30.06
265.00	39.87	39.54	38.49	35.54	38.92	36.76	32.38	30.79	30.07
270.00	39.92	39.63	38.52	35.60	39.01	36.83	32.42	30.81	30.07
275.00	39.95	39.72	38.56	35.66	39.09	36.89	32.47	30.82	30.08
280.00	39.98	39.80	38.58	35.71	39.17	36.95	32.51	30.84	30.09
285.00	40.00	39.87	38.60	35.77	39.25	37.00	32.55	30.86	30.09
290.00	40.02	39.95	38.61	35.82	39.32	37.05	32.59	30.87	30.10
295.00	40.03	40.01	38.63	35.86	39.38	37.10	32.62	30.89	30.11
300.00	40.03	40.08	38.63	35.91	39.44	37.14	32.66	30.90	30.11
305.00	40.02	40.13	38.64	35.95	39.50	37.17	32.69	30.92	30.12
310.00	40.02	40.18	38.64	35.99	39.55	37.21	32.72	30.93	30.12
315.00	40.00	40.23	38.63	36.03	39.59	37.24	32.76	30.94	30.13
320.00	39.98	40.27	38.62	36.05	39.64	37.26	32.78	30.95	30.13
325.00	39.95	40.31	38.61	36.08	39.67	37.29	32.81	30.96	30.14
330.00	39.92	40.35	38.60	36.11	39.71	37.30	32.84	30.97	30.14
335.00	39.89	40.38	38.58	36.13	39.73	37.32	32.86	30.98	30.15
340.00	39.83	40.40	38.56	36.15	39.76	37.33	32.89	30.99	30.15
345.00	39.77	40.42	38.53	36.16	39.77	37.33	32.91	31.00	30.15
350.00	39.71	40.43	38.50	36.17	39.79	37.33	32.93	31.01	30.16
355.00	39.64	40.44	38.47	36.18	39.79	37.33	32.94	31.02	30.16
360.00	39.57	40.44	38.43	36.19	39.80	37.33	32.96	31.02	30.16
365.00	39.50	40.44	38.39	36.19	39.80	37.33	32.97	31.03	30.17
370.00	39.42	40.43	38.35	36.19	39.79	37.32	32.99	31.03	30.17
375.00	39.34	40.42	38.30	36.19	39.78	37.30	33.00	31.04	30.17
380.00	39.26	40.41	38.26	36.18	39.77	37.29	33.01	31.04	30.17
385.00	39.17	40.39	38.20	36.17	39.75	37.27	33.01	31.04	30.17
390.00	39.08	40.36	38.15	36.15	39.72	37.25	33.02	31.05	30.17
395.00	38.98	40.33	38.09	36.13	39.70	37.22	33.02	31.05	30.17
400.00	38.88	40.30	38.03	36.11	39.66	37.19	33.03	31.05	30.17
405.00	38.78	40.26	37.96	36.08	39.63	37.16	33.03	31.05	30.17
410.00	38.68	40.21	37.89	36.05	39.59	37.13	33.03	31.05	30.17
415.00	38.57	40.17	37.82	36.01	39.54	37.09	33.02	31.04	30.17
420.00	38.46	40.11	37.74	35.97	39.49	37.05	33.02	31.04	30.17

Timecum	UCIL8 (%)	UCIL7 (%)	UCIL6 (%)	UCIL5 (%)	UCIL4 (%)	UCIL3 (%)	UCIL2 (%)	UCIL2_a (%)	UCIL2_b (%)
0.00	42.60	42.62	42.62	42.62	42.61	42.69	42.57	42.62	42.62
5.00	65.89	46.52	66.58	63.67	45.21	69.65	52.08	37.66	33.21
10.00	65.06	47.19	65.67	62.75	45.25	68.64	51.51	37.03	32.57
15.00	63.75	46.95	64.62	62.44	45.10	68.25	51.66	37.06	32.56
20.00	62.40	46.28	63.68	62.08	44.50	67.79	51.72	37.10	32.60
25.00	61.18	45.54	62.82	61.81	43.97	67.35	51.77	37.10	32.57
30.00	60.09	44.77	62.05	61.59	43.23	66.98	51.83	37.12	32.57
35.00	59.14	43.98	61.33	61.43	42.52	66.67	51.88	37.14	32.58
40.00	58.19	43.29	60.63	61.22	42.09	66.38	51.95	37.16	32.58
45.00	57.33	42.66	59.99	61.06	41.52	66.10	52.02	37.17	32.59
50.00	56.60	41.94	59.42	60.94	40.78	65.85	52.08	37.20	32.59
55.00	55.88	41.29	58.86	60.80	40.30	65.62	52.16	37.21	32.60
60.00	55.21	40.79	58.37	60.73	40.00	65.43	52.23	37.24	32.61
65.00	54.66	40.22	57.89	60.52	39.38	65.22	52.31	37.26	32.61
70.00	54.22	39.61	57.76	61.11	38.77	65.04	52.29	37.29	32.63
75.00	53.50	39.19	57.06	60.44	38.64	64.92	52.42	37.31	32.63
80.00	52.94	38.81	56.62	60.31	38.43	64.79	52.47	37.34	32.65
85.00	52.51	38.40	56.26	60.24	38.07	64.66	52.53	37.37	32.66
90.00	52.10	37.98	55.92	60.19	37.72	64.55	52.58	37.40	32.67
95.00	51.71	37.58	55.61	60.13	37.41	64.45	52.64	37.43	32.68
100.00	51.35	37.17	55.32	60.09	37.02	64.36	52.70	37.46	32.69
105.00	50.99	36.79	55.04	60.06	36.68	64.28	52.76	37.49	32.70
110.00	50.67	36.45	54.79	60.03	36.46	64.22	52.83	37.52	32.72
115.00	50.38	36.10	54.56	60.02	36.15	64.16	52.90	37.56	32.73
120.00	50.13	35.73	54.36	60.02	35.76	64.12	52.98	37.59	32.74
125.00	49.87	35.41	54.16	60.01	35.52	64.09	53.05	37.62	32.75
130.00	49.66	35.13	54.00	60.01	35.35	64.07	53.13	37.66	32.77
135.00	49.47	34.87	53.85	60.03	35.08	64.07	53.21	37.69	32.78
140.00	49.30	34.62	53.71	60.05	34.88	64.07	53.29	37.73	32.79
145.00	49.19	34.39	53.60	60.09	34.81	64.07	53.37	37.76	32.81
150.00	49.05	34.14	53.50	60.13	34.60	64.09	53.45	37.80	32.82
155.00	48.90	33.88	53.42	60.16	34.26	64.13	53.53	37.83	32.83
160.00	48.86	33.66	53.35	60.22	34.20	64.16	53.61	37.87	32.85
165.00	48.81	33.50	53.30	60.27	34.06	64.21	53.69	37.91	32.86
170.00	48.74	33.28	53.28	60.34	33.83	64.27	53.78	37.94	32.88
175.00	48.74	33.12	53.27	60.42	33.78	64.35	53.86	37.98	32.89
180.00	48.73	32.97	53.28	60.49	33.73	64.44	53.95	38.02	32.90
185.00	48.74	32.81	53.29	60.58	33.55	64.52	54.03	38.06	32.92
190.00	48.78	32.67	53.31	60.67	33.46	64.61	54.12	38.09	32.93
195.00	48.79	32.54	53.34	60.75	33.44	64.71	54.21	38.13	32.95
200.00	48.80	32.38	53.38	60.84	33.22	64.80	54.29	38.17	32.96
205.00	48.90	32.18	53.45	60.94	32.94	64.89	54.38	38.21	32.98
210.00	48.99	32.06	53.55	61.02	32.93	64.99	54.47	38.25	32.99
215.00	49.06	31.95	53.68	61.11	32.82	65.10	54.55	38.28	33.01
220.00	49.22	31.81	53.84	61.23	32.61	65.20	54.64	38.32	33.02
225.00	49.34	31.70	53.99	61.32	32.62	65.31	54.72	38.36	33.04
230.00	49.40	31.61	54.14	61.40	32.59	65.42	54.81	38.40	33.05
235.00	49.54	31.48	54.30	61.53	32.32	65.53	54.89	38.43	33.07

240.00	49.69	31.43	54.46	61.62	32.40	65.64	54.97	38.47	33.08
245.00	49.83	31.42	54.61	61.72	32.41	65.75	55.05	38.51	33.10
250.00	50.01	31.34	54.78	61.83	32.26	65.86	55.13	38.54	33.11
255.00	50.13	31.33	54.94	61.92	32.35	65.98	55.21	38.58	33.12
260.00	50.25	31.29	55.12	62.04	32.26	66.10	55.29	38.61	33.14
265.00	50.43	31.16	55.31	62.15	32.01	66.23	55.37	38.65	33.15
270.00	50.54	31.09	55.50	62.24	32.01	66.36	55.44	38.68	33.16
275.00	50.70	31.10	55.69	62.35	32.08	66.49	55.51	38.71	33.18
280.00	50.90	31.05	55.90	62.47	31.99	66.63	55.58	38.74	33.19
285.00	51.06	31.05	56.11	62.56	32.05	66.76	55.65	38.78	33.20
290.00	51.20	31.09	56.31	62.66	32.21	66.90	55.72	38.81	33.21
295.00	51.45	31.07	56.54	62.79	32.12	67.03	55.78	38.83	33.22
300.00	51.68	30.96	56.76	62.88	31.87	67.17	55.85	38.86	33.24
305.00	51.81	30.95	56.96	62.96	31.93	67.32	55.91	38.89	33.25
310.00	52.02	31.00	57.17	63.09	32.09	67.46	55.97	38.92	33.26
315.00	52.28	31.01	57.39	63.18	32.05	67.60	56.02	38.94	33.27
320.00	52.56	31.05	57.63	63.29	32.12	67.74	56.08	38.97	33.28
325.00	52.80	31.08	57.86	63.40	32.15	67.89	56.13	38.99	33.28
330.00	53.03	31.10	58.08	63.50	32.17	68.03	56.18	39.01	33.29
335.00	53.31	31.15	58.30	63.62	32.30	68.18	56.22	39.03	33.30
340.00	53.57	31.17	58.52	63.71	32.32	68.32	56.27	39.05	33.31
345.00	53.87	31.18	58.74	63.81	32.30	68.47	56.31	39.07	33.32
350.00	54.20	31.21	58.96	63.92	32.39	68.61	56.35	39.09	33.32
355.00	54.48	31.22	59.18	64.00	32.40	68.74	56.38	39.10	33.33
360.00	54.71	31.21	59.39	64.09	32.24	68.88	56.42	39.12	33.33
365.00	55.03	31.21	59.61	64.20	32.23	69.00	56.45	39.13	33.34
370.00	55.39	31.23	59.83	64.30	32.39	69.13	56.47	39.14	33.34
375.00	55.62	31.27	60.03	64.36	32.37	69.25	56.50	39.15	33.35
380.00	55.97	31.34	60.24	64.47	32.43	69.37	56.52	39.16	33.35
385.00	56.27	31.44	60.45	64.55	32.56	69.48	56.54	39.17	33.35
390.00	56.60	31.53	60.66	64.65	32.64	69.60	56.55	39.17	33.35
395.00	56.92	31.60	60.87	64.74	32.74	69.71	56.56	39.18	33.36
400.00	57.21	31.67	61.07	64.83	32.78	69.81	56.57	39.18	33.36
405.00	57.54	31.73	61.27	64.93	32.77	69.91	56.58	39.18	33.36
410.00	57.83	31.77	61.47	65.02	32.87	70.01	56.58	39.18	33.36
415.00	58.08	31.85	61.66	65.10	32.97	70.10	56.58	39.18	33.36
420.00	58.40	31.96	61.86	65.21	33.08	70.19	56.58	39.18	33.35

Timecum	UCIL8 degC	UCIL7 degC	UCIL6 degC	UCIL5 degC	UCIL4 degC	UCIL3 degC	UCIL2 degC	UCIL2_a degC	UCIL2_b degC
0.00	23.20	23.20	23.20	23.20	23.20	23.20	23.20	23.20	23.20
5.00	23.72	23.51	23.62	23.40	23.50	23.47	23.25	23.22	23.21
10.00	24.28	23.96	24.08	23.63	23.90	23.76	23.32	23.25	23.22
15.00	24.81	24.39	24.51	23.86	24.29	24.05	23.39	23.28	23.23
20.00	25.32	24.81	24.93	24.08	24.67	24.32	23.46	23.31	23.25
25.00	25.81	25.22	25.34	24.29	25.04	24.59	23.53	23.34	23.26
30.00	26.28	25.62	25.73	24.50	25.39	24.85	23.60	23.37	23.27
35.00	26.74	26.00	26.11	24.70	25.74	25.11	23.67	23.40	23.29
40.00	27.17	26.37	26.47	24.90	26.07	25.35	23.74	23.43	23.30
45.00	27.60	26.74	26.82	25.10	26.39	25.60	23.82	23.46	23.31
50.00	28.00	27.09	27.17	25.29	26.71	25.83	23.89	23.49	23.33
55.00	28.40	27.43	27.50	25.48	27.01	26.06	23.96	23.53	23.34
60.00	28.77	27.77	27.82	25.67	27.31	26.29	24.04	23.56	23.35
65.00	29.14	28.10	28.14	25.85	27.60	26.51	24.11	23.59	23.37
70.00	29.49	28.42	28.45	26.03	27.88	26.73	24.19	23.62	23.38
75.00	29.83	28.73	28.74	26.21	28.16	26.94	24.26	23.65	23.39
80.00	30.16	29.03	29.04	26.38	28.42	27.15	24.34	23.68	23.41
85.00	30.48	29.33	29.32	26.55	28.69	27.36	24.41	23.72	23.42
90.00	30.78	29.62	29.60	26.72	28.95	27.56	24.49	23.75	23.43
95.00	31.08	29.90	29.87	26.89	29.20	27.76	24.56	23.78	23.45
100.00	31.36	30.18	30.13	27.05	29.44	27.95	24.64	23.81	23.46
105.00	31.64	30.44	30.39	27.21	29.68	28.14	24.72	23.84	23.47
110.00	31.91	30.71	30.63	27.36	29.91	28.32	24.79	23.88	23.49
115.00	32.16	30.97	30.88	27.52	30.14	28.51	24.87	23.91	23.50
120.00	32.41	31.22	31.11	27.67	30.37	28.68	24.94	23.94	23.51
125.00	32.65	31.46	31.34	27.82	30.58	28.86	25.01	23.97	23.53
130.00	32.88	31.71	31.56	27.96	30.79	29.03	25.09	24.00	23.54
135.00	33.11	31.94	31.77	28.11	31.00	29.20	25.16	24.03	23.55
140.00	33.32	32.17	31.98	28.25	31.20	29.36	25.24	24.06	23.57
145.00	33.52	32.39	32.18	28.38	31.40	29.52	25.31	24.09	23.58
150.00	33.72	32.61	32.37	28.52	31.59	29.68	25.38	24.12	23.59
155.00	33.91	32.83	32.56	28.65	31.78	29.84	25.45	24.15	23.60
160.00	34.09	33.04	32.73	28.77	31.97	29.98	25.52	24.18	23.62
165.00	34.26	33.24	32.91	28.90	32.15	30.13	25.59	24.21	23.63
170.00	34.42	33.44	33.07	29.02	32.32	30.27	25.66	24.24	23.64
175.00	34.58	33.62	33.23	29.14	32.49	30.41	25.73	24.27	23.65
180.00	34.73	33.81	33.37	29.25	32.65	30.53	25.80	24.30	23.66
185.00	34.87	33.98	33.52	29.36	32.81	30.66	25.87	24.32	23.68
190.00	35.00	34.16	33.66	29.47	32.96	30.79	25.93	24.35	23.69
195.00	35.13	34.33	33.79	29.57	33.11	30.91	26.00	24.38	23.70
200.00	35.26	34.49	33.92	29.68	33.25	31.03	26.06	24.41	23.71
205.00	35.37	34.65	34.05	29.78	33.40	31.14	26.13	24.43	23.72
210.00	35.47	34.81	34.15	29.88	33.53	31.26	26.19	24.46	23.73
215.00	35.56	34.95	34.24	29.98	33.67	31.37	26.25	24.48	23.74
220.00	35.65	35.10	34.33	30.08	33.80	31.48	26.31	24.51	23.75
225.00	35.73	35.24	34.40	30.17	33.93	31.58	26.37	24.53	23.76
230.00	35.81	35.37	34.47	30.26	34.05	31.68	26.43	24.56	23.77
235.00	35.88	35.50	34.55	30.34	34.17	31.78	26.49	24.58	23.78

240.00	35.95	35.63	34.62	30.43	34.28	31.88	26.54	24.60	23.79
245.00	35.99	35.74	34.68	30.51	34.40	31.97	26.60	24.63	23.80
250.00	36.05	35.85	34.75	30.59	34.50	32.06	26.65	24.65	23.81
255.00	36.12	35.96	34.81	30.67	34.61	32.14	26.70	24.67	23.82
260.00	36.17	36.06	34.85	30.74	34.71	32.22	26.75	24.69	23.83
265.00	36.22	36.16	34.90	30.81	34.80	32.29	26.80	24.71	23.84
270.00	36.26	36.25	34.94	30.87	34.89	32.36	26.85	24.73	23.85
275.00	36.29	36.33	34.97	30.94	34.97	32.43	26.90	24.75	23.85
280.00	36.32	36.41	35.00	31.00	35.06	32.49	26.94	24.77	23.86
285.00	36.35	36.49	35.02	31.05	35.13	32.55	26.99	24.78	23.87
290.00	36.37	36.57	35.04	31.11	35.20	32.60	27.03	24.80	23.88
295.00	36.38	36.64	35.05	31.16	35.27	32.65	27.07	24.82	23.88
300.00	36.39	36.70	35.06	31.21	35.33	32.70	27.11	24.83	23.89
305.00	36.39	36.76	35.07	31.25	35.39	32.74	27.15	24.85	23.90
310.00	36.39	36.81	35.07	31.30	35.44	32.78	27.18	24.86	23.90
315.00	36.38	36.86	35.07	31.34	35.49	32.81	27.22	24.88	23.91
320.00	36.37	36.90	35.06	31.37	35.54	32.84	27.25	24.89	23.91
325.00	36.34	36.94	35.05	31.40	35.58	32.87	27.28	24.90	23.92
330.00	36.31	36.97	35.04	31.43	35.61	32.89	27.31	24.92	23.92
335.00	36.28	37.00	35.02	31.46	35.64	32.91	27.34	24.93	23.93
340.00	36.23	37.03	35.00	31.48	35.67	32.93	27.36	24.94	23.93
345.00	36.17	37.05	34.98	31.50	35.69	32.94	27.39	24.95	23.94
350.00	36.12	37.06	34.95	31.52	35.70	32.94	27.41	24.96	23.94
355.00	36.05	37.08	34.92	31.53	35.71	32.95	27.43	24.96	23.94
360.00	35.99	37.08	34.88	31.54	35.72	32.95	27.45	24.97	23.95
365.00	35.92	37.08	34.84	31.54	35.72	32.95	27.47	24.98	23.95
370.00	35.84	37.08	34.80	31.55	35.71	32.94	27.49	24.99	23.95
375.00	35.77	37.07	34.76	31.55	35.71	32.93	27.50	24.99	23.95
380.00	35.69	37.05	34.71	31.54	35.69	32.92	27.51	25.00	23.96
385.00	35.60	37.04	34.66	31.53	35.68	32.90	27.53	25.00	23.96
390.00	35.51	37.01	34.61	31.52	35.66	32.88	27.53	25.00	23.96
395.00	35.42	36.99	34.55	31.51	35.63	32.86	27.54	25.01	23.96
400.00	35.32	36.95	34.49	31.49	35.60	32.84	27.55	25.01	23.96
405.00	35.21	36.92	34.42	31.46	35.57	32.81	27.55	25.01	23.96
410.00	35.11	36.88	34.36	31.44	35.53	32.78	27.55	25.01	23.96
415.00	35.01	36.83	34.29	31.40	35.48	32.74	27.55	25.01	23.96
420.00	34.90	36.78	34.21	31.37	35.43	32.71	27.55	25.01	23.96

Timecum	UCIL8 (%)	UCIL7 (%)	UCIL6 (%)	UCIL5 (%)	UCIL4 (%)	UCIL3 (%)	UCIL2 (%)	UCIL2_a (%)	UCIL2_b (%)
0.00	42.60	42.62	42.62	42.62	42.61	42.69	42.57	42.62	42.62
5.00	68.33	50.48	68.34	69.46	50.68	74.90	60.95	48.64	44.78
10.00	67.12	51.59	67.10	69.02	51.38	74.24	60.97	48.64	44.78
15.00	65.67	50.76	65.98	68.62	50.70	73.65	60.99	48.64	44.78
20.00	64.20	49.79	64.93	68.25	49.86	73.09	61.00	48.65	44.78
25.00	62.92	48.86	63.98	67.91	49.05	72.59	61.03	48.65	44.78
30.00	61.75	47.94	63.12	67.60	48.20	72.14	61.06	48.66	44.78
35.00	60.64	47.08	62.30	67.32	47.46	71.72	61.09	48.67	44.78
40.00	59.63	46.27	61.55	67.06	46.76	71.34	61.12	48.68	44.78
45.00	58.69	45.52	60.88	66.83	46.09	70.99	61.16	48.69	44.78
50.00	57.83	44.83	60.23	66.59	45.52	70.67	61.20	48.70	44.79
55.00	57.04	44.18	59.65	66.41	44.95	70.38	61.24	48.71	44.79
60.00	56.31	43.53	59.09	66.24	44.39	70.11	61.29	48.73	44.79
65.00	55.65	42.88	58.58	66.06	43.81	69.87	61.34	48.74	44.79
70.00	55.03	42.35	58.12	65.93	43.37	69.66	61.39	48.76	44.80
75.00	54.45	41.79	57.67	65.81	42.89	69.46	61.44	48.77	44.80
80.00	53.90	41.28	57.26	65.66	42.42	69.31	61.50	48.79	44.81
85.00	53.43	40.83	56.88	65.58	42.06	69.13	61.56	48.81	44.81
90.00	52.97	40.34	56.53	65.52	41.57	68.99	61.62	48.83	44.82
95.00	52.56	39.87	56.19	65.45	41.17	68.87	61.68	48.85	44.83
100.00	52.18	39.47	55.90	65.36	40.92	68.76	61.74	48.88	44.83
105.00	51.81	39.09	55.61	65.31	40.55	68.67	61.81	48.90	44.84
110.00	51.52	38.73	55.36	65.28	40.22	68.60	61.88	48.93	44.85
115.00	51.23	38.38	55.13	65.24	39.99	68.54	61.95	48.95	44.86
120.00	50.97	38.07	54.92	65.22	39.71	68.49	62.02	48.98	44.87
125.00	50.73	37.73	54.73	65.21	39.43	68.46	62.10	49.01	44.87
130.00	50.52	37.42	54.56	65.21	39.16	68.44	62.17	49.03	44.88
135.00	50.32	37.12	54.42	65.22	38.89	68.42	62.25	49.06	44.89
140.00	50.16	36.79	54.29	65.23	38.62	68.42	62.32	49.09	44.90
145.00	49.99	36.49	54.16	65.26	38.33	68.42	62.40	49.12	44.91
150.00	49.89	36.26	54.08	65.29	38.19	68.44	62.48	49.15	44.92
155.00	49.79	36.00	54.01	65.34	37.97	68.47	62.56	49.19	44.94
160.00	49.69	35.76	53.94	65.39	37.70	68.51	62.65	49.22	44.95
165.00	49.64	35.51	53.90	65.44	37.55	68.55	62.73	49.25	44.96
170.00	49.59	35.30	53.88	65.50	37.35	68.61	62.81	49.28	44.97
175.00	49.57	35.12	53.88	65.58	37.21	68.69	62.90	49.32	44.98
180.00	49.57	34.94	53.89	65.67	37.10	68.78	62.98	49.35	44.99
185.00	49.57	34.76	53.92	65.76	36.92	68.88	63.07	49.39	45.01
190.00	49.59	34.61	53.95	65.85	36.81	68.97	63.15	49.42	45.02
195.00	49.60	34.43	53.97	65.94	36.66	69.07	63.24	49.46	45.03
200.00	49.64	34.30	54.02	66.03	36.55	69.17	63.32	49.49	45.05
205.00	49.71	34.15	54.08	66.13	36.43	69.27	63.41	49.53	45.06
210.00	49.77	33.98	54.17	66.19	36.26	69.37	63.50	49.57	45.07
215.00	49.90	33.84	54.32	66.32	36.13	69.47	63.58	49.60	45.08
220.00	50.03	33.75	54.47	66.42	36.11	69.58	63.67	49.64	45.10
225.00	50.16	33.67	54.64	66.53	36.04	69.70	63.76	49.68	45.11
230.00	50.28	33.57	54.81	66.64	35.95	69.81	63.84	49.71	45.13
235.00	50.41	33.42	54.98	66.76	35.80	69.92	63.93	49.75	45.14

240.00	50.54	33.35	55.14	66.85	35.76	70.04	64.01	49.79	45.15
245.00	50.73	33.27	55.31	66.96	35.66	70.16	64.09	49.82	45.17
250.00	50.88	33.15	55.46	67.07	35.55	70.28	64.18	49.86	45.18
255.00	51.00	33.15	55.63	67.18	35.56	70.40	64.26	49.89	45.19
260.00	51.16	33.11	55.83	67.29	35.54	70.53	64.34	49.93	45.21
265.00	51.33	33.04	56.02	67.41	35.43	70.67	64.42	49.97	45.22
270.00	51.49	32.94	56.23	67.52	35.34	70.82	64.50	50.00	45.23
275.00	51.68	32.89	56.44	67.64	35.33	70.97	64.58	50.03	45.25
280.00	51.88	32.93	56.66	67.77	35.36	71.12	64.65	50.07	45.26
285.00	52.06	32.91	56.88	67.88	35.33	71.26	64.73	50.10	45.27
290.00	52.26	32.88	57.11	68.00	35.29	71.41	64.80	50.13	45.28
295.00	52.47	32.83	57.34	68.12	35.27	71.56	64.87	50.16	45.30
300.00	52.68	32.84	57.57	68.24	35.28	71.72	64.94	50.20	45.31
305.00	52.90	32.83	57.81	68.36	35.26	71.87	65.01	50.23	45.32
310.00	53.14	32.81	58.05	68.47	35.25	72.04	65.07	50.26	45.33
315.00	53.37	32.83	58.29	68.59	35.27	72.20	65.14	50.28	45.34
320.00	53.62	32.83	58.54	68.71	35.25	72.36	65.20	50.31	45.35
325.00	53.87	32.81	58.78	68.83	35.21	72.51	65.26	50.34	45.36
330.00	54.14	32.80	59.02	68.95	35.25	72.67	65.32	50.36	45.37
335.00	54.41	32.86	59.27	69.06	35.31	72.84	65.37	50.39	45.38
340.00	54.73	32.89	59.51	69.17	35.33	73.00	65.42	50.41	45.39
345.00	55.03	32.92	59.75	69.29	35.37	73.16	65.47	50.43	45.40
350.00	55.36	32.95	60.00	69.41	35.40	73.33	65.52	50.45	45.41
355.00	55.66	32.98	60.24	69.52	35.43	73.48	65.57	50.47	45.42
360.00	55.98	33.02	60.49	69.63	35.47	73.64	65.61	50.49	45.42
365.00	56.30	33.05	60.73	69.74	35.53	73.79	65.65	50.51	45.43
370.00	56.64	33.12	60.97	69.85	35.58	73.93	65.68	50.53	45.44
375.00	56.97	33.17	61.21	69.96	35.64	74.08	65.72	50.54	45.44
380.00	57.29	33.23	61.45	70.07	35.70	74.22	65.75	50.55	45.45
385.00	57.61	33.29	61.67	70.18	35.76	74.36	65.78	50.57	45.45
390.00	57.95	33.35	61.91	70.28	35.83	74.49	65.80	50.58	45.46
395.00	58.28	33.42	62.13	70.39	35.89	74.62	65.82	50.59	45.46
400.00	58.64	33.49	62.37	70.51	35.97	74.75	65.84	50.59	45.46
405.00	58.97	33.57	62.59	70.62	36.05	74.87	65.86	50.60	45.46
410.00	59.29	33.65	62.81	70.73	36.13	74.99	65.87	50.61	45.47
415.00	59.64	33.70	63.03	70.84	36.21	75.10	65.88	50.61	45.47
420.00	59.97	33.80	63.25	70.97	36.29	75.21	65.88	50.61	45.47

Timecum	UCIL8 degC	UCIL7 degC	UCIL6 degC	UCIL5 degC	UCIL4 degC	UCIL3 degC	UCIL2 degC	UCIL2_a degC	UCIL2_b degC
0.00	23.20	23.20	23.20	23.20	23.20	23.20	23.20	23.20	23.20
5.00	26.80	25.25	26.68	27.65	26.11	27.47	28.51	28.92	29.04
10.00	28.02	27.04	27.77	28.52	27.84	28.38	29.03	29.37	29.46
15.00	28.58	27.69	28.21	28.73	28.39	28.64	29.10	29.41	29.48
20.00	29.09	28.15	28.60	28.95	28.78	28.88	29.14	29.43	29.48
25.00	29.55	28.54	28.96	29.12	29.12	29.10	29.19	29.46	29.51
30.00	29.98	28.92	29.31	29.29	29.45	29.31	29.23	29.48	29.52
35.00	30.40	29.28	29.64	29.45	29.77	29.50	29.28	29.51	29.53
40.00	30.79	29.64	29.96	29.60	30.09	29.69	29.32	29.53	29.54
45.00	31.17	29.99	30.27	29.75	30.39	29.87	29.37	29.56	29.55
50.00	31.53	30.33	30.58	29.90	30.69	30.05	29.42	29.58	29.57
55.00	31.87	30.66	30.87	30.04	30.98	30.22	29.46	29.61	29.58
60.00	32.23	30.98	31.15	30.17	31.26	30.39	29.51	29.64	29.59
65.00	32.52	31.30	31.44	30.36	31.53	30.56	29.55	29.66	29.61
70.00	32.90	31.61	31.67	30.35	31.79	30.73	29.60	29.69	29.62
75.00	33.13	31.91	31.94	30.56	32.05	30.87	29.65	29.71	29.63
80.00	33.41	32.20	32.19	30.69	32.31	31.03	29.70	29.74	29.64
85.00	33.67	32.49	32.43	30.81	32.55	31.17	29.74	29.77	29.65
90.00	33.93	32.77	32.66	30.93	32.79	31.31	29.79	29.79	29.67
95.00	34.18	33.04	32.88	31.04	33.03	31.45	29.84	29.82	29.68
100.00	34.42	33.30	33.10	31.15	33.25	31.59	29.88	29.85	29.69
105.00	34.65	33.56	33.31	31.26	33.48	31.72	29.93	29.87	29.70
110.00	34.87	33.81	33.51	31.36	33.69	31.85	29.98	29.90	29.71
115.00	35.09	34.06	33.71	31.47	33.90	31.97	30.02	29.92	29.73
120.00	35.29	34.30	33.90	31.57	34.11	32.09	30.07	29.95	29.74
125.00	35.48	34.53	34.08	31.66	34.31	32.21	30.12	29.97	29.75
130.00	35.67	34.76	34.26	31.76	34.51	32.33	30.17	30.00	29.76
135.00	35.84	34.99	34.42	31.85	34.70	32.44	30.21	30.02	29.77
140.00	36.00	35.20	34.59	31.94	34.88	32.54	30.26	30.05	29.78
145.00	36.16	35.42	34.74	32.03	35.07	32.65	30.31	30.07	29.79
150.00	36.31	35.63	34.89	32.11	35.24	32.75	30.35	30.10	29.80
155.00	36.45	35.83	35.03	32.19	35.41	32.84	30.40	30.12	29.81
160.00	36.58	36.03	35.16	32.27	35.58	32.94	30.44	30.14	29.83
165.00	36.70	36.22	35.29	32.35	35.74	33.03	30.49	30.17	29.84
170.00	36.81	36.40	35.41	32.42	35.89	33.11	30.53	30.19	29.85
175.00	36.92	36.58	35.52	32.49	36.04	33.19	30.57	30.21	29.86
180.00	37.02	36.75	35.63	32.56	36.19	33.27	30.62	30.23	29.87
185.00	37.11	36.92	35.73	32.62	36.33	33.34	30.66	30.26	29.88
190.00	37.20	37.08	35.82	32.68	36.47	33.41	30.70	30.28	29.89
195.00	37.28	37.24	35.92	32.74	36.60	33.48	30.74	30.30	29.90
200.00	37.36	37.39	36.00	32.80	36.73	33.55	30.78	30.32	29.90
205.00	37.43	37.54	36.08	32.86	36.85	33.62	30.82	30.34	29.91
210.00	37.48	37.68	36.14	32.91	36.97	33.68	30.86	30.36	29.92
215.00	37.52	37.82	36.19	32.97	37.09	33.74	30.90	30.38	29.93
220.00	37.56	37.96	36.24	33.02	37.21	33.80	30.94	30.40	29.94
225.00	37.60	38.09	36.28	33.07	37.32	33.86	30.98	30.41	29.95
230.00	37.64	38.21	36.31	33.11	37.43	33.91	31.01	30.43	29.96
235.00	37.67	38.33	36.35	33.16	37.53	33.97	31.05	30.45	29.96

240.00	37.70	38.44	36.38	33.20	37.63	34.01	31.08	30.47	29.97
245.00	37.72	38.55	36.41	33.24	37.73	34.06	31.11	30.48	29.98
250.00	37.74	38.65	36.44	33.28	37.82	34.11	31.14	30.50	29.99
255.00	37.76	38.73	36.46	33.32	37.91	34.15	31.17	30.52	30.00
260.00	37.78	38.82	36.47	33.35	37.99	34.18	31.20	30.53	30.00
265.00	37.78	38.91	36.48	33.38	38.07	34.21	31.23	30.55	30.01
270.00	37.79	38.98	36.48	33.41	38.14	34.24	31.26	30.56	30.02
275.00	37.79	39.06	36.49	33.44	38.21	34.27	31.29	30.57	30.02
280.00	37.78	39.13	36.48	33.46	38.28	34.29	31.31	30.59	30.03
285.00	37.77	39.19	36.48	33.49	38.34	34.31	31.34	30.60	30.03
290.00	37.76	39.25	36.46	33.51	38.39	34.33	31.36	30.61	30.04
295.00	37.74	39.31	36.45	33.53	38.45	34.35	31.38	30.62	30.04
300.00	37.72	39.36	36.43	33.54	38.50	34.36	31.40	30.63	30.05
305.00	37.69	39.41	36.41	33.56	38.54	34.37	31.42	30.64	30.05
310.00	37.65	39.46	36.38	33.57	38.58	34.37	31.44	30.65	30.06
315.00	37.62	39.49	36.36	33.58	38.62	34.37	31.46	30.66	30.06
320.00	37.57	39.53	36.33	33.58	38.65	34.37	31.47	30.67	30.07
325.00	37.52	39.56	36.29	33.59	38.67	34.37	31.49	30.68	30.07
330.00	37.46	39.59	36.26	33.59	38.70	34.37	31.50	30.69	30.07
335.00	37.40	39.61	36.22	33.59	38.71	34.36	31.52	30.69	30.08
340.00	37.32	39.62	36.18	33.59	38.73	34.35	31.53	30.70	30.08
345.00	37.24	39.64	36.13	33.58	38.74	34.33	31.54	30.71	30.08
350.00	37.16	39.64	36.09	33.57	38.74	34.31	31.55	30.71	30.09
355.00	37.08	39.65	36.04	33.56	38.74	34.30	31.55	30.72	30.09
360.00	36.99	39.64	35.98	33.55	38.74	34.27	31.56	30.72	30.09
365.00	36.90	39.64	35.93	33.54	38.73	34.25	31.57	30.72	30.09
370.00	36.81	39.63	35.87	33.52	38.72	34.23	31.57	30.73	30.09
375.00	36.71	39.61	35.82	33.50	38.70	34.20	31.57	30.73	30.09
380.00	36.61	39.59	35.76	33.48	38.68	34.17	31.57	30.73	30.09
385.00	36.51	39.56	35.69	33.46	38.65	34.14	31.57	30.73	30.10
390.00	36.41	39.54	35.63	33.43	38.62	34.11	31.57	30.73	30.10
395.00	36.30	39.50	35.56	33.40	38.59	34.07	31.57	30.73	30.10
400.00	36.20	39.47	35.49	33.37	38.55	34.03	31.57	30.73	30.10
405.00	36.09	39.42	35.42	33.33	38.51	33.99	31.56	30.73	30.09
410.00	35.98	39.37	35.35	33.29	38.46	33.95	31.55	30.72	30.09
415.00	35.87	39.32	35.27	33.25	38.41	33.91	31.55	30.72	30.09
420.00	35.75	39.26	35.19	33.20	38.35	33.87	31.54	30.72	30.09

Timecum	UCIL8 (%)	UCIL7 (%)	UCIL6 (%)	UCIL5 (%)	UCIL4 (%)	UCIL3 (%)	UCIL2 (%)	UCIL2_a (%)	UCIL2_b (%)
0.00	42.60	42.62	42.62	42.62	42.61	42.69	42.57	42.62	42.62
5.00	65.80	46.50	66.45	63.58	45.19	69.55	52.05	37.65	33.20
10.00	64.84	47.13	65.39	62.55	45.20	68.42	51.43	37.00	32.56
15.00	63.40	46.84	64.19	62.14	45.00	67.90	51.54	37.02	32.54
20.00	61.94	46.12	63.09	61.67	44.35	67.31	51.56	37.04	32.57
25.00	60.59	45.32	62.08	61.26	43.76	66.74	51.57	37.02	32.54
30.00	59.39	44.49	61.14	60.92	42.97	66.23	51.58	37.03	32.54
35.00	58.30	43.66	60.28	60.61	42.21	65.77	51.59	37.03	32.54
40.00	57.23	42.92	59.42	60.28	41.72	65.35	51.61	37.04	32.54
45.00	56.25	42.23	58.63	59.98	41.12	64.94	51.62	37.03	32.54
50.00	55.40	41.48	57.91	59.74	40.35	64.56	51.63	37.03	32.53
55.00	54.55	40.79	57.21	59.48	39.83	64.22	51.64	37.03	32.53
60.00	53.69	40.23	56.54	59.25	39.49	63.87	51.67	37.04	32.53
65.00	53.10	39.62	55.89	58.87	38.84	63.54	51.68	37.04	32.53
70.00	52.50	38.98	55.54	59.23	38.21	63.21	51.68	37.04	32.53
75.00	51.75	38.51	54.80	58.59	38.03	62.93	51.70	37.04	32.53
80.00	51.11	38.02	54.24	58.37	37.61	62.66	51.72	37.05	32.53
85.00	50.55	37.56	53.76	58.20	37.27	62.41	51.74	37.05	32.53
90.00	50.06	37.08	53.30	58.04	36.82	62.16	51.76	37.05	32.53
95.00	49.56	36.61	52.85	57.87	36.38	61.93	51.77	37.06	32.53
100.00	49.08	36.18	52.42	57.70	36.09	61.71	51.79	37.06	32.54
105.00	48.66	35.76	52.03	57.56	35.74	61.50	51.81	37.06	32.54
110.00	48.25	35.32	51.67	57.44	35.30	61.30	51.82	37.07	32.54
115.00	47.84	34.94	51.30	57.30	34.98	61.12	51.84	37.07	32.54
120.00	47.49	34.57	50.95	57.16	34.73	60.95	51.85	37.07	32.54
125.00	47.18	34.19	50.66	57.06	34.37	60.78	51.87	37.08	32.54
130.00	46.87	33.89	50.36	56.96	34.15	60.63	51.88	37.08	32.54
135.00	46.60	33.63	50.08	56.85	33.99	60.49	51.89	37.09	32.55
140.00	46.35	33.35	49.83	56.76	33.70	60.36	51.90	37.09	32.55
145.00	46.12	33.07	49.58	56.66	33.58	60.23	51.92	37.10	32.55
150.00	45.90	32.78	49.37	56.59	33.33	60.11	51.93	37.11	32.55
155.00	45.71	32.48	49.16	56.51	32.98	60.01	51.94	37.11	32.56
160.00	45.53	32.21	48.96	56.44	32.77	59.91	51.96	37.12	32.56
165.00	45.38	31.97	48.79	56.38	32.62	59.82	51.97	37.13	32.56
170.00	45.23	31.72	48.64	56.32	32.32	59.76	51.98	37.13	32.57
175.00	45.14	31.49	48.50	56.28	32.17	59.70	51.99	37.14	32.57
180.00	45.00	31.28	48.38	56.25	32.11	59.64	52.00	37.15	32.57
185.00	44.89	31.07	48.28	56.21	31.87	59.60	52.01	37.16	32.57
190.00	44.83	30.82	48.16	56.18	31.57	59.56	52.02	37.16	32.58
195.00	44.75	30.63	48.06	56.15	31.52	59.51	52.03	37.17	32.58
200.00	44.68	30.49	47.98	56.12	31.42	59.47	52.04	37.18	32.58
205.00	44.65	30.39	47.92	56.09	31.39	59.43	52.05	37.19	32.59
210.00	44.67	30.21	47.90	56.07	31.19	59.40	52.06	37.19	32.59
215.00	44.67	30.02	47.89	56.05	30.98	59.37	52.07	37.20	32.59
220.00	44.65	29.89	47.89	56.03	30.95	59.34	52.08	37.21	32.60
225.00	44.67	29.73	47.92	56.01	30.83	59.32	52.09	37.22	32.60
230.00	44.70	29.53	47.96	56.01	30.53	59.31	52.10	37.22	32.60
235.00	44.67	29.38	47.97	55.99	30.37	59.29	52.11	37.23	32.61

240.00	44.69	29.27	47.98	55.97	30.38	59.28	52.12	37.24	32.61
245.00	44.79	29.11	48.03	55.99	30.23	59.27	52.13	37.24	32.61
250.00	44.79	29.00	48.06	55.98	29.96	59.26	52.14	37.25	32.61
255.00	44.88	28.97	48.09	55.97	30.10	59.26	52.14	37.25	32.62
260.00	44.92	28.96	48.15	55.97	30.13	59.27	52.15	37.26	32.62
265.00	44.98	28.87	48.22	55.98	29.97	59.29	52.16	37.27	32.62
270.00	45.04	28.79	48.30	55.99	29.88	59.31	52.16	37.27	32.62
275.00	45.12	28.73	48.38	56.01	29.89	59.34	52.17	37.27	32.63
280.00	45.19	28.63	48.46	56.02	29.74	59.37	52.17	37.28	32.63
285.00	45.26	28.55	48.55	56.03	29.63	59.40	52.18	37.28	32.63
290.00	45.37	28.50	48.65	56.05	29.66	59.43	52.18	37.29	32.63
295.00	45.46	28.44	48.76	56.07	29.63	59.47	52.19	37.29	32.63
300.00	45.54	28.36	48.86	56.08	29.45	59.52	52.19	37.29	32.64
305.00	45.68	28.30	48.97	56.11	29.39	59.57	52.19	37.29	32.64
310.00	45.82	28.27	49.08	56.14	29.45	59.62	52.19	37.30	32.64
315.00	45.91	28.22	49.20	56.15	29.36	59.67	52.19	37.30	32.64
320.00	46.07	28.16	49.33	56.18	29.21	59.73	52.19	37.30	32.64
325.00	46.26	28.14	49.44	56.22	29.24	59.79	52.19	37.30	32.64
330.00	46.42	28.16	49.58	56.25	29.31	59.85	52.19	37.30	32.64
335.00	46.63	28.19	49.71	56.30	29.34	59.92	52.19	37.30	32.64
340.00	46.84	28.20	49.84	56.33	29.38	59.99	52.18	37.30	32.64
345.00	47.03	28.18	49.97	56.37	29.36	60.06	52.18	37.30	32.64
350.00	47.26	28.15	50.11	56.41	29.25	60.14	52.17	37.30	32.64
355.00	47.48	28.13	50.25	56.46	29.21	60.21	52.17	37.29	32.64
360.00	47.67	28.17	50.39	56.50	29.37	60.29	52.16	37.29	32.63
365.00	47.92	28.20	50.54	56.54	29.43	60.37	52.15	37.29	32.63
370.00	48.17	28.18	50.69	56.60	29.31	60.44	52.15	37.28	32.63
375.00	48.35	28.18	50.83	56.65	29.28	60.51	52.14	37.28	32.63
380.00	48.57	28.23	50.97	56.69	29.41	60.60	52.12	37.27	32.63
385.00	48.86	28.24	51.12	56.75	29.46	60.68	52.12	37.27	32.63
390.00	49.06	28.25	51.29	56.82	29.38	60.75	52.11	37.26	32.62
395.00	49.23	28.31	51.41	56.86	29.42	60.83	52.09	37.26	32.62
400.00	49.55	28.35	51.56	56.93	29.57	60.92	52.08	37.25	32.62
405.00	49.80	28.44	51.74	57.00	29.60	60.99	52.06	37.24	32.61
410.00	50.02	28.51	51.88	57.06	29.62	61.06	52.05	37.23	32.61
415.00	50.36	28.57	52.05	57.17	29.80	61.15	52.03	37.22	32.61
420.00	50.62	28.64	52.23	57.26	29.91	61.22	52.02	37.22	32.60

Timecum	UCIL8 degC	UCIL7 degC	UCIL6 degC	UCIL5 degC	UCIL4 degC	UCIL3 degC	UCIL2 degC	UCIL2_a degC	UCIL2_b degC
0.00	23.20	23.20	23.20	23.20	23.20	23.20	23.20	23.20	23.20
5.00	23.69	23.51	23.59	23.37	23.50	23.43	23.23	23.22	23.21
10.00	24.20	23.94	24.00	23.56	23.87	23.67	23.29	23.24	23.22
15.00	24.69	24.36	24.40	23.75	24.25	23.91	23.34	23.27	23.23
20.00	25.15	24.76	24.77	23.92	24.61	24.13	23.39	23.30	23.24
25.00	25.60	25.15	25.14	24.10	24.95	24.35	23.44	23.32	23.26
30.00	26.02	25.54	25.49	24.27	25.29	24.56	23.50	23.35	23.27
35.00	26.43	25.91	25.82	24.43	25.62	24.77	23.55	23.38	23.28
40.00	26.82	26.27	26.15	24.59	25.93	24.96	23.60	23.40	23.29
45.00	27.20	26.61	26.46	24.74	26.24	25.15	23.66	23.43	23.30
50.00	27.57	26.95	26.76	24.90	26.54	25.34	23.71	23.46	23.32
55.00	27.92	27.29	27.05	25.04	26.83	25.52	23.77	23.48	23.33
60.00	28.25	27.61	27.34	25.19	27.11	25.69	23.82	23.51	23.34
65.00	28.57	27.93	27.61	25.33	27.39	25.86	23.88	23.54	23.35
70.00	28.88	28.23	27.87	25.46	27.65	26.03	23.93	23.56	23.37
75.00	29.17	28.53	28.13	25.60	27.91	26.19	23.99	23.59	23.38
80.00	29.46	28.82	28.38	25.73	28.16	26.35	24.04	23.62	23.39
85.00	29.73	29.11	28.62	25.86	28.41	26.50	24.10	23.65	23.40
90.00	29.99	29.38	28.85	25.98	28.65	26.65	24.15	23.67	23.42
95.00	30.25	29.65	29.08	26.10	28.88	26.79	24.21	23.70	23.43
100.00	30.49	29.91	29.30	26.22	29.11	26.94	24.26	23.73	23.44
105.00	30.72	30.17	29.51	26.33	29.33	27.07	24.31	23.75	23.45
110.00	30.94	30.42	29.72	26.44	29.55	27.21	24.37	23.78	23.47
115.00	31.15	30.66	29.92	26.55	29.76	27.33	24.42	23.81	23.48
120.00	31.36	30.90	30.11	26.66	29.97	27.46	24.48	23.84	23.49
125.00	31.55	31.14	30.29	26.76	30.17	27.58	24.53	23.86	23.50
130.00	31.74	31.36	30.47	26.86	30.36	27.70	24.58	23.89	23.51
135.00	31.92	31.58	30.64	26.96	30.55	27.82	24.63	23.91	23.52
140.00	32.09	31.80	30.80	27.06	30.74	27.93	24.69	23.94	23.54
145.00	32.25	32.01	30.96	27.15	30.92	28.04	24.74	23.97	23.55
150.00	32.40	32.22	31.11	27.24	31.09	28.15	24.79	23.99	23.56
155.00	32.55	32.42	31.26	27.33	31.27	28.25	24.84	24.02	23.57
160.00	32.69	32.61	31.39	27.41	31.43	28.35	24.89	24.04	23.58
165.00	32.82	32.80	31.53	27.49	31.59	28.45	24.94	24.07	23.59
170.00	32.94	32.98	31.65	27.57	31.75	28.54	24.99	24.09	23.60
175.00	33.05	33.16	31.76	27.64	31.90	28.62	25.04	24.11	23.62
180.00	33.15	33.33	31.87	27.71	32.05	28.70	25.08	24.14	23.63
185.00	33.25	33.49	31.97	27.78	32.19	28.78	25.13	24.16	23.64
190.00	33.34	33.65	32.07	27.85	32.33	28.86	25.18	24.18	23.65
195.00	33.43	33.81	32.17	27.91	32.46	28.93	25.22	24.21	23.66
200.00	33.51	33.96	32.26	27.98	32.59	29.01	25.27	24.23	23.67
205.00	33.58	34.10	32.34	28.04	32.71	29.08	25.31	24.25	23.68
210.00	33.64	34.24	32.40	28.10	32.84	29.15	25.35	24.27	23.69
215.00	33.69	34.38	32.45	28.15	32.95	29.21	25.39	24.29	23.70
220.00	33.73	34.51	32.50	28.21	33.07	29.27	25.44	24.31	23.71
225.00	33.78	34.64	32.54	28.26	33.18	29.33	25.48	24.33	23.71
230.00	33.81	34.76	32.58	28.31	33.29	29.39	25.52	24.35	23.72
235.00	33.86	34.87	32.62	28.36	33.39	29.45	25.55	24.37	23.73

240.00	33.88	34.98	32.65	28.41	33.49	29.50	25.59	24.39	23.74
245.00	33.90	35.09	32.69	28.45	33.59	29.55	25.63	24.41	23.75
250.00	33.92	35.19	32.72	28.50	33.68	29.60	25.66	24.42	23.76
255.00	33.94	35.28	32.74	28.54	33.77	29.64	25.70	24.44	23.76
260.00	33.95	35.37	32.76	28.57	33.85	29.69	25.73	24.46	23.77
265.00	33.96	35.46	32.77	28.61	33.93	29.72	25.76	24.47	23.78
270.00	33.97	35.54	32.78	28.64	34.01	29.75	25.79	24.49	23.79
275.00	33.96	35.61	32.78	28.67	34.08	29.78	25.82	24.51	23.79
280.00	33.96	35.69	32.78	28.70	34.15	29.81	25.85	24.52	23.80
285.00	33.95	35.75	32.78	28.73	34.21	29.83	25.88	24.53	23.81
290.00	33.94	35.82	32.77	28.75	34.27	29.86	25.91	24.55	23.81
295.00	33.92	35.88	32.76	28.77	34.32	29.88	25.93	24.56	23.82
300.00	33.89	35.93	32.74	28.79	34.37	29.89	25.96	24.57	23.82
305.00	33.86	35.98	32.72	28.81	34.42	29.90	25.98	24.58	23.83
310.00	33.82	36.03	32.70	28.83	34.46	29.91	26.00	24.60	23.84
315.00	33.79	36.07	32.68	28.84	34.49	29.92	26.02	24.61	23.84
320.00	33.75	36.10	32.65	28.85	34.53	29.92	26.04	24.62	23.84
325.00	33.71	36.14	32.61	28.86	34.55	29.92	26.06	24.63	23.85
330.00	33.64	36.16	32.58	28.86	34.58	29.92	26.08	24.63	23.85
335.00	33.58	36.19	32.54	28.87	34.60	29.91	26.09	24.64	23.86
340.00	33.51	36.20	32.50	28.87	34.61	29.91	26.11	24.65	23.86
345.00	33.42	36.21	32.46	28.86	34.62	29.89	26.12	24.66	23.86
350.00	33.35	36.22	32.41	28.86	34.63	29.88	26.13	24.66	23.87
355.00	33.27	36.23	32.36	28.85	34.63	29.87	26.14	24.67	23.87
360.00	33.18	36.23	32.31	28.85	34.63	29.85	26.15	24.67	23.87
365.00	33.09	36.22	32.26	28.83	34.62	29.83	26.16	24.68	23.87
370.00	33.00	36.21	32.20	28.82	34.61	29.81	26.17	24.68	23.88
375.00	32.91	36.19	32.14	28.80	34.59	29.78	26.17	24.69	23.88
380.00	32.81	36.17	32.08	28.79	34.57	29.76	26.18	24.69	23.88
385.00	32.72	36.15	32.02	28.77	34.55	29.73	26.18	24.69	23.88
390.00	32.62	36.12	31.96	28.74	34.52	29.70	26.18	24.69	23.88
395.00	32.52	36.09	31.89	28.72	34.49	29.67	26.18	24.69	23.88
400.00	32.41	36.06	31.82	28.69	34.46	29.63	26.18	24.69	23.88
405.00	32.31	36.01	31.76	28.65	34.42	29.60	26.18	24.69	23.88
410.00	32.20	35.97	31.68	28.62	34.38	29.56	26.18	24.69	23.88
415.00	32.09	35.92	31.61	28.58	34.33	29.52	26.17	24.69	23.88
420.00	31.98	35.86	31.53	28.54	34.27	29.48	26.17	24.69	23.88

Timecum	UCIL8 (%)	UCIL7 (%)	UCIL6 (%)	UCIL5 (%)	UCIL4 (%)	UCIL3 (%)	UCIL2 (%)	UCIL2_a (%)	UCIL2_b (%)
0.00	42.60	42.62	42.62	42.62	42.61	42.69	42.57	42.62	42.62
5.00	68.04	49.41	68.32	69.40	49.89	74.76	60.92	48.62	44.78
10.00	66.74	50.80	66.88	68.83	50.76	73.99	60.89	48.61	44.77
15.00	65.21	50.41	65.61	68.35	50.36	73.29	60.86	48.60	44.76
20.00	63.77	49.60	64.45	67.88	49.63	72.63	60.83	48.58	44.75
25.00	62.40	48.70	63.38	67.42	48.88	72.01	60.81	48.56	44.75
30.00	61.11	47.78	62.37	66.99	48.13	71.44	60.79	48.55	44.74
35.00	59.95	46.90	61.44	66.61	47.34	70.90	60.76	48.54	44.73
40.00	58.86	46.05	60.56	66.25	46.54	70.39	60.74	48.52	44.72
45.00	57.80	45.25	59.73	65.88	45.86	69.91	60.72	48.51	44.72
50.00	56.86	44.51	58.96	65.55	45.24	69.45	60.71	48.50	44.71
55.00	55.96	43.80	58.22	65.22	44.64	69.02	60.69	48.49	44.70
60.00	55.14	43.13	57.53	64.93	44.07	68.62	60.67	48.48	44.70
65.00	54.37	42.48	56.88	64.65	43.49	68.24	60.66	48.47	44.69
70.00	53.66	41.87	56.27	64.37	42.96	67.88	60.64	48.46	44.69
75.00	52.97	41.27	55.69	64.12	42.42	67.54	60.63	48.45	44.68
80.00	52.34	40.70	55.14	63.87	41.94	67.21	60.61	48.44	44.68
85.00	51.75	40.17	54.63	63.65	41.50	66.91	60.60	48.43	44.67
90.00	51.20	39.66	54.14	63.43	41.03	66.62	60.59	48.43	44.67
95.00	50.68	39.17	53.67	63.22	40.60	66.35	60.58	48.42	44.66
100.00	50.20	38.71	53.23	63.03	40.19	66.09	60.56	48.41	44.66
105.00	49.74	38.26	52.82	62.84	39.79	65.85	60.55	48.40	44.65
110.00	49.32	37.83	52.43	62.67	39.44	65.62	60.54	48.40	44.65
115.00	48.92	37.42	52.06	62.50	39.06	65.41	60.53	48.39	44.64
120.00	48.53	37.01	51.70	62.34	38.66	65.21	60.53	48.39	44.64
125.00	48.20	36.61	51.38	62.20	38.34	65.02	60.52	48.38	44.64
130.00	47.88	36.25	51.07	62.06	38.03	64.83	60.51	48.38	44.63
135.00	47.57	35.90	50.78	61.92	37.69	64.67	60.51	48.37	44.63
140.00	47.32	35.55	50.52	61.81	37.41	64.51	60.50	48.37	44.63
145.00	47.06	35.24	50.27	61.70	37.16	64.36	60.49	48.36	44.62
150.00	46.80	34.93	50.03	61.59	36.85	64.22	60.49	48.36	44.62
155.00	46.60	34.59	49.82	61.49	36.53	64.09	60.48	48.36	44.62
160.00	46.40	34.32	49.62	61.40	36.35	63.98	60.48	48.36	44.62
165.00	46.25	34.04	49.44	61.32	36.05	63.86	60.48	48.35	44.62
170.00	46.09	33.81	49.28	61.26	35.90	63.78	60.47	48.35	44.61
175.00	45.98	33.56	49.15	61.20	35.64	63.71	60.47	48.35	44.61
180.00	45.88	33.32	49.04	61.16	35.43	63.65	60.47	48.35	44.61
185.00	45.75	33.14	48.92	61.11	35.34	63.59	60.47	48.35	44.61
190.00	45.66	32.92	48.81	61.06	35.11	63.53	60.47	48.35	44.61
195.00	45.60	32.64	48.71	61.03	34.77	63.48	60.47	48.35	44.61
200.00	45.50	32.49	48.61	60.98	34.77	63.42	60.47	48.35	44.61
205.00	45.47	32.31	48.54	60.94	34.55	63.37	60.47	48.35	44.61
210.00	45.47	32.05	48.53	60.92	34.22	63.33	60.47	48.35	44.61
215.00	45.45	31.89	48.53	60.89	34.13	63.30	60.47	48.35	44.61
220.00	45.43	31.75	48.52	60.85	34.09	63.27	60.47	48.35	44.61
225.00	45.43	31.57	48.56	60.84	33.82	63.24	60.47	48.35	44.61
230.00	45.49	31.46	48.58	60.83	33.76	63.22	60.47	48.35	44.61
235.00	45.49	31.35	48.60	60.81	33.73	63.20	60.48	48.36	44.61

240.00	45.57	31.21	48.64	60.80	33.54	63.19	60.48	48.36	44.61
245.00	45.61	31.09	48.67	60.78	33.42	63.18	60.48	48.36	44.61
250.00	45.65	31.02	48.70	60.78	33.43	63.17	60.48	48.36	44.61
255.00	45.72	30.89	48.76	60.78	33.24	63.17	60.49	48.36	44.61
260.00	45.78	30.73	48.83	60.78	33.02	63.18	60.49	48.36	44.61
265.00	45.83	30.64	48.89	60.78	32.98	63.20	60.49	48.37	44.61
270.00	45.88	30.60	48.95	60.79	32.98	63.22	60.49	48.37	44.61
275.00	46.01	30.51	49.06	60.80	32.84	63.26	60.49	48.37	44.61
280.00	46.11	30.48	49.14	60.82	32.89	63.29	60.50	48.37	44.61
285.00	46.23	30.41	49.25	60.83	32.80	63.32	60.50	48.37	44.61
290.00	46.32	30.34	49.36	60.85	32.70	63.36	60.50	48.37	44.61
295.00	46.44	30.30	49.46	60.88	32.72	63.40	60.50	48.37	44.61
300.00	46.58	30.24	49.58	60.90	32.65	63.45	60.50	48.38	44.61
305.00	46.70	30.12	49.70	60.91	32.44	63.52	60.50	48.38	44.61
310.00	46.85	30.07	49.82	60.94	32.37	63.58	60.50	48.38	44.61
315.00	47.01	30.07	49.95	60.98	32.46	63.64	60.50	48.38	44.61
320.00	47.15	30.03	50.09	61.01	32.36	63.71	60.50	48.38	44.61
325.00	47.30	30.00	50.23	61.05	32.29	63.77	60.50	48.38	44.61
330.00	47.53	30.01	50.36	61.09	32.40	63.85	60.50	48.38	44.61
335.00	47.72	29.97	50.52	61.14	32.42	63.93	60.50	48.38	44.61
340.00	47.93	29.93	50.67	61.18	32.28	64.01	60.49	48.38	44.61
345.00	48.16	29.94	50.81	61.23	32.21	64.09	60.49	48.37	44.60
350.00	48.41	29.94	50.98	61.28	32.35	64.18	60.49	48.37	44.61
355.00	48.61	29.95	51.15	61.33	32.30	64.27	60.48	48.37	44.60
360.00	48.86	29.98	51.29	61.39	32.26	64.36	60.48	48.37	44.60
365.00	49.13	29.98	51.46	61.45	32.35	64.45	60.47	48.37	44.60
370.00	49.36	29.97	51.64	61.51	32.37	64.54	60.47	48.36	44.60
375.00	49.58	29.99	51.79	61.56	32.30	64.63	60.47	48.36	44.60
380.00	49.89	30.05	51.96	61.64	32.48	64.72	60.46	48.36	44.60
385.00	50.12	30.08	52.13	61.70	32.50	64.82	60.45	48.35	44.60
390.00	50.39	30.15	52.30	61.77	32.54	64.91	60.44	48.35	44.59
395.00	50.67	30.21	52.47	61.86	32.67	65.01	60.44	48.35	44.59
400.00	50.92	30.25	52.65	61.94	32.68	65.11	60.43	48.34	44.59
405.00	51.20	30.31	52.81	62.02	32.66	65.20	60.42	48.34	44.59
410.00	51.48	30.36	52.98	62.11	32.74	65.29	60.41	48.33	44.59
415.00	51.73	30.41	53.16	62.21	32.81	65.39	60.40	48.33	44.58
420.00	52.01	30.49	53.35	62.32	32.89	65.48	60.39	48.32	44.58

Timecum	**2x1RH**	**2x1T**	**2x1flux**	**2x1aRH**	**2x1aT**	**2x1aflux**	**2x2RH**
0.00	0.949330	23.205000	-266.190000	0.946180	23.201000	-264.490000	0.943690
5.00	0.970610	29.292000	623.650000	0.972320	29.004000	577.590000	0.973920
10.00	0.970990	29.500000	653.430000	0.972490	29.208000	606.650000	0.973720
15.00	0.971620	29.672000	678.010000	0.973130	29.365000	628.930000	0.974440
20.00	0.972140	29.844000	702.470000	0.973590	29.518000	650.620000	0.974890
25.00	0.972660	30.020000	727.500000	0.974050	29.674000	672.730000	0.975330
30.00	0.973180	30.197000	752.710000	0.974520	29.832000	695.010000	0.975770
35.00	0.973710	30.376000	778.180000	0.974990	29.991000	717.470000	0.976220
40.00	0.974240	30.557000	803.770000	0.975470	30.151000	740.090000	0.976670
45.00	0.974780	30.738000	829.430000	0.975950	30.313000	762.910000	0.977120
50.00	0.975330	30.923000	855.590000	0.976440	30.477000	785.930000	0.977580
55.00	0.975900	31.106000	881.420000	0.976940	30.641000	809.020000	0.978040
60.00	0.976440	31.293000	907.860000	0.977440	30.808000	832.400000	0.978510
65.00	0.977030	31.478000	933.870000	0.977950	30.974000	855.730000	0.978980
70.00	0.977580	31.665000	960.200000	0.978450	31.142000	879.310000	0.979450
75.00	0.978150	31.850000	986.190000	0.978970	31.311000	902.870000	0.979930
80.00	0.978720	32.036000	1012.200000	0.979490	31.480000	926.490000	0.980410
85.00	0.979280	32.221000	1038.100000	0.980010	31.649000	950.120000	0.980890
90.00	0.979840	32.405000	1063.900000	0.980530	31.819000	973.770000	0.981370
95.00	0.980400	32.589000	1089.500000	0.981050	31.989000	997.410000	0.981860
100.00	0.980960	32.772000	1115.100000	0.981570	32.159000	1021.000000	0.982350
105.00	0.981520	32.955000	1140.600000	0.982100	32.328000	1044.500000	0.982830
110.00	0.982080	33.137000	1165.900000	0.982620	32.498000	1068.000000	0.983320
115.00	0.982630	33.318000	1191.000000	0.983140	32.666000	1091.300000	0.983820
120.00	0.983190	33.498000	1216.000000	0.983670	32.834000	1114.500000	0.984310
125.00	0.983740	33.677000	1240.800000	0.984190	33.001000	1137.500000	0.984800
130.00	0.984280	33.854000	1265.300000	0.984700	33.166000	1160.300000	0.985290
135.00	0.984820	34.031000	1289.700000	0.985210	33.330000	1183.000000	0.985770
140.00	0.985360	34.206000	1313.800000	0.985720	33.493000	1205.300000	0.986260
145.00	0.985900	34.379000	1337.700000	0.986230	33.654000	1227.500000	0.986740
150.00	0.986430	34.551000	1361.300000	0.986730	33.814000	1249.400000	0.987220
155.00	0.986960	34.721000	1384.700000	0.987230	33.972000	1271.100000	0.987690
160.00	0.987470	34.890000	1407.900000	0.987710	34.129000	1292.500000	0.988150
165.00	0.987990	35.057000	1430.700000	0.988210	34.284000	1313.700000	0.988620
170.00	0.988500	35.222000	1453.300000	0.988690	34.436000	1334.500000	0.989080
175.00	0.989010	35.384000	1475.400000	0.989170	34.587000	1355.000000	0.989540
180.00	0.989510	35.544000	1497.300000	0.989640	34.735000	1375.200000	0.989990
185.00	0.990000	35.702000	1518.800000	0.990100	34.882000	1395.100000	0.990440
190.00	0.990480	35.857000	1539.900000	0.990560	35.025000	1414.700000	0.990880
195.00	0.990960	36.009000	1560.600000	0.991000	35.167000	1433.800000	0.991310
200.00	0.991420	36.159000	1580.900000	0.991450	35.306000	1452.700000	0.991730
205.00	0.991880	36.305000	1600.800000	0.991880	35.442000	1471.200000	0.992150
210.00	0.992320	36.449000	1620.200000	0.992300	35.576000	1489.300000	0.992560
215.00	0.992760	36.589000	1639.200000	0.992720	35.707000	1507.000000	0.992960
220.00	0.993190	36.727000	1657.700000	0.993130	35.835000	1524.300000	0.993360
225.00	0.993610	36.861000	1675.800000	0.993530	35.961000	1541.200000	0.993750
230.00	0.994010	36.991000	1693.500000	0.993920	36.083000	1557.700000	0.994130
235.00	0.994410	37.119000	1710.600000	0.994300	36.202000	1573.700000	0.994490
240.00	0.994790	37.243000	1727.300000	0.994660	36.319000	1589.300000	0.994850

245.00	0.995160	37.363000	1743.400000	0.995020	36.432000	1604.500000	0.995200
250.00	0.995530	37.479000	1759.100000	0.995370	36.541000	1619.200000	0.995540
255.00	0.995870	37.592000	1774.200000	0.995710	36.648000	1633.500000	0.995870
260.00	0.996200	37.701000	1788.800000	0.996030	36.751000	1647.300000	0.996190
265.00	0.996530	37.806000	1802.800000	0.996340	36.850000	1660.600000	0.996500
270.00	0.996840	37.907000	1816.400000	0.996650	36.946000	1673.400000	0.996800
275.00	0.997130	38.004000	1829.400000	0.996940	37.038000	1685.800000	0.997090
280.00	0.997420	38.097000	1841.800000	0.997220	37.127000	1697.600000	0.997360
285.00	0.997690	38.186000	1853.700000	0.997480	37.212000	1709.000000	0.997630
290.00	0.997950	38.271000	1865.000000	0.997740	37.294000	1719.800000	0.997890
295.00	0.998190	38.352000	1875.700000	0.997980	37.371000	1730.200000	0.998130
300.00	0.998420	38.428000	1885.900000	0.998210	37.445000	1740.000000	0.998360
305.00	0.998630	38.500000	1895.500000	0.998430	37.515000	1749.300000	0.998590
310.00	0.998830	38.568000	1904.500000	0.998630	37.581000	1758.100000	0.998790
315.00	0.999010	38.631000	1912.900000	0.998820	37.643000	1766.300000	0.998990
320.00	0.999180	38.690000	1920.700000	0.998990	37.701000	1774.000000	0.999170
325.00	0.999340	38.744000	1927.900000	0.999150	37.755000	1781.200000	0.999340
330.00	0.999480	38.794000	1934.500000	0.999300	37.805000	1787.800000	0.999500
335.00	0.999600	38.839000	1940.500000	0.999440	37.851000	1793.900000	0.999650
340.00	0.999710	38.880000	1945.900000	0.999560	37.892000	1799.400000	0.999780
345.00	0.999800	38.916000	1950.700000	0.999660	37.930000	1804.400000	0.999900
350.00	0.999880	38.947000	1954.800000	0.999750	37.963000	1808.800000	1.000000
355.00	0.999940	38.974000	1958.400000	0.999830	37.992000	1812.700000	1.000000
360.00	0.999980	38.996000	1961.300000	0.999900	38.017000	1815.900000	1.000000
365.00	1.000000	39.013000	1963.600000	0.999940	38.038000	1818.700000	1.000000
370.00	1.000000	39.026000	1965.300000	0.999980	38.054000	1820.800000	1.000000
375.00	1.000000	39.034000	1966.300000	1.000000	38.066000	1822.400000	1.000000
380.00	**1.000000**	**39.037000**	**1966.700000**	**1.000000**	**38.074000**	**1823.500000**	**1.000000**
385.00	0.999970	39.035000	1966.500000	0.999990	38.077000	1823.900000	1.000000
390.00	0.999920	39.029000	1965.700000	0.999970	38.076000	1823.800000	1.000000
395.00	0.999850	39.018000	1964.200000	0.999930	38.071000	1823.100000	1.000000
400.00	0.999770	39.002000	1962.100000	0.999880	38.062000	1821.900000	1.000000
405.00	0.999670	38.982000	1959.400000	0.999810	38.048000	1820.100000	1.000000
410.00	0.999560	38.956000	1956.100000	0.999730	38.030000	1817.700000	1.000000
415.00	0.999430	38.926000	1952.100000	0.999630	38.008000	1814.700000	1.000000
420.00	0.999280	38.891000	1947.500000	0.999520	37.981000	1811.100000	1.000000

2x2T	2x2flux	2x21RH	2x21T	2x21flux	2x3RH	2x3T	2x3flux
23.200000	-262.960000	0.939640	23.200000	-261.950000	0.939500	23.200000	-262.460000
28.768000	540.430000	0.973460	28.582000	512.190000	0.973900	28.465000	496.600000
28.966000	568.460000	0.972840	28.775000	539.340000	0.973030	28.659000	524.070000
29.116000	589.660000	0.973690	28.925000	560.510000	0.974020	28.813000	545.820000
29.260000	609.900000	0.974170	29.066000	580.310000	0.974550	28.951000	565.320000
29.406000	630.460000	0.974640	29.208000	600.330000	0.974990	29.089000	584.690000
29.551000	651.010000	0.975080	29.349000	620.150000	0.975450	29.227000	604.170000
29.699000	671.730000	0.975530	29.492000	640.190000	0.975900	29.367000	623.870000
29.847000	692.590000	0.975980	29.636000	660.310000	0.976350	29.508000	643.610000
29.998000	713.660000	0.976440	29.780000	680.540000	0.976800	29.649000	663.370000
30.148000	734.760000	0.976910	29.925000	700.780000	0.977260	29.790000	683.200000
30.301000	756.080000	0.977370	30.071000	721.200000	0.977730	29.932000	703.120000
30.454000	777.490000	0.977840	30.218000	741.630000	0.978200	30.075000	723.140000
30.608000	799.010000	0.978300	30.365000	762.170000	0.978670	30.219000	743.170000
30.763000	820.650000	0.978770	30.513000	782.720000	0.979140	30.362000	763.250000
30.919000	842.410000	0.979230	30.661000	803.370000	0.979620	30.507000	783.380000
31.076000	864.200000	0.979700	30.810000	824.020000	0.980090	30.651000	803.480000
31.233000	886.060000	0.980170	30.959000	844.710000	0.980560	30.795000	823.600000
31.391000	907.980000	0.980630	31.109000	865.440000	0.981030	30.940000	843.710000
31.549000	929.910000	0.981100	31.259000	886.180000	0.981500	31.085000	863.820000
31.707000	951.840000	0.981570	31.409000	906.910000	0.981960	31.230000	883.900000
31.866000	973.730000	0.982040	31.559000	927.630000	0.982430	31.375000	903.980000
32.024000	995.570000	0.982510	31.708000	948.290000	0.982900	31.520000	924.040000
32.181000	1017.300000	0.982980	31.858000	968.910000	0.983370	31.664000	944.070000
32.338000	1039.000000	0.983460	32.008000	989.510000	0.983840	31.809000	964.070000
32.495000	1060.600000	0.983930	32.157000	1010.100000	0.984320	31.954000	984.030000
32.651000	1082.000000	0.984410	32.307000	1030.600000	0.984790	32.098000	1003.900000
32.806000	1103.300000	0.984890	32.455000	1051.000000	0.985270	32.242000	1023.800000
32.959000	1124.300000	0.985360	32.603000	1071.200000	0.985750	32.386000	1043.600000
33.112000	1145.200000	0.985840	32.750000	1091.400000	0.986220	32.530000	1063.200000
33.263000	1165.900000	0.986310	32.896000	1111.400000	0.986700	32.672000	1082.800000
33.413000	1186.400000	0.986790	33.042000	1131.200000	0.987180	32.814000	1102.200000
33.561000	1206.700000	0.987250	33.186000	1150.900000	0.987640	32.955000	1121.500000
33.708000	1226.700000	0.987720	33.329000	1170.400000	0.988120	33.094000	1140.600000
33.853000	1246.500000	0.988190	33.470000	1189.600000	0.988580	33.232000	1159.400000
33.997000	1265.900000	0.988650	33.610000	1208.600000	0.989050	33.369000	1178.100000
34.138000	1285.200000	0.989110	33.749000	1227.400000	0.989510	33.504000	1196.500000
34.278000	1304.100000	0.989560	33.885000	1246.000000	0.989960	33.638000	1214.700000
34.415000	1322.700000	0.990000	34.020000	1264.200000	0.990410	33.769000	1232.600000
34.550000	1341.000000	0.990440	34.153000	1282.100000	0.990850	33.899000	1250.200000
34.683000	1359.000000	0.990870	34.283000	1299.800000	0.991280	34.026000	1267.500000
34.813000	1376.700000	0.991300	34.411000	1317.100000	0.991710	34.152000	1284.500000
34.942000	1394.000000	0.991720	34.537000	1334.100000	0.992140	34.275000	1301.200000
35.067000	1410.900000	0.992130	34.661000	1350.700000	0.992550	34.396000	1317.700000
35.190000	1427.500000	0.992530	34.782000	1367.000000	0.992960	34.515000	1333.700000
35.311000	1443.700000	0.992920	34.900000	1383.000000	0.993360	34.632000	1349.500000
35.428000	1459.500000	0.993310	35.016000	1398.600000	0.993750	34.746000	1364.800000
35.543000	1475.000000	0.993690	35.129000	1413.700000	0.994140	34.857000	1379.800000
35.655000	1490.000000	0.994050	35.239000	1428.500000	0.994510	34.966000	1394.500000

35.764000	1504.600000	0.994410	35.347000	1442.900000	0.994870	35.072000	1408.800000
35.870000	1518.800000	0.994760	35.451000	1456.900000	0.995230	35.175000	1422.600000
35.973000	1532.500000	0.995100	35.553000	1470.600000	0.995580	35.275000	1436.100000
36.072000	1545.900000	0.995430	35.652000	1483.800000	0.995910	35.373000	1449.200000
36.169000	1558.800000	0.995750	35.747000	1496.500000	0.996240	35.467000	1461.900000
36.262000	1571.200000	0.996060	35.840000	1508.900000	0.996560	35.559000	1474.200000
36.352000	1583.200000	0.996360	35.929000	1520.800000	0.996860	35.648000	1486.100000
36.438000	1594.700000	0.996640	36.015000	1532.300000	0.997160	35.733000	1497.500000
36.521000	1605.800000	0.996920	36.098000	1543.300000	0.997450	35.815000	1508.500000
36.601000	1616.400000	0.997190	36.178000	1553.900000	0.997720	35.894000	1519.100000
36.677000	1626.600000	0.997440	36.254000	1564.000000	0.997990	35.970000	1529.200000
36.750000	1636.200000	0.997690	36.327000	1573.700000	0.998240	36.043000	1538.900000
36.819000	1645.400000	0.997920	36.396000	1582.900000	0.998480	36.112000	1548.100000
36.884000	1654.100000	0.998140	36.462000	1591.700000	0.998710	36.178000	1556.900000
36.946000	1662.300000	0.998350	36.525000	1600.000000	0.998930	36.240000	1565.300000
37.004000	1670.100000	0.998540	36.584000	1607.900000	0.999130	36.299000	1573.100000
37.059000	1677.300000	0.998730	36.639000	1615.200000	0.999320	36.355000	1580.500000
37.109000	1684.000000	0.998900	36.691000	1622.100000	0.999510	36.407000	1587.400000
37.156000	1690.200000	0.999060	36.739000	1628.500000	0.999680	36.455000	1593.900000
37.199000	1695.900000	0.999210	36.784000	1634.400000	0.999830	36.500000	1599.900000
37.238000	1701.100000	0.999350	36.825000	1639.800000	0.999970	36.542000	1605.300000
37.274000	1705.800000	0.999470	36.862000	1644.700000	1.000000	36.579000	1610.300000
37.305000	1709.900000	0.999580	36.895000	1649.200000	1.000000	36.613000	1614.800000
37.333000	1713.500000	0.999680	36.925000	1653.100000	1.000000	36.643000	1618.900000
37.356000	1716.700000	0.999760	36.951000	1656.500000	1.000000	36.670000	1622.400000
37.376000	1719.200000	0.999840	36.973000	1659.400000	1.000000	36.692000	1625.400000
37.391000	1721.300000	0.999900	36.991000	1661.800000	1.000000	36.711000	1627.900000
37.403000	**1722.800000**	0.999940	37.006000	1663.700000	1.000000	36.727000	1629.900000
37.410000	1723.800000	0.999970	37.016000	1665.100000	1.000000	36.738000	1631.500000
37.414000	1724.300000	0.999990	37.023000	1666.000000	1.000000	36.745000	1632.500000
37.413000	1724.200000	**1.000000**	**37.026000**	**1666.400000**	**1.000000**	**36.749000**	**1633.000000**
37.409000	1723.600000	0.999990	37.025000	1666.300000	1.000000	36.749000	1632.900000
37.400000	1722.500000	0.999970	37.020000	1665.600000	1.000000	36.745000	1632.400000
37.388000	1720.800000	0.999940	37.011000	1664.400000	1.000000	36.737000	1631.400000
37.371000	1718.600000	0.999890	36.998000	1662.700000	1.000000	36.726000	1629.800000
37.350000	1715.900000	0.999830	36.981000	1660.500000	1.000000	36.710000	1627.700000

2x31RH	2x31T	2x31flux	2x4RH	2x4T	2x4flux	2x41RH	2x41T	2x41flux
0.941710	23.200000	-263.360000	0.941530	23.200000	-262.650000	0.940130	23.200000	-261.430000
0.975370	28.365000	484.120000	0.976280	28.246000	465.870000	0.976840	28.124000	446.510000
0.974370	28.564000	512.270000	0.975300	28.454000	495.340000	0.975920	28.343000	477.450000
0.975470	28.715000	533.810000	0.976520	28.603000	516.520000	0.977250	28.490000	498.140000
0.975990	28.845000	552.210000	0.977000	28.725000	533.750000	0.977680	28.605000	514.340000
0.976420	28.974000	570.430000	0.977400	28.846000	550.830000	0.978080	28.719000	530.450000
0.976860	29.104000	588.810000	0.977830	28.968000	568.090000	0.978480	28.835000	546.630000
0.977290	29.236000	607.490000	0.978250	29.094000	585.750000	0.978880	28.953000	563.250000
0.977710	29.369000	626.170000	0.978670	29.220000	603.530000	0.979290	29.073000	580.140000
0.978140	29.501000	644.800000	0.979080	29.345000	621.210000	0.979700	29.193000	596.940000
0.978560	29.633000	663.490000	0.979490	29.471000	638.950000	0.980110	29.314000	613.860000
0.978990	29.766000	682.190000	0.979910	29.598000	656.670000	0.980520	29.434000	630.750000
0.979420	29.899000	700.920000	0.980320	29.724000	674.400000	0.980920	29.555000	647.680000
0.979860	30.033000	719.630000	0.980730	29.850000	692.100000	0.981320	29.676000	664.560000
0.980300	30.166000	738.340000	0.981150	29.976000	709.760000	0.981710	29.796000	681.350000
0.980740	30.300000	757.070000	0.981560	30.103000	727.500000	0.982110	29.917000	698.250000
0.981170	30.433000	775.770000	0.981980	30.229000	745.190000	0.982510	30.038000	715.110000
0.981610	30.566000	794.440000	0.982400	30.356000	762.880000	0.982900	30.159000	731.960000
0.982040	30.700000	813.080000	0.982810	30.482000	780.540000	0.983300	30.281000	748.810000
0.982460	30.833000	831.670000	0.983220	30.609000	798.170000	0.983700	30.402000	765.640000
0.982890	30.966000	850.210000	0.983640	30.735000	815.750000	0.984100	30.523000	782.440000
0.983320	31.099000	868.730000	0.984050	30.861000	833.290000	0.984500	30.643000	799.210000
0.983740	31.232000	887.220000	0.984460	30.987000	850.790000	0.984900	30.764000	815.950000
0.984170	31.364000	905.680000	0.984870	31.112000	868.240000	0.985300	30.885000	832.630000
0.984590	31.497000	924.100000	0.985280	31.238000	885.640000	0.985710	31.005000	849.260000
0.985020	31.629000	942.470000	0.985690	31.363000	903.000000	0.986110	31.125000	865.830000
0.985440	31.762000	960.810000	0.986100	31.488000	920.320000	0.986510	31.244000	882.350000
0.985870	31.894000	979.110000	0.986510	31.613000	937.580000	0.986900	31.363000	898.780000
0.986300	32.026000	997.360000	0.986910	31.737000	954.770000	0.987300	31.482000	915.110000
0.986720	32.157000	1015.500000	0.987320	31.861000	971.860000	0.987700	31.600000	931.330000
0.987150	32.288000	1033.600000	0.987730	31.984000	988.860000	0.988090	31.717000	947.440000
0.987580	32.419000	1051.600000	0.988130	32.106000	1005.700000	0.988480	31.833000	963.430000
0.988000	32.548000	1069.500000	0.988530	32.228000	1022.500000	0.988860	31.948000	979.310000
0.988420	32.678000	1087.300000	0.988930	32.349000	1039.200000	0.989240	32.063000	995.030000
0.988840	32.806000	1104.900000	0.989330	32.469000	1055.700000	0.989620	32.176000	1010.600000
0.989260	32.932000	1122.300000	0.989730	32.588000	1072.000000	0.990000	32.289000	1025.900000
0.989670	33.058000	1139.600000	0.990120	32.705000	1088.100000	0.990370	32.400000	1041.200000
0.990080	33.182000	1156.600000	0.990510	32.822000	1104.000000	0.990740	32.509000	1056.200000
0.990490	33.304000	1173.400000	0.990890	32.936000	1119.700000	0.991100	32.617000	1070.900000
0.990890	33.425000	1189.900000	0.991270	33.049000	1135.200000	0.991470	32.724000	1085.500000
0.991290	33.544000	1206.200000	0.991650	33.161000	1150.500000	0.991820	32.829000	1099.900000
0.991690	33.662000	1222.200000	0.992020	33.271000	1165.500000	0.992180	32.933000	1114.000000
0.992080	33.778000	1238.000000	0.992390	33.379000	1180.300000	0.992530	33.035000	1127.900000
0.992460	33.891000	1253.500000	0.992750	33.485000	1194.800000	0.992870	33.136000	1141.600000
0.992830	34.003000	1268.700000	0.993110	33.590000	1209.000000	0.993210	33.235000	1155.000000
0.993200	34.112000	1283.600000	0.993460	33.692000	1223.000000	0.993540	33.332000	1168.200000
0.993570	34.219000	1298.100000	0.993810	33.793000	1236.600000	0.993870	33.427000	1181.100000
0.993920	34.324000	1312.400000	0.994140	33.891000	1250.000000	0.994190	33.520000	1193.800000
0.994270	34.426000	1326.200000	0.994470	33.987000	1263.000000	0.994500	33.611000	1206.200000

0.994600	34.526000	1339.800000	0.994790	34.081000	1275.800000	0.994810	33.700000	1218.200000
0.994940	34.623000	1352.900000	0.995110	34.172000	1288.200000	0.995110	33.787000	1230.000000
0.995260	34.717000	1365.800000	0.995420	34.261000	1300.300000	0.995400	33.872000	1241.500000
0.995570	34.809000	1378.200000	0.995710	34.348000	1312.000000	0.995690	33.955000	1252.700000
0.995870	34.898000	1390.200000	0.996000	34.432000	1323.400000	0.995970	34.036000	1263.600000
0.996160	34.985000	1401.900000	0.996280	34.514000	1334.400000	0.996240	34.114000	1274.200000
0.996450	35.068000	1413.200000	0.996560	34.593000	1345.100000	0.996500	34.190000	1284.400000
0.996720	35.149000	1424.100000	0.996820	34.669000	1355.400000	0.996760	34.263000	1294.300000
0.996990	35.226000	1434.500000	0.997070	34.743000	1365.400000	0.997000	34.334000	1303.900000
0.997240	35.301000	1444.600000	0.997320	34.813000	1374.900000	0.997240	34.403000	1313.200000
0.997490	35.372000	1454.200000	0.997550	34.881000	1384.100000	0.997470	34.469000	1322.000000
0.997720	35.441000	1463.400000	0.997780	34.947000	1392.900000	0.997690	34.532000	1330.600000
0.997950	35.506000	1472.200000	0.997990	35.009000	1401.300000	0.997900	34.593000	1338.700000
0.998160	35.568000	1480.600000	0.998200	35.068000	1409.300000	0.998110	34.651000	1346.500000
0.998360	35.627000	1488.500000	0.998390	35.125000	1416.900000	0.998300	34.706000	1354.000000
0.998550	35.683000	1496.000000	0.998570	35.178000	1424.100000	0.998480	34.759000	1361.000000
0.998730	35.735000	1503.000000	0.998750	35.229000	1430.900000	0.998650	34.809000	1367.700000
0.998900	35.784000	1509.600000	0.998910	35.276000	1437.300000	0.998820	34.856000	1374.100000
0.999050	35.830000	1515.800000	0.999070	35.321000	1443.200000	0.998970	34.900000	1380.000000
0.999200	35.873000	1521.500000	0.999210	35.362000	1448.800000	0.999110	34.941000	1385.500000
0.999330	35.912000	1526.700000	0.999340	35.400000	1453.900000	0.999250	34.979000	1390.700000
0.999450	35.947000	1531.500000	0.999460	35.435000	1458.600000	0.999370	35.015000	1395.400000
0.999560	35.980000	1535.800000	0.999560	35.467000	1462.900000	0.999480	35.047000	1399.700000
0.999660	36.008000	1539.700000	0.999660	35.496000	1466.700000	0.999590	35.077000	1403.700000
0.999750	36.034000	1543.100000	0.999750	35.521000	1470.100000	0.999680	35.103000	1407.200000
0.999820	36.056000	1546.000000	0.999820	35.543000	1473.100000	0.999760	35.126000	1410.300000
0.999880	36.074000	1548.500000	0.999890	35.562000	1475.600000	0.999830	35.147000	1413.100000
0.999930	36.089000	1550.500000	0.999940	35.578000	1477.700000	0.999890	35.164000	1415.400000
0.999970	36.100000	1552.000000	0.999980	35.590000	1479.400000	0.999940	35.178000	1417.200000
0.999990	36.108000	1553.000000	1.000000	35.599000	1480.600000	0.999970	35.189000	1418.700000
1.000000	**36.113000**	**1553.600000**	**1.000000**	**35.605000**	**1481.300000**	**1.000000**	**35.197000**	**1419.800000**
1.000000	36.113000	1553.700000	1.000000	35.607000	1481.700000	1.000000	35.202000	1420.400000
1.000000	36.111000	1553.400000	1.000000	35.606000	1481.500000	1.000000	35.203000	1420.600000
0.999970	36.104000	1552.500000	1.000000	35.602000	1481.000000	1.000000	35.201000	1420.400000
0.999930	36.094000	1551.200000	0.999970	35.594000	1479.900000	1.000000	35.197000	1419.800000
0.999890	36.081000	1549.300000	0.999930	35.583000	1478.500000	0.999970	35.189000	1418.700000

2x5RH	2x5T	2x5flux	2x51RH	2x51T	2x51flux	2x6RH	2x6T	2x6flux
0.936620	23.200000	-258.250000	0.929740	23.200000	-255.970000	0.919470	23.200000	-254.310000
0.977040	27.999000	423.600000	0.975060	27.897000	405.790000	0.970740	27.830000	393.950000
0.976080	28.227000	455.460000	0.974020	28.138000	439.120000	0.969640	28.098000	430.770000
0.977560	28.378000	476.440000	0.975680	28.294000	460.620000	0.971520	28.268000	454.090000
0.977980	28.489000	491.900000	0.976100	28.404000	475.910000	0.972010	28.391000	470.980000
0.978340	28.598000	507.130000	0.976450	28.512000	490.800000	0.972440	28.511000	487.420000
0.978730	28.709000	522.520000	0.976840	28.622000	505.960000	0.972890	28.633000	504.150000
0.979120	28.823000	538.380000	0.977230	28.736000	521.570000	0.973360	28.758000	521.350000
0.979530	28.940000	554.700000	0.977650	28.854000	537.810000	0.973860	28.889000	539.190000
0.979940	29.057000	570.930000	0.978080	28.971000	553.980000	0.974380	29.019000	556.920000
0.980350	29.176000	587.330000	0.978510	29.090000	570.290000	0.974880	29.149000	574.670000
0.980760	29.294000	603.740000	0.978940	29.209000	586.680000	0.975400	29.279000	592.500000
0.981170	29.414000	620.250000	0.979370	29.329000	603.140000	0.975900	29.409000	610.210000
0.981570	29.532000	636.640000	0.979800	29.449000	619.590000	0.976430	29.541000	628.100000
0.982000	29.654000	653.450000	0.980230	29.571000	636.240000	0.976810	29.675000	646.320000
0.982390	29.772000	669.690000	0.980670	29.691000	652.680000	0.977420	29.803000	663.730000
0.982800	29.892000	686.220000	0.981100	29.812000	669.240000	0.977920	29.934000	681.520000
0.983210	30.012000	702.750000	0.981530	29.934000	685.830000	0.978430	30.066000	699.360000
0.983610	30.132000	719.260000	0.981970	30.055000	702.430000	0.978940	30.198000	717.230000
0.984020	30.252000	735.750000	0.982400	30.177000	718.990000	0.979440	30.330000	735.050000
0.984430	30.372000	752.210000	0.982830	30.298000	735.510000	0.979940	30.461000	752.830000
0.984830	30.491000	768.640000	0.983250	30.419000	751.980000	0.980440	30.593000	770.580000
0.985240	30.611000	785.010000	0.983680	30.540000	768.390000	0.980930	30.724000	788.290000
0.985650	30.730000	801.320000	0.984100	30.660000	784.730000	0.981430	30.855000	805.950000
0.986050	30.848000	817.560000	0.984520	30.780000	800.990000	0.981920	30.986000	823.560000
0.986460	30.967000	833.740000	0.984950	30.900000	817.180000	0.982410	31.116000	841.130000
0.986860	31.085000	849.860000	0.985370	31.019000	833.310000	0.982910	31.247000	858.620000
0.987260	31.202000	865.880000	0.985790	31.137000	849.340000	0.983400	31.376000	875.990000
0.987660	31.319000	881.790000	0.986210	31.255000	865.270000	0.983880	31.505000	893.220000
0.988060	31.435000	897.600000	0.986630	31.372000	881.100000	0.984370	31.632000	910.340000
0.988460	31.550000	913.290000	0.987050	31.489000	896.820000	0.984850	31.759000	927.340000
0.988860	31.665000	928.870000	0.987470	31.604000	912.420000	0.985330	31.885000	944.200000
0.989240	31.779000	944.350000	0.987870	31.720000	927.920000	0.985800	32.011000	960.960000
0.989630	31.892000	959.690000	0.988290	31.834000	943.300000	0.986280	32.135000	977.580000
0.990020	32.004000	974.900000	0.988700	31.947000	958.590000	0.986750	32.259000	994.080000
0.990400	32.115000	989.960000	0.989100	32.060000	973.740000	0.987220	32.382000	1010.500000
0.990780	32.225000	1004.900000	0.989510	32.172000	988.750000	0.987690	32.504000	1026.700000
0.991160	32.334000	1019.600000	0.989910	32.283000	1003.600000	0.988150	32.625000	1042.700000
0.991530	32.441000	1034.100000	0.990300	32.392000	1018.200000	0.988610	32.744000	1058.600000
0.991900	32.547000	1048.400000	0.990690	32.499000	1032.600000	0.989070	32.863000	1074.300000
0.992270	32.652000	1062.500000	0.991080	32.606000	1046.900000	0.989520	32.979000	1089.700000
0.992630	32.755000	1076.400000	0.991470	32.711000	1060.900000	0.989970	33.094000	1105.000000
0.992980	32.856000	1090.100000	0.991840	32.814000	1074.700000	0.990410	33.208000	1120.000000
0.993330	32.956000	1103.600000	0.992220	32.916000	1088.200000	0.990840	33.320000	1134.800000
0.993680	33.054000	1116.800000	0.992580	33.016000	1101.600000	0.991270	33.430000	1149.300000
0.994020	33.151000	1129.700000	0.992940	33.114000	1114.700000	0.991690	33.538000	1163.600000
0.994350	33.245000	1142.400000	0.993300	33.210000	1127.500000	0.992100	33.644000	1177.600000
0.994680	33.338000	1154.900000	0.993640	33.305000	1140.100000	0.992510	33.748000	1191.300000
0.994990	33.428000	1167.000000	0.993980	33.397000	1152.300000	0.992900	33.850000	1204.700000

0.995300	33.517000	1178.900000	0.994310	33.488000	1164.400000	0.993290	33.950000	1217.800000
0.995610	33.604000	1190.500000	0.994640	33.576000	1176.100000	0.993680	34.047000	1230.700000
0.995910	33.688000	1201.800000	0.994960	33.662000	1187.500000	0.994050	34.142000	1243.100000
0.996200	33.770000	1212.800000	0.995260	33.746000	1198.700000	0.994410	34.235000	1255.300000
0.996480	33.850000	1223.500000	0.995570	33.828000	1209.500000	0.994760	34.325000	1267.200000
0.996750	33.928000	1233.900000	0.995860	33.907000	1220.000000	0.995110	34.413000	1278.700000
0.997020	34.003000	1243.900000	0.996140	33.984000	1230.200000	0.995440	34.498000	1289.800000
0.997280	34.076000	1253.700000	0.996420	34.059000	1240.100000	0.995770	34.581000	1300.600000
0.997530	34.147000	1263.100000	0.996690	34.131000	1249.700000	0.996080	34.661000	1311.100000
0.997770	34.215000	1272.200000	0.996950	34.201000	1258.900000	0.996390	34.738000	1321.200000
0.998000	34.281000	1280.900000	0.997200	34.269000	1267.800000	0.996680	34.813000	1330.900000
0.998220	34.344000	1289.300000	0.997440	34.333000	1276.300000	0.996960	34.884000	1340.200000
0.998440	34.404000	1297.400000	0.997670	34.395000	1284.500000	0.997230	34.952000	1349.200000
0.998640	34.462000	1305.000000	0.997890	34.454000	1292.300000	0.997490	35.018000	1357.700000
0.998830	34.517000	1312.400000	0.998090	34.511000	1299.700000	0.997740	35.080000	1365.900000
0.999020	34.569000	1319.300000	0.998290	34.565000	1306.800000	0.997970	35.140000	1373.600000
0.999190	34.619000	1325.900000	0.998480	34.616000	1313.500000	0.998190	35.196000	1380.900000
0.999360	34.666000	1332.100000	0.998660	34.664000	1319.900000	0.998400	35.249000	1387.900000
0.999520	34.710000	1338.000000	0.998830	34.709000	1325.900000	0.998600	35.300000	1394.400000
0.999660	34.751000	1343.400000	0.998980	34.752000	1331.500000	0.998790	35.347000	1400.500000
0.999790	34.789000	1348.500000	0.999130	34.792000	1336.700000	0.998960	35.391000	1406.200000
0.999920	34.825000	1353.200000	0.999270	34.828000	1341.500000	0.999120	35.431000	1411.500000
1.000000	34.857000	1357.500000	0.999390	34.862000	1346.000000	0.999270	35.469000	1416.400000
1.000000	34.887000	1361.500000	0.999510	34.893000	1350.000000	0.999400	35.503000	1420.800000
1.000000	34.914000	1365.000000	0.999610	34.921000	1353.700000	0.999520	35.534000	1424.800000
1.000000	34.937000	1368.200000	0.999700	34.946000	1357.000000	0.999630	35.561000	1428.400000
1.000000	34.958000	1370.900000	0.999780	34.968000	1359.900000	0.999730	35.586000	1431.600000
1.000000	34.976000	1373.300000	0.999850	34.987000	1362.400000	0.999810	35.607000	1434.300000
1.000000	34.991000	1375.200000	0.999910	35.003000	1364.500000	0.999880	35.624000	1436.500000
1.000000	35.002000	1376.800000	0.999960	35.016000	1366.200000	0.999940	35.638000	1438.400000
1.000000	**35.011000**	**1377.900000**	**1.000000**	**35.026000**	**1367.500000**	0.999980	35.649000	1439.800000
1.000000	35.017000	1378.700000	1.000000	35.033000	1368.400000	**1.000000**	**35.656000**	**1440.700000**
1.000000	35.019000	1379.000000	1.000000	35.037000	1368.900000	1.000000	35.660000	1441.200000
1.000000	35.019000	1379.000000	1.000000	35.037000	1369.000000	1.000000	35.660000	1441.200000
1.000000	35.015000	1378.500000	1.000000	35.035000	1368.600000	1.000000	35.657000	1440.800000
1.000000	35.008000	1377.600000	1.000000	35.029000	1367.900000	0.999990	35.650000	1440.000000

2x61RH	2x61T	2x61flux	2x7RH	2x7T	2x7flux	2x71RH	2x71T	2x71flux
0.916700	23.200000	-252.080000	0.922810	23.200000	-249.050000	0.914330	23.200000	-244.520000
0.969960	27.753000	379.960000	0.972880	27.667000	363.720000	0.971530	27.565000	343.570000
0.968760	28.039000	418.970000	0.971540	27.962000	403.590000	0.970120	27.884000	385.900000
0.970880	28.214000	442.830000	0.973900	28.136000	426.920000	0.972680	28.053000	408.330000
0.971370	28.338000	459.750000	0.974330	28.252000	442.660000	0.973030	28.168000	423.530000
0.971810	28.459000	476.200000	0.974750	28.366000	457.870000	0.973440	28.280000	438.220000
0.972280	28.583000	492.990000	0.975190	28.481000	473.430000	0.973860	28.393000	453.250000
0.972770	28.709000	510.160000	0.975630	28.599000	489.200000	0.974290	28.508000	468.390000
0.973280	28.840000	527.870000	0.976090	28.719000	505.350000	0.974730	28.626000	483.860000
0.973810	28.970000	545.490000	0.976560	28.839000	521.420000	0.975170	28.744000	499.430000
0.974320	29.100000	563.060000	0.977030	28.959000	537.420000	0.975630	28.864000	515.270000
0.974830	29.230000	580.680000	0.977460	29.078000	553.400000	0.976100	28.984000	530.950000
0.975370	29.360000	598.240000	0.977960	29.198000	569.350000	0.976540	29.116000	548.350000
0.975850	29.497000	616.720000	0.978320	29.336000	587.850000	0.977230	29.213000	561.060000
0.976520	29.602000	630.960000	0.979250	29.386000	594.560000	0.977550	29.443000	591.130000
0.976920	29.754000	651.360000	0.979340	29.564000	618.300000	0.978030	29.481000	596.210000
0.977430	29.885000	669.080000	0.979820	29.687000	634.620000	0.978510	29.604000	612.290000
0.977950	30.017000	686.750000	0.980280	29.809000	650.870000	0.978980	29.727000	628.380000
0.978470	30.149000	704.480000	0.980750	29.932000	667.210000	0.979470	29.852000	644.700000
0.978990	30.281000	722.190000	0.981220	30.055000	683.560000	0.979960	29.979000	661.170000
0.979500	30.413000	739.870000	0.981680	30.178000	699.830000	0.980450	30.105000	677.600000
0.980010	30.544000	757.530000	0.982150	30.300000	716.060000	0.980940	30.231000	694.010000
0.980520	30.676000	775.150000	0.982610	30.423000	732.280000	0.981440	30.357000	710.410000
0.981030	30.808000	792.740000	0.983070	30.545000	748.470000	0.981920	30.483000	726.760000
0.981540	30.939000	810.290000	0.983520	30.667000	764.610000	0.982410	30.608000	743.060000
0.982040	31.070000	827.780000	0.983980	30.789000	780.700000	0.982890	30.734000	759.300000
0.982540	31.201000	845.210000	0.984430	30.910000	796.710000	0.983370	30.858000	775.440000
0.983040	31.331000	862.490000	0.984880	31.031000	812.600000	0.983840	30.982000	791.460000
0.983540	31.460000	879.640000	0.985330	31.151000	828.370000	0.984310	31.105000	807.340000
0.984040	31.588000	896.670000	0.985780	31.270000	844.020000	0.984780	31.227000	823.090000
0.984530	31.715000	913.560000	0.986220	31.388000	859.550000	0.985240	31.348000	838.710000
0.985020	31.842000	930.320000	0.986660	31.505000	874.950000	0.985700	31.468000	854.200000
0.985500	31.967000	946.970000	0.987100	31.621000	890.250000	0.986160	31.587000	869.580000
0.985990	32.092000	963.490000	0.987540	31.737000	905.410000	0.986610	31.705000	884.820000
0.986470	32.216000	979.860000	0.987980	31.852000	920.430000	0.987060	31.823000	899.930000
0.986950	32.339000	996.100000	0.988410	31.966000	935.310000	0.987510	31.939000	914.880000
0.987420	32.461000	1012.200000	0.988830	32.078000	950.060000	0.987960	32.055000	929.710000
0.987890	32.582000	1028.100000	0.989260	32.190000	964.630000	0.988400	32.169000	944.360000
0.988360	32.701000	1043.900000	0.989680	32.300000	979.020000	0.988840	32.282000	958.830000
0.988820	32.819000	1059.400000	0.990090	32.409000	993.220000	0.989270	32.393000	973.120000
0.989280	32.936000	1074.800000	0.990500	32.516000	1007.200000	0.989690	32.504000	987.220000
0.989740	33.051000	1090.000000	0.990900	32.622000	1021.000000	0.990120	32.612000	1001.100000
0.990180	33.165000	1104.900000	0.991300	32.727000	1034.600000	0.990530	32.720000	1014.800000
0.990620	33.277000	1119.600000	0.991690	32.830000	1048.000000	0.990940	32.825000	1028.300000
0.991060	33.387000	1134.000000	0.992070	32.931000	1061.200000	0.991350	32.930000	1041.600000
0.991490	33.496000	1148.200000	0.992450	33.031000	1074.100000	0.991750	33.032000	1054.600000
0.991910	33.602000	1162.100000	0.992830	33.128000	1086.800000	0.992140	33.132000	1067.400000
0.992320	33.707000	1175.800000	0.993190	33.224000	1099.200000	0.992530	33.231000	1080.000000
0.992720	33.809000	1189.100000	0.993550	33.318000	1111.400000	0.992900	33.328000	1092.300000

0.993120	33.909000	1202.200000	0.993890	33.410000	1123.300000	0.993270	33.423000	1104.400000
0.993510	34.007000	1215.000000	0.994240	33.500000	1134.900000	0.993640	33.516000	1116.100000
0.993880	34.103000	1227.400000	0.994570	33.588000	1146.300000	0.993990	33.606000	1127.600000
0.994250	34.196000	1239.600000	0.994900	33.674000	1157.300000	0.994340	33.695000	1138.900000
0.994610	34.287000	1251.400000	0.995220	33.757000	1168.100000	0.994680	33.781000	1149.800000
0.994960	34.375000	1262.900000	0.995530	33.838000	1178.600000	0.995010	33.865000	1160.400000
0.995300	34.461000	1274.000000	0.995830	33.917000	1188.700000	0.995330	33.947000	1170.800000
0.995630	34.544000	1284.800000	0.996120	33.993000	1198.500000	0.995650	34.026000	1180.800000
0.995950	34.624000	1295.200000	0.996400	34.067000	1208.100000	0.995950	34.103000	1190.500000
0.996270	34.702000	1305.300000	0.996680	34.139000	1217.300000	0.996250	34.177000	1199.900000
0.996570	34.777000	1315.000000	0.996940	34.208000	1226.200000	0.996530	34.249000	1209.000000
0.996850	34.849000	1324.300000	0.997200	34.274000	1234.700000	0.996810	34.318000	1217.700000
0.997130	34.918000	1333.300000	0.997440	34.338000	1242.900000	0.997070	34.385000	1226.100000
0.997390	34.984000	1341.800000	0.997680	34.399000	1250.700000	0.997330	34.449000	1234.100000
0.997640	35.047000	1350.000000	0.997900	34.457000	1258.200000	0.997570	34.510000	1241.800000
0.997880	35.107000	1357.800000	0.998110	34.513000	1265.300000	0.997800	34.568000	1249.200000
0.998110	35.164000	1365.100000	0.998310	34.566000	1272.100000	0.998020	34.624000	1256.200000
0.998320	35.218000	1372.100000	0.998500	34.616000	1278.500000	0.998230	34.677000	1262.800000
0.998530	35.269000	1378.700000	0.998690	34.663000	1284.600000	0.998430	34.727000	1269.100000
0.998720	35.317000	1384.800000	0.998860	34.707000	1290.200000	0.998620	34.774000	1275.000000
0.998890	35.361000	1390.500000	0.999020	34.749000	1295.500000	0.998800	34.818000	1280.600000
0.999060	35.403000	1395.900000	0.999160	34.787000	1300.500000	0.998960	34.859000	1285.700000
0.999210	35.441000	1400.800000	0.999300	34.823000	1305.000000	0.999120	34.897000	1290.500000
0.999350	35.476000	1405.300000	0.999420	34.856000	1309.200000	0.999260	34.933000	1295.000000
0.999480	35.507000	1409.300000	0.999540	34.885000	1313.000000	0.999390	34.965000	1299.000000
0.999590	35.536000	1413.000000	0.999640	34.912000	1316.400000	0.999510	34.994000	1302.600000
0.999690	35.560000	1416.200000	0.999730	34.935000	1319.400000	0.999620	35.020000	1305.900000
0.999770	35.582000	1419.000000	0.999810	34.956000	1322.000000	0.999710	35.043000	1308.800000
0.999850	35.600000	1421.300000	0.999870	34.973000	1324.200000	0.999790	35.063000	1311.200000
0.999900	35.615000	1423.200000	0.999930	34.987000	1326.000000	0.999850	35.079000	1313.300000
0.999950	35.626000	1424.600000	0.999970	34.998000	1327.500000	0.999910	35.093000	1315.000000
0.999980	35.634000	1425.600000	1.000000	35.006000	1328.500000	0.999960	35.103000	1316.300000
1.000000	**35.638000**	**1426.200000**	**1.000000**	**35.011000**	**1329.100000**	0.999990	35.110000	1317.200000
1.000000	35.639000	1426.300000	1.000000	35.013000	1329.300000	**1.000000**	**35.114000**	**1317.700000**
0.999990	35.636000	1425.900000	1.000000	35.011000	1329.100000	1.000000	35.114000	1317.700000
0.999960	35.630000	1425.100000	0.999990	35.007000	1328.500000	1.000000	35.112000	1317.400000

2x8RH	2x8T	2x8flux	2x81RH	2x81T	2x81flux	2x9RH	2x9T	2x9flux
0.900300	23.200000	-239.370000	0.885050	23.200000	-231.430000	0.868900	23.200000	-221.790000
0.968470	27.464000	323.320000	0.965840	27.340000	297.040000	0.964710	27.208000	268.760000
0.966940	27.808000	367.990000	0.964460	27.721000	344.820000	0.963490	27.619000	318.220000
0.969690	27.977000	389.900000	0.967240	27.885000	365.470000	0.966170	27.775000	337.050000
0.970030	28.096000	405.260000	0.967570	28.010000	381.050000	0.966550	27.902000	352.320000
0.970440	28.208000	419.820000	0.968030	28.128000	395.900000	0.967030	28.023000	366.830000
0.970870	28.324000	434.750000	0.968490	28.249000	411.050000	0.967510	28.146000	381.600000
0.971290	28.439000	449.660000	0.968940	28.371000	426.290000	0.967970	28.271000	396.510000
0.971730	28.557000	464.900000	0.969410	28.495000	441.690000	0.968440	28.396000	411.530000
0.972170	28.677000	480.360000	0.969890	28.621000	457.430000	0.968930	28.524000	426.790000
0.972670	28.802000	496.450000	0.970410	28.751000	473.610000	0.969470	28.656000	442.550000
0.973150	28.930000	512.860000	0.970920	28.886000	490.400000	0.970000	28.790000	458.600000
0.973740	29.058000	529.370000	0.971560	29.015000	506.440000	0.970590	28.926000	474.850000
0.974250	29.187000	545.890000	0.972110	29.139000	521.880000	0.971300	29.033000	487.640000
0.974740	29.377000	570.320000	0.972170	29.372000	550.850000	0.970720	29.329000	522.780000
0.975210	29.438000	578.160000	0.973110	29.418000	556.570000	0.972210	29.335000	523.550000
0.975790	29.573000	595.450000	0.973720	29.551000	572.940000	0.972830	29.464000	538.870000
0.976290	29.701000	611.820000	0.974250	29.689000	590.040000	0.973390	29.607000	555.790000
0.976800	29.830000	628.300000	0.974800	29.827000	607.120000	0.973940	29.749000	572.690000
0.977340	29.962000	645.070000	0.975370	29.965000	624.160000	0.974530	29.890000	589.400000
0.977870	30.093000	661.870000	0.975940	30.103000	641.160000	0.975110	30.031000	606.080000
0.978410	30.225000	678.640000	0.976510	30.240000	658.130000	0.975690	30.172000	622.740000
0.978950	30.357000	695.400000	0.977080	30.378000	675.090000	0.976280	30.313000	639.380000
0.979480	30.488000	712.120000	0.977650	30.516000	692.010000	0.976860	30.454000	655.990000
0.980020	30.619000	728.820000	0.978220	30.653000	708.900000	0.977440	30.595000	672.550000
0.980550	30.751000	745.470000	0.978790	30.791000	725.750000	0.978030	30.735000	689.070000
0.981080	30.881000	762.050000	0.979360	30.928000	742.550000	0.978610	30.875000	705.520000
0.981610	31.011000	778.540000	0.979920	31.064000	759.250000	0.979180	31.014000	721.850000
0.982140	31.141000	794.900000	0.980480	31.200000	775.840000	0.979750	31.152000	738.050000
0.982660	31.269000	811.140000	0.981040	31.334000	792.310000	0.980320	31.289000	754.110000
0.983180	31.397000	827.250000	0.981600	31.468000	808.660000	0.980890	31.425000	770.020000
0.983700	31.523000	843.240000	0.982150	31.601000	824.890000	0.981460	31.560000	785.800000
0.984200	31.649000	859.110000	0.982690	31.733000	841.000000	0.982000	31.694000	801.460000
0.984710	31.774000	874.860000	0.983240	31.865000	856.980000	0.982560	31.828000	817.010000
0.985220	31.898000	890.450000	0.983780	31.995000	872.830000	0.983100	31.960000	832.440000
0.985720	32.021000	905.890000	0.984320	32.124000	888.550000	0.983650	32.092000	847.790000
0.986220	32.143000	921.190000	0.984850	32.253000	904.140000	0.984190	32.223000	863.060000
0.986710	32.263000	936.310000	0.985380	32.380000	919.570000	0.984730	32.353000	878.200000
0.987200	32.383000	951.250000	0.985910	32.506000	934.830000	0.985270	32.482000	893.190000
0.987690	32.500000	966.000000	0.986430	32.631000	949.900000	0.985810	32.610000	908.020000
0.988170	32.617000	980.560000	0.986950	32.754000	964.790000	0.986350	32.737000	922.670000
0.988640	32.731000	994.910000	0.987470	32.876000	979.480000	0.986880	32.861000	937.120000
0.989110	32.845000	1009.000000	0.987970	32.996000	993.970000	0.987390	32.985000	951.370000
0.989580	32.956000	1023.000000	0.988470	33.114000	1008.200000	0.987910	33.106000	965.420000
0.990040	33.066000	1036.700000	0.988970	33.231000	1022.300000	0.988420	33.226000	979.260000
0.990490	33.174000	1050.100000	0.989470	33.346000	1036.100000	0.988920	33.344000	992.880000
0.990940	33.280000	1063.300000	0.989950	33.459000	1049.700000	0.989420	33.460000	1006.300000
0.991380	33.384000	1076.300000	0.990430	33.570000	1063.000000	0.989910	33.575000	1019.400000
0.991810	33.486000	1089.000000	0.990890	33.679000	1076.100000	0.990390	33.687000	1032.300000

0.992230	33.586000	1101.400000	0.991350	33.785000	1088.900000	0.990860	33.797000	1045.000000
0.992650	33.684000	1113.500000	0.991810	33.890000	1101.400000	0.991330	33.905000	1057.300000
0.993060	33.780000	1125.400000	0.992250	33.992000	1113.700000	0.991780	34.010000	1069.500000
0.993460	33.873000	1137.000000	0.992690	34.092000	1125.600000	0.992230	34.114000	1081.300000
0.993850	33.965000	1148.300000	0.993100	34.190000	1137.300000	0.992660	34.215000	1092.900000
0.994220	34.053000	1159.200000	0.993520	34.284000	1148.600000	0.993090	34.313000	1104.100000
0.994600	34.139000	1169.800000	0.993930	34.376000	1159.600000	0.993510	34.408000	1115.000000
0.994960	34.223000	1180.200000	0.994320	34.467000	1170.400000	0.993910	34.502000	1125.700000
0.995310	34.305000	1190.300000	0.994700	34.555000	1180.800000	0.994310	34.593000	1136.100000
0.995650	34.383000	1200.000000	0.995070	34.640000	1191.000000	0.994690	34.681000	1146.200000
0.995980	34.459000	1209.300000	0.995430	34.721000	1200.600000	0.995070	34.766000	1155.800000
0.996300	34.533000	1218.500000	0.995780	34.801000	1210.100000	0.995420	34.849000	1165.300000
0.996610	34.603000	1227.000000	0.996120	34.876000	1219.100000	0.995780	34.928000	1174.300000
0.996900	34.671000	1235.400000	0.996440	34.950000	1227.800000	0.996110	35.004000	1183.000000
0.997180	34.736000	1243.500000	0.996740	35.021000	1236.200000	0.996430	35.078000	1191.400000
0.997450	34.798000	1251.000000	0.997040	35.088000	1244.200000	0.996740	35.149000	1199.400000
0.997710	34.857000	1258.300000	0.997330	35.151000	1251.700000	0.997040	35.216000	1207.000000
0.997960	34.913000	1265.200000	0.997600	35.213000	1259.000000	0.997330	35.281000	1214.400000
0.998200	34.966000	1271.700000	0.997860	35.271000	1265.900000	0.997600	35.342000	1221.300000
0.998420	35.016000	1277.800000	0.998100	35.326000	1272.400000	0.997860	35.400000	1227.900000
0.998630	35.063000	1283.600000	0.998330	35.377000	1278.500000	0.998100	35.455000	1234.100000
0.998820	35.107000	1289.000000	0.998550	35.426000	1284.200000	0.998330	35.506000	1239.900000
0.999000	35.148000	1294.000000	0.998750	35.471000	1289.500000	0.998550	35.554000	1245.400000
0.999170	35.185000	1298.600000	0.998940	35.512000	1294.400000	0.998750	35.599000	1250.500000
0.999320	35.219000	1302.800000	0.999120	35.550000	1298.900000	0.998940	35.640000	1255.100000
0.999470	35.251000	1306.700000	0.999280	35.587000	1303.200000	0.999120	35.679000	1259.500000
0.999590	35.278000	1309.900000	0.999420	35.616000	1306.700000	0.999280	35.713000	1263.300000
0.999700	35.302000	1312.900000	0.999550	35.644000	1310.000000	0.999420	35.744000	1266.800000
0.999800	35.325000	1315.700000	0.999670	35.670000	1313.100000	0.999550	35.772000	1270.000000
0.999880	35.343000	1317.900000	0.999760	35.692000	1315.600000	0.999660	35.796000	1272.700000
0.999950	35.357000	1319.700000	0.999850	35.709000	1317.700000	0.999760	35.816000	1275.100000
1.000000	35.369000	1321.100000	0.999920	35.723000	1319.400000	0.999840	35.834000	1277.000000
1.000000	35.376000	1322.000000	0.999970	35.734000	1320.600000	0.999910	35.847000	1278.500000
1.000000	**35.382000**	**1322.700000**	**1.000000**	**35.742000**	**1321.500000**	0.999960	35.857000	1279.600000
1.000000	35.382000	1322.700000	1.000000	35.745000	1321.900000	0.999990	35.863000	1280.300000
1.000000	35.380000	1322.400000	1.000000	35.744000	1321.800000	**1.000000**	**35.866000**	**1280.600000**

2x91RH	2x91T	2x91flux	2x10RH	2x10T	2x10flux	2x101RH	2x101T	2x101flux
0.831210	23.200000	-208.680000	0.770730	23.200000	-188.670000	0.603960	23.200000	-149.660000
0.961200	27.097000	240.260000	0.957210	26.985000	205.810000	0.943950	26.925000	158.530000
0.960050	27.540000	290.590000	0.955970	27.461000	254.630000	0.942710	27.484000	204.120000
0.962580	27.696000	308.220000	0.958540	27.620000	270.950000	0.945640	27.674000	219.590000
0.963150	27.831000	323.550000	0.959150	27.760000	285.310000	0.946770	27.844000	233.430000
0.963660	27.960000	338.060000	0.959780	27.898000	299.400000	0.947960	28.008000	246.720000
0.964200	28.091000	352.820000	0.960410	28.038000	313.750000	0.949070	28.174000	260.150000
0.964720	28.222000	367.680000	0.961040	28.181000	328.310000	0.950130	28.341000	273.680000
0.965280	28.356000	382.710000	0.961700	28.326000	343.100000	0.951200	28.508000	287.160000
0.965820	28.490000	397.840000	0.962350	28.472000	358.040000	0.952130	28.680000	300.990000
0.966430	28.628000	413.300000	0.963060	28.621000	373.200000	0.953160	28.846000	314.410000
0.967010	28.768000	429.020000	0.963720	28.774000	388.760000	0.953960	29.026000	328.950000
0.967670	28.910000	445.060000	0.964370	28.927000	404.280000	0.954650	29.205000	343.330000
0.968460	29.027000	458.120000	0.965360	29.088000	420.590000	0.956290	29.368000	356.420000
0.967150	29.393000	499.280000	0.962940	29.415000	453.750000	0.949230	29.932000	401.750000
0.969430	29.339000	493.110000	0.966400	29.386000	450.760000	0.957480	29.743000	386.460000
0.970160	29.473000	508.060000	0.967110	29.532000	465.520000	0.958480	29.912000	400.030000
0.970750	29.622000	524.640000	0.967740	29.691000	481.560000	0.959500	30.097000	414.760000
0.971340	29.771000	541.240000	0.968340	29.850000	497.620000	0.960500	30.276000	429.060000
0.971980	29.918000	557.630000	0.968970	30.006000	513.270000	0.961520	30.454000	443.250000
0.972610	30.065000	573.990000	0.969600	30.160000	528.830000	0.962560	30.631000	457.340000
0.973240	30.212000	590.360000	0.970250	30.315000	544.310000	0.963620	30.807000	471.320000
0.973860	30.359000	606.710000	0.970910	30.468000	559.670000	0.964680	30.982000	485.220000
0.974470	30.506000	622.990000	0.971570	30.620000	574.910000	0.965720	31.156000	499.050000
0.975090	30.652000	639.230000	0.972240	30.771000	590.060000	0.966750	31.330000	512.800000
0.975700	30.799000	655.430000	0.972920	30.921000	605.090000	0.967780	31.503000	526.480000
0.976330	30.945000	671.550000	0.973620	31.071000	620.060000	0.968790	31.675000	540.080000
0.976950	31.089000	687.550000	0.974310	31.220000	634.960000	0.969780	31.847000	553.620000
0.977570	31.233000	703.390000	0.975000	31.369000	649.790000	0.970760	32.018000	567.070000
0.978200	31.376000	719.090000	0.975700	31.517000	664.540000	0.971720	32.187000	580.400000
0.978830	31.517000	734.640000	0.976390	31.664000	679.200000	0.972670	32.356000	593.640000
0.979450	31.657000	750.060000	0.977090	31.811000	693.770000	0.973620	32.523000	606.760000
0.980060	31.797000	765.400000	0.977770	31.957000	708.300000	0.974540	32.690000	619.810000
0.980670	31.936000	780.650000	0.978460	32.103000	722.750000	0.975470	32.855000	632.770000
0.981270	32.074000	795.810000	0.979140	32.248000	737.100000	0.976380	33.019000	645.580000
0.981870	32.212000	810.910000	0.979810	32.392000	751.360000	0.977280	33.182000	658.250000
0.982470	32.349000	825.940000	0.980480	32.536000	765.530000	0.978170	33.343000	670.800000
0.983070	32.486000	840.870000	0.981150	32.678000	779.580000	0.979050	33.502000	683.190000
0.983670	32.622000	855.670000	0.981820	32.819000	793.480000	0.979920	33.659000	695.380000
0.984260	32.756000	870.320000	0.982480	32.959000	807.240000	0.980780	33.814000	707.400000
0.984850	32.889000	884.810000	0.983140	33.097000	820.830000	0.981630	33.966000	719.230000
0.985440	33.020000	899.090000	0.983790	33.234000	834.250000	0.982460	34.116000	730.860000
0.986010	33.150000	913.150000	0.984430	33.368000	847.480000	0.983280	34.264000	742.270000
0.986580	33.277000	927.010000	0.985060	33.501000	860.510000	0.984090	34.409000	753.480000
0.987140	33.403000	940.660000	0.985690	33.632000	873.360000	0.984880	34.551000	764.470000
0.987690	33.527000	954.080000	0.986310	33.762000	885.980000	0.985660	34.691000	775.240000
0.988240	33.649000	967.290000	0.986920	33.889000	898.400000	0.986430	34.828000	785.780000
0.988780	33.769000	980.250000	0.987520	34.013000	910.580000	0.987180	34.962000	796.090000
0.989310	33.887000	992.970000	0.988110	34.136000	922.530000	0.987900	35.093000	806.150000

0.989830	34.002000	1005.400000	0.988690	34.256000	934.240000	0.988610	35.221000	815.970000
0.990340	34.115000	1017.600000	0.989270	34.374000	945.710000	0.989320	35.345000	825.530000
0.990840	34.226000	1029.600000	0.989830	34.489000	956.910000	0.990000	35.467000	834.820000
0.991340	34.335000	1041.300000	0.990380	34.602000	967.880000	0.990650	35.585000	843.890000
0.991810	34.441000	1052.700000	0.990910	34.712000	978.560000	0.991290	35.700000	852.670000
0.992290	34.544000	1063.700000	0.991440	34.819000	989.010000	0.991900	35.812000	861.210000
0.992760	34.644000	1074.500000	0.991950	34.924000	999.170000	0.992500	35.920000	869.460000
0.993200	34.742000	1085.100000	0.992450	35.026000	1009.000000	0.993080	36.025000	877.420000
0.993640	34.838000	1095.300000	0.992940	35.125000	1018.600000	0.993640	36.125000	885.080000
0.994060	34.930000	1105.200000	0.993410	35.221000	1027.800000	0.994170	36.223000	892.490000
0.994480	35.019000	1114.700000	0.993870	35.313000	1036.800000	0.994690	36.316000	899.590000
0.994870	35.106000	1124.000000	0.994320	35.403000	1045.500000	0.995180	36.406000	906.400000
0.995270	35.189000	1132.900000	0.994750	35.490000	1053.800000	0.995650	36.492000	912.940000
0.995640	35.269000	1141.500000	0.995170	35.573000	1061.800000	0.996110	36.573000	919.140000
0.995990	35.346000	1149.700000	0.995560	35.653000	1069.600000	0.996530	36.652000	925.080000
0.996340	35.421000	1157.600000	0.995950	35.730000	1077.000000	0.996920	36.726000	930.720000
0.996680	35.492000	1165.200000	0.996320	35.803000	1084.000000	0.997290	36.796000	936.030000
0.996990	35.559000	1172.400000	0.996670	35.873000	1090.800000	0.997650	36.862000	941.040000
0.997300	35.623000	1179.200000	0.997010	35.940000	1097.200000	0.997990	36.924000	945.730000
0.997590	35.684000	1185.700000	0.997330	36.003000	1103.200000	0.998290	36.982000	950.120000
0.997860	35.742000	1191.800000	0.997630	36.063000	1108.900000	0.998570	37.036000	954.180000
0.998120	35.796000	1197.600000	0.997920	36.119000	1114.300000	0.998830	37.086000	957.920000
0.998360	35.847000	1203.000000	0.998180	36.171000	1119.300000	0.999060	37.131000	961.350000
0.998580	35.894000	1208.000000	0.998440	36.220000	1124.000000	0.999270	37.172000	964.450000
0.998800	35.937000	1212.600000	0.998680	36.265000	1128.300000	0.999450	37.209000	967.220000
0.998990	35.978000	1216.900000	0.998890	36.306000	1132.300000	0.999600	37.242000	969.710000
0.999180	36.014000	1220.800000	0.999090	36.343000	1135.800000	0.999740	37.270000	971.810000
0.999340	36.047000	1224.300000	0.999270	36.377000	1139.000000	0.999850	37.294000	973.610000
0.999470	36.076000	1227.400000	0.999420	36.407000	1141.900000	0.999930	37.314000	975.130000
0.999600	36.102000	1230.100000	0.999570	36.433000	1144.400000	0.999980	37.329000	976.300000
0.999710	36.123000	1232.400000	0.999690	36.455000	1146.600000	1.000000	37.340000	977.110000
0.999800	36.141000	1234.300000	0.999790	36.474000	1148.300000	**1.000000**	**37.347000**	**977.610000**
0.999880	36.156000	1235.800000	0.999880	36.488000	1149.700000	0.999990	37.349000	977.770000
0.999940	36.167000	1237.000000	0.999950	36.499000	1150.700000	0.999930	37.347000	977.610000
0.999980	36.174000	1237.700000	0.999990	36.505000	1151.300000	0.999860	37.340000	977.120000
1.000000	**36.176000**	**1238.000000**	**1.000000**	**36.508000**	**1151.600000**	0.999760	37.329000	976.290000

2_l1116RH	2_l1116T	2_l1116flux	2x11RH	2x11T	2x11flux
0.620700	23.200000	-96.550000	0.698330	23.200000	-80.162000
0.940620	26.753000	93.178000	0.941890	26.738000	76.491000
0.939370	27.417000	128.010000	0.940600	27.525000	110.840000
0.942210	27.668000	141.070000	0.943510	27.866000	125.640000
0.943310	27.902000	153.250000	0.944830	28.175000	139.050000
0.944330	28.128000	165.010000	0.946010	28.468000	151.690000
0.945360	28.348000	176.470000	0.947350	28.748000	163.760000
0.946430	28.566000	187.730000	0.948660	29.025000	175.690000
0.947560	28.782000	198.950000	0.949990	29.302000	187.590000
0.948760	28.996000	209.980000	0.951310	29.576000	199.360000
0.949940	29.212000	221.110000	0.952600	29.853000	211.210000
0.951180	29.426000	232.130000	0.953870	30.129000	222.970000
0.952190	29.648000	243.580000	0.955200	30.405000	234.760000
0.953830	29.852000	254.020000	0.955990	30.686000	246.710000
0.952470	30.202000	272.160000	0.957850	30.984000	259.350000
0.956060	30.280000	275.970000	0.958900	31.217000	269.220000
0.957340	30.483000	286.360000	0.960200	31.475000	280.120000
0.958570	30.693000	297.050000	0.961420	31.740000	291.300000
0.959760	30.902000	307.710000	0.962570	32.003000	302.360000
0.960940	31.109000	318.260000	0.963740	32.262000	313.270000
0.962100	31.316000	328.760000	0.964880	32.520000	324.070000
0.963240	31.521000	339.180000	0.966020	32.774000	334.720000
0.964360	31.726000	349.540000	0.967130	33.026000	345.240000
0.965470	31.929000	359.850000	0.968240	33.276000	355.650000
0.966570	32.132000	370.090000	0.969330	33.523000	365.930000
0.967670	32.333000	380.250000	0.970420	33.767000	376.070000
0.968750	32.533000	390.330000	0.971480	34.008000	386.070000
0.969830	32.731000	400.290000	0.972540	34.245000	395.900000
0.970900	32.928000	410.160000	0.973590	34.479000	405.560000
0.971960	33.122000	419.920000	0.974620	34.709000	415.070000
0.973010	33.314000	429.540000	0.975650	34.936000	424.400000
0.974040	33.504000	439.050000	0.976660	35.158000	433.540000
0.975050	33.692000	448.450000	0.977630	35.378000	442.560000
0.976070	33.878000	457.710000	0.978620	35.593000	451.380000
0.977070	34.061000	466.830000	0.979590	35.804000	460.000000
0.978060	34.241000	475.800000	0.980550	36.011000	468.420000
0.979040	34.419000	484.630000	0.981490	36.213000	476.680000
0.980000	34.593000	493.300000	0.982410	36.411000	484.730000
0.980930	34.765000	501.820000	0.983300	36.604000	492.580000
0.981850	34.934000	510.170000	0.984180	36.793000	500.240000
0.982760	35.099000	518.370000	0.985040	36.978000	507.710000
0.983650	35.262000	526.400000	0.985880	37.158000	514.990000
0.984520	35.421000	534.260000	0.986690	37.333000	522.070000
0.985370	35.577000	541.940000	0.987490	37.503000	528.950000
0.986200	35.730000	549.440000	0.988260	37.669000	535.620000
0.987010	35.878000	556.760000	0.989020	37.830000	542.090000
0.987800	36.024000	563.910000	0.989750	37.986000	548.360000
0.988570	36.166000	570.870000	0.990460	38.137000	554.420000
0.989310	36.304000	577.630000	0.991140	38.283000	560.280000

0.990030	36.438000	584.200000	0.991800	38.424000	565.920000
0.990740	36.568000	590.570000	0.992450	38.560000	571.340000
0.991420	36.694000	596.730000	0.993070	38.690000	576.550000
0.992070	36.816000	602.710000	0.993650	38.816000	581.550000
0.992690	36.934000	608.470000	0.994210	38.935000	586.300000
0.993300	37.048000	614.000000	0.994750	39.048000	590.800000
0.993870	37.157000	619.340000	0.995260	39.156000	595.090000
0.994420	37.263000	624.470000	0.995740	39.258000	599.170000
0.994950	37.363000	629.380000	0.996210	39.355000	603.030000
0.995450	37.460000	634.080000	0.996650	39.447000	606.670000
0.995930	37.552000	638.570000	0.997060	39.533000	610.090000
0.996390	37.640000	642.830000	0.997460	39.614000	613.280000
0.996810	37.724000	646.890000	0.997820	39.689000	616.270000
0.997220	37.802000	650.730000	0.998160	39.759000	619.040000
0.997590	37.877000	654.350000	0.998460	39.823000	621.580000
0.997940	37.947000	657.750000	0.998750	39.882000	623.900000
0.998260	38.012000	660.910000	0.999010	39.935000	626.000000
0.998560	38.073000	663.860000	0.999240	39.982000	627.880000
0.998830	38.129000	666.590000	0.999450	40.024000	629.530000
0.999070	38.180000	669.090000	0.999620	40.060000	630.960000
0.999290	38.227000	671.350000	0.999770	40.091000	632.170000
0.999480	38.269000	673.390000	0.999890	40.116000	633.150000
0.999640	38.306000	675.200000	0.999990	40.135000	633.910000
0.999780	38.338000	676.790000	1.000000	40.148000	634.450000
0.999890	38.366000	678.130000	1.000000	40.156000	634.760000
0.999970	38.389000	679.250000	1.000000	40.158000	634.840000
1.000000	38.406000	680.130000	1.000000	40.154000	634.700000
1.000000	38.419000	680.780000	1.000000	40.145000	634.340000
1.000000	38.428000	681.210000	**1.000000**	**40.130000**	**633.740000**
1.000000	**38.431000**	**681.400000**	0.999950	40.109000	632.920000
0.999990	38.430000	681.350000	0.999840	40.082000	631.880000
0.999910	38.423000	681.080000	0.999690	40.050000	630.610000
0.999800	38.412000	680.560000	0.999520	40.012000	629.110000
0.999660	38.396000	679.820000	0.999320	39.968000	627.400000
0.999490	38.375000	678.840000	0.999090	39.919000	625.460000
0.999300	38.349000	677.620000	0.998840	39.864000	623.290000

Timecum	case4 (gm/S)	case3 (gm/S)	case2 (gm/S)	case1 (gm/S)
0.00	4.52	4.52	4.52	4.52
5.00	1.58	2.40	1.59	2.42
10.00	1.59	2.43	1.62	2.46
15.00	1.61	2.46	1.64	2.50
20.00	1.62	2.47	1.66	2.53
25.00	1.63	2.49	1.69	2.56
30.00	1.65	2.50	1.71	2.59
35.00	1.66	2.52	1.74	2.62
40.00	1.67	2.53	1.76	2.65
45.00	1.69	2.54	1.79	2.68
50.00	1.70	2.56	1.82	2.71
55.00	1.71	2.58	1.84	2.74
60.00	1.72	2.59	1.87	2.78
65.00	1.74	2.61	1.90	2.80
70.00	1.75	2.64	1.92	2.84
75.00	1.76	2.64	1.95	2.88
80.00	1.78	2.65	1.98	2.90
85.00	1.79	2.66	2.01	2.94
90.00	1.81	2.68	2.04	2.97
95.00	1.82	2.69	2.07	3.00
100.00	1.83	2.71	2.10	3.04
105.00	1.85	2.72	2.13	3.07
110.00	1.86	2.74	2.16	3.11
115.00	1.87	2.75	2.19	3.14
120.00	1.89	2.77	2.22	3.18
125.00	1.90	2.78	2.25	3.21
130.00	1.91	2.80	2.28	3.25
135.00	1.93	2.81	2.31	3.28
140.00	1.94	2.83	2.34	3.32
145.00	1.95	2.84	2.37	3.35
150.00	1.97	2.85	2.41	3.39
155.00	1.98	2.87	2.44	3.43
160.00	1.99	2.88	2.47	3.46
165.00	2.00	2.90	2.50	3.49
170.00	2.02	2.91	2.53	3.53
175.00	2.03	2.92	2.56	3.57
180.00	2.04	2.94	2.59	3.60
185.00	2.05	2.95	2.62	3.64
190.00	2.07	2.96	2.66	3.67
195.00	2.08	2.98	2.69	3.71
200.00	2.09	2.99	2.72	3.74
205.00	2.10	3.00	2.75	3.78
210.00	2.11	3.01	2.78	3.81
215.00	2.12	3.02	2.81	3.84
220.00	2.14	3.04	2.84	3.88
225.00	2.15	3.05	2.87	3.91
230.00	2.15	3.06	2.90	3.94
235.00	2.16	3.07	2.93	3.98
240.00	2.17	3.08	2.95	4.01

245.00	2.18	3.09	2.98	4.04
250.00	2.19	3.10	3.01	4.07
255.00	2.20	3.11	3.04	4.10
260.00	2.21	3.12	3.06	4.13
265.00	2.22	3.12	3.09	4.16
270.00	2.23	3.13	3.11	4.19
275.00	2.23	3.14	3.14	4.21
280.00	2.24	3.15	3.16	4.24
285.00	2.25	3.16	3.19	4.26
290.00	2.25	3.16	3.21	4.29
295.00	2.26	3.17	3.23	4.32
300.00	2.27	3.17	3.25	4.34
305.00	2.27	3.18	3.28	4.36
310.00	2.28	3.19	3.29	4.39
315.00	2.28	3.19	3.31	4.40
320.00	2.29	3.19	3.33	4.42
325.00	2.29	3.20	3.35	4.44
330.00	2.30	3.20	3.37	4.46
335.00	2.30	3.20	3.38	4.48
340.00	2.30	3.20	3.40	4.50
345.00	2.31	3.21	3.42	4.51
350.00	2.31	3.21	3.43	4.52
355.00	2.31	3.21	3.44	4.54
360.00	2.31	3.21	3.45	4.55
365.00	2.32	3.21	3.47	4.56
370.00	2.32	3.21	3.47	4.57
375.00	2.32	3.21	3.48	4.58
380.00	2.32	3.21	3.49	4.58
385.00	2.32	3.21	3.50	4.59
390.00	2.32	3.21	3.51	4.59
395.00	2.32	3.20	3.51	4.60
400.00	2.31	3.20	3.52	4.60
405.00	2.31	3.20	3.52	4.60
410.00	2.31	3.19	3.52	4.60
415.00	2.31	3.19	3.52	4.60
420.00	2.31	3.18	3.52	4.60

	Case 1	Case 1	Case 1	Case 3
Fetch(x)	NoShadingInversionHeight(z)	NSIHRHHigh	NSIHRHLow	ShadingInversionHeight(z)
0.0000000000	0.0038500000	0.0044920000	0.0033525000	0.0034700000
0.4687500000	0.0039090000	0.0045720000	0.0033933000	0.0032820000
0.9375000000	0.0040000000	0.0047540000	0.0034970000	0.0030300000
1.4062500000	0.0043600000	0.0051588000	0.0037470000	0.0029630000
1.8750000000	0.0047000000	0.0057260000	0.0040930000	0.0030200000
2.3437500000	0.0049000000	0.0058640000	0.0041780000	0.0032320000
2.8125000000	0.0049700000	0.0059780000	0.0042285000	0.0032900000
3.2812500000	0.0050500000	0.0061077000	0.0042790000	0.0032940000
3.7500000000	0.0050000000	0.0062050000	0.0043157000	0.0031800000
4.2187500000	0.0054400000	0.0066485000	0.0045795000	0.0030920000
4.6875000000	0.0064000000	0.0078520000	0.0053600000	0.0029400000
5.1562500000	0.0067290000	0.0082685000	0.0056100000	0.0028730000
5.6250000000	0.0063100000	0.0077640000	0.0052760000	0.0029100000
6.0937500000	0.0065800000	0.0081190000	0.0054860000	0.0027680000
6.5625000000	0.0072000000	0.0089220000	0.0060000000	0.0025800000
7.0312500000	0.0077500000	0.0095950000	0.0064490000	0.0023680000
7.5000000000	0.0079400000	0.0098300000	0.0066000000	0.0021400000
7.9687500000	0.0085600000	0.0106000000	0.0071100000	0.0018910000
8.4375000000	0.0093900000	0.0117100000	0.0077650000	0.0016000000
8.9062500000	0.0132500000	0.0164300000	0.0109800000	0.0015315000
9.2430000000	0.0165429187	0.0199650000	0.0140170000	0.0039800000
9.3750000000	0.0167000000	0.0197090000	0.0144240000	0.0040000000

Case 3	Case 3	Case 2	Case 4	Case 1	Case 1
SIHRHHigh	SIHRHLow	NoShadingHeight(z)	ShadingHeight(z)	RHNSI	TNSI
0.0040626500	0.0030767500	0.0028800000	0.0024000000	1.0000000000	39.0370000000
0.0038680000	0.0028910000	0.0028370000	0.0021200000	1.0000000000	38.0740000000
0.0036080500	0.0026421800	0.0028600000	0.0017300000	1.0000000000	37.4030000000
0.0035700000	0.0025736000	0.0031030000	0.0014670000	1.0000000000	37.0260000000
0.0036770000	0.0026099000	0.0034800000	0.0013500000	1.0000000000	36.7490000000
0.0039334600	0.0027880000	0.0032530000	0.0013252000	1.0000000000	36.1130000000
0.0040270000	0.0028358000	0.0031600000	0.0012200000	1.0000000000	35.6050000000
0.0040445000	0.0028290000	0.0031200000	0.0010570000	1.0000000000	35.1970000000
0.0039375000	0.0027275500	0.0031400000	0.0009000000	1.0000000000	35.0110000000
0.0038475000	0.0026309000	0.0035140000	0.0007390000	1.0000000000	35.0260000000
0.0037202000	0.0024765000	0.0047000000	0.0005100000	1.0000000000	35.6560000000
0.0036601000	0.0023985000	0.0050000000	0.0003570000	1.0000000000	35.6380000000
0.0037032500	0.0024390000	0.0043000000	0.0002900000	1.0000000000	35.0110000000
0.0035371200	0.0023090000	0.0047600000	0.0001200000	1.0000000000	35.1140000000
0.0033195000	0.0021520000	0.0057000000	0.0000100000	1.0000000000	35.3820000000
0.0030598000	0.0019547000	0.0065800000	0.0000000001	1.0000000000	35.7420000000
0.0027865000	0.0017615000	0.0069000000	0.0000100000	1.0000000000	35.8660000000
0.0024702000	0.0015440000	0.0080800000	0.0000000001	1.0000000000	36.1760000000
0.0021849000	0.0013454000	0.0096000000	0.0000100000	1.0000000000	36.5080000000
0.0020630000	0.0012094300	0.0156400000	0.0000000001	1.0000000000	37.3470000000
0.0049225000	0.0033870000	0.0195000000	0.0020500000	1.0000000000	38.4310000000
0.0050630000	0.0034745000	0.0189800000	0.0016130000	1.0000000000	40.1300000000

Case 1	Case 1	Case 1	Case 1	Case 1	Case 1
tefluxxNSI	HighRHNSI	HighTNSI	HightefluxxNSI	LowRHNSI	LowTNSI
1966.7000000000	1.0000000000	39.2210000000	1996.4000000000	1.0000000000	38.8380000000
1823.5000000000	1.0000000000	38.2510000000	1852.1000000000	1.0000000000	37.8870000000
1722.8000000000	1.0000000000	37.5890000000	1753.2000000000	1.0000000000	37.2320000000
1666.4000000000	1.0000000000	37.2060000000	1696.0000000000	1.0000000000	36.8400000000
1633.0000000000	1.0000000000	36.9370000000	1665.0000000000	1.0000000000	36.5520000000
1553.6000000000	1.0000000000	36.2800000000	1582.0000000000	1.0000000000	35.9380000000
1481.3000000000	1.0000000000	35.7630000000	1508.3000000000	1.0000000000	35.4450000000
1419.8000000000	1.0000000000	35.3540000000	1446.7000000000	1.0000000000	35.0490000000
1377.9000000000	1.0000000000	35.1650000000	1405.1000000000	1.0000000000	34.8720000000
1367.5000000000	1.0000000000	35.1830000000	1395.0000000000	1.0000000000	34.8890000000
1440.7000000000	1.0000000000	35.8120000000	1469.7000000000	1.0000000000	35.4980000000
1426.2000000000	1.0000000000	35.7900000000	1455.0000000000	1.0000000000	35.4760000000
1329.1000000000	1.0000000000	35.1620000000	1356.4000000000	1.0000000000	34.8580000000
1317.7000000000	1.0000000000	35.2620000000	1345.1000000000	1.0000000000	34.9600000000
1322.7000000000	1.0000000000	35.5240000000	1350.8000000000	1.0000000000	35.2290000000
1321.5000000000	1.0000000000	35.8810000000	1350.2000000000	1.0000000000	35.5920000000
1280.6000000000	1.0000000000	35.9960000000	1308.4000000000	1.0000000000	35.7170000000
1238.0000000000	1.0000000000	36.2860000000	1264.4000000000	1.0000000000	36.0400000000
1151.6000000000	1.0000000000	36.5900000000	1175.5000000000	1.0000000000	36.3900000000
977.6100000000	1.0000000000	37.2640000000	990.6100000000	1.0000000000	37.3420000000
681.4000000000	1.0000000000	38.3920000000	698.2300000000	1.0000000000	38.3980000000
633.7400000000	1.0000000000	40.0860000000	650.5200000000	1.0000000000	40.1600000000

Case 1	Case 3	Case 3	Case 3	Case 3	Case 3
LowtefluxxNSI	RHSI	TSI	tefluxxSI	HighRHSI	HighTSI
1936.4000000000	1.0000000000	38.4650000000	1888.0000000000	1.0000000000	38.6430000000
1794.7000000000	1.0000000000	36.6690000000	1632.1000000000	1.0000000000	36.8740000000
1696.5000000000	1.0000000000	35.3500000000	1442.8000000000	1.0000000000	35.5510000000
1637.4000000000	1.0000000000	34.4300000000	1311.5000000000	1.0000000000	34.6230000000
1602.7000000000	1.0000000000	33.8500000000	1234.8000000000	1.0000000000	34.0530000000
1525.8000000000	1.0000000000	33.5360000000	1196.9000000000	1.0000000000	33.7130000000
1455.7000000000	1.0000000000	33.1730000000	1144.6000000000	1.0000000000	33.3390000000
1395.8000000000	1.0000000000	32.7990000000	1088.3000000000	1.0000000000	32.9460000000
1355.8000000000	1.0000000000	32.4510000000	1027.9000000000	1.0000000000	32.5990000000
1344.7000000000	1.0000000000	32.1000000000	969.6700000000	1.0000000000	32.2550000000
1414.1000000000	1.0000000000	31.6810000000	903.7500000000	1.0000000000	31.8700000000
1398.8000000000	1.0000000000	31.4100000000	858.8300000000	1.0000000000	31.6090000000
1304.0000000000	1.0000000000	31.2800000000	833.2800000000	1.0000000000	31.4620000000
1292.2000000000	1.0000000000	31.0020000000	780.7500000000	1.0000000000	31.1850000000
1296.8000000000	1.0000000000	30.6980000000	722.9600000000	1.0000000000	30.8860000000
1295.4000000000	1.0000000000	30.3620000000	654.9200000000	1.0000000000	30.5610000000
1254.7000000000	1.0000000000	30.0630000000	590.6600000000	1.0000000000	30.2640000000
1213.3000000000	1.0000000000	29.7550000000	518.6700000000	1.0000000000	29.9650000000
1129.2000000000	1.0000000000	29.4560000000	436.3400000000	1.0000000000	29.6760000000
963.4300000000	1.0000000000	29.0700000000	308.0100000000	1.0000000000	29.3220000000
665.9500000000	1.0000000000	30.8440000000	272.4400000000	1.0000000000	31.0460000000
620.8700000000	1.0000000000	33.4980000000	318.3400000000	1.0000000000	33.6640000000

Case 3	Case 3	Case 3	Case 3	Case 2	Case 2
HightefluxxSI	LowRHSI	LowTSI	LowtefluxxSI	RHNS	TNS
1916.3000000000	1.0000000000	38.2900000000	1861.8000000000	1.0000000000	34.4630000000
1663.6000000000	1.0000000000	36.4910000000	1605.6000000000	1.0000000000	33.5830000000
1473.4000000000	1.0000000000	35.1780000000	1417.4000000000	1.0000000000	33.0090000000
1340.9000000000	1.0000000000	34.2660000000	1287.3000000000	1.0000000000	32.7280000000
1265.7000000000	1.0000000000	33.6710000000	1208.5000000000	1.0000000000	32.5230000000
1224.3000000000	1.0000000000	33.3850000000	1174.3000000000	1.0000000000	31.8060000000
1170.4000000000	1.0000000000	33.0370000000	1124.2000000000	1.0000000000	31.3240000000
1111.4000000000	1.0000000000	32.6740000000	1069.4000000000	1.0000000000	30.9720000000
1050.8000000000	1.0000000000	32.3270000000	1009.3000000000	1.0000000000	30.8520000000
993.4000000000	1.0000000000	31.9690000000	950.4600000000	1.0000000000	30.9510000000
931.7400000000	1.0000000000	31.5140000000	880.0200000000	1.0000000000	31.7170000000
887.7700000000	1.0000000000	31.2410000000	834.9700000000	1.0000000000	31.7520000000
859.6900000000	1.0000000000	31.1310000000	812.3600000000	1.0000000000	31.1130000000
806.7400000000	1.0000000000	30.8490000000	759.8500000000	1.0000000000	31.2650000000
748.9200000000	1.0000000000	30.5420000000	702.1700000000	1.0000000000	31.6010000000
681.2100000000	1.0000000000	30.1930000000	633.3700000000	1.0000000000	32.0610000000
615.9400000000	1.0000000000	29.8940000000	570.1300000000	1.0000000000	32.2610000000
543.0600000000	1.0000000000	29.5800000000	498.8700000000	1.0000000000	32.6390000000
459.1500000000	1.0000000000	29.2790000000	418.6200000000	1.0000000000	32.9900000000
327.9900000000	1.0000000000	28.8600000000	291.7400000000	1.0000000000	33.6680000000
284.1300000000	1.0000000000	30.6630000000	262.7100000000	1.0000000000	34.8810000000
328.2200000000	1.0000000000	33.3320000000	310.4100000000	1.0000000000	36.7390000000

Case 2	Case 4	Case 4	Case 4
tefluxxNS	RHS	TS	tefluxxS
1343.5000000000	1.0000000000	33.7210000000	1239.4000000000
1211.8000000000	1.0000000000	32.1260000000	1008.7000000000
1125.2000000000	1.0000000000	30.8890000000	829.9000000000
1082.1000000000	1.0000000000	29.9780000000	699.1900000000
1056.7000000000	1.0000000000	29.4300000000	623.8800000000
960.7100000000	1.0000000000	29.0960000000	579.3900000000
891.2200000000	1.0000000000	28.7440000000	528.6600000000
838.3100000000	1.0000000000	28.3910000000	476.7200000000
811.7300000000	1.0000000000	28.1210000000	433.3700000000
817.2600000000	1.0000000000	27.8410000000	390.2700000000
914.7300000000	1.0000000000	27.5080000000	340.9400000000
911.7400000000	1.0000000000	27.2970000000	309.0200000000
816.4800000000	1.0000000000	27.1950000000	292.3200000000
821.3300000000	1.0000000000	26.9860000000	259.1600000000
846.7700000000	0.9997000000	26.7620000000	224.0000000000
875.3500000000	0.9989800000	26.5360000000	187.9800000000
862.3500000000	0.9982600000	26.3420000000	156.8000000000
854.8000000000	0.9976300000	26.1360000000	124.1900000000
811.0500000000	0.9968800000	25.9360000000	91.8770000000
706.0000000000	0.9962100000	25.6550000000	49.7450000000
519.4700000000	1.0000000000	27.5810000000	118.2400000000
509.1100000000	1.0000000000	30.4080000000	198.7300000000

	E-W axis H/W=1	NE-SW axis H/W=1	N-S axis H/W=1	E-W axis H/W=1	NE-SW axis H/W=1
Timecum	T1_90d17FEB24	T1_45d17FEB24	T1_0d17FEB24	T1_90d16OCT21	T1_45d16OCT21
0.00	23.337	23.329	23.329	23.337	23.329
5.00	23.668	23.562	23.575	23.665	23.567
10.00	23.993	23.793	23.820	23.991	23.798
15.00	24.313	24.019	24.064	24.315	24.030
20.00	24.631	24.241	24.309	24.635	24.271
25.00	24.950	24.460	24.553	24.952	24.504
30.00	25.262	24.672	24.806	25.267	24.732
35.00	25.577	24.879	25.060	25.580	24.967
40.00	25.893	25.100	25.316	25.895	25.200
45.00	26.207	25.319	25.591	26.210	25.428
50.00	26.518	25.532	25.865	26.523	25.650
55.00	26.828	25.749	26.142	26.843	25.878
60.00	27.134	25.969	26.422	27.169	26.142
65.00	27.439	26.181	26.746	27.492	26.408
70.00	27.742	26.386	27.072	27.810	26.670
75.00	28.043	26.586	27.404	28.123	26.930
80.00	28.342	26.818	27.771	28.416	27.186
85.00	28.637	27.057	28.134	28.706	27.434
90.00	28.930	27.302	28.504	28.991	27.692
95.00	29.220	27.546	28.872	29.273	28.005
100.00	29.507	27.790	29.236	29.552	28.315
105.00	29.790	28.028	29.650	29.826	28.649
110.00	30.070	28.265	30.060	30.097	28.990
115.00	30.356	28.548	30.472	30.358	29.323
120.00	30.638	28.838	30.891	30.615	29.667
125.00	30.917	29.147	31.307	30.865	30.003
130.00	31.192	29.477	31.727	31.108	30.330
135.00	31.463	29.799	32.173	31.348	30.654
140.00	31.731	30.131	32.610	31.582	30.983
145.00	31.989	30.461	33.046	31.810	31.316
150.00	32.243	30.783	33.487	32.032	31.665
155.00	32.489	31.100	33.965	32.249	32.009
160.00	32.727	31.417	34.439	32.461	32.346
165.00	32.962	31.743	34.902	32.670	32.709
170.00	33.191	32.081	35.366	32.875	33.073
175.00	33.414	32.422	35.818	33.075	33.447
180.00	33.629	32.755	36.260	33.275	33.825
185.00	33.840	33.111	36.719	33.471	34.196
190.00	34.047	33.467	37.181	33.665	34.565
195.00	34.250	33.830	37.629	33.857	34.921
200.00	34.449	34.210	38.069	34.045	35.264
205.00	34.644	34.580	38.469	34.231	35.595
210.00	34.839	34.949	38.846	34.412	35.940
215.00	35.029	35.309	39.213	34.588	36.277
220.00	35.219	35.657	39.567	34.767	36.609
225.00	35.405	35.991	39.904	34.946	36.963
230.00	35.588	36.329	40.230	35.122	37.306
235.00	35.769	36.667	40.536	35.292	37.647

240.00	35.945	36.997	40.778	35.457	38.027
245.00	36.120	37.348	41.011	35.616	38.389
250.00	36.296	37.696	41.230	35.770	38.733
255.00	36.472	38.033	41.437	35.917	39.060
260.00	36.641	38.409	41.595	36.064	39.377
265.00	36.805	38.785	41.745	36.208	39.680
270.00	36.962	39.142	41.884	36.347	39.970
275.00	37.114	39.482	42.008	36.469	40.248
280.00	37.250	39.806	42.121	36.576	40.531
285.00	37.369	40.121	42.209	36.678	40.811
290.00	37.485	40.420	42.256	36.774	41.073
295.00	37.598	40.710	42.294	36.862	41.320
300.00	37.704	40.989	42.322	36.945	41.546
305.00	37.806	41.282	42.337	37.024	41.735
310.00	37.901	41.559	42.339	37.097	41.906
315.00	37.991	41.819	42.309	37.164	42.063
320.00	38.077	42.066	42.271	37.226	42.204
325.00	38.158	42.281	42.215	37.273	42.332
330.00	38.234	42.468	42.116	37.286	42.448
335.00	38.304	42.635	42.016	37.295	42.514
340.00	38.368	42.791	41.909	37.301	42.562
345.00	38.428	42.929	41.802	37.314	42.583
350.00	38.482	43.056	41.666	37.325	42.586
355.00	38.524	43.166	41.532	37.333	42.577
360.00	38.549	43.226	41.394	37.343	42.558
365.00	38.573	43.268	41.243	37.348	42.518
370.00	38.595	43.285	41.094	37.345	42.456
375.00	38.612	43.282	40.940	37.334	42.371
380.00	38.632	43.269	40.788	37.323	42.269
385.00	38.645	43.246	40.635	37.312	42.159
390.00	38.645	43.203	40.479	37.295	42.030
395.00	38.616	43.138	40.325	37.268	41.880
400.00	38.589	43.048	40.156	37.230	41.713
405.00	38.561	42.939	39.986	37.188	41.544
410.00	38.528	42.819	39.819	37.146	41.364
415.00	38.490	42.686	39.656	37.100	41.183
420.00	38.448	42.538	39.496	37.049	40.996

N-S axis H/W=1	E-W axis H/W=2	NE-SW axis H/W=2	N-S axis H/W=2	E-W axis H/W=3	NE-SW axis H/W=3
T1_0d16OCT21	T2_90d17FEB24	T2_45d17FEB24	T2_0d17FEB24	T3_90d17FEB24	T3_45d17FEB24
23.329	23.709	23.697	23.686	23.709	23.704
23.615	23.962	23.862	23.873	23.945	23.854
23.894	24.210	24.024	24.061	24.173	24.000
24.185	24.450	24.183	24.247	24.396	24.144
24.483	24.688	24.342	24.438	24.613	24.285
24.786	24.919	24.496	24.630	24.824	24.420
25.092	25.148	24.651	24.825	25.026	24.553
25.416	25.376	24.807	25.026	25.225	24.682
25.764	25.602	24.963	25.231	25.423	24.812
26.114	25.826	25.115	25.437	25.619	24.934
26.486	26.047	25.267	25.640	25.812	25.051
26.872	26.269	25.413	25.846	26.003	25.162
27.255	26.489	25.557	26.058	26.194	25.273
27.640	26.707	25.698	26.272	26.379	25.378
28.024	26.920	25.838	26.492	26.560	25.479
28.426	27.121	25.980	26.715	26.728	25.580
28.852	27.316	26.120	26.937	26.890	25.684
29.282	27.509	26.259	27.160	27.047	25.789
29.710	27.687	26.402	27.386	27.191	25.900
30.145	27.860	26.553	27.611	27.328	26.018
30.573	28.029	26.711	27.850	27.463	26.138
31.024	28.195	26.869	28.091	27.596	26.261
31.474	28.356	27.026	28.349	27.722	26.386
31.921	28.507	27.182	28.615	27.837	26.509
32.361	28.654	27.349	28.892	27.948	26.628
32.844	28.795	27.520	29.205	28.054	26.752
33.332	28.933	27.694	29.542	28.153	26.885
33.808	29.069	27.876	29.899	28.250	27.028
34.280	29.205	28.063	30.258	28.345	27.173
34.744	29.335	28.248	30.628	28.433	27.319
35.198	29.464	28.429	31.024	28.520	27.465
35.656	29.588	28.607	31.426	28.602	27.615
36.130	29.702	28.790	31.832	28.676	27.765
36.589	29.813	28.977	32.264	28.746	27.924
37.039	29.921	29.165	32.701	28.813	28.084
37.461	30.026	29.368	33.168	28.878	28.251
37.850	30.124	29.574	33.626	28.935	28.423
38.227	30.219	29.777	34.084	28.989	28.595
38.595	30.308	29.988	34.555	29.039	28.770
38.942	30.394	30.219	35.024	29.088	28.949
39.283	30.481	30.450	35.461	29.138	29.135
39.608	30.571	30.689	35.874	29.192	29.333
39.865	30.665	30.919	36.264	29.252	29.528
40.110	30.759	31.187	36.630	29.313	29.727
40.341	30.855	31.471	36.955	29.376	29.925
40.564	30.951	31.774	37.248	29.442	30.133
40.734	31.046	32.086	37.503	29.507	30.344
40.900	31.144	32.396	37.737	29.577	30.577

41.051	31.241	32.705	37.949	29.646	30.818
41.190	31.347	33.027	38.116	29.727	31.073
41.316	31.458	33.354	38.267	29.815	31.342
41.418	31.567	33.709	38.411	29.907	31.645
41.479	31.677	34.077	38.517	30.003	31.965
41.530	31.784	34.443	38.595	30.098	32.287
41.570	31.888	34.797	38.633	30.191	32.617
41.600	31.991	35.154	38.661	30.283	32.972
41.617	32.091	35.514	38.678	30.372	33.349
41.601	32.194	35.881	38.674	30.468	33.724
41.578	32.303	36.281	38.659	30.572	34.108
41.534	32.415	36.665	38.632	30.681	34.512
41.457	32.525	37.036	38.597	30.789	34.931
41.376	32.635	37.396	38.560	30.896	35.339
41.282	32.745	37.765	38.514	31.003	35.748
41.183	32.854	38.117	38.471	31.112	36.148
41.062	32.959	38.439	38.413	31.218	36.509
40.946	33.063	38.730	38.353	31.323	36.841
40.827	33.164	38.997	38.287	31.428	37.140
40.695	33.262	39.246	38.211	31.530	37.397
40.558	33.355	39.451	38.130	31.629	37.621
40.417	33.445	39.619	38.048	31.727	37.808
40.280	33.537	39.762	37.962	31.829	37.956
40.139	33.638	39.885	37.872	31.940	38.069
39.999	33.731	39.976	37.774	32.046	38.155
39.858	33.817	40.026	37.671	32.147	38.205
39.698	33.894	40.057	37.565	32.243	38.235
39.541	33.966	40.068	37.454	32.339	38.248
39.388	34.032	40.056	37.342	32.428	38.249
39.237	34.093	40.015	37.230	32.513	38.240
39.089	34.157	39.963	37.115	32.600	38.222
38.940	34.217	39.893	37.000	32.685	38.194
38.775	34.273	39.815	36.885	32.765	38.157
38.612	34.322	39.731	36.768	32.838	38.115
38.452	34.367	39.641	36.646	32.907	38.066
38.294	34.410	39.548	36.526	32.977	38.011
38.140	34.452	39.449	36.405	33.044	37.950

N-S axis H/W=3	E-W axis H/W=4	NE-SW axis H/W=4	N-S axis H/W=4
T3_0d17FEB24	T4_90d17FEB24	T4_45d17FEB24	T4_0d17FEB24
23.686	23.693	23.698	23.676
23.857	23.957	23.834	23.841
24.028	24.211	23.966	24.009
24.197	24.454	24.096	24.175
24.369	24.691	24.224	24.340
24.544	24.919	24.346	24.505
24.721	25.134	24.464	24.671
24.899	25.336	24.579	24.841
25.079	25.529	24.691	25.013
25.256	25.720	24.799	25.187
25.433	25.901	24.904	25.360
25.610	26.079	25.006	25.531
25.797	26.253	25.105	25.705
25.984	26.422	25.199	25.885
26.171	26.585	25.290	26.065
26.363	26.739	25.380	26.249
26.553	26.891	25.468	26.432
26.746	27.041	25.557	26.618
26.945	27.182	25.653	26.809
27.146	27.321	25.753	27.004
27.352	27.454	25.856	27.200
27.565	27.581	25.960	27.399
27.782	27.694	26.064	27.602
28.004	27.798	26.171	27.809
28.228	27.899	26.277	28.019
28.464	27.995	26.389	28.242
28.713	28.089	26.507	28.477
28.978	28.176	26.639	28.716
29.267	28.256	26.771	28.976
29.573	28.324	26.903	29.237
29.905	28.387	27.034	29.512
30.257	28.444	27.166	29.813
30.634	28.493	27.300	30.169
31.046	28.541	27.440	30.558
31.466	28.586	27.582	30.976
31.907	28.625	27.731	31.418
32.368	28.652	27.883	31.880
32.843	28.671	28.038	32.383
33.325	28.689	28.194	32.897
33.815	28.708	28.352	33.418
34.263	28.727	28.519	33.895
34.688	28.754	28.692	34.326
35.066	28.791	28.867	34.700
35.404	28.832	29.049	35.034
35.714	28.877	29.235	35.318
35.978	28.924	29.424	35.550
36.196	28.973	29.619	35.731
36.384	29.025	29.826	35.850

36.539	29.080	30.040	35.946
36.655	29.143	30.266	36.023
36.752	29.215	30.496	36.090
36.816	29.295	30.748	36.135
36.867	29.377	31.017	36.172
36.897	29.457	31.300	36.193
36.919	29.538	31.610	36.204
36.931	29.618	31.941	36.208
36.938	29.698	32.283	36.207
36.934	29.782	32.651	36.197
36.920	29.875	33.041	36.179
36.896	29.970	33.448	36.150
36.864	30.064	33.873	36.116
36.827	30.156	34.309	36.075
36.781	30.247	34.744	36.032
36.736	30.338	35.172	35.985
36.683	30.433	35.559	35.932
36.626	30.529	35.913	35.878
36.566	30.624	36.220	35.812
36.493	30.718	36.498	35.741
36.418	30.810	36.734	35.670
36.345	30.899	36.932	35.600
36.271	30.984	37.095	35.526
36.194	31.071	37.223	35.448
36.111	31.161	37.319	35.364
36.023	31.256	37.394	35.276
35.932	31.350	37.445	35.187
35.838	31.441	37.483	35.099
35.744	31.536	37.508	35.007
35.650	31.633	37.519	34.911
35.556	31.726	37.521	34.813
35.454	31.814	37.514	34.716
35.352	31.905	37.499	34.621
35.249	31.992	37.476	34.524
35.144	32.077	37.446	34.429
35.040	32.158	37.410	34.335
34.938	32.235	37.370	34.242